Identification of mechanisms of acquired resistance to taxanes in triple negative breast cancer using patient-derived xenografts: a step closer to clinics

Jorge Gómez Miragaya

University of Barcelona

Faculty of Pharmacy

Cancer Epigenetics and Biology Programme

Programme of Biomedicine

Identification of mechanisms of acquired resistance to taxanes in triple negative breast cancer using patient-derived xenografts: a step closer to clinics

Memory presented by Jorge Gómez Miragaya to obtain the tithle of doctor by the

University of Barcelona

Thesis director: Eva González Suárez

PhD student: Jorge Gómez Miragaya

Thesis tutor: Francesc Ventura Pujol

Jorge Gómez Miragaya. 2018.

AGRADECIMIENTOS

Me gustaría empezar agradeciendo a la Dra. Eva González Suárez la oportunidad que me dio hace ya más de cinco años para empezar el doctorado en su laboratorio. Ha sido un camino arduo y difícil, a lo largo del cual hemos aprendido mucho juntos, sobre todo técnicas de última generación. Ambos hemos hecho grandes esfuerzos y dedicado mucho tiempo para sacar la tesis adelante, pero finalmente lo hemos conseguido.

Agradecer todo el apoyo que desde el PEBC y otros departamentos nos han brindado. Tanto por los análisis bioinformáticos (Toni Gómez, Sebas, Maren, Laia Paré, Luis Palomero, etc.) como por los reactivos prestados. Hay que destacar que lo mejor del PEBC siempre ha sido su gente, desde el lab 1 hasta el 7, y tiene que seguir siendo así porque es lo que lo ha hecho grande. Al echar la vista atrás uno se acuerda de esos antiretreats para compensar los fines de semana de retreat "secuestrados", las tonterías en cultivos hasta horas intempestivas, las bromas y sustos en el estabulario, etc. Todo esto siempre ha sido lo mejor. Vuestra inestimable ayuda ha sido imprescindible y ha hecho más llevadero el camino.

Gracias también a los compañeros del laboratorio, tanto de Eva como de Puri. A los que ya no están (Álex, Pili, Gonzalo, María, Héctor, Fran, etc.) como a los que aún continúan (Guille, Eva T., Sandra, Marina, Clara, Ana, Adrià, Laura, Marta). La verdad es que creo que me costará encontrar un grupo con gente tan buena como vosotros. Me alegro de haber compartido todo este tiempo con vosotros y de haberos conocido!

También agradecérselo a todos amigos, tanto a los de toda la vida (Bombi, Abel, Agus, Javi, etc.) como a la gente que más tarde se ha incorporado a mi vida y estoy muy contento de ello (Ceru, Gregor, Sara, Meri, Silvia, etc.). Gracias por aguantarme durante tanto tiempo (sé que no os ha sido tarea fácil ;-)), por estar ahí en los malos momentos y por seguir juntándonos. Eso no lo podemos perder a pesar de todo lo demás.

Mis exjefes del bar Córdoba: Paco, Peri y Sevi. Bien sabeis que os echo mucho de menos y que me alegro un montón de haberos conocido, así como a vuestras familias y gente del bar. Me habeis hecho sentir como en una gran familia. Gracias!

Qué decir de mis padres? Son los que me han hecho ser tal como soy y a ellos les debo haber emprendido este camino. Gracias por todo lo que habeis hecho por mi. En especial a ti, mama, que pasaste por esta enfermedad. Ya he puesto mi granito de arena para mejorar el día a día de la gente. Estamos más cerca de la cura!

Gracias también a mis abuelos, que se que me vigilan y protegen allá donde estén, y al resto de mi familia. Os quiero.

Y finalmente gracias a Marta. Por aguantarme más que nadie, en los días difíciles sacarme una sonrisa y hacer más llevadero el día a día. Eres un apoyo fundamental y único, sin ti

TODO hubiera sido mucho más complicado y tú, con tu forma de ser, lo has facilitado. Y sí, ya nos iremos de viaje muuuuy lejos para celebrarlo…

La tesis va dedicada a ti mamá,

porque te prometí de pequeño que iba a intentar curar a la gente de esta enfermedad y seguimos luchando con la misma fuerza por ello y porque nadie tenga que volver a pasar por lo que tu pasaste. Te quiero.

INDEX

ABBREVIATIONS

ABBREVIATIONS

A647: alexa 647

ABCC1: ATP Binding Cassette Subfamily C Member 1

ABCG2: ATP Binding Cassette Subfamily G Member 2

Akt: Protein kinase B

ALDH1: aldehyde dehydrogenase 1 family, member A1

APC: allophycocyanin

BAX: Bcl-2-associated X protein

Bcl2: B-cell lymphoma 2

Bcl-xL: B-cell lymphoma-extra large

BCSC: breast cancer stem cell

BIRC5: baculoviral IAP repeat containing 5

BRCA1: breast cancer 1

BRCA2: breast cáncer 2

CCNE1: cyclin E1

cDNA: complementary deoxyribonucleic acid

CD10: cluster of differentiation 10, common acute lymphocytic leukemia antigen

CD133: cluster of differentiation 133, prominin

CD24: cluster of differentiation 24

CD44: cluster of differentiation 44

CD49f: cluster of differentiation 49, integrin alpha 6

CK: cytokeratin

CNV: copy number variation

CSC: cancer stem cell

DMEM: Dulbecco's modified Eagle's medium

DNA: deoxyribonucleic acid

EDTA: ethylenediaminetetraacetic acid

EGF: epidermal growth factor

EGFR: epidermal growth factor receptor

ELDA: extreme limiting dilution assay

EpCAM: epitelial cell adhesión molecule

ER: estrogen receptor

ERK:extracelular signal-regulated kinases

ESR1: estrogen receptor 1

FACS: fluorescence-activated cell sorting

FBS: fetal bovine serum

FISH: fluorescence *in situ* hybridization

FITC: fluorescein isothiocyanate

GATA3: GATA Binding Protein 3

GSEA: gene set enrichment analysis

HER2: human epidermal growth factor receptor 2

H&E: hematoxilin and eosin

IGF1: insulin growth factor 1

INPP4B: inositol polyphosphate 4-phosphatase type II

KO: knock-out

MAPs: microtubule-associated proteins

MAPKs: microtubule-associated protein kinases

METABRIC: Molecular Taxonomy of Breast Cancer International Consortium

MLL3: mixed-lineage leukemia protein 3

MKI67: marker of proliferation Ki-67

NF-κB: nuclear factor-kappa B

NOD: non-obese/diabetic

OPG: osteoprotegerin

PE: phycoerythrin

PI3K: phosphatidylinositol-4,5-bisphosphate 3-kinase

PIK3CA: phosphoinositide-3-kinase, catalytic, alpha polypeptide

PIK3R1: phosphoinositide-3-kinase regulatory subunit 1

PPiA: peptidylprolyl Isomerase A

PR: progesterone receptor

PTEN: phosphatase and tensin homolog

RANK: receptor activator of nuclear factor kappa B

RANKL: receptor activator of nuclear factor kappa B ligand

RAS: rat sarcoma viral oncogene

SCID: severe combined immunodeficient

SNV: single nucleotide variant

R-Fc: RANK-Fc

RNA: ribonucleic acid

ROS: reactive oxygen species

TCGA: the cáncer genome atlas

TIC: tumor initiating cells

TGF-beta: tumor growth factor-beta

TNF: tumor necrosis factor

TP53: tumor protein p53

Wnt: Wingless-type MMTV integration site family

INTRODUCTION

INTRODUCTION

Cancer

Cancer definition

Cancer is a general term that covers more than 200 different types of diseases, which can be considered independent diseases, with their specific causes, evolution and treatment. The common denominator is the ability to multiply and spread throughout the organism that cancer cells present (**Figure 1**) (https://www.aacrfoundation.org/Pages/what-is-cancer.aspx).

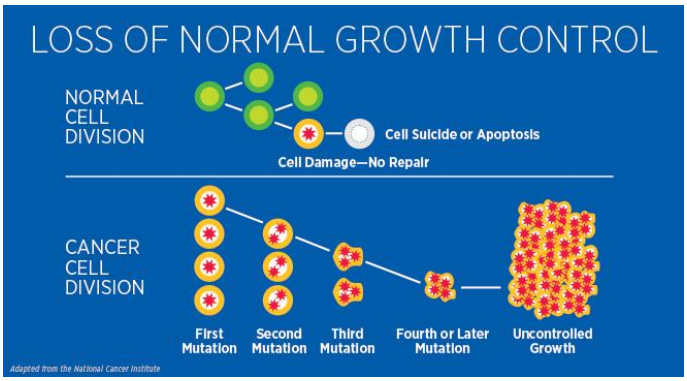

Figure 1. Scheme related to cell proliferation, normal growth control loss. Adapted from the National Cancer Institute (NCI).

Cancer types

Cancer is classified in different types according to the organ or cell of origin where it takes place (https://www.aacrfoundation.org/Pages/what-is-cancer.aspx). In that way, different cancer types are grouped into:

- Carcinomas, those which take place in the skin or internal epithelial tissues.
- Sarcomas, those which occur in bones, cartilage, fat, muscle, blood vessels and other connective or supportive tissues.
- Leukaemia, those which take place on blood and bone marrow cells.

- Lymphomas, those which occur in immune system cells (normally they appear in the lymphatic system).
- Central nervous system cancer, those which take place on cerebrum and spinal cord.

Breast cancer

Breast cancer is the cancer type originated in the mammary gland. Normally breast cancer is developed from epithelial cells, which can be from lobular or ductal compartment, and rarely it is developed from stromal cells, as fat or fibrous connective tissue.

Incidence of breast cancer

Breast cancer is the most common cancer type, with the exception non-melanoma skin tumors, and the second leading cause of cancer death among women worldwide, presenting in 2012 overall figures of 1.7 millions of diagnostics and near to 522.000 deaths in women worldwide (GLOBOCAN 2012, Fitzmaurice et al., 2017).

It is estimated that woman's risk to suffer breast cancer is approximately 13% and the incidence is increasing around the world, due mainly to an earlier diagnostic but also due to the ageing population in the developed countries (GLOBOCAN 2012, Fitzmaurice et al., 2017).

In Spain the incidence is lower than in other European countries, such as UK, France, Switzerland, Belgium or Germany. However, around 28.000 new cases were diagnosed in 2015 in our country (REDECAN), which accounts approximately for 30% of all tumors diagnosed in women. The age of greatest population incidence ranges between 45 to 65 years old (AECC).

Prognosis of breast cancer

Thanks to early diagnosis, in Spain over the past 20 years survival has increased by 1.4% per annum, by making it 5 years form diagnosis the overall survival is 83%, which is above the European average (EURCOARE-4). In this way, breast cancer mortality in Spain is among the lowest in Europe and the number of deaths has stabilised in recent years. However, the

number of deaths due to breast cancer represents a 17% of all deaths due to cancer in women (AECC).

Types of breast cancer

There are several types of breast cancer, which can be classified according to different parameters, such as the cells of origin, the location in the breast, the degree of invasion, the histologic grade, or gene expression patterns. The different types of breast cancer are detailed below.

Cell of Origin

Carcinoma: it develops from the cells that line the organs and tissues, called epithelial cells.

Adenocarcinoma: it is a type of carcinoma that develops from glandular epithelial cells, which may be ductal or lobular. It is the type of breast cancer most common.

Sarcoma: it develops from muscle cells, fat or connective tissue located in the breast and that supports the ducts and lobules. It is a very rare type of breast cancer, accounting for less than 1% of the primary breast cancer.

Histologic Classification

Carcinoma *in situ* (CIS): Injury composed of abnormal epithelial cells that are completely confined within the ducts and lobules of the breast. These lack or incompletely several of the hallmarks of invasive cancers and that the molecular changes involved in progression to invasive carcinoma does not always occur (Ward et al., 2015). This type of carcinoma comprises a heterogeneous group of lesions that can be divided mainly in ductal, originating in breast ductal cells, and lobular, originating in lobular or alveolar cells. The ductal carcinoma *in situ* (DCIS) is considerably more common than lobular carcinoma *in situ* (LCIS) (Malhotra et al., 2010).

Invasive carcinoma (IC): Group of malignant epithelial tumors characterized by the invasion of adjacent tissues and a marked tendency to metastasize to distant organs. It is believed

that they may derive from the breast parenchymal tissue (WHO, 2012). They are subdivided into:

- Invasive ductal carcinoma (IDC), a heterogeneous group of tumors that are originated in ductal cells.
- Invasive lobular carcinoma (ILC), composed of non-cohesive individually dispersed or arranged in a linear pattern in a fibrous stroma.
- Invasive tubular carcinoma (ITC), composed of well-differentiated tubular structures with open lumen lined by a single layer of epithelial cells. It has a particularly favorable prognosis.
- Invasive cribriform carcinoma (ICC), characterized by growing up with a cribriform pattern and mixed with a tubular component. It is usually associated with an excellent prognosis.
- Medullary Carcinoma (MC), composed of poorly differentiated cells without glandular structures, little stroma and a prominent lymphoplasmocytic infiltrate.
- Mucin-producing carcinoma, defined by the abundant production of intra- and/or extracellular mucin.
- Neuroendocrine carcinomas, defined by morphological characteristics similar to pancreatic neuroendocrine tumors of the gastrointestinal tract and the lung. Express neuroendocrine markers in more than 50% of its population.
- Invasive papillary carcinoma, similar to infiltrating ductal carcinomas with papillary architecture. It comprises less than 1-2% of invasive breast tumors and are characterized by a relatively good prognosis.
- Apocrine carcinoma, constituted by the cytological and immunohistochemical features of the apocrine cells in more than 90% of the tumor cells.
- Metaplastic carcinomas, formed by a mixture of adenocarcinoma with key areas of spindle cells, squamous cell and/or mesenchymal differentiation. Fusiform cells and squamous cells may also occur without any mixture of adenocarcinoma.

Other rare types of breast tumors are Pagget's disease of the nipple, where the cancer cells are generated in the nipple or areola; Phyllodes tumors, which form in the stroma and tend to grow in the form of sheet quickly but rarely metastasize; angiosarcoma, which is formed

in the blood vessels and/or lymph vessels; and inflammatory breast cancer, a rare type of tumor but very aggressive in which cancer cells block the lymph vessels in the skin of the breast, giving rise to the breast will be swollen and reddened (WHO 2012, Pourteimoor et al., 2016).

Histologic Grade

Normal adult cells are differentiated in order to carry out their function in the organs; however the cancerous cells lose this differentiation and become disorganized and highly proliferative. In this way, the histologic grade is an assessment of differentiation (tubular formation and nuclear pleomorphism) and proliferative activity (mitotic index). Currently, the Notthingam system, also known as the Bloom-Richardson-Elston system, is mostly used worldwide for histologic classification (Pourteimoor et al., 2016). In this way, there are three histologic grades:

- Grade 1, which corresponds to well-differentiated tumors, and a good prognosis. The cells look like normal cells, and tumors grow slowly.
- Grade 2, which corresponds to tumors of moderate differentiation and intermediate prognosis. They still keep some phenotypic similarity with the cells of origin and their growth is most fast.
- Grade 3, which corresponds to poorly differentiated tumors and poor prognosis. Cells from these tumors do not resemble the cells of origin and tumors grow quickly. Tumors belonging to this histological grade are the most frequently metastasizing.

TNM classification

TNM staging system used in breast cancer is a classification system based on the progression and stage of breast cancer, so it is representative of the severity of the tumor progression (Pourteimoor et al., 2016). The factors that this system takes into account are 3:

1. Location of the primary tumor and tumor size (T);
2. Involvement of the lymph nodes (N);
3. Presence or absence of distant metastases (M).

Once the variables T, N, and M are measured separately, they are combined and a comprehensive stage is assigned, which can be:

1. Stage 0: they are carcinoma *in situ* (CIS). Tumor cells are located exclusively in the lobules or ducts.
2. Stage I (T1, N0, M0): The size of the tumor is less than 2 cms. There is no involvement of lymph nodes or distant metastases.
3. Stage II: Tumor between 2 and 5 cms, with or without axillary node involvement.
4. Stage III: The tumor affects axillary nodes, and/or skin and chest wall (muscles or ribs).
5. Stage IV: The primary tumor has metastasized, affecting other distant organs, such as bone, liver, lungs, and brain (the most common metastatic sites in breast cancer).

This staging classification is closely related to the prognosis of the disease and the survival. The percentage of 5-year survival i 100% in stage I and about 20% in stage IV.

Clinical Classification

Clinical classification is based on a characterization by immunohistochemistry (IHC) of hormone receptors for estrogen receptor (ER) and progesterone receptor (PR), the human epidermal growth factor receptor 2 (HER2) and the proliferation marker Ki67 (Goldhirsch et al., 2011). In this way, breast tumors can be classified as:

- Luminal (60 - 80%): those which present expression of ER and/or PR without amplification or overexpression of HER2 in tumor cells. It can be divided into luminal A, those with expression of Ki67 less than 14%, and luminal B, those with high Ki67 expression. These tumors have a better clinical prognosis, specially the Luminal A subtype.
- HER2-positive (20 - 30%): those which have genomic amplification or protein overexpression of HER2, independently on expression of ER and/or PR. HER2-positive breast cancer is more aggressive and has a less favourable prognosis than HER2-negative breast cancer.

- Triple Negative Breast Cancer (TNBC) (10 - 20%): those which do not present expression of ER, PR, or amplification or overexpression of HER2. These tumors have a worse clinical prognosis.

Treatment decisions are principally based in the clinical classification but also other clinicopathologic factors are taken into account, including age, tumor size, histological grade, metastases in lymph nodes and lymphovascular invasion. These parameters have been consolidated into guidelines, such as those of St. Gallen consensus criteria, the Nottingham Prognostic Index (NPI), and the National Comprehensive Cancer Network (NCCN) guidelines (Pourteimoor et al., 2016).

Intrinsic molecular subtypes

While the histological and clinical classifications of breast cancer have prognostic value, the lack of a molecular component limits the ability to predict the response to anticancer therapies (Pourteimoor et al., 2016). In this way, breast cancer patients with the same histological and clinical subtype have great heterogeneity as well as diverse evolution and response to treatments. In the last 15 years, the identification of the intrinsic molecular subtypes of breast cancer through the analysis of microarray-based gene expression has filled this gap (Perou et al., 2000; Prat et al., 2010; Sørlie et al., 2001; Sorlie et al., 2003). Thus, the different intrinsic molecular subtypes of breast cancer are classified in (Figure 2):

- Basal-like: at RNA and protein level these tumours are characterized by a very high expression of epithelial genes characteristic from basal cells, as well as very low expression of genes typically luminal and intermediate expression of *HER2*-related genes. They also show a high expression of proliferation-related genes, as *MKI67*, and keratins typically expressed in the basal layer of the skin, such as *KRT5*, *KRT14* and *KRT17* (Prat et al., 2015). At DNA level, these tumors show the second highest rate of mutations and chromosomal aberrations throughout the genome, being *TP53* and *PIK3CA* the most commonly mutated genes. Hereditary breast tumors carrying *BRCA1* mutations are associated with this

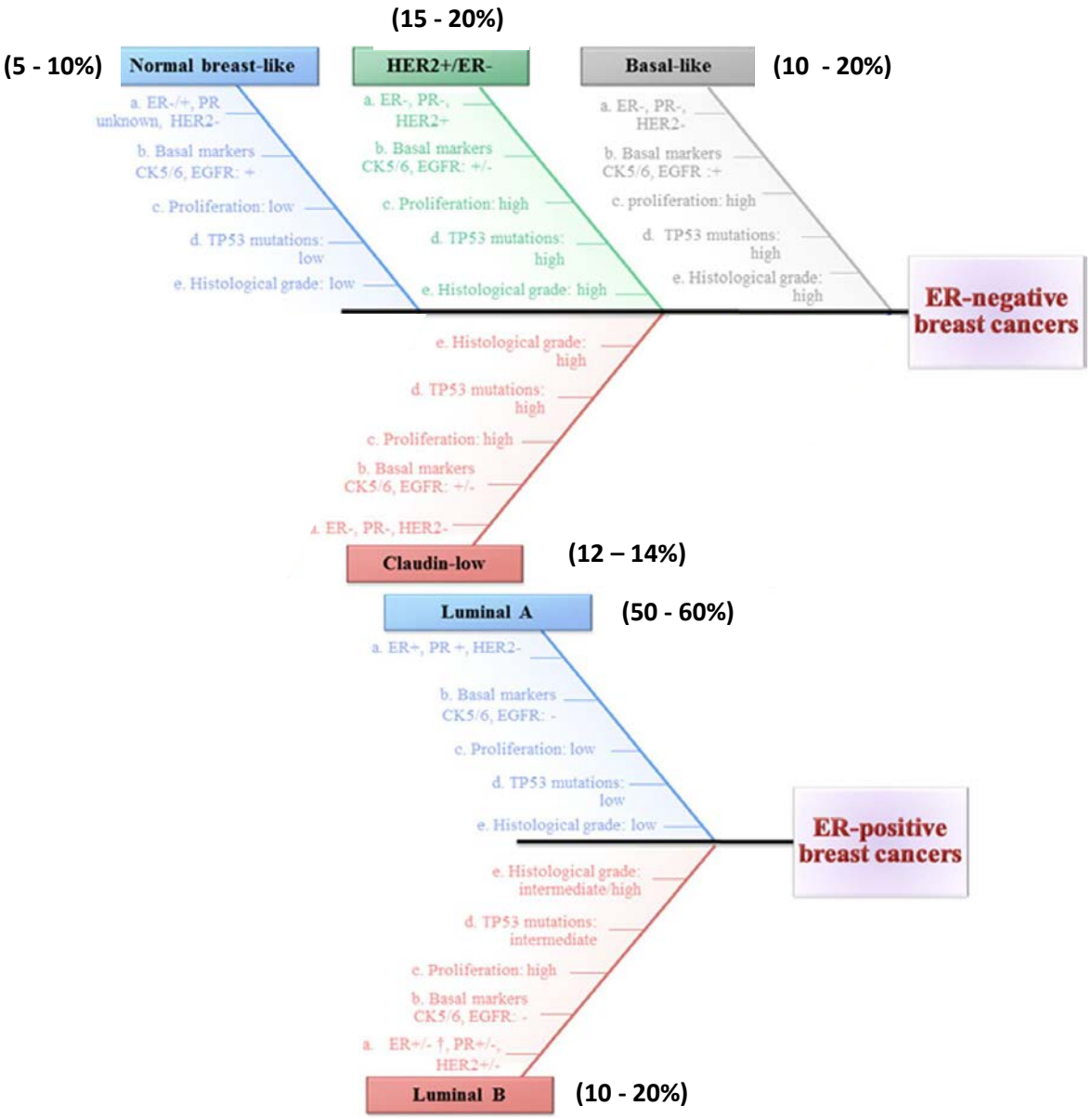

Figura 2. Scheme of the intrinsic molecular subtypes of breast cáncer, indicating the main features and the percentage of total breast tumors that represent (Eroles et al., 2012). Modified from (Pourteimoor et al., 2016).

subtype (Network, 2012; Prat et al., 2015). Most of basal-like tumors are TNBC and, therefore, do not have targeted treatment and clinical management mainly consists in (neo)adjuvant combinations of chemotherapeutic agents (Prat et al., 2015). Lower survival and greater risk of relapse correlate also with this subtype (Sørlie et al., 2001).

- Claudin-low: at RNA and protein level these tumors are characterized by low expression of intercellular binding proteins, such as *CLDN3*, *CLDN4* and *CLDN7*, and luminal genes, such as *ER* and *GATA3*, enrichment in markers of epithelial-mesenchymal transition (EMT), such as *VIM*, *TWIST2* and *ZEB2*, immune response genes and features of CSC (Prat et al., 2010; Sabatier et al., 2014). At DNA level, these tumors display several gains and losses suggesting a high genomic instability, showing no clear differences when compared to basal-like tumors (Sabatier et al., 2014). They are usually TNBC, so tumors with poor prognosis, and high frequency of medullary and metaplastic differentiation (Prat et al., 2010; Sabatier et al., 2014). As TNBC, they are mainly treated with combinations of chemotherapeutic agents.

- Luminal A: similarly to luminal B, these tumors are characterized by the expression of genes associated to luminal epithelial cells. Two major biological processes are regulated in this tumor subtype: downregulation of cell cycle- and proliferation-associated pathways and upregulation of hormone- and luminal-regulated pathways. Tumors from these subtype are usually ER/PR-positive and they show also the highest expression levels of *ESR1*, *GATA3* and *HNF3α* among other genes (Sørlie et al., 2001). Tumors from this subtype display lower number of mutations throughout the genome, lower number of chromosomal aberrations, lower mutation rate of *TP53*, similar of *GATA3* and higher of *PIK3CA* and *MAP3K1* regarding to the luminal B subtype (Prat et al., 2015). They show the best prognosis among all molecular subtypes (Sørlie et al., 2001) and the treatment is based primarily on endocrine therapy; they do not respond to chemotherapy (Prat et al., 2015), presenting the lower rates of pathological complete response to this systemic treatment (Bonnefoi et al., 2014; Sabatier et al., 2014).

- Luminal B: these tumours have higher expression of proliferation- and cell cycle-related genes, such as *MKI67* and *AURKA*, and lower expression of several luminal-related genes, such as *PGR* and *FOXA1*, but not the *ESR1*, which is found similarly expressed between the two luminal subtypes (Prat et al., 2015). They present an intermediate clinical prognosis (Sørlie et al., 2001) and the treatment is mostly with endocrine therapy; as luminal A tumors, they do not respond to chemotherapy (Prat

et al., 2015). However, in that point is important to mention that there is now a controversial in the use of chemotherapy in ER-positive/luminal tumors, as those revealing a 'high' Ki67 score, expressing moderate to low ER levels, with a luminal B gene expression signature or having a high recurrence score are likely a subtype responding to chemotherapy (Albain et al., 2010; Lønning, 2012).

- HER2-enriched: tumors from these subtype are characterized at RNA and protein level by the expression of proliferation-related genes and HER2 pathway, as *HER2* and *GRB7*, intermediate expression of luminal genes, such as *ESR1* and *PGR*, and low expression of basal genes, such as *KRT5* and *FOXC1*. At DNA level, these tumors have the highest rate of mutations and chromosomal aberrations. Despite the fact that most present overexpression/amplification of *HER2*, there are tumors without this feature that are classified by gene expression as HER2-enriched (Prat et al., 2015). The overexpression of the HER2 oncoprotein is associated with worse survival in breast cancer, so tumors of this subtype, along with the basal-like subtype, show the worst survival and recurrence prognosis (Sørlie et al., 2001). This subtype of tumors is treated primarily with HER2 pathway inhibitors combined normally with chemotherapy (Prat et al., 2015).

- Normal-like: these tumors are defined by the expression of many genes known to be expressed in adipose tissue and in other types of non-epithelial cells. They express high levels of basal genes and low levels of luminal genes (Sørlie et al., 2001). Patients harbouring these tumors present an intermediate clinical prognosis (Sørlie et al., 2001). However, some studies have questioned the existence of this subtype based on the small number of breast tumors that fall into the normal-like subtype, showing low tumor cellularity when examined pathologically, which likely explains why they cluster with the true normal breast samples (Prat and Perou, 2011).

The usefulness of this new molecular classification depends on how it can be transferred to the clinics. Initially, intrinsic molecular subtypes were carried out through the use of gene expression microarrays (Sørlie et al., 2001; Sorlie et al., 2003), which made it prohibitive in the clinical setting, due to its high cost. To overcome this impediment, the list of genes used

for the classification of the intrinsic molecular subtypes has been declining (Hu et al., 2006), until being reduced to a gene signature of only 50 genes, known as PAM50 (Parker et al., 2009), maintaining its subtypying predictive capacity. In addition, it was demonstrated that PAM50 gene signature improved the prediction of the risk of recurrence compared with the classical model of clinical classification that uses only variables such as tumor size, lymph node involvement, histologic grade, and the expression of biomarkers such as hormone receptor and HER2. It also has the property of being able to predict pathologic complete response (IARC 2003; Pourteimoor et al., 2016).

Lim and colleagues proposed a model describing how the intrinsic molecular subtypes of breast cancer would be associated with gene expression patterns from subpopulations of normal mammary gland at different stages of differentiation (Lim et al., 2009) (Figure 3). They directly compared the gene expression profiles of normal mammary epithelial subsets [i.e. basal/mammary stem cell

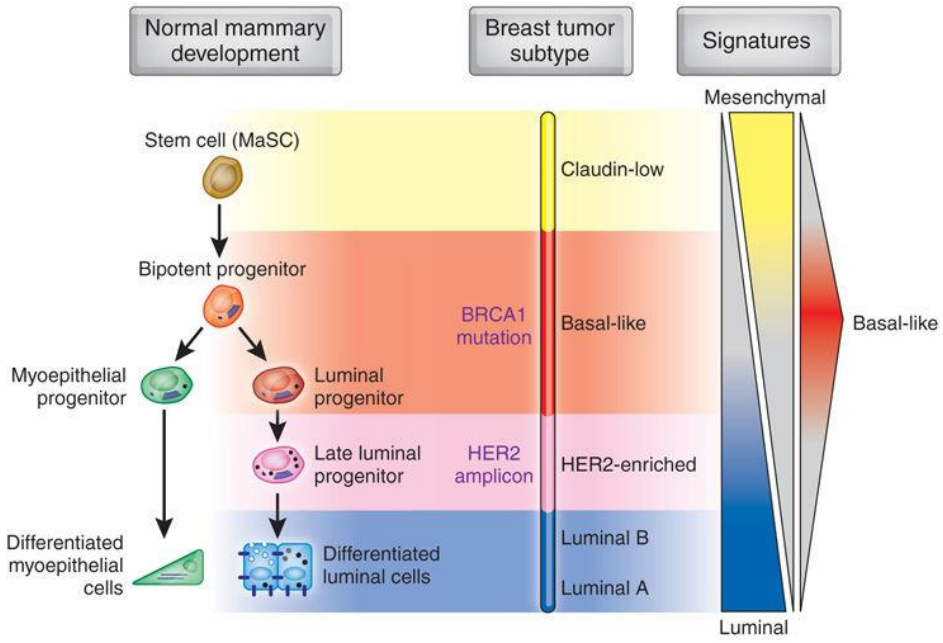

Figure 3. Model of the human mammary epithelial hierarchy related to breast cancer molecular subtypes (Prat and Perou, 2009).

(MaSC), luminal progenitor and mature luminal cells] to those of breast tumors falling into each of the intrinsic subtypes, including basal, luminal A/B, and claudin-low. They found that the luminal A and B subtypes were most similar to the mature luminal cells, while

unexpectedly, the luminal progenitor gene expression signature was most highly associated with the basal-like/BRCA1-mutated subtype. Meanwhile, the MaSC-signature was closely in line with the claudin-low subtype. This observation has since been noted by other groups as well (Prat and Perou, 2011). In fact, many of the immunohistochemical and molecular markers that define the basal-like subtype, such as cytokeratins 5/6 and cytokeratin 14, are also expressed by luminal cells in human tissues, including mammary gland ducts and also terminal duct lobular units (Gusterson et al., 2005). Therefore, the so-called “basal-like” gene expression signature may actually be a luminal progenitor signature. Likewise, the claudin-low tumors show similarities with the basal/MaSC subpopulation of epithelial cells, a finding that is in line with the generation of metaplastic, poorly-differentiated tumors from basal precursors. Finally, the HER2-enriched subtype would be mostly generated from luminal progenitor cells. Currently there is an emerging consensus that most common subtypes arise as a result of transformation of normal mammary cells at different stages of differentiation (Pfefferle et al., 2015; Skibinski and Kuperwasser, 2015).

Hereditary breast cancer

Hereditary breast cancer accounts for about 10% of all diagnosed breast cancers (Pharoah et al., 2002), its transmission follows an autosomal dominant pattern and the pathology usually happens in women at early age. Two genes accumulate most of the cases of hereditary breast cancer, *BRCA1* and *BRCA2*. These are tumor suppressor genes discovered in the mid 1990 (Hall et al., 1990; Wooster et al., 1994). *BRCA1* and *BRCA2* act as "DNA-keepers" being responsible to repair DNA when it is damaged (McCarthy and Armstrong, 2014). In such a way mutations in *BRCA1* and *BRCA2* genes confer a risk of developing breast cancer of about 60% and 50%, respectively, as well as increases the risk of bilateral breast cancer and ovarian cancer (Chen and Parmigiani, 2007). Interestingly, the Ashkenazi Jewish population is more likely to suffer from hereditary breast cancer due to identified mutations in *BRCA1* and *BRCA2*, which occurs in greater proportion in this population, due to their ancestral inbreeding (Struewing et al., 1997).

In recent times the genome-wide association studies have led to the discovery of new mutations that increase the risk of breast cancer (Peng et al., 2011). Hence mutations identified in genes such as *PTEN*, *TP53*, *STK11*, *CDH1* and *PALB2*, among others, have been associated with a higher risk of developing hereditary breast cancer (Shiovitz and Korde, 2015).

Breast cancer treatment

Different types of treatment are available for patients with breast cancer. The treatments known as "standard of care" are the most commonly used, which have been accepted by medical experts as the most appropriate treatments due to scientific studies and clinical responses. New treatments in continuous development can be found under clinical trials, being subject to strict protocols and controls. Clinical trials are research studies that have as their objective the gathering of information and approval of new treatments as well as the improvement in the treatment using existing drugs (i.e. different combinations or drug regimens). When clinical trials show that a new treatment is better than the standard of care, this is adopted as a new standard of care.

To choose a treatment, different clinical factors are taken into account, such as the expression of hormone receptors (ER and PR) and HER2 overexpression, the histologic grade of the tumor, the TNM classification, as well as other prognostic factors.

The types of treatments can be classified according to two parameters:

- Affectation, divided into local treatment, when it is directed to the tumor's place of origin or to any particular location (e.g. surgery, radiation therapy), and systemic treatment, when it affects the entire body (e.g. chemotherapy, hormone therapy).

- Administration time, divided in adjuvant treatment, when therapy is managed as a local or systemic treatment after the prophylactic surgery with the aim to reduce the risk of breast cancer recurrence, and neoadjuvant treatment, when therapy is managed as a local or systemic treatment prior to surgery with the aim of reducing tumor size.

The standard treatments can be divided into 5 groups:

- Surgery has been the common treatment of breast cancer for centuries with the idea of eliminating the breast cancer from its primary site completely. Initially a radical mastectomy was used (i.e. removal of the breast tissue, the nipple, areola, skin, lymph nodes, and pectoral muscles) (Halsted, 1894). Fisher and colleagues showed that total and simple mastectomy (i.e. removal of the breast tissue, the nipple, areola and skin) have similar effectiveness, demonstrating that simple mastectomy could replace total mastectomy (Fisher et al., 2002a). Also a new study comparing mastectomy against lumpectomy (i.e. removal of the breast tumor and a piece of healthy breast tissue while retaining the rest of the breast and lymph nodes) accompanied by radiation showed that does not change survival, becoming lumpectomy the standard surgery (Fisher et al., 2002b). Currently, in certain cases administration of chemotherapy can replace radiation therapy.
  It is also very common the removal of the sentinel node (i.e. axillary node closest to the tumor on the first draining the breast) along with a lumpectomy. The affectation of the sentinel node is an important prognostic factor, and its affectation implies the study of the rest of nodes.

- Chemotherapy, based on the use of antineoplastic agents in both systemic neoadjuvant and adjuvant regimen. Its use is mainly suitable for TNBC, which lack targeted therapies, as well as for metastatic or high histologic grade breast tumors of any subtype. Chemotherapy is given in the form of cycles, alternating periods of treatment with periods of rest, being these cycles weekly, fortnightly, tri-weekly, etc. depending on the type of antineoplastic agent administered and the drug combination (Rapoport et al., 2014).

  The most commonly used chemotherapeutic agents are:
  Anthracyclines (e.g. doxorubicin, epirubicin): discovered and extracted from bacteria of the genus *Streptomyces*. There are two proposed mechanisms by which anthracyclines act on tumor cells: by insertion in the DNA and the consequent disruption of the DNA repair mediated by topoisomerase-II, avoiding DNA replication

and RNA synthesis; by generation of reactive oxygen species (ROS) that damage cell membranes, DNA and proteins (Gewirtz, 1999). The use of anthracycline-based regimens has been shown to increase the benefits of the treatment in combination with other types of chemotherapeutic agents, as cyclophosphamide, methotrexate, and fluorouracil (Poole et al., 2006).

Taxanes (e.g. docetaxel, paclitaxel): diterpens discovered and extracted initially from plants of the genus *Taxus*. They are considered microtubule stabilizers (Figure 4), as they bind to tubulin, stabilize it and prevent its depolymerization, inducing cell cycle arrest, cell death and apoptosis (Bines et al., 2014). The incorporation of taxanes to anthracycline-based treatment has improved the response of patients to treatment (Gianni et al., 2009).
The standard treatment in TNBC is the combination of anthracyclines and taxanes (Coates et al., 2015).

Platinum-based agents (e.g. cisplatin, carboplatin): platinum-coordinated structural complexes whose mechanism of action is based on the DNA inducing intra- and intercatenary connections (Poklar et al., 1996; Rudd et al., 1995), inhibiting DNA repair as well as synthesis during tumor cell division. They are also called “similar to alkylating agents” due to their similar effects (Cruet-Hennequart et al., 2008). Platinum-based agents have aroused great interest in the treatment of TNBC because they are associated with better response in tumors with defects in DNA repair mechanisms (i.e. mutated *BRCA1* tumors) and high proliferation ratios, making TNBC/*BRCA1*-mutated tumors highly sensitive to DNA intercalating agents (Byrski et al., 2010; Silver et al., 2010).

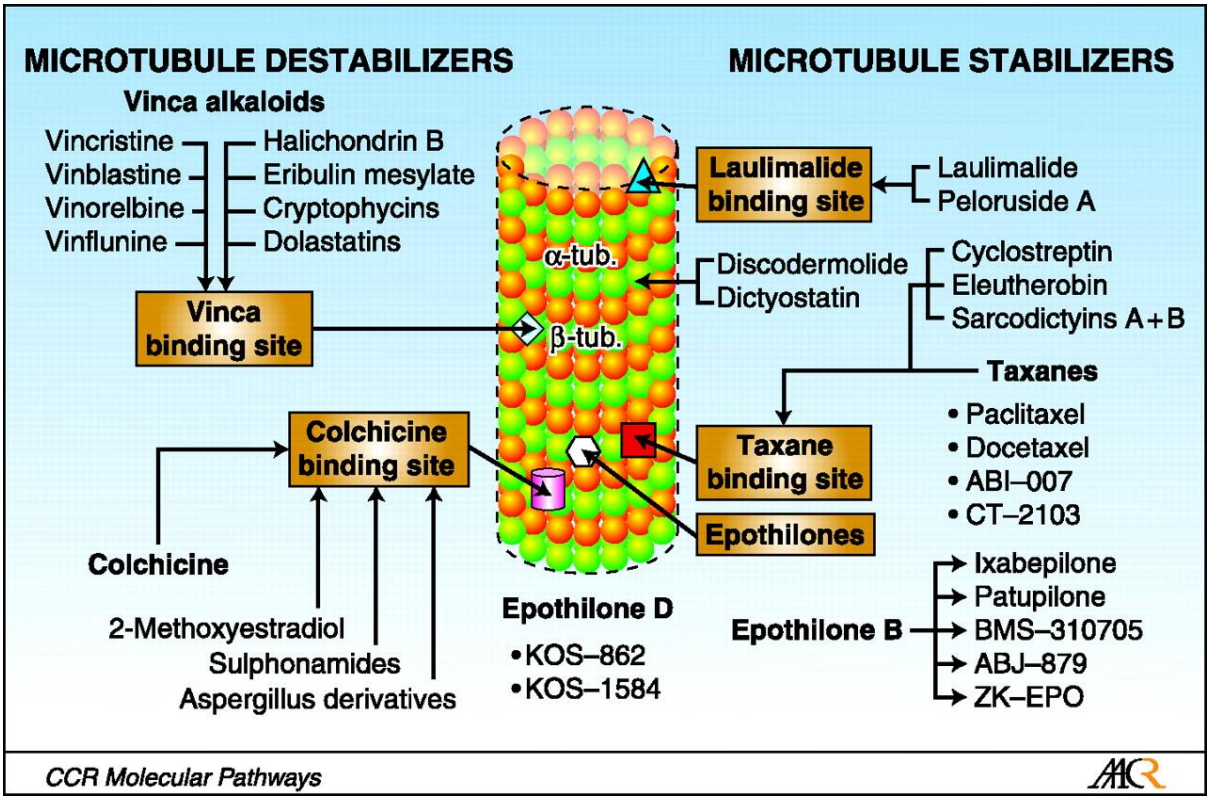

Figure 4. Chemotherapeutic agents acting as microtubule stabilizers or destabilizers, including taxanes, and their binding site to microtubules (Morris and Fornier, 2008).

- Radiotherapy: based on the use of ionizing radiation for the treatment of breast cancer using high-energy X-rays. There are two main types of treatments, external radiation, which comes from a machine located on the outside of patient's body, and internal radiation or brachytherapy, where the radioactive source is inside the body during a short period of time. Radiation therapy is associated with lower rates of recurrence and longer survival after lumpectomy (Early Breast Cancer Trialists' Collaborative Group (EBCTCG) et al., 2011; Fisher et al., 2002b).

- Endocrine or hormonal therapy (e.g. tamoxifen, fulvestrant): used exclusively for the treatment of hormone-positive tumors (ER and/or PR-positive), also called hormone sensitive tumors, in pre- and post-menopausal women. They act by stopping or slowing cell growth by blocking the production of hormones or by interfering with the effect of hormones in breast tumor cells. Endocrine therapy is the first type of systemic treatment directed at a specific target, the hormone-dependent cancer

cells, and may be referred to as "targeted therapy", but normally is separated from that group of treatments as they can act in non-cancer cells.

The hormones, particularly oestrogen and progesterone in women, are chemical messengers produced mainly by the ovaries, but also by other tissues, such as fat and skin. They act in an endocrine manner, affecting organs far away from where they are produced, through transport by bloodstream. In hormone-positive breast tumors, once hormones reach the breast cancer cells, they are internalized in the cells where bind to hormone receptors. Active hormone receptors translocate to nucleus, where they function as transcription factors inducing the expression of cell proliferation-related genes (Daniel et al., 2011; Klinge, 2001). The standard hormonal treatment during the past 30 - 40 years has been based on the use of tamoxifen (Jones and Buzdar, 2004; Matsen and Neumayer, 2013), a selective estrogen receptor modulator (SERM) that blocks the effects of estrogen in the breast cancer by attaching to the ER in breast cells. However, side effects from tamoxifen have led to the development of new hormonal therapies, such as aromatase inhibitors and the use of the luteinizing hormone-releasing hormone (Jones and Buzdar, 2004; Matsen and Neumayer, 2013).

- Biological or targeted therapies: based on the use of drugs that attack specifically cancer cells without harming normal cells. In breast cancer treatment, the targeted therapies used are mostly monoclonal antibodies, tyrosine kinase inhibitors, cyclin-dependent kinase inhibitors, mTOR pathway inhibitors, PARP inhibitors and antiangiogenic drugs.

  HER2-targeted therapies for the treatment of HER2-positive breast cancer have been developed. They are mainly anti-HER2 monoclonal antibodies, such as trastuzumab and pertuzumab, and tyrosine kinase inhibitors, such as lapatinib, which have led to an increase in survival and a lower recurrence rate in HER2-positive tumors, with fewer side effects than other systemic therapies (Geyer et al., 2006; Slamon et al., 2011; Swain et al., 2015). The use of specific inhibitors of the PI3K/AKT/mTOR pathway in ER-positive breast tumors, such as everolimus, has made possible an

improvement in the survival of these patients regarding to patients just treated with aromatase inhibitors (Yardley et al., 2013). Similarly, the use of CDK4/6 inhibitors in ER-positive breast tumors has improved disease-free survival (Finn et al., 2015), and sensitisized breast tumors to other drugs (Vora et al., 2014). On the other hand, the use of antiangiogenic therapy is controversial, due to the existence of studies that show a better progression of patients treated with this type of therapeutic agents (Miller et al., 2007; Saux et al., 2014) but no improvement in overall survival (Miller et al., 2007; Robert et al., 2011), or even, counter-productive effects, as increasing numbers of breast CSC, metastases and tumor aggressiveness (Conley et al., 2012; Pàez-Ribes et al., 2009).

In the last years increased evidences of PARP inhibitors effectiveness have been unravelled. PARP inhibitors are a group of novel oral anticancer drugs highly active in a subgroup of TNBC with selected mutations or epigenetic silencing of *BRCA1* and *BRCA2* (Geenen et al., 2017). Several studies with PARP inhibitors have demonstrated promising results in the treatment of *BRCA*-mutated breast and ovarian cancer, both as monotherapy and in combination with cytotoxic therapy or radiotherapy (Geenen et al., 2017).

Currently, new avenues for treatment of breast cancer are emerging, including immunotherapy, androgen receptor (AR) targeted therapy and glycoprotein NMB (gpNMB) targeted therapy, among others. The immunotherapy can be categorized as active immunization, using specific stimulation of the immune system, with vaccines against cancer, or passive immunization, using specific antibodies, such as anti-tumor immune modulators, or adoptive cell therapy that inhibits the function or directly kills the tumor cells (Bianchini and Gianni, 2014; Criscitiello et al., 2014). The androgen receptor has been identified as another possible predictive biomarker for antiandrogen therapy in breast cancer, mainly in AR-positive, ER-negative breast cancer (Gucalp et al., 2013), being bicalutamide and enzalutamide promising treatments. Another strategy targeting TNBC is through the gpNMB, a transmembrane protein expressed in approximately 40% to 60% of breast cancers. A recent phase I/II study investigated a fully humanized anti-gpNMB monoclonal antibody conjugated to antimitotic, chemotherapeutic agents in patients with

metastatic breast cancer. Progression-free survival was particularly improved in gpNMB-positive and TNBC, and phase II studies are under way (Bendell et al., 2014).

Cancer stem cells (CSC)

The concept of the CSC was first hypothesized in the 20th century by Bonnet and Dick in their studies of human acute myeloid leukaemia (AML) (Bonnet and Dick, 1997). Their studies indicated the presence of a unique cellular hierarchy in AML, reflecting a similar order identified during normal haematopoiesis. Leukemic stem cells identified in this hierarchy, originally termed as CSCs, were categorized as $CD34^{+}/CD38^{-}$.

The terms TIC and CSC are used interchangeably, when they really are not synonymous. In this way, TICs are the cancer-initiating cells that give raise a tumor and it is determined by xenotransplantation assays (Rycaj and Tang, 2015). On the other hand, the CSCs are cancer-propagating cells that show not only TICs features, but they also are defined by two attributes, self-renewal and multipotency (Rycaj and Tang, 2015). This two features of CSCs contribute to tumor heterogeneity, tumor propagation, recurrence, metastasis and resistance to chemotherapy (Clevers, 2011; Visvader, 2011; Visvader and Lindeman, 2010). Initially these cells were identified as minor tumor subpopulations, so that only a small fraction of the cells that make up the tumor presents the characteristics of self-renewal, self-replication and tumor initiation (Al-Hajj et al., 2004); but recently, this idea has been revised, showing that tumors present different frequencies of cancer stem cells (Clevers, 2011). In breast cancer, these are the so-called breast cancer stem cells (BCSC) and the rest are considered differentiated cancer cells.

As mentioned before, different features or processes have been associated to CSCs, as epithelial-to-mesenchymal transition (EMT), self-renewal and differentiation, metastasis and therapy resistance. The epithelial–mesenchymal transition (EMT) is a process by which epithelial cells lose their cell polarity and cell-cell adhesion, and gain migratory and invasive properties to become mesenchymal stem cells. Multiple studies have associated EMT with stemness and BCSCs (Ansieau, 2013). During EMT, a series of changes take place, including the shutdown of transcription factors and down regulation of epithelial markers such as E-cadherin, and the appearance of mesenchymal markers such as vimentin, fibronectin, and

N-cadherin. These changes lead to unstable structures and functions in these cells (Thiery et al., 2009), inducing EMT in normal and neoplastic human mammary epithelial cells , highlighting the role of EMT in BCSC niche maintenance.

CSCs have also the ability to self-renew and a potential to differentiate, generating cells with a variety of phenotypes within tumors. Several pathways with key roles during embryonic development and adult tissue homeostasis have been implicated in the regulation of BCSCs self-renewal, including Notch, Hedgehog, and Wnt among others (Karamboulas and Ailles, 2013; Peitzsch et al., 2013). CSCs are also responsible for the metastatic dissemination of tumors. Different lines of evidence indicate that BCSCs play an important role in metastasis, by displaying these cells increased cell motility, invasion, and overexpressed genes that promote metastasis (Charafe-Jauffret et al., 2009; Geng et al., 2014; Liu et al., 2010; Shipitsin et al., 2007; Velasco-Velázquez et al., 2011).

Taken together these observations, it has been postulated that identification and targeting of these population will benefit patient survival and outcome.

Intratumoral heterogeneity

Previously it has been exposed the great intertumoral heterogeneity of breast cancer, reflected by the multiple subtypes and classifications that can be performed. But there is also intratumoral heterogeneity in breast cancer, which refers to the existence of different cell populations within tumors (Bruna et al., 2016; Swanton, 2012; Yates et al., 2015; Zhang et al., 2015b). Thus, as aforementioned, the tumors can be composed by CSC and differentiated tumor cells in different proportions (Batlle and Clevers, 2017; Clevers, 2011). This intratumoral heterogeneity can be usually seen at histological level by the presence of cells with different phenotypes (Denisov et al., 2014; Gerashchenko et al., 2017; Tashireva et al., 2017). However, the intratumoral heterogeneity can also be described in functional terms, characterized by specific genomic, epigenomic or expression signature subclones.

Two models have been mainly proposed for the generation and maintenance of intratumoral heterogeneity: the clonal evolution and the cancer stem cell model (Figure 5).

Both models are able to explain the intratumoral heterogeneity in different ways. Different studies have also demonstrated that these hypothesis are not exclusive, but they are mainly inclusive (Marusyk et al., 2012). In the clonal evolution model, cells acquire (epi)genetic changes that not only give rise to derivatives with different functionalities and behaviour but also serve as a platform for further acquisition of (epi)genetic alterations. In the continuum of evolution, this process produces tumors with noticeably distinct and variant abilities for survival, malignancy, and therapy tolerance at the regional and distant metastatic sites. This model predicts that cancers arise from a single cell, which over time can develop various combinations of mutations resulting in (epi)genetic drift and selection of the fittest. According to the clonal evolution model, cancer progression is non-linear with clones branching out to produce diverse clones, which leads to heterogeneity (Marusyk and Polyak, 2010; Marusyk et al., 2012). One of the disadvantages of this model is that it ignores non-(epi)genetic variability and does not take into consideration the interactions among clones within the tumor ecosystem and the interaction with the microenvironment (Janiszewska and Polyak, 2015).

In contrast, the CSC model proposes that only a subpopulation of tumor cells with stem cell properties drives tumor initiation, progression, and recurrence because of their indefinite self-renewal capability (Bapat, 2007; Kreso and Dick, 2014; Marusyk et al., 2012), and eradication of this subpopulation is critical for tumor elimination. CSCs share fundamental properties of stem cells (as mentioned before, self-renewal, undifferentiated state and ability to give rise differentiated cells), but harbour tumor-initiating mutations which can be transferred to the progeny (Bjerkvig et al., 2005). Heterogeneity in CSCs has been revealed by generation of a variety of differentiation states (Kreso and Dick, 2014).

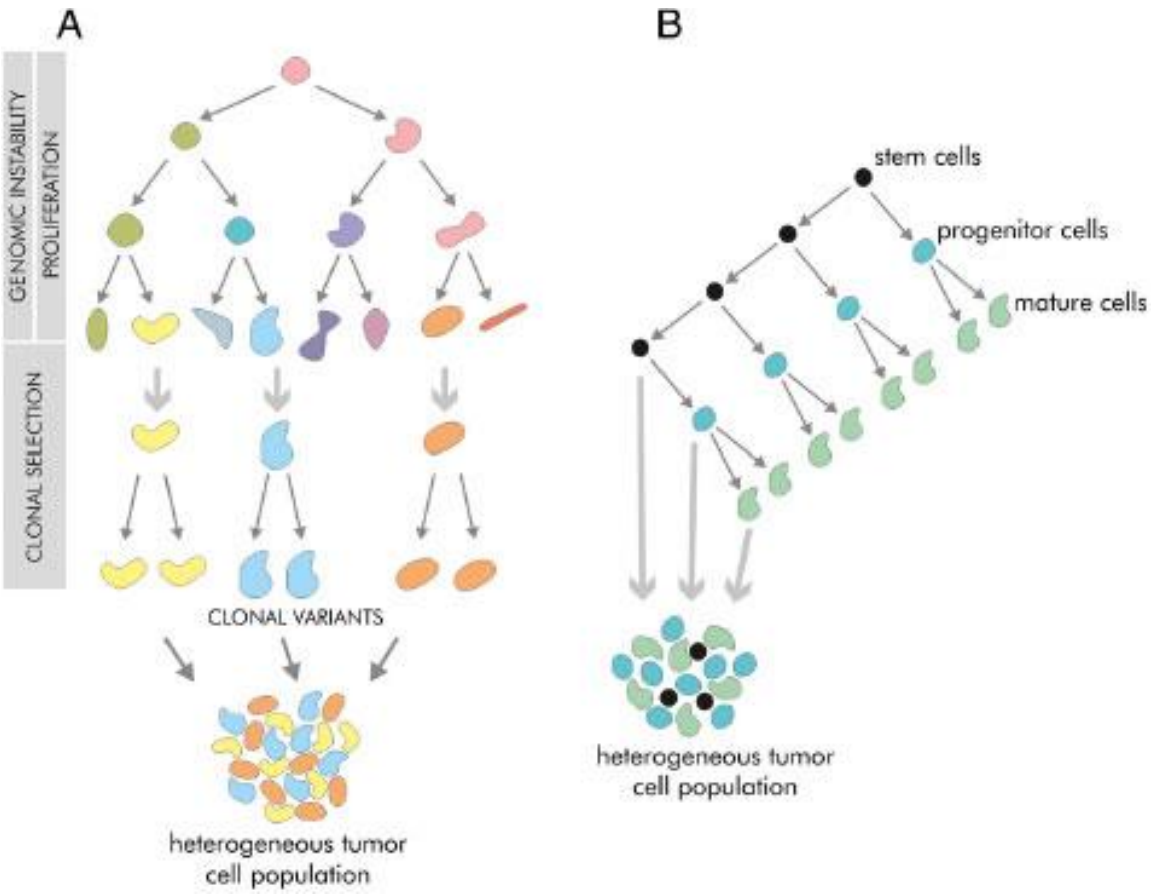

Figure 5. Models of intratumour heterogeneity. **A)** Clonal evolution model. High proliferation and genomic instability result in a large number of cells differing in genotype and thus phenotype. The best fitted cells are selected by Darwinian processes to generate clonal variants of the tumour. **B)** Cancer stem cell model. CSC population is capable of unlimited number of divisions. Tumour heterogeneity results from existence of phenotypically diverse populations of different stages of cell maturation.

The main difference between both hypotheses is that while the first is a competition between populations of tumor cells with different phenotypes, the second takes into account a program of aberrant differentiation from CSCs. In addition, the target cell of transformation is different in both cases, as in the first case this cell initially transformed is a mammary differentiated cell while in the second hypothesis is a mammary stem cell (Marusyk and Polyak, 2010).

This intratumoral heterogeneity may play an important role not only in tumor development but also in clinical behaviour as in therapy response. The (epi)genomic sequencing has

allowed to analyze the clonal evolution in breast cancer through the single cell sequencing during tumor progression (Alevizos et al., 2014; Braun et al., 2005; Ding et al., 2010; Eirew et al., 2015; Wang et al., 2014)

In this way, some genome-wide studies of paired primary-metastatic breast cancer provided an initial view of intratumoral heterogeneity in primary breast cancer and its evolution in metastatic disease (Ding et al., 2010; Shah et al., 2009). Also, genome-wide analysis of primary and different lung metastatic samples from a single patient showed that each metastatic site harboured distinct mutational events, with a common inactivating mutations in PTEN indicating convergent and parallel evolution (Juric et al., 2015). This mutations would be the cause of PI3K inhibitors resistance in the primary tumor (Juric et al., 2015), allowing this first mutational event the recurrence in primary site and then the spread to other distant organs.

Importantly, these studies have mainly focused on single nucleotide variants (SNV). However, breast cancer has on average one of the lowest levels of SNVs in solid tumors (Kandoth et al., 2013), and a “panomic” analysis by TCGA categorized breast cancer into a copy number variant (CNV)-driven disease (Ciriello et al., 2013). Early studies using CNV arrays revealed genome-wide changes in DNA copy number between primary tumors and metastases (Nishizaki et al., 1997). Studies analyzing CNVs in single disseminated cancer cells confirmed that CNVs are both gained and lost during progression, but interestingly, the lower number of CNVs found in disseminated tumor cells compared with the primary tumor suggested that tumor cells disseminate very early in a less progressed evolutionary state (Schmidt-Kittler et al., 2003). Focused analysis of CNV changes in breast cancer has recently given insight into tumor evolution and the timing of different genetic changes (Janiszewska and Polyak, 2015).

The intratumoral heterogeneity in breast cancer has also a clear clinical translation. It has been demonstrated that a tumor in early stage will present fewer (epi)genetic changes that a larger tumor detected later (Corte et al., 2010; Shafi et al., 2013). There is also a greater likelihood that a tumor with greater heterogeneity present worse prognosis because some of these clones can present an evolutionary advantage to the treatment (De Palma and Hanahan, 2012; Ramos and Bentires-Alj, 2015). Increasing evidences highlight the existence

of the low-frequency resistant clones within a tumor that expand under selective pressure with drug treatment (Turner and Reis-Filho, 2012). Genetic changes, environmental differences, and dynamic conversion among tumor cells within a tumor may all lead to phenotypic and functional heterogeneity (Meacham and Morrison, 2013). Technically, it remains a challenge in cancer genomics to detect minor and genetically distinct subpopulations within tumors, a problem that actually is solved with single cell genomic analysis. Another handicap is to determine individual cell fate after drug treatment or environmental changes without applications of lineage tracing and deep sequencing, which may help to determine the extent to which intratumoral heterogeneity accounts for therapy resistance and disease progression (Meacham and Morrison, 2013).

Taking into account that high levels of intratumoral heterogeneity are in general associated with a worse outcome, this indicates the importance of genome-based stratification for the treatment of breast cancer, which will be an important prerequisite for personalized genomic medicine (Aparicio and Caldas, 2013; Baird and Caldas, 2013). In addition, using deep-genome and single-cell sequencing methods, Eirew and colleagues analyzed (during the period of this thesis) DNAs from patient-derived xenograft (PDX) lines as well as their matched patient samples to identify any clonal variations or dynamics during engraftments at the single-cell level. Varying degrees of clonal selection, from rare clone (<5% of starting population) to moderate, polyclonal engraftment, were observed in all ten primary and five metastatic breast tumors. PDX models were shown to recapitulate the clonal heterogeneity, with some drift (Eirew et al., 2015).

Markers of breast cancer stem cells

The identification of CSCs is a very hard and complicated issue that has been improved during last years. The advances in demonstrating the existence of CSCs were due to the development of the flow cytometry technology, the use of fluorescent antibodies and immunodeficient mice. The first CSC from solid tumors were identified and isolated in breast cancer in 2003 (Al-Hajj et al., 2003); subsequently, CSCs have been described in colonic, pancreatic, prostatic, ovarian, hepatic, lung, gastric, melanoma and brain tumours (https://stemcells.nih.gov/info/Regenerative_Medicine/2006chapter9.htm#ref14).

Cancer stem cells are detected and isolated using mainly cell surface markers, but some intracellular, enzymatic markers (ALDH) and activity of certain ATP-binding cassette transporter proteins (side populations), which are able to transport fluorescent dyes out of the cells, are also used (Greve et al., 2012). CSC features are then interrogated after isolation by others *in vitro* or *in vivo* assays. Fluorescent-activated cell sorting (FACS) is the golden isolation method capable of sorting via fluorochromes in direct or indirect immune fluorescence staining (Al-Hajj et al., 2003; Ponti et al., 2005; Maeda et al., 2008). Generally, FACS separation uses fluorochromes with different emission wavelengths, what allows the separation of CSCs via multiple markers simultaneously (Al-Hajj et al., 2003; Ponti et al., 2005; Maeda et al., 2008). Intracellular, enzymatic markers, which are more stable than surface markers, are also used for CSC detection and isolation (Ginestier et al., 2007).

But all these methodologies to isolate CSCs have also shown some limitations. As stem cell features like side population and ALDH or cell surface markers are measured exclusively, they have disadvantages to identify CSCs unequivocally, especially in tumor tissue (Liu et al., 2011b). For example, SP analysis alone was not sufficient to define a CSC phenotype in glioblastoma multiforme (Broadley et al., 2011) and this was also the case for CD44+/CD24- cells in breast cancer (Fillmore and Kuperwasser, 2008). Thus, it might be more advantageous to use several markers and properties in combination. Some new technologies using metal-conjugated antibodies will facilitate analysis of CSCs by combining more than 40 parameters.

CSCs reveal also a unique gene expression profile consisting of stem cell-specific genes (Bolós et al., 2009; Leis et al., 2012; Liu et al., 2011a; Okano et al., 2002). These predominantly intracellular markers would be useable for a specific labeling of CSCs if suitable molecular probes were available which are capable of entering living cells. New methods based on using a molecular beacon to visualize mRNA in live mouse embryonic carcinoma stem cells have been developed (Rhee and Bao, 2009). However, the construction of molecular beacons and the transfection procedure require further development and testing, thus limiting the applicability of this innovative technique at the present time. The most common markers actually available to select BCSCs are described below.

CD44

It is a cell surface glycoprotein and specific receptor to hyaluronan that is involved in cell-cell interactions, cancer adhesion, motion, migration and invasion (Herrera-Gayol and Jothy, 1999). Its interaction with osteopontin leads also to tumor progression (Rangaswami et al., 2006). CD44 has an important role in cell proliferation and tumor angiogenesis (Götte and Yip, 2006). It is a marker not only of BCSCs, but also of CSCs from other tissues (Guzmán-Ramírez et al., 2009; Wei et al., 2010), which is also involved in metastasis. The injection of CD44+ cells from breast cancer patients in the cleared mammary fat pad from NOD/SCID mice as well as the use of non-invasive imaging strategies to localize the injected cells demonstrate the increased tumorigenicity and lung metastatic ability of these cells (Liu et al., 2010). Beside standard CD44 (sCD44), it was discovered that expression of variant isoforms of CD44 (vCD44), created by alternate splicing of the mRNA that elongates extracellular domain, induced a metastatic phenotype in locally growing tumour cells (Günthert et al., 1991). Notably, ectodomain cleavage of CD44 is highly prevalent in tumours, and soluble CD44 levels after cleavage were detected in the serum not only of breast cancer patients, but also in other cancer types, correlating its expression with tumour burden (Okamoto et al., 2002).

CD24

CD24 is another surface glycoprotein expressed at low levels that increases the ability of tumors to grow and metastasize (Schabath et al., 2006). As mentioned before, in 2003, Al-Hajj and colleagues reported for the first time that breast cancer can originate from BCSCs (Al-Hajj et al., 2003). They identified and isolated a small subset of cells based on CD24 expression in combination with CD44. Thus, CD44+/CD24- expression within primary breast cancer cells identified BCSCs of which a few cancer cells were able to form palpable tumors after injection in the mammary fat pad of NOD/SCID mice. Since then, the CD44+/CD24- phenotype has been used as a reliable phenotype for the isolation of BCSCs (Perrone et al., 2012; Ponti et al., 2005; Wright et al., 2008).

EpCAM

This transmembrane glycoprotein mediates the calcium-independent, homophilic cell-cell adhesion in the epithelium (epithelial cell adhesion molecule, CD326) (Litvinov et al., 1994). In the mammary gland, EpCAM has been widely used in combination with other markers to select mammary stem cells, bipotent progenitors and mature luminal cells (Al-Hajj et al., 2003; Eirew et al., 2008). It participates in cell signaling (Maetzel et al., 2009), migration (Osta et al., 2004), proliferation and differentiation (Litvinov et al., 1996), as well as in tumorigenesis and metastasis by acting as a prognostic marker and potential immunotherapeutic target (Armstrong and Eck, 2003). Different clinical studies have shown that high expression of EpCAM in breast cancer is associated with worse prognosis (Gastl et al., 2000; Schmidt et al., 2008). Different antibodies that targets EpCAM have been even developed and they are under clinical evaluation for the treatment of EpCAM-positive breast cancer (Schmidt et al., 2012). EpCAM is also used for the detection of circulating tumor cells in blood (Rack et al., 2014; Yap et al., 2014) and disseminated tumor cells in bone marrow (Braun et al., 2005; Choesmel et al., 2004), and also as a predictor marker of clinical response.

CD49f

Also known as integrin α6, CD49f is a transmembrane glycoprotein belonging to integrin protein family, an unusual signalling protein family that function to signal from the extracellular environment into the cell, but also from the cytoplasm to the external of the cell. CD49f acts on platelets and epithelial cells as a receptor for laminins. The intracellular signalling cascades associated with integrin activation focus on protein kinase activities, such as focal adhesion kinase and Src (Giancotti and Ruoslahti, 1999). Integrins are heterodimeric integral membrane proteins composed of an alpha (α) chain and a beta (β) chain, being the most common partners for integrin α6 the integrin β1 and β4 chains. In epithelial cells CD49f plays a critical structural role in the hemidesmosome. It also acts as a mediator of the cell-cell adhesion and cell matrix (Giancotti and Ruoslahti, 1999; Hehlgans et al., 2007). It has been described that heterodimers formed by CD49f can bind directly to both neuregulin-1, due to the EGF-like domains of neuregulin-1 (Ieguchi et al., 2010), as well as IGF1 (Fujita et al., 2012), giving rise to the intracellular activation of these pathways. Pece and coworkers described that CD49f+ mammary cells enrich for anchorage-independent and

sphere-forming cells (mammospheres) (Pece et al., 2010). In breast cancer cell lines the subpopulation of CD49f+ cells has been denoted as highly tumorigenic (Cariati et al., 2008). Also, high expression in breast cancer primary tumors is associated with worse prognosis and with lower survival in patients (Friedrichs et al., 1995). In particular, the expression of CD49f by itself has been shown as a valuable independent prognostic marker of reduced survival in ER- tumors, superior to other BCSC markers (Ali et al., 2011). As occurs with EpCAM, CD49f+ cells have been detected as circulating tumor cells in blood of breast cancer patients (Mostert et al., 2012). Numerous studies have demonstrated the role of CD49f in breast cancer contributing to the regulation of processes such as cell adhesion, migration, invasion and survival (Kim et al., 2008; Mukhopadhyay et al., 1999; Shaw, 1999; Wewer et al., 1997). Studies demonstrating the potential of CD49f inhibition to sensitizes tumors cells to conventional radiotherapy in prostate cancer have been also carried out (PAWAR et al., 2007).

CD10

Also known as common acute lymphoblastic leukemia antigen (CALLA), it is a neutral endopeptidase that in the mammary gland contributes to maintain the niche of stem and progenitor cells (Bachelard-Cascales et al., 2010). The use of CD10 and EpCAM to discriminate basal from luminal breast epithelial subpopulations has been demonstrated (Keller et al., 2012). Also various functional assays have established that EpCAM separates luminal progenitors from other epithelial populations present in the CD10+ fraction (stem cells, bipotent progenitors, and differentiated myoepithelial cells) (Bachelard-Cascales et al., 2010). In tumor tissues, CD10-peptidase activity modulates the accumulation of peptides during cell proliferation and is involved in tumor progression.

CD133

It is a pentaspan transmembrane cell surface glycoprotein also known as prominin-1, and located in plasma membrane protrusions. It was initially considered to be a marker of hematopoietic stem cells (Miraglia et al., 1997), but it has been demonstrated to be also a marker for other CSCs (Cherciu et al., 2014; Li et al., 2015; Qu et al., 2013). Biological functions of CD133 on breast cancer include tumor initiation, cellular migration,

vasculogenic mimicry, and drug resistance (Nadal et al., 2013). CD133 expression was the highest in TNBC specimens compared to another breast cancer subtypes (Liu et al., 2013).

ALDH

Aldehyde dehydrogenase 1 (ALDH1) is a detoxifying agent responsible for the removal of intracellular aldehydes and retinoic acid (Sládek, 2003). ALDH enzymatic activity can also be used to enrich for BCSCs and normal mammary stem cells and progenitor cells. The combination of ALDH+ and CD44+/CD24- phenotypes, which present very few overlap between cell subpopulations, enriches further for cells with tumorigenic activity (Ginestier et al., 2007). ALDH1 activity identifies human and murine neural and haematopoietic stem cells (Armstrong et al., 2004; Hess et al., 2004), as well as for multiple myeloma and acute myeloid leukaemia stem cells (Pearce et al., 2005). Also, ALDH1-positive tumors were associated with ERBB2 overexpression and absence of estrogen and progesterone receptor expression (Ginestier et al., 2007).

Functional contribution of breast cancer stem cell markers

Questions still remain whether these cell-surface markers are only phenotypic markers or functional markers. Despite the growing list of CSC markers shown here, some researchers do not consider all these markers suitable for identifying CSCs. For example, one report shows that CD44+CD24- BCSC population is not expressed in all breast cancers (Pattabiraman and Weinberg, 2014). For that reason, the functional significance of these proteins is an important area of investigation, but it still remains poorly understood. However, some studies have elucidated a functional contribution of these markers in the acquisition of stem cell features on CSCs.

It has been suggested that CD44 has an important role in metastasis because a non-metastatic rat glioma cell line after ectopically overexpression of a CD44 splice variant acquired metastatic properties (Günthert et al., 1991). In addition, CD44 variant isoforms are differentially expressed during pregnancy and involution, indicating a role in normal breast epithelial homeostasis (Hebbard et al., 2000). Moreover, sCD44, CD44v3, and CD44v6 levels are increased in invasive breast carcinomas (Auvinen et al., 2005), and blocking

antibodies against CD44s reduced adhesion, motility, and matrigel invasion, whereas CD44v6 antibodies only inhibited motility in breast cancer cell lines (Afify et al., 2009), indicating a functional direct and specific role in BCSC features. These results, among others, are promising for the therapeutic targeting of CD44 with monoclonal antibodies and blocking peptides.

CD24 is functionally identified as an alternate ligand for P-selectin, an adhesion receptor on platelets and endothelial cells (Aigner et al., 1997, 1998), through which their interaction facilitates the passage of tumour cells in blood stream during metastasis. It increases proliferation and adhesion of tumour cells to fibronectin, collagen, and lamin (Baumann et al., 2005; Zheng et al., 2011). The function of CD24 in cell signaling has been tied to its possible role as the “gatekeeper” of lipid rafts, and it is involved in the recruitment of integrins to the complex (Runz et al., 2008). Along with increased cell adhesion, CD24 may have important roles in migration and invasion as measured by several in vitro assays (Runz et al., 2008) and association with metastasis in vivo (Sano et al., 2009; Yang et al., 2009). However, results in breast and prostate CSC have called into question the role CD24 plays in migration and invasion in cancer, as CD44+/CD24- cells have been postulated as CSCs (aforementioned).

ALDH plays a special role in the oxidation of toxic aldehydes such as acetaldehyde during alcohol metabolism. This cellular function is likely crucial for SC longevity and probably a key explanation for the reported resistance of CSCs to chemotherapies, especially those that generate toxic aldehyde intermediates. HNSCC cells expressing high levels of ALDH1, compared with cells with low expression, were found to be resistant to cisplatin and cyclophosphamide, which are both converted into toxic aldehyde intermediates (Visus et al., 2007). Separate groups have found that shRNA and siRNA knockdown of ALDH1 in colorectal xenografts and lung cells, respectively, sensitized ALDH+ CSCs to cyclophosphamide and 4-hydroperoxycyclophosphamide treatment (Dylla et al., 2008; Moreb et al., 2007).

Regardless of the biologic activities of these markers, it is remarkable that the same cell surface markers enrich for tumor stem cells across many solid tumor types. Nearly all studies on the prospective identification of human solid tumor stem cells have either xenografted the primary tumor into a NOD/SCID mouse, or briefly conditioned the tumor

cells in culture before enriching for tumor initiating cells (Al-Hajj et al., 2003; Li et al., 2007; O'Brien et al., 2007). Therefore, perhaps the markers that are currently used to identify "stem cells" from solid tumors could only be enriching for cells with certain functional properties *in vivo* or *in vitro*, namely to engraft successfully in mouse or to adhere and expand in culture. If these cell-surface molecules turn out to be functional markers and are retained during clonal evolution of cancer to an aggressive clone with CSC properties, they can also serve as therapeutic targets. More functional analysis of these cell-surface markers are required to elucidate its role in breast cancer.

Breast cancer chemoresistance

Despite advances in early detection and understanding of the molecular bases of breast cancer biology, about 30% of patients with early-stage breast cancer have recurrent disease which is metastatic in most cases (Pisani et al., 2002). Systemic treatment of breast cancer includes cytotoxic, hormonal, and immunotherapeutic agents. These medications are used in the adjuvant, neoadjuvant, and metastatic settings. It is well established that TNBC is an aggressive group of breast cancer subtypes despite having a good initial response to chemotherapy. In general, systemic agents are active at the beginning of therapy in 90% of primary TNBC and 50% of metastases (Gonzalez-Angulo et al., 2007). However, it is well established that patients with residual TNBC disease post neo-adjuvant chemotherapy have a worse prognosis than those presenting with non-TNBC (Carey et al., 2007). Also it is common that after a variable period of time, recurence occurs. At that point, resistance to therapy is not only common but expected.

There is incomplete understanding of the role of diverse gene expression, (epi)genetic, protein and non-coding RNA changes in the heterogeneous manifestations of clinical resistance (Miller et al., 2012). There is a lack of equivalence between clinical, pathological, proliferative and molecular resistance that needs to be addressed. Furthermore, multiple mechanisms have also been implicated in acquired chemoresistance, as the expression of multidrug-resistance proteins [ATP-binding cassette transporters (ABC transporters)], the overexpression of some isoforms of the tubulin preventing access to the microtubules, or

tubulin mutations that prevent the binding of the taxanes (McGrogan et al., 2008). However, their relationship to intrinsic chemoresistance remains to be defined. Some chemoresistant mechanisms are outlined below.

Breast cancer stem cells and resistance

A trait of BCSC is the intrinsic resistance to therapy and this feature in BCSC has been shown to radio and chemotherapy (Al-Hajj et al., 2004; Creighton et al., 2009; Li et al., 2008). Neoadjuvant treatment with chemotherapy in breast cancer patients has been shown to enrich in $CD44^+/CD24^-$ cells, and this remaining cells displayed a greater capacity of mammosphere formation *in vitro* (Yu et al., 2007). In addition, it has been observed that the percentage of ALDH1+ cells increases in breast tumors that have been treated with epirubicin/paclitaxel-based chemotherapy (Tanei et al., 2009). Radiotherapy also increases the proportion of CD44+/CD24- cells in patient-derived xenografts (PDX) (Phillips et al., 2006; Zielske et al., 2011).

Resistance on BCSCs is associated but not limited to the ability of self-renewal and differentiation that BCSC present, giving rise to the differentiated cancer progeny and maintaining the niche of BCSC. Certain cellular pathways are associated to BCSC, their self-renewal ability and resistance, such as the aforementioned Notch, Wnt and hedgehog. For example, the activation of Notch promotes the increase of the levels of the antiapoptotic gene *BIRC5* and the induction of *CCND1* (Stahl et al., 2006); *BIRC5* throws numerous mitotic control points, contributing to the genetic instability and inhibiting apoptosis induced by drugs (Ponti et al., 2005).

Other mechanisms of resistance associated with BCSC are the overexpression of transmembrane transporters, the modulation of DNA repair mechanisms and the elimination of reactive oxygen species (ROS).

Membrane proteins from the ATP-binding cassette (ABC) family as well as solute carriers are proteins involved in the traffic of compounds and small molecules from inside to outside of the cell (and vice versa) and between cellular organelles. They play a key role in the maintenance of homeostasis and cell survival in unfavourable conditions, as cytotoxic

treatment and/or stress (DeGorter et al., 2012). In addition, ABC transporters have been shown to confer resistance to multiple drugs (multiple drug resistance proteins, MDR) in several cancer types (Doyle and Ross, 2003; Doyle et al., 1998; Gottesman et al., 2002), what is in concordance with the idea of CSC resistance mechanisms to different compounds and across different cancer types.

Some chemotherapeutic agents work by damaging the DNA through various mechanisms such as the inhibition of DNA synthesis, the inhibition of topoisomerases or through intra- and intercatenary DNA binding, inducing cell death due to the inability to repair the DNA damage (Cheung-Ong et al., 2013). However, CSC have proved to be resistant to radiotherapy and DNA damaging chemotherapy through mechanisms to counteract these effects on DNA (Peitzsch et al., 2013).

Reactive oxygen species (ROS) are active free radicals that are produced in the inner cell due the oxidative metabolism during physiological conditions, such as cell migration, proliferation and angiogenesis (Sena and Chandel, 2012). The ROS intracellular accumulation gives rise to effects on DNA, proteins and lipids, inducing cell death (Cook et al., 2004). In that way, differentiated cells under stress or starving conditions undergo senescence or cell death. However, CSC show hyperactive mechanisms for their removal, as the activation of catalases, glutathione peroxidases, superoxide dismutases and tiorredoxins (Trachootham et al., 2009), being able to overpass these cell death signals to continue proliferating.

Due to the mechanisms of treatment resistance and in accordance with the cancer stem cell hypothesis, BCSC have been clearly associated with relapse, being these cells the responsible for that event (Donnenberg and Donnenberg, 2005; Frank et al., 2010; Greaves and Maley, 2012; Reya et al., 2001). The BCSC that survive to the selective pressure exerted by the therapy, could transmit their resistance to the progeny, thus promoting the emergence and evolution toward more aggressive tumors, as this resistance is largely thought to be a stable and heritable process. Thus, reuse of therapeutic agents that have failed is generally contraindicated. This is a established dogma in oncology for managing recurrent or refractory disease that dictates that therapy has to be changed at disease progression, because the cancer is assumed to have become drug-resistant (Kuczynski et al.,

2013). However, there are many examples from the clinic that compete with the archetype of managing recurrent or refractory disease. Thus, patients' tumours can be sensitive to the agent(s) they had originally experienced disease progression on, and that could be because the CSC are not stable (He et al., 2011; Quintana et al., 2010).

Methylation and resistance

Methylation is a heritable epigenetic change of the DNA that implies the addition of a methyl group to a cytosine that form part of a CpG dinucleotide (Esteller, 2007). These CpG are not stochastically distributed in the DNA, but they are distributed forming clusters of DNA regions enriched in CpG dinucleotides, also called CpG islands (Esteller, 2007). These CpG islands are mainly located in the promoter and the first exon of more than half of the human genes, controlling their expression (Takai and Jones, 2002). In this way, methylation of the promoter-located CpG islands of a gene usually induces silencing while the demethylation of these promoter-located CpG islands usually activates the expression of the gene (Esteller, 2007).

Methylation is an epigenetic process coordinated by DNA methyltransferases (DNMTs) which are the enzymes responsible to transfer and bind a methyl group to the cytosine of a CpG dinucleotide (Brenner and Fuks, 2006). There are known 5 enzymes with DNMT activity, one of them is responsible for transmitting the methylation from the mother to the daughter strand during cell division, it means, to transfer or reply the methylation from the mother cell to the daughter cell (Tajima and Suetake, 1998), and 3 of them are responsible for the *de novo* methylation in adult cells (Chedin et al., 2002; Okano et al., 1999).

Extensive studies on epigenome changes in breast cancer have been undertaken to understand the role of epigenetics in breast cancer and to develop novel epigenetic therapies. Such studies have demonstrated that oftenly the DNMT3b enzyme is overexpressed, which correlates with a worse prognosis and a hypermethylator phenotype (Girault et al., 2003; Roll et al., 2008). That process in many cases includes promoter hypermethylation of tumor suppressor genes, which induces a change in the opened euchromatin to a compacted, closed heterochromatin, repressing gene expression, as mentioned before (Esteller and Almouzni, 2005; Jones and Baylin, 2002, 2007). Also, the

epigenetic silencing of tumor suppressor genes by promoter methylation in one of the alleles as a second carcinogenic event after mutation of the other allele, is something which has been observed in breast epithelial cells, such as in *BRCA1* or *APC* genes (Birgisdottir et al., 2006; Jin et al., 2001), inducing breast tumorogenesis.

Less studied that the hypermethylation, the global hypomethylation also occurs in different types of cancer, including breast cancer, when compared with healthy tissue, correlating with some characteristics such as the clinical stage, tumor size and histologic grade (Soares et al., 1999). Also some proto-oncogenes involved in proliferation, metastasis, or resistance to endocrine therapy are overexpressed in breast cancer due to the hypomethylation of their promoters (Fan et al., 2006; Gupta et al., 2003; Pakneshan et al., 2004).

Epigenetic signatures have proven to be powerful biomarkers for the detection of cancer. In addition, gene-specific hypermethylation has been considered as a powerful and promising line of research for the detection and risk factor prediction of breast cancer. For example breast cancer-specific methylation could be detected in circulating tumour DNA in serum, which can be used as an early detection biomarker, or as a prognostic indicator (Müller et al., 2003; Widschwendter and Menon, 2006; Yazici et al., 2009). Recently, the ENCODE study provided a wide-ranging analysis of epigenetic marks on a small fraction of the genome (ENCODE Project Consortium, 2012). The first candidate gene epigenetic risk factor that could usefully be included in breast cancer risk models (once fully validated) has been identified (Brennan et al., 2012).

Methylation has proven also to participate in resistance acquisition to different therapeutic drugs in breast cancer. When gene function is involved in mediating effects of certain chemotherapy agents, the silencing of these genes may influence the treatment response. Studies have shown that the expression silencing of *ESR1* mediated by the hypermethylation of its promoter (Ottaviano et al., 1994) makes ER-positive breast tumors independent on estrogens and resistant to endocrine therapies. In a similar way, other studies have shown that promoter hypermethylation in cyclin-dependent kinases results in their downregulation, inducing resistance to tamoxifen in patients with ER-positive breast tumors (Iorns et al., 2008). These evidences show that tumors are able to use methylation mechanisms as a source of intrinsic or acquired chemoresistance.

Epigenetic factors also provide molecular measures of long-term exposure to potentially oncogenic agents. Epigenetic alterations are reversible, making this reversibility attractive targets for epigenetic therapy of cancer. There are two main types of epigenetic drug: DNMTis (e.g. azatidine, decitabine), which are used to prevent DNA re-methylation after cell division (Martinet et al., 2012); and HDACis (e.g.entinostat, vorinostat), which chelate the zinc co-enzyme factor, thereby blocking HDACs catalytic activity (Cai et al., 2011). Preclinical and recent clinical testing of epigenetic-targeted therapies such as entinostat and vorinostat (both histone deacetylase inhibitors) indicate that such drugs may prove effective in combination with other therapies (Azad et al., 2013; Tsai et al., 2012). Currently, epigenetic drugs are used in the treatment of cancer, mostly of leukemias (Piekarz et al., 2009; Whittaker et al., 2010), but also of breast cancer (Munster et al., 2011; Ramaswamy et al., 2012).

Many methods are available to study DNA methylation status at single base resolution (Cokus et al., 2008; Hing et al., 2015; Lee et al., 2014; Magdalena and Goval, 2009). These methods can be classified into two main categories: microarrays-based or next-generation sequencing techniques. The microarray-based technology, as the Infinium HumanMethylation450 (Infinium 450k) from Illumina Inc, uses a fixed number of probes to study specific genomic loci throughout the whole genome (Bibikova et al., 2011). Infinium 450K has been the most broadly used platform in epigenome-wide association studies of diseases, due to the low-cost, the modest requirement of DNA and the reduced sample processing time, making possible a high-performance processing of a large number of clinical samples (Bibikova et al., 2011).

Genomics and resistance

Our knowledge of the heritability of breast cancer has increased significantly during last years, as aforementioned. Known breast cancer genes (*BRCA1*, *BRCA2*, *CHEK2*, *ATM*, *PALB2*, *BRIP1*, *TP53*, *PTEN*, *CDH1* and *STK11*) make up 25 to 30% of the heritability (Melchor and Benítez, 2013). Genome-wide association studies and the recent international collaborative analyses have confirmed 77 common polymorphisms individually associated with breast cancer risk, which add a further 14% (Melchor and Benítez, 2013; Michailidou et al., 2013). If we assume the risk estimates for polygenic markers are log additive, the cumulative risk

associated with these SNPs has a median of 9% to age 80 (95% confidence intervals 5 to 15%). In the familiar setting, we have learnt that common genetic SNPs can modify the risk associated with BRCA2, which may be relevant when considering risk reducing surgery (Antoniou et al., 2010; Ingham et al., 2013).

New genome-wide studies have revealed the heterogeneity in the genomic landscape of breast cancer (Curtis et al., 2012; Stephens et al., 2012) and have also allowed to establish associations between genomics and histologic/molecular intrinsic subtypes, describing the main characteristics of breast cancer (Curtis et al., 2012; Turner et al., 2010). The different breast tumor subtypes show also different genomic landscape, what may explain the differences on biological characteristics, clinical behavior and response to therapies. Analysis in primary breast tumors have shown that missense mutations are common in luminal/ER-positive and HER2 positive tumors, while TNBC have a higher proportion of nonsense mutations, frameshifts and complex mutations (Forbes et al., 2011). TNBC subtype is the most heterogeneous, which shows great variability both in mutations and, above all, in chromosome aberrations (Lehmann et al., 2011).

TNBC/basal-like subtype and HER2-positive tumors are the ones displaying higher mutational rates per megabase among breast cancer subtypes (Hu et al., 2009; Network, 2012). Mutated genes are relatively subtype-specific, being significantly mutated genes in luminal tumors near absent in basal-like breast tumors (Network, 2012). Thus, while tumor suppressor genes *TP53*, *RB1* and *BRCA1* are frequently mutated in basal-like tumors, the oncogenes *PIK3CA*, *MAP3K1* and *GATA3* are mainly mutated in luminal breast cancer subtypes (Network, 2012). The genomic landscape of TNBC tumors is also characterized by numerous chromosomal aberrations, suggesting a high chromosomal instability, and even chromothripsis (Andre et al., 2009; Bergamaschi et al., 2006; Network, 2012; Turner et al., 2010).

Several breast cancer studies have described multiple genomic alterations associated with therapy resistance to many drugs in, but not limited to, TNBC (Dey et al., 2015; Gurden et al., 2015; Li et al., 2013; Murray et al., 2012; Printz, 2017). In this way, some resistance mechanisms come through *de novo* mutations, which generate new resistant populations not present in the tumors initially sensitive (Swanton, 2012; Zardavas et al., 2015). But, as

aforementioned, the existence of different genetic clones in the same tumor (intratumoral heterogeneity) and subsequent clonal selection in response to the drug pressure has been suggested as an explanation for the development of resistance to treatment by selection of a subpopulation present in initially sensitive breast cancer (Metzger-Filho et al., 2012; Wang et al., 2014)(Metzger-Filho et al., 2012; Wang et al., 2014). Also, the existence of intratumoral heterogeneity in terms CNV has been demonstrated (Yates et al., 2015). Studies based on FISH showed that the heterogeneity in the CNV predicts response to neoadjuvant chemotherapy (Almendro et al., 2014), demonstrating that lower genetic diversity at CNV level was significantly associated with pathologic complete response.

These evidences make plausible the idea of the acquisition of *de novo* mutations and CNV during treatment as well as the selection of subclones within initially sensitive breast tumors as mechanisms responsible of chemoresistance acquisition. However, most of the published works try to uncover biomarkers or response predictors and not really new mutations or variations in the CNV, since they rarely posses paired sensitive and resistant tumors. The elucidation of the genomic mechanisms involved in chemoresistance acquisition is necessary to improve chemotherapy treatments as well as the management regimens.

The exome is the genomic region coding for proteins. It represents less than 2% of the entire genome, however, it contains about 85% of the variants or mutations known to be associated with disease (van Dijk et al., 2014). The exome sequencing, in contrast to the whole-genome sequencing, gives rise to an enrichment in these important changes associated with disease and a smaller and manageable data set, making easier the analysis and achieving greater coverage of coding regions. In this way, the whole-exome sequencing emerges as a credible alternative to the sequencing of the human genome and converts it into the sequencing method more extensively used. Exome sequencing makes possible to detect not only point mutations, but also small insertions and deletions (INDELs) and CNV (Gonzaga-Jauregui et al., 2012; Valdés-Mas et al., 2012). There are different platforms to carry out exome sequencing studies. However, comparative studies of different platforms have shown that the Illumina HiSeq 2000 platform along with the Agilent SureSelect Human All Exon kit are those that provide best results of precision (Clark et al., 2011; Ergüner et al., 2015; Zhang et al., 2015a).

Gene expression and resistance

Gene expression profiling has had a considerable impact on our understanding of breast cancer biology. During the last 15 years, the five intrinsic molecular subtypes of breast cancer (Luminal A, Luminal B, HER-2 enriched, Basal-like and Claudin-low) and a normal breast-like group have been extensively characterized (Network, 2012; Perou et al., 2000; Prat and Perou, 2011; Prat et al., 2010). These entities have shown significant differences in terms of their incidence, risk factors, prognosis and treatment sensitivity. Regarding prognosis, the Luminal A subtype has shown repeatedly to have a better outcome than the rest of subtypes across many datasets of patients with early breast cancer. To date, numerous studies have evaluated and compared the classification of tumours based on the PAM50 gene expression predictor with the pathology-based surrogate definitions (Bastien et al., 2012; Prat et al., 2013, 2014), with high discordance rate between both classifications, suggesting that both methods to identify intrinsic biology should not be considered the same.

Lehmann and colleagues analyzed gene-expression profiles from 21 breast cancer datasets and confirmed the concept that a significant heterogeneity within TNBC and breast cancer tumors occurs (Lehmann et al., 2011). According to this analysis, there are six different TNBC subtypes: two basal-like (BL1 and BL2), an immunomodulatory, a mesenchymal, a mesenchymal stem-like, and a luminal androgen receptor (Lehmann et al., 2011). That unravels gene expression and biological diversity between, not only intrinsic molecular subtypes, but also the intertumoral heterogeneity in the TNBC tumors. These results constitute the basis for future approaches in TNBC, using new drugs not classically used in breast cancer and alternative schedules.

Hoadley and co-workers studied 12 different cancer types in a multiplatform manner, where they combined methylation, gene expression, CNV and RPPA data to identify a multitissue, molecular signature-based classification of cancer (Hoadley et al., 2014). Breast cancer (BRCA) gene expression exhibits a pattern of divergence in which two main groups of samples are distinctly identifiable. One group contains essentially all of the luminal (estrogen receptor-positive) and HER2-positive tumors, whereas the other contains the vast majority of the breast basal-like tumors. Although it has previously been appreciated that

basal-like breast cancers (the majority subset of triple-negative breast cancers) form a distinct subtype (Network, 2012; Prat et al., 2013), their findings provide a more refined, quantitative picture of the extent of difference from luminal and basal-like breast cancers. Whereas tissue of origin is the dominant signal for combined data on almost all of the other cancer types in the Pan-Cancer-12 collection, breast basal-like cancers are as different from luminal/ER+ breast cancers as they are from cancers of the lung. In that way, this study strongly reinforces the idea that basal-like breast cancers constitute a unique disease entity. The rest of the multiplatform analyses also associate these basal-like breast tumors closer to other tumors types than with the rest of breast cancer subtypes.

Gene expression studies have been also useful to identify mechanisms of resistance in breast cancer. Then, resistance acquisition takes place due to a complex set of molecular changes, which also includes gene expression deregulation, running these as one of the most studied mechanisms of resistance acquisition. Thus, some resistance mechanisms to taxanes involving gene expression changes are:

- ABC transporters: many cancer types overexpress this type of transmembrane family proteins, giving rise to cross-resistance of tumor cells to very different, not structurally related cytotoxic agents (Cordon-Cardo et al., 1990; Ling, 1992). Increased expression of these proteins has been extensively detected and characterized in taxane-resistant breast carcinomas, not only at mRNA but also at IHC level, (Trock et al., 1997). The MDR-1 gene is the most well studied gene conferring resistance in breast cancer (Merkel et al., 1989; Sanfilippo et al., 1991). This gene encodes for a transmembrane protein of about 170 kDa and its expression correlates with the acquisition of resistance to taxanes, vinca alkaloids, epipodophyllotoxins and anthracyclines (Ling, 1992). Other important, well known members of this protein family involved in breast cancer resistance are the breast cancer resistant protein (BCRP)/*ABCG2* and the multidrug resistance protein (MRP-1)/*ABCC1*, which confer a resistance phenotype to a high number of different drugs (Kruh and Belinsky, 2003; Mao and Unadkat, 2015; Szakács et al., 2004). Other solute carrier family with similar functions but less studied are of the SLC (Joyce et al., 2015).

- Tubulin: these are the microtubule-forming structures. Tubulin heterodimers are formed by α- and β-tubulin subunits that are also bound to the microtubule association proteins (MAPs). Microtubule dynamics is influenced by the presence/absence of GTP and the MAPs, which includes MAP2, MAP4, Mip-90, tau and STOP (Dumontet and Sikic, 1999). There are studies performed in several breast cancer cell lines showing that deregulation in the expression of the α- and β-tubulin subunits are mechanism underlying resistance to taxanes (Yusuf et al., 2003). Some other studies indicate that an increase in the tubulin expression (Han et al., 2000), the expression of alternative tubulin isoforms (not α- and β-tubulin isoforms) (Minotti et al., 1991) and an increase in the expression levels of the MAPs (Rouzier et al., 2005) are also mechanisms mediating resistance acquisition to taxanes in breast cancer. The importance of tubulin expression imbalances in resistance to taxanes is due to microbules and, therefore, tubulin are the targets of this type of drugs.
- β-tubulin isoforms: there are different β-tubulin isoforms that have demonstrated lower affinity for taxanes. Usually the β-tubulin isoform III appears to be unique destabilizing the microtubules and, in combination with the β-tubulin isoform I, is considered to be the most important in breast cancer as predictive of response to taxanes (Bernard-Marty et al., 2002; Noguchi, 2006).
- Apoptosis: some studies indicate that the overexpression of proteins associated with apoptotic pathways, such as anti-apoptotic signaling proteins Bcl2 and Bcl-xL, contributes to taxane resistance (Huang et al., 1997). Other studies showed the opposite, that the overexpression of proapoptotic genes, such as *BAX*, is associated with a better response to taxanes (Strobel et al., 1996). Many of these anti-apoptotic genes are under the transcriptional control of the NF-κB pathway, which is constitutively activated in many breast cancers; the inhibition of this pathway seems to favor the sensitization of tumor cells to taxanes (Ganta and Amiji, 2009; Mabuchi et al., 2004). In addition to NF-κB pathway, Akt, a mediator of the signaling pathway, is active in half of breast cancers and controls the activation of the Bcl2 as well as the mentioned NF-kB pathway, acting as a mechanism of resistance relating clearly both the anti-apoptotic signaling and the NF-κB pathway (Bratton et al., 2010; Coloff et al., 2011).

- Other important mechanisms related to chemoresistance acquisition to taxanes in breast cancer are the overexpression of glutathione-s-transferase (Traverso et al., 2013), mechanisms of epithelial-mesenchymal transition (EMT) due to loss of cell-cell adhesion and gain of motility, which is mediated by essential aforementioned EMT-inductor pathways TGF-beta, Wnt/beta-catenin, Notch and Hedgehog (Lee et al., 2006; Voulgari and Pintzas, 2009), as well as novel mechanisms as the deregulation of microRNAs (Mulrane et al., 2013; Muluhngwi and Klinge, 2015).

Patient-derived xenografts (PDX)

Conventional preclinical models

The use of preclinical models is a core component in every aspect of translational cancer research, ranging from the biologic understanding of the disease to the development of new treatments. The use of human cancer models for drug screening began at the NCI in the 1970s (Venditti et al., 1984). A number of studies have established basic methodology and a systematic approach for preclinical testing of anticancer agents both *in vitro* and *in vivo,* through injection of human cancer cell lines in inmunodeficient mice (Venditti et al., 1984). Currently, the NCI-60 cancer cell line panel represents the best-characterized and most frequently used collection of human cancer cell line models for *in vitro* drug screening and development (Abaan et al., 2013). These cancer cell lines were derived from patients with cancer, where tumor cells from primary tumors or metastatic pleural effusions were isolated, plated and then adapted to grow indefinitely in *in vitro* culture conditions. Xenografts developed by growing these cell lines subcutaneously in immunodeficient mice are the most commonly used *in vivo* platform in preclinical drug development.

Although these conventional cell lines are convenient and easy to use, they have important limitations in preclinical drug development. The most relevant is their lack of predictive value with regard to activity in specific cancer types in clinical trials (Johnson et al., 2001). Despite the underlying cause of this limited predictive value is not fully understood, evidences suggest that the process of generating cancer cell lines results in major and irreversible alterations in biologic properties. This include gain and loss of genetic information, alteration in growth and invasion properties, and loss of specific cell

populations (Gillet et al., 2011; Hausser and Brenner, 2005), as well as loss of the initial heterogeneity present in the population of origin, due to a clonal selection for more aggressive subpopulations. For all these reasons, the establishment of cancer cell lines is not an appropriate strategy for personalized medicine applications. Also, it has been demonstrated that due to the continuous passages *in vitro* and the differences in cell culture among different laboratories, the same cell line can present enormous differences in genomics and gene expression (Nugoli et al., 2003). In spite of this, cancer cell lines are broadly used for the cancer research community and present some advantages in front of other cancer models (Wilding and Bodmer, 2014). However, novel models, such as short-term primary cultures or organoids, are being developed, although important validation studies are still required before broad application in conventional preclinical screening projects.

Beginning and importance of patient-derived xenografts

To circumvent these major troubles in preclinical models, an increasing interest in the development of more advanced models has been exposed. That includes the development of genetically engineered mouse models (GEEM), but mostly the establishment of patient-derived tumor xenografts (PDX) which were initially supposed to retain key characteristics of the donor tumor and that these characteristics would be maintained through successive mouse-to-mouse passages *in vivo*. PDX models started approximately in the 1980s and since then they showed a high degree of correlation between PDX and tumors of origin. In that way, clinical response to cytotoxic agents in adult patients and response to the same agent in PDX models generated from these patients was demonstrated (Fiebig et al., 1985; Houghton et al., 1982).

Initially, it was difficult to establish PDX models. This was reflected by the lower xenografting rates, approximately around 10% (Naundorf et al., 1992; Rae-Venter and Reid, 1980; Sakakibara et al., 1996). Actually, development of new, more immunodeficient mice allow the increase of xenografting rates (Al-Hajj et al., 2003; DeRose et al., 2011; Zhang et al., 2013).

In recent years, there has been a renewed interest in the development of PDX models from different tumor types (Byrne et al., 2017; Dobrolecki et al., 2016; Whittle et al., 2015). Indeed, these models are becoming the preferred preclinical tool in both the industry and academic groups in an attempt to improve the drug development process (Siolas and Hannon, 2013; Tentler et al., 2012). Currently, there are several collections of extensively characterized PDX models in use for different translational research applications. These collections broadly represent the complex clinical tumor heterogeneity and molecular diversity of human cancers (Byrne et al., 2017; Dobrolecki et al., 2016; Whittle et al., 2015).

Breast cancer patient-derived xenograft models

The establishment of well-characterized breast cancer PDX complemented with the information of the patients/tumors of origin is nowadays an important goal achieved. Big panels of breast cancer PDX model have been established for different breast cancer subtypes, representing all the intertumoral heterogeneity from patients in the TNBC, luminal and HER2+ PDX models.

Breast cancer PDX models have shown to be stable during passages in mice, avoiding the selective pressure of *in vitro* culture, and being a source of renewable cancer tissue. They also maintain most of the initial heterogeneity present in tumors of origin (Bruna et al., 2016; Eirew et al., 2015), highlighting these models for the study of complex processes as metastasis and treatment response. In general, most of the studies showed that breast cancer PDX models retain the principal characteristics of primary breast tumors.

At the histological level, some studies have demonstrated that breast cancer PDX models mimic the tumor of origin phenotypically, from the hematoxilin-eosin staining to the most common clinical biomarkers as ER, PR, HER2, Ki67, etc. (DeRose et al., 2011; Zhang et al., 2013). At the biologic level, most studies also showed good concordance between tumors and the PDX models derived from them. Analysis of gene expression profiles showed that there are no substantial changes between donor tumors and their corresponding PDX (DeRose et al., 2011; Zhang et al., 2013). Indeed, using unsupervised clustering analysis, paired donor tumor and PDX models cluster together in most of the studies. Analyses of copy-number alterations (CNA) and exome sequencing data also show extraordinary

concordance between paired samples (Marangoni et al., 2007; Reyal et al., 2012). Furthermore, mouse-to-mouse propagation does not substantially change the functional characteristics of the xenografted tumors (Bruna et al., 2016; DeRose et al., 2011; Zhang et al., 2013). In contrast, an interesting study compared the gene expression profiles of a donor tumor with those of PDX models and cell lines developed from that tumor, both *in vitro* and *in vivo* in conventional xenograft models. The data show that while the gene expression profile of breast cancer PDX models is similar to the original tumor, breast cancer cell lines developed from the same specimen display a different gene expression profile that is not restored by *in vivo* subcutaneous propagation in mice (Daniel et al., 2009). Also the metastatic patterns shown in humans seems to be maintained in the PDX models, as demonstrate some studies (DeRose et al., 2011; Zhang et al., 2013). All this data seems to demonstrate that breast cancer PDX models reflect human tumors of origin, that they are stable during passages in mice and that they are useful tools for the cancer research studies, been closer to the clinical scenario than breast cancer cell lines.

Breast cancer PDX models and resistance

Breast cancer PDX models have been asserted as important tools for the study of mechanisms of resistance, among other therapeutic applications. The xenografting of primary tumors as breast cancer PDX models is by itself a predictive independent factor of clinical response, being the TNBC and most aggressive breast tumors the ones showing higher xenografting rates. However, immune system deficiency in PDX bearing mice and the absence of human stromal component have created some controversy.

Breast cancer PDX models are showing increasing utility for the identification of mechanisms of resistance and potential targetable pathways, as it is exemplified below. Although most of the ER-positive breast tumors respond to endocrine therapy, their efficacy is limited by intrinsic and acquired resistance. Deregulation of ER-mediated gene transcription has been recently identified as a cause of endocrine resistance using luminal breast cancer PDX models (Cottu et al., 2014). In another study, Li and colleagues recently invoked intertumoral heterogeneity to explain *de novo* endocrine-therapy resistance in ER-positive breast cancer and discovered point mutations or rearrangements affecting the *ESR1* ligand-binding domain (Li et al., 2013). These findings suggest that functional *ESR1* variants

may be selected in a subset of endocrine-resistant luminal tumors. Data from these PDX models are consistent with clinical observations and highlight the different forms of endocrine resistance that probably occur in patients. Also, aberrant PI3K signaling has been demonstrated as a resistance mechanism to endocrine resistance through studies performed in breast cancer PDX models. Other studies using reverse phase protein assay analysis in combination with an integrated bioinformatic model established upregulation of the PI3K/Akt/mTOR signaling pathway as a candidate driver of resistance to anti-angiogenic agents (Lindholm et al., 2014). Another mechanisms of resistance has been identified to targeted-therapy but also to chemotherapy using PDX models of different cancer types (Cassidy et al., 2016), increasing our understanding of cancer biology and therapy resistance.

RANK/RANKL signaling pathway

The RANK/RANKL signaling pathway is composed by three members: the receptor activator of nuclear factor (NF)-κB (RANK), its ligand (RANKL) and the soluble decoy receptor osteoprotegerin (OPG). These proteins are members of the superfamily of tumor necrosis factor (TNF). This pathway plays a fundamental role in controlling the activation and survival of osteoclasts. Thus, secretion of RANKL by osteoblasts and its binding to RANK in osteoclasts promotes bone resorption and remodeling, due to the reabsorption of organic and inorganic bone matrix by these cells (Kearns et al., 2008). In contrast, OPG, an atypical member of the superfamily of TNF receptors since it lacks a transmembrane domain and it is soluble (Yasuda et al., 1998), suppresses the bone resorption due to its specific binding to RANKL, kidnapping it and preventing its bind to RANK (Kearns et al., 2008). In this way, knockout-mice lacking either RANK or RANKL showed an identical phenotype, due to the absence of osteoclasts and bone resorption: osteopetrosis (Dougall et al., 1999).

In osteoclasts, RANKL binding to RANK induces the homotrimerization of RANK, forming as a result a heterohexamer, and the recruitment of intracellular adapter proteins, called TNF receptor-associated factors (TRAF), mainly TRAF6. These proteins bind to the cytoplasmic region of RANK and activate intracellular signaling pathways as NF-κB, ERK, JNK, AKT and p38 (Boyle et al., 2003; Wada et al., 2006). The activation of similar pathways through this

interaction has been observed in 293T cells that overexpress RANK (Mizukami et al., 2002), in macrophages (Liu et al., 2004), in dendritic cells (Darnay et al., 1998) and in breast cells (Palafox et al., 2012).

RANK/RANKL role in mammary gland

RANK and RANKL pathway has also been shown to have an important role in other tissues beyond bone, as in mammary gland, where this pathway participates in the proper development and activity. RANK expression promotes proliferation and survival of mammary epithelial cells (Fata et al., 2000). It has been reported that the paracrine signaling through RANKL is responsible for the expansion and maintenance of the mammary stem cell compartment promoted by progesterone (Asselin-Labat et al., 2010; Joshi et al., 2010; Schramek et al., 2010). In this way the overexpression of RANK leads to the expansion of progenitors and mammary stem cells and prevents the differentiation of alveolar lineage (Pellegrini et al., 2013).

Role of RANK/RANKL signaling pathway in breast cancer

It has been described that RANK signaling promotes carcinogenesis in the murine mammary gland, induced by RANKL acting as a mediator of the action of progesterone on breast epithelium (Gonzalez-Suarez et al., 2010; Schramek et al., 2010). The pharmacological inhibition of RANK through treatment with RANK-Fc, a recombinant antagonist of RANKL formed by the extracellular domain of RANK bind to the constant fragment (Fc) of a human immunoglobulin (Sordillo and Pearse, 2003), attenuates mammary carcinogenesis not only in hormone- and carcinogen-treated MMTV-RANK and wild-type mice, but also in the MMTV-Neu and the MMTV-PyMT mouse models (Gonzalez-Suarez et al., 2010; Yoldi et al., 2016). In addition, RANK activation through RANKL induces the formation of lung metastases in a model of ErbB-driven mammary tumours (Tan et al., 2011) and features of CSCs, such as tumorsphere, anchorage-independent growth and resistance to both radio and chemotherapy (Schramek et al., 2010).

In humans, low levels of RANK expression have been described in some human breast cancer cell lines (www.proteinatlas.org). RANK overexpression in immortalized, non-

transformed breast cell lines and breast cancer cell lines causes constitutive activation of the pathway, independently of RANKL (Palafox et al., 2012). In non-transformed breast cell lines induces a stem cell phenotype and transformation, with ability to reconstitute a murine mammary gland, epithelial-mesenchymal transition, increase in migration ability and mammosphere, anchorage-independent growth (Palafox et al., 2012) In BRCA1-mutated breast cancer cell lines, RANK overexpression stimulates invasiveness *in vitro* and increases tumorigenesis and metastatic disease in immunodeficient mice, which is accompanied by an increase in the $CD44^{+}/CD24^{-}$ cancer stem cell population (Palafox et al., 2012). In human breast cancer, RANK expression is associated with TNBC, high histologic grade, high proliferative index and metastatic capacity (Palafox et al., 2012). The RANK expression in primary breast cancer also is associated with a higher pathological complet response and lower disease-free survival and overall survival (Pfitzner et al., 2014; Santini et al., 2011). In contrast, RANKL expression is very rare in human breast cancer cells and was not clearly correlated with any clinical features (Gonzalez-Suarez et al., 2010; Pfitzner et al., 2014).

RANK/RANKL signaling pathway as therapeutic target

RANK/RANKL signaling pathway has been studied as therapeutic target, mainly due to its key role in bone remodelling. Based on the critical role of RANK/RANKL in osteoclastogenesis, denosumab, a fully human monoclonal antibody that specifically binds to RANKL with high affinity and neutralizes its activity, has been developed and approved for clinical use to reduce risk of osteoporosis in postmenopausal women and for the prevention of skeletal-related events (SRE) in patients with solid tumors which have metastasized to bone (Coleman et al., 2012).

In breast cancer, bone metastases are frequent. Breast cancer patients with bone metastasis showed increased expression levels of RANKL and OPG (Dougall and Chaisson, 2006). Osteoclast-derived proteolytic enzymes aid in the colonization of disseminated tumor cells by promoting angiogenesis, cancer cell invasiveness, and engraftment at metastatic sites. Once cancer cells metastasize to bone, produce soluble factors that activate directly, as RANKL, or indirectly osteoclast differentiation and maturation, inducing bone remodelling and more releasement of growth factors. This vicious cycle has been proposed to explain the tumor development in bone (Ando et al., 2008; Coleman et al., 2012). Blockade of

postmenopausal bone loss by use of an antiresorptive agent such as zoledronic acid or denosumab has potent downstream antitumor effects at sites of bone metastases (Coleman et al., 2012).

Both chemotherapy and endocrine therapy, using selective estrogen-receptor modulators, used in premenopausic women with breast cancer induces loss of bone mass (Lønning, 2012; Shapiro et al., 2001). Combination of this treatment with denosumab has shown to reduce this side effects on bone mass (Ellis et al., 2008).

OBJECTIVES

Objectives

The objectives of this PhD thesis could be mainly summarized in:

1. Characterization of breast cancer patient-derived xenografts (PDX) and their use for the identification of biomarkers and mechanisms of resistance to docetaxel in triple negative breast cancer (TNBC): analyses of cancer stem cell populations, next generation sequencing, genome wide methylation and gene expression studies.
2. Identification of human breast cancer PDX models expressing RANK for the study of RANK signalling pathway.

RESULTS

I hereby certify that the PhD student **JORGE GÓMEZ MIRAGAYA** will present his thesis as a compendium of five publications. His contribution to each work is as follows:

ARTICLE 1: Jorge Gómez-Miragaya*, Marta Palafox*, Laia Paré, Guillermo Yoldi, Irene Ferrer, Sergi Vila, Patricia Galván, Pasquale Pellegrini, Hector Pérez-Montoyo, Ana Igea, Purificación Muñoz, Manel Esteller, Angel R. Nebreda, Ander Urruticoechea, Idoia Morilla, Sonia Pernas, Fina Climent, María Teresa Soler-Monso, Ana Petit, Violeta Serra, Aleix Prat, and Eva González-Suárez.

* contributed equally

TITLE: "Resistance to Taxanes in Triple-Negative Breast Cancer Associates with the Dynamics of a CD49f+ Tumor-Initiating Population".

JOURNAL: Stem Cell Reports j Vol. 8 j 1392–1407 j May 9, 2017. Impact factor (2016): 7.338

In this article Jorge Gómez participated in the characterization of the breast cancer PDX models by FACs, the FACs analysis of the chemoresistant TNBC PDX models, performed qRT-PCR analysis for EpCAM and CD49f, performed functional assays (sorting, ELDA, docetaxel treatment), residual disease experiments (*in vivo* and *in vitro*), infections of breast cancer cell lines with CD49f shRNAs, screened public databases to find clinical associations to CD49f expression, data collection and interpretation and manuscript preparation. Some data from this article has been incorporated to the thesis of Marta Palafox Sánchez.

ARTICLE 2: F Mateo*, E J Arenas*, H Aguilar*, J Serra-Musach, G Ruiz de Garibay, J Boni, M Maicas, S Du, F Iorio, C Herranz-Ors, A Islam, X Prado, A Llorente, A Petit, A Vidal, I Català, T Soler, G Venturas, A Rojo-Sebastian, H Serra, D Cuadras, I Blanco, J Lozano, F Canals, A M Sieuwerts, V de Weerd, M P Look, S Puertas, N García, A S Perkins, N Bonifaci, M Skowron, L Gómez-Baldó, V Hernández, A Martínez-Aranda, M Martínez-Iniesta, X Serrat, J Cerón, J Brunet, M P Barretina, M Gil, C Falo, A Fernández, I Morilla, S Pernas, M J Plà, X Andreu, M A Seguí, R Ballester, E Castellà, M Nellist, S Morales, J Valls, A Velasco, X Matias-Guiu, A Figueras, J V Sánchez-Mut, M Sánchez-Céspedes, A Cordero, **J Gómez-Miragaya**, L Palomero, A Gómez, T F Gajewski, E E W Cohen, M Jesiotr, L Bodnar, M Quintela-Fandino, N López-Bigas, R Valdés-Mas, X S Puente, F Viñals, O Casanovas, M Graupera, J Hernández-Losa, S Ramón y Cajal, L García-Alonso, J Saez-Rodriguez, M Esteller, A Sierra, N Martín-Martín, A Matheu, A Carracedo, E González-Suárez, M Nanjundan, J Cortés, C Lázaro, M D Odero, J W M Martens, G Moreno-Bueno, M H Barcellos-Hoff, A Villanueva, R R Gomis & M A Pujana

* contributed equally

TITLE: “Stem cell-like transcriptional reprogramming mediates metastatic resistance to mTOR inhibition”.

JOURNAL: Oncogene (2017) 36, 2737–2749 (11 May 2017). Impact factor (2016): 7.519

In this article Jorge Gómez participated in the characterization of the breast cancer stem cell population enriched in the chemoresistant breast cancer cell lines MCF7 and HCC1937.

ARTICLE 3: Jorge Gómez-Miragaya, Raúl Tonda, Sergi Beltrán, Miguel Angel Pujana, Eva González-Suárez*

TITLE: “Chromosome 12p amplification in TNBC/basal-like breast cancer associates with resistance to docetaxel”.

JOURNAL: Manuscript in preparation.

In this article Jorge Gómez performed DNA and RNA extraction, analysis of exome-sequencing data, validation of the amplification by qPCR, transcriptomic analysis by qRT-PCR of the genes located in chr12p amplified region in IDB-02 PDX model and additional models at residual disease, screening of public databases to find clinical associations to chr12p amplification, data collection and interpretation and manuscript preparation.

ARTICLE 4: Jorge Gómez-Miragaya, Sebastián Morán, Maria Eréndira Calleja-Cervantes, Antonio Gómez, Laia Paré, Aleix Prat, Manel Esteller, Eva González-Suárez.

TITLE: “Identification of epigenetic and transcriptomic pathways leading docetaxel resistance acquisition in triple-negative breast cancer patient derived xenografts”.

JOURNAL: Manuscript in preparation.

In this article Jorge Gómez participated in the DNA and RNA extraction, analysis of the methylation and gene expression microarray data, correlations between methylation and gene expression data, analysis of gene pathways, qRT-PCRs of *ERBB3* and *EGFR*, western blotting for EGFR pathway, data collection and interpretation and manuscript preparation.

ARTICLE 5: Guillermo Yoldi, Pasquale Pellegrini, Eva M. Trinidad, Alex Cordero, Jorge Gómez-Miragaya, Jordi Serra-Musach, William C. Dougall, Purificación Muñoz, Miguel-Angel Pujana, Lourdes Planelles, and Eva González-Suárez.

TITLE: “RANK Signaling Blockade Reduces Breast Cancer Recurrence by Inducing Tumor Cell Differentiation”.

JOURNAL: Cancer Research (2016). Oct 1;76(19):5857-5869. Impact factor: 9.122.

In this article Jorge Gómez participated in the docetaxel treatment of RANK-WT and RANK-KO mice, data interpretation and manuscript preparation.

Annex

In witness whereof, I hereby sign this in Hospitalet de Llobregat,

Barcelona, December 19th, 2017

Eva González Suárez, PhD

Metastases and Transformation group, leader; Cancer Epigenetics and Biology Programme (PEBC); Bellvitge Biomedical Research Institute (IDIBELL); Avda. Gran Via 199-203; 08908 L'Hospitalet de Llobregat, Barcelona, Spain. +34 932607500 ext. 3171. +34 932607219. egsuarez@idibell.cat

ARTICLE 1

“Resistance to Taxanes in Triple-Negative Breast Cancer Associates with the Dynamics of a CD49f+ Tumor-Initiating Population”

Stem Cell Reports
Article

OPEN ACCESS

Resistance to Taxanes in Triple-Negative Breast Cancer Associates with the Dynamics of a CD49f+ Tumor-Initiating Population

Jorge Gómez-Miragaya,[1,10] Marta Palafox,[1,10,11] Laia Paré,[2] Guillermo Yoldi,[1] Irene Ferrer,[1,12] Sergi Vila,[1,13] Patricia Galván,[2,3] Pasquale Pellegrini,[1,14] Hector Pérez-Montoyo,[1,15] Ana Igea,[4] Purificación Muñoz,[1] Manel Esteller,[1,5,6] Angel R. Nebreda,[4,6] Ander Urruticoechea,[7,16] Idoia Morilla,[7] Sonia Pernas,[7] Fina Climent,[8] María Teresa Soler-Monso,[8] Ana Petit,[8] Violeta Serra,[9] Aleix Prat,[2,3] and Eva González-Suárez[1,*]

[1]Cancer Epigenetics and Biology Program (PEBC), Bellvitge Biomedical Research Institute (IDIBELL), Avinguda de la Gran Via, 199 – 203, L'Hospitalet de Llobregat, 08908 Barcelona, Spain
[2]Translational Genomics and Targeted Therapeutics in Solid Tumors, August Pi i Sunyer Biomedical Research Institute (IDIBAPS), 08036 Barcelona, Spain
[3]Translational Genomics Group, Vall d'Hebron Institute of Oncology (VHIO), 08035 Barcelona, Spain
[4]Institute for Research in Biomedicine (IRB Barcelona), Barcelona Institute of Science and Technology, 08028 Barcelona, Spain
[5]Unitat de Bioquímica i Biologia Molecular, Departament de Ciències Fisiològiques II, Universitat de Barcelona-IDIBELL, 08908 Barcelona, Spain
[6]Institució Catalana de Recerca i Estudis Avançats (ICREA), Pg. Lluís Companys 23, 08010 Barcelona, Spain
[7]Breast Cancer Unit, Catalan Institute of Oncology, IDIBELL, 08908 Barcelona, Spain
[8]Pathology Department, University Hospital of Bellvitge, IDIBELL, 08908 Barcelona, Spain
[9]Experimental Therapeutics Group, Vall d'Hebron Institute of Oncology (VHIO), 08035 Barcelona, Spain
[10]Co-first author
[11]Present address: Experimental Therapeutics Group, Vall d'Hebron Institute of Oncology (VHIO), 08035 Barcelona, Spain
[12]Present address: Lung Cancer Clinical Research Unit, CNIO, 28029 Madrid, Spain
[13]Present address: August Pi i Sunyer Institute for Biomedical Research (IDIBAPS), Hospital Clínic - CIBEREHD, University of Barcelona Medical School, 08036 Barcelona, Spain
[14]Present address: Gladstone Institutes, San Francisco, CA 94107, USA
[15]Present address: Ability Pharmaceuticals, SL, 08290 Barcelona, Spain
[16]Present address: Oncologic Center (Onkologikoa), San Sebastian, 20014 Gipuzkoa, Spain
*Correspondence: egsuarez@idibell.cat
http://dx.doi.org/10.1016/j.stemcr.2017.03.026

SUMMARY

Taxanes are a mainstay of treatment for breast cancer, but resistance often develops followed by metastatic disease and mortality. Aiming to reveal the mechanisms underlying taxane resistance, we used breast cancer patient-derived orthoxenografts (PDX). Mimicking clinical behavior, triple-negative breast tumors (TNBCs) from PDX models were more sensitive to docetaxel than luminal tumors, but they progressively acquired resistance upon continuous drug administration. Mechanistically, we found that a CD49f+ chemoresistant population with tumor-initiating ability is present in sensitive tumors and expands during the acquisition of drug resistance. In the absence of the drug, the resistant CD49f+ population shrinks and taxane sensitivity is restored. We describe a transcriptional signature of resistance, predictive of recurrent disease after chemotherapy in TNBC. Together, these findings identify a CD49f+ population enriched in tumor-initiating ability and chemoresistance properties and evidence a drug holiday effect on the acquired resistance to docetaxel in triple-negative breast cancer.

INTRODUCTION

Triple-negative breast cancer (TNBC) is a heterogeneous disease with divergent profiles of chemosensitivity and prognosis (Perou et al., 2000; Prat et al., 2010; Shah et al., 2012; Yu et al., 2013). Standard chemotherapy with anthracyclines and taxanes is the mainstay treatment. A subset of TNBCs shows increased chemosensitivity compared with other breast cancer subtypes; however, for a significant number of patients, overall prognosis is poorer, with high risk of early relapse. Once metastases appear the patient median survival is drastically reduced (Andre and Zielinski, 2012). Despite enormous efforts, the cause of resistance to chemotherapy agents, including taxanes, is unclear (Bonnefoi et al., 2011). There remains an urgent unmet need to identify the population of patients that will benefit from taxanes, on one hand, and to determine the mechanisms of resistance, on the other.

There is increasing evidence that in a variety of neoplasia, including breast cancer, only a subset of cancer cells are capable of reconstituting the tumor after transplantation. These cells called cancer stem cells (CSCs) or tumor-initiating cells (TICs), have the ability to self-renew and regenerate tumor heterogeneity (Al-Hajj et al., 2003) and show intrinsic resistance to conventional chemotherapies, leading to recurrence or metastasis. In fact, breast tumors from patients who received neoadjuvant chemotherapy are substantially enriched for CSCs compared with tumors of untreated patients (Yu et al., 2007), suggesting that anticancer agents kill the bulk of tumor cells, but spare the CSCs (Dean et al., 2005). In breast cancer, a variety of markers (CD44, CD24, EpCAM, CD49f, CD133/2, CD10, and ALDH activity) have been shown to identify CSCs (Al-Hajj et al., 2003; Bachelard-Cascales et al., 2008; Li et al., 2008; Lim et al., 2009; Stingl et al., 2006). However, it is still unclear whether all these markers are appropriate

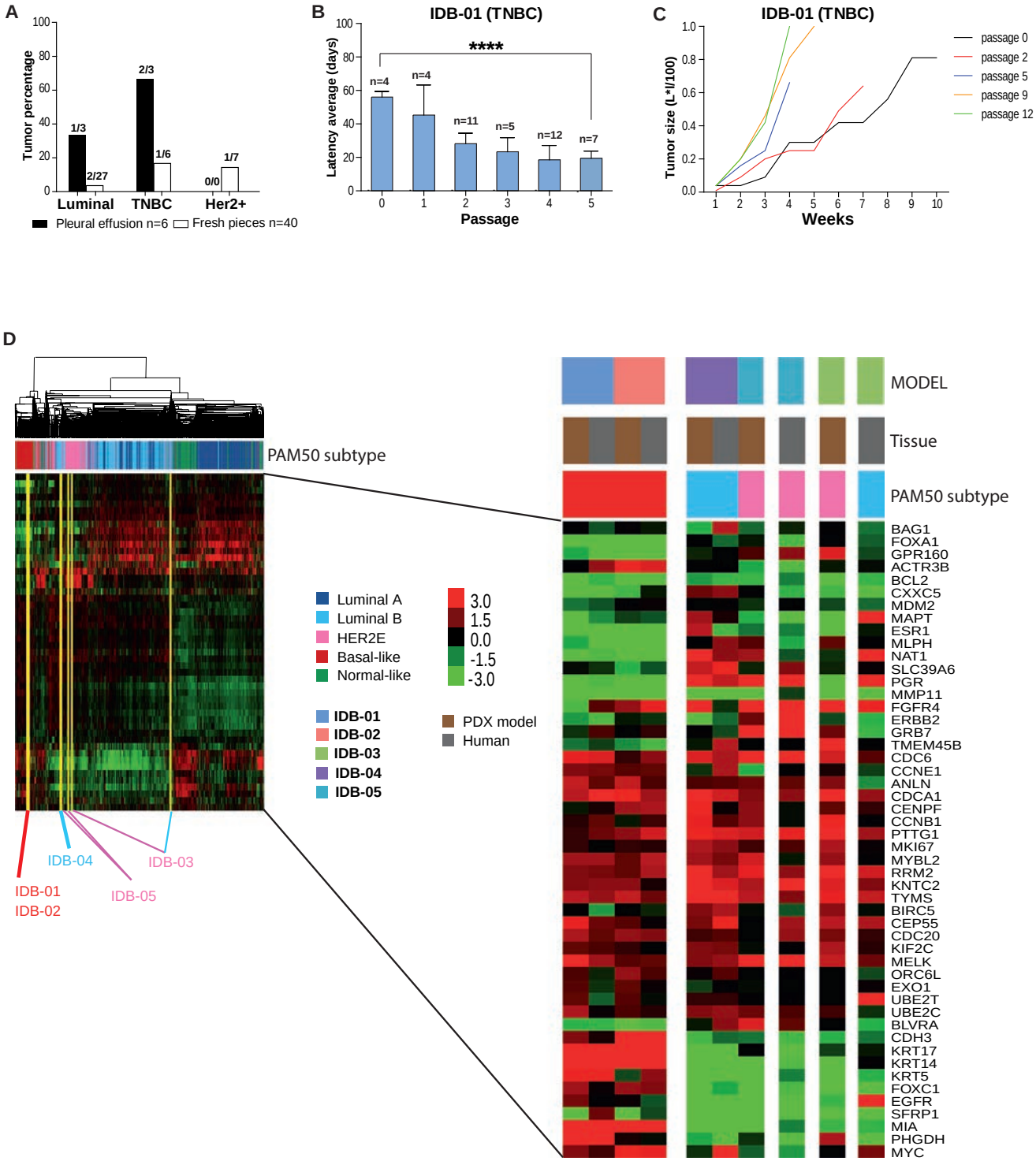

Figure 1. Generation and Characterization of PDX Models of Human Breast Cancer

(A) Percentage of palpable tumors that engrafted relative to total number of independent patient samples, classified by subtype and source. The total number of original patient samples is indicated and mice that did not survive for at least 60 days after surgery were excluded.

(B) Tumor latency in IDB-01 at the indicated passages. Total number of tumors (n), mean, SD, and t test p values are shown. ****$p < 0.0001$.

(legend continued on next page)

for the different breast cancer subtypes, and further studies are necessary to identify the population of TICs and their functionality in each type of tumors.

The lack of appropriate tools and models has hindered our efforts to gain insight into the mechanisms of drug resistance. The best approach to investigate acquired resistance requires analysis of primary or metastatic samples collected before and after recurrence, but these paired sensitive/resistant samples are often difficult to obtain. To advance our knowledge in clinical breast cancer and the molecular mechanisms of resistance, we have generated breast cancer patient-derived orthoxenografts (PDXs), which allow the amplification and perpetuation of human tumors by serial passages. Our panel of breast cancer PDXs recapitulates the heterogeneity of the clinical disease and constitutes a unique tool for studying the biological mechanisms of clinical response to taxanes and acquisition of resistance. We demonstrate that a CD49f+ cell population with tumor-initiating ability and increased resistance to taxanes is present in the initially sensitive TNBC tumors and expands during continued exposure to the drug in vivo, contributing to taxane resistance and tumor recurrence. Remarkably, the transcriptional differences observed between the CD49f+ population of sensitive and resistant tumors accompany and may contribute to the acquisition of chemoresistance. Finally, we demonstrate that docetaxel sensitivity is recovered in the absence of the drug and associates with changes in the CD49f+ population.

RESULTS

PDX Models Resemble Human Tumors of Origin in Early Passages

PDX were generated as described (DeRose et al., 2011; Zhang et al., 2013; Table S1). Increased tumor rates and shorter latency to tumor formation was observed in samples derived from pleural effusions compared with tumor pieces. The TNBC engrafted better than luminal tumors and all palpable tumors derived from grade 3 human samples (Figures 1A, S1A, and S1B). Of the mammary glands, 52% with no palpable tumor contained human mammary epithelium, mostly normal ducts and grade 1 intraductal carcinoma indicating engraftment of these low-grade lesions (Figures S1C and S1D; Table S1). Tumor lines (Table 1, yellow in Table S1) were maintained by consecutive rounds of transplantation, and include two TNBC models derived from pleural effusions, the second one a BRCA1 mutant (IDB-01, IDB-02); two luminal/HER2-negative models (IDB-03 and IDB-04) derived from tumor pieces and pleural effusion, respectively; and one (IDB-05) derived from a tumor piece of a triple-positive (ER+ PR+ HER2+) breast cancer. In most models, shorter latency and faster tumor growth were observed in late passages (Figures 1B, 1C, S1E, and S1F). Thus, as demonstrated previously (DeRose et al., 2011; Dobrolecki et al., 2016; Zhang et al., 2013), establishment of PDX models was associated with increased tumor aggressiveness and poor prognosis.

Expression analyses of markers used in the clinical setting for histopathological tumor classification and selection of treatment (ER, PR, HER2, CK5/6, CK18, and p53), in parental human tumors and PDX tumors at early (0–1) and late passages (4–8) demonstrate that PDX retain most human characteristics in the early passages, but occasional changes are observed in some models (Table 1; Figures S1G and S2A). ER and PR mRNA and protein expression was detected in tumors from all passages of the luminal models IDB-04 and IDB-05 (Figures S2A and S1G), but only IDB-05 required estrogen/progesterone pellets to grow (Figure S1H). IDB-03, ER+ and PR+ in the patient, lost ER and PR expression in the PDX and a population of p53+ cells was enriched (Table 1; Figure S2A and S1G). After surgically resection of tumors, most models developed local relapses and metastases to clinical relevant sites (Table 1; Figure S2B).

Next, we performed intrinsic subtyping of our 5 PDX models and their corresponding human tumors of origin using the PAM50 subtype predictor (Parker et al., 2009), and clustered these samples with 1,834 breast tumor samples representing all subtypes (Prat et al., 2015b). Mimicking the intrinsic subtypes of their corresponding human tumors, the two TNBC models were identified as basal-like, IDB-04 (HR+/HER2–) as luminal B, and the HER2+ IDB-05 as HER2 enriched (HER2-E). Interestingly, the human tumor of origin for IDB-03 was identified as luminal B but the PDX was identified as HER2-E by PAM50 without HER2 overexpression (Figure 1D). As reported in similar PDX collections (Dobrolecki et al., 2016), our mouse grafts retain initial human tumor characteristics, but some models change during serial passages in mice, which may reflect evolution of the clinical disease.

(C) Tumor growth in IDB-01, calculated as L × I (mm × mm)/100 versus time (weeks). Each line represents a representative tumor.
(D) Unsupervised clustering using the PAM50 genes across the PDX models, human tumors of origin, and 1,834 human breast cancer clinical samples (Prat et al., 2015b). The type of sample and the subtype call of each sample are shown. Each square represents the relative transcript abundance. All PDX tumors were from passage 5.
See also Table S1; Figures S1 and S2.

Table 1. Main Characteristics of Human Tumor of Origin and Mouse Grafts in Five Established IDB Models

	Model	IDB-01 (TNBC)	IDB-02 (TNBC)	IDB-03 (Luminal)	IDB-04 (Luminal)	IDB-05 (HER2+)
Mouse	phenotype early passage	ER-PR-HER2-CK5/6+ CK18+ p53-	ER-PR-HER2-CK5/6+ CK18+ p53- BRCA1 mut	ER+ PR+ HER2-CK5/6- CK18+ p53+ BRCA2 mut	ER+ PR+ HER2-CK5/6- CK18+ p53-	ER+ PR+ HER2+ CK5/6-CK18+ p53-
	phenotype late passage	no change	no change	loss of ER and PR	no change	no change
	passage	13	8	16	7	9
	latency (p5) (days)	19	42	18	63	27
	growth without hormone pellets	yes	yes	yes	yes	no
	Local relapse (%)	17.24 (n = 116)	6.94 (n = 144)	20.79 (n = 178)	23.40 (n = 94)	8.54 (n = 94)
	axillary metastasis (%)	10	10	46	0	8
	lymph ND metastasis (%)	14	33	41.2	0	50
	lung metastasis (%)	20	20	10	0	20
	metastasis to other sites	ND	Yes (brain, axillary, subcutaneous)	Yes (bone, kidney)	Yes (liver)	ND
Human	subtype	TNBC grade 3	TNBC grade 3	luminal grade 3	luminal grade 3	HER2+ grade 3
	IHC	ER-PR-HER2-CK5/6+ CK18+ p53-	ER-PR-HER2-CK5/6+ CK18+ p53- BRCA1mut	ER+ PR+ HER2-CK5/6- CK18+ p53+	ER+ PR+ HER2-CK5/6- CK18+ p53-	ER+ PR+ HER2+ CK5/6-CK18+ p53-
	source	pleural	pleural	tumor pieces	pleural	tumor pieces
	treatment	FEC, docetaxel, capecitabine	FEC, docetaxel	not treated	paclitaxel, carboplatin, capecitabine	not treated

ER, estrogen receptor; PR, progesterone receptor; CK, cytokeratin, FEC, triple treatment composed of 5-fluorouracil, epirubicin and cyclophosphamide. Frequency of tumor relapse per mammary gland (local relapse) and metastasis is indicated in each model. Only mice that survived for at least 60 days after primary tumor excision with no relapse/metastasis were considered as relapse/metastasis free. All metastases were confirmed by pathologists. ND, not determined. See also Table S1.

Basal-like PDX Are Initially Sensitive to Docetaxel but Acquire Resistance after Continuous Exposure to the Drug In Vivo

Next, we tested the sensitivity of orthotopic mouse models to docetaxel, one of the most commonly used chemotherapeutics in breast cancer and other solid tumors (Figure S3A). According to docetaxel response, tumors were classified as sensitive when the treatment induced complete tumor regression; partially sensitive when the treatment interfered with tumor growth inducing complete regression in some tumors but not in others; and resistant when tumors continued growing despite docetaxel treatment. In line with these criteria, luminal tumors from IDB-03 and IDB-04 were resistant to docetaxel, the TNBC IDB-01 model was sensitive (IDB-01S), and the TNBC IDB-02 was partially sensitive to the drug (Figures 2A, 2B, and S3B). Despite the initial pathological complete response, all IDB-01 tumors started growing again 30–60 days after treatment interruption. In the second round of treatment, more doses of docetaxel were required to eliminate tumors and a more heterogeneous response between individual tumors was observed (partially sensitive tumors). This behavior was accentuated during consecutive docetaxel treatments and the tumors became resistant in passage 3 (Figures 2B and 2C). Resistance was retained for at least two passages in the absence of docetaxel, as IDB-01-resistant tumors (IDB-01R, passage 5) grew at comparable growth rates irrespective of docetaxel treatment (Figure 2D). Importantly, tumors growing without the selective pressure of docetaxel partially regained sensitivity after five passages (IDB-01R, passage 8), which demonstrates that taxane resistance can be reverted

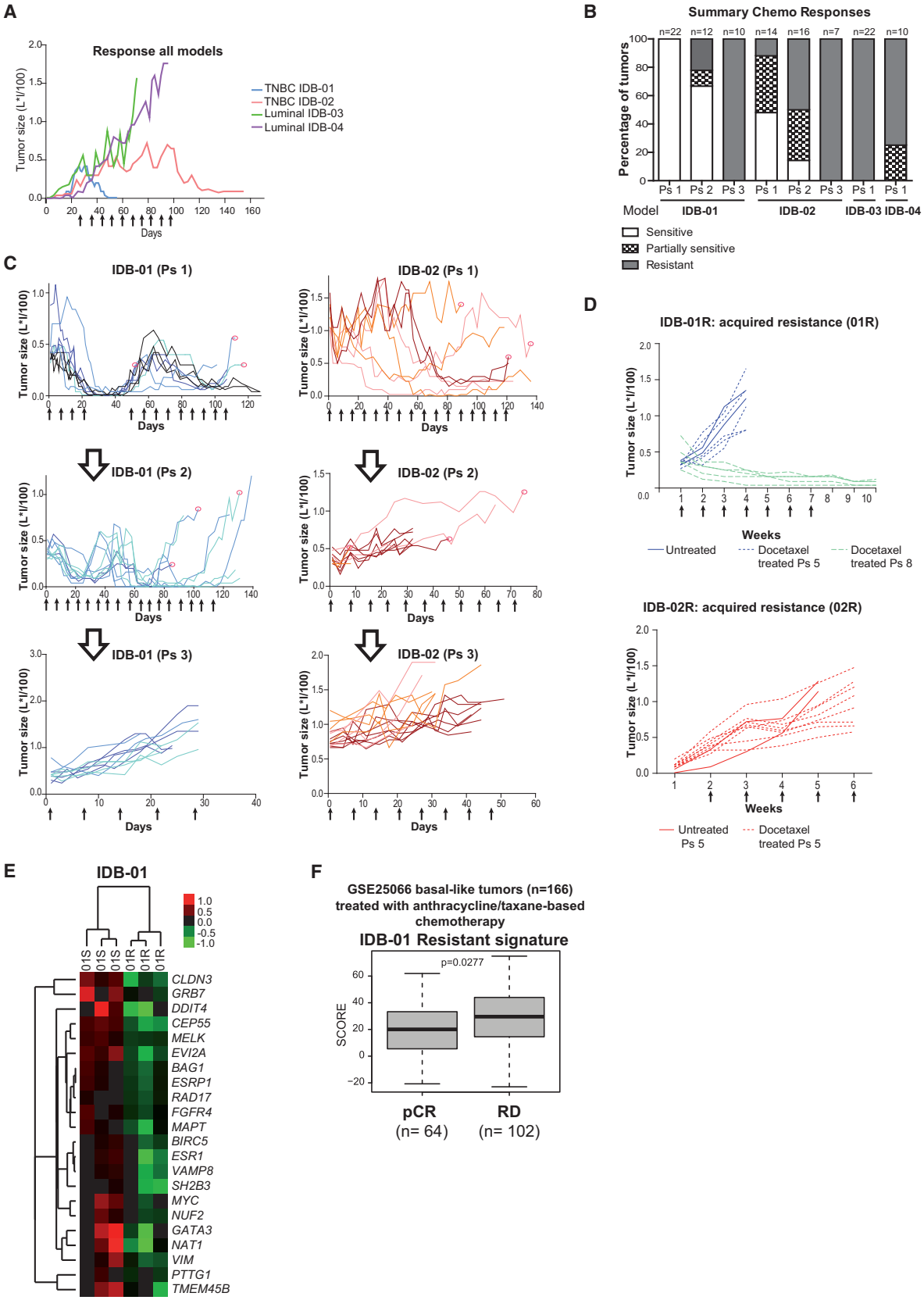

(legend on next page)

(Figure 2D). No differences in latency to tumor formation or tumor growth were observed between IDB-01S (sensitive tumors of origin) and the resistant ones, IDB-01R, derived from them (Figures S3C and S3D). Gene expression analyses of IDB-01S and IDB-01R tumors identified a signature (22 downregulated genes in IDB-01R) that was predictive of residual disease after anthracycline/taxane-based therapy in 166 patients with basal-like disease (GSE25066) (Hatzis et al., 2011) and poor survival in the TCGA dataset, highlighting the clinical relevance of our sensitive and resistant PDX pairs (Figures 2E, 2F, and S3E). In IDB-02 an already heterogeneous response was observed after the first doses, and docetaxel treatment could not be interrupted in most mice (Figures 2B, 2C, and S3B). Tumors started growing very fast after interruption of the treatment and became resistant in passage 2. A third passage and additional docetaxel treatments did not change tumor growth, demonstrating that tumors had acquired resistance to docetaxel, which was retained for at least two passages (Figures 2B–2D). IDB-02R resistant tumors showed similar latency as IDB-02S sensitive tumors but grew significantly faster (Figures S3C and S3D). These results demonstrate that our triple-negative PDX tumors are more sensitive to docetaxel than the luminal ones. In the clinic, a better response to chemotherapy is observed in TNBC compared with luminal tumors, and in some studies taxanes have been shown to be superior to anthracyclines in this subtype (Kim et al., 2010; Martin et al., 2011). Moreover, initially sensitive PDX tumors gradually became less responsive to docetaxel and acquired resistance after continuous exposure to the drug, mimicking the clinical scenario.

Docetaxel Acquired Resistance Is Accompanied by an Increase in the CD49f+ Population

It has been shown that chemotherapy efficiently eliminates the bulk tumor cells but spares the CSC population (Li et al., 2008). Thus, we analyzed the expression of markers previously shown to identify CSCs in our PDX tumor collection including paired sensitive and resistant tumors from IDB-01 and IDB-02 (Figure S4A-B). Variability in marker expression was detected between models with the same histological and molecular subtype. Docetaxel-resistant luminal tumors (IDB-03 and IDB-04) showed the highest percentages of EpCAM, CD49f, and CD24 cells, but the CD133 population was scarce. IDB-03 contained an abundant CD44+ population and ALDH activity, and is the only one expressing CD10. A CD133+ population was found in basal-like and HER2+ PDX. The CD44+ CD24– population, shown to identify human breast CSCs (Al-Hajj et al., 2003), was only detected in the TNBC IDB-02 (Figures S4B and S4C).

No significant changes in the expression of CD44, CD24, CD133, or CD10 were found between sensitive and resistant TNBC paired samples, neither in IDB-01 nor in IDB-02. The CD44+ CD24– population remained barely detectable in the chemoresistant models, and the ALDH+ population, based on ALDH enzymatic activity, was also comparable between paired sensitive and resistant tumors (Figure 3A). In contrast, the frequency of CD49f+ cells significantly increased in TNBC-resistant tumors compared with paired sensitive ones in both models. A significant increase in the frequency of EpCAM+ cells was also observed in IDB-01R compared with IDB-01S tumors (Figure 3A). Resistant tumors from IDB-01 and IDB-02 showed significantly higher mRNA expression levels of *CD49f* (*ITGA6*) but not *EpCAM*, than the corresponding sensitive tumors (Figure 3B).

We next sought to investigate the clinical relevance of our findings by analyzing different clinical datasets. In basal-like tumors from the EORTC 10994/BIG-1-00 clinical trial (Bonnefoi et al., 2011), higher expression of *CD49f* and *EpCAM* was associated with a non-pathological

Figure 2. TNBC PDX Tumors were Sensitive to Docetaxel and Acquired Resistance after Continuous Treatment, whereas the Luminal Tumors were Resistant

(A) Representative kinetics of tumor growth during docetaxel treatment. Docetaxel treatment (20 mg/kg i.p., once per week) started when tumors reached 6 × 6 mm. Each line illustrates a representative tumor (passages 4–14).

(B) Percentage of sensitive, partially sensitive or resistant tumors of each model to docetaxel. Total number of tumors (n) and passage are indicated.

(C) Representative kinetics of tumor growth during acquisition of resistance to docetaxel in the basal-like IDB-01 and IDB-02. Each line represents one tumor and each color represents an independent sensitive tumor of origin. Ps, passage treated with docetaxel. Red circles indicate the tumors that were transplanted.

(D) Representative kinetics of tumor growth during docetaxel treatment after acquisition of resistance to taxanes. Each line represents one tumor. IDB-01R tumors were analyzed after growing for two and five passages, respectively, in the absence of docetaxel.

(E) Supervised expression analysis of the genes found differentially expressed between IDB-01R and IDB-01S tumors. Each square represents the relative transcript abundance.

(F) Association of IDB-01 resistant signature with chemotherapy response in 166 patients with basal-like breast cancer (Hatzis et al., 2011). Response was measured as pathological complete response (pCR) or residual disease (RD). Mean values, box and whiskers (min to max) and t test p values are shown.

(A, C, and D) Arrows represent docetaxel doses. See also Figure S3.

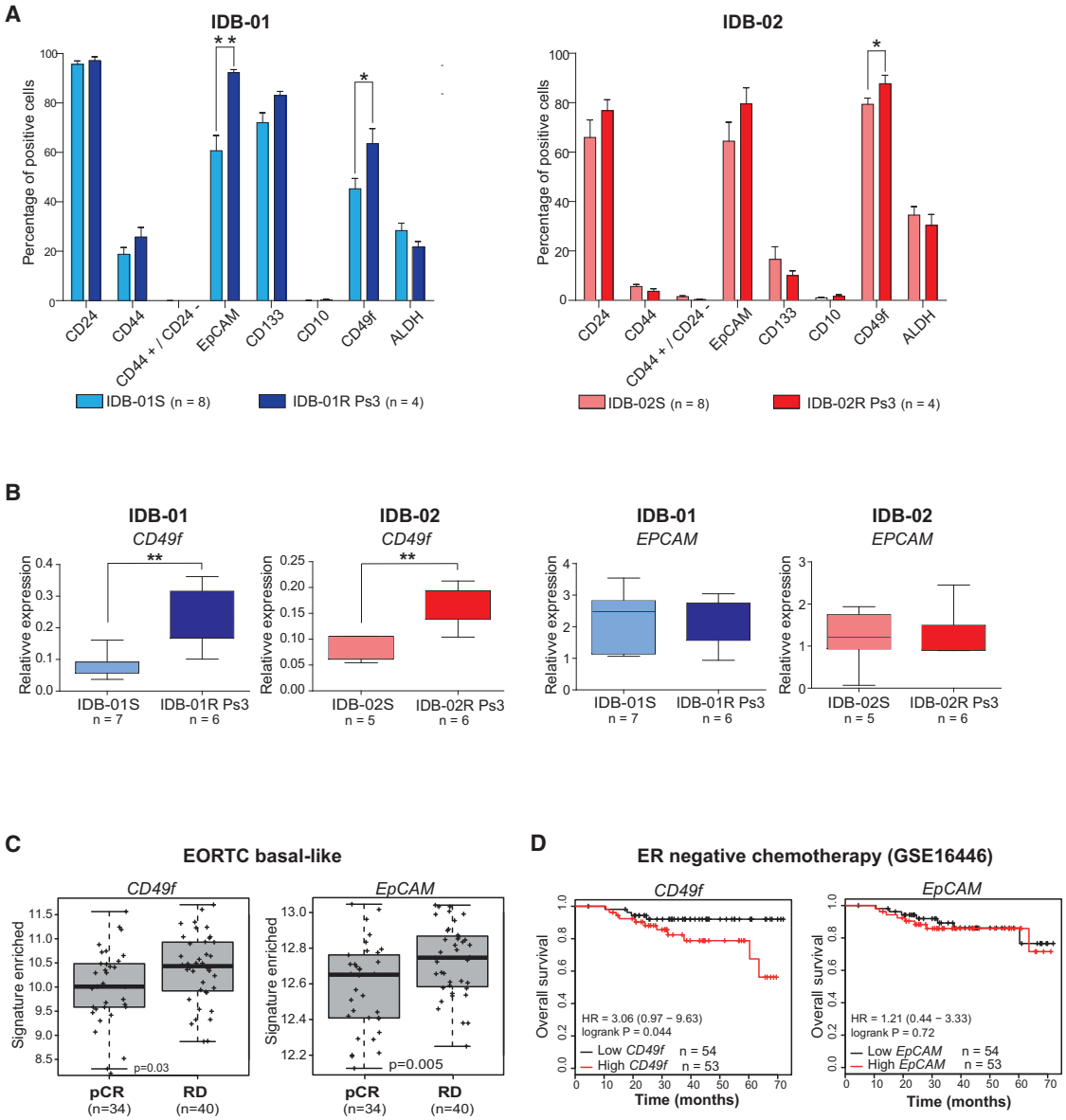

Figure 3. The CD49f+ Population Is Enriched after Acquisition of Resistance to Docetaxel

(A) Frequency of indicated markers within the H2Kd– population in IDB-01 and IDB-02, sensitive and resistant tumors analyzed by flow cytometry at passage 3, at least 5 days after the last docetaxel treatment. Total number of tumors analyzed (n) mean values, SDs and t test p values are shown. *0.01 < p < 0.05; **0.001 < p < 0.01.

(B) Box and whiskers (min to max) graph showing expression levels of *CD49f* and *EpCAM* mRNA relative to *PPiA* in additional sensitive and resistant tumors measured by qRT-PCR. Determinations were done in triplicate and means are used. t test p values for significant differences are shown. **0.001 < p < 0.01.

(C) Box and whiskers (min to max) graph showing association of *CD49f* and *EpCAM* with chemotherapy response in 74 patients with basal-like breast cancer EORTC (Bonnefoi et al., 2011). Response was measured as pathological complete response (pCR) or residual disease (RD). t test p values are shown.

(D) Kaplan-Meier analysis of overall survival of ER-tumors all treated with chemotherapy using *CD49f* and *EpCAM* mRNA expression in the clinical dataset (GSE16446) from the TOP TRIAL (Desmedt et al., 2011).

See also Figures S3 and S4.

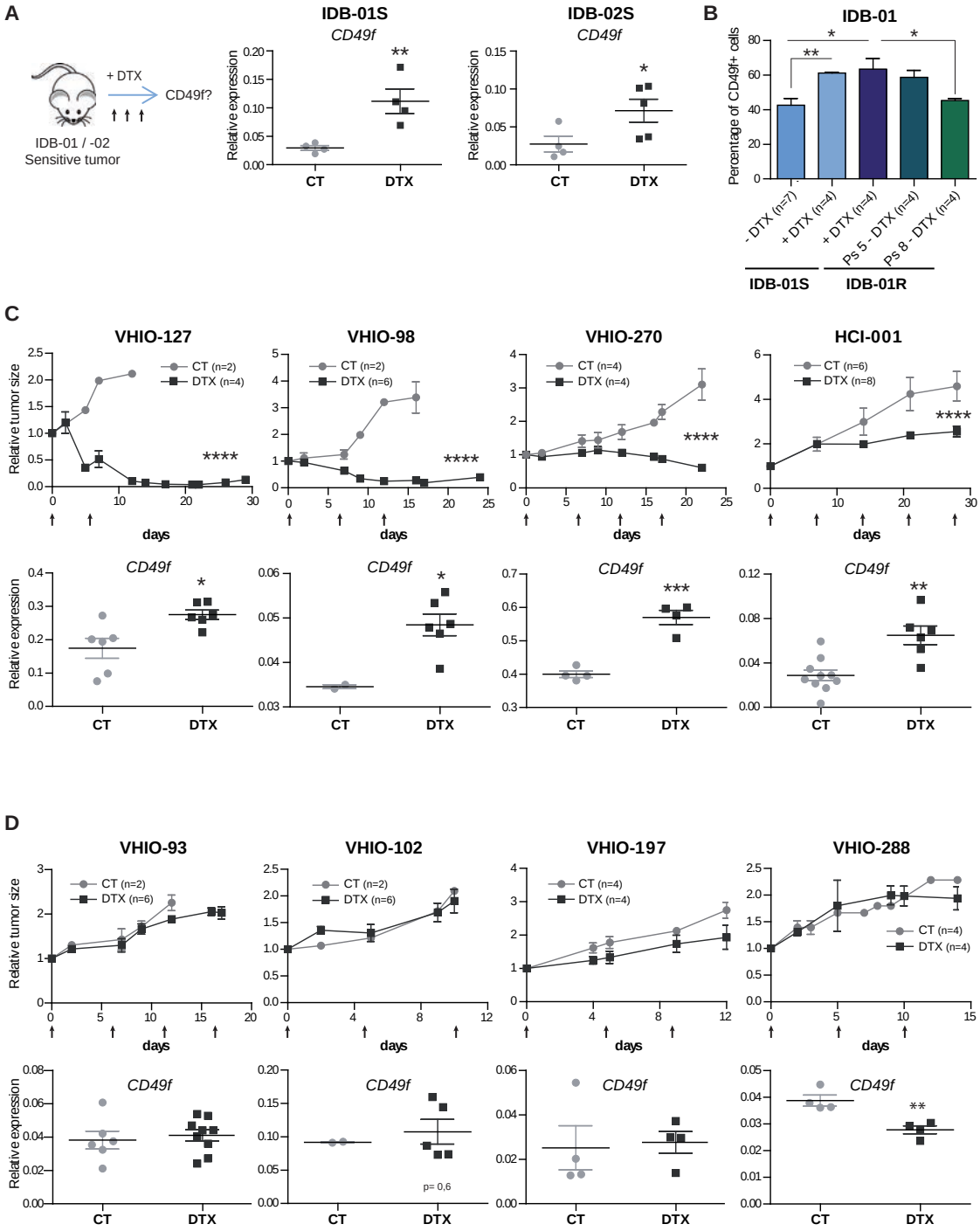

Figure 4. CD49f Expression Increases in Residual Disease of Most TNBC PDX Tumors after Treatment with Docetaxel, but Not on Resistant Tumors

(A) Scheme of short-term docetaxel treatment and *CD49f* mRNA expression levels in sensitive tumors from IDB-01S and IDB-02S after short-term treatment with docetaxel (DTX) and in untreated controls (CT). Each dot represents one tumor. *0.01 < p < 0.05; **0.001 < p < 0.01.

(B) Frequency of CD49f+ cells within H2Kd– in IDB-01S tumors after two to three doses of docetaxel and in IDB-01R tumors that have been treated with docetaxel (at least 5 days after last treatment) or growing in the absence of docetaxel for two and five passages. *0.01 < p < 0.05; **0.001 < p < 0.01.

(legend continued on next page)

complete response (non-pCR) after chemotherapy (Figure 3C). Using GOBO, the Gene expression-based Outcome for Breast cancer Online tool (Ringner et al., 2011), high expression levels of *EpCAM* and *CD49f* combined predicted a reduction in distal metastasis-free survival in basal-like tumors (Figure S3F). Associations with poor overall survival were obtained for *CD49f*, but not *EpCAM*, in other ER-negative or basal-like tumor samples after chemotherapy treatment (Clarke et al., 2013; Desmedt et al., 2011) (Figures 3D, S3G, and S3H). These results demonstrate that, whereas CD44+ CD24– and ALDH activity are not altered, the percentage of the CD49f+ population significantly increases during the acquisition of resistance to docetaxel in basal-like breast cancer.

A Chemoresistant CD49f+ Population Is Present in Most TNBC Tumors

We hypothesized that a chemoresistant CD49f+ population is present in the original sensitive tumors. To test this hypothesis we analyzed *CD49f* mRNA expression in IDB-01S and IDB-02S tumors after two to three doses of docetaxel treatment when tumors were shrinking, and found a significant increase in *CD49f* mRNA expression in the residual disease of both PDX tumors (Figure 4A). Next, we evaluated by flow cytometry the percentage of cells expressing CD49f in residual disease and found that the frequency of CD49f+ cells in residual disease of IDB-01S after docetaxel treatment increases by 20%; these levels are comparable with those of resistant IDB-01R tumors, indicating that the surviving population is enriched in CD49f+ cells (Figure 4B). Importantly, in IDB-01R tumors that regained sensitivity to taxanes after growing in the absence of docetaxel (passage 8), the frequency of the CD49f+ population decreases again to basal levels, similar to those found in sensitive tumors of origin (Figure 4B).

To evaluate whether a chemoresistant CD49f+ population could be found in other TNBC tumors, we analyzed *CD49f* expression after short-term in vivo treatment with docetaxel in 12 additional TNBC PDX tumors derived from patient samples (Bruna et al., 2016; DeRose et al., 2011). Four of these PDX tumors were resistant to docetaxel (no differences in tumor growth after docetaxel treatment), and eight showed different grades of sensitivity to the drug (tumors either shrank or showed tumor growth stabilization after two to four doses of docetaxel). After docetaxel treatment, an increase in *CD49f* mRNA expression levels was observed in residual disease of five out of the eight TNBC-sensitive tumors treated, whereas in resistant tumors *CD49f* expression remained unaltered (Figures 4C, 4D, and S5A). No changes in the expression of the most common partners of CD49f, CD29 (*ITGB1*) and CD104 (*ITGB4*), were observed between sensitive, resistant and residual disease in TNBC tumors (Figure S5B-D). The increase in *CD49f* expression in residual tumors suggests that CD49f+ chemoresistant cells are present in docetaxel-sensitive tumors and get enriched in residual disease.

In addition, we analyzed *CD49f* mRNA expression in five independent TNBC cell lines after 72 h of treatment with increasing concentrations of docetaxel. Different cell lines showed different grades of sensitivity to taxanes but, in four out of the five cell lines tested, a significant increase in *CD49f* mRNA expression was found in cells that survive docetaxel treatment compared with the untreated ones (Figure 5A). No changes in *CD49f* expression were observed at shorter time points with negligible cell death, suggesting that docetaxel does not induce *CD49f* expression and that the observed increase in residual disease, most probably represents the survival of a pre-existing CD49f+ population (Figure 5B). Higher levels of *CD49f* mRNA after paclitaxel treatment were also observed in some cell lines (Figure S5E). No changes in docetaxel sensitivity were observed in MDA-MB-436 cells upon stable reduction of CD49f expression with two independent short hairpin RNA constructs, ruling out a functional role for CD49f itself in chemoresistance of these cells (Figures 5C–5E and S5F).

Together these results demonstrate that higher expression of CD49f was observed in residual disease after docetaxel treatment for most TNBC-sensitive models (seven out of ten PDX models and four out of five cell lines), suggesting that despite the heterogeneity of the TNBC subtype a chemoresistant CD49f+ population is present in most TNBC.

CD49f+/hi Cells Show Enhanced Tumor-Initiating Ability and Resistance to Docetaxel

Next, we asked whether chemoresistant CD49f+ cells showed a higher tumor-initiating potential than CD49f– cells and could be responsible for tumor recurrence. Using fluorescence-activated cell sorting (FACS), we sorted the higher and lower quartile of tumor cells based on CD49f expression from IDB-01S and IDB-02S tumors and functionally tested their tumor-initiating potential (Figure 6A).

(C and D) Docetaxel-sensitive tumors (C) and docetaxel-resistant tumors (D). Top panels: tumor size of the indicated PDX tumors treated with docetaxel (20 mg/kg, arrows) and corresponding controls relative to the size at the first day of treatment. n = total number of tumors. ****$p < 0.0001$. Bottom panels: *CD49f* mRNA expression levels in PDX tumors after short-term treatment with docetaxel and in untreated controls. Each dot represents one tumor. *$0.01 < p < 0.05$; **$0.001 < p < 0.01$; ***$0.001 < p < 0.0001$.
(A–D) Mean values, SEM, and t test p values are shown in all cases.
See also Figure S5.

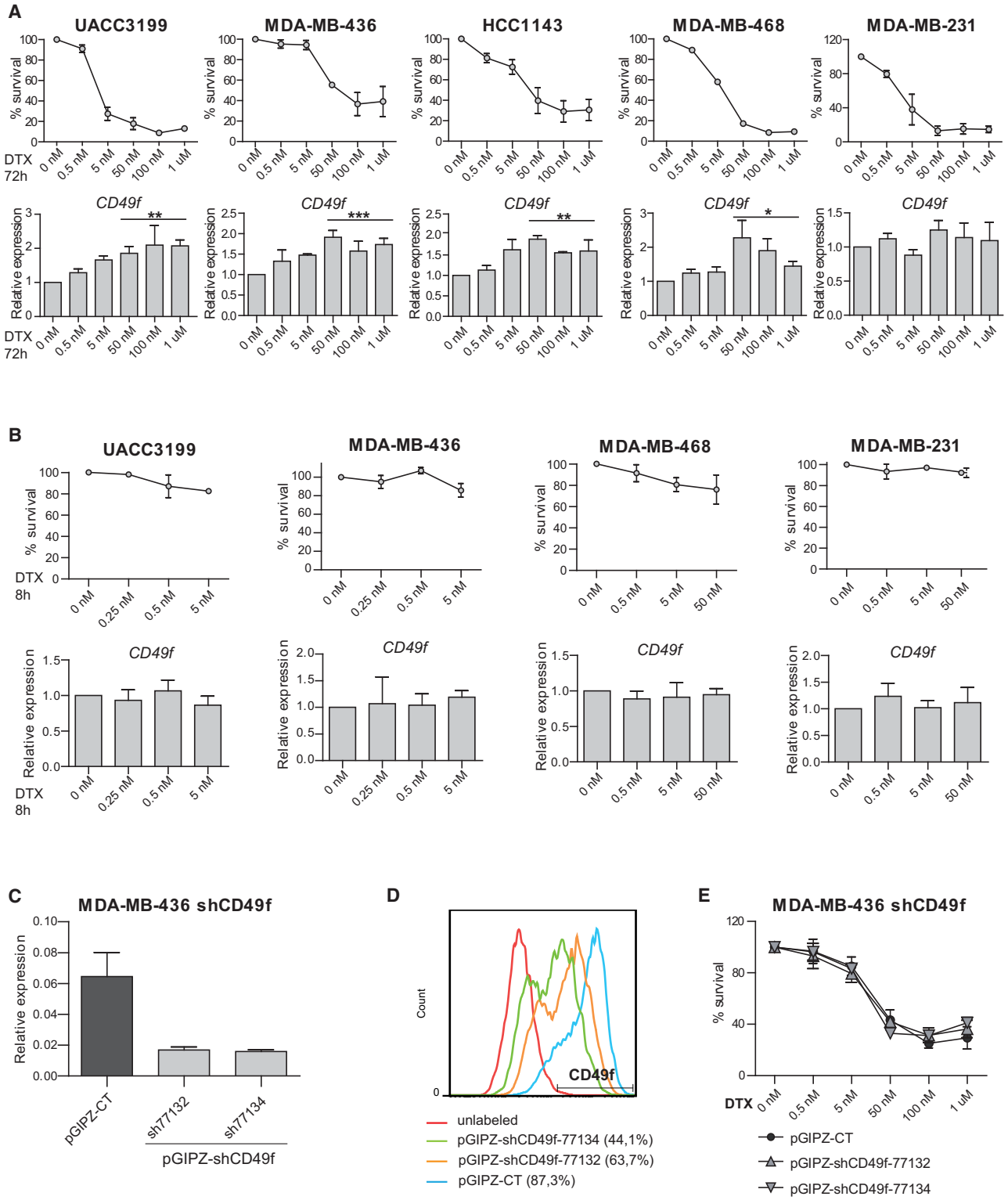

Figure 5. CD49f Expression Increases in Surviving TNBC Cells after Treatment with Docetaxel

(A and B) Top panels: percentage of surviving cells treated with docetaxel for 72 h (A) or 8 h (B). Bottom panels: *CD49f* mRNA expression levels in the indicated TNBC cell lines treated with docetaxel relative to untreated controls. *0.01 < p < 0.05; **0.001 < p < 0.01; ***0.001 < p < 0.0001.

(legend continued on next page)

Indeed, only CD49f+/hi cells, but not the CD49f− in the IDB-01S model, were able to give rise to tumors when re-implanted in mice (Figure 6B). Tumors derived from the IDB-01S-CD49f+/hi cells contained a more abundant CD49f+ population, but also CD49f– cells demonstrating that the tumor-initiating CD49f+/hi cells were able to give rise to non-TICs CD49f− cells (Figure 6C). Docetaxel attenuated growth in tumors derived from IDB-01S-CD49f+/hi cells, but tumors were still palpable after ten doses of docetaxel, in contrast to sensitive tumors of origin IDB-01S that were not detectable after four doses (Figure 6D). Thus, IDB-01S-CD49f+/hi derived tumors are more resistant to docetaxel than the original IDB-01S tumors.

In IDB-02, where tumors were partially sensitive to docetaxel and contained a higher proportion of CD49f+ cells, both CD49f+/hi and CD49f− cells gave rise to tumors. However, limiting dilution assays and extreme limiting dilution analyses (ELDA) revealed that the CD49f+/hi population showed a 5-fold increase in tumor-initiating ability compared with the CD49f− cells (Figure 6E). In addition, the CD49f+/hi cells gave rise to tumors with shorter latency than CD49f− cells (Figure 6F). CD49f+ cells were more abundant in CD49f+/hi than in tumors derived from CD49f−, but tumors from both groups contained CD49f+ and CD49f− cells (Figure 6G), demonstrating that CD49f− cells can also give rise to CD49f+ cells. Again, IDB-02S-CD49f−/lo-derived tumors were more sensitive to docetaxel than the ones derived from IDB-02S-CD49f+ cells (Figure 6H).

Unsupervised gene expression profiling of FACS-sorted CD49f+/hi and CD49f− cells from IDB-01S and -01R, using 105 breast cancer-selected genes, revealed two main clusters which broadly represents the CD49f+ and CD49f− populations (Figures 6I and S6A). Compared with CD49f− cells, CD49f+ cells showed downregulation of keratins, claudins and *CDH3*, and upregulation of *SFRP1*, *MIA* and proliferation-related genes (*UBE2C*, *CDC6* and *CDC20*) (Figure 6I). Further gene expression analyses revealed significant transcriptome differences between CD49f+/hi cells from resistant and sensitive tumors, including enhanced decrease in tight junction proteins, claudins, and *CDH3*, which may suggest a more claudin-low phenotype (Prat et al., 2010). Downregulation of tumor suppressors (e.g., *PTEN* and *RAB25*) is also observed in CD49f+ cells from resistant tumors (Figure S6A). Interestingly, CD49f+/hi cells showed increased proliferation by gene expression analysis than CD49f− cells, especially within sensitive tumors (Figure S6B). Among the two CD49f+ signatures, the IDB-01R/CD49f+ signature was found to predict residual disease following anthracycline/taxane-based therapy in breast tumors (GSE25066), concordant with our preclinical observations (Figure S6C). On the other hand, the IDB-01S/CD49f+ signature was found to predict pathological complete response (pCR) following anthracycline/taxane-based therapy, likely due to the large difference in proliferation between CD49f+ and CD49f− cells in IDB-01S tumors (Figures S6B and S6C) (Hatzis et al., 2011). The IDB-01S/CD49f+ signature was associated with lower recurrence-free survival in an additional dataset of breast cancer patients (Prat et al., 2010) (Figure S6D). Together, these results demonstrate that sensitive tumors of origin contain a tumorigenic and docetaxel-resistant CD49f+ population that changes and expands during the acquisition of taxane resistance; whereas in the absence of the drug, the CD49f+ chemoresistant population shrinks and taxane sensitivity is restored.

DISCUSSION

Patient-derived xenograft (PDX) models have emerged as an important intermediate tool between basic research and clinical trials to expedite the translation of basic research findings into effective therapies for patients. We have generated a panel of PDX models that recapitulates the heterogeneity of human breast tumors. Initial collections of breast PDX were reported to remain phenotypically identical to human tumors during serial passages (DeRose et al., 2011; Zhang et al., 2013). However, in agreement with our findings, there is increasing evidence that tumors in PDX are not "static" and can evolve, as observed in patients (Eirew et al., 2015).

Our PDX models constitute a unique tool to investigate resistance in cancer as they mimic clinical responses: TNBC tumors are more sensitive to chemotherapy than the luminal tumors, confirming previous clinical results (Berry et al., 2006; Colleoni et al., 2004; Guarneri et al., 2006; Martin et al., 2011), and even initially sensitive tumors develop resistance upon continuous exposure to taxanes. Both basal-like tumors (IDB-01 and IDB-02) derived from metastatic samples that were heavily exposed to multiple treatments including taxanes showed minimal clinical response. Strikingly, sensitivity to docetaxel was restored upon xenografting and was retained for months. Moreover, we observed that in PDX tumors with acquired resistance, sensitivity is partially restored when maintained in the

(C and D) *CD49f* mRNA expression levels (C) and CD49f protein expression measured by flow cytometry (D) in cells stably infected with two independent shCD49f knockdown constructs and control vector (pGIPZ).
(E) Percentage of surviving shCD49f-infected and control pGIPZ-infected cells treated with indicated doses of docetaxel for 72 hr.
RT-PCR Determinations were done in triplicate and means are used in the calculations. Mean values of three independent experiments, SEM, and t test p values for the higher concentrations are shown. See also Figure S5.

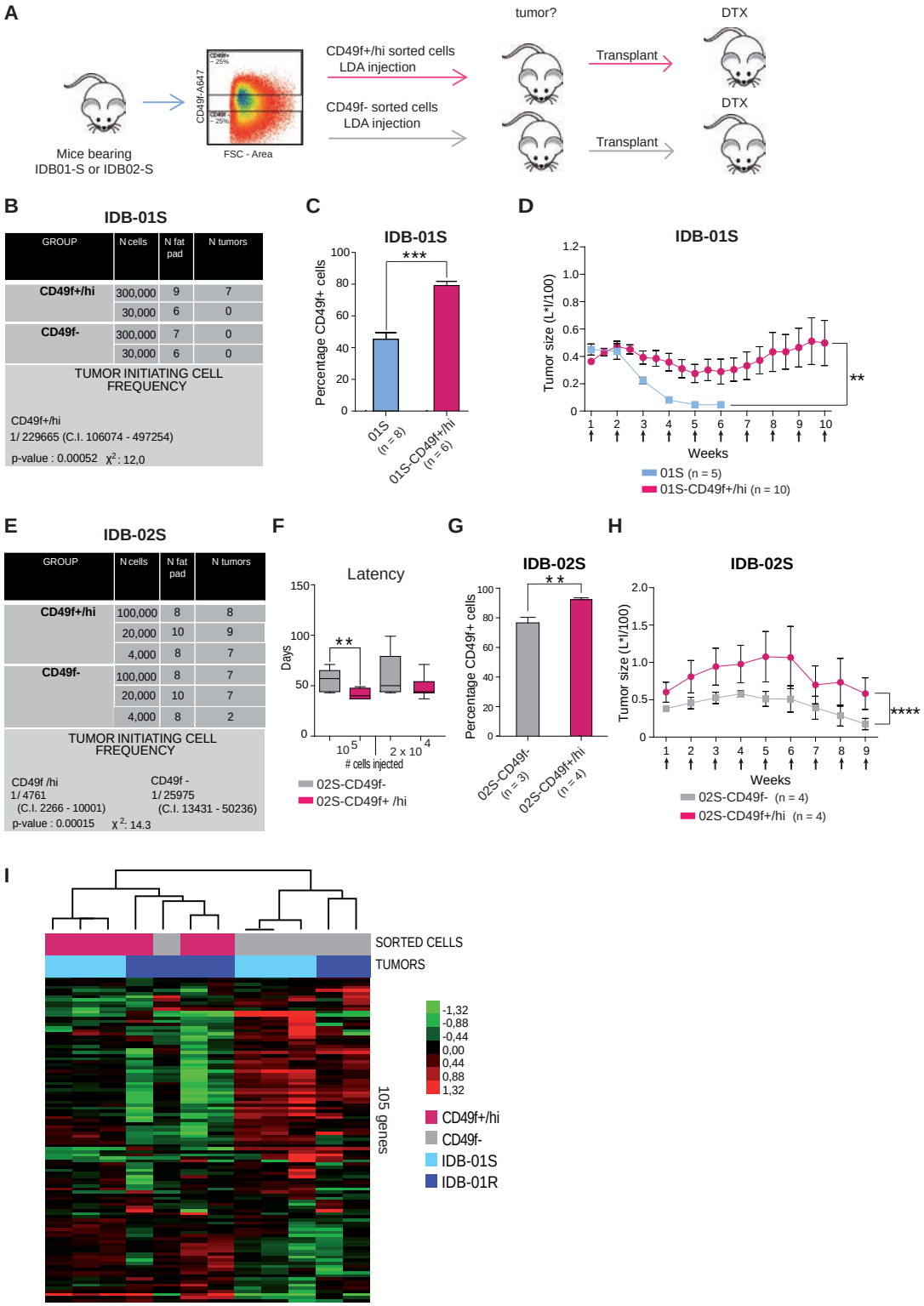

Figure 6. CD49f+ Population Is Enriched in Tumor-Initiating Cells with Increased Resistance to Docetaxel

(A) Scheme of functional experiments.

(B and E) Table showing limiting dilution assay of CD49f+/hi and CD49f− tumor cells from IDB-01 (B) and IDB-02 (E) cells. Tumor-initiating cell frequency (with confidence intervals) for each group was calculated by ELDA; chi-square values and associated probabilities are shown.

(legend continued on next page)

absence of the drug. This regain of sensitivity, the so-called "drug holiday," has been described for targeted therapies in melanoma (Das Thakur et al., 2013; Sun et al., 2014). We now demonstrate that the same is true for cytotoxics such as docetaxel, with important implications for clinical decisions and drug scheduling, as resistant metastatic disease may benefit from intermittent docetaxel treatment.

Our data demonstrate that a pre-existing and chemoresistant CD49f+ subpopulation is present in most sensitive TNBC, expands during long-term therapy, and has the ability to generate novel tumors contributing to recurrence and acquisition of chemoresistance (as shown in the graphical abstract), and importantly that this population shrinks again in the absence of taxanes, restoring drug sensitivity. Previous reports have also shown the increased tumor-initiating ability of CD49f+ cells in breast and other solid tumors (Haraguchi et al., 2013; Lo et al., 2012; Meyer et al., 2010; Vassilopoulos et al., 2014). These findings do not imply that the CD49f+ cells are the CSC in TNBC, but demonstrate that the CD49f+ population is associated with taxane resistance.

Aiming to further characterize the chemoresistant CD49f+ population, an unbiased approach was undertaken. Gene expression analysis revealed important differences, not only between CD49f+ and CD49f− cells, but also between CD49f+ cells from sensitive and resistant tumors. These changes may suggest that the chemoresistant CD49f+ population has expanded during the exposure to docetaxel, and can provide novel therapeutic targets for the metastatic chemoresistant basal-like tumors. Given the heterogeneity of the TNBC subtype, the significant increase in CD49f expression observed in residual or stabilized disease of most TNBC cell lines and PDX models is remarkable and indicates that modulation of CD49f positivity as a biomarker of taxane resistance is not a peculiarity of a single PDX model but a general event in TNBC, which can be exploited for clinical benefit.

These findings can be clinically validated in the neoadjuvant setting, evaluating whether an enrichment of the CD49f population is observed in residual disease following taxane-based chemotherapy. However, as the rates of pCR in TNBC are high (30%–40%), a dynamic study of early changes in the CD49f population after the first cycles of taxane treatment and occurrence of pCR could be a better approach. The clinical utility of the biomarker could be tested in a prospective clinical trial in the neoadjuvant setting where patients are randomized based on the biomarker modulation to change treatment or continue with taxane-based therapy. Improvement of clinical outcomes (pCR rates or survival) should be the final objective. The effect of novel drugs can be evaluated in the subgroup of chemoresistant CD49f-enriched TNBC. In clinical series the presence of CD49f+ in breast cancer is associated with a poor clinical outcome (Friedrichs et al., 1995; Ye et al., 2015). Moreover, within several CSC markers (CD44, CD24, ALDH1A3, and CD49f) analyzed by IHC in breast cancer samples, only CD49f retained prognostic value in a multivariate analyses in ER– disease (Ali et al., 2011). Our results provide a functional rationale for the poor outcome associated with CD49f expression in hormone receptor-negative breast cancer. Further studies will reveal whether this population can be manipulated in order to unveil the ever-elusive status of tumor drug resistance and recurrence.

EXPERIMENTAL PROCEDURES

Patient Characteristics and Generation of PDX

IDB PDX were generated by orthotopic transplantation of primary tumor pieces obtained directly after surgery or cancer cells isolated from pleural effusions and transplanted into the fat pad of immunodeficient mice, as described previously (DeRose et al., 2011). The clinical characteristics from original patient samples, the number and strain of recipient mice, and the outcome of the implant are indicated in Table S1 (IDB-01-05 models). All experimental procedures were performed according to Spanish regulations. Informed consent was obtained from all subjects and the study received approval from the institutional Ethics Committee. Additional models were generated following similar procedures (Bruna et al., 2016). All research involving animals was performed at the IDIBELL animal facility in compliance with protocols approved by the IDIBELL Committee on Animal Care and following national and European Union regulations.

Breast Cancer Cell Isolation, Flow Cytometry, and Sorting

Single cells were isolated from tumors as described previously (Smalley, 2010). Single cells were resuspended and blocked with

(C and G) Frequency of CD49f+ cells in tumors derived from indicated cells. Mean values, SEM, and significant t test p values are shown. **0.001 < p < 0.01; ***0.001 < p < 0.0001.

(D and H) Kinetics of tumor growth during docetaxel treatment in tumors derived from indicated cells. Mean values, SEM, and t test p values are shown. **0.001 < p < 0.01; ****p <0.0001.

(F) Latency of tumors derived from the injection of the indicated number of IDB-02S-CD49f+/hi and 02S-CD49f− tumor cells. Mean values, SEM and significant t test p values are shown. **0.001 < p < 0.01.

(I) Unsupervised analysis of all CD49f sorted samples from IDB-01S and -01R tumors using 105 breast cancer-related genes. The type of sample and tumor are shown below the array tree. Each square represents the relative transcript abundance.

See also Figure S6.

PBS 2% fetal bovine serum (FBS), 2 mM EDTA, and immunoglobulin G blocking reagent for 10 min on ice. Then they were labeled with antibodies against CD24-PE (555428), CD44-APC (559942), EpCAM-FITC (347197), CD10-PECy5 (555376), and CD49f-A647 (562473) (all from BD Pharmingen), CD133/1-PE (130-098-826 from Miltenyi Biotec), and CD49f-APC (FAB13501A from R&D Systems). Mouse cells were excluded in flow cytometry using H2Kd-PECy7 (116622 from BioLegend). Gating was based on "Fluorescence Minus One" controls. Single cells were assessed for their ALDH activity using the ALDEFLUOR assay system (01700 from STEMCELL Technologies) following the manufacturer's procedures. A population of 10,000 living cells was captured in all FACS experiments. FACS analysis and sorting was performed using Gallios and MoFlo (Beckman Coulter) flow cytometers, respectively. Data was analyzed using the FlowJo software (see Figure S4).

Therapeutic and Limiting Dilution Assays

Docetaxel (Hospira/Actavis, 20 mg/kg) was administered intraperitoneally once per week (unless reported otherwise), followed 24 hr later by Fortecortin (Dexametasona, 0.132 mg/kg, Merck). The treatment scheme of resistant variants generation is shown in Figure S3. For orthotopic ELDA, isolated tumor cells were mixed 1:1 with Matrigel Basement Membrane (BD Biosciences) and orthotopically implanted in the inguinal mammary gland of non-obese diabetic/severe combined immunodeficiency females. Tumor development was monitored once per week for a maximum of 25 weeks. In all assays the tumor-initiating potential was defined as the ability to form palpable, growing tumors of $\geq$2 mm diameter.

Culture and Treatment of Human Breast Cancer Cells

All cell lines were purchased from the American Type Culture Collection (Rockville, MD), except for UACC3199 which was obtained from the Arizona Cancer Center (Tucson, AZ). All cells but HCC1143, which was cultured in RPMI 1640, were maintained in DMEM high glucose, containing 10% FBS (Gibco), L-glutamate (Gibco), and penicillin/streptomycin (PAA Laboratories) at 37°C in 5% CO_2. At 60%–70% confluence the indicated concentrations of docetaxel or paclitaxel were added. Cells were collected at the indicated time points and counted with trypan blue to exclude dead ones. All cell lines were routinely tested for mycoplasma, and were shown to be free of contamination.

Gene Expression-Based Analyses

A minimum of ~100 ng of total RNA was used to measure the expression of 105 breast cancer-related genes and five house-keeping genes using the nCounter platform (Nanostring Technologies). Data was log base 2 transformed and normalized using five housekeeping genes (*ACTB, MRPL19, PSMC4, RPLP0* and *SF3A1*). The list of 105 genes includes genes from the following three signatures: PAM50 intrinsic subtype predictor (n = 50) (Parker et al., 2009), claudin-low subtype predictor (n = 43) (Prat et al., 2010), 13-VEGF/hypoxia signature (n = 13) (Hu et al., 2009), and eight individual genes that have been found to play an important role in breast cancer (e.g., CD24). Raw gene expression data and signatures can be found in Table S2. All tumors were assigned to an intrinsic molecular subtype of breast cancer (luminal A, luminal B, HER2-enriched, basal-like, and claudin-low) and the normal-like group using the previously reported PAM50 subtype and the claudin-low subtype predictors (Parker et al., 2009; Prat et al., 2010, 2015b).

Gene Expression-Based Signatures

Genes differentially expressed between the two groups were identified using a two-class unpaired Significance Analysis of Microarrays (SAM) (Tusher et al., 2001) and a false discovery rate of <5%. The final signature of up- and/or downregulated genes was then summarized as a single "enrichment/activity score" by multiplying the SAM score of each gene by its expression value in the tested sample and then summing all the values of each sample. Each signature was evaluated in GSE25066, a microarray-based dataset of patients treated with neoadjuvant anthracycline/taxane-based chemotherapy (Hatzis et al., 2011) and the Perou-extended dataset GSE18229 (Prat et al., 2010). This microarray dataset was normalized as described previously (Prat et al., 2015a). Raw data can be found in Table S2.

Statistical Analyses

All data are expressed as mean ± SEM. Statistical comparison was performed by Student's t test using GraphPad Prism version 5.04. $p \leq 0.05$ was considered statistically significant. The statistical significance of difference between groups is expressed by asterisks: *$0.01 < p < 0.05$; **$0.001 < p < 0.01$; ***$0.001 < p < 0.0001$; ****$p < 0.0001$.

SUPPLEMENTAL INFORMATION

Supplemental Information includes Supplemental Experimental Procedures, six figures, and two tables and can be found with this article online at http://dx.doi.org/10.1016/j.stemcr.2017.03.026.

AUTHOR CONTRIBUTIONS

J.G.M., M.P., and L.P., collection and assembly of data, data analysis and interpretation, writing, and final approval of manuscript; J.G.M., identified the enrichment in the CD49f+ population and performed functional assays and analyses of residual disease; M.P., generated the PDX models and docetaxel-resistant variants; I.F., S.V., P.P., H.P.M., A.I., G.Y., P.G., A.U., T.S.M., J.C., I.M., M.E., A.N., V.S., A.P., and S.P., collection and assembly of data and final approval of manuscript; P.M., data analysis and interpretation and final approval of manuscript; A.P. and E.G.S., conception and design, financial support, collection and assembly of data, data analysis and interpretation, writing, and final approval of manuscript.

ACKNOWLEDGMENTS

We thank A. Villanueva, C. Saura, C. Cruz, A. Fernández, E. Nadal, M. Martin, and R. Iggo for reagents and helpful advice, A. Welm and Y. DeRose for sharing PDX models, V. Peg, X. Serres, J. Balmaña, J. Pérez, and C. Hierro for providing samples, S. Hernández-Ortega, R. Gil, L. Barberá, and G. Boigues, the Pathology Department of the University Hospital of Bellvitge, the IDIBELL animal facility, histology service and UB-SCT, for technical support, and members of the laboratory for useful discussions and reading of the manuscript. This work

was supported by grants to E. González Suárez by the Spanish Ministry of Economy and Competitivity MINECO and from the Health Institute Carlos III (ISCIII) SAF2008-01975, SAF2011-22893, SAF2014-55997, PIE13/00022, co-funded by FEDER funds/European Regional Development Fund (ERDF – a way to build Europe), by a Career Catalyst Grant from the Susan G Komen Foundation CCR13262449 and by funds to A. Prat from ISCIII-PI13/01718, by a Career Catalyst Grant from the Susan G. Komen Foundation, by Banco Bilbao Vizcaya Argentaria (BBVA) Foundation, and by a Sociedad Española de Oncología Médica (SEOM) grant. The PDX from VHIO were supported by a "GHD-pink" research support via the FERO Foundation to V. Serra. V.S. is recipient of ISCIII grants (PI13/01714 and CP14/0028). M.P., J.G.M., and P.P. were recipients of FPU/FPI grants from the MINECO.

Received: October 13, 2016
Revised: March 31, 2017
Accepted: March 31, 2017
Published: April 27, 2017

REFERENCES

Al-Hajj, M., Wicha, M.S., Benito-Hernandez, A., Morrison, S.J., and Clarke, M.F. (2003). Prospective identification of tumorigenic breast cancer cells. Proc. Natl. Acad. Sci. USA *100*, 3983–3988.

Ali, H.R., Dawson, S.J., Blows, F.M., Provenzano, E., Pharoah, P.D., and Caldas, C. (2011). Cancer stem cell markers in breast cancer: pathological, clinical and prognostic significance. Breast Cancer Res. *13*, R118.

Andre, F., and Zielinski, C.C. (2012). Optimal strategies for the treatment of metastatic triple-negative breast cancer with currently approved agents. Ann. Oncol. *23*, vi46–51.

Bachelard-Cascales, E., Chapellier, M., Delay, E., Pochon, G., Voeltzel, T., Puisieux, A., Caron de Fromentel, C., and Maguer-Satta, V. (2008). The CD10 enzyme is a key player to identify and regulate human mammary stem cells. Stem Cells *28*, 1081–1088.

Berry, D.A., Cirrincione, C., Henderson, I.C., Citron, M.L., Budman, D.R., Goldstein, L.J., Martino, S., Perez, E.A., Muss, H.B., Norton, L., et al. (2006). Estrogen-receptor status and outcomes of modern chemotherapy for patients with node-positive breast cancer. JAMA *295*, 1658–1667.

Bonnefoi, H., Piccart, M., Bogaerts, J., Mauriac, L., Fumoleau, P., Brain, E., Petit, T., Rouanet, P., Jassem, J., Blot, E., et al. (2011). TP53 status for prediction of sensitivity to taxane versus non-taxane neoadjuvant chemotherapy in breast cancer (EORTC 10994/BIG 1-00): a randomised phase 3 trial. Lancet Oncol. *12*, 527–539.

Bruna, A., Rueda, O.M., Greenwood, W., Batra, A.S., Callari, M., Batra, R.N., Pogrebniak, K., Sandoval, J., Cassidy, J.W., Tufegdzic-Vidakovic, A., et al. (2016). A biobank of breast cancer explants with preserved intra-tumor heterogeneity to screen anticancer compounds. Cell *167*, 260–274.e22.

Clarke, C., Madden, S.F., Doolan, P., Aherne, S.T., Joyce, H., O'Driscoll, L., Gallagher, W.M., Hennessy, B.T., Moriarty, M., Crown, J., et al. (2013). Correlating transcriptional networks to breast cancer survival: a large-scale coexpression analysis. Carcinogenesis *34*, 2300–2308.

Colleoni, M., Viale, G., Zahrieh, D., Pruneri, G., Gentilini, O., Veronesi, P., Gelber, R.D., Curigliano, G., Torrisi, R., Luini, A., et al. (2004). Chemotherapy is more effective in patients with breast cancer not expressing steroid hormone receptors: a study of preoperative treatment. Clin. Cancer Res. *10*, 6622–6628.

Das Thakur, M., Salangsang, F., Landman, A.S., Sellers, W.R., Pryer, N.K., Levesque, M.P., Dummer, R., McMahon, M., and Stuart, D.D. (2013). Modelling vemurafenib resistance in melanoma reveals a strategy to forestall drug resistance. Nature *494*, 251–255.

Dean, M., Fojo, T., and Bates, S. (2005). Tumour stem cells and drug resistance. Nat. Rev. Cancer *5*, 275–284.

DeRose, Y.S., Wang, G., Lin, Y.C., Bernard, P.S., Buys, S.S., Ebbert, M.T., Factor, R., Matsen, C., Milash, B.A., Nelson, E., et al. (2011). Tumor grafts derived from women with breast cancer authentically reflect tumor pathology, growth, metastasis and disease outcomes. Nat. Med. *17*, 1514–1520.

Desmedt, C., Di Leo, A., de Azambuja, E., Larsimont, D., Haibe-Kains, B., Selleslags, J., Delaloge, S., Duhem, C., Kains, J.P., Carly, B., et al. (2011). Multifactorial approach to predicting resistance to anthracyclines. J. Clin. Oncol. *29*, 1578–1586.

Dobrolecki, L.E., Airhart, S.D., Alferez, D.G., Aparicio, S., Behbod, F., Bentires-Alj, M., Brisken, C., Bult, C.J., Cai, S., Clarke, R.B., et al. (2016). Patient-derived xenograft (PDX) models in basic and translational breast cancer research. Cancer Metastasis Rev. *35*, 547–573.

Eirew, P., Steif, A., Khattra, J., Ha, G., Yap, D., Farahani, H., Gelmon, K., Chia, S., Mar, C., Wan, A., et al. (2015). Dynamics of genomic clones in breast cancer patient xenografts at single-cell resolution. Nature *518*, 422–426.

Friedrichs, K., Ruiz, P., Franke, F., Gille, I., Terpe, H.J., and Imhof, B.A. (1995). High expression level of alpha 6 integrin in human breast carcinoma is correlated with reduced survival. Cancer Res. *55*, 901–906.

Guarneri, V., Broglio, K., Kau, S.W., Cristofanilli, M., Buzdar, A.U., Valero, V., Buchholz, T., Meric, F., Middleton, L., Hortobagyi, G.N., and Gonzalez-Angulo, A.M. (2006). Prognostic value of pathologic complete response after primary chemotherapy in relation to hormone receptor status and other factors. J. Clin. Oncol. *24*, 1037–1044.

Haraguchi, N., Ishii, H., Mimori, K., Ohta, K., Uemura, M., Nishimura, J., Hata, T., Takemasa, I., Mizushima, T., Yamamoto, H., et al. (2013). CD49f-positive cell population efficiently enriches colon cancer-initiating cells. Int. J. Oncol. *43*, 425–430.

Hatzis, C., Pusztai, L., Valero, V., Booser, D.J., Esserman, L., Lluch, A., Vidaurre, T., Holmes, F., Souchon, E., Wang, H., et al. (2011). A genomic predictor of response and survival following taxane-anthracycline chemotherapy for invasive breast cancer. JAMA *305*, 1873–1881.

Hu, Z., Fan, C., Livasy, C., He, X., Oh, D.S., Ewend, M.G., Carey, L.A., Subramanian, S., West, R., Ikpatt, F., et al. (2009). A compact VEGF signature associated with distant metastases and poor outcomes. BMC Med. *7*, 9.

Kim, S.I., Sohn, J., Koo, J.S., Park, S.H., Park, H.S., and Park, B.W. (2010). Molecular subtypes and tumor response to neoadjuvant

chemotherapy in patients with locally advanced breast cancer. Oncology *79*, 324–330.

Li, X., Lewis, M.T., Huang, J., Gutierrez, C., Osborne, C.K., Wu, M.F., Hilsenbeck, S.G., Pavlick, A., Zhang, X., Chamness, G.C., et al. (2008). Intrinsic resistance of tumorigenic breast cancer cells to chemotherapy. J. Natl. Cancer Inst. *100*, 672–679.

Lim, E., Vaillant, F., Wu, D., Forrest, N.C., Pal, B., Hart, A.H., Asselin-Labat, M.L., Gyorki, D.E., Ward, T., Partanen, A., et al. (2009). Aberrant luminal progenitors as the candidate target population for basal tumor development in BRCA1 mutation carriers. Nat. Med. *15*, 907–913.

Lo, P.K., Kanojia, D., Liu, X., Singh, U.P., Berger, F.G., Wang, Q., and Chen, H. (2012). CD49f and CD61 identify Her2/neu-induced mammary tumor-initiating cells that are potentially derived from luminal progenitors and maintained by the integrin-TGFbeta signaling. Oncogene *31*, 2614–2626.

Martin, M., Romero, A., Cheang, M.C., López García-Asenjo, J.A., García-Saenz, J.A., Oliva, B., Román, J.M., He, X., Casado, A., de la Torre, J., et al. (2011). Genomic predictors of response to doxorubicin versus docetaxel in primary breast cancer. Breast Cancer Res. Treat. *128*, 127–136.

Meyer, M.J., Fleming, J., Lin, A.F., Hussnain, S.A., Ginsburg, E., and Vonderhaar, B.K. (2010). CD44posCD49fhiCD133/2hi defines xenograft-initiating cells in estrogen receptor-negative breast cancer. Cancer Res. *70*, 4624–4633.

Parker, J.S., Mullins, M., Cheang, M.C., Leung, S., Voduc, D., Vickery, T., Davies, S., Fauron, C., He, X., Hu, Z., et al. (2009). Supervised risk predictor of breast cancer based on intrinsic subtypes. J. Clin. Oncol. *27*, 1160–1167.

Perou, C.M., Sorlie, T., Eisen, M.B., van de Rijn, M., Jeffrey, S.S., Rees, C.A., Pollack, J.R., Ross, D.T., Johnsen, H., Akslen, L.A., et al. (2000). Molecular portraits of human breast tumours. Nature *406*, 747–752.

Prat, A., Parker, J.S., Karginova, O., Fan, C., Livasy, C., Herschkowitz, J.I., He, X., and Perou, C.M. (2010). Phenotypic and molecular characterization of the claudin-low intrinsic subtype of breast cancer. Breast Cancer Res. *12*, R68.

Prat, A., Fan, C., Fernandez, A., Hoadley, K.A., Martinello, R., Vidal, M., Viladot, M., Pineda, E., Arance, A., Munoz, M., et al. (2015a). Response and survival of breast cancer intrinsic subtypes following multi-agent neoadjuvant chemotherapy. BMC Med. *13*, 303.

Prat, A., Pineda, E., Adamo, B., Galvan, P., Fernandez, A., Gaba, L., Diez, M., Viladot, M., Arance, A., and Munoz, M. (2015b). Clinical implications of the intrinsic molecular subtypes of breast cancer. Breast *24* (*Suppl 2*), S26–S35.

Ringner, M., Fredlund, E., Hakkinen, J., Borg, A., and Staaf, J. (2011). GOBO: gene expression-based outcome for breast cancer online. PLoS One *6*, e17911.

Shah, S.P., Roth, A., Goya, R., Oloumi, A., Ha, G., Zhao, Y., Turashvili, G., Ding, J., Tse, K., Haffari, G., et al. (2012). The clonal and mutational evolution spectrum of primary triple-negative breast cancers. Nature *486*, 395–399.

Smalley, M.J. (2010). Isolation, culture and analysis of mouse mammary epithelial cells. Methods Mol. Biol. *633*, 139–170.

Stingl, J., Eirew, P., Ricketson, I., Shackleton, M., Vaillant, F., Choi, D., Li, H.I., and Eaves, C.J. (2006). Purification and unique properties of mammary epithelial stem cells. Nature *439*, 993–997.

Sun, C., Wang, L., Huang, S., Heynen, G.J., Prahallad, A., Robert, C., Haanen, J., Blank, C., Wesseling, J., Willems, S.M., et al. (2014). Reversible and adaptive resistance to BRAF(V600E) inhibition in melanoma. Nature *508*, 118–122.

Tusher, V.G., Tibshirani, R., and Chu, G. (2001). Significance analysis of microarrays applied to the ionizing radiation response. Proc. Natl. Acad. Sci. USA *98*, 5116–5121.

Vassilopoulos, A., Chisholm, C., Lahusen, T., Zheng, H., and Deng, C.X. (2014). A critical role of CD29 and CD49f in mediating metastasis for cancer-initiating cells isolated from a Brca1-associated mouse model of breast cancer. Oncogene *33*, 5477–5482.

Ye, F., Qiu, Y., Li, L., Yang, L., Cheng, F., Zhang, H., Wei, B., Zhang, Z., Sun, L., and Bu, H. (2015). The presence of EpCAM(-)/CD49f(+) cells in breast cancer is associated with a poor clinical outcome. J. Breast Cancer *18*, 242–248.

Yu, F., Yao, H., Zhu, P., Zhang, X., Pan, Q., Gong, C., Huang, Y., Hu, X., Su, F., Lieberman, J., and Song, E. (2007). let-7 regulates self renewal and tumorigenicity of breast cancer cells. Cell *131*, 1109–1123.

Yu, K.D., Zhu, R., Zhan, M., Rodriguez, A.A., Yang, W., Wong, S., Makris, A., Lehmann, B.D., Chen, X., Mayer, I., et al. (2013). Identification of prognosis-relevant subgroups in patients with chemoresistant triple-negative breast cancer. Clin. Cancer Res. *19*, 2723–2733.

Zhang, X., Claerhout, S., Prat, A., Dobrolecki, L.E., Petrovic, I., Lai, Q., Landis, M.D., Wiechmann, L., Schiff, R., Giuliano, M., et al. (2013). A renewable tissue resource of phenotypically stable, biologically and ethnically diverse, patient-derived human breast cancer xenograft models. Cancer Res. *73*, 4885–4897.

Graphical abstract

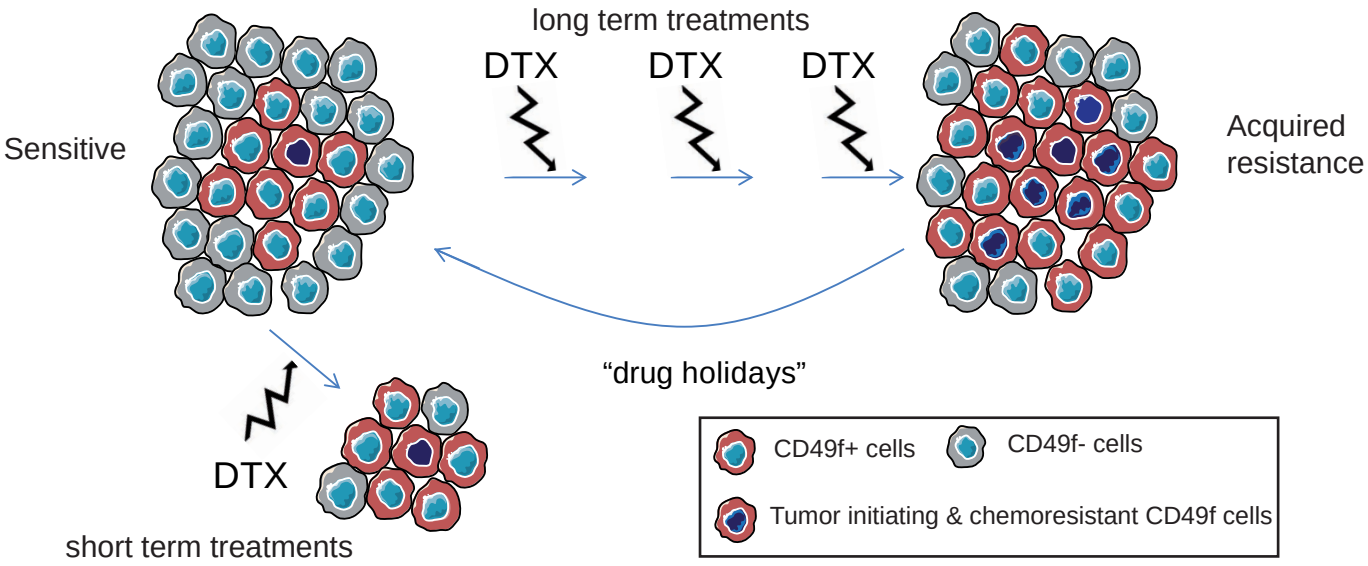

Supplementary Figure S1

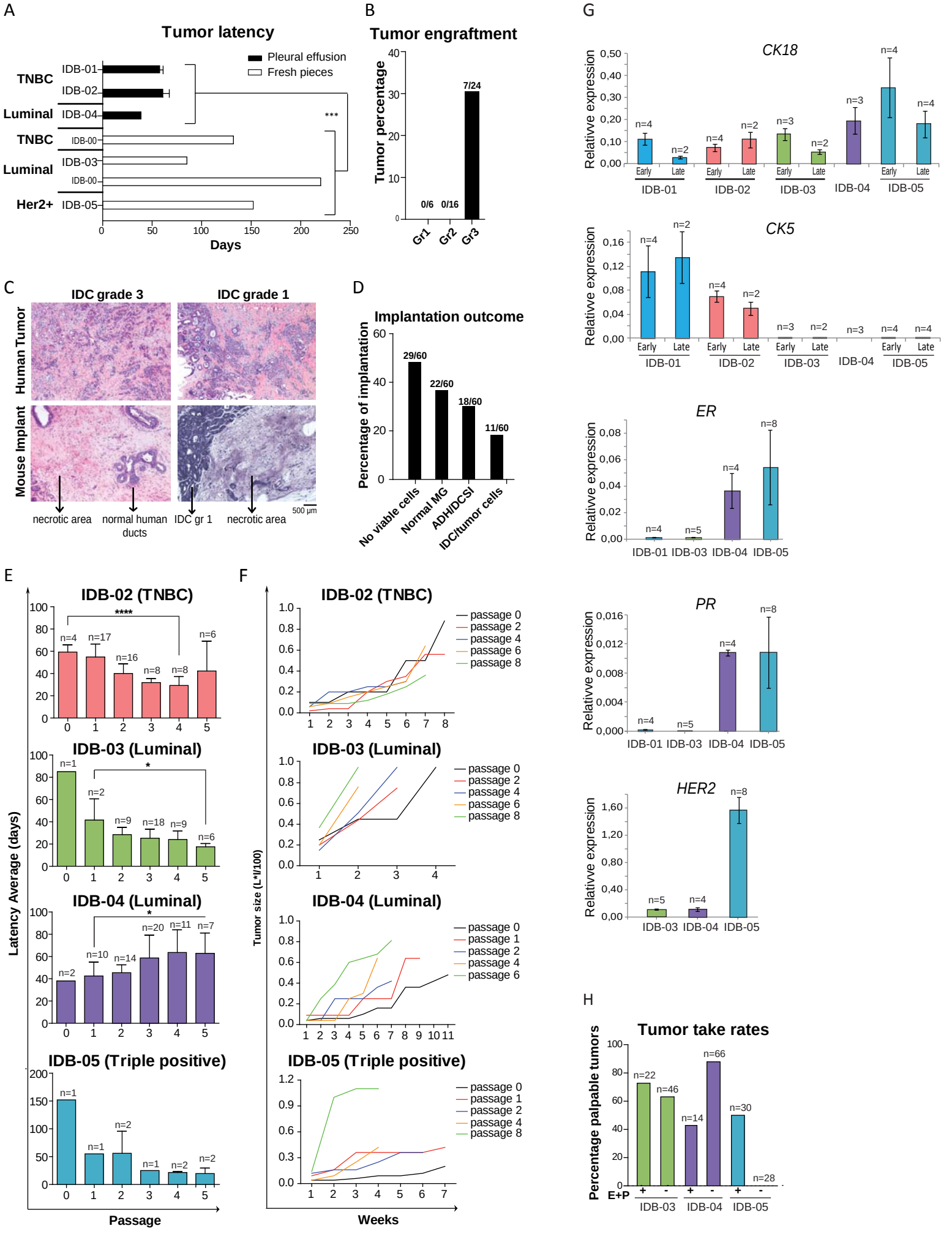

Supplemental Figure S2

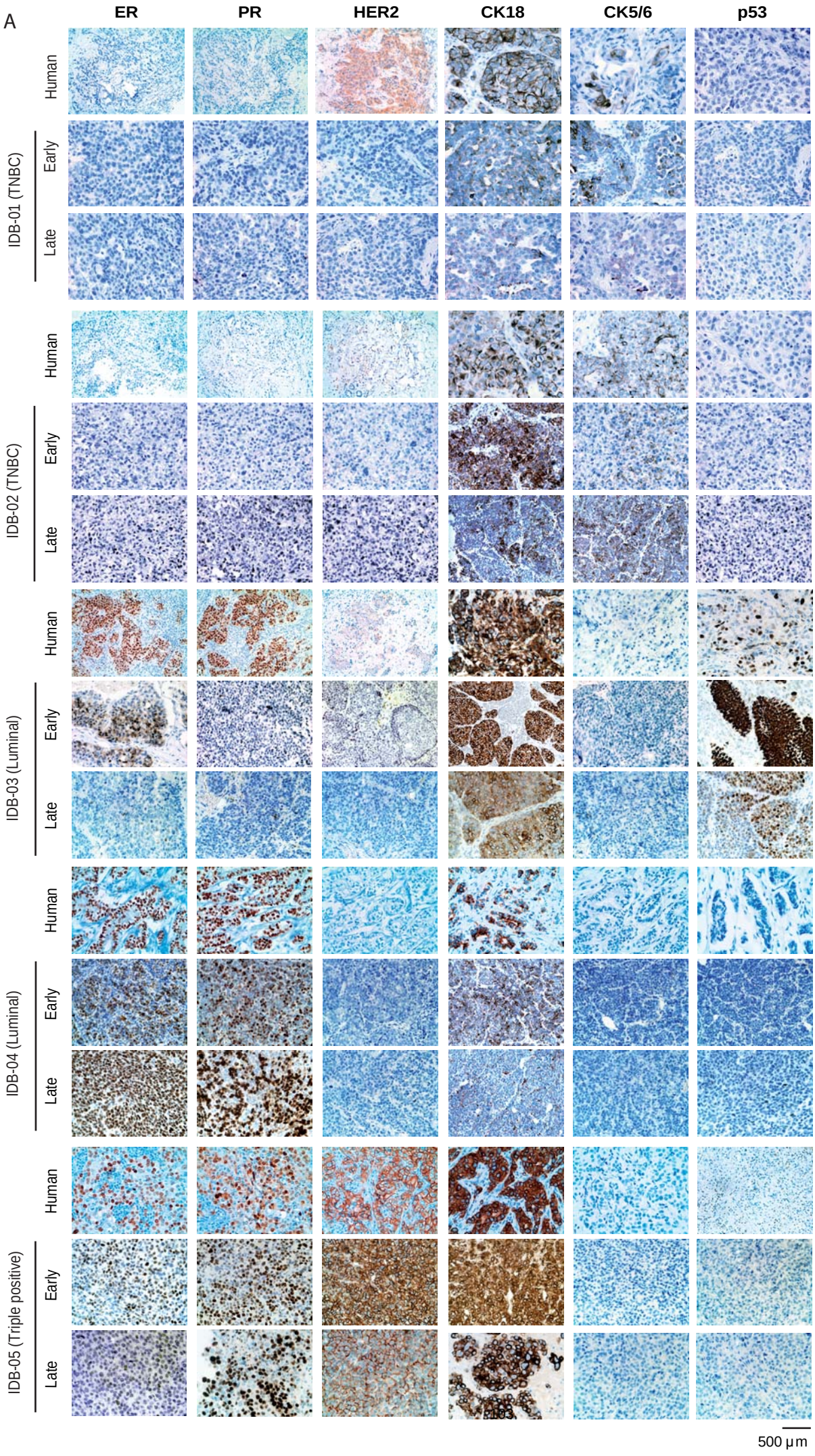

Supplemental Figure S3

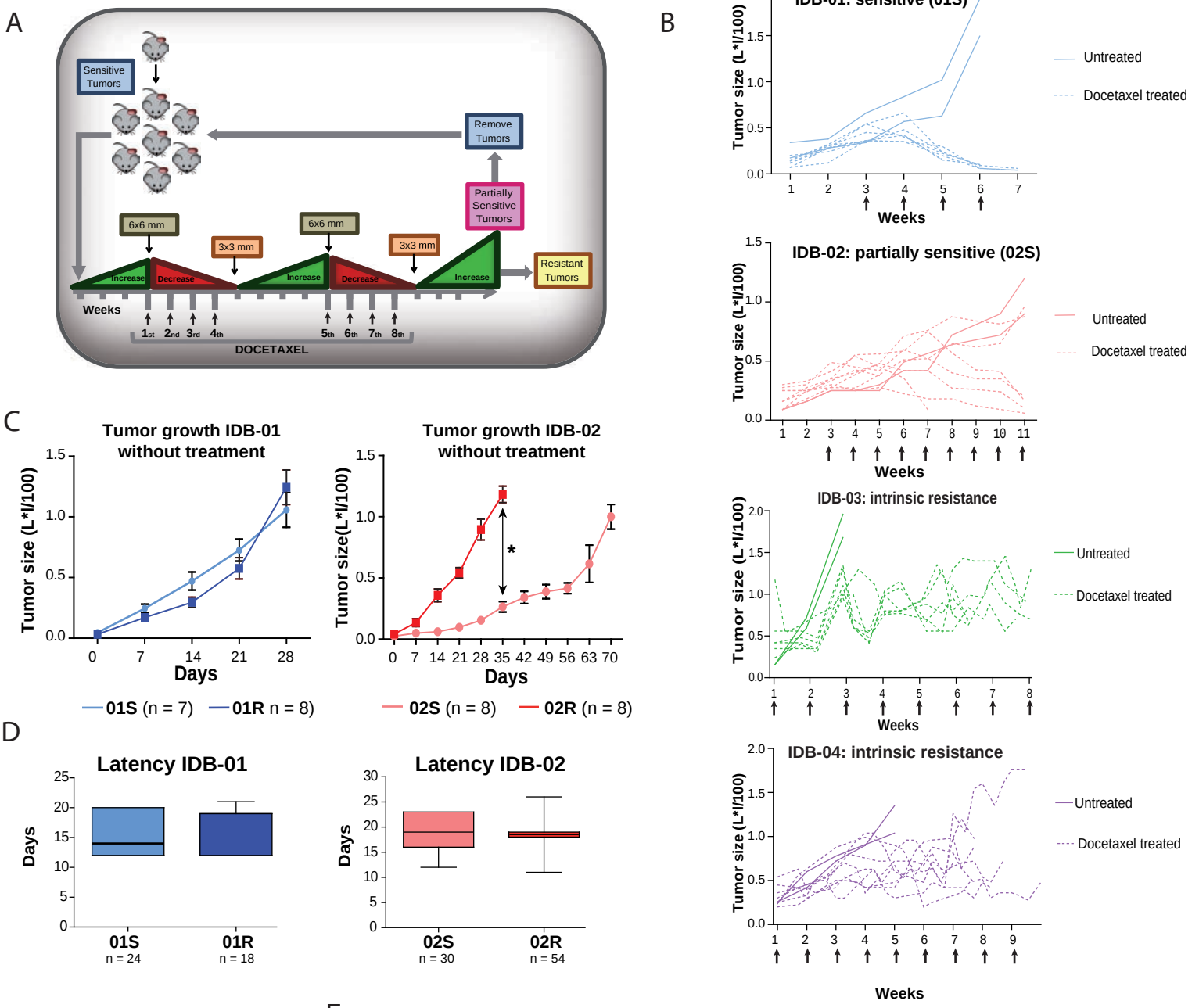

Supplemental Figure S4

A

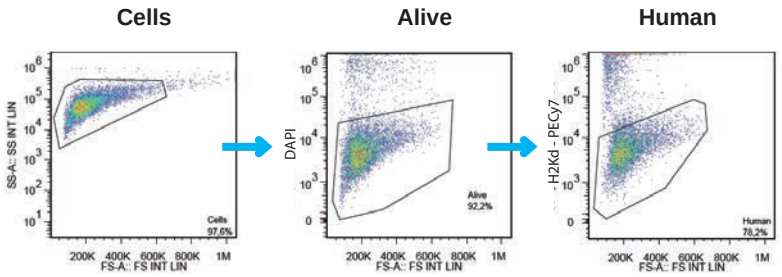

B

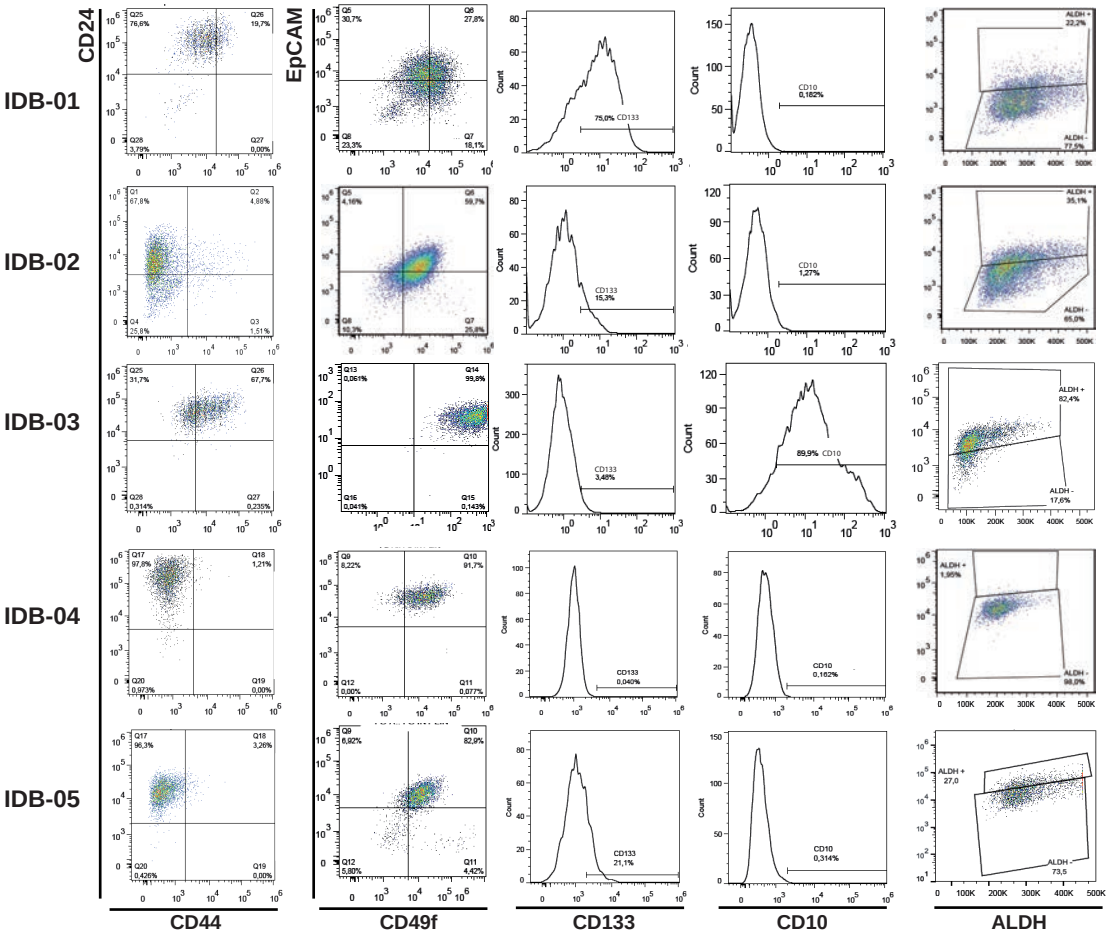

C

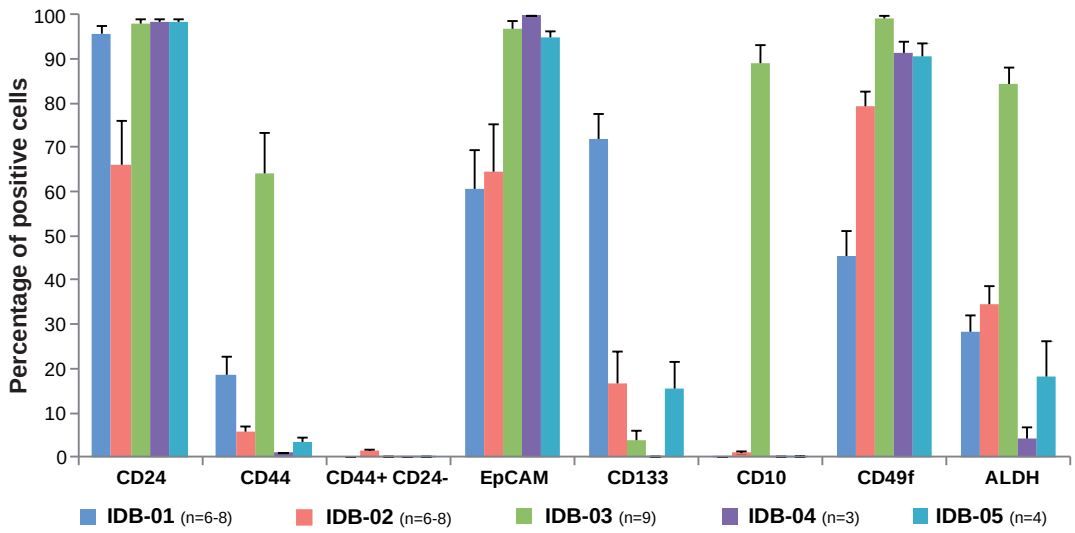

Supplementary Figure S5

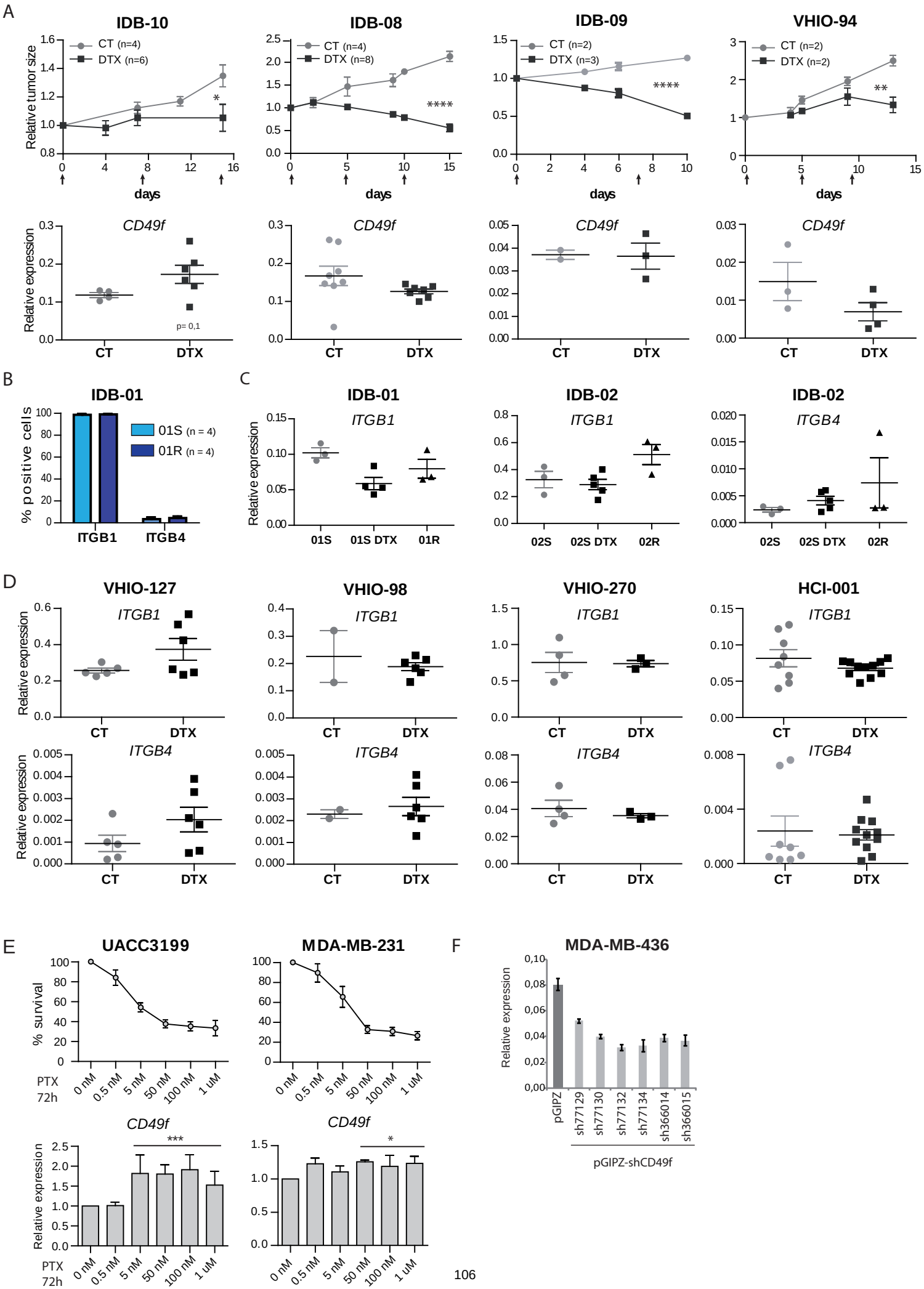

Supplemental Figure S6

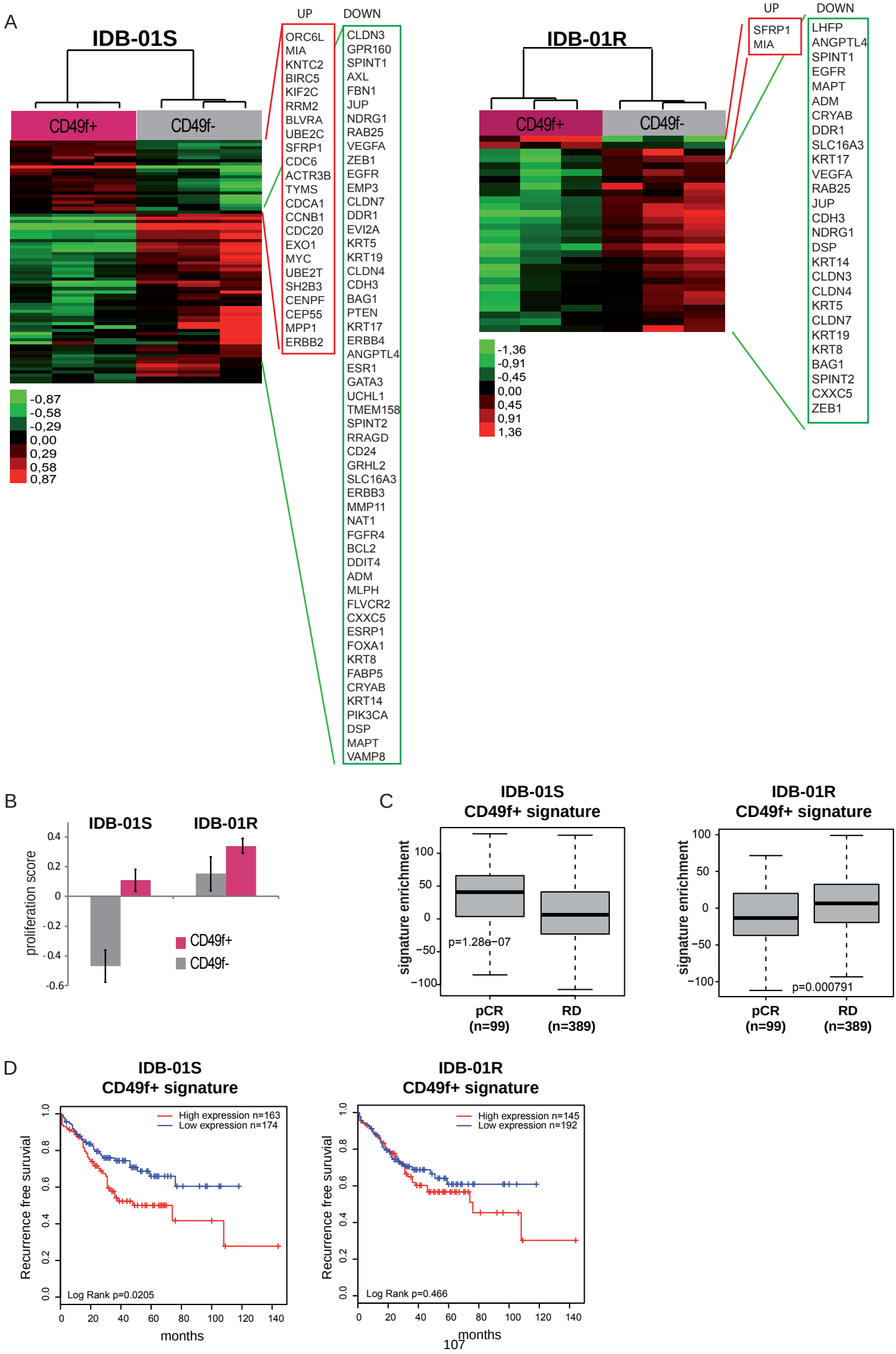

Supplemental Figure legends

Supplemental Figure S1. Generation of breast cancer PDX models (related to Figure 1 and Table 1)
A. Time in days until palpable lesions are detected in mice at first passage according to the source. All engrafted tumors were grade 3 and their subtype is shown.
B. Percentage of palpable tumors engrafted relative to the total number of independent patient samples, depicted in pathological grade classification. Mice that did not survive for at least 60 days after surgery were excluded from the analyses. Total number of samples is indicated (n). Gr1 = grade 1; Gr2 = grade 2; Gr3 = grade 3.
C. Representative images of H&E staining of the original human tumors and the mouse mammary glands where they were implanted. No palpable lesions were detected in these mice and accordingly extensive necrotic areas were observed. However, viable human epithelial structures, mainly normal ducts, ADH (atypical ductal hyperplasia), DCIS (ductal carcinoma in situ) and occasionally IDC (invasive ductal carcinoma) or viable tumor cells were detected. Note that the morphology of IDC grade 1 is maintained in the mouse implant.
D. Percentage of mouse mammary glands showing human structures but not tumor growth. Quantification of indicated human structures in mouse mammary glands where no palpable lesions were detected is represented. MG = mammary glands. Only mice that survived for at least 60 days after tumor implantation were considered. Total number of MG analyzed is indicated (n).
E. Tumor latency (days) in each mouse tumor model at the indicated passages. Total number of tumors considered (n), mean, standard deviation and t-test p values for significant differences are shown.
F. Tumor growth in mice, calculated as L x I (mm x mm)/100 versus time (weeks). Each line represents a representative tumor and each color represents a different passage as indicated. Week 1 is the time at which palpable tumors were first detected.
G. mRNA expression levels of indicated genes relative to *PPiA* at indicated passages: early (1^{st} to 5^{th}) and late (more than 10^{th}) measured by qRT-PCR. Total number of tumors analyzed is indicated (n). Determinations were done in triplicate and mean values were used for the calculations. Mean values for "n" independent tumors and standard deviations are shown.
H. Percentage of palpable tumors relative to the total number of tumors implanted with (+) or without (-) exogenous 17β-estradiol and progesterone pellets in luminal models. Total number of implanted mammary glands is indicated (n).

Supplemental Figure S2. Mouse PDX grafts resemble human tumors of origin at early passages but changes are observed at late passages in some models (related to Figure 1 and Table 1)
A. Representative images of estrogen receptor (ER), progesterone receptor (PR), HER2, cytokeratins (CK18, CK5/6) and p53 protein expression in human tumors of origin and tumors growing in mice of the indicated models at early (1^{st} to 2^{nd}) and later passages (4^{th} to 8^{th}) as determined by immunohistochemistry.
B. Representative H&E pictures of macroscopic metastasis.

Supplemental Figure S3. Docetaxel treatment in PDX models and association of CD49f and EpCAM expression with survival (related to Figure 2 and 3)
A. Schematic representation of docetaxel resistant tumors generation. Several tumors from each model were implanted in both mammary inguinal glands of 8 recipient NOD/Scid females. Tumor-bearing animals were individually identified and when tumors reached 6x6 of size, mice were treated with docetaxel (20 mg/kg i.p.) once a week as indicated. If the tumor volume decreases below 3x3 size treatment was interrupted and re-initiated when tumor volume increased again over the size of 6x6. After 10 to 12 doses, mice were sacrificed, tumors were excised and re-implanted in mice (second passage) to repeat the process until tumors become resistant.
B. Representative kinetics of tumor growth during docetaxel treatment in sensitive TNBC IDB-01S and IDB-02S tumors and resistant luminal tumors IDB-03 and IDB-04. Tumor size (v = Lxl/100) is shown over time (weeks). Each line represents one tumor and arrows indicate docetaxel treatments.
C. Tumor growth in the initially sensitive (IDB-01S and IDB-02S) and after resistance to taxanes was acquired (IDB-01R and IDB-02R). Total number of tumors analyzed (n), mean values and SEM are shown.
D. Time in days until palpable tumors are detected (tumor latency) in the initially sensitive (IDB-01S and IDB-02S) and after resistance to taxanes was acquired (IDB-01R and IDB-02R).

E. Kaplan-Meier analyses of disease free survival (DFS) of the resistant signature identified in the TCGA database for breast tumors.
F. Kaplan-Meier analyses of distal metastasis free survival of basal-like tumors using *CD49f* and *EpCAM* mRNA expression independently and combined in the online GOBO database (Ringner et al., 2011).
G. Kaplan-Meier analyses of overall survival of basal-like tumors using *CD49f* and *EpCAM* mRNA expression in the clinical data set (GSE16446) from the TOP TRIAL (Desmedt et al., 2011) .
H. Kaplan-Meier analyses of overall survival of basal-like tumors using *CD49f* and *EpCAM* mRNA expression in the clinical data set (GSE42568) (Clarke et al., 2013) .

Supplemental Figure S4. Heterogeneous expression of CSC markers in PDX models and FACs gating (related to Figure 3)
A. Gating scheme. Analyzed cells were first gated as DAPI negatives (live cells) and H2Kd- (human cells).
B. Representative dot-plots and histograms of indicated markers in H2kD- human cells from each tumor model. The axes were established according to fluorescence minus one (FMO) controls or ALDH negative control.
C. Frequency of indicated markers within the human H2Kd- population analyzed by flow cytometry on established PDX. Total number of tumors analyzed (n), mean values and SEM are shown. Passage 7-14 was analyzed for all models

Supplemental Figure S5. No changes in ITGB1 and ITGB4 in docetaxel resistant tumors or residual disease (related to Figure 4 and 5)
A. Top panels: Tumor size of the indicated PDX tumors treated with docetaxel (20 mg/kg arrows) and corresponding controls relative to the size at the first day of treatment. Total number of tumors (n), mean, SEM and t-test p values are shown. Bottom panels: *CD49f* mRNA expression levels relative to *PPiA* in tumors treated with docetaxel and untreated controls measured by qRT-PCR. Determinations were done in triplicates and means are used.
B. Frequency of ITGB1+ and ITGB4+ cells in H2Kd- human cells in IDB-01S and IDB-01R tumors measured by flow cytometry. Total number of tumors analyzed (n), mean values and SEM are shown.
C. *ITGB1* and *ITGB4* mRNA expression levels relative to *PPiA* in sensitive untreated tumors, residual disease after docetaxel treatment and tumors with acquired resistance in IDB-01 and IDB-02 models measured by qRT-PCR. No expression of *ITGB4* was found in IDB-01 tumors. Determinations were done in triplicates. Means and SEM are shown.
D. *ITGB1* and *ITGB4* mRNA expression levels relative to *PPiA* in tumors treated with docetaxel and in untreated controls of indicated PDX models measured by qRT-PCR. Determinations were done in triplicates.Means and SEM are shown.
E. Top panels. Percentage of surviving cells treated with indicated doses of paclitaxel for 72h. Bottom panels: *CD49f* mRNA expression levels in cells treated with paclitaxel relative to untreated controls. Mean values of 3 independent experiments, SEM and t-test p values for the higher concentrations are shown.
F. Bars show *CD49f* mRNA expression levels relative to *PPiA* in the indicated TNBC cell lines stably infected with six independent shCD49f knock-down constructs and control vector (pGIPZ) measured by qRT-PCR. Determinations were done in triplicates and means are used.

Supplemental Figure S6. Molecular characterization of CD49f+ and CD49f- cell populations (related to Figure 6)
A. Supervised expression analysis of the genes found differentially expressed between CD49f+ and CD49f- cells within IDB-01S and -01R tumors. Each square represents the relative transcript abundance.
B. Expression of the PAM50 proliferation score across CD49f+ and CD49f- cells within IDB-01S and -01R tumors.
C. Association of IDB-01S-CD49f+ or 01R-CD49f+ signatures with chemotherapy response in 508 patients with breast cancer (GSE25066). Response was measured as pathological complete response or residual disease.
D. Kaplan-Meier analysis of overall survival and distant metastasis free survival using sensitive and resistant CD49f+ signatures in the Perou extended database (Prat et al., 2010).

Supplemental Items

Supplemental Table S1. Characteristics of human tumors of origin and recipient mice (related to Table 1, Figure 1 and 2)

Source, histopathological status and clinical data available of the 61 human samples implanted; number, strain, survival of recipient mice and outcome after H&E examination of recipient mammary glands are shown. Samples excluded from the analysis are shown in red. Samples highlighted in yellow indicate established tumor models. IDC: invasive ductal carcinoma; ADH: atypical ductal hyperplasia; DCIS: ductal carcinoma in situ; QT: chemotherapy; HTP: hormonotherapy, n.d.: no data, n.e. not evaluable. MG: mammary gland.

Supplemental Table S2. Gene expression signatures and raw data (related to Figure 2, Figure 6 and S6)

Supplemental Experimental Procedures

Generation of PDX

A total of 61 samples from breast cancer patients, 54 from fresh primary tumor pieces obtained directly after surgery and 7 from cancer cells isolated from pleural effusions were transplanted into the fat pad of 90 immunodeficient mice. Three strains of immunodeficient mice have been used. Nude mice (Athymic Nude - Foxn1nu Harlan), NOD/ Scid (NOD.CB17-Prkdcscid/J; JAX via Charles River) and Scid/Beige (CB17.Cg-PrkdcscidLystbg-J/Crl, JAX via CR) mice (Carroll and Bosma, 1991). Mice were maintained in specific pathogen-free animal housing (IDIBELL). NOD/Scid and Scid/Beige mice were bred in our animal facility. Fresh primary human breast tumor fragments and cells isolated from pleural effusion were obtained from patients at the time of surgery or thoracocentesis, with informed written patient consent. Fragments of 30 to 60 mm^3 were implanted into cleared fat pad from 4^{th} mammary glands of 3-weeks-old NOD/Scid or Nude females and pellets of 17β-estrogen (0,1 mg) (Innovative Research of America) were implanted into the intraescapular fad pat; in the case of tumor cells isolated from pleural effusions, $3x10^6$ tumor cells were injected in 4th mammary glands of Nude, Scid/Beige or NOD/Scid females. Pathological characteristics of implanted samples, number and strain of host mice and engraftment outcome are shown in Supplementary Table S1. Orthotopic tumors appeared at the graft site 30 to 152 days after implantation and they were subsequently transplanted from mouse to mouse without clearing epithelia. In each passage, samples were collected, cryopreserved in DMSO-fetal bovine serum solution (1:10) as stock, or directly at -80ºC for gene expression analysis, and fixed with phosphate buffered saline (PBS) 10% formol, for histological studies.

Mice that died within 60 days after tumor implantation without developing tumor or samples without pathological data available were excluded from the analyses (15 samples, in red in Table S1). Tumor growth (engraftment) was analyzed in 46 patients´ samples implanted in 71 immunodeficient mice. In the first passage, palpable tumors from 7 patients were obtained; all of them derived from grade 3 tumors. We were able to successfully maintain 5 tumor lines by consecutive rounds of transplantation (yellow in table S1, indicated as IDB-01-IDB-05). To evaluate the influence of hormones ER+PR+ tumors were maintained in mice with or without 17β-estrogen (0,1 mg) progesterone (32,5 mg) pellets (Innovative Research of America) implanted into their intraescapular fad pat.

The additional models included (IDB-08-IDB-10) were generated following similar procedures, after implantation of fresh tumor pieces in the cleared fat pad of NSG (NOD.Cg-Prkdc^{scid} Il2rg^{tm1Wjl}/SzJ, JAX via Charles River) mice. All the *in house* generated PDX models were maintained by serial transplantation in the intact fat pad of Nod/Scid mice, except for IDB-08 which was maintained in NSG mice.

Model HCI001 (TNBC) was donated by A Welm and Y DeRose (DeRose et al., 2011) and was maintained in passage by serial transplantation over time in the fat pad of NSG mice. Models VHIO-93, -94, -98, -102, -127, -197, -270 and -288 (all of them TNBC, VHIO-127 is a BRCA1 mutant) were generated by subcutaneous implantation of primary tumor pieces (except for VHIO-127 and VHIO-288 which derived from metastasis) on the back of Nude mice as described previously (Bruna et al., 2016; Garcia-Garcia et al., 2012). The models from VHIO were collected and implanted in the intact fact pad of Nod/Scid mice in our animal facility to perform docetaxel treatments.

Tumor growth

Every mice was monitored for tumor incidence by palpation and visual inspection and for weight variations. Mice were sacrificed before tumors reached a diameter of 1,5 cm, or when 20% loss of their initial weight or deterioration of health was observed. Individual tumor size was calculated as L*l/100, with "L" being the largest diameter and "l" the smallest. Growth curves were established as a function of time. Tumor latency was recorded for all palpable tumors and mice. To emulate the clinical procedure tumors were surgically removed before they reached 1,5 cm of diameter and mice were left alive to determine the incidence of relapse and metastasis. We randomly sectioned the axillary mammary gland, lymph nodes and lungs of mice that survived longer than 60 days after primary tumor excision.

Histology and immunohistochemistry

Samples from patient or mouse tumors, and mammary fat pads of host mice that did not develope tumors were fixed in formalin immediately after resection and embedded into paraffin. Lungs, brain, liver, kidneys and other organs were collected following the same protocol. Bones were treated with 10% formic acid before were formalin fixation and paraffin embedding. For light microscopic examination 3-µm-thick sections were

stained with hematoxylin and eosin (H&E). Selected lungs from all models and brains from Model B were sectioned every 75-100 µm, stained with H&E and scored for metastasis. For immunohistochemical (IHC) studies 3-µm-thick sections were embedded in paraffin and incubated with antibodies against ER (1:30; DAKO, clon 1D5, IR657), PR (diluted; DAKO, clon 636, IR68), HER2 (1:350; DAKO, SK001), CK18 (diluted; DAKO, clon DC10, IR 618), CK5/6 (1:100; Zymed, clon D5/16B4, MAB1620) and p53 (1:50; Biogenex, AM195). Pre-treatment with citrate pH6 was done on slides stained for ER, PR, HER2, CK18 and p53 and with citrate pH9 on CK5/6 stained slides. Antibodies were detected using biotin-conjugated secondary antibodies (HRP; DAKO). The antigen-antibody complex was conjugated with streptavidin horseradish peroxidase and visualized with diaminobenzidine (Kit DAKO LSAB). Sections were counterstained with hematoxylin and appropriate positive and negative controls were used.

Breast cancer cells isolation

Fresh tissues were mechanically cut using the McIlwain tissue chopper and enzymatically digested with appropriate medium (Dulbecco's modified Eagle's medium [DMEM] F-12 (PAA), 0.3% Collagenase A (Roche Diagnostics, S.L.), 2.5U/mL Dispase (Gibco), 20 mM HEPES (Sigma-Aldrich), and antibiotics) 60 minutes at 37ºC with shacking. Samples were washed with Leibowitz-L15 medium (Gibco) supplemented with 10% fetal bovine serum (FBS) and penicillin/streptomycin between each step. Erythrocytes were eliminated by treating samples with hypotonic lysis buffer (ACK lysing buffer, Lonza Iberica) and incubated over night at 4ºC in the 4ºC in the aforementioned Leibowitz-L15 medium. Tje following day, single epithelial cells were isolated by treating with trypsin (PAA Laboratories) 5 minutes at 37ºC and a mix of Dispase (Gibco life technologies, Invitrogen) DNAse (Invitrogen) for 10 minutes at 37ºC. Dead cells were first excluded by centrifugation with Lympholyte (Cedarlane laboratories) 800xg for 20 minutes and then 250xg for 10 minutes at room temperature. Cell aggregates were removed by filtering cell suspension with 40 µm filter and counted with Trypan Blue.

ALDH assay

Single cells were assessed for their ALDH activity using the ALDEFLUOR assay system (STEMCELL technologies). 4 x 10^5 cells were re-suspended in ALDEFLUOR buffer and activated ALDEFLUOR substrate was added. Immediately, half of them were separated in other tube with the inhibitor DEAB. The incubation was performed during 30 minutes at 37ºC. Mouse cells were excluded in flow cytometry using H2Kd-PECy7 (116622 from BioLegend). A population of 10,000 living cells was captured in all fluorescence-activated cell sorting (FACS) experiments. FACS analysis was performed using FACS Gallios cytometer (Beckman Coulter, Inc) and the FlowJo software package.

Therapeutic assays

For the generation of the docetaxel resistant-derived tumors, treatment started in mice bearing tumors of 6x6 mm size (L*l/100). Tumor growth and weight were evaluated twice a week. When tumor volume decreased below 3x3 mm, treatment was interrupted, and reinitiated when tumors re-grew over of 6x6 mm. Mice were ethically sacrificed after 10 to 12 doses of docetaxel when the tumor size surpassed a diameter of 1,5 cm or mouse weight decreased by 20%. Tumors were then excised, cut in pieces and re-implanted into new host mice (passage 2) in which docetaxel treatment was reinitiated following the same criteria, as shown in Supplementary Figure S3A.

For short term treatments, tumor bearing mice were treated with 2 to 5 doses of docetaxel, every 5-7 days for a period of 10 to 30 days, depending on tumors response. Mice were then sacrificed and tumors were analyzed for CD49f expression 3-5 days after the last dose of docetaxel, except for the most sensitive models that needed longer time to grow.

Lentiviral infection

Lentiviral infection was done following the manufacturer´s indications (Invitrogen). Briefly 293FT cells were used for the production of the virus. 293FT cells (5x106) were transfected with lentiviral pGIPZ empty or pGIPZ-shCD49f vectors (Dharmacon GE) and packaging (gag-pol, vsvg, rev) plasmids (Addgene) by calcium phosphate method. 25mM HEPES was added 16 h later. Virus supernatants were harvested 72h post transfection, centrigufated at 250G 5' and filtered with 0.22 µm filters. MDA-MB-436 cell lines were transduced in a ratio 1:3 with fresh growth medium and with 8µg/ml of polybrene. Plates were centrifuged 1 hour at 1.000 rpm at 37ºC to improve the infection. Selection started with puromycin antibiotic (Sigma-

Aldrich) at 1,5µg/ml. The resulting stable cell lines infected were maintained with 0,5 µg/ml . Medium was refreshed every three days. The following shCD49f sequences were tested: 77129: TATTCCATCTGCCTTGCTG; 77130:TAGTTACTGAATCTGAGAG; 77132: TTCTGAATATTAATCACAG; 77134: TTAGAAACAATACCTTTCC; 326014: ATTTCTAAAGCAATATCCT and 326015: TCAGTTGTACTTAAAACCA, and based on the results 77132 and 77134 were selected.

RNA extraction and RT-PCR

Total RNA from tissue was prepared with Tripure Isolation Reagent (Roche). Frozen tumor tissues were fractionated using the POLYTRON® system PT 1200 E (Kinematica). cDNA was produced by reverse transcription using 1 µg of RNA in a 35 µL reaction following manufacturer's instructions (Applied Biosystems). 20 ng/well of cDNA were used for the analysis performed in triplicate. Quantitative PCR was performed using the LightCycler® 480 SYBR green. Primer sequences are indicated below. Ct analysis was performed using LightCycler 480 software (Roche). All primers indicated below are in 5' → 3' direction.

hCD49f Forward	CTGGCCTCTTCATTTGGCTA
hCD49f Reverse	AAAATACTGTGGGGCTCCAAT
hEpCAM Forward	AATCGTCAATGCCAGTGTACTT
hEpCAM Reverse	TCTCATCGCAGTCAGGATCATAA
hPPiA Forward	ATGCTGGACCCAACACAAAT
hPPiA Reverse	TCTTTCACTTTGCCAAACACC
hCK18 Forward	TCAGCAGATTGAGGAGAGCA
hCK18 Reverse	GAGCTGCTCCATCTGTAGG
hCK5 Forward	ATCGCCACTTACCGCAAGCTGCTGGAG
hCK5 Reverse	AAACACTGCTTGTGACAACAGAG
hER Forward	ATCTCGGTTCCGCATGATGAATCTGC
hER Reverse	TGCTGGACAGAAATGTGTACACTCCAGA
hPR Forward	GGCATGGTCCTTGGAGGT
hPR Reverse	CACTGGCTGTGGGAGAGC
hHER2 Forward	TTCCTTCCTGCTTGAGTTCC
hHER2 Reverse	GRGCTGTTCCTCTTCCAACG
hITGB1 Forward	GCCGCGCGGAAAAGATG
hITGB1 Reverse	ACAATTTGGCCCTGCTTGTA
hITGB4 Forward	CCCCGAGGTAGGTCCAGG
hITGB4 Reverse	GTTTGCCAAGGTCCCAGAGA

Public clinical tools:

The web-based tools used include: Gene expression-based Outcome for Breast cancer Online (GOBO), comprising 1881 breast cancer-samples (Ringner et al., 2011) http://co.bmc.lu.se/gobo/gsa_information.pl, Kaplan Meier plotter (KM plotter), capable to assess the effect of 54,675 genes on survival using 5,143 breast cancer patients (Szasz et al., 2016) http://kmplot.com/analysis/, and PROGgeneV2, a tool that can be used to study prognostic implications of genes in various cancers, including breast (Goswami and Nakshatri, 2014) http://watson.compbio.iupui.edu/chirayu/proggene/database/index.php

Supplemental References

Bruna, A., Rueda, O. M., Greenwood, W., Batra, A. S., Callari, M., Batra, R. N., Pogrebniak, K., Sandoval, J., Cassidy, J. W., Tufegdzic-Vidakovic, A., *et al.* (2016). A Biobank of Breast Cancer Explants with Preserved Intra-tumor Heterogeneity to Screen Anticancer Compounds. Cell *167*, 260-274 e222.

Carroll, A. M., and Bosma, M. J. (1991). T-lymphocyte development in scid mice is arrested shortly after the initiation of T-cell receptor delta gene recombination. Genes Dev *5*, 1357-1366.

Clarke, C., Madden, S. F., Doolan, P., Aherne, S. T., Joyce, H., O'Driscoll, L., Gallagher, W. M., Hennessy, B. T., Moriarty, M., Crown, J., *et al.* (2013). Correlating transcriptional networks to breast cancer survival: a large-scale coexpression analysis. Carcinogenesis *34*, 2300-2308.

DeRose, Y. S., Wang, G., Lin, Y. C., Bernard, P. S., Buys, S. S., Ebbert, M. T., Factor, R., Matsen, C., Milash, B. A., Nelson, E., *et al.* (2011). Tumor grafts derived from women with breast cancer authentically reflect tumor pathology, growth, metastasis and disease outcomes. Nat Med *17*, 1514-1520.

Desmedt, C., Di Leo, A., de Azambuja, E., Larsimont, D., Haibe-Kains, B., Selleslags, J., Delaloge, S., Duhem, C., Kains, J. P., Carly, B., *et al.* (2011). Multifactorial approach to predicting resistance to anthracyclines. J Clin Oncol *29*, 1578-1586.

Garcia-Garcia, C., Ibrahim, Y. H., Serra, V., Calvo, M. T., Guzman, M., Grueso, J., Aura, C., Perez, J., Jessen, K., Liu, Y., *et al.* (2012). Dual mTORC1/2 and HER2 blockade results in antitumor activity in preclinical models of breast cancer resistant to anti-HER2 therapy. Clin Cancer Res *18*, 2603-2612.

Goswami, C. P., and Nakshatri, H. (2014). PROGgeneV2: enhancements on the existing database. BMC Cancer *14*, 970.

Prat, A., Parker, J. S., Karginova, O., Fan, C., Livasy, C., Herschkowitz, J. I., He, X., and Perou, C. M. (2010). Phenotypic and molecular characterization of the claudin-low intrinsic subtype of breast cancer. Breast Cancer Res *12*, R68.

Ringner, M., Fredlund, E., Hakkinen, J., Borg, A., and Staaf, J. (2011). GOBO: gene expression-based outcome for breast cancer online. PLoS One *6*, e17911.

Szasz, A. M., Lanczky, A., Nagy, A., Forster, S., Hark, K., Green, J. E., Boussioutas, A., Busuttil, R., Szabo, A., and Gyorffy, B. (2016). Cross-validation of survival associated biomarkers in gastric cancer using transcriptomic data of 1,065 patients. Oncotarget *7*, 49322-49333.

ARTICLE 2

“Stem cell-like transcriptional reprogramming mediates metastatic resistance to mTOR inhibition”

OPEN

Oncogene (2017) **36,** 2737–2749

www.nature.com/onc

ORIGINAL ARTICLE

Stem cell-like transcriptional reprogramming mediates metastatic resistance to mTOR inhibition

F Mateo[1,49], EJ Arenas[2,49], H Aguilar[1,49], J Serra-Musach[1], G Ruiz de Garibay[1], J Boni[1], M Maicas[3], S Du[4], F Iorio[5,6], C Herranz-Ors[1], A Islam[7], X Prado[1], A Llorente[1], A Petit[8], A Vidal[8], I Català[8], T Soler[8], G Venturas[8], A Rojo-Sebastian[9], H Serra[10], D Cuadras[11], I Blanco[12], J Lozano[13], F Canals[14], AM Sieuwerts[15], V de Weerd[15], MP Look[15], S Puertas[16], N García[1], AS Perkins[17], N Bonifaci[1], M Skowron[1], L Gómez-Baldó[1], V Hernández[18], A Martínez-Aranda[18], M Martínez-Iniesta[16], X Serrat[19], J Cerón[19], J Brunet[20], MP Barretina[21], M Gil[22], C Falo[22], A Fernández[22], I Morilla[22], S Pernas[22], MJ Plà[23], X Andreu[24], MA Seguí[25], R Ballester[26], E Castellà[27], M Nellist[28], S Morales[29], J Valls[29], A Velasco[29], X Matias-Guiu[29], A Figueras[10], JV Sánchez-Mut[30], M Sánchez-Céspedes[30], A Cordero[30], J Gómez-Miragaya[30], L Palomero[1], A Gómez[30], TF Gajewski[31], EEW Cohen[32], M Jesiotr[33], L Bodnar[34], M Quintela-Fandino[35], N López-Bigas[36,37], R Valdés-Mas[38], XS Puente[38], F Viñals[10], O Casanovas[10], M Graupera[10], J Hernández-Losa[39], S Ramón y Cajal[39], L García-Alonso[5], J Saez-Rodriguez[5], M Esteller[30,37,40], A Sierra[41], N Martín-Martín[42], A Matheu[43,44], A Carracedo[42,44,45], E González-Suárez[30], M Nanjundan[46], J Cortés[47], C Lázaro[12], MD Odero[3], JWM Martens[15], G Moreno-Bueno[48], MH Barcellos-Hoff[4], A Villanueva[16], RR Gomis[2,37] and MA Pujana[1]

Inhibitors of the mechanistic target of rapamycin (mTOR) are currently used to treat advanced metastatic breast cancer. However, whether an aggressive phenotype is sustained through adaptation or resistance to mTOR inhibition remains unknown. Here, complementary studies in human tumors, cancer models and cell lines reveal transcriptional reprogramming that supports metastasis in response to mTOR inhibition. This cancer feature is driven by EVI1 and SOX9. EVI1 functionally cooperates with and positively regulates SOX9, and promotes the transcriptional upregulation of key mTOR pathway components (REHB and RAPTOR) and of lung metastasis mediators (FSCN1 and SPARC). The expression of *EVI1* and *SOX9* is associated with stem cell-like and metastasis signatures, and their depletion impairs the metastatic potential of breast cancer cells. These results establish the mechanistic link between resistance to mTOR inhibition and cancer metastatic potential, thus enhancing our understanding of mTOR targeting failure.

Oncogene (2017) **36,** 2737–2749; doi:10.1038/onc.2016.427; published online 19 December 2016

[1]Breast Cancer and Systems Biology Laboratory, Program Against Cancer Therapeutic Resistance (ProCURE), Catalan Institute of Oncology (ICO), Bellvitge Institute for Biomedical Research (IDIBELL), L'Hospitalet del Llobregat, Barcelona, Spain; [2]Oncology Program, Institute for Research in Biomedicine (IRB Barcelona), The Barcelona Institute of Science and Technology, Barcelona, Spain; [3]Centre for Applied Medical Research (CIMA) and Department of Biochemistry and Genetics, University of Navarra, Pamplona, Spain; [4]Department of Radiation Oncology, New York University School of Medicine, New York, NY, USA; [5]European Molecular Biology Laboratory-European Bioinformatics Institute (EMBL-EBI), Wellcome Trust Genome Campus, Cambridge, UK; [6]Cancer Genome Project, Wellcome Trust Sanger Institute, Hinxton, UK; [7]Department of Genetic Engineering and Biotechnology, University of Dhaka, Dhaka, Bangladesh; [8]Department of Pathology, University Hospital of Bellvitge, IDIBELL, L'Hospitalet del Llobregat, Barcelona, Spain; [9]Department of Pathology, MD Anderson Cancer Center, Madrid, Spain; [10]Angiogenesis Research Group, ProCURE, ICO, IDIBELL, L'Hospitalet del Llobregat, Barcelona, Spain; [11]Statistics Unit, IDIBELL, L'Hospitalet del Llobregat, Barcelona, Spain; [12]Hereditary Cancer Programme, ICO, IDIBELL, L'Hospitalet del Llobregat, Barcelona, Spain; [13]Department of Molecular Biology and Biochemistry, Málaga University, and Molecular Oncology Laboratory, Mediterranean Institute for the Advance of Biotechnology and Health Research (IBIMA), University Hospital Virgen de la Victoria, Málaga, Spain; [14]ProteoRed-Instituto de Salud Carlos III, Proteomic Laboratory, Vall d'Hebron Institute of Oncology (VHIO), Vall d'Hebron University Hospital, Barcelona, Spain; [15]Department of Medical Oncology, Erasmus University Medical Center, Daniel den Hoed Cancer Center, Cancer Genomics Centre, Rotterdam, The Netherlands; [16]Chemoresistance and Predictive Factors Laboratory, ProCURE, ICO, IDIBELL, L'Hospitalet del Llobregat, Barcelona, Spain; [17]University of Rochester Medical Center, School of Medicine and Dentistry, Rochester, NY, USA; [18]Biological Clues of the Invasive and Metastatic Phenotype Laboratory, IDIBELL, L'Hospitalet del Llobregat, Barcelona, Spain; [19]Cancer and Human Molecular Genetics, IDIBELL, Hospitalet de Llobregat, Barcelona, Spain; [20]Hereditary Cancer Programme, ICO, Girona Biomedical Research Institute (IDIBGI), Girona, Spain; [21]Department of Medical Oncology, ICO, IDIBGI, Girona, Spain; [22]Department of Medical Oncology, ICO, IDIBELL, L'Hospitalet del Llobregat, Barcelona, Spain; [23]Department of Gynecology, University Hospital of Bellvitge, IDIBELL, L'Hospitalet del Llobregat, Barcelona, Spain; [24]Department of Pathology, Parc Taulí Hospital Consortium, Sabadell, Barcelona, Spain; [25]Medical Oncology Service, Parc Taulí Hospital Consortium, Sabadell, Barcelona, Spain; [26]Department of Radiation Oncology, University Hospital Germans Trias i Pujol, ICO, Germans Trias i Pujol Research Institute (IGTP), Badalona, Barcelona, Spain; [27]Department of Pathology, University Hospital Germans Trias i Pujol, ICO, IGTP, Badalona, Barcelona, Spain; [28]Department of Clinical Genetics, Erasmus Medical Centre, Rotterdam, The Netherlands; [29]Hospital Arnau de Vilanova, University of Lleida, Biomedical Research Institute of Lleida (IRB Lleida), Lleida, Spain; [30]Cancer Epigenetics and Biology Program (PEBC), IDIBELL, L'Hospitalet del Llobregat, Barcelona, Spain; [31]Departments of Pathology and Medicine, University of Chicago, Chicago, IL, USA; [32]Moores Cancer Center, University of California San Diego, La Jolla, CA, USA; [33]Department of Pathology, Military Institute of Medicine, Warsaw, Poland; [34]Department of Oncology, Military Institute of Medicine, Warsaw, Poland; [35]Breast Cancer Clinical Research Unit, Spanish National Cancer Research Center (CNIO), Madrid, Spain; [36]Department of Experimental and Health Sciences, Barcelona Biomedical Research Park, Pompeu Fabra University (UPF), Barcelona, Spain; [37]Institució Catalana de Recerca i Estudis Avançats (ICREA), Barcelona, Spain; [38]Department of Biochemistry and Molecular Biology, University Institute of Oncology of Asturias, University of Oviedo, Oviedo, Spain; [39]Department of Pathology, Vall d'Hebron University Hospital, Barcelona, Spain; [40]Department of Physiological Sciences II, School of Medicine, University of Barcelona, Barcelona, Spain; [41]Molecular and Translational Oncology Laboratory, Biomedical Research Center CELLEX-CRBC, Biomedical Research Institute 'August Pi i Sunyer' (IDIBAPS), and Systems Biology Department, Faculty of Science and Technology, University of Vic, Central University of Catalonia, Barcelona, Spain; [42]Center for Cooperative Research in Biosciences (CIC bioGUNE), Derio, Spain; [43]Neuro-Oncology Section, Oncology Department, Biodonostia Research Institute, San Sebastian, Spain; [44]Ikerbasque, Basque Foundation for Science, Bilbao, Spain; [45]Department of Biochemistry and Molecular Biology, University of the Basque Country (UPV/EHU), Bilbao, Spain; [46]Department of Cell Biology, Microbiology, and Molecular Biology, University of South Florida, Tampa, FL, USA; [47]Department of Medical Oncology, VHIO, Vall d'Hebron University Hospital, Barcelona, Spain and [48]Department of Biochemistry, Autonomous University of Madrid (UAM), Biomedical Research Institute 'Alberto Sols' (Spanish National Research Council (CSIC)-UAM), Translational Research Laboratory, Hospital La Paz Institute for Health Research (IdiPAZ), and MD Anderson International Foundation, Madrid, Spain. Correspondence: Dr RR Gomis, Oncology Program, Institute for Research in Biomedicine (IRB Barcelona), The Barcelona Institute of Science and Technology, Baldiri Reixac 10, Barcelona 08028, Spain or Dr MA Pujana, ProCURE, Catalan Institute of Oncology, IDIBELL, Hospital Duran i Reynals, Gran via 199, L'Hospitalet del Llobregat, Barcelona 08028, Spain.

E-mail: roger.gomis@irbbarcelona.org or mapujana@iconcologia.net

[49]These authors contributed equally to this work.

Received 10 March 2016; revised 31 August 2016; accepted 10 October 2016; published online 19 December 2016

INTRODUCTION

The mechanistic target of rapamycin (mTOR) kinase integrates cues from nutrients and growth factors and is thus a master regulator of cell growth and metabolism.[1] As such, mTOR is activated in most cancer types and is frequently associated with poor prognosis.[2] Moreover, oncogenic mTOR signaling has a direct role in promoting cancer progression by inducing a pro-invasion translational program.[3] This program includes the downregulation of the tuberous sclerosis complex 2 (*TSC2*) gene, whose product, in a heterodimer with the *TSC1* product, serves as a negative regulator of mTOR complex 1 (mTORC1).[4] Consequently, loss of *Tsc2* in mice promotes breast cancer progression and metastasis.[5] Collectively, current knowledge supports the notion that mTOR signaling has a key role in cancer initiation, progression and metastasis.

As mTOR is a key factor in cancer biology, therapies based on its inhibition have been widely studied[6] and are central to the treatment of advanced metastatic breast cancer.[7] However, the success of monotherapy assays has been limited. Critically, within a relatively short term, allosteric mTOR inhibition concomitantly induces upstream receptor kinase signaling, which mediates therapeutic resistance.[8] Thus, therapies that combine allosteric inhibitors (rapamycin (sirolimus) and rapalogs) with inhibitors of growth factor signaling have been extensively evaluated.[9] Intriguingly, recent studies have further linked mTOR activity to a stem cell-like cancer phenotype that mediates breast cancer metastasis[10,11] and, using triple-negative (TN) breast cancer cell lines, have described that mTORC1/2 inhibition spares a cell population with stem cell-like properties and enhanced NOTCH activity.[12] These results are consistent with previous observations concerning the required activation of mTOR signaling in breast cancer stem-like viability and maintenance,[13] the enhancement of NOTCH signaling in poorly differentiated breast tumors[14] and the increase of tumor-initiating capacities with mTOR inhibition in liver cancer.[15] In this scenario, a fundamental question emerges as to whether relative long-term adaptation or resistance to mTOR inhibition is functionally linked to tumor-initiating properties and, eventually, metastasis.

Here, we explored the hypothesis that mTOR signaling supports metastasis and remains active in therapeutic resistance in metastatic breast cancer. We found that abnormal mTOR signaling enhances tumor-initiating properties and metastatic potential. This activity is dependent on EVI1, which in cooperation with SOX9 sustains a transcriptional reprogramming response.

RESULTS

Active mTORC1 signaling associates with distant metastasis

mTORC1 is the target of one of the latest drugs approved for the treatment of breast cancer in the advanced metastatic setting,[7] which suggests that this protein complex has a potential role in supporting metastasis and aggressive features. To study this relationship, a tissue microarray of primary breast tumors was assessed for mTORC1 activity by means of immunohistochemical determination of phospho-Ser235/236-ribosomal protein S6 (pS6), a well-established downstream target of mTORC1.[1] An association between pS6 positivity and the basal-like tumor phenotype or CK5 positivity was observed (Figure 1a; Mann–Whitney test $P < 0.01$). Most importantly, an association was also detected between medium-high pS6 positivity and the development of distant metastases (Fisher's exact test $P = 0.02$; odds ratio (OR) = 2.64, 95% confidence interval (CI) 0.95–7.35). Intriguingly, whereas the analyses by tumor subtypes were underpowered, both estrogen receptor (ER)-positive and ER-negative cases suggested a trend toward increased metastatic risk (ORs = 4.44 and 1.96, respectively). Thus, enhanced mTOR activity and breast cancer metastatic potential appear to be linked.

Metastasis dependence on mTORC1 signaling

To test the contribution of mTOR signaling to metastasis, we used the well-defined MDA-MB-231 breast cancer cell line, including its parental poorly metastatic population and the lung metastatic derivatives LM1 and LM2.[16] Western blot analyses showed increased levels in LM2 cells of several components of the mTORC1 signaling pathway, and particularly of RAPTOR and RHEB across the sub-populations (Figure 1b). The enhanced signaling in LM2 cells compared with the poorly metastatic parental population was confirmed by quantification of immunohistochemical staining of pS6 in the lung metastases that developed the cells upon tail vein injection (Figure 1c). Expanding on these observations, analysis of TCGA data showed negative correlations between *TSC1/2* and an upregulated gene set whose expression was clinically and experimentally associated with breast cancer metastasis to lung (lung metastasis signature (LMS)-up; Pearson's correlation coefficients (PCCs) < -0.25; *P*-values $< 10^{-8}$). Notably, this set was derived from the study of LM2 cells.[16]

Next, we tested the causal role of mTOR activity in the experimental model of lung metastasis. The capacity of LM2 cells to colonize the lung was assessed in the presence or absence of an allosteric mTOR inhibitor. LM2 cells stably expressing green fluorescent protein (GFP) and luciferase were injected into the lateral tail vein of immunocompromised mice, which were then randomly allocated to a group treated with dimethyl sulfoxide (DMSO) or a group treated with everolimus, both for 38 days. A significant reduction of lung colonization (and, as expected, of pS6 intensity) was observed in the latter group, both by measurements of *in vivo* photon flux and the relative lung metastasis area *ex vivo* by histology (Figure 1d). Collectively, these data suggest that mTORC1 signaling is associated with breast cancer metastatic potential and that inhibition of mTOR prevents lung metastasis. However, it is unclear whether this association persists in settings of resistance to mTOR inhibitors.

Metastatic resistance to mTOR inhibition

To evaluate the mechanisms responsible for resistance to mTOR inhibitors, we used two independent metastatic tumor models, namely a human TN *BRCA1*-mutated breast tumor orthotopically engrafted in nude mice (hereafter ortho-xenograft; Supplementary Figure 1) and the TN 4T1 murine breast carcinoma cell line engrafted in syngeneic background mice. Cells from both tumor models showed substantial mTORC1 signaling activity, particularly at the tumor invasive front (Supplementary Figure 1).[17] Unexpectedly, although systemic treatment with sirolimus or everolimus blunted primary tumor growth in each model, it did not reduce the number or size of lung metastases (Figure 2a). In addition, and contrary to expectations, the intensity of pS6 staining at the invasive tumor fronts of the primary lesion and in the lung metastases of the sirolimus-treated ortho-xenografts was significantly higher than in the control animals (Figure 2b). Similarly, a key factor in cancer metastasis initially identified in LM2 cells and human data analyses (thus included in LMS-up), FSCN1,[16,18] was found to be significantly overexpressed in both experimental models exposed to mTOR inhibitors (Figure 2c). Subsequent gene expression analysis of the treated tumors revealed coordinated changes concurrent with mTOR inhibition that were associated with LMS activation (Supplementary Figure 2). These changes included overexpression of LMS-up in the sirolimus-treated ortho-xenografts and underexpression of LMS-down in the everolimus-treated 4T1 tumors (as measured by the gene set expression analysis (GSEA), *P*-values < 0.05; Supplementary Figure 2).

To further study resistance to allosteric mTOR inhibition, we subjected MCF7 ER-positive and HCC1937 TN cells to long-term exposure to 50 and 150 nM of everolimus, respectively. After a period of sensitivity defined by undetectable or very low levels of

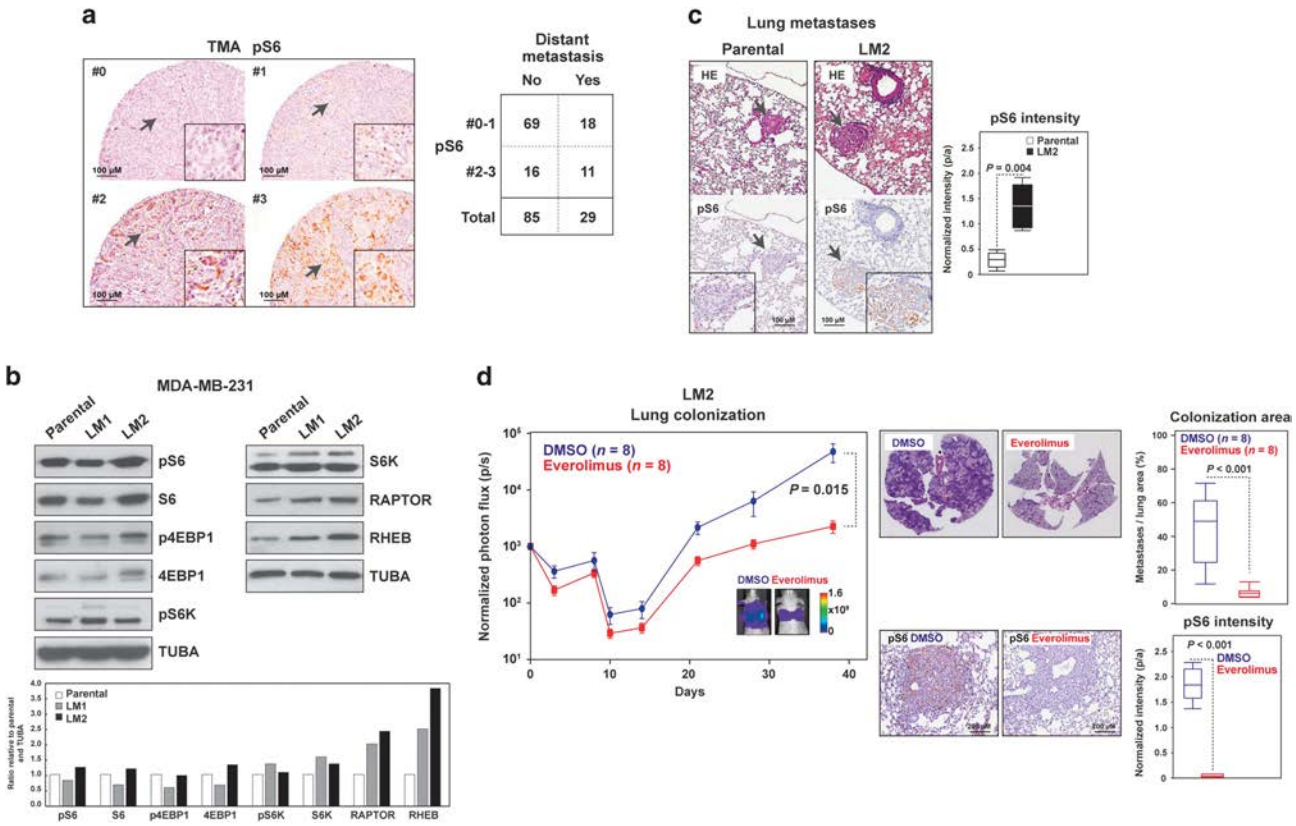

Figure 1. mTORC1 activity concurrent with enhanced metastatic potential. (**a**) Left panels, representative immunohistochemical scores (0, negative, to 3, highest expression) of pS6 staining in the tissue microarray (TMA) of primary breast tumors. Right panel, results for the association between pS6 staining and distant metastasis. (**b**) Increased expression of mTORC1 pathway components with enhanced metastatic potential of MDA-MB-231 cells. The loading control (α-tubulin, TUBA) is shown. Bottom panel, graph showing quantifications of protein levels relative to parental and TUBA (per sample). (**c**) Increased pS6 expression in lung metastases developed by LM2 cells. The arrows mark magnified fields. Right panel, box-and-whisker plots for the quantification (pixels/area, p/a) of pS6 intensity; three mice and three similar lung metastases were analyzed in each setting. The *P*-value of the two-tailed Mann–Whitney test is shown. (**d**) Left panel, graph showing the *in vivo* photon flux quantification in mice injected with LM2 and treated with DMSO or everolimus. Representative images from bioluminescence in lungs from DMSO- or everolimus-treated mice are shown. The scale bar depicts the range of photon flux values as a pseudo-color display, with red and blue representing high and low values, respectively. Right top panels, quantification of lung colonization (total metastasis area normalized per total lung area, based on HE). Right bottom panels, representative immunohistochemical results for pS6 and quantification of normalized intensities.

pS6, both cell lines recovered canonical mTORC1 signaling in 90–120 days (Figure 2d, top panels). Similarly to the *in vivo* observations, FSCN1 increased concurrently with adaptation to everolimus in both cell settings (Figure 2d, bottom panels). Subsequently, transcriptome analyses showed a significant change of the LMS in both cell lines, and particularly of the LMS-up in HCC1937 cells (Supplementary Figure 3).

Interestingly, both everolimus-adapted cell models showed significantly higher colony-forming capacity, with the higher relative difference found in HCC1937 cells (Figure 2e). Accordingly, fluorescence-activated cell sorting revealed an increase of CD49f+ and of CD44+/CD24− cells in everolimus-adapted MCF7 and HCC1937 cultures, respectively (Figure 2f). Although MCF7 did not show an increase in CD44+/CD24−, CD49f positivity has been linked to cancer stem cell-like properties.[19] In addition, quantitative gene expression analysis revealed a significant increase of *SOX2* in everolimus-adapted MCF7 cells and, in turn, an increase of *NANOG* and *OCT4* (but not *SOX2*) in everolimus-adapted HCC1937 cells (Supplementary Figure 4). Notably, an increase in *SOX2*, but not the two additional stem cell-like markers, has also been described in MCF7 cells resistant to tamoxifen.[20] Therefore, by combining *in vivo* and *in vitro* models of breast cancer, we reveal that exposure to allosteric mTOR inhibitors consistently promotes metastatic and tumor initiation properties. However, the precise regulators of this aggressive reprogramming remain to be determined.

TSC1/2 expression correlates negatively with tumor-initiating features

Given that differences in colony formation assays and tumor initiation properties were observed in mTOR inhibitor-resistant cell populations, we then explored the association between mTOR signaling and cancer cell initiation features in gene expression profiles from patient samples. To this end, we computed the expression correlations between *TSC1* or *TSC2* (*TSC1/2*) and 20 previously defined gene expression signatures using breast cancer data from The Cancer Genome Atlas (TCGA).[21] The signatures (full annotation is provided in Supplementary Table 1) include a consensus set derived from the study of embryonic stem cell-like cells (sESCs),[22] a consensus set of correlated master regulators of breast cancer stemness-like functions (hereafter sMRS),[23] and a MYC-centered regulatory network (sMYC);[24] importantly, these signatures were originally associated with poor prognosis and/or metastatic potential of ER-negative breast cancer and other types of cancer.[22–24] The expression profiles of

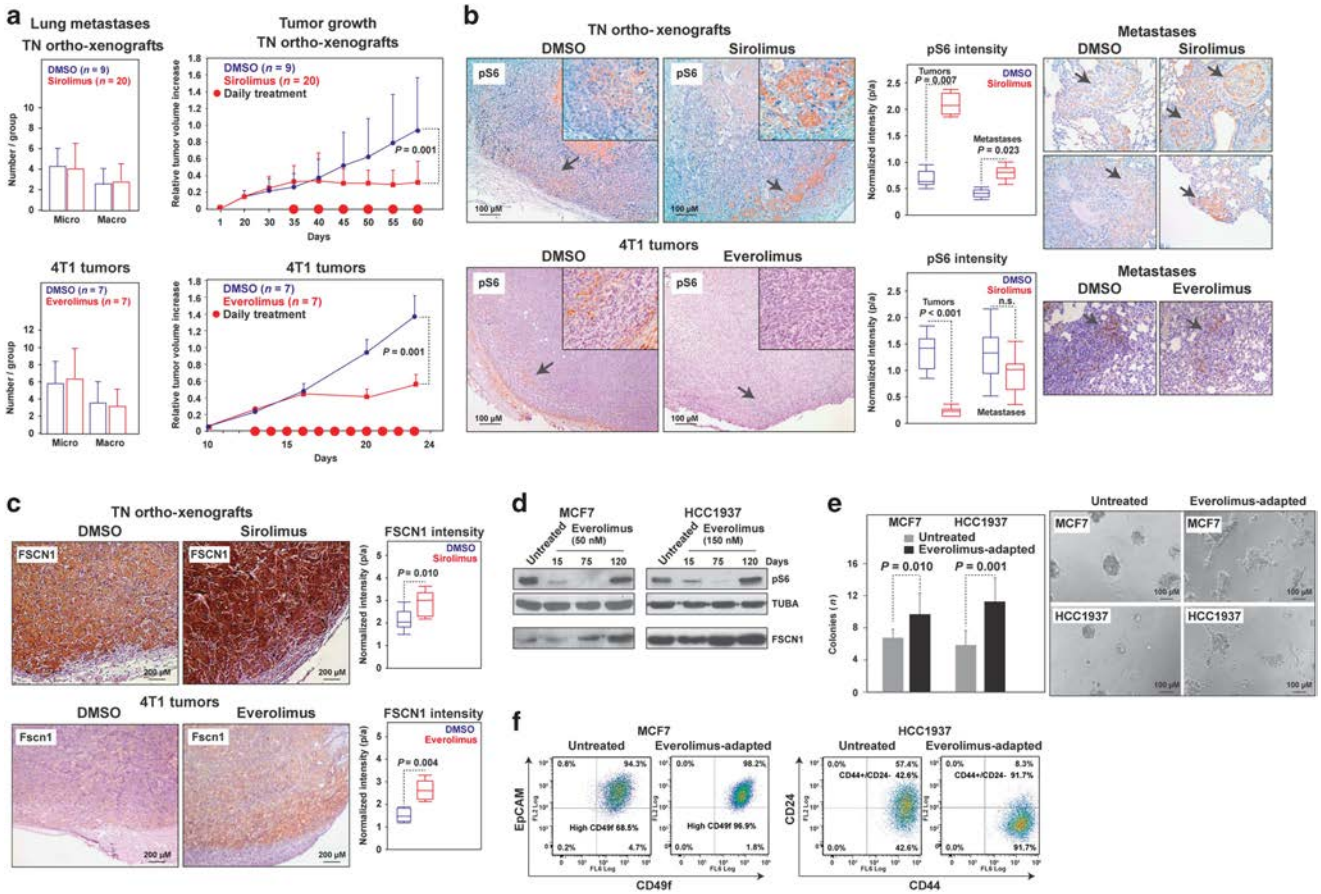

Figure 2. Metastatic resistance to mTOR inhibition. (**a**) Left panels, graphs showing the average and standard deviation of micro- and macro-metastases observed in the lungs of the DMSO- and sirolimus- or everolimus-treated orthoxenografts and 4T1 tumors, respectively. The results correspond to the last day of treatment, and micro- versus macro-metastases were defined using a 2 mm width threshold, and by examining at least three tissue levels separated by $> 20\,\mu m$. Right panels, growth rates of the DMSO- and sirolimus- or everolimus-treated tumors. (**b**) Representative immunohistochemical results for pS6 at the invasive tumor fronts (magnifications; top right panels) and the lung metastases (right panels) of DMSO- or sirolimus/everolimus-treated mice. The middle panels show quantifications, which correspond to three tumors, three equal front areas, and three metastases in each case. (**c**) Representative immunohistochemical tumor results for FSCN1/Fscn1 in DMSO- or sirolimus/everolimus-treated mice; quantifications are shown in right panels. (**d**) Recovered pS6 signal with concurrent FSCN1 overexpression through adaptation to everolimus in MCF7 and HCC1937 cells. Days of treatment are shown. (**e**) Left panel, graph showing the quantification of colonies from untreated and everolimus-adapted cells (12 culture fields were analyzed). The one-tailed *t*-test *P*-values are shown. Representative images of cell cultures are shown in right panels. (**f**) Flow cytometry results showing the cell counts for CD49f/EpCAM and of CD44/CD24 positivity in untreated or everolimus-adapted MCF7 and HCC1937 cells, respectively.

TSC1/2 were found to be negatively correlated (PCCs < -0.10; *P*-values < 0.05) with most of the signatures (Figure 3a). In turn, positive correlations were observed with the downregulated genes that characterize mammary epithelial basal and luminal progenitor cells (Figure 3a).[25] Moreover, the expression of *TSC1* was positively correlated with a downregulated gene expression signature associated with oncogenic PI3KCA activity in breast cancer.[26,27] Collectively, these results confirmed that mTOR activity is associated with stem cell-like gene expression profiles in breast cancer.

Next, we observed that the sESC, sMRS and sMYC largely distinguished the expression profiles of mTOR inhibitor-treated tumors from those treated with DMSO (Figure 3b). The regulators of the sMRS (originally defined as Core-9)[23] were commonly overexpressed upon mTOR inhibition (Figure 3c). Furthermore, a strong overexpression of the three signatures was detected when the ortho-xenografts were allowed to re-grow following treatment with sirolimus (relative to the DMSO-treated re-growth, GSEA *P*-values < 0.001; Figure 3d and Supplementary Table 2). Analysis of the three signatures defined above did not reveal significant changes in the cell line models, but most of the regulators of sMRS were found to be overexpressed in HCC1937 cells (Figure 3e). These results were confirmed by western blot analysis of HMGA1 (Figure 3f), which has been associated with poor prognosis and metastatic breast cancer.[28] The observed differences between the *in vitro* and *in vivo* expression changes may be due to the molecular specificity and/or biological conditions involved in each setting. Globally, however, inhibition of mTOR appears to be coupled to the transcriptional reprogramming that sustains metastatic and tumor initiation features.

EVI1 couples mTOR signaling to metastasis

Feedback activation of known mediators of resistance to rapalogs was not observed in the sirolimus-treated ortho-xenografts, but an increase in phospho-Thr202/Tyr204 ERK (pERK) was detected in 4T1 tumors treated with everolimus (Supplementary Figure 5). Exome sequence comparison between one DMSO- and one sirolimus-treated ortho-xenograft did not identify acquired mutations affecting components of the canonical TSC/mTOR pathway (Supplementary Table 3). *In vitro*, only modest time-dependent

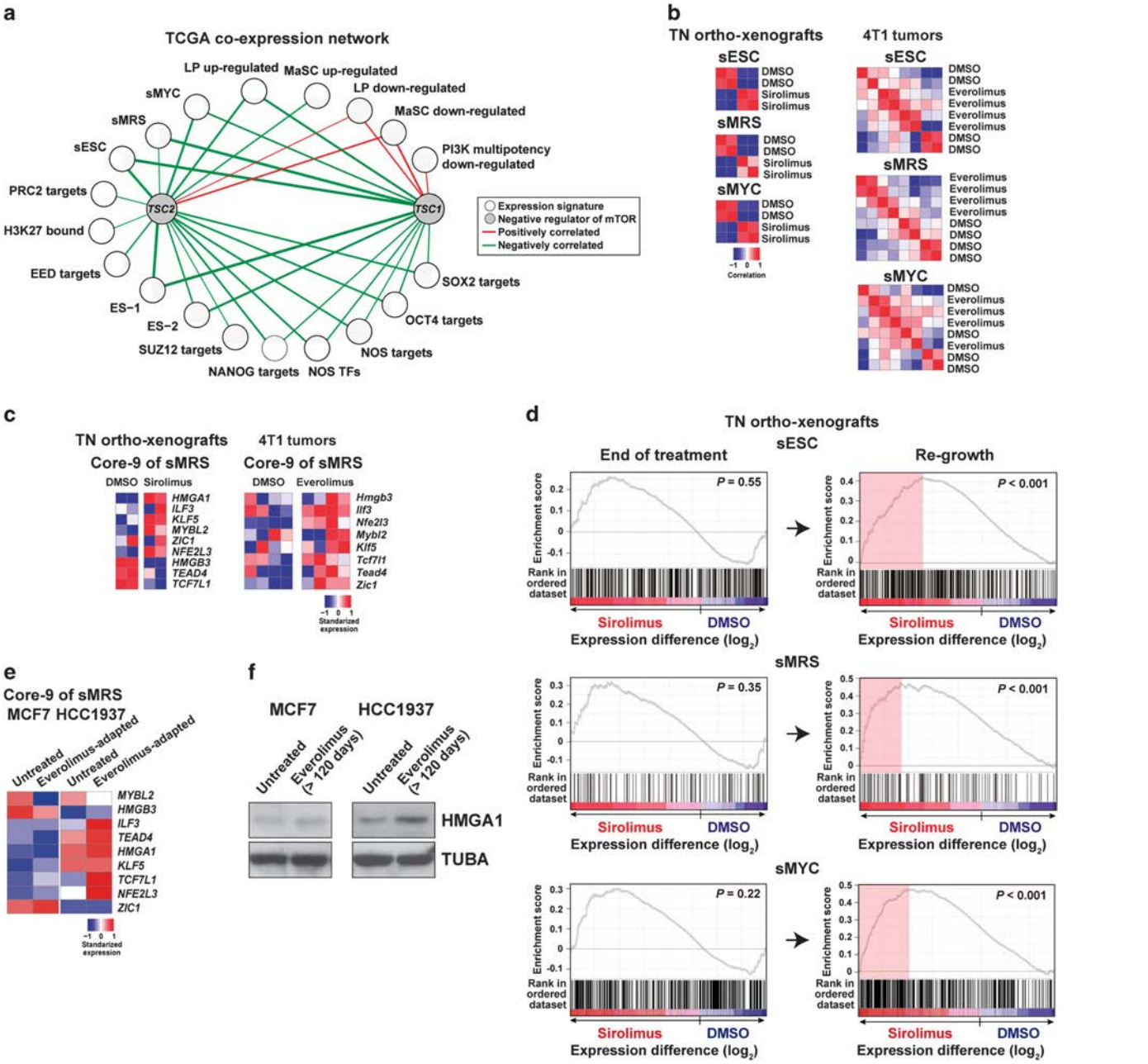

Figure 3. Co-expression analysis and stem cell-like signatures. (**a**) TCGA network of significant co-expression levels (PCC *P*-values < 0.05) between *TSC1* or *TSC2* and signatures derived from stem cell-like cell studies (Supplementary Table 1). The nodes represent *TSC1/2* and the signatures, and the edges positive (red) or negative (green) correlations. Edge width is proportional to the corresponding PCC value. (**b**) Clustering correlation of sESC, sMRS and sMYC. The ortho-xenografts are differentially clustered relative to the treatment, and a similar trend is observed for 4T1 tumors. (**c**) The master regulators of the sMRS (that is, Core-9) are found to be relatively overexpressed upon mTOR inhibition. (**d**) Significant overexpression of sESC, sMRS and sMYC in regrown ortho-xenografts after sirolimus treatment. The GSEA ESs and the nominal *P*-values are shown. (**e**) Most of the regulators of sMRS are relatively overexpressed in everolimus-adapted HCC1937 cells. (**f**) HMGA1, which is encoded in Core-9, is upregulated upon adaptation to mTOR inhibition, particularly in HCC1937 cells.

changes of phospho-S473 AKT (pAKT) and phospho-Y703 STAT3 (pSTAT3) were observed (Supplementary Figure 6). Although the lack of detection of known factors of resistance in our *in vitro* and *in vivo* analyses may be due to long-term treatments, we next sought to analyze a different mechanism that could be common to all models.

Given the transcriptomic changes observed across the *in vivo* and *in vitro* models, the data were analyzed to identify alternative regulators. A significant association (false discovery rate $< 5\%$) was observed in the gene expression profiles from ortho-xenograft samples and a target gene set of the ecotropic viral integration site-1 (EVI1) proto-oncogene (Transfac V$EVI1_02; Supplementary Figure 7). Similar associations for predicted EVI1 target sets were observed using data from the 4T1 tumors and MCF7 cells (Supplementary Figure 7). Importantly, expression analysis using TCGA data revealed positive correlations between *EVI1* and stem cell-like signatures (sMYC and from mammary stem and progenitor cells),[25] in addition to metastatic signatures,

including LMS-up,[16] a signature from low-burden breast cancer metastatic cells,[10] and of breast cancer multipotency promoted by oncogenic PI3KCA[26,27] (Figure 4a). Moreover, a set of 79 commonly overexpressed genes (>0.25 $\log_2$; Supplementary Table 4) across the *in vivo* and *in vitro* models of mTOR inhibitor resistance showed significant positive co-expression with *EVI1* (Figure 4b). Of note, this set included *LEF1*, which regulates stem cell maintenance in different contexts and is functionally connected to SOXs.[29] In addition, this set showed over-representation of gene products involved in actin-cytoskeleton remodeling (Supplementary Table 4).

EVI1 is essential for hematopoietic stem cell self-renewal[30] and its overexpression has been associated with worse recurrence-free, overall and distant metastasis-free survival of ER-negative breast cancer.[31] *In vitro* depletion of EVI1 reduced the levels of pS6, particularly in everolimus-adapted HCC1937 cells (60% reduction, and MCF7 showed a reduction of 10% in any condition; Figure 4c), whereas GFP-EVI1 overexpression conferred higher cellular viability in response to everolimus (Figure 4d). Of note, the levels of pS6 in the GFP-EVI1 overexpression assays were relatively low (Figure 4d), which could be due to the lack of full adaptation and/or the need for EVI1 co-factors.

To further validate the direct transcriptional role of EVI1, chromatin immunoprecipitation (ChIP) assays of predicted transcriptional targets were performed. This analysis revealed increased (one-tailed *P*-values < 0.01) EVI1 binding at the following *loci* with adaptation to everolimus in at least one cell model: *FSCN1* and *SPARC* (from the LMS-up); *SCUBE3* and *TCF4* (from V $EVI1_02); and *RHEB*, *RPS6KA1* and *RAPTOR* (from the mTOR pathway) (Figure 4e). In addition, RAPTOR and RHEB were found to be overexpressed as a function of everolimus adaptation in MCF7 and HCC1937 cells, respectively (Figure 4f; RAPTOR showed transitory underexpression in HCC1937), and EVI1 depletion reduced the expression of both proteins in the everolimus-

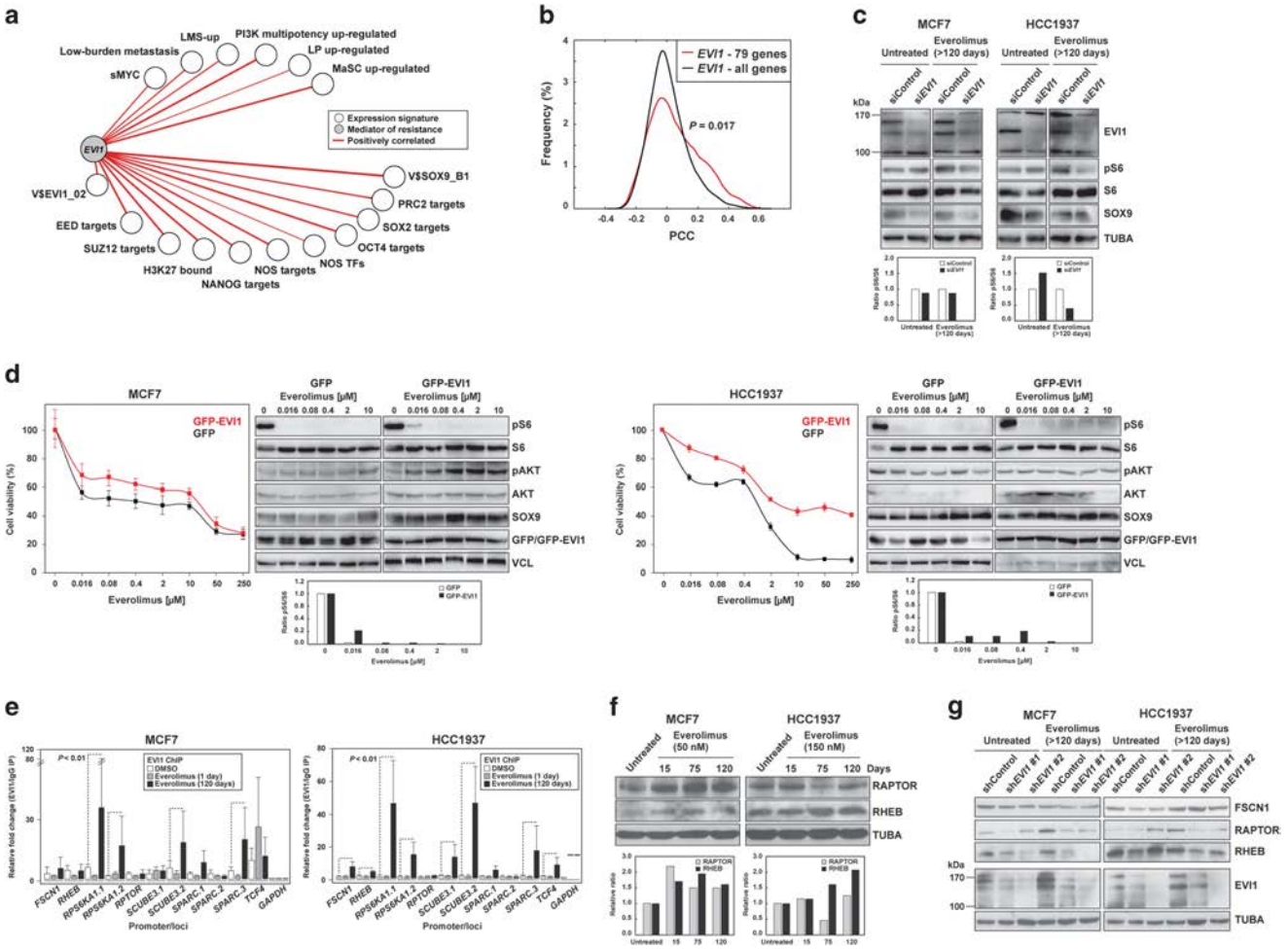

Figure 4. EVI1 couples stemness, metastatic potential and resistance to mTOR inhibition. (**a**) TCGA network of significant co-expression (PCC *P*-values < 0.05) between *EVI1* and signatures derived from stem cell-like cells and/or metastatic settings (Supplementary Table 1). (**b**) Distributions of PCCs between *EVI1* and the commonly overexpressed 79 genes across the studied models or the complete microarray gene list as background control. The *P*-value of the Mann–Whitney test for the comparison of the distributions is shown. (**c**) Reduced pS6 levels with *EVI1* depletion in cell models. The quantification of pS6/S6 signal ratios is show at the bottom (relative to siControl). (**d**) Ectopic overexpression of GFP-EVI1 in MCF7 (left panels) and HCC1937 (right panels) cells provides higher viability upon exposure to everolimus, relative to GFP-only overexpression. Also shown are the western blot results for defined markers across the drug-exposed cell cultures. The quantification of pS6/S6 signal ratios is show at the bottom (relative to TUBA per sample). (**e**) Increased EVI1 binding at predicted target promoters/gene loci with adaptation to everolimus. The fold changes are relative to the immunoglobulin control and the promoter gene targets are shown in the *X* axis. (**f**) Relative overexpression of RAPTOR and/or RHEB with adaptation to everolimus in MCF7 and HCC1937 cells. The quantification is show at the bottom (relative to untreated and TUBA per sample). (**g**) Relative reduction of RAPTOR and RHEB expression following EVI1 depletion, in particular in the everolimus-adapted setting.

adapted settings (Figure 4g). However, the expression of FSCN1 was not significantly reduced with EVI1 depletion (Figure 4g) and, in turn, EVI1 was found to be overexpressed with FSCN1 depletion (Supplementary Figure 8). Therefore, these results may reflect the initial response towards mTOR inhibition; in fact, a similar effect was observed for RAPTOR and RHEB when EVI1 was depleted in parental HCC1937 cells (Figure 4g, right panels).

EVI1 cooperates with SOX9

Based on the strong association between EVI1 and stem cell-like/tumor initiation gene expression signatures, we searched for potential EVI1-transcriptional target genes mediating such functions. The V$EVI1_02 gene set and several other stem cell-like cells and/or metastasis-associated gene signatures were positively co-expressed with a key regulator of these functions, *SOX9* (Figure 5a).[32,33] Subsequently, whole-genome EVI1 ChIP data corroborated the positive correlation between EVI1 and SOX9 binding sites in HCC1937 cells (Supplementary Figure 9). Interestingly, EVI1 ChIP data also showed a positive correlation with SLUG targets[34] in both cell models, and with SNAIL targets[34] in HCC1937 (Supplementary Figure 9). Notably, MCF7 differentiation to a basal-like phenotype requires SLUG activity.[35]

Expanding on the above results, sirolimus-treated ortho-xenografts and everolimus-adapted cells showed increased SOX9 expression compared with their corresponding controls

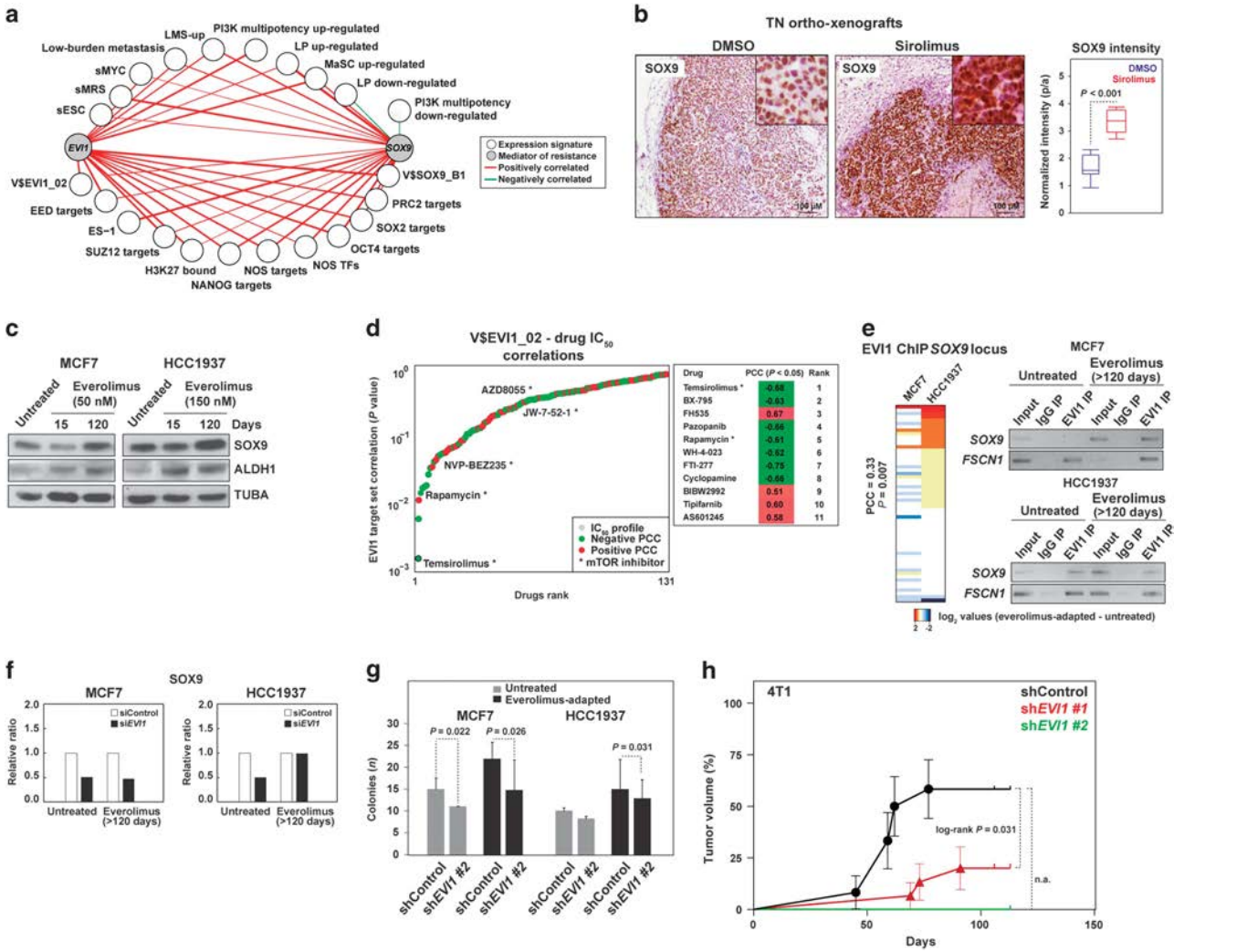

Figure 5. EVI1 cooperates with SOX9 and regulates its expression. (**a**) TCGA network of significant co-expression (PCC *P*-values < 0.05) between *EVI1* or *SOX9* and signatures derived from stem cell-like cells and/or metastatic settings (Supplementary Table 1). (**b**) Increased SOX9 expression in ortho-xenograft tumor fronts of mice treated with sirolimus; the results correspond to at least three ortho-xenografts of each group. (**c**) Increased SOX9 and ALDH1 expression in everolimus-adapted cells. (**d**) Graph showing the results from the analysis of the complete drug panel for the correlation between IC_{50} profiles and the expression of the V$EVI1_02 gene set; drugs are ranked according to PCC log *P*-values. Negative and positive PCCs are indicated with different colors, and the mTOR inhibitors in the panel are denoted. (**e**) Left panel, unsupervised clustering and correlation analysis of the difference in EVI1 ChIP results at the *SOX9* locus between everolimus-adapted and untreated cells. Right panels, results of ChIP assays targeting a predicted EVI1-binding site in the *SOX9* promoter (Supplementary Table 5); the input, control immunoglobulin immunoprecipitation (IP), and EVI1-IP results are shown. The control results for the binding site in *FSCN1* are also shown. (**f**) Depletion of EVI1 leads to a reduction of SOX9 expression in three cell conditions (the results correspond to Figure 4c; the ratios are relative to siControl and TUBA per sample). (**g**) Depletion of EVI1 leads to a reduction of colony-forming capacity. The results of the one-tailed *t*-test are shown. (**h**) Depletion of Evi1 impairs the tumorigenic potential of 4T1 cells. The log-rank *P*-value is shown for the comparison between the shControl and short hairpin RNA (shRNA)-*EVI1* #1; note that transduction with shRNA-*EVI1* #2 completely impaired tumor formation so a *P*-value could not be computed (n.a.).

(Figures 5b and c, respectively; the same antibody did not recognize mouse Sox9). The expression of ALDH1—canonical stem/progenitor marker in normal breast tissue and tumors, and also associated with poor prognosis[36]—was also detected to be increased with adaptation to everolimus in both MCF7 and HCC1937 cells (Figure 5c). The higher expression at the tumor invasive front is consistent with previous observations of invasive leader cells showing positivity for basal/stem cell-like markers.[10,37]

In addition to the results from the models, the analysis of data from hundreds of cell lines[38] revealed significant positive correlations between *EVI1* and *SOX9* expression, and with *EVI1* locus copy number (PCCs >0.20, *P*-values $<10^{-4}$). Moreover, in this data set, both *EVI1* and *SOX9* expression correlated positively (that is, linked to resistance) with the half maximal inhibitory concentration (IC_{50}) of temsirolimus (PCCs = 0.22 and 0.24, respectively, *P*-values $<10^{-4}$). In fact, a ranking-based analysis using the V$EVI1_02 gene set as a surrogate of EVI1 activity showed equivalent results, and the second and fourth most correlated drugs, respectively, were BX-795 (inhibitor of PDK1 activity) and rapamycin (Figure 5d). To further assess these findings, an ER-positive and HER2-positive breast cancer cell model, BT-474, was exposed to 150 nM of everolimus for approximately 100 days and subsequently profiled for gene expression changes; the results showed significant associations with EVI1 and SOX9 targets, and with the commonly over-expressed genes detected across the above *in vitro* and *in vivo* models (Supplementary Figure 10).

Further analysis of the predicted functional relationship between *EVI1* and *SOX9* revealed a positive correlation in the differential (between control and everolimus-adapted) binding of EVI1 at the *SOX9* locus (Figure 5e, left panel). Next, targeted ChIP assays confirmed that EVI1 binds at the *SOX9* locus in untreated HCC1937 and both everolimus-adapted cell models (Figure 5e, right panel). Thus, depletion of EVI1 reduced the expression of SOX9 in three out of four conditions; however, it remains to be determined which co-factor(s) may maintain SOX9 expression at normal levels in everolimus-adapted HCC1939 cells (Figure 5f). In parallel, depletion of EVI1/Evi1 reduced the colony-forming capacity of both models of everolimus adaptation (Figure 5g) and impaired *in vivo* tumorigenic potential of 4T1 cells (Figure 5h). Collectively, ChIP, gene/protein expression analyses and *in vivo* functional assays depict a link between EVI1 and SOX9 in the regulation of stem cell-like and tumor initiation features.

In vivo evaluation of the EVI1, SOX9 and mTOR relationship

The functional cooperation between EVI1 and SOX9 was evaluated *in vivo* using LM2 and 4T1 cells transduced with a short-hairpin RNA scrambled control or directed against *EVI1*, and with or without concomitant overexpression of Sox9 (mouse protein). Thus, EVI1 depletion significantly reduced the capacity to colonize the lungs, and concurrent *Sox9* overexpression partially rescued metastatic potential (Figures 6a and b). As shown in everolimus-adapted cell lines, EVI1/Evi1 depletion caused a significant decrease of both SOX9 and pS6 expression in the corresponding metastasis (Supplementary Figure 11). Concurrent Sox9 over-expression recovered pS6 signal in 4T1 but not in LM2 cells (Supplementary Figure 11), which suggest differences in the precise regulation of mTOR activity between the models.

In addition to EVI1, depletion of SOX9 in LM2 cells led to a significant decrease in lung colonization capacity and, conversely, Sox9 overexpression increased this capacity (Figure 6c and Supplementary Figure 12). Depletion of Sox9 in 4T1 cells and everolimus treatment of both cell models also reduced lung colonization (Figures 6c and d). In addition, depletion of FSCN1 in both models also led to a substantial impairment of lung colonization (Figures 6e and f). Moreover, a greater effect was observed when the animals were simultaneously treated with everolimus (Figures 6e and f), which fully suppressed pS6 signal (Supplementary Figure 11). Collectively, these results indicate that transcriptional reprogramming mediated by EVI1-SOX9 is one of the key factors in metastatic resistance to mTOR inhibition.

DISCUSSION

We provide evidence of the association between EVI1-SOX9 function, mTOR inhibition resistance and metastasis in breast cancer. We also show that EVI1-SOX9-mediated transcriptional reprogramming drives the molecular processes that support breast cancer tumor initiation features and metastatic potential in therapeutic resistance (Figure 7). These data are coherent and expand on the concept that cancer stem cell-like cell populations have high tumor-initiating capacity and are frequently the source of therapy resistance and metastasis.[39] Data from hundreds of cell lines[38] suggest that the proposed mechanism is relevant in settings beyond breast cancer. Importantly, *EVI1* maps in a genomic region (including *PI3KCA* and *SOX2*) whose amplification is an independent predictor of breast cancer recurrence.[40] This region is frequently found to be amplified in basal-like and *BRCA1*-mutated breast cancer,[21] as well as in non-small cell lung and ovarian cancers.[41] In addition, *EVI1* amplification is independent of *PIK3CA* mutations,[41] which further reinforces the link with basal-like breast cancer and is consistent with a role in resistance to allosteric mTOR inhibition. It remains to be determined whether *EVI1* expression is upregulated through genomic amplification and/or whether its function is enhanced by biochemical modifications by casein kinase II[42] and/or ERK signaling as seen to be activated in our 4T1 assays.

Our preclinical findings and mechanistic model are consistent with and expand on recent observations across different neoplastic settings. EVI1 contributes to epithelial-to-mesenchymal transition (EMT) and invasion of acute myeloid leukemia,[43] and influences EMT in ovarian cancer cells,[44] whereas EMT mediates resistance to rapamycin.[45] In the latter study, MCF7 cells transfected with constitute active SNAIL showed increased ERK signaling and decreased sensitivity to rapamycin. Thus, our study provides a mechanistic explanation for these observations. In addition, it has recently been shown that SOX2 and SOX9 mediated the maintenance of latent metastatic stem cell-like cells,[46] and it was previously demonstrated that SLUG and SOX9 cooperatively determine mammary stem cell state,[32] and that SOX9 function links tumor initiation and invasion.[33] Moreover, a stem cell-like cancer phenotype that mediates breast cancer metastasis is predicted to exhibit abnormal mTORC1 signaling[10] and, in turn, mTORC1/2 inhibition promotes stem cell-like properties and enhanced NOTCH1 activity in TN breast cancer cell lines.[12] Thus, enhanced mTOR signaling impairs cell differentiation by potentiating NOTCH1 activity, and this signaling is found to be increased in poorly differentiated breast tumors.[14] Intriguingly, NOTCH may also regulate *SOX9* expression,[47] which, in turn, is a master regulator of stem and progenitor cells.[48] In parallel, allosteric mTOR inhibition increases the number of tumor-initiating cells in a model of liver cancer[15] and the metastatic potential in a model of pancreatic neuroendocrine cancer.[49] In this scenario, our study proposes that EVI1 and SOX9 functionally cooperate to sustain mTORC1 activity, EMT and metastatic potential, thereby providing new insights into therapeutic resistance.

Our findings—particularly those from MCF7 cell assays—may have clinical implications for the established use of mTOR inhibitors in endocrine-resistant ER-positive advanced metastatic breast cancer,[7] in which resistance to treatment is eventually reported. Our results indicate that exposure to allosteric mTOR inhibition selects a stem cell-like cancer cell population with metastatic capacity, which may therefore promote disease progression. Although *in vivo* assays may be warranted to further

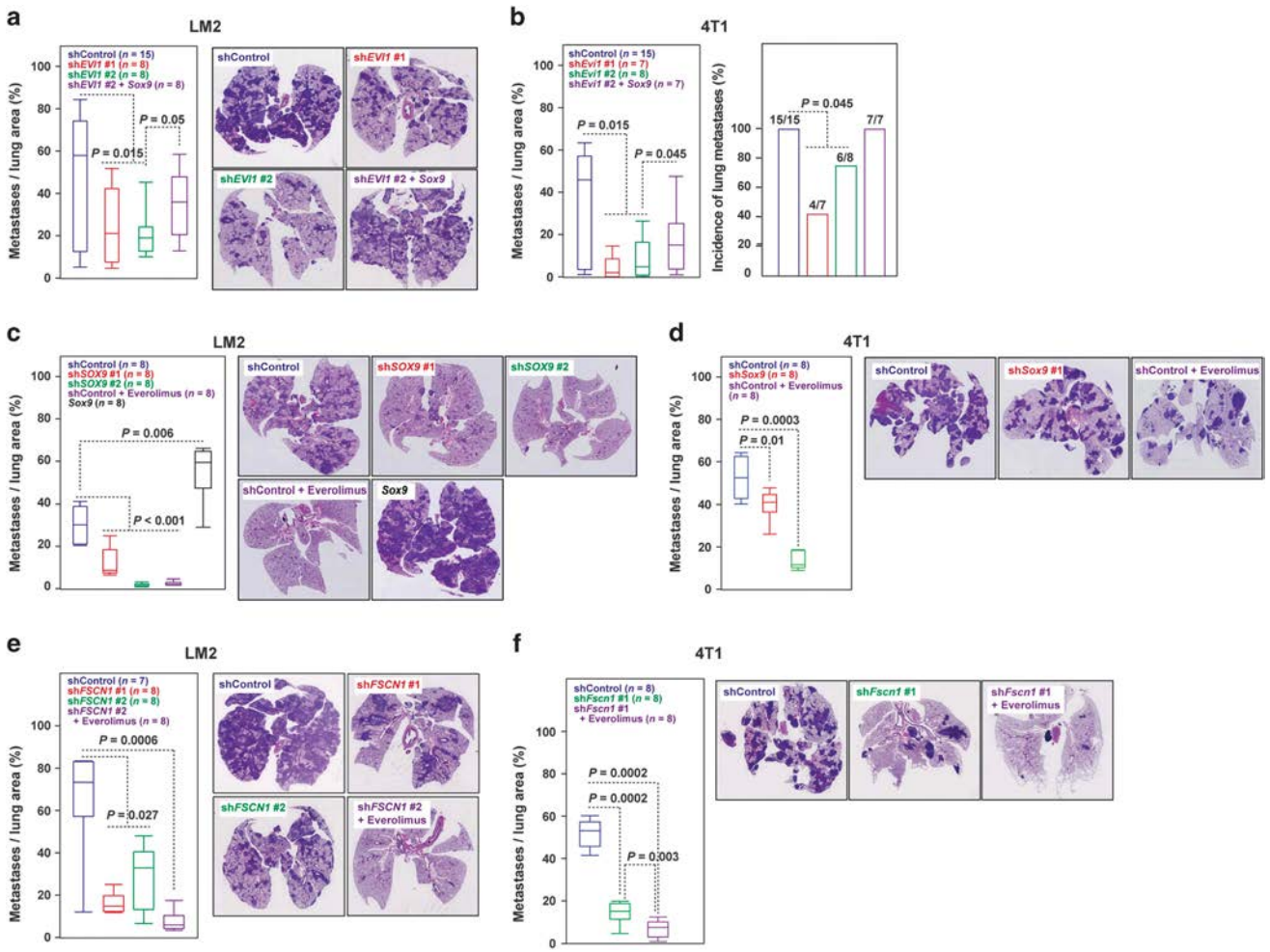

Figure 6. *In vivo* assessment of the role of EVI1 and SOX9. (**a**, **b**) Depletion of *EVI1*/*Evi11* expression (using two different short hairpin RNAs (shRNAs)) in LM2 and 4T1 cells reduced lung colonization, and *Sox9* overexpression partially recovered this potential, left panels. (**a**) Right panels show representative images of lungs and their respective HE staining. (**c**) Depletion of *SOX9* and overexpression of *Sox9* reduced and increased, respectively, lung colonization of LM2 cells. Treatment with everolimus of shControl LM2 cells also reduced lung colonization. (**d**) Depletion of *Sox9* or treatment with everolimus of 4T1 cells reduced lung colonization. (**e**, **f**) Depletion of *FSCN1*/*Fscn1* expression in LM2 and 4T1 cells reduced lung colonization, and concurrent treatment with everolimus further impaired this potential.

assess this observation, and while we cannot rule out that the specific population may arise through the acquisition of new mutations, it is noteworthy that the Breast Cancer Trials of Oral Everolimus-2 (BOLERO-2) study for the efficacy of everolimus plus exemestane in endocrine resistance showed similar benefits for patients with or without visceral metastases.[50] Nevertheless, full and durable pathway inhibition—such as obtained that by the next generation of targeted drugs[51]—may fully impair metastatic resistance.

MATERIALS AND METHODS

Tissue microarray

The tissue microarray included 138 infiltrating ductal breast carcinoma tumors collected at the Department of Pathology of the MD Anderson Cancer Center, Madrid (Spain). The patients underwent surgery between 2003 and 2004, and all tumors were classified as grade 3. According to the TNM system, 45 tumors belonged to stage I, 48 to stage II and 45 to stage III-IV. The linked data included ER ($n = 104$), progesterone receptor ($n = 127$) and epidermal growth factor receptor 2 (HER2; $n = 125$) status, and CK5 expression ($n = 128$), absence/presence of lymph node metastasis ($n = 124$), and absence/presence of distant metastasis ($n = 127$). The tissue microarray contained duplicated cases and normal tissue, and the immunohistochemical results were scored independently and blindly (to molecular and clinical status). Selection of the highest value for a given case, blindly to its status, solved discordant scores. The study was approved by the ethics committee of the MD Anderson Cancer Center and written informed consent was obtained from all patients.

Gene expression analyses

Pre-processed and normalized data of human breast cancer were taken from the corresponding publication[16] and from the TCGA repository (http://tcga-data.nci.nih.gov/tcga/tcgaHome2.jsp).[52] RNA samples were extracted using TRIzol Reagent (Invitrogen, Karlsruhe, Germany) and RNeasy Kit (Qiagen, Venlo, Netherlands), and quality was evaluated in an Agilent Bioanalyzer (Foster City, CA, USA) 2100. The RNAs were amplified using the Ribo-SPIA system (NuGEN Technologies Inc., San Carlos, CA, USA) and subsequently hybridized on the Human Genome U219 microarray platform (Affymetrix, Santa Clara, CA, USA; IRB Core Facility, Barcelona, Spain). Gene expression data from the ortho-xenograft, and MCF7 and HCC1937 cell lines have been deposited under the GEO reference GSE39694. Gene expression data from the 4T1 tumors and BT-474 cells have been deposited under the GEO references GSE50712 and GSE85801, respectively. The GSEA and DAVID (for functional term analyses) tools were used with standard parameters.[53,54] The signature correlations were computed by selecting genes with s.d. >1.0 and using the average *Z*-score value per gene set. The quantification of *NANOG*, *OCT4* and *SOX2* gene expression was performed as previously described.[55]

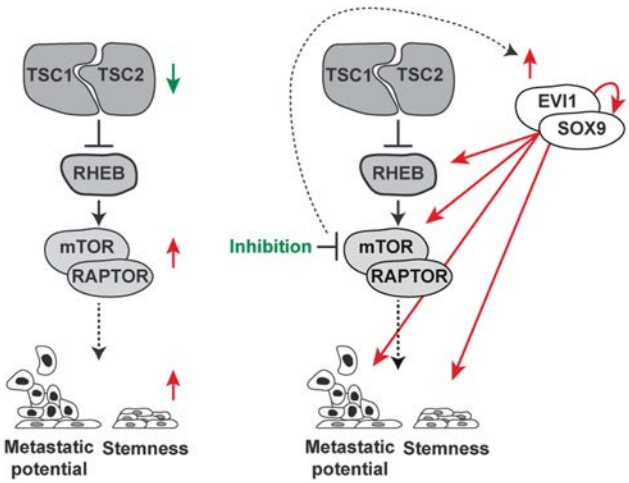

Figure 7. Proposed mechanistic model. In untreated cancer, low *TSC1/2* expression is associated with enhanced mTORC1 activity and, therefore, with a primary metastatic and stemness phenotype. In cancer treated for mTOR inhibition, EVI1-SOX9 become activated (in part by overexpression) and positively sustain the following features: mTOR signaling (through upregulation of RHEB and RAPTOR), metastatic potential (through LMS-up and other signatures) and stemness (through at least SOX9).

Antibodies

Anti-total and pAKT (#9272 and #9271, respectively, Cell Signaling Technology, Danvers, MA, USA; #4060 for immunohistochemistry assays), anti-ALDH1 (#611194, BD Biosciences, Oxford, UK), anti-4EBP1 (#9452, Cell Signaling Technology), anti-p4EBP1 (#2855 and #9451, Cell Signaling Technology), anti-ER (#IR151, Dako, Glostrup, Denmark), anti-total and phospho-Thr202/Tyr204 ERK (#4695 and #4376, respectively, Cell Signaling Technology), anti-EVI1 (#2265 and #2593, Cell Signaling Technology; and #A301-691A, Bethyl Laboratories, Montgomery, TX, USA), anti-FSCN1 (#SC-56531, Santa Cruz Biotechnology, Dallas, TX, USA), anti-GFP ChIP grade (#ab290, Abcam, Cambridge, UK), anti-GLUT1 (#652, Abcam), anti-HER2 (#790-100, Ventana, Tucson, AZ, USA), anti-HMGA1 (#129153, Abcam), anti-pIGF1R (#39398, Abcam), anti-IRS1 (#2382 and #9451, Cell Signaling Technology), anti-KI67 (#IR626, Dako), anti-CK19 (#IR615, Dako), anti-PR (#IR168, Dako), anti-RAPTOR (#SC-81537, Santa Cruz Biotechnology), anti-RHEB (#SC-6341, Santa Cruz Biotechnology), anti-S6 (#SC-74459, Santa Cruz Biotechnology), anti-pS6 (#4858, Cell Signaling Technology), anti-S6K (#9202, Cell Signaling Technology), anti-pS6K (#9205, Cell Signaling Technology), anti-SOX9 (#5535, Abcam), anti-total and pSTAT3 (#9132 and #9145, respectively, Cell Signaling Technology), anti-TUBA (#44928, Abcam) and anti-VCL (V9131, Sigma-Aldrich, St Louis, MO, USA). The antibodies used for fluorescence-activated cell sorting were anti-CD24-PE, anti-CD44-APC, anti-CD49f-Alexa-647, and anti-EPCAM-FITC (#555428, 559942, 562473, and 347197, respectively; BD Biosciences).

Immunohistochemistry

The assays were performed on serial paraffin sections (3–4 μm thick) using the EnVision (Dako) or Ultraview (Ventana) systems. Antigen retrieval was performed using citrate- or EDTA-based buffers. Endogenous peroxidase was blocked by pre-incubation in a solution of 3% H_2O_2 and blocking was performed in 1X phosphate-buffered saline with 5% goat serum or 1% bovine serum albumin and 0.1% Tween 20 (Sigma-Aldrich). In all experiments, equivalent sections were processed without incubation with the primary antibody, which did not reveal immunostaining in any case. Sections were hematoxylin and eosin (HE)-counterstained and examined with an Olympus BX51 (Tokyo, Japan) microscope. The immunohistochemistry microscopic images were color deconvoluted and quantitated using the regions of interest methodology in ImageJ (http://rsb.info.nih.gov/ij). Quantification of tumor fronts was based on rectangular areas of 25 μM × 50–300 μM. When quantifying the results from lung metastases, the complete metastatic area was considered because the fronts were often difficult to outline histologically.

Cell culture

The LM2 cell derivative is a lung metastatic sub-line originated from MDA-MB-231 breast cancer cells from the laboratory of Professor Massagué.[16] The 4T1 cells derived from a spontaneous BALB/c mouse breast cancer tumor[56] and were obtained from the ATCC (Rockville, MD, USA). The LM2 cells were cultured in Dulbecco's modified Eagle's medium (GIBCO, Karlsruhe, Germany) supplemented with 10% fetal bovine serum (GIBCO), 1x L-glutamine (Biowest, Nuaillé, France) and 1% penicillin/streptomycin (Biowest). The 4T1 cells were cultured in Roswell Park Memorial Institute (RPMI)-1640 medium (Sigma-Aldrich) supplemented with 10% fetal bovine serum, 1x L-glutamine and 1% penicillin/streptomycin. All MDA-MB-231 cells/sub-lines were stably transfected with a thymidine kinase and GFP luciferase construct and sorted for GFP expression. The MCF7 and HCC1937 cell lines were obtained from ATCC and cultured in supplemented Dulbecco's modified Eagle's medium and RPMI-1640 medium, respectively. The Matrigel (BD Biosciences) colony formation assays were performed using standard protocols with 5% fetal bovine serum. Everolimus was purchased from Selleck Chemicals (Houston, TX, USA) and LC Laboratories (Woburn, MA, USA). Fluorescence-activated cell sorting was performed using FACS Canto (Becton Dickinson, Franklin Lakes, NJ, USA) and Diva software (Becton Dickinson) package, and antibody-based cell labeling was performed as previously described.[55]

Western blotting

To analyze extracts, cells were lysed in standard 150 mM NaCl buffer supplemented with protease inhibitor cocktail (Roche Molecular Biochemicals, Mannheim, Germany) and, in some instances, a phosphatase inhibitor was added (1 mM NaF, Sigma-Aldrich). Lysates were clarified twice by centrifugation at 13 000 × *g* and protein concentration was measured using the Bradford method (Bio-Rad, Solna, Sweden). Lysates were resolved in sodium dodecyl sulfate–polyacrylamide gel electrophoresis gels and transferred to Immobilon-P (Merck Millipore, Billerica, MA, USA) or PVDF membranes (Roche Molecular Biochemicals). Target proteins were identified by detection of horseradish peroxidase-labeled antibody complexes with chemiluminescence using the ECL Western Blotting Detection Kit (GE Healthcare, Amersham, UK).

Lung colonization assays

The Animal Care and Use Committee of IRB Barcelona approved the following animal studies. Female BALB/c nude (MDA-MB- 231 cells) or BALB/c wild-type mice (4T1 cells) were used. For tail vein injections, cells were suspended in 1x phosphate-buffered saline (GIBCO; 200 μl per mouse) and injected into the lateral tail vein of mice using a 26G needle, as previously described.[57] Before the injection of cells, mice were anesthetized with ketamine (100 mg/kg body weight) and xylazine (10 mg/kg body weight), and immediately after injection they were imaged for luciferase activity by injecting 50 μl of beetle luciferin potassium salt (Promega, Madison, WI, USA) at 15 mg/ml. To induce the expression of short hairpin RNA *in vivo,* doxycycline (1 mg/ml, Sigma-Aldrich) was administered *ad libitum* in drinking water containing 25 mg/ml sucrose (Sigma-Aldrich). When indicated, DMSO solution (at the same concentration as for the compound test, 5%) or everolimus (5 mg/kg; SC-218452, Santa Cruz Biotechnology) was administered daily by intraperitoneal injection. Mice were monitored weekly using IVIS imaging, unless otherwise indicated. Lung tumor development was followed up once a week by bioluminescence imaging of the upper dorsal region that corresponds to lung position. Bioluminescent images were quantified with Living Image 2.60.1 software (Perkin-Elmer, Waltham, MA, USA). All values were normalized to those obtained at day 0. The HE staining of lung sections scored the lung colonization capacity of 4T1 cells 3 weeks post-inoculation. Five sections, separated by 50 μm, per mouse lung were counted. The average of the total metastatic area normalized to total lung area was measured. The average total lung metastasis area for all mice was then plotted. The tissue was dissected, fixed in 10% buffered formalin (Sigma-Aldrich), and embedded in paraffin. Sections (3 μm thick) were stained with HE. To analyze the metastatic area, images were taken with a scanner, and the area of each metastatic lesion was quantified with the ImageJ software. Five images per section/animal were evaluated, and the average area was plotted. The Fiji Trainable Weka segmentation, an ImageJ plugin based on the Weka[58] Java machine learning library, was used to classify images on the basis of local colorimetric, textural and structural features in the neighborhood of each pixel. Images were processed with a custom macro created at the Microscopy Core Facility of IRB Barcelona.

The two-tailed non-parametric Mann–Whitney test was used to assess significance of the immunohistochemical staining results.

Ortho-xenograft

The patient was a 33-year-old woman with a pathological germline *BRCA1* mutation and diagnosed with breast cancer shortly after pregnancy. At diagnosis she presented a locally advanced TN ductal infiltrating carcinoma of the breast (T4) with involvement of ipsilateral nodes (N2) and lung metastasis. Primary systemic chemotherapy was initiated with TAC regimen for four cycles, followed by mastectomy to prevent local complications because of extensive breast involvement. Following surgery, the patient received further chemotherapy with the same regimen. The patient was diagnosed with brain metastases shortly after and died 8 months post-diagnosis as a result of disease progression. Mutational analysis of *BRCA1* was carried out by the Molecular Diagnostics Unit (Catalan Institute of Oncology, Barcelona, Spain) following standards for genetic testing and pathological determination. The patient provided written informed consent, and the study was approved by the IDIBELL Ethics Committee. Female athymic (*nu/nu*) mice (Harlan, Harlan Laboratories, Barcelona, Spain) between 4 and 6 weeks of age were used for engraftment. The orthotopic model developed histologically detectable lung metastases in a period of approximately 50 days after engraftment. The protocol was reviewed and approved by the IDIBELL Animal Care and Use Committee. A daily oral treatment with sirolimus (Rapamune) or control solution (DMSO, Sigma-Aldrich) was applied.

Exome analysis

The National Centre for Genomic Analysis (CNAG) carried out exome sequencing. Sequence capture and amplification was performed using Agilent (Agilent Technologies, Palo Alto, CA, USA) SureSelect Human All Exon kit (Agilent) according to the manufacturer's instructions. Paired-end sequencing was performed on a HiSeq2000 instrument (Illumina, San Diego, CA, USA) using 76-base reads. Reads were aligned to the reference genome (GRCh37) and BAM files were generated using SAMtools. Duplicates were removed using SAMtools and custom scripts, and single-nucleotide variant calling was performed using a combination of SAMtools and Sidrón algorithms as described previously.[59] The reads were first aligned to mouse genome (mm9), and those read-pairs that did not align to mouse were then aligned to the human genome following the same pipeline as above. Only mismatch variants were taken into account and small insertions and deletions were not counted. Common variants, defined as those present in dbSNP135 with a minor allele frequency $> 1\%$, were filtered out.

4T1 tumors

The animal studies were conducted using protocols that had undergone appropriate review and approval at the New York University School of Medicine. Balb/C mice were injected subcutaneously with 5×10^4 4T1 cells, measured for tumor size at day 10, and randomly organized in two equivalent groups that were treated with DMSO solution (the same concentration as for the compound test) or everolimus (5 mg/kg; SC-218452, Santa Cruz Biotechnology) daily by intraperitoneal injection. Tumors were excised at day 23 and processed. Half of each tissue sample was used for immunohistochemistry and half for gene expression microarray analysis. For the tumorigenicity assays, 250 000 4T1 cells were injected at the orthotopic site, mixed with growth factor-reduced Matrigel (BD Biosciences) before inoculation (1:1). Once palpable, tumors were measured with a digital caliper, and the tumor volume was calculated. The ethics committee of the CIC bioGUNE approved these assays.

ChIP assays

Assays were prepared using 10^7 cells of each cell line per condition. Chromatin was fragmented by sonication (Bioruptor, Diagenode, Denville, NJ, USA) for 30 min (30-s pulses, 30-s pauses) and assays were carried out following the manufacturer's protocol (kch-mahigh-A16, HighCell# ChIP Kit, Diagenode), using anti-EVI1 (#2593, Cell Signaling Technology) or an equal amount of IgG isotype as negative control (#2729, Cell Signaling Technology). The amount of DNA was analyzed by real-time polymerase chain reactions using SYBR Green-based assays (Applied Biosystems, Life Technologies, Foster City, CA, USA). The results were calculated using the ΔCt method. A genomic region of the *GAPDH* gene was used as negative control (Diagenode). The corresponding human genome coordinates, EVI1-binding sites and primers designed for the assays are detailed in Supplementary Table 5. Whole-genome ChIP data were obtained by hybridization to SurePrint G3 Human Promoter 1x1M microarrays (IRB Core Facility) and analyzed by MACS (version 2.0.9).[60] The data have been deposited under the GEO reference GSE50905. The complete ranking of differential EVI1 binding between adapted and sensitive MCF7 or HCC1937 cells was used as input for the GSEA of transcription factor targets.

Gene expression alterations

Stable LM2 and 4T1 cell lines expressing short hairpin RNAs were generated as described previously.[57] The sh*FSCN1/Fscn1* (that is, targeting both human and mouse gene expression) #1 and sh*EVI1/Evi1* #2 were encoded in lentiviral vectors (inducible pTRIPZ lentiviral short hairpin RNAs, GE Dharmacon, Lafayette, CO, USA). The short hairpins were induced by 1 μg/ml doxycycline for 72 h. The shControl and sh*EVI1/Evi1* #1 were encoded in a retrovirus pGFP-V-RS (OriGene, Rockville, MD, USA). The sh*FSCN1/Fscn1* #1 was encoded in a pSUPER (Addgene, Cambridge, MA, USA) vector. The sh*Sox9* (against mouse gene sequence) and sh*SOX9* (human) were obtained from the MISSION library (SHCLND-NM_011448 and SHCLND-NM_000346, respectively; Sigma-Aldrich). An additional sh*SOX9* was obtained from Addgene, catalog #40644. For *Sox9* overexpression, the corresponding coding sequence was cloned into a lentiviral pWXL vector. Stable cell lines expressing the various constructs described above were generated under puromycin selection for 48 h. The siRNA against *EVI1* expression was an ON-TARGETplus SMARTpool (L-006530-02-0010, Dharmacon). The following primer sequences were used to assess gene expression changes in real-time (using SYBR Green, Applied Biosystems) polymerase chain reaction assays: *EVI1*, 5′-CATT GGGAACAGCAACCAT-3′ and 5′-GGTCACCAAAGCCTTTTCAT-3′; *Evi1*, 5′-CAC AGAAAGTCCAAATCACAGG-3′ and 5′-GCCACACGTTGGAGGAAC-3′; *Sox9*, 5′-GTACCCGCATCTGCACAAC-3′ and 5′-CTCCTCCACGAAGGGTCTCT-3′; *ACTB*, 5′-GGAGTGGGTGGAGGCAG-3′ and 5′-AACTAAGGTGTGCACTTTTGTTC-3′; and *mL32*, 5′-GAAACTGGCGGAAACCCA-3′ and 5′-GGATCTGGCCCTTGAACCTT-3′.

Genomics of drug sensitivity data analyses

For the correlation analysis between the basal expression of *EVI1*, its predicted target genes and the drug responses across cancer cell lines, data were downloaded from the GDS project (web-release April 2012).[38] This data set included IC_{50} values for 131 drugs that were assessed in a panel of 638 human cancer cell lines. The basal gene expression data were downloaded from ArrayExpress reference E-MTAB-783. Non-annotated probes were removed and expression values were averaged when multiple probes mapped to the same gene. Correlation scores and *P*-values were computed using the PCC. The EVI1 target set included 20 genes that were represented by at least one microarray probe (Supplementary Table 6). The extent of the basal expression of the EVI1 targets was quantified using an enrichment score (ES) computed with a Matlab implementation of the GSEA algorithm. To estimate ES significance, a null model was created by generating 10 000 random gene sets (of the same size as the EVI1 target set) and used to query the data set through GSEA. Next, two inverse Gaussian distributions (for positive and negative ES values) were fitted on the resulting empirical distribution and used to compute *P*-values. The correlations between IC_{50} profiles and ESs were computed by considering only cell lines whose basal expression profile yielded a significant ES ($P < 0.05$), according to the null model. The enrichment *P*-values of mTOR inhibitors among drugs whose IC_{50} profile was anti-correlated with the EVI1 target ES were computed using Fisher's exact test and considering the total set of 131 drugs.

CONFLICT OF INTEREST

The authors declare no conflict of interest.

ACKNOWLEDGEMENTS

We thank Ander Urruticoechea, Gabriel Capellá and George Thomas for helpful discussion; Ana Isabel Extremera, Antoni Xaubet and Julio Ancochea for administrative support; and Sebastien Tosi from the Advanced Digital Microscopy Facility at IRB Barcelona for image analysis. We also thank Xiyun Deng, Yanna Cao, Tien C Ko, Yi Zhang (The University of Texas Health Science Centre at Houston) and Adrian W Moore (RIKEN Brain Science Institute) for their support in evaluating antibodies against EVI1. This study was supported by the following bodies and grants:

the Scientific Foundation 'Asociación Española Contra el Cáncer' (AECC, Stable Coordinated Group, Hereditary Cancer); the BBVA Foundation; the Eugenio Rodríguez Pascual Foundation grant 2012; Generalitat de Catalunya AGAUR SGR 2012 grants 283, 290 and 312, and SGR 2014 grants 364, 530, and 535; Spanish Ministry of Health ISCIII FIS grants PI10/00057, PI10/00222, PI10/01422, PI12/01528, PI13/00132, and PI14/00336. ISCIII RTICC grants RD06/0020/1051, RD12/0036/0007, RD12/0036/0008 and RD12/0036/0063; Spanish Ministry of Science and Innovation, 'Fondo Europeo de Desarrollo Regional (FEDER), una manera de hacer Europa', MINECO grants SAF2010-20203 and SAF2013-46196; and the Telemaraton 2014 'Todos Somos Raros, Todos Somos Únicos' grant P35. EJA was supported by 'la Caixa' PhD fellowship program, F Iorio was supported by a fellowship from the EMBL-EBI and the Wellcome Trust Sanger Institute Postdoctoral (ESPOD) program, and NL-B, ME and RRG were supported by ICREA. No funding bodies had any role in study design, data collection and analysis, decision to publish, or preparation of the manuscript, either in the submission form or the text of the manuscript.

AUTHOR CONTRIBUTIONS

RRG and MAP: performed the design and interpretation of experiments, and wrote the manuscript; FM, EJA, HA, GRG, J Boni, XP, CH, AL, HS, MS, LG-B, XS, J Cerón and JG-M: molecular and cell biology experiments; FM, EJA, HA, SD, MHB-H and A Villanueva: *in vivo* studies; FM, HA, MM and MDO: chromatin immunoprecipitation assays; JS-M, FI, AI, DC, NB, LP, AG, NL-B, LG-A and JS-R: bioinformatic analyses; FM, HA, J Boni, S Puertas, NG, VH, MM-I and AF: immunohistochemistry experiments; AR-S, A Martínez, MPB, M Gil, CF, AF, IM, S Pernas, MJP, XA, MAS, RB, EC, SM, JV, A Velasco, XM-G, MAQ, AS and GM-B: tissue microarray studies; RV-M and XSP: exome analyses; A Petit, A Vidal, IC, TS and GV: pathological evaluations; AMS, VW, MPL, M Nellist, JVS-M, ME, MJ, LB and JWMM: genetic analyses; FM, HA, J Boni, EG-S and A Cordero: three-dimensional cell culture experiments; JH-L, SRC and J Cortés: breast cancer tumor analyses; JL, FC, IB, A Perkins, J Brunet, FV, OC, M Graupera, NM-M, A Matheu, A Carracedo, TFG, EEWC, MS-C, M Nanjundan and CL: experimental design and interpretation.

REFERENCES

1 Zoncu R, Efeyan A, Sabatini DM. mTOR: from growth signal integration to cancer, diabetes and ageing. *Nat Rev Mol Cell Biol* 2011; **12**: 21–35.
2 Courtney KD, Corcoran RB, Engelman JA. The PI3K pathway as drug target in human cancer. *J Clin Oncol* 2010; **28**: 1075–1083.
3 Hsieh AC, Liu Y, Edlind MP, Ingolia NT, Janes MR, Sher A *et al.* The translational landscape of mTOR signalling steers cancer initiation and metastasis. *Nature* 2012; **485**: 55–61.
4 Crino PB, Nathanson KL, Henske EP. The tuberous sclerosis complex. *N Engl J Med* 2006; **355**: 1345–1356.
5 Nasr Z, Robert F, Porco Jr JA, Muller WJ, Pelletier J. eIF4F suppression in breast cancer affects maintenance and progression. *Oncogene* 2013; **32**: 861–871.
6 Fruman DA, Rommel C. PI3K and cancer: lessons, challenges and opportunities. *Nat Rev Drug Discov* 2014; **13**: 140–156.
7 Baselga J, Campone M, Piccart M, Burris HA 3rd, Rugo HS, Sahmoud T *et al.* Everolimus in postmenopausal hormone-receptor-positive advanced breast cancer. *N Engl J Med* 2012; **366**: 520–529.
8 Chandarlapaty S. Negative feedback and adaptive resistance to the targeted therapy of cancer. *Cancer Discov* 2012; **2**: 311–319.
9 Markman B, Dienstmann R, Tabernero J. Targeting the PI3K/Akt/mTOR pathway--beyond rapalogs. *Oncotarget* 2010; **1**: 530–543.
10 Lawson DA, Bhakta NR, Kessenbrock K, Prummel KD, Yu Y, Takai K *et al.* Single-cell analysis reveals a stem-cell program in human metastatic breast cancer cells. *Nature* 2015; **526**: 131–135.
11 Ruiz de Garibay G, Herranz C, Llorente A, Boni J, Serra-Musach J, Mateo F *et al.* Lymphangioleiomyomatosis biomarkers linked to lung metastatic potential and cell stemness. *PLoS One* 2015; **10**: e0132546.
12 Bhola NE, Jansen VM, Koch JP, Li H, Formisano L, Williams JA *et al.* Treatment of triple-negative breast cancer with TORC1/2 inhibitors sustains a drug-resistant and Notch-dependent cancer stem cell population. *Cancer Res* 2016; **76**: 440–452.
13 Zhou J, Wulfkuhle J, Zhang H, Gu P, Yang Y, Deng J *et al.* Activation of the PTEN/mTOR/STAT3 pathway in breast cancer stem-like cells is required for viability and maintenance. *Proc Natl Acad Sci USA* 2007; **104**: 16158–16163.
14 Ma J, Meng Y, Kwiatkowski DJ, Chen X, Peng H, Sun Q *et al.* Mammalian target of rapamycin regulates murine and human cell differentiation through STAT3/p63/Jagged/Notch cascade. *J Clin Invest* 2010; **120**: 103–114.
15 Yang Z, Zhang L, Ma A, Liu L, Li J, Gu J *et al.* Transient mTOR inhibition facilitates continuous growth of liver tumors by modulating the maintenance of CD133+ cell populations. *PLoS One* 2011; **6**: e28405.
16 Minn AJ, Gupta GP, Siegel PM, Bos PD, Shu W, Giri DD *et al.* Genes that mediate breast cancer metastasis to lung. *Nature* 2005; **436**: 518–524.
17 Issa A, Gill JW, Heideman MR, Sahin O, Wiemann S, Dey JH *et al.* Combinatorial targeting of FGF and ErbB receptors blocks growth and metastatic spread of breast cancer models. *Breast Cancer Res* 2013; **15**: R8.
18 Chen L, Yang S, Jakoncic J, Zhang JJ, Huang XY. Migrastatin analogues target fascin to block tumour metastasis. *Nature* 2010; **464**: 1062–1066.
19 Cariati M, Naderi A, Brown JP, Smalley MJ, Pinder SE, Caldas C *et al.* Alpha-6 integrin is necessary for the tumourigenicity of a stem cell-like subpopulation within the MCF7 breast cancer cell line. *Int J Cancer* 2008; **122**: 298–304.
20 Piva M, Domenici G, Iriondo O, Rabano M, Simoes BM, Comaills V *et al.* Sox2 promotes tamoxifen resistance in breast cancer cells. *EMBO Mol Med* 2014; **6**: 66–79.
21 TCGA. Comprehensive molecular portraits of human breast tumours. *Nature* 2012; **490**: 61–70.
22 Wong DJ, Liu H, Ridky TW, Cassarino D, Segal E, Chang HY. Module map of stem cell genes guides creation of epithelial cancer stem cells. *Cell Stem Cell* 2008; **2**: 333–344.
23 Ben-Porath I, Thomson MW, Carey VJ, Ge R, Bell GW, Regev A *et al.* An embryonic stem cell-like gene expression signature in poorly differentiated aggressive human tumors. *Nat Genet* 2008; **40**: 499–507.
24 Kim J, Woo AJ, Chu J, Snow JW, Fujiwara Y, Kim CG *et al.* A Myc network accounts for similarities between embryonic stem and cancer cell transcription programs. *Cell* 2010; **143**: 313–324.
25 Lim E, Wu D, Pal B, Bouras T, Asselin-Labat ML, Vaillant F *et al.* Transcriptome analyses of mouse and human mammary cell subpopulations reveal multiple conserved genes and pathways. *Breast Cancer Res* 2010; **12**: R21.
26 Koren S, Reavie L, Couto JP, De Silva D, Stadler MB, Roloff T *et al.* PIK3CA(H1047R) induces multipotency and multi-lineage mammary tumours. *Nature* 2015; **525**: 114–118.
27 Van Keymeulen A, Lee MY, Ousset M, Brohee S, Rorive S, Giraddi RR *et al.* Reactivation of multipotency by oncogenic PIK3CA induces breast tumour heterogeneity. *Nature* 2015; **525**: 119–123.
28 Huang R, Huang D, Dai W, Yang F. Overexpression of HMGA1 correlates with the malignant status and prognosis of breast cancer. *Mol Cell Biochem* 2015; **404**: 251–257.
29 Kormish JD, Sinner D, Zorn AM. Interactions between SOX factors and Wnt/beta-catenin signaling in development and disease. *Dev Dyn* 2010; **239**: 56–68.
30 Kataoka K, Sato T, Yoshimi A, Goyama S, Tsuruta T, Kobayashi H *et al.* Evi1 is essential for hematopoietic stem cell self-renewal, and its expression marks hematopoietic cells with long-term multilineage repopulating activity. *J Exp Med* 2011; **208**: 2403–2416.
31 Patel JB, Appaiah HN, Burnett RM, Bhat-Nakshatri P, Wang G, Mehta R *et al.* Control of EVI-1 oncogene expression in metastatic breast cancer cells through microRNA miR-22. *Oncogene* 2011; **30**: 1290–1301.
32 Guo W, Keckesova Z, Donaher JL, Shibue T, Tischler V, Reinhardt F *et al.* Slug and Sox9 cooperatively determine the mammary stem cell state. *Cell* 2012; **148**: 1015–1028.
33 Larsimont JC, Youssef KK, Sanchez-Danes A, Sukumaran V, Defrance M, Delatte B *et al.* Sox9 controls self-renewal of oncogene targeted cells and links tumor initiation and invasion. *Cell Stem Cell* 2015; **17**: 60–73.
34 Ye X, Tam WL, Shibue T, Kaygusuz Y, Reinhardt F, Ng Eaton E *et al.* Distinct EMT programs control normal mammary stem cells and tumour-initiating cells. *Nature* 2015; **525**: 256–260.
35 Sflomos G, Dormoy V, Metsalu T, Jeitziner R, Battista L, Scabia V *et al.* A preclinical model for ERalpha-positive breast cancer points to the epithelial microenvironment as determinant of luminal phenotype and hormone response. *Cancer Cell* 2016; **29**: 407–422.
36 Ginestier C, Hur MH, Charafe-Jauffret E, Monville F, Dutcher J, Brown M *et al.* ALDH1 is a marker of normal and malignant human mammary stem cells and a predictor of poor clinical outcome. *Cell Stem Cell* 2007; **1**: 555–567.
37 Cheung KJ, Gabrielson E, Werb Z, Ewald AJ. Collective invasion in breast cancer requires a conserved basal epithelial program. *Cell* 2013; **155**: 1639–1651.
38 Garnett MJ, Edelman EJ, Heidorn SJ, Greenman CD, Dastur A, Lau KW *et al.* Systematic identification of genomic markers of drug sensitivity in cancer cells. *Nature* 2012; **483**: 570–575.
39 Clevers H. The cancer stem cell: premises, promises and challenges. *Nat Med* 2011; **17**: 313–319.
40 Janssen EA, Baak JP, Guervos MA, van Diest PJ, Jiwa M, Hermsen MA. In lymph node-negative invasive breast carcinomas, specific chromosomal aberrations are strongly associated with high mitotic activity and predict outcome more accurately than grade, tumour diameter, and oestrogen receptor. *J Pathol* 2003; **201**: 555–561.

41 Hagerstrand D, Tong A, Schumacher SE, Ilic N, Shen RR, Cheung HW *et al.* Systematic interrogation of 3q26 identifies TLOC1 and SKIL as cancer drivers. *Cancer Discov* 2013; **3**: 1044–1057.
42 Bard-Chapeau EA, Gunaratne J, Kumar P, Chua BQ, Muller J, Bard FA *et al.* EVI1 oncoprotein interacts with a large and complex network of proteins and integrates signals through protein phosphorylation. *Proc Natl Acad Sci USA* 2013; **110**: E2885–E2894.
43 Stavropoulou V, Kaspar S, Brault L, Sanders MA, Juge S, Morettini S *et al.* MLL-AF9 expression in hematopoietic stem cells drives a highly invasive AML expressing EMT-related genes linked to poor outcome. *Cancer Cell* 2016; **30**: 43–58.
44 Dutta P, Bui T, Bauckman KA, Keyomarsi K, Mills GB, Nanjundan M. EVI1 splice variants modulate functional responses in ovarian cancer cells. *Mol Oncol* 2013; **7**: 647–668.
45 Holder AM, Akcakanat A, Adkins F, Evans K, Chen H, Wei C *et al.* Epithelial to mesenchymal transition is associated with rapamycin resistance. *Oncotarget* 2015; **6**: 19500–19513.
46 Malladi S, Macalinao DG, Jin X, He L, Basnet H, Zou Y *et al.* Metastatic latency and immune evasion through autocrine inhibition of WNT. *Cell* 2016; **165**: 45–60.
47 Chao CH, Chang CC, Wu MJ, Ko HW, Wang D, Hung MC *et al.* MicroRNA-205 signaling regulates mammary stem cell fate and tumorigenesis. *J Clin Invest* 2014; **124**: 3093–3106.
48 Malhotra GK, Zhao X, Edwards E, Kopp JL, Naramura M, Sander M *et al.* The role of Sox9 in mouse mammary gland development and maintenance of mammary stem and luminal progenitor cells. *BMC Dev Biol* 2014; **14**: 47.
49 Pool SE, Bison S, Koelewijn SJ, van der Graaf LM, Melis M, Krenning EP *et al.* mTOR inhibitor RAD001 promotes metastasis in a rat model of pancreatic neuroendocrine cancer. *Cancer Res* 2013; **73**: 12–18.
50 Campone M, Bachelot T, Gnant M, Deleu I, Rugo HS, Pistilli B *et al.* Effect of visceral metastases on the efficacy and safety of everolimus in postmenopausal women with advanced breast cancer: subgroup analysis from the BOLERO-2 study. *Eur J Cancer* 2013; **49**: 2621–2632.
51 Rodrik-Outmezguine VS, Okaniwa M, Yao Z, Novotny CJ, McWhirter C, Banaji A *et al.* Overcoming mTOR resistance mutations with a new-generation mTOR inhibitor. *Nature* 2016; **534**: 272–276.
52 Koboldt DC, Fulton RS, McLellan MD, Schmidt H, Kalicki-Veizer J, McMichael JF *et al.* Comprehensive molecular portraits of human breast tumours. *Nature* 2012; **490**: 61–70.
53 Subramanian A, Tamayo P, Mootha VK, Mukherjee S, Ebert BL, Gillette MA *et al.* Gene set enrichment analysis: a knowledge-based approach for interpreting genome-wide expression profiles. *Proc Natl Acad Sci USA* 2005; **102**: 15545–15550.
54 Huang DW, Sherman BT, Tan Q, Collins JR, Alvord WG, Roayaei J *et al.* The DAVID gene functional classification tool: a novel biological module-centric algorithm to functionally analyze large gene lists. *Genome Biol* 2007; **8**: R183.
55 Palafox M, Ferrer I, Pellegrini P, Vila S, Hernandez-Ortega S, Urruticoechea A *et al.* RANK induces epithelial-mesenchymal transition and stemness in human mammary epithelial cells and promotes tumorigenesis and metastasis. *Cancer Res* 2012; **72**: 2879–2888.
56 Aslakson CJ, Miller FR. Selective events in the metastatic process defined by analysis of the sequential dissemination of subpopulations of a mouse mammary tumor. *Cancer Res* 1992; **52**: 1399–1405.
57 Morales M, Arenas EJ, Urosevic J, Guiu M, Fernandez E, Planet E *et al.* RARRES3 suppresses breast cancer lung metastasis by regulating adhesion and differentiation. *EMBO Mol Med* 2014; **6**: 865–881.
58 Witten IH, Frank E, Trigg L, Hall M, Holmes G, Cunningham SJ. Weka: practical machine learning tools and techniques with Java implementations. *Proceedings of the ICONIP/ANZIIS/ANNES'99 Workshop on Emerging Knowledge Engineering and Connectionist-Based Information Systems* 1999, pp 192–196.
59 Puente XS, Pinyol M, Quesada V, Conde L, Ordonez GR, Villamor N *et al.* Whole-genome sequencing identifies recurrent mutations in chronic lymphocytic leukaemia. *Nature* 2011; **475**: 101–105.
60 Zhang Y, Liu T, Meyer CA, Eeckhoute J, Johnson DS, Bernstein BE *et al.* Model-based analysis of ChIP-Seq (MACS). *Genome Biol* 2008; **9**: R137.

Supplementary Information accompanies this paper on the Oncogene website (http://www.nature.com/onc)

Figure S1

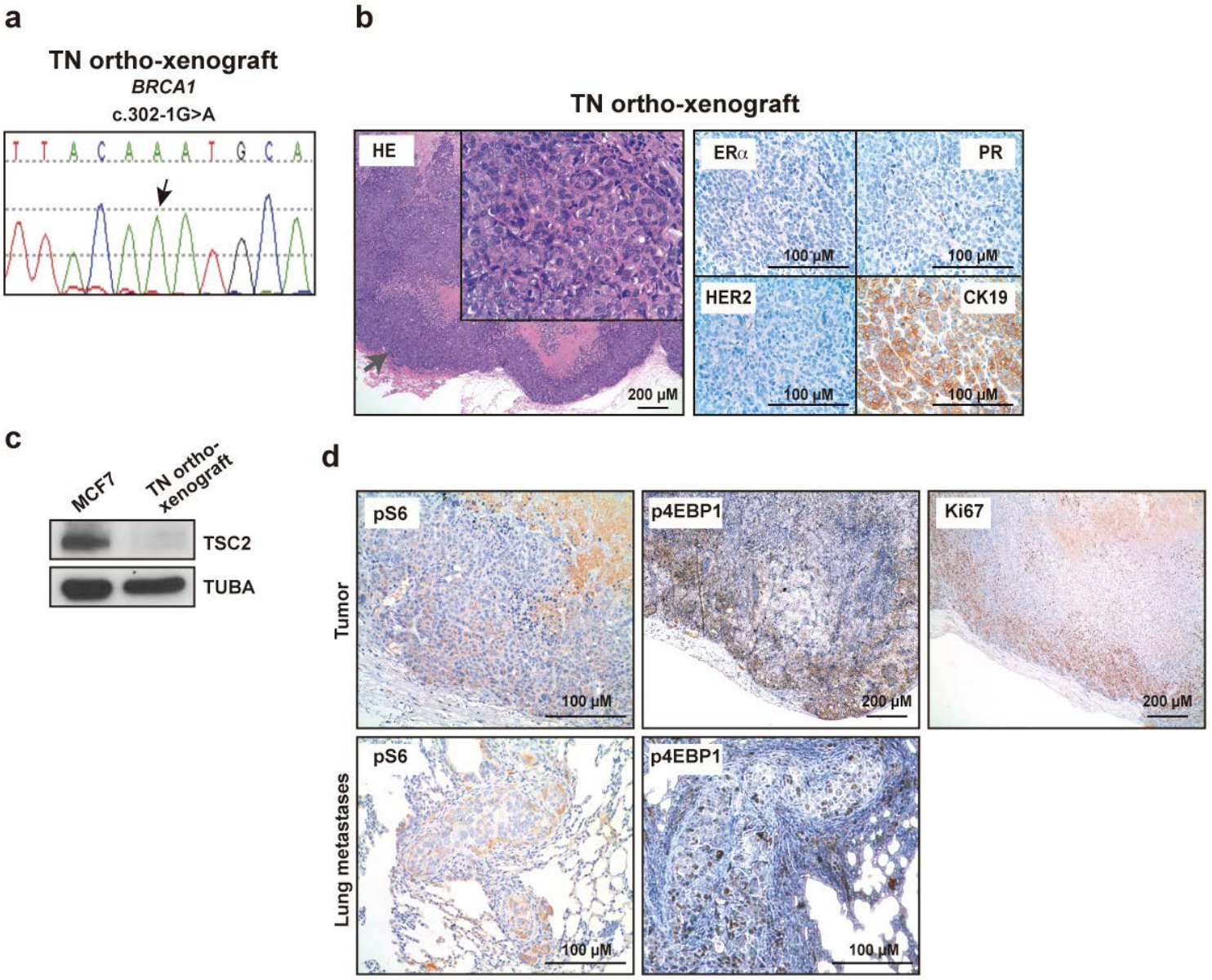
a
TN ortho-xenograft
BRCA1
c.302-1G>A
T T A C A A A T G C A
b
TN ortho-xenograft
HE
200 µM
ERα
PR
HER2
CK19
100 µM
c
MCF7
TN ortho-xenograft
TSC2
TUBA
d
Tumor
Lung metastases
pS6
p4EBP1
Ki67
100 µM
200 µM

Figure S2

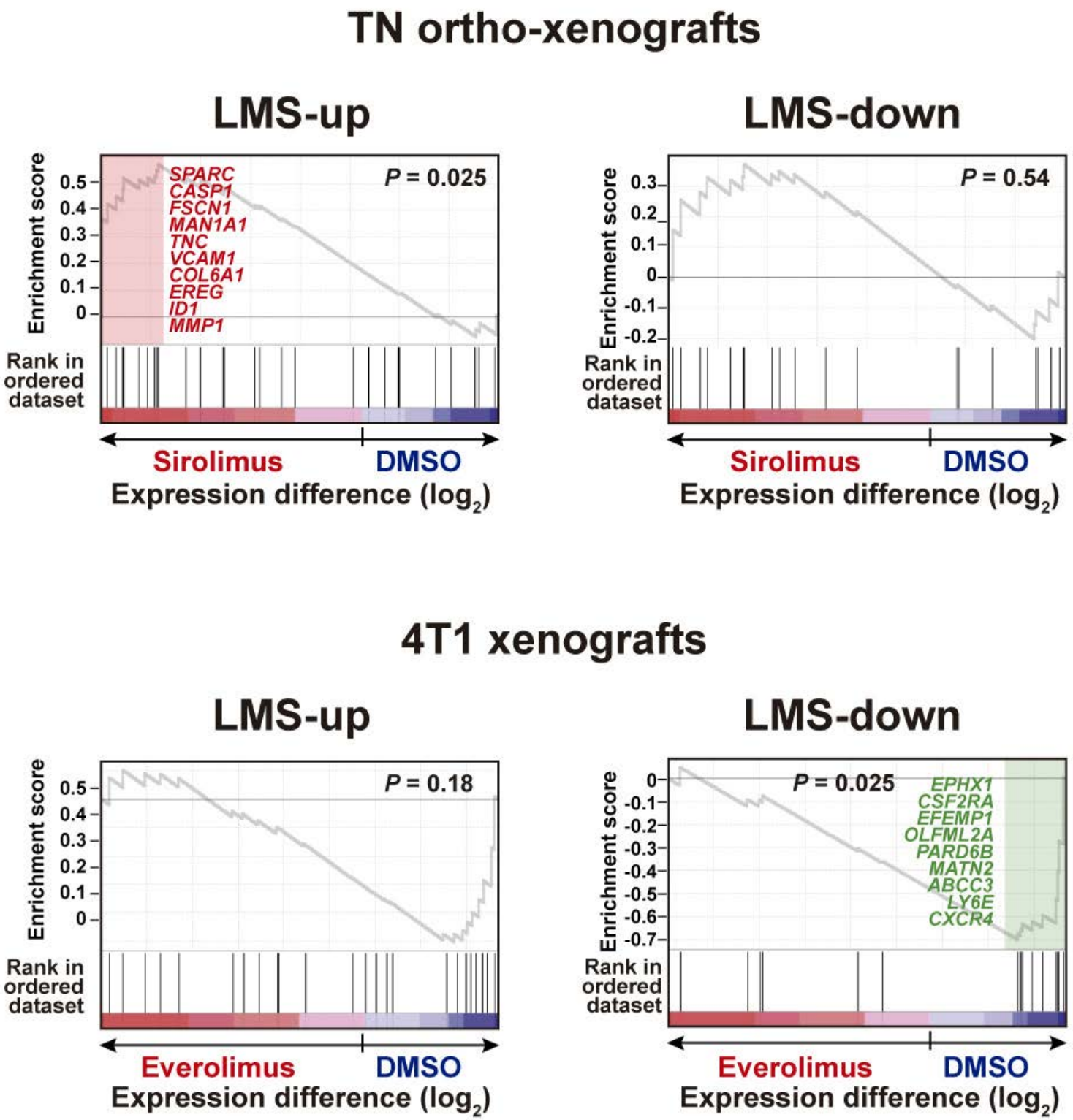
TN ortho-xenografts
LMS-up
LMS-down
Enrichment score
Rank in ordered dataset
SPARC
CASP1
FSCN1
MAN1A1
TNC
VCAM1
COL6A1
EREG
ID1
MMP1
P = 0.025
P = 0.54
Sirolimus
DMSO
Expression difference (log2)
4T1 xenografts
LMS-up
LMS-down
P = 0.18
P = 0.025
EPHX1
CSF2RA
EFEMP1
OLFML2A
PARD6B
MATN2
ABCC3
LY6E
CXCR4
Everolimus
DMSO
Expression difference (log2)

Figure S3

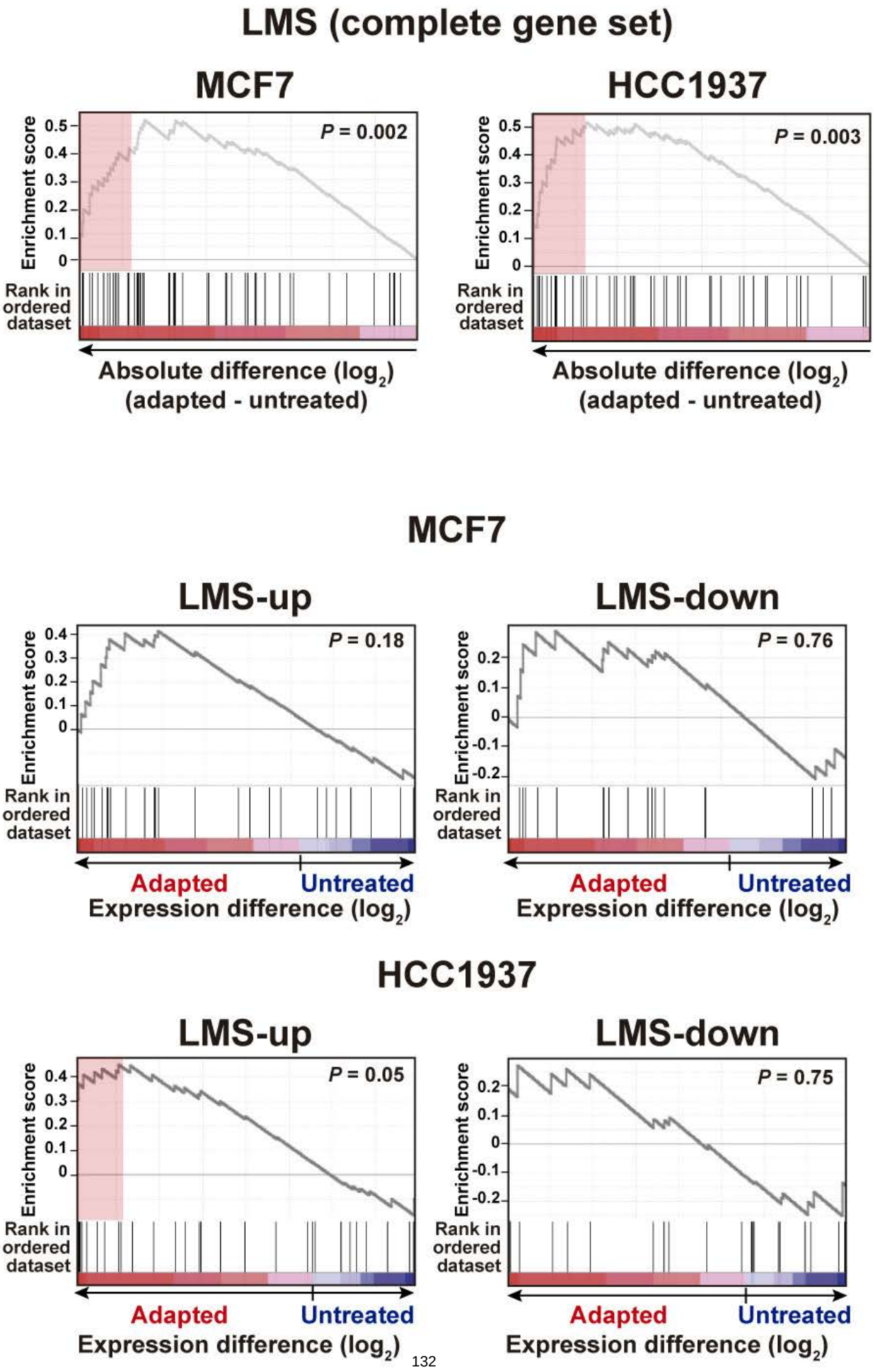
LMS (complete gene set)
MCF7
HCC1937
Enrichment score
Rank in ordered dataset
P = 0.002
P = 0.003
Absolute difference (log2)
(adapted - untreated)
MCF7
LMS-up
LMS-down
P = 0.18
P = 0.76
Adapted
Untreated
Expression difference (log2)
HCC1937
LMS-up
LMS-down
P = 0.05
P = 0.75

Figure S4

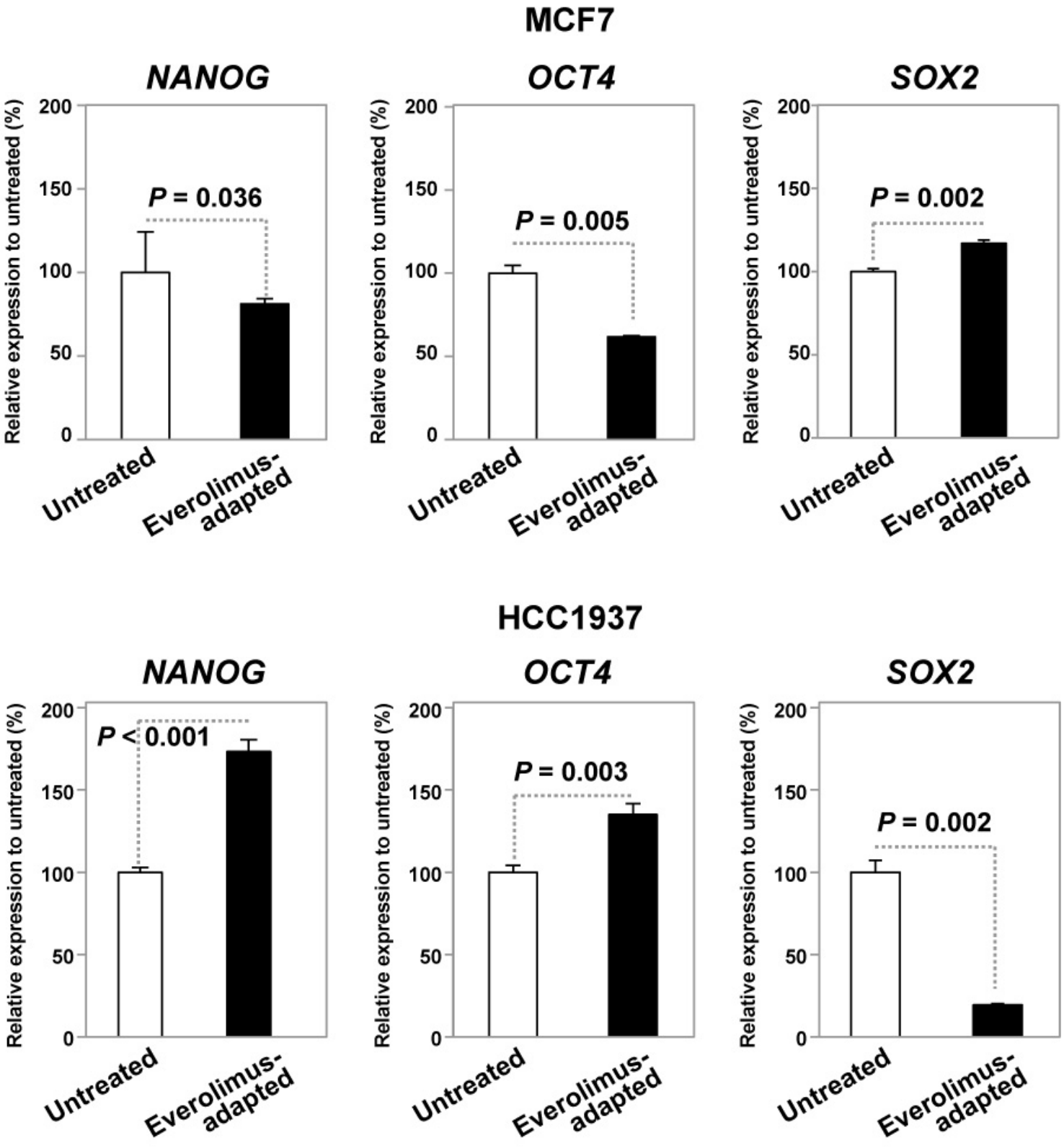
MCF7
NANOG
OCT4
SOX2
Relative expression to untreated (%)
200
150
100
50
0
P = 0.036
P = 0.005
P = 0.002
Untreated
Everolimus-adapted
HCC1937
NANOG
OCT4
SOX2
P < 0.001
P = 0.003
P = 0.002
Untreated
Everolimus-adapted

Figure S5

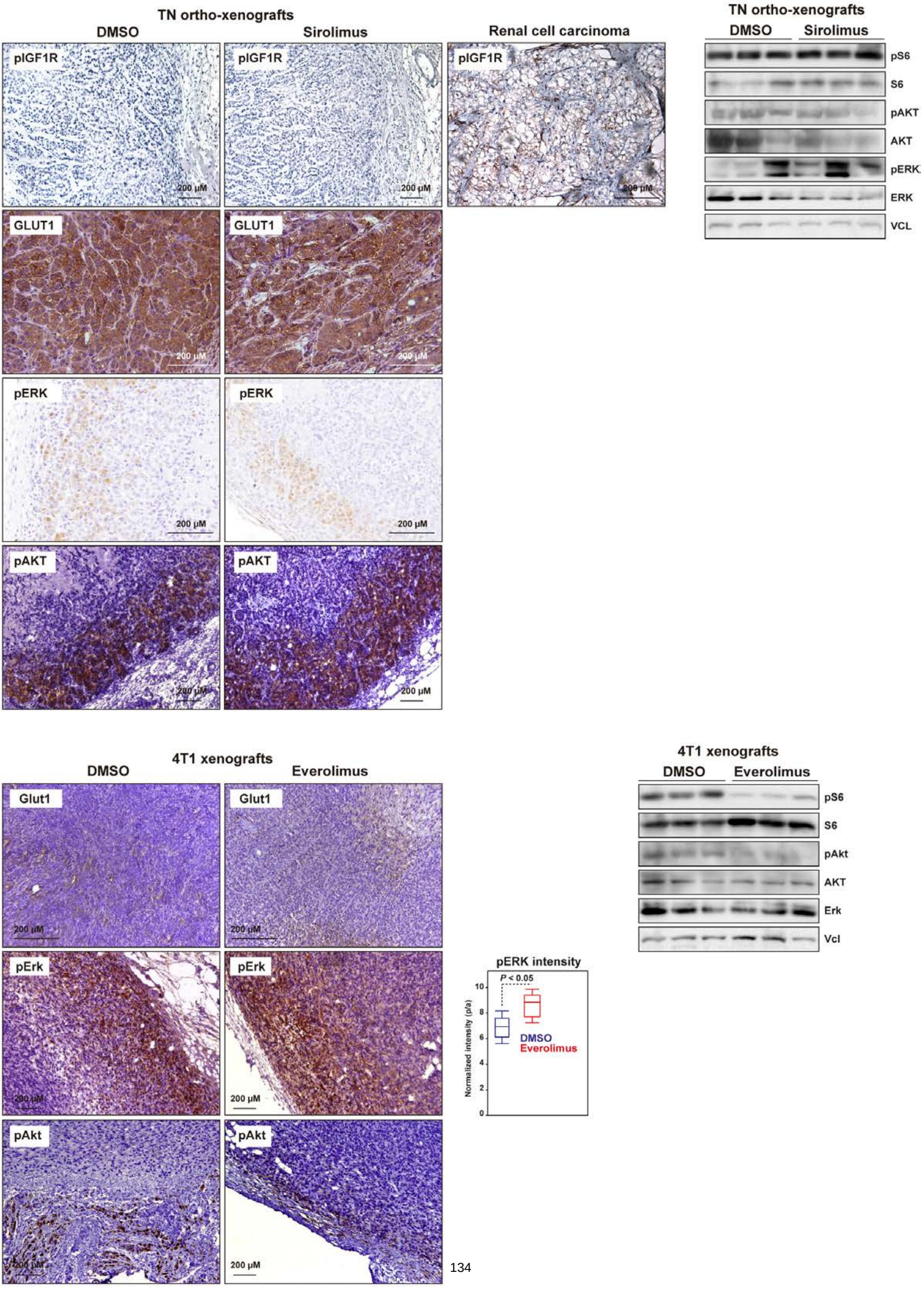
TN ortho-xenografts
DMSO
Sirolimus
Renal cell carcinoma
pIGF1R
GLUT1
pERK
pAKT
200 μM
TN ortho-xenografts
DMSO
Sirolimus
pS6
S6
pAKT
AKT
pERK
ERK
VCL
4T1 xenografts
DMSO
Everolimus
Glut1
pErk
pAkt
pERK intensity
P < 0.05
Normalized intensity (p/a)
DMSO
Everolimus
4T1 xenografts
DMSO
Everolimus
pS6
S6
pAkt
AKT
Erk
Vcl

Figure S6

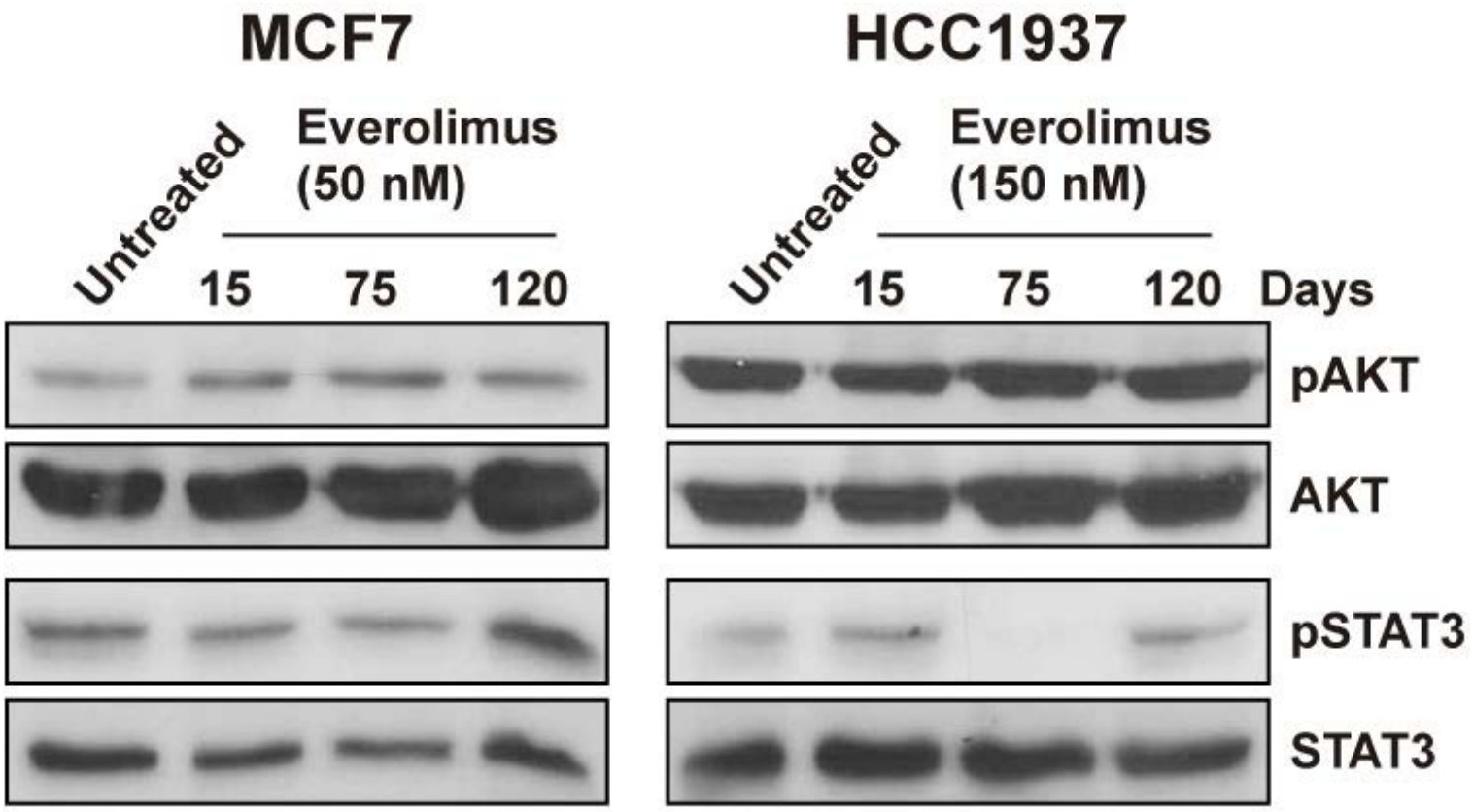
MCF7
HCC1937
Untreated
Everolimus (50 nM)
Everolimus (150 nM)
15
75
120
Days
pAKT
AKT
pSTAT3
STAT3

Figure S7

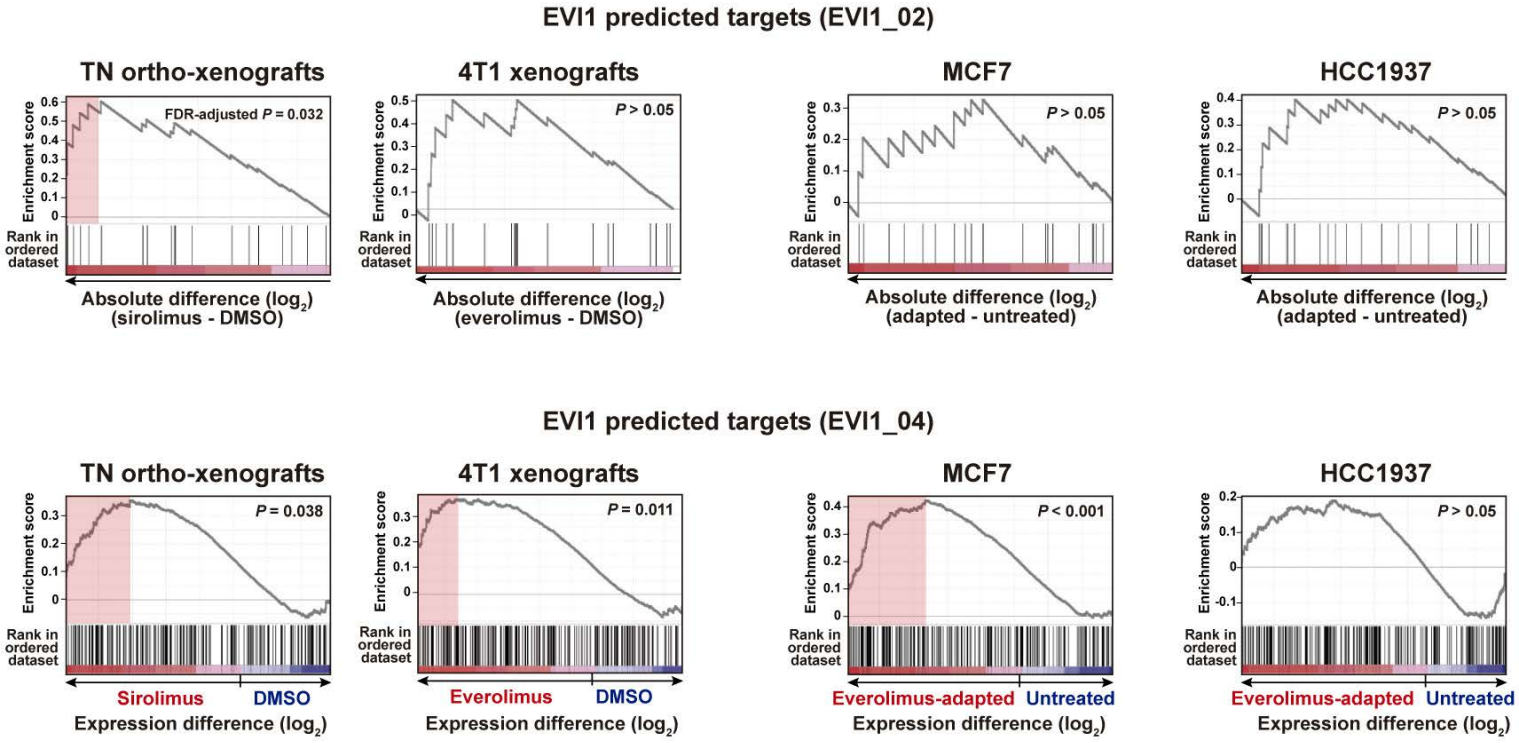
EVI1 predicted targets (EVI1_02)
TN ortho-xenografts
FDR-adjusted P = 0.032
Enrichment score
Rank in ordered dataset
Absolute difference (log2) (sirolimus - DMSO)
4T1 xenografts
P > 0.05
Absolute difference (log2) (everolimus - DMSO)
MCF7
P > 0.05
Absolute difference (log2) (adapted - untreated)
HCC1937
P > 0.05
Absolute difference (log2) (adapted - untreated)

EVI1 predicted targets (EVI1_04)
TN ortho-xenografts
P = 0.038
Enrichment score
Rank in ordered dataset
Sirolimus
DMSO
Expression difference (log2)
4T1 xenografts
P = 0.011
Everolimus
DMSO
Expression difference (log2)
MCF7
P < 0.001
Everolimus-adapted
Untreated
Expression difference (log2)
HCC1937
P > 0.05
Everolimus-adapted
Untreated
Expression difference (log2)

Figure S8

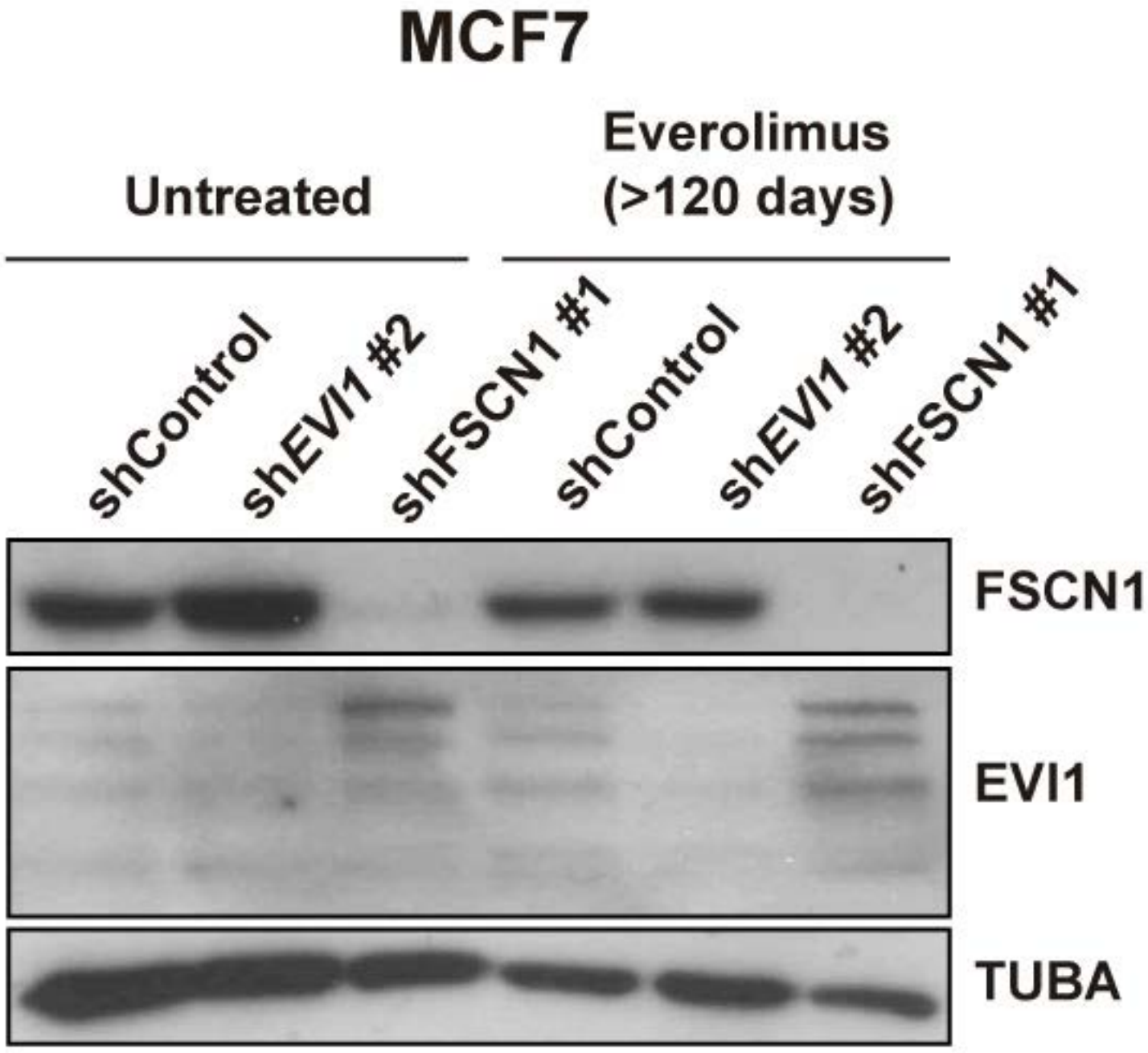
MCF7
Untreated
Everolimus
(>120 days)
shControl
shEVI1 #2
shFSCN1 #1
shControl
shEVI1 #2
shFSCN1 #1
FSCN1
EVI1
TUBA

Figure S9

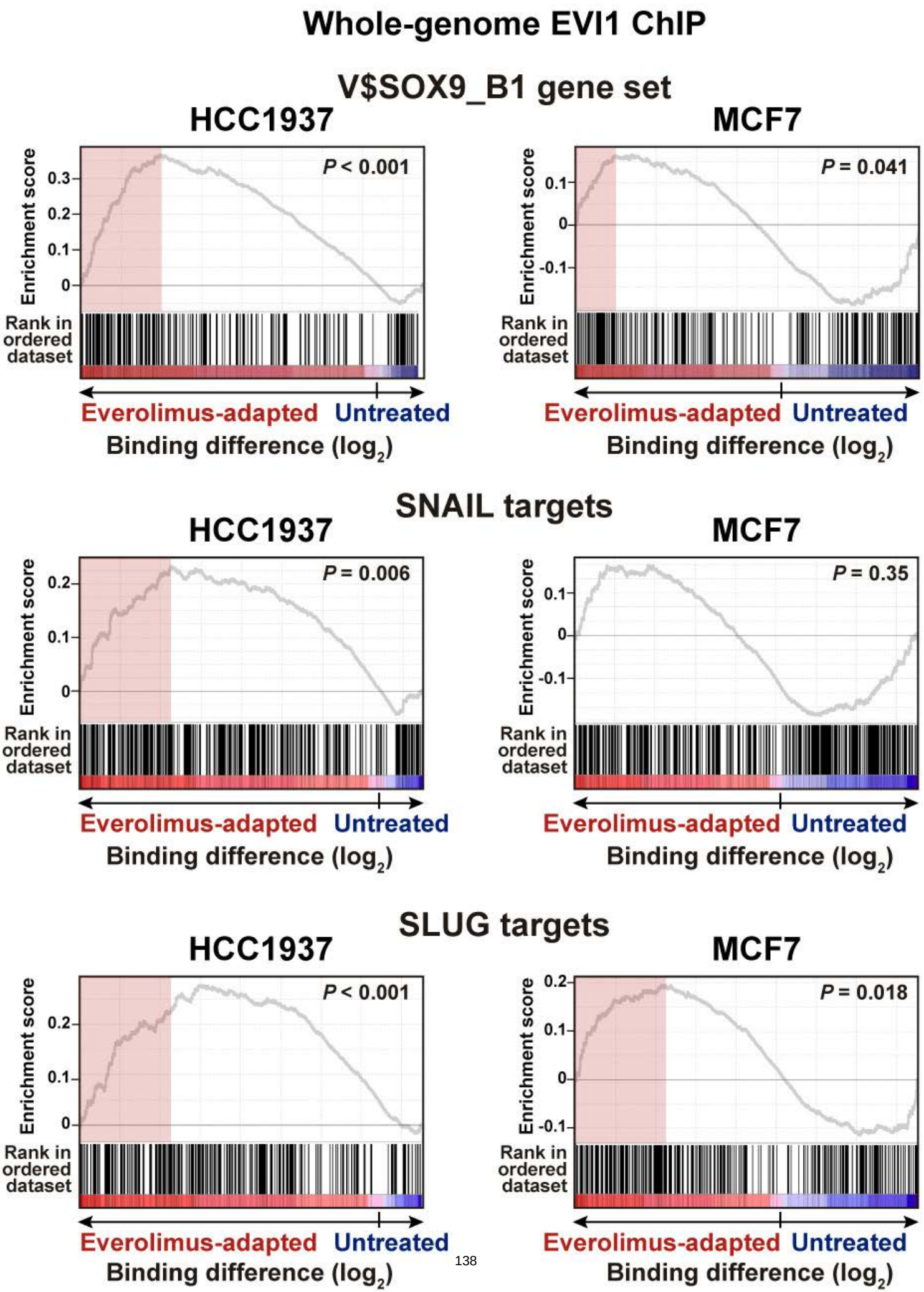
Whole-genome EVI1 ChIP
V$SOX9_B1 gene set
HCC1937
MCF7
Enrichment score
Rank in ordered dataset
P < 0.001
P = 0.041
Everolimus-adapted
Untreated
Binding difference (log2)
SNAIL targets
HCC1937
MCF7
P = 0.006
P = 0.35
Everolimus-adapted
Untreated
Binding difference (log2)
SLUG targets
HCC1937
MCF7
P < 0.001
P = 0.018
Everolimus-adapted
Untreated
Binding difference (log2)

Figure S10

BT-474 long-term exposed to everolimus

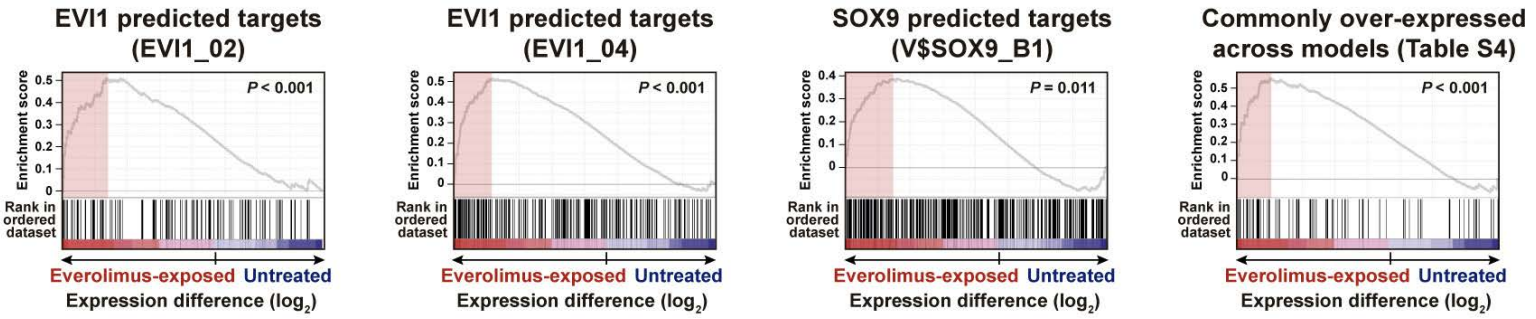

Figure S11

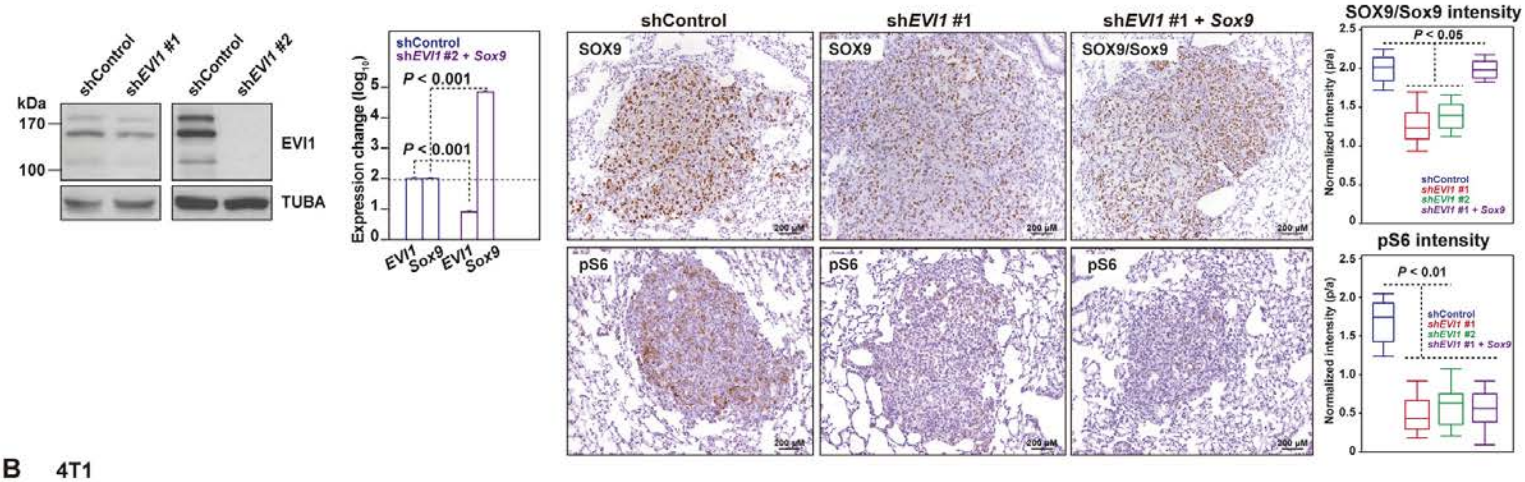
A
MDA-MB-231 LM2
Control assays for conditions shControl, shEVI1, and Sox9 over-expression
shControl
shEVI1 #1
shControl
shEVI1 #2
kDa
170
100
EVI1
TUBA
shControl
shEVI1 #2 + Sox9
P < 0.001
P < 0.001
Expression change (log10)
EVI1
Sox9
EVI1
Sox9
shControl
shEVI1 #1
shEVI1 #1 + Sox9
SOX9
SOX9
SOX9/Sox9
pS6
pS6
pS6
200 μM
SOX9/Sox9 intensity
P < 0.05
Normalized intensity (p/a)
shControl
shEVI1 #1
shEVI1 #2
shEVI1 #1 + Sox9
pS6 intensity
P < 0.01
Normalized intensity (p/a)
shControl
shEVI1 #1
shEVI1 #2
shEVI1 #1 + Sox9

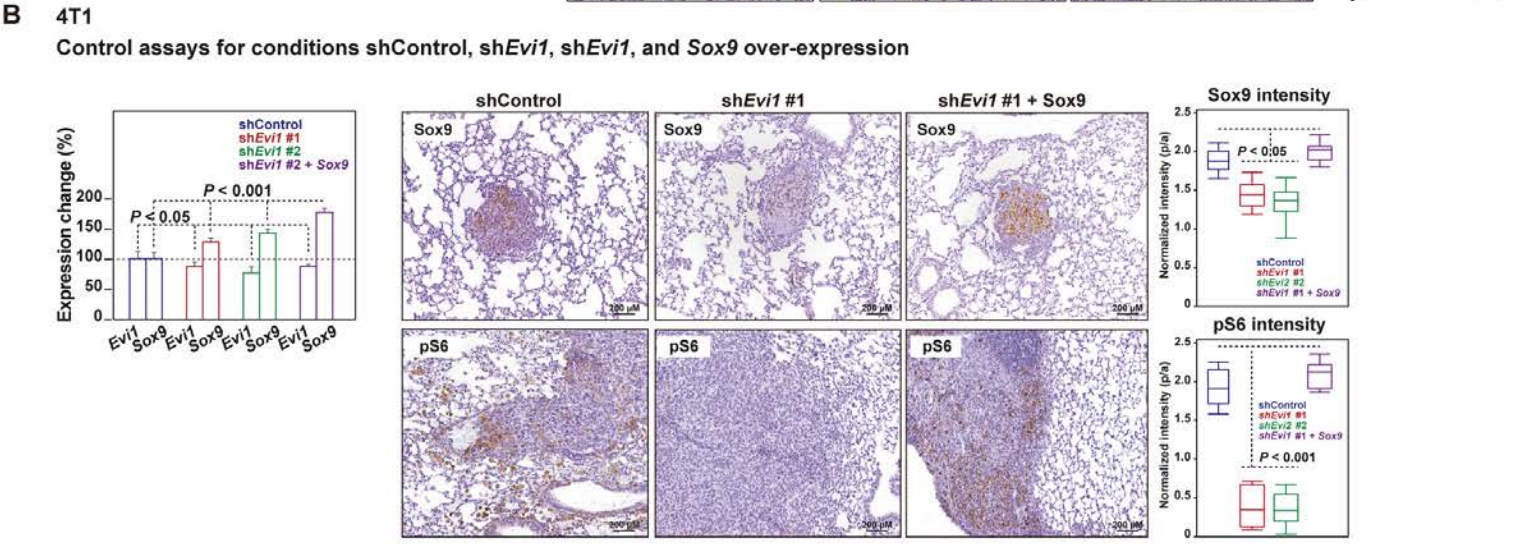
B
4T1
Control assays for conditions shControl, shEvi1, shEvi1, and Sox9 over-expression
shControl
shEvi1 #1
shEvi1 #2
shEvi1 #2 + Sox9
P < 0.001
P < 0.05
Expression change (%)
Evi1
Sox9
Evi1
Sox9
Evi1
Sox9
Evi1
Sox9
shControl
shEvi1 #1
shEvi1 #1 + Sox9
Sox9
Sox9
Sox9
pS6
pS6
pS6
200 μM
Sox9 intensity
P < 0.05
Normalized intensity (p/a)
shControl
shEvi1 #1
shEvi2 #2
shEvi1 #1 + Sox9
pS6 intensity
shControl
shEvi1 #1
shEvi2 #2
shEvi1 #1 + Sox9
P < 0.001
Normalized intensity (p/a)

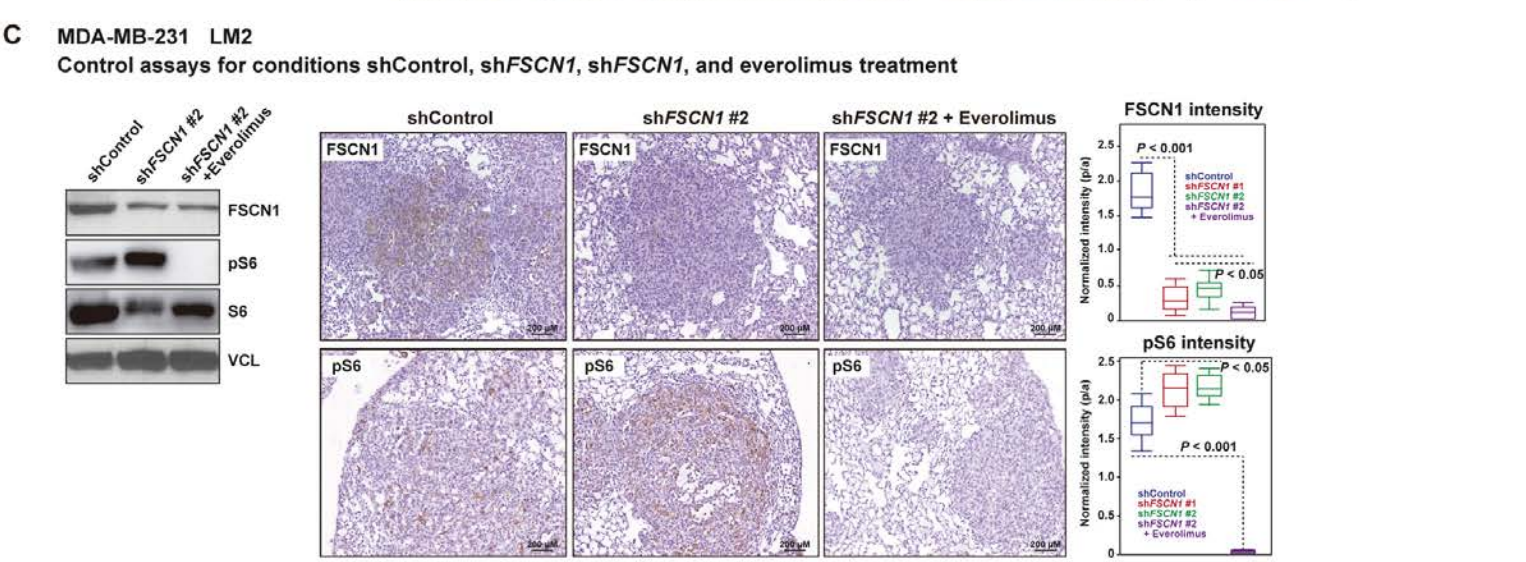
C
MDA-MB-231 LM2
Control assays for conditions shControl, shFSCN1, shFSCN1, and everolimus treatment
shControl
shFSCN1 #2
shFSCN1 #2 +Everolimus
FSCN1
pS6
S6
VCL
shControl
shFSCN1 #2
shFSCN1 #2 + Everolimus
FSCN1
FSCN1
FSCN1
pS6
pS6
pS6
200 μM
FSCN1 intensity
P < 0.001
P < 0.05
Normalized intensity (p/a)
shControl
shFSCN1 #1
shFSCN1 #2
shFSCN1 #2
+ Everolimus
pS6 intensity
P < 0.05
P < 0.001
Normalized intensity (p/a)
shControl
shFSCN1 #1
shFSCN1 #2
shFSCN1 #2
+ Everolimus

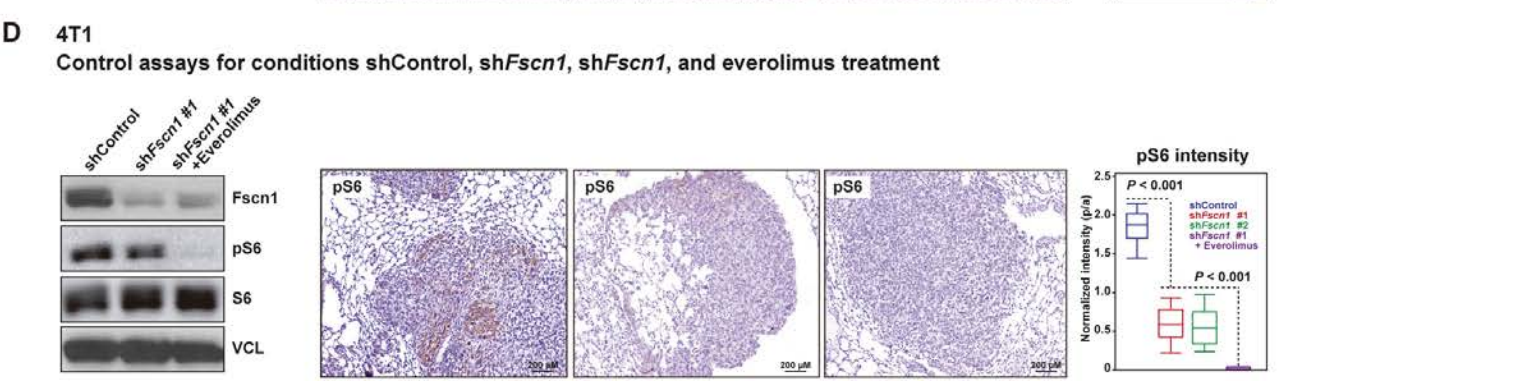
D
4T1
Control assays for conditions shControl, shFscn1, shFscn1, and everolimus treatment
shControl
shFscn1 #1
shFscn1 #1 +Everolimus
Fscn1
pS6
S6
VCL
pS6
pS6
pS6
200 μM
pS6 intensity
P < 0.001
P < 0.001
Normalized intensity (p/a)
shControl
shFscn1 #1
shFscn1 #2
shFscn1 #1
+ Everolimus

Figure S12

A LM2

Control assays for conditions shControl, sh*Sox9* + Everolimus

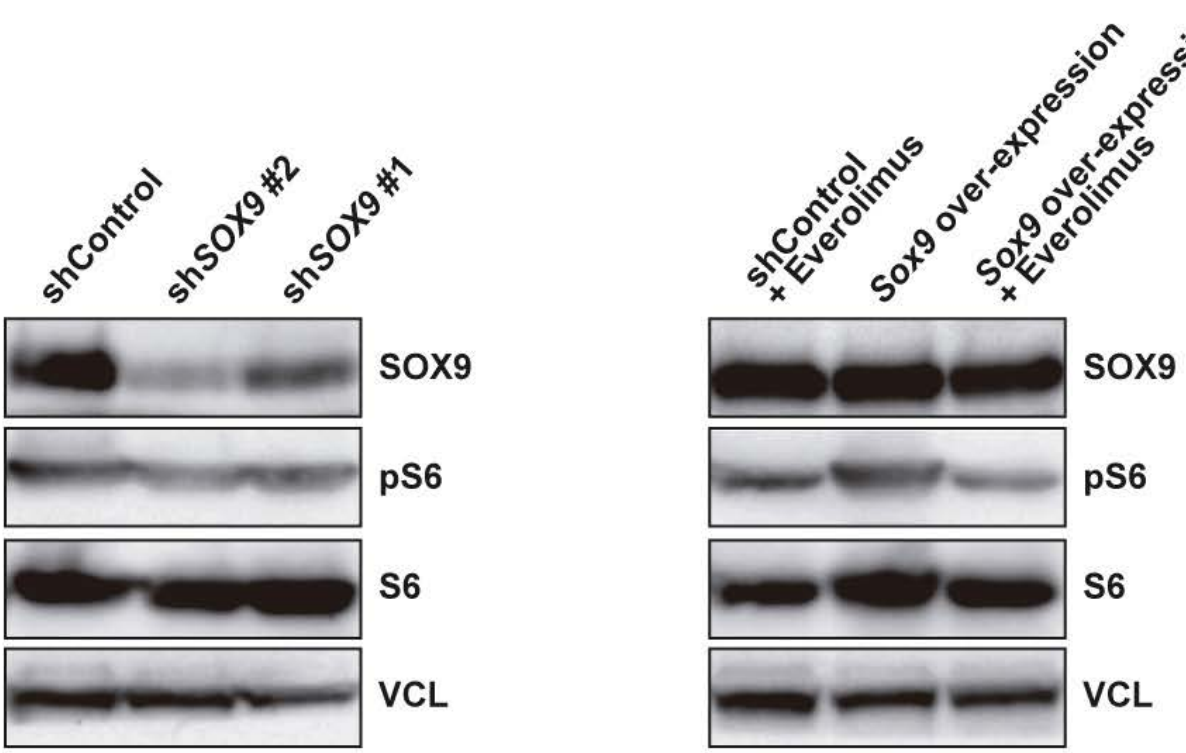

B 4T1

Control assays for conditions shControl and sh*Sox9*

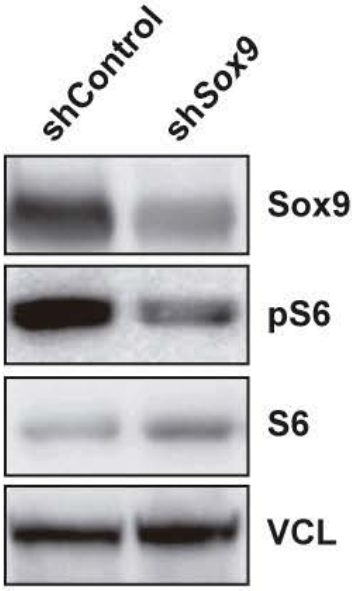

ARTICLE 3

“Chromosome 12p amplification in TNBC/basal-like breast cancer associates with resistance to docetaxel”

Chromosome 12p amplification in TNBC/basal-like breast cancer associates with resistance to docetaxel

Jorge Gómez-Miragaya[1], Raúl Tonda[2,3], Sergi Beltrán[2,3], Luis Palomero[4], Miguel Angel Pujana[4], Violeta Serra[5,6], Eva González-Suárez[1,*]

[1] Cancer Epigenetics and Biology Program (PEBC), Bellvitge Biomedical Research Institute (IDIBELL), Avinguda de la Gran Via, 199 – 203, L'Hospitalet deLlobregat, 08908 Barcelona, Spain

[2] CNAG-CRG, Centre for Genomic Regulation (CRG), Institute of Science and Technology (BIST), Centre for Genomic Analysis (CNAG), Barcelona, Spain.

[3] Universitat Pompeu Fabra (UPF), Barcelona, Spain.

[4] ProCURE, Catalan Institute of Oncology, IDIBELL (Bellvitge Biomedical Research Institute), Barcelona, Spain.

[5] Experimental Therapeutics Group, Vall d'Hebron Institute of Oncology, Barcelona, Spain.

[6] CIBERONC, Vall d'Hebron Institute of Oncology, Barcelona, Spain.

[*] Corresponding author: Eva González Suárez.

Cancer Epigenetics and Biology Program, Bellvitge Institute for Biomedical Research, IDIBELL.
Av.Gran Via de L'Hospitalet, 199. 08908 L'Hospitalet de Llobregat. Barcelona. Spain
egsuarez@idibell.cat www.pebc.cat Phone: +34 932607139 Fax: +34 932607219

Abstract

Taxane-based regimens constitute the most common therapeutic option in patients with triple-negative breast cancer (TNBC). Resistance to treatment often arises leading to death, although the molecular mechanisms responsible for this process are unknown. To unravel chemoresistance mechanisms, exome sequencing was performed on matched sensitive and docetaxel resistant TNBC patient-derived xenografts (PDX). Multiple mutations, small insertion/deletions and copy number variation (CNV) changes were detected in the original human metastatic samples, and most of them were maintained in serially passaged TNBC PDX models even after long term treatment with docetaxel, with very few changes being detected between paired sensitive and resistant tumors.. However, we identified a chromosomal amplification of chr12p arm present in the metastatic sample and chemosresistant PDXs of one BRCA1 mutant models which was absent in docetaxel-sensitive PDXs. Increased expression levels of genes located at chr12p correlated with amplificacion in chemoresistant tumors. Clinical data from TCGA and METABRIC studies confirmed that chr12p amplification was associated with a small subset of TNBC/basal-like breast cancer patients with increased gene expression of genes from that region and poor survival after chemotherapy. Our findings suggest that there is a subset of TNBC/basal-like breast cancer harbouring chr12p amplification that may be associated with resistance to docetaxel treatment in clinical setting.

Introduction

Triple negative breast cancer (TNBC) is the most aggressive subtype of this disease and most tumors display basal-like features (Dent et al., 2007; Ismail-Khan and Bui, 2010; Oakman et al., 2010). As no targetable therapies are available, chemotherapy is the most common treatment for TNBC patients, mostly using taxanes in combination with other drugs (Oakman et al., 2010). *De novo* or intrinsic chemoresistance to taxanes consistently occurs in TNBCs (Oakman et al., 2010), leading to resistant relapse or distant metastasis that cause death in TNBC patients (Dent et al., 2007; Oakman et al., 2010). Some mechanisms of resistance to taxanes have been described as potentially targetable (Balko et al., 2012, 2014; Bauer et al., 2010) with little success in the clinic, so better understanding of these mechanisms is essential to improve patient outcome.

Tumors from the basal-like and HER2+ subtype display higher chromosomal aberrations and mutational rates per megabase than luminal subtypes (Hu et al., 2009; Network, 2012). A lot of mutations in several genes and rearregements involving different chromosomal locations have been elucidated (Banerji et al., 2012; Network, 2012; Shah et al., 2012; Stephens et al., 2012). Mutated cancer driver genes are relatively subtype-specific, i.e. significantly mutated genes in luminal tumors are near absent in basal-like breast tumors (Network, 2012). Thus, while tumor suppressor genes *TP53*, *RB1* and *BRCA1* are frequently mutated in basal-like tumors whereas the oncogenes *PIK3CA*, *MAP3K1* and *GATA3* are preferentially mutated in luminal breast tumors (Network, 2012). Furthermore, germline mutations in *BRCA1* and *BRCA2* genes have been associated with up to 15% of TNBC, and TNBC accounts for 70% of breast tumors arising in *BRCA1* mutation carriers (Foulkes et al., 2010; Stevens et al., 2013).

Genomic alterations inducing drug resistance have been described in breast and other cancer types (Li et al., 2013; Paolillo et al., 2017; Walerych et al., 2016). For example, point mutations involving ESR1 (Jeselsohn et al., 2015; Li et al., 2013) and downstream signaling pathways of HER2 (Rexer and Arteaga, 2012) have been reported to induce resistance to endocrine and HER2-targeted therapy, respectively. Furthermore, chromosomal alterations have been shown to induce resistance to antiestrogen therapy (Miller et al., 2011) and targeted therapy (Scaltriti et al., 2011; Sun et al., 2015). In TNBC/basal-like tumors some genomic alterations have been identified and associated to sensitivity to some drugs, indicating a potential benefit in the outcome of these patients (Balko et al., 2016; Geenen et al., 2017). However, mutations and chromosomal rearrangements in TNBC/basal-like tumors have been poorly associated with resistance to chemotherapy, probably because there are no clean studies with single chemotherapy as most patients are treated with drug combinations.

Nowadays, integrative genomics combining molecular data as DNA copy number alterations, mRNA and protein expression are emerging approaches in the study of tumor aggressiveness and response to therapy facilitating an easier translation into clinics (Kristensen et al., 2014). Gene signatures extracted from sensitive and resistant breast cancer cell lines have demonstrated to be useful in elucidating mechanisms of resistance (Györffy et al., 2005; Lee et al., 2007), but most of the *in vitro* cell line-derived signatures are not able to predict response in the clinical setting (Liedtke et al., 2010).

In this regard, patient-derived xenografts (PDX) represent a better model for the study of tumor progression, tumor clonal evolution and for assessing novel therapies (Byrne et al., 2017; Dobrolecki et al., 2016; Hidalgo et al., 2014). PDX models have been described as important tools for translational research, as they maintain the main features from patient tumors, as transcriptomic,

genomic and histologic patterns (Byrne et al., 2017; Dobrolecki et al., 2016; Hidalgo et al., 2014). Interestingly, treatment response to drugs as chemotherapy or targeted compounds is also closely correlated with patients from which PDX models derived (Byrne et al., 2017; Dobrolecki et al., 2016; Hidalgo et al., 2014).Thus, PDX models have been reported to be suitable models for the study of chemoresistance acquisition.

Using a panel of breast cancer PDX we have shown previously that unlike luminal tumors, basal-like PDX models were initially sensitive to docetaxel (IDB-01S and IDB-02S) but they progressively acquired resistance after continuous *in vivo* docetaxel treatment (IDB-01R and IDB-02R), mimicking the clinical scenario (Gómez-Miragaya et al., 2017). A gene expression signature predictive of residual disease after anthracycline/taxane-based therapy in patients with basal-like disease was identified using our paired sensitive and resistant basal-like PDX models, highlighting the clinical relevance of these models (Gómez-Miragaya et al., 2017).

In this study, we hypothesized that acquisition of genomic changes could underlie docetaxel resistance in TNBC patients. Using matched sensitive and docetaxel resistant TNBC PDXs models, association of point mutations, small INDELs and copy number variation with resistance was investigated. We identified an amplification in chr12p in the *BRCA1*-mutant IDB-02R model that correlates with overexpression of the genes encoded in that genomic region. Finally, validation in a clinical setting revealed that this amplification is associated with a subset of TNBC/basal-like tumors with decreased overall survival, highlighting the clinical value of our findings.

Materials and methods

Patient Characteristics and Generation of PDX

IDB PDX were generated by orthotopic transplantation of cancer cells isolated from pleural effusions and transplanted into the fat pad of immunodeficient mice, as previously described (Gómez-Miragaya et al., 2017). Generation of resistant TNBC PDX models from the original sensitive ones and maintenance of PDX models by serial transplantation in the intact fat pad of Nod/Scid mice was described (Gómez-Miragaya et al., 2017). All experimental procedures were performed according to Spanish regulations. Informed consent was obtained from all subjects and the study received approval from the institutional Ethics Committee. Additional models were generated following similar procedures (Bruna et al., 2016). All research involving animals was performed at the IDIBELL animal facility in compliance with protocols approved by the IDIBELL Committee on Animal Care and following national and European Union regulations.

Whole exome sequencing

Exome sequence capture and amplification was performed using Agilent SureSelect Human All Exon kit (Agilent, Santa Clara, CA, US) according to the manufacturer's instructions. Paired-end sequencing was performed on a HiSeq2000 instrument (Illumina) using 100-base reads. Reads were aligned to the reference genome (GRCh37) using BWA (Li and Durbin, 2009) and a BAM file was generated using SAMtools (Li et al., 2009). PCR duplicates were removed using SAMtools and custom scripts, and somatic substitutions and indels were called using Sidrón as described previously (Puente et al., 2011). For orthoxenograft-derived samples, reads were first aligned to mouse genome (mm9), and those read-pairs which did not align to mouse were then aligned to the human genome following the same pipeline as above. This procedure removed murine-derived reads, which might interfere in the analysis by artificially increasing the number of variants. CNVs were determined using exome2cnv (Valdés-Mas et al., 2012) by comparing each tumor sample or PDX to its normal counterpart or a normal sample in case of IBD-01 model.

Therapeutic *in vivo* PDX assays

Short term treatments with 2 to 5 doses of docetaxel (Hospira/Actavis, 20 mg/kg) administered intraperitoneally, followed 24 hr later by Fortecortin (Dexametasona, 0.132 mg/kg, Merck), every 5-7 days for a period of 10 to 30 days, depending on tumors response were performed in tumor bearing mice. Mice were then sacrificed and tumors were collected 3-5 days after the last dose of docetaxel. Tumors were frozen at -80ºC prior to DNA or RNA extraction.

RNA extraction, DNAse treatment and qRT-PCR

Total RNA from tissue was prepared with Tripure Isolation Reagent (Roche). Frozen tumor tissues were fractionated using the POLYTRON® system PT 1200 E (Kinematica) and treated with DNA-free DNase I kit (Ambion, AM1906). cDNA was produced by reverse transcription using 1 µg of DNA-free RNA in a 35 µL reaction following TaqMan™ Reverse Transcription instructions (Applied Biosystems, N8080234). 20 ng/well of cDNA were used for the analysis performed in triplicate. Quantitative PCR was performed using the LightCycler® 480 SYBR green. Primer sequences are indicated below. Ct

analysis was performed using LightCycler 480 software (Roche). All primers indicated below are in 5' → 3' direction.

hA2ML1 Forward	GGCAGCAAGTGTATTTCCGC
hA2ML1 Reverse	ATGCCTTGCTCAGGTACCAC
hCMAS Forward	AGAAAAGAAATGGGCCTGTGC
hCMAS Reverse	TAGAACAGGCATCAGCAGGAG
hDERA Forward	AACAGAAGCTTGGTGCTGACA
hDERA Reverse	GCCTTGCGAAACTGACGAATC
hETV6 Forward	TGACAGCAACACGTTTGAAAT
hETV6 Reverse	AGGAGTTCATAGAGCACATCACC
hGABARAPL1 Forward	ACCATGGGCCAACTGTATGA
hGABARAPL1 Reverse	TGGGCTTCCAACCACTCATTT
hITPR2 Forward	CCTTGGGGTTAGTGGATGACAG
hITPR2 Reverse	TGGCTTGCTTTGCTTTCCAAT
hKLHL42 Forward	CGCCCTTACCCAATCCTCTG
hKLHL42 Reverse	GTCCACATGTCGGAAGAGGG
hM6PR Forward	GCTACTCCAGTTTCCCACGA
hM6PR Reverse	GTAGCAGTCCAGTCCTCCAG
hMGST1 Forward	AATTGTATTTCTGTCCCCGTGC
hMGST1 Reverse	TCCATTACCTGGGTGAGGTCAA
hSTRAP Forward	ACAGCAGCTGCAGATTTCACA
hSTRAP Reverse	CCTGTCCCCCGGTTAACAA
hPPiA Forward	ATGCTGGACCCAACACAAAT
hPPiA Reverse	TCTTTCACTTTGCCAAACACC

DNA extraction and RNAse treatment

Total DNA from tissue was prepared with in house lysis buffer (100mM NaCl, 10mM Tris-Cl pH 8, 25mM EDTA). Frozen tumor tissues were fractionated using the POLYTRON® system PT 1200 E (Kinematica) and incubated 12-16 hours with 0.25% SDS (Invitrogen, 24730020), 0.25 mg/ml Proteinase K (Sigma Aldrich, P4850) and RNAse A (Sigma Aldrich, R5503) at 55ºC in a termal block. For DNA purification, the homogenized sample was transferred to a phase lock gel heavy tube (VWR, 713-2538). Two steps of removal of proteins from nucleic acids using Phenol:Chloroform:Isoamyl Alcohol 25:24:1 (Sigma Aldrich, P3803) and three steps of nucleic acid washing with chloroform (VWR, 1024311000) were performed, centrifuging each time at 1500G during 5 minutes. After last spinning, remaining volume containing DNA was recovered and transferred to a solution containing 2.5x absolute ethanol (Merck Millipore, 1009832500) and 30 mM of sodium acetate pH 5.2 (Sigma Aldrich, S2889), mix and centrifuge at maximum for 5 minutes. Wash two times with 70% ethanol centrifuging at maximum for 5 minutes. Finally resuspension in TE buffer (10 mM Tris-HCl, 1 mM disodium EDTA, pH 8.0) or ultrapure water (MilliQ purification system) was performed. DNA concentrations were determined using a Nano Drop ND-1000 Spectrophotometer (Thermo Scientific, Inc. USA). The DNA was diluted to a final concentration of 50 ng/µL prior to conventional PCR and to 5 ng/µL prior to quantitative real-time PCR.

qRT-PCR using Taqman probes and data analysis

GABARAPL1 (Life Technologies, 4400291, Hs02787462_cn), ETV6 (Life Technologies, 4400291, Hs02036151_cn) and KLHL42 (Life Technologies, 4400291, Hs01571843_cn) pre-designed copy number assays with a FAM™ dye labeled MGB probe were used and a RNase P pre-designed copy number reference assay with a VIC® dye-labeled TAMRA™ probe (TaqMan® Copy Number Reference Assay RNase P, Life Technologies, 4403326) was used. RNase P is recommended as the standard reference gene in CNV experiments. Copy number assays were performed in a duplex real-time PCR reaction with the TaqMan® Copy Number Reference Assay for RNase P, using a QuantStudio 5 Real-Time PCR System (Life Technologies) in a standard 384 well format in a total volume of 10 µl. The PCR was carried out using 5 µl 2x TaqMan® Universal PCR Master Mix (cat. no. 4304437, Life Technologies), 0.5 µl 20x TaqMan® Copy Number Reference Assay RNase P (Life Technologies), 0.5 µl 20x TaqMan® Copy Number Assay mix, 2 µl DNase free water and 2 µl genomic DNA (initial concentration 5ng/µl). The final concentration of genomic DNA was 20 ng/µL in all reactions. All samples were amplified in three replicates and one non-template control per primer pair was included in each run together with a calibrator sample. The cycling conditions comprised 10 minute polymerase activation at 95°C followed by 40 cycles of 95°C for 15 s and 60°C for 1 minute.

The amplification curves were analyzed using QuantStudio 5 software (Life Technologies). To determine the copy number for the targets in each sample, the real-time PCR data were exported into an Excel and calculated manually in a comparative quantification cycle (Cq) relative quantification on the real-time data manner to determine the calculated copy numbers. First, the difference between the Cq of the target and reference assay is calculated (ΔCq) in each sample for both the patient sample and the calibrator sample. Then, the method compares the ΔCq values of the patient sample and the calibrator sample (ΔΔCq). With this approach, the predicted copy number of normal samples with two copies of each gene will be 2 for all assays. The predicted copy number of a sample with one gene deleted will be 1 in the respective assay. Due to the mathematics of the $2^{-\Delta\Delta Cq}$ method, the calculated copy numbers deviates from whole numbers. Predicted copy numbers are based on the calculated copy numbers and are specified as whole numbers.

Sanger sequencing

PCR reactions were set up using 25 µL final volume according with Immolase DNA Polymerase manufacturer's recommendations (Bioline, BIO-21047), and 1 µl of template DNA (initial concentration 50 ng/µl) with specific primers for each point mutation or small INDEL and performed on an Applied Biosystems 2720 thermal cycler machine using the following conditions: 95**°**C for 10 min, 35 cycles of 94**°**C for 30 s, 55**°**C for 30 s, 72**°**C for 30 s, and a final extension of 5 min at 72**°**C. PCR products were separated by electrophoresis on a 2% agarose gel. Successful PCR products were cleaned with *in house* ExoSAP mix of Exonuclease I (New England Biolabs, M0293S) and Shrink Anctarctic Phosphatase (New England Biolabs, M0289S) heating them at 37ºC for 15 minutes and inactivating both at 80ºC for 15 minutes. The purified PCR reactions were finally amplified with the BigDye™ Terminator v3.1 Cycle Sequencing Kit (Applied Biosystems, 4337455) using manufacturer's instructions on an Applied Biosystems 2720 thermal cycler machine using just one specific primer and the following conditions: 96**°**C for 3 minutes, 25 cycles of 96**°**C for 15 s, 50**°**C for 10 s, 60**°**C for 2 minutes, and a final extension of 4 min at 60**°**C. Final step with the Big Dye X-Terminator was carried out (Applied Biosystems, 4376487) with agitation in dark during 30 minutes and a last centrifugation

of 2 minutes at 1000G. Capillary sequencing was then performed in the Applied Biosystems 3730 DNA analyzer and analysis of the retrieved sequences was performed with Chromas software (Technelysium Pty Ltd.). Primers are indicated below in 5' → 3' direction.

hKLHL42 Forward	AGCAGCAGATGGTGTCTGTG
hKLHL42 Reverse	CCCTTGGAATGGGACACCAC
hBRCA1 Forward	GCTTCTCTTTCTCTTATCCTGATG
hBRCA1 Reverse	AATCCAAATTACACAGCCTCTC

Databases analysis

The largest METABRIC data set (n = 2509) and TCGA data set (n = 825), which includes patients with copy number, gene expression and follow-up, among other data, within the cBioPortal database (Cerami et al., 2012; Gao et al., 2013) (http://www.cbioportal.org/) was extracted.

Statistical Analyses

All data are expressed as mean ± SEM. Statistical comparison was performed by Student's t test using GraphPad Prism version 5.04. $p \leq 0.05$ was considered statistically significant. The statistical significance of difference between groups is expressed by asterisks: *0.01 < p < 0.05; **0.001 < p < 0.01; ***0.001 < p < 0.0001; ****p < 0.0001.

Results and discussion

Stable exome profiles in breast cancer PDX during implantation, passaging and resistance acquisition

Whole exome sequencing was performed using DNA from paired sensitive and resistant IDB-01 and IDB-02 TNBC PDX models at different passages and "branches" (passages are indicated in Supplementary Figure S1A), the metastatic sample of origin in both models and primary tumor and normal lymphocytic DNA from the patient from whom IDB-02 models were originated. Mean coverage for all samples was 95x and more than 84% of target bases had 15x coverage in all samples.

Metastatic sample of origin from IDB-01 model showed mutations in the most significantly mutated genes in basal-like breast cancer (Network, 2012), including *TP53* (p.N238fs) and *PIK3CA* (p.E545K) (Table 2). Although germline DNA was not available for this patient to establish the somatic status of these mutations, they were recurrent mutations present in the COSMIC database, suggesting that they constitute *bona fide* somatic mutations.

We observed a very low number of somatic substitutions and small insertions/deletions (INDEL) between the primary breast tumor of model IDB-02 and normal lymphocytic DNA (Table 1), probably reflecting a low percentage of tumor cells in the sample, so we conclude that it mostly represents peritumoral tissue. This finding highlights the need to perform microdissection in tumor samples to prevent low sensitivity due to contamination with normal DNA from non-tumor cells.

The comparison of point mutations between metastatic sample of origin from model IDB-02 and normal lymphocytic DNA revealed that there were 91 somatic point mutations accumulated during breast carcinogenesis in whole exome (Table 1). This data shows that the mutation burden of the TNBC metastatic sample from whom IDB-02 was originated (1.82) is similar to the mutational rate described for primary TNBC from the TCGA data (1.68) (Network, 2012). Interestingly, analysis of germline variants revealed the presence of a heterozygous frameshift mutation in *BRCA1* (p.Q1777fs) in both normal lymphocytic DNA and in the primary tumor from the patient (Table 1) that was validated as heterozygous by Sanger sequencing,however, in the human metastatic sample as well as in IDB-02 PDX tumors this mutation was present in homozygosis (Figure 1A).

These data evidence enrichment of a population carrying *BRCA1* mutation in metastatic pleural effusion of IDB-02 model and suggests that an aggressive subclone harbouring common oncogenic mutations present in breast tumors from origin could be selected during engraftment in mice as well as during metastatic events in patients. Moreover, itn correlates with the fact that most aggressive tumors are the ones with higher rates of engraftment (Dobrolecki et al., 2016; Whittle et al., 2015).

In the last years, it has been described that breast cancer PDXs stably maintain genomic features present in initial primary and metastatic breast tumors from patients, with different percentages of subclonal intratumor selection (Bruna et al., 2016; Eirew et al., 2015). Accordingly, a high level of similarity in point mutations and small insertions/deletions (INDELs) was observed between metastatic human samples of origin and breast cancer PDX tumors during tumor engraftment but also during serial transplantation in mice of IDB-01 (more than 96% of genotype was shared; Supplementary Figure S1B) and IDB-02 (more than 87% of genotype was shared; Figure 1B) PDX

tumors. This observation confirms a conserved, stable genotype between metastatic sample of origin and PDX tumors and during serial transplantation of PDX in mice, demonstrating the genomic stability of basal-like breast cancer PDX despite the high rate of mutations and CNVs.

In order to identify point mutations or small INDELs that could be acting as drivers of docetaxel chemoresistance, comparisons of whole exome-sequencing data between paired sensitive and resistant samples from each TNBC PDX model were carried out. The results showed that more than 95% in IDB-01 model (Supplementary Figure S1B) and 97% in IDB-02 model (Figure 1B) of the genotype was shared between sensitive and resistant tumors. Next, mutations present in homo- or heterozygosis in chemoresistant tumors and absent in chemosensitive PDX and metastatic sample in both IDB-01 and IDB-02 models were screened (Supplementary Figure S1C). Very few point mutations or small INDELs were shared between resistant tumors from each model and absent in sensitive tumors. Point mutations or small INDELs that could be potentially affecting protein function (non-synonymous changes, frameshift, or insertion/deletion of amino acids) were selected in IDB-01 and IDB-02 PDX models (Figure 1C), but only one point mutation was shared by all chemoresistant tumors from IDB-02 model (Figure 1C). This mutation was affecting *KLHL42* gene and it was detected as a heterozygotic mutation in resistant IDB-02R tumors, while it was not detected in sensitive IDB-02S tumors. However, validation by Sanger in the exome-sequenced and in independent sensitive and resistant IDB-02 tumors showed that it was a false negative, as by Sanger sequencing all tumors showed equally the heterozygotic mutation (Supplementary Figure S1D).

Taken together, our results reveal that very few point mutations appear de novo in the exome of TNBC PDX models during engraftment, serial passages in mice and with the acquisition of resistance to docetaxel. Although TNBC PDX models show mutations in key DNA mismatch repair genes, as a germline mutation in *BRCA1* in IDB-02, or they pertain to the subtype showing the highest mutational rates per megabase (Network, 2012), TNBC PDX models do not acquire novel mutations or small INDELs during engraftment, serial passages or after long term treatment with docetaxel, showing a very stable genome. However, it is important to note that a more homogeneous population is present in the IDB-02 PDX model than in the human metastatic sample of origin. This result was unravelled due to the higher genotype similarity between sensitive PDX tumors than between sensitive PDX and metastatic sample of origin and by the selection of a *BRCA1* homogeneously mutated population in the PDX models. High genomic similarity between breast tumors of origin and matched PDX has been previously described, as well as that breast cancer PDX models are genomically very stable models during serial transplantation in mice (Bruna et al., 2016; Li et al., 2013). Also, it was described that alterations in oncogenic drivers or tumor suppressors are not enriched in chemotherapy-resistant breast tumors (Goetz et al., 2017). Our data supports these findings in breast cancer PDX, mimicking what happens in clinics and validating matched PDX models for genomic studies.

Amplification in chromosome 12p is detected in metastatic and chemoresistant-derived PDX tumors, but not in sensitive PDX tumors

It has been demonstrated that copy number variation (CNV) is involved in the acquisition of drug resistance in breast cancer (Gay-Bellile et al., 2016; Järvinen et al., 2000). CNV can be inferred from whole-exome sequencing data (Kadalayil et al., 2015; Serratì et al., 2016; Valdés-Mas et al., 2012). Thus, CNV was studied aiming to elucidate chromosomal changes modulating docetaxel response in

our TNBC PDX models. Note that due to the low fraction of tumor cells in patient's primary tumor of IDB-02 PDX model, very few CNVs were detected when compared to normal lymphocytes (Supplementary Figure S2A). In contrast, analysis of CNV in metastasis of origin from IDB-02 PDX model showed a high number of chromosomal abnormalities compared to the normal lymphocytic DNA (Figure 2A and Table 3). In the case of IDB-01 model, the absence of non-tumor DNA avoided the comparison, but an estimation of CNV done using a human normal DNA sample of reference, also showed an aberrant chromosomal landscape (Supplementary Figure S2B), although with less genomic alterations in agreement with IDB-02 bearing a BRCA1 mutation.

Comparison of CNV from metastatic sample of origin and the corresponding TNBC PDX models revealed that most of the chromosomal variations detected in the human metastatic samples were maintained in the corresponding TNBC PDX models (Figure 2A and Supplementary Figure S2B and Table 3 and 4), once again indicating a stable chromosomal copy number change during PDX generation and passage in mice as occurs with point mutations. It is important to highlight that all tumors from IDB-01 PDX model compared to the metastatic sample of origin showed amplification in chromosome 5p15.2-p12 of 35 megabases and, interestingly, duplication in *ERBB2*, suggesting that these changes have been selected during xenograft expansion (Table 4). Duplication in *ERBB2* does not seem to be correlated with increase in protein expression as shown in (Gómez-Miragaya et al., 2017). IDB-02 model showed a CNV profile characterized by amplifications in 1q, 8q and 10p and losses of 1p, 4p, 5q, 10q, 15q and Xp (Figure 2A and Table 3). This profile is associated to basal-like tumors (Natrajan et al., 2009a; Network, 2012), making our PDX model a valuable tool to study the importance of these chromosomal aberration patterns in basal-like breast cancer.

To find differential CNV that could mediate chemoresistance acquisition, comparisons between sensitive and resistant tumors from each TNBC PDX were conducted. Again very few changes at CNV level were detected in resistant IDB-01 tumors and none shared between resistant and absent in sensitive tumors (Supplementary Figure S2B and Table 4). However in IDB-02, two CNV were consistently shared between resistant but absent in sensitive tumors. These were amplifications of a region of chromosome 3p, including around 50 exons from 4 genes, and a region of chromosome 12p including 23 megabases, from 12p13.31 to 12p11.21 and 225 genes (chr12p, Figure 2B and Table 3). Amplification of the same chr12 region was also detected in the human metastatic sample of origin (Figure 2B and Table 3). Chr12p amplification includes two small regions that were initially amplified in sensitive tumors with three copies (Figure 2B – C and Table 3), but they were overamplified in resistant IDB-02 tumors and also in metastatic sample of origin (Figure 2B and Table 3) and a central region showing amplification only in the resistant tumors and the human metastasis. Then we focused on this chr12p amplified region.

Gene expression analysis was previously conducted in both sensitive and resistant TNBC PDX models by Agilent platform (unpublished data). Using this microarray data obtained from three sensitive and three resistant independent IDB-02 tumors indirect validation of chr12p amplification was carried out. Taking into account the overexpressed genes from the entire chromosome 12 in resistant tumors as compared to sensitive (25 out of 1382), and the overexpressed genes located at chr12p amplified region (16 out of 225), a statistical analysis estimated that there was a correlation between amplification and overexpression (Supplementary figure 2C). A direct validation of DNA amplification was performed in additional sensitive and resistant IDB-02 tumors not previously

characterized by exome sequencing. For this purpose three different exonic Taqman probes against exonic regions of genes located at different positions in the chr12p amplified region were selected (Figure 2C) taking into account three criteria: distribution throughout the chr12p amplified region; genes with potential function in resistance; and localized in the diploid or amplified copy number region in sensitive IDB-02 tumors (Figure 2C). Then the *GABARAPL1*, *ETV6* and *KLHL42* exonic probes were selected accomplishing these criteria. The three genomic probes demonstrated to be amplified in chemoresistant compared to chemosensitive IDB-02 tumors (Figure 2D), validating chr12p region as amplified.

Amplification in chr12p is a common chromosomal alteration detected in different types of cancer, as testicular germ cell tumors (Litchfield et al., 2016), CLL (Coll-Mulet and Gil, 2009), ovarian (Network, 2012), but also in some breast tumors (Natrajan et al., 2009a). Here we show for the first time that chr12p amplification in basal-like breast cancer associates with docetaxel resistance in paired sensitive and resistant TNBC PDX tumors.

Identification of gene expression changes associated to chr12p during resistance and residual disease

Amplification is one known mechanism of many that cancer uses to overexpress genes involved in oncogenesis and drug resistance in breast and other types of cancer (Lockwood et al., 2008; Reichenberger et al., 2005; Suriano et al., 2005). Gene expression data suggested that genes located in the amplified chr12p region were associated with being overexpressed. Then, trying to find functional candidate genes involved in chemoresistance,gene expression analysis from genes located in amplified chr12p region in additional sensitive and resistant IDB-02 tumors were conducted. For that purpose, 6 out 16 genes differentially expressed by microarray data and 4 additional ones scattered, functionally interesting genes in the amplified chr12p region (Figure 2C) were selected. As shown in Figure 3A all the analyzed genes showed a trend to be overexpressed in chemoresistant IDB-02R tumors as compared to IDB-02S, which was significant for GABARAPL1, ETV6 and MGST1 . Taking into account that amplification of chr12p in resistant IDB-02 tumors implies one copy gain (Figure 2B), expected gene expression changes will be minimal. The fact that all the analyzed genes from chr12p amplified region come in the same direction strengthen the idea that chr12p amplification leads to gene overexpression, as not always CNV associates with changes in gene expression (Jia et al., 2016).

Intratumoral heterogeneity in breast cancer is an accepted phenomenon and breast tumor subclones harbouring different genomic profiles show different grade of response to treatment, being enriched the chemoresistant subclones after neoadjuvant chemotherapy treatment (Yates et al., 2015; Yu et al., 2007). Suggested by the presence of the amplification in the human metastasis which was heavily treated with taxanes, we hypothesized that chr12p amplification was diluted during engraftment and serial passages in the absence of docetaxel, being undetectable in IDB-02S tumorsand enriched after continuous exposure to docetaxel treatment. To test this hypothesis DNA copy number and mRNA expression levels were analyzed by qPCR and qRT-PCR, repectively, in IDB-02 sensitive tumors after three to four doses of docetaxel treatment, when tumors were shrinking (Supplementary Figure S3A). We found that in residual disease there was no chr12p copy number gain associated to the three screened genes, but copy number variability was highly reduced compared to untreated tumors (Supplementary Figure S3B). However, some genes located at

chr12p amplified region showed increased gene expression in docetaxel treated compared to untreated tumors (Figure 3B). Decrease in copy number variability in residual disease of sensitive IDB-02 tumors demonstrates a selection of a definite population. This population has no amplification of chr12p region but it shows overexpression of genes encoded in that chr12p region.

To evaluate whether genes located in chr12p region are overexpressed in residual disease from other TNBC PDX tumors, expression analysis in residual disease after short-term *in vivo* treatment with docetaxel in 2 additional TNBC PDX tumors was conducted (VHIO98 and the BRCA1 mutant VHIO127 (Gómez-Miragaya et al., 2017)). A gene expression increase in most of the analyzed genes located in the chr12p region was found in these additional basal-like PDXs (Figure 3C) indicating a common pattern between different TNBC PDX tumors during residual disease. These data suggestthat overexpression of some chr12p-located genes is selected after taxane treatment in a subset of TNBC. Interestingly, the gene encoding the mannose-6-phosphate receptor (*M6PR*) was overexpressed in chemoresistant but also in all residual disease PDX models, suggesting a potential role for this gene in taxane resistance.

Taken together, these results evidence an association between docetaxel resistance tumors and chr12p amplification and/or overexpression of genes encoded in that region. The fact that chr12p amplification is present in the human metastasis of origin, diluted masked in sensitive IDB-02 tumors and reappears in resistant IDB-02R tumors suggests that the amplification identifies a subclonal population that is overcome by the non-amplified chr12p population during long term drug interruption. We recently described for the first time in breast cancer this phenomenon called “drug holidays” for chemotherapy regimens using TNBC PDXs (Gómez-Miragaya et al., 2017). No selection of a population harbouring chr12p amplification was shown after docetaxel treatment in IDB-02 tumors but overexpression of chr12p-located genes was observed. It has been recently described that genomic “targetable” alterations were not enriched in tumors after neoadjuvant chemotherapy during residual disease (Goetz et al., 2017), what could be related with no chr12p amplification detection during residual disease in our model. It has been proposed that modulation of gene expression has a central role and that it is different and dynamic during cellular adaptation to short- or long-term environmental changes, with extensive regulation occurring at both the transcriptional and post-transcriptional level (López-Maury et al., 2008). So in an evolutionary manner, at short term it will be easier to select a population expressing genes just to survive to short-term chemotherapy treatment (residual disease state); while after a long-term exposure to the drug, it will be easier to select the population harbouring the amplification for the survival genes to get a rapid response to treatment (chemoresistant tumor state), similar to what occurs with memory immune cells. For that, we propose chemoresistance acquisition in a two-step model: first, selection of a population overexpressing genes associated to taxane resistance , and second, selection of a population with chr12p amplification as a mechanism to maintain high expression of these genes.

Basal-like breast cancer tumors harbouring chr12p amplification show a gene expression signature of chemoresistance to docetaxel

In the last years, curated datasets of breast cancer have been widely used to demonstrate association of genes or sets of genes with clinical outcomes and to elucidate useful biomarkers (Wu et al., 2017; Xu et al., 2016; Yen et al., 2017). To better understand the importance of chr12p amplification in the clinical setting, we queried the cBioPortal (Cerami et al., 2012; Gao et al., 2013)

for patients from TCGA and METABRIC studies with alterations in genes located at different regions of chr12p. We selected *GABARAPL1*, *ETV6* and *KLHL42* genes for the study due to their location at different chr12p regions, their amplification and overexpression in chemoresistant IDB-02 tumors and that trend to be overexpressed in TNBC PDX during residual disease. Similarly to chr12p amplification, amplification of *GABARAPL1*, *ETV6* and *KLHL42* occurred in a high proportion of testicular germ cell tumors, ovarian and lung tumors (Supplementary Figure S4A). In around 4% of breast tumors amplifications of these 3 genes were detected, with relative consistency between breast cancer datasets (Supplementary Figure S4A).

METABRIC dataset was selected because it includes a higher number of samples and more curated information about tumor subtype, patient status and follow-up. Amplification of *ETV6, GABARAPL1 and KLHL42* tends to co-occur in METABRIC breast cancer patients (Supplementary Table 1), but also there is a significant co-occurrence of amplification between these three genes and all the genes from the chr12p amplified region (Supplementary Table 2),. Analyses of breast cancer samples in METABRIC (or TCGA) did not revealed amplification of minimal region, suggesting that the whole 12p arm is co-amplified. This data also suggest that selection of these three amplified genes can be used as markers of chr12p amplification in METABRIC breast cancer patients, simplifying the analysis.

To know if this amplification was enriched in any molecular breast cancer subtype using not only invasive ductal carcinomas, 3 gene-classifier subtype and PAM50 subtype were used in the whole cohort of METABIRC breast cancer patients. Association between chr12p amplification and ER-status (5 – 10% vs 2%, Supplementary Figure S4B) and basal-like and claudin-low subtypes (5 – 10% vs 2%, Figure 4B), the most aggressive subtypes among breast cancer, was found. Also the tumors harbouring amplification of chr12p showed increased gene expression of those amplified genes (Supplementary Figure S4C). These results are in agreement with previous finding of Natrajan et al using an immunohistochemical panel of markers (Natrajan et al., 2009b). Moreover, basal-like tumors with amplification on chr12p had associated other chromosomal alterations, such as chr5q (Natrajan et al., 2009b) which is also observed in IDB-02R PDX model. In our study we have heavily increased the number of breast cancer patients analysed (Natrajan et al., 2009, n=95; METABRIC, 2016, n=2051) and we have associated this genotype to *BRCA1*-mutated breast cancer patients (data not shown).

Overall survival was predicted to be 50% lower in breast cancer patients retaining amplification and gain in chr12p (Figure 4C). If the analysis is performed specifically in the basal-like and claudin-low subtypes, where the amplification and gain is more frequent, chr12p seems to predict a lower percentage of overall survival mainly between 50 and 150 months (Supplementary Figure S4DB), indicating again the high aggressiveness of tumors harbouring chr12p amplification even within the basal-like subtype.

Finally, for the purpose to extract a gene expression signature related with amplification of chr12p that could be associated with chemotherapy resistance to docetaxel, gene expression data from METABRIC was screened. Comparison of basal-like and claudin-low tumors harbouring or not chr12p amplification revealed many genes detected as differentially expressed with statistically significance (Supplementary Table 3). DAVID bioinformatics analysis (https://david.ncifcrf.gov/) conducted with the 500 most differentially expressed genes demonstrates that there is a subset of ER-, basal-

like/claudin-low breast cancer tumors harbouring chr12p amplification that show a gene expression profile enriched for cell cycle, mitosis, cell division and cytoskeletal pathways (Supplementary Figure 4E and Supplementary Table 4).

Ten different integrative clusters (IntClust) have been described on breast cancer clinical tumors based on germline variants and somatic aberration that were associated with alterations in gene expression (Curtis et al., 2012; Dawson et al., 2013). Each IntClust correlates with different CNV and gene expression changes, affecting CNV not only to *cis* but also to *trans* gene expression changes. Also each IntClust associates with distinct clinical features and outcomes (Dawson et al., 2013). IntClust10 includes mostly triple-negative/basal-like tumors with poor prognosis characterized by 5q loss and 8q, 10p and 12p gain. This group of tumors represent a high-risk group during the first 5 years after diagnoses but they also show better pCR, associate to young women, high histological grade, high Nothingam prognostic index, poorly differentiated tumors and high mitotic index. Also Curtis and colleagues showed that these tumors are enriched for DNA damage repair and apoptosis genes, as *BCL2*, *IGF1R* and *AURKB* (Curtis et al., 2012). Here our investigation suggest that patients classified as IntClust10 and with chr12p amplification may not respond to taxane therapy and we hypothesize that they would benefit from treatment with other chemotherapy regimens, mainly DNA damaging agents. We hypothesize also that chr12p amplification is the key as the rest of the IntClust10 associated CNV were present in the sensitive PDX IDB-02. Clinical trials dividing tumors harbouring all CNV of IntClust10 and with chr12p amplification in arms treated with or without taxanes would be needed to validate this hypothesis.

References

Balko, J.M., Cook, R.S., Vaught, D.B., Kuba, M.G., Miller, T.W., Bhola, N.E., Sanders, M.E., Granja-Ingram, N.M., Smith, J.J., Meszoely, I.M., et al. (2012). Profiling of residual breast cancers after neoadjuvant chemotherapy identifies DUSP4 deficiency as a mechanism of drug resistance. Nat. Med. *18*, 1052–1059.

Balko, J.M., Giltnane, J.M., Wang, K., Schwarz, L.J., Young, C.D., Cook, R.S., Owens, P., Sanders, M.E., Kuba, M.G., Sánchez, V., et al. (2014). Molecular profiling of the residual disease of triple-negative breast cancers after neoadjuvant chemotherapy identifies actionable therapeutic targets. Cancer Discov. *4*, 232–245.

Balko, J.M., Schwarz, L.J., Cook, R.S., Estrada, M.V., Giltnane, J.M., Sanders, M.E., Sánchez, V., Dean, P.T., Wang, K., Combs, S.E., et al. (2016). Triple negative breast cancers with amplification of JAK2 at the 9p24 loci demonstrate JAK2-specific dependence. Sci. Transl. Med. *8*, 334ra53.

Banerji, S., Cibulskis, K., Rangel-Escareno, C., Brown, K.K., Carter, S.L., Frederick, A.M., Lawrence, M.S., Sivachenko, A.Y., Sougnez, C., Zou, L., et al. (2012). Sequence analysis of mutations and translocations across breast cancer subtypes. Nature *486*, 405–409.

Bauer, J.A., Chakravarthy, A.B., Rosenbluth, J.M., Mi, D., Seeley, E.H., Granja-Ingram, N.D.M., Olivares, M.G., Kelley, M.C., Mayer, I.A., Meszoely, I.M., et al. (2010). Identification of Markers of Taxane Sensitivity Using Proteomic and Genomic Analyses of Breast Tumors from Patients Receiving Neoadjuvant Paclitaxel and Radiation. Clin. Cancer Res. *16*, 681–690.

Bruna, A., Rueda, O.M., Greenwood, W., Batra, A.S., Callari, M., Batra, R.N., Pogrebniak, K., Sandoval, J., Cassidy, J.W., Tufegdzic-Vidakovic, A., et al. (2016). A Biobank of Breast Cancer Explants with Preserved Intra-tumor Heterogeneity to Screen Anticancer Compounds. Cell *167*, 260–274.e22.

Byrne, A.T., Alférez, D.G., Amant, F., Annibali, D., Arribas, J., Biankin, A.V., Bruna, A., Budinská, E., Caldas, C., Chang, D.K., et al. (2017). Interrogating open issues in cancer precision medicine with patient-derived xenografts. Nat. Rev. Cancer *17*, 254–268.

Cerami, E., Gao, J., Dogrusoz, U., Gross, B.E., Sumer, S.O., Aksoy, B.A., Jacobsen, A., Byrne, C.J., Heuer, M.L., Larsson, E., et al. (2012). The cBio Cancer Genomics Portal: An Open Platform for Exploring Multidimensional Cancer Genomics Data. Cancer Discov. *2*, 401–404.

Coll-Mulet, L., and Gil, J. (2009). Genetic alterations in chronic lymphocytic leukaemia. Clin. Transl. Oncol. Off. Publ. Fed. Span. Oncol. Soc. Natl. Cancer Inst. Mex. *11*, 194–198.

Curtis, C., Shah, S.P., Chin, S.-F., Turashvili, G., Rueda, O.M., Dunning, M.J., Speed, D., Lynch, A.G., Samarajiwa, S., Yuan, Y., et al. (2012). The genomic and transcriptomic architecture of 2,000 breast tumours reveals novel subgroups. Nature *486*, 346–352.

Dawson, S.-J., Rueda, O.M., Aparicio, S., and Caldas, C. (2013). A new genome-driven integrated classification of breast cancer and its implications. EMBO J. *32*, 617–628.

Dent, R., Trudeau, M., Pritchard, K.I., Hanna, W.M., Kahn, H.K., Sawka, C.A., Lickley, L.A., Rawlinson, E., Sun, P., and Narod, S.A. (2007). Triple-negative breast cancer: clinical features and patterns of recurrence. Clin. Cancer Res. Off. J. Am. Assoc. Cancer Res. *13*, 4429–4434.

Dobrolecki, L.E., Airhart, S.D., Alferez, D.G., Aparicio, S., Behbod, F., Bentires-Alj, M., Brisken, C., Bult, C.J., Cai, S., Clarke, R.B., et al. (2016). Patient-derived xenograft (PDX) models in basic and translational breast cancer research. Cancer Metastasis Rev. *35*, 547–573.

Eirew, P., Steif, A., Khattra, J., Ha, G., Yap, D., Farahani, H., Gelmon, K., Chia, S., Mar, C., Wan, A., et al. (2015). Dynamics of genomic clones in breast cancer patient xenografts at single cell resolution. Nature *518*, 422–426.

Foulkes, W.D., Smith, I.E., and Reis-Filho, J.S. (2010). Triple-negative breast cancer. N. Engl. J. Med. *363*, 1938–1948.

Gao, J., Aksoy, B.A., Dogrusoz, U., Dresdner, G., Gross, B., Sumer, S.O., Sun, Y., Jacobsen, A., Sinha, R., Larsson, E., et al. (2013). Integrative analysis of complex cancer genomics and clinical profiles using the cBioPortal. Sci. Signal. *6*, pl1.

Gay-Bellile, M., Romero, P., Cayre, A., Véronèse, L., Privat, M., Singh, S., Combes, P., Kwiatkowski, F., Abrial, C., Bignon, Y., et al. (2016). ERCC1 and telomere status in breast tumours treated with neoadjuvant chemotherapy and their association with patient prognosis. J. Pathol. Clin. Res. *2*, 234–246.

Geenen, J.J.J., Linn, S.C., Beijnen, J.H., and Schellens, J.H.M. (2017). PARP Inhibitors in the Treatment of Triple-Negative Breast Cancer. Clin. Pharmacokinet. 1–11.

Goetz, M.P., Kalari, K.R., Suman, V.J., Moyer, A.M., Yu, J., Visscher, D.W., Dockter, T.J., Vedell, P.T., Sinnwell, J.P., Tang, X., et al. (2017). Tumor Sequencing and Patient-Derived Xenografts in the Neoadjuvant Treatment of Breast Cancer. JNCI J. Natl. Cancer Inst. *109*.

Gómez-Miragaya, J., Palafox, M., Paré, L., Yoldi, G., Ferrer, I., Vila, S., Galván, P., Pellegrini, P., Pérez-Montoyo, H., Igea, A., et al. (2017). Resistance to Taxanes in Triple-Negative Breast Cancer Associates with the Dynamics of a CD49f+ Tumor-Initiating Population. Stem Cell Rep. *8*, 1392–1407.

Györffy, B., Serra, V., Jürchott, K., Abdul-Ghani, R., Garber, M., Stein, U., Petersen, I., Lage, H., Dietel, M., and Schäfer, R. (2005). Prediction of doxorubicin sensitivity in breast tumors based on gene expression profiles of drug-resistant cell lines correlates with patient survival. Oncogene *24*, 7542–7551.

Hidalgo, M., Amant, F., Biankin, A.V., Budinská, E., Byrne, A.T., Caldas, C., Clarke, R.B., de Jong, S., Jonkers, J., Mælandsmo, G.M., et al. (2014). Patient-derived xenograft models: an emerging platform for translational cancer research. Cancer Discov. *4*, 998–1013.

Hu, X., Stern, H.M., Ge, L., O'Brien, C., Haydu, L., Honchell, C.D., Haverty, P.M., Peters, B.A., Wu, T.D., Amler, L.C., et al. (2009). Genetic Alterations and Oncogenic Pathways Associated with Breast Cancer Subtypes. Mol. Cancer Res. *7*, 511–522.

Ismail-Khan, R., and Bui, M.M. (2010). A review of triple-negative breast cancer. Cancer Control J. Moffitt Cancer Cent. *17*, 173–176.

Järvinen, T.A.H., Tanner, M., Rantanen, V., Bärlund, M., Borg, Å., Grénman, S., and Isola, J. (2000). Amplification and Deletion of Topoisomerase IIα Associate with ErbB-2 Amplification and Affect Sensitivity to Topoisomerase II Inhibitor Doxorubicin in Breast Cancer. Am. J. Pathol. *156*, 839–847.

Jeselsohn, R., Buchwalter, G., De Angelis, C., Brown, M., and Schiff, R. (2015). ESR1 mutations—a mechanism for acquired endocrine resistance in breast cancer. Nat. Rev. Clin. Oncol. *12*, 573–583.

Jia, Y., Chen, L., Jia, Q., Dou, X., Xu, N., and Liao, D.J. (2016). The well-accepted notion that gene amplification contributes to increased expression still remains, after all these years, a reasonable but unproven assumption. J. Carcinog. *15*.

Kadalayil, L., Rafiq, S., Rose-Zerilli, M.J.J., Pengelly, R.J., Parker, H., Oscier, D., Strefford, J.C., Tapper, W.J., Gibson, J., Ennis, S., et al. (2015). Exome sequence read depth methods for identifying copy number changes. Brief. Bioinform. *16*, 380–392.

Kristensen, V.N., Lingjærde, O.C., Russnes, H.G., Vollan, H.K.M., Frigessi, A., and Børresen-Dale, A.-L. (2014). Principles and methods of integrative genomic analyses in cancer. Nat. Rev. Cancer *14*, 299–313.

Lee, J.K., Havaleshko, D.M., Cho, H., Weinstein, J.N., Kaldjian, E.P., Karpovich, J., Grimshaw, A., and Theodorescu, D. (2007). A strategy for predicting the chemosensitivity of human cancers and its application to drug discovery. Proc. Natl. Acad. Sci. U. S. A. *104*, 13086–13091.

Li, H., and Durbin, R. (2009). Fast and accurate short read alignment with Burrows-Wheeler transform. Bioinforma. Oxf. Engl. *25*, 1754–1760.

Li, H., Handsaker, B., Wysoker, A., Fennell, T., Ruan, J., Homer, N., Marth, G., Abecasis, G., Durbin, R., and 1000 Genome Project Data Processing Subgroup (2009). The Sequence Alignment/Map format and SAMtools. Bioinforma. Oxf. Engl. *25*, 2078–2079.

Li, S., Shen, D., Shao, J., Crowder, R., Liu, W., Prat, A., He, X., Liu, S., Hoog, J., Lu, C., et al. (2013). Endocrine-Therapy-Resistant ESR1 Variants Revealed by Genomic Characterization of Breast-Cancer-Derived Xenografts. Cell Rep. *4*, 1116–1130.

Liedtke, C., Wang, J., Tordai, A., Symmans, W.F., Hortobagyi, G.N., Kiesel, L., Hess, K., Baggerly, K.A., Coombes, K.R., and Pusztai, L. (2010). Clinical evaluation of chemotherapy response predictors developed from breast cancer cell lines. Breast Cancer Res. Treat. *121*, 301–309.

Litchfield, K., Levy, M., Huddart, R.A., Shipley, J., and Turnbull, C. (2016). The genomic landscape of testicular germ cell tumours: from susceptibility to treatment. Nat. Rev. Urol. *13*, 409–419.

Lockwood, W., Chari, R., Coe, B., Girard, L., MacAulay, C., Lam, S., Gazdar, A., Minna, J., and Lam, W. (2008). DNA amplification is a ubiquitous mechanism of oncogene activation in lung and other cancers. Oncogene *27*, 4615–4624.

López-Maury, L., Marguerat, S., and Bähler, J. (2008). Tuning gene expression to changing environments: from rapid responses to evolutionary adaptation. Nat. Rev. Genet. *9*, 583–593.

Miller, T.W., Balko, J.M., and Arteaga, C.L. (2011). Phosphatidylinositol 3-Kinase and Antiestrogen Resistance in Breast Cancer. J. Clin. Oncol. *29*, 4452–4461.

Natrajan, R., Lambros, M.B., Rodríguez-Pinilla, S.M., Moreno-Bueno, G., Tan, D.S.P., Marchió, C., Vatcheva, R., Rayter, S., Mahler-Araujo, B., Fulford, L.G., et al. (2009a). Tiling Path Genomic Profiling of Grade 3 Invasive Ductal Breast Cancers. Clin. Cancer Res. *15*, 2711–2722.

Natrajan, R., Lambros, M.B., Rodríguez-Pinilla, S.M., Moreno-Bueno, G., Tan, D.S.P., Marchió, C., Vatcheva, R., Rayter, S., Mahler-Araujo, B., Fulford, L.G., et al. (2009b). Tiling Path Genomic Profiling of Grade 3 Invasive Ductal Breast Cancers. Clin. Cancer Res. *15*, 2711–2722.

Network, T.C.G.A. (2012). Comprehensive molecular portraits of human breast tumours. Nature *490*, 61–70.

Oakman, C., Viale, G., and Leo, A.D. (2010). Management of triple negative breast cancer. The Breast *19*, 312–321.

Paolillo, C., Mu, Z., Rossi, G., Schiewer, M.J., Nguyen, T., Austin, L., Capoluongo, E., Knudsen, K.E., Cristofanilli, M., and Fortina, P. (2017). Detection of Activating Estrogen Receptor Gene (ESR1) Mutations in Single Circulating Tumor Cells. Clin. Cancer Res. Off. J. Am. Assoc. Cancer Res.

Puente, X.S., Pinyol, M., Quesada, V., Conde, L., Ordóñez, G.R., Villamor, N., Escaramis, G., Jares, P., Beà, S., González-Díaz, M., et al. (2011). Whole-genome sequencing identifies recurrent mutations in chronic lymphocytic leukaemia. Nature *475*, 101–105.

Reichenberger, K.J., Coletta, R.D., Schulte, A.P., Varella-Garcia, M., and Ford, H.L. (2005). Gene Amplification Is a Mechanism of *Six1* Overexpression in Breast Cancer. Cancer Res. *65*, 2668–2675.

Rexer, B.N., and Arteaga, C.L. (2012). Intrinsic and acquired resistance to HER2-targeted therapies in HER2 gene-amplified breast cancer: mechanisms and clinical implications. Crit. Rev. Oncog. *17*, 1–16.

Scaltriti, M., Eichhorn, P.J., Cortés, J., Prudkin, L., Aura, C., Jiménez, J., Chandarlapaty, S., Serra, V., Prat, A., Ibrahim, Y.H., et al. (2011). Cyclin E amplification/overexpression is a mechanism of trastuzumab resistance in HER2+ breast cancer patients. Proc. Natl. Acad. Sci. U. S. A. *108*, 3761–3766.

Serratì, S., De Summa, S., Pilato, B., Petriella, D., Lacalamita, R., Tommasi, S., and Pinto, R. (2016). Next-generation sequencing: advances and applications in cancer diagnosis. OncoTargets Ther. *9*, 7355–7365.

Shah, S.P., Roth, A., Goya, R., Oloumi, A., Ha, G., Zhao, Y., Turashvili, G., Ding, J., Tse, K., Haffari, G., et al. (2012). The clonal and mutational evolution spectrum of primary triple-negative breast cancers. Nature *486*, 395–399.

Stephens, P.J., Tarpey, P.S., Davies, H., Van Loo, P., Greenman, C., Wedge, D.C., Nik-Zainal, S., Martin, S., Varela, I., Bignell, G.R., et al. (2012). The landscape of cancer genes and mutational processes in breast cancer. Nature *486*, 400–404.

Stevens, K.N., Vachon, C.M., and Couch, F.J. (2013). Genetic Susceptibility to Triple-Negative Breast Cancer. Cancer Res. *73*, 2025–2030.

Sun, Z., Shi, Y., Shen, Y., Cao, L., Zhang, W., and Guan, X. (2015). Analysis of different HER-2 mutations in breast cancer progression and drug resistance. J. Cell. Mol. Med. *19*, 2691–2701.

Suriano, G., Vrcelj, N., Senz, J., Ferreira, P., Masoudi, H., Cox, K., Nabais, S., Lopes, C., Machado, J.C., Seruca, R., et al. (2005). beta-catenin (CTNNB1) gene amplification: a new mechanism of protein overexpression in cancer. Genes. Chromosomes Cancer *42*, 238–246.

Valdés-Mas, R., Bea, S., Puente, D.A., López-Otín, C., and Puente, X.S. (2012). Estimation of copy number alterations from exome sequencing data. PloS One *7*, e51422.

Walerych, D., Lisek, K., Sommaggio, R., Piazza, S., Ciani, Y., Dalla, E., Rajkowska, K., Gaweda-Walerych, K., Ingallina, E., Tonelli, C., et al. (2016). Proteasome machinery is instrumental in a

common gain-of-function program of the p53 missense mutants in cancer. Nat. Cell Biol. *18*, 897–909.

Whittle, J.R., Lewis, M.T., Lindeman, G.J., and Visvader, J.E. (2015). Patient-derived xenograft models of breast cancer and their predictive power. Breast Cancer Res. *17*, 17.

Wu, H.-T., Liu, J., Li, G.-W., Shen, J.-X., and Huang, Y.-T. (2017). The transcriptional STAT3 is a potential target, whereas transcriptional STAT5A/5B/6 are new biomarkers for prognosis in human breast carcinoma. Oncotarget *8*, 36279–36288.

Xu, Z., Shen, J., Wang, M.H., Yi, T., Yu, Y., Zhu, Y., Chen, B., Chen, J., Li, L., Li, M., et al. (2016). Comprehensive molecular profiling of the B7 family of immune-regulatory ligands in breast cancer. Oncoimmunology *5*, e1207841.

Yates, L.R., Gerstung, M., Knappskog, S., Desmedt, C., Gundem, G., Loo, P.V., Aas, T., Alexandrov, L.B., Larsimont, D., Davies, H., et al. (2015). Subclonal diversification of primary breast cancer revealed by multiregion sequencing. Nat. Med. *21*, 751–759.

Yen, M.-C., Kan, J.-Y., Hsieh, C.-J., Kuo, P.-L., Hou, M.-F., and Hsu, Y.-L. (2017). Association of long-chain acyl-coenzyme A synthetase 5 expression in human breast cancer by estrogen receptor status and its clinical significance. Oncol. Rep. *37*, 3253–3260.

Yu, F., Yao, H., Zhu, P., Zhang, X., Pan, Q., Gong, C., Huang, Y., Hu, X., Su, F., Lieberman, J., et al. (2007). let-7 Regulates Self Renewal and Tumorigenicity of Breast Cancer Cells. Cell *131*, 1109–1123.

Figure 1

A

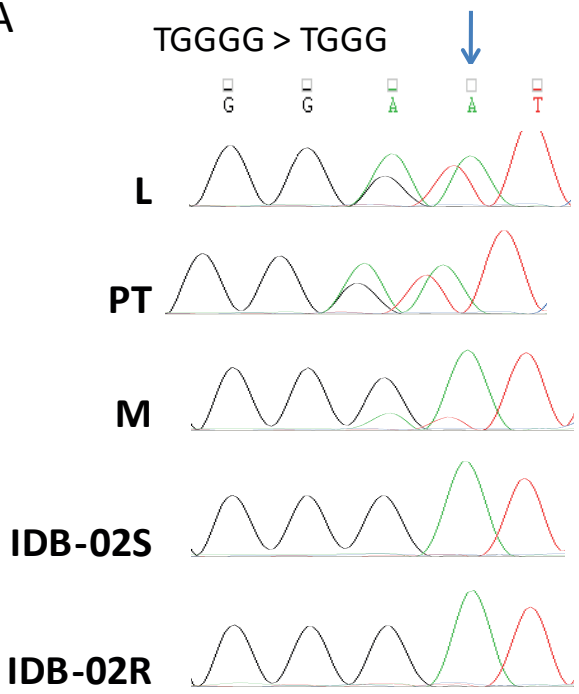
TGGGG > TGGG
G
G
A
A
T
L
PT
M
IDB-02S
IDB-02R

B

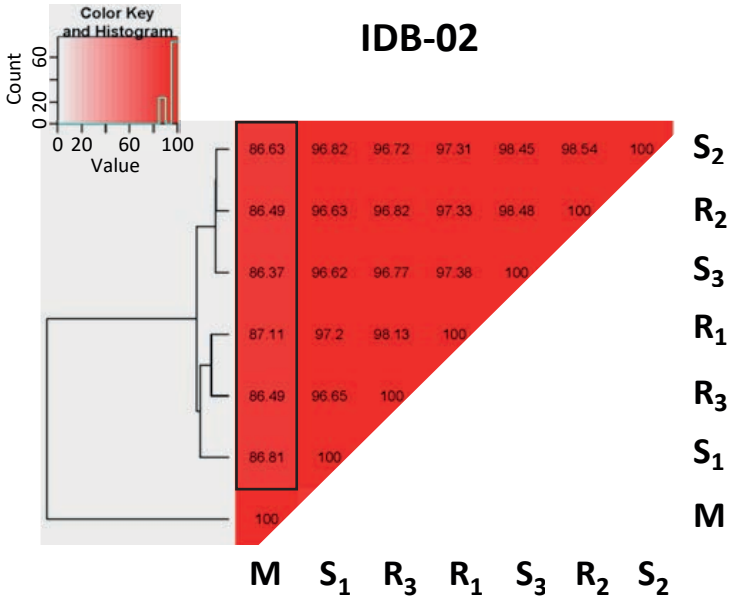
Color Key and Histogram
Count
0 20 60
0 20 60 100
Value
IDB-02
86.63 96.82 96.72 97.31 98.45 98.54 100
86.49 96.63 96.82 97.33 98.48 100
86.37 96.62 96.77 97.38 100
87.11 97.2 98.13 100
86.49 96.65 100
86.81 100
100
S2
R2
S3
R1
R3
S1
M
M S1 R3 R1 S3 R2 S2

C

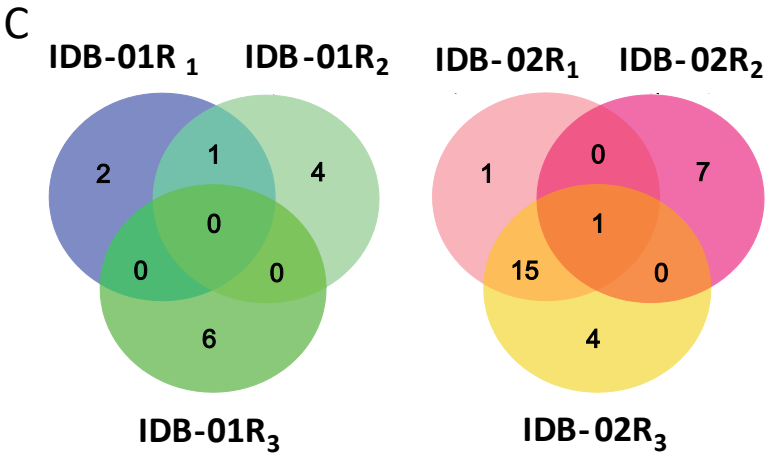
IDB-01R 1
IDB-01R2
IDB-02R1
IDB-02R2
2
1
4
0
0
0
6
1
0
7
1
15
0
4
IDB-01R3
IDB-02R3

Figure 2

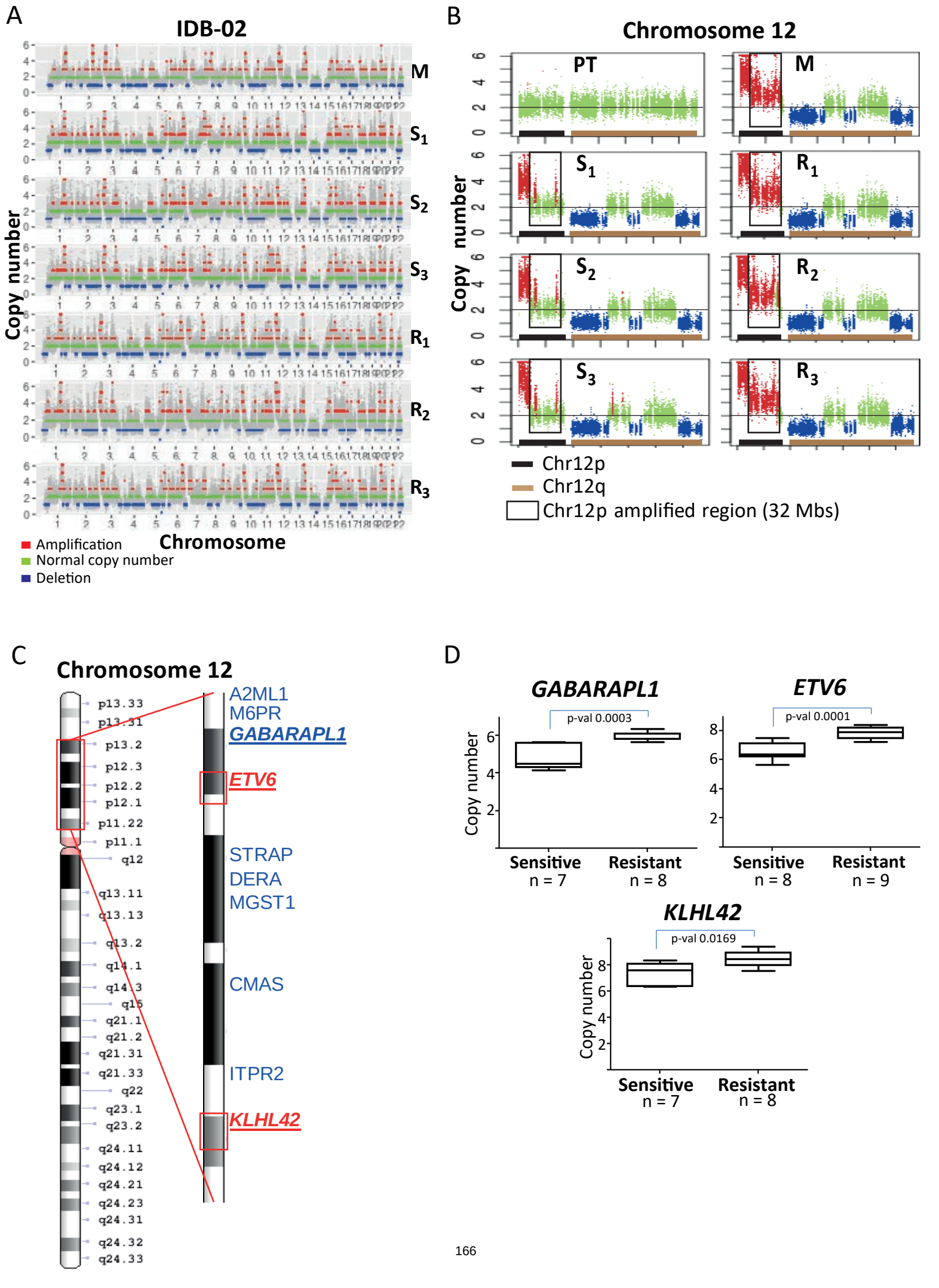
A
IDB-02
M
S1
S2
S3
R1
R2
R3
Copy number
Chromosome
Amplification
Normal copy number
Deletion
B
Chromosome 12
PT
M
S1
R1
S2
R2
S3
R3
Copy number
Chr12p
Chr12q
Chr12p amplified region (32 Mbs)
C
Chromosome 12
A2ML1
M6PR
GABARAPL1
ETV6
STRAP
DERA
MGST1
CMAS
ITPR2
KLHL42
D
GABARAPL1
p-val 0.0003
Copy number
Sensitive
n = 7
Resistant
n = 8
ETV6
p-val 0.0001
Sensitive
n = 8
Resistant
n = 9
KLHL42
p-val 0.0169
Copy number
Sensitive
n = 7
Resistant
n = 8

Figure 3

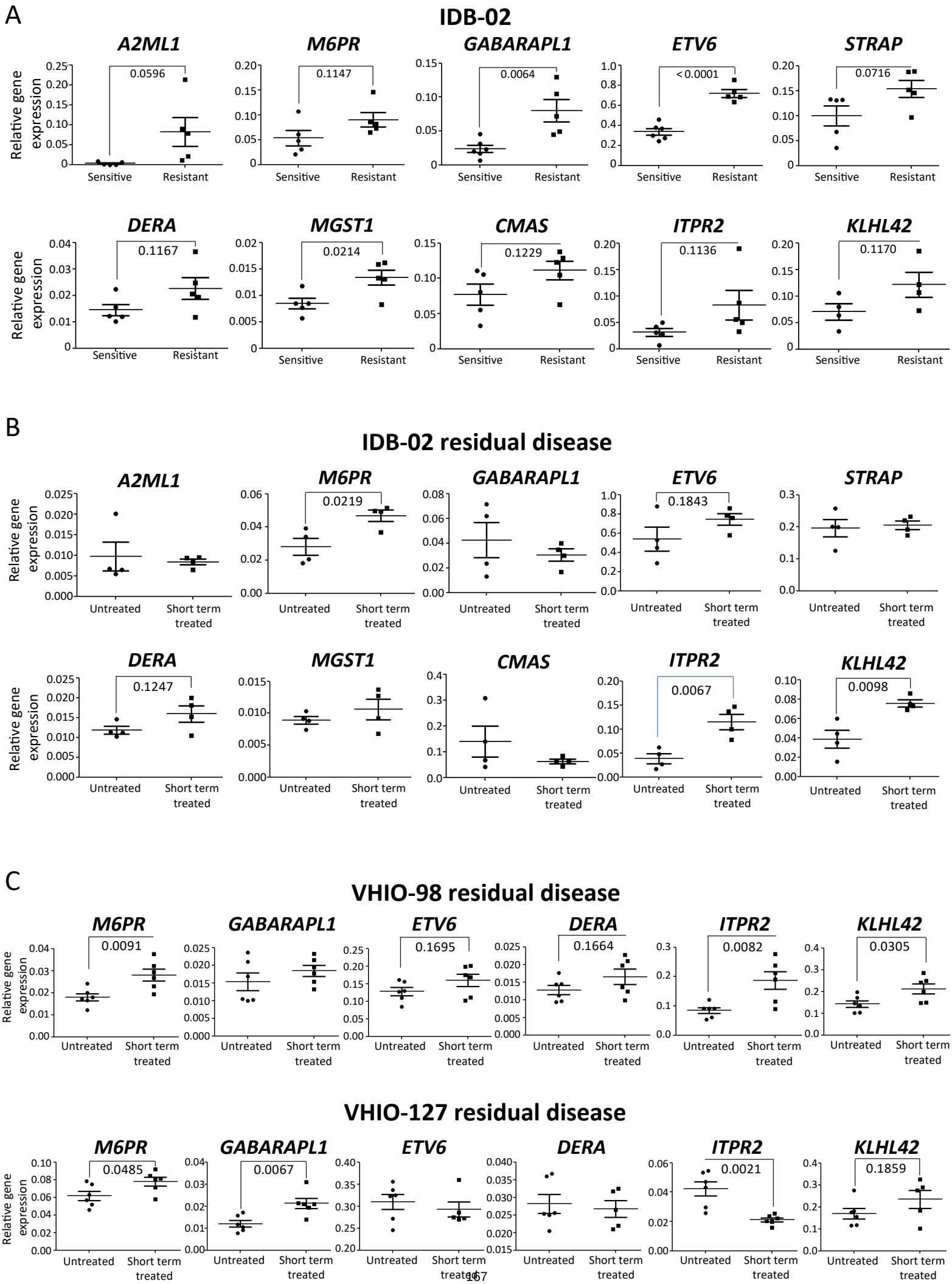
A
IDB-02
A2ML1
M6PR
GABARAPL1
ETV6
STRAP
DERA
MGST1
CMAS
ITPR2
KLHL42
Relative gene expression
0.0596
0.1147
0.0064
< 0.0001
0.0716
0.1167
0.0214
0.1229
0.1136
0.1170
Sensitive
Resistant
B
IDB-02 residual disease
0.0219
0.1843
0.1247
0.0067
0.0098
Untreated
Short term treated
C
VHIO-98 residual disease
0.0091
0.1695
0.1664
0.0082
0.0305
VHIO-127 residual disease
0.0485
0.0067
0.0021
0.1859

Figure 4

A

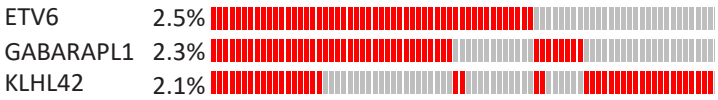

B

PAM50 + claudin-low subtype

	Deep Deletion	Shallow Deletion	Diploid	Gain	Amplification	
ETV6 copy number	1	39	102	29	27	Basal
	2	49	150	16	1	Her2
	1	52	588	32	0	LumA
	1	74	345	33	1	LumB
	0	2	4	0	0	NC
	0	19	109	7	0	Normal
	1	25	134	10	12	Claudin-low
GABARAPL1 copy number	1	37	103	34	23	Basal
	1	48	154	13	2	Her2
	1	44	597	31	0	LumA
	0	67	353	33	1	LumB
	0	2	4	0	0	NC
	0	17	111	7	0	Normal
	1	25	134	12	10	Claudin-low
KLHL42 copy number	41	115	26	16		Basal
	44	148	17	9		Her2
	28	608	34	3		LumA
	45	369	37	3		LumB
	1	5	0	0		NC
	12	115	7	1		Normal
	23	140	15	4		Claudin-low

C

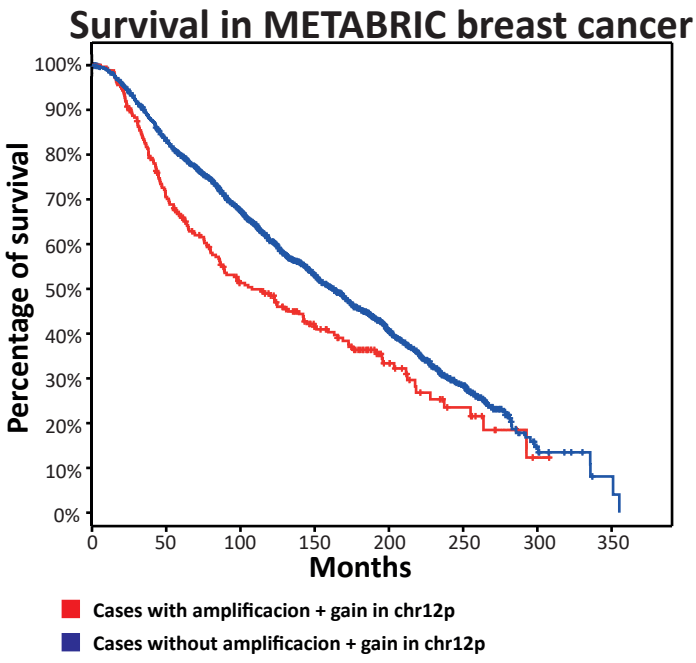

Log-rank t-test p-value: 2.632e-4

	Total cases	Deceased cases	Median months survival
Chr12p amplified + gain	249	156	107.8
Chr12p non-amplified + gain	1731	987	162.8

Supplementary Figure 1

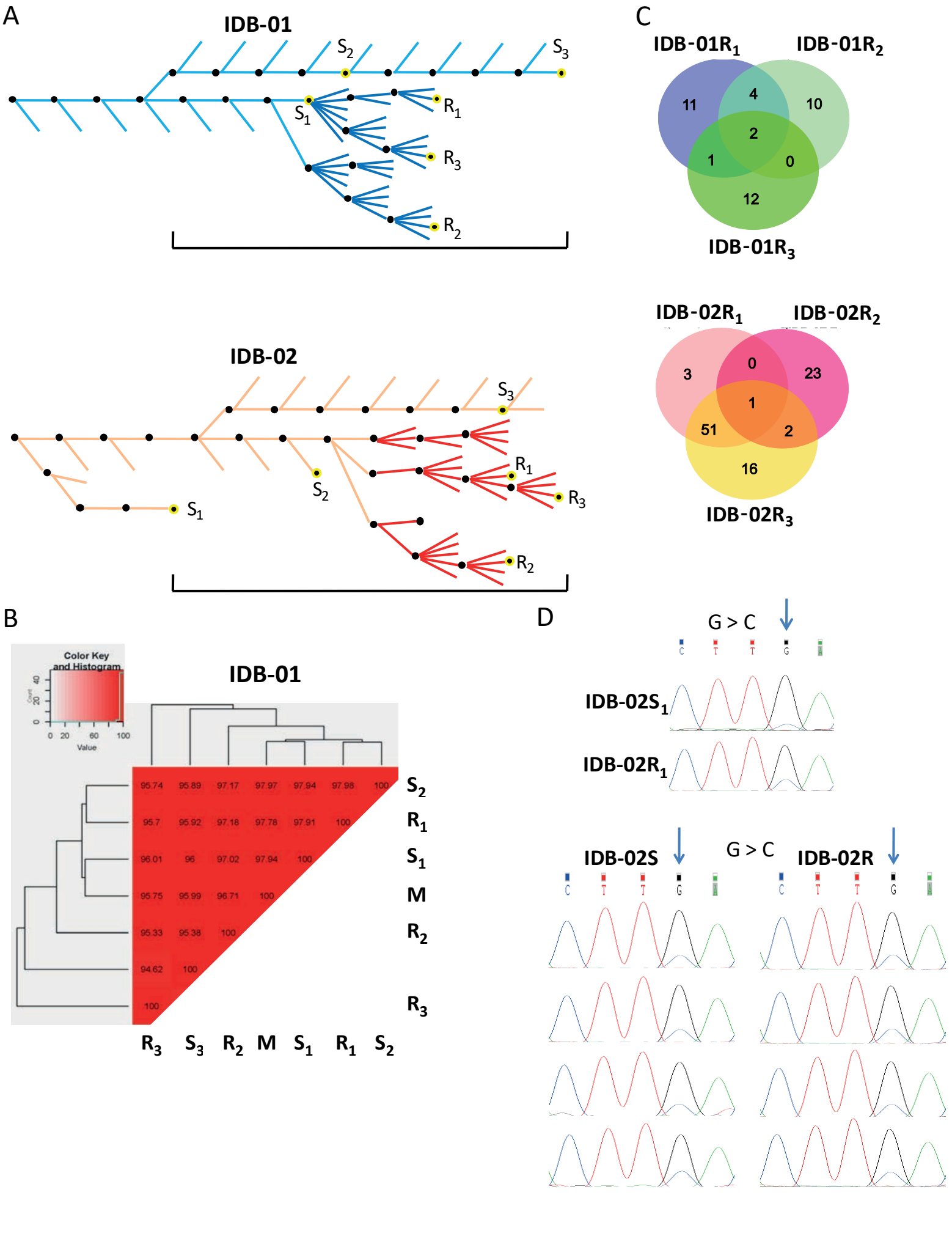

Supplementary Figure 2

A

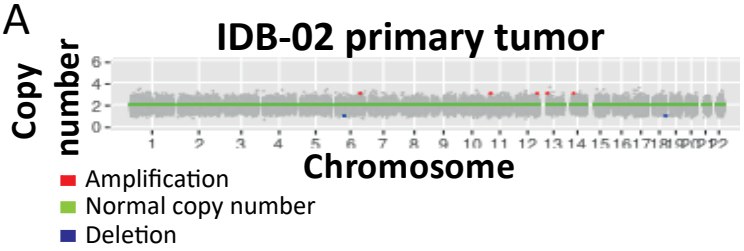

B

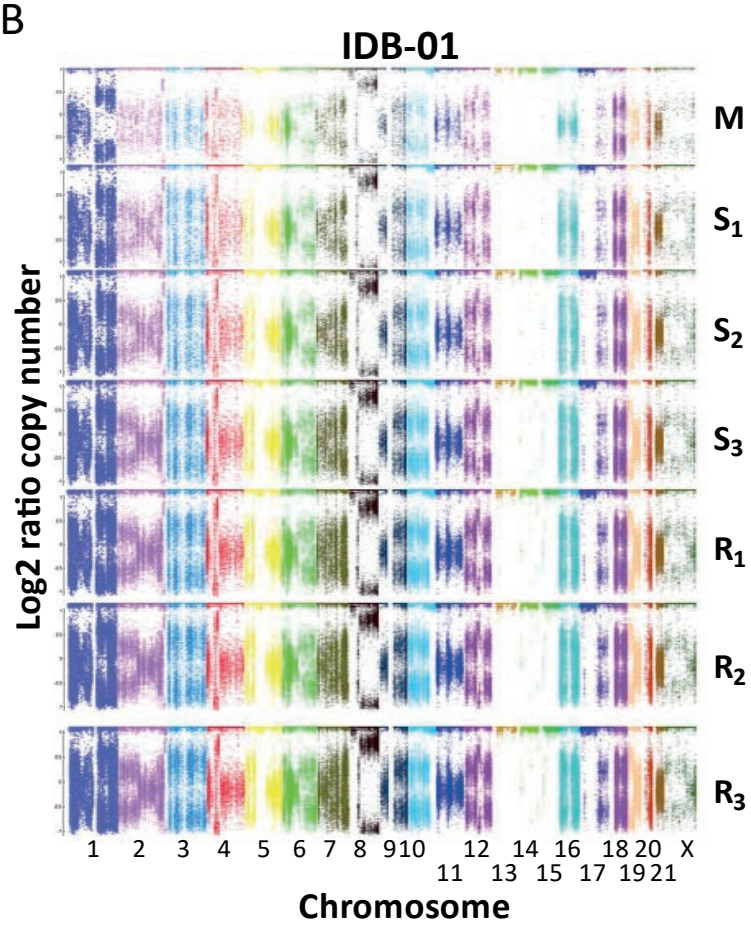

C

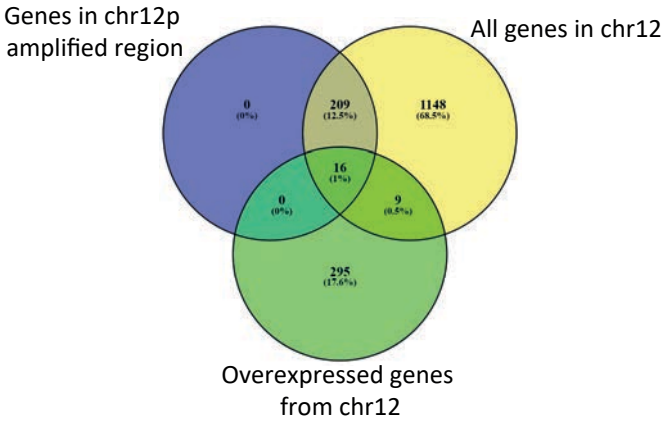

	Total genes	Overexpressed genes	*Marginal Rox Totals*
All chr12	1382 (1372) [0.07]	25 (35) [2.86]	1407
Chr12p	225 (235) [0.43]	16 (6) [16.69]	241
Marginal Column Totals	1607	41	1648 (Grand Total)

chi-square 20.0507

p-value $8x10^{-6}$

Supplementary Figure 3

A

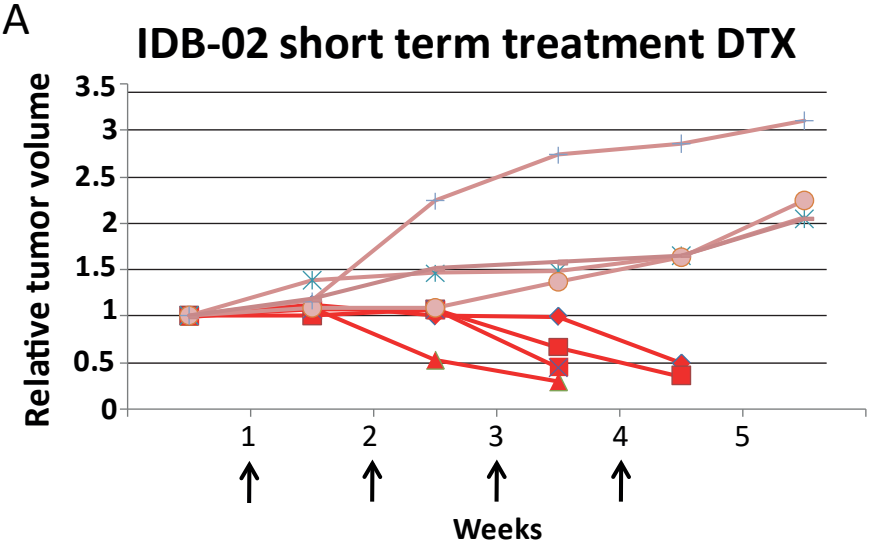

B

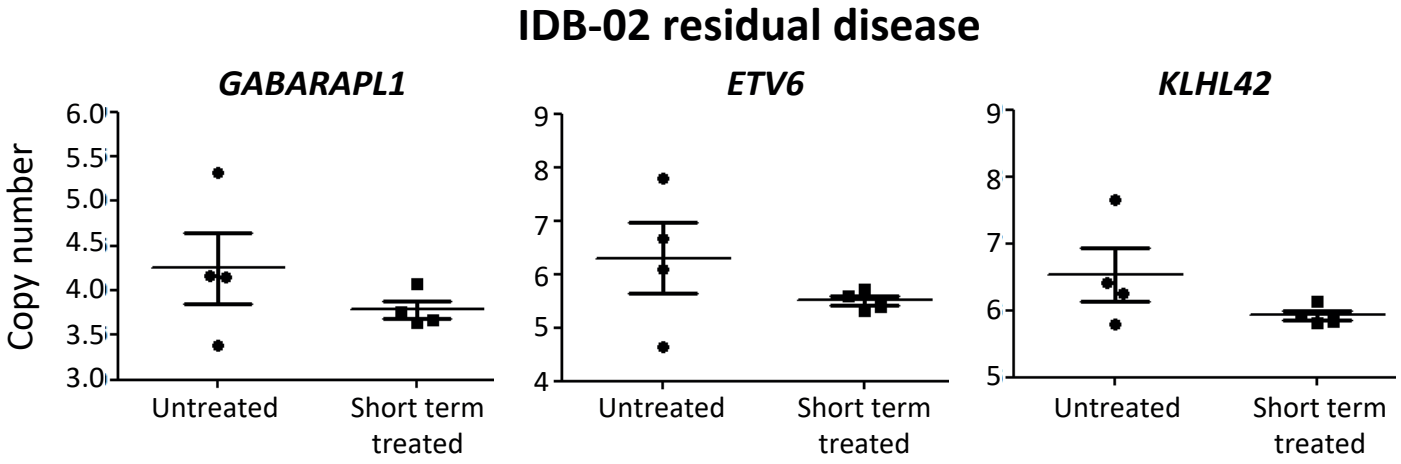

Supplementary Figure 4

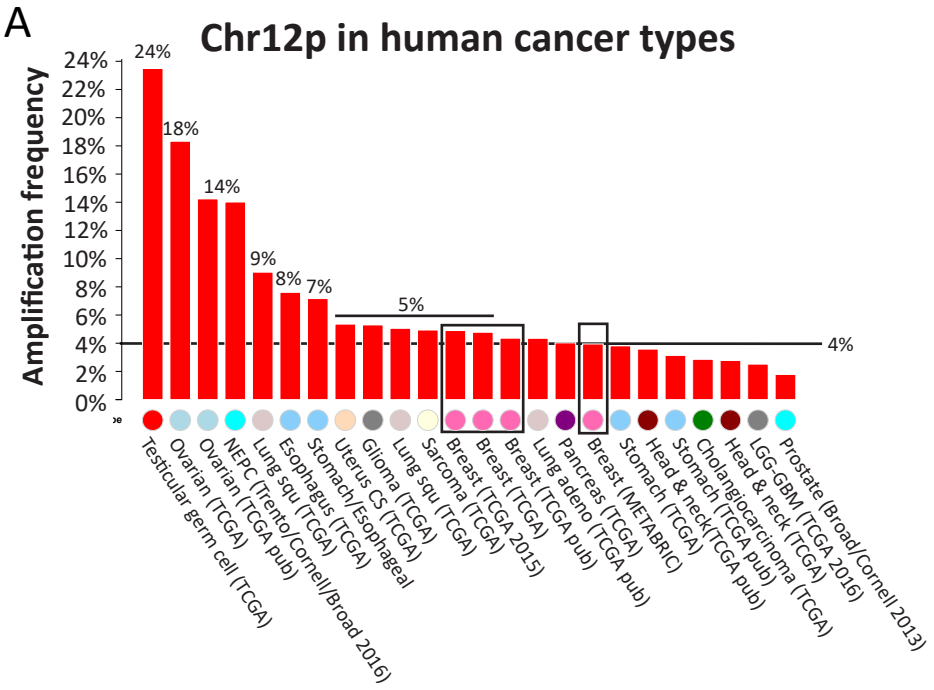

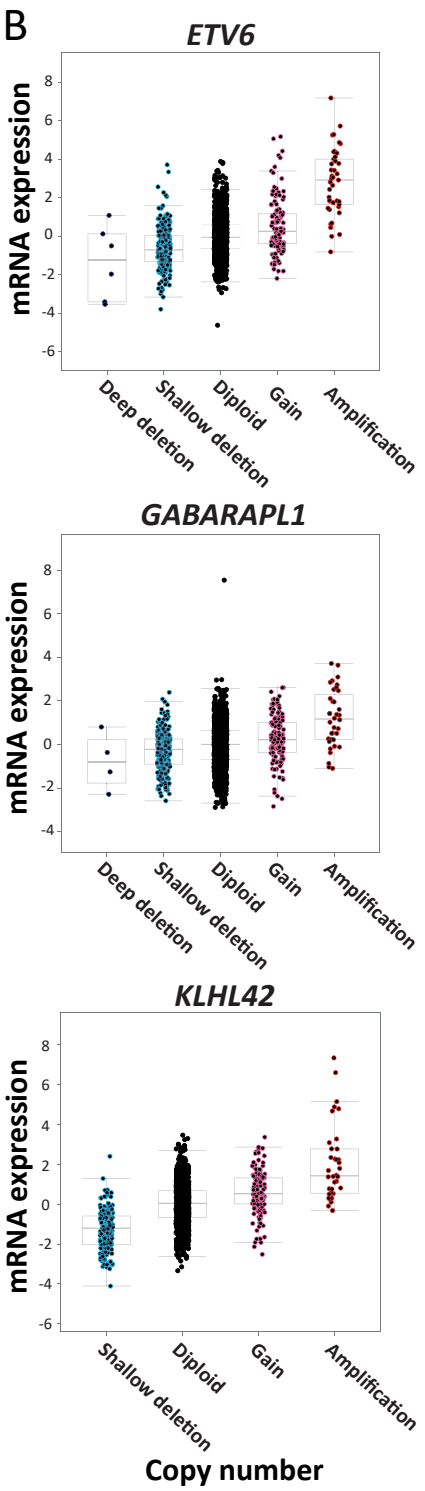

C

3-Gene classifier subtype

Deep Deletion	Shallow Deletion	Diploid	Gain	Amplification	
2	91	452	50	1	ER+/HER2- High Prolif
0	43	550	14	2	ER+/HER2- Low Prolif
2	55	160	33	29	ER-/HER2-
1	42	130	9	1	HER2+

ETV6 copy number

1	80	461	53	1	ER+/HER2- High Prolif
0	38	557	12	2	ER+/HER2- Low Prolif
1	54	162	40	22	ER-/HER2-
1	40	133	7	2	HER2+

GABARAPL1 copy number

54	478	56	8	ER+/HER2- High Prolif
25	569	14	1	ER+/HER2- Low Prolif
55	176	34	14	ER-/HER2-
38	129	9	7	HER2+

KLHL42 copy number

D

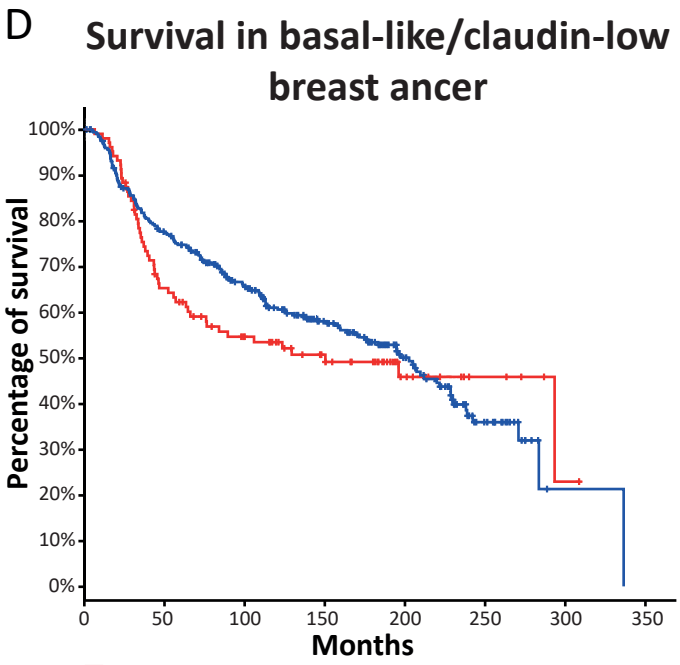

	Total cases	Deceased cases	Median months survival
Chr12p amplified + gain	48	24	105
Chr12p non-amplified + gain	379	185	202

E

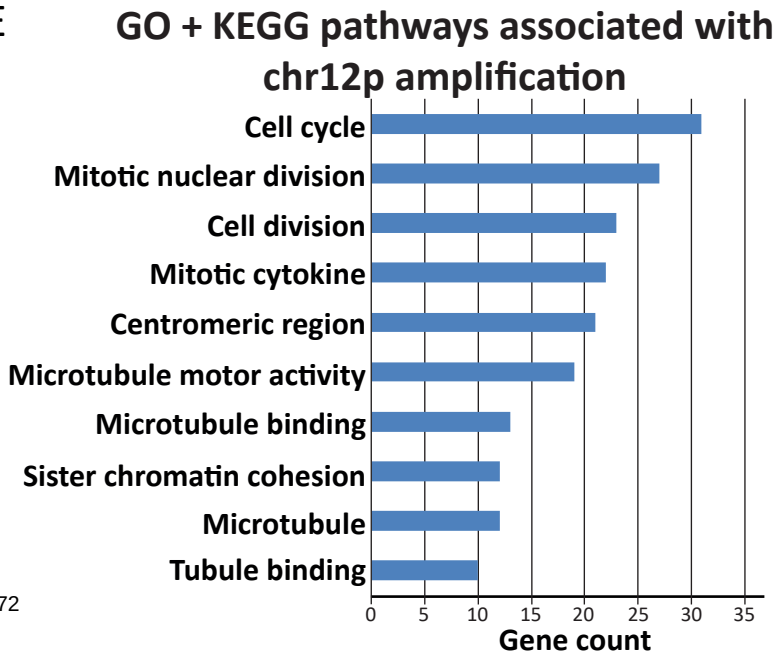

Figure legends

Figure 1. Point mutations or small INDELs are not associated to docetaxel chemoresistance acquisition in TNBC PDX. A) Sanger sequencing traces for *BRCA1* point mutation inducing a frameshift in IDB-02 PDX tumors and samples from patient. *L*, lymphocytic DNA; *PT*, primary tumor DNA; *M*, pleural effusion metastases. **B)** Unsupervised hierarchical clustering using genotype similarity extracted from whole-exome sequencing data between the human metastatic sample of origin, sensitive and resistant TNBC PDX tumors from IDB-02. Note sensitive and resistant samples do not cluster separately. The percentage of similarity between metastasis and the IDB-02 PDX model is framed. **C)** Venn's diagrams showing the comparisons between point mutations or small INDELs potentially affecting protein function present in the three resistant PDX tumors and absent in metastases or sensitive PDX tumors from IDB-01 (left) and IDB-02 (right).

Figure 2. High copy number stability during passages and acquisition of resistance to docetaxel in model IDB-02 and amplification of chr12p in resistant tumors. A) Copy number analysis performed in the human metastasis of origin (M) and sensitive (S) and resistant (R) IDB-02 PDX tumors compared to normal lymphocytic DNA from the pacient.. **B)** Zoom in on chromosome 12 of the primary tumor (PT), metastasis of origin (M) and sensitive (S) and resistant (R) tumors from IDB-02 compared to normal lymphocytic DNA. Amplifications are indicated in red while deletions are indicated in blue. Chromosome 12p amplified region in chemoresistant tumors was indicated, as well as chr12p and chr12q regions. **C)** Idiogram showing chromosome 12 relative size and its banding pattern used to describe the location of genes in the chromosome. Amplified region in IDB-02R tumors is highlighted and genes analyzed by Taqman probe (in italics and underlined) and qRT-PCR are distributed across the amplification. The amplified regions in IDB-02S and overamplified in IDB-02R tumors are also highlighted by red boxes and genes included in that region are indicated (in italics, underlined and red). **D**) Copy number analysis by qPCR using three different Taqman probes for the indicated genes located at different genomic positions of chr12p in sensitive and resistant IDB-02 tumors relative to RNAase P copies. Number of copies was divided by half, as RNAase P is located in 5p which losses 1 copy. Number of analyzed tumors, mean values, box and whiskers (min tomax) and t test p values are shown.

Figure 3. Overexpression of genes located at chr12p amplification in IDB-02R and IDB-02S and additional basal like PDX models during residual disease. mRNA expression levels of indicated genes located at chr12p amplification relative to *PPiA* in IDB-02S and IDB-02R tumors (**A**) or in IDB-02S control and after short term treatment (**B**) by qRT-PCR. Each dot represents a tumor. Mean, SEM and t-test p-values are indicated. **C)** mRNA expression levels of indicated geneslocated at chr12p amplification relative to *PPiA*in sensitive control and after short term treatment in two additional basal-like PDX models VHIO-98 and VHIO-127 (BRCA1 mutant). Each dot represents a tumor. Mean, SEM and t-test p-values are indicated.

Figure 4. Integrative genomic analysis using cBioPortal of samples from METABRIC and TCGA clinical setting. A) Representation of breast tumors from METABRIC dataset harbouring amplification and gain of three selected genes located at chr12p amplified region. **B)** Association between copy number of three selected genes located at chr12p amplified region and PAM50 + claudin-low molecular subtype in METABRIC dataset. **C)** Overall survival analysis of METABRIC dataset patients separated by harboring or not the amplification and gain of *ETV6, GABARAP and*

KLH42 genes located at chr12p amplified region. Number of cases, median month's survival and log-rank t-test p value are indicated.

Supplementary Figure S1. *BRCA1* mutation validation in IDB-02 model and common point mutations or small INDELs present in docetaxel chemoresistance TNBC PDX. A) Diagrams showing the transplant history from IDB-01 and IDB-02 TNBC PDX models. Black spheres indicate the passage of a tumor to another set of mice. Clear lines correspond to sensitive tumors while dark lines correspond to docetaxel treated tumors during chemoresistance acquisition. Tumors used for whole exome sequencing are indicated with a yellow circle and the name. Tumors used for Sanger sequencing validation are indicated with a line under genealogical tree. **B)** Unsupervised hierarchical clustering using genotype similarity extracted from whole-exome sequencing data between metastatic sample of origin, sensitive and resistant TNBC PDX tumors from IDB-01. Note sensitive and resistant samples do not cluster separately. **C)** Venn's diagrams showing the comparisons between point mutations or small INDELs present in the three resistant PDX tumors and absent in metastases or sensitive PDX tumors from IDB-01 and IDB-02 . **D)** Sanger sequencing traces for *KLHL42* point mutation in sensitive (left) and resistant (right) IDB-02 tumors. Arrows indicate the changed base and expected > alternative nucleotide was indicated at the top.

Supplementary Figure S2. High copy number stability during passages and acquisition of resistance to docetaxel in model IDB-01 and indirect validation of chr12p amplification using microarray data for IDB-02 model. A) Copy number analysis performed between primary tumor and normal lymphocytic DNA in IDB-02.. Note high normal stromal DNA in primary tumor drives genotype. **B)** Copy number analysis performed in metastasis of origin (M) and sensitive (S) and resistant (R) IDB-01 PDX tumors compared to a human non transformed genome of reference **C)** Venn's diagrams showing the comparisons between all genes located and overexpressed in chromosome 12 and specifically in chr12p amplification in IDB-02 model. Chi square t test p value demonstrating significance is shown.

Supplementary Figure S3. Tumor regression during docetaxel treatment in sensitive IDB-02 tumors. A) Relative tumor volume over time in sensitive untreated (pink) and sensitive docetaxel-treated (red) IDB-02 tumors. Mice were sacrificed one week after the last dose and at end point tumors were collected. Each line represents a tumor and arrows indicate the doses of docetaxel.
B) Copy number analysis using three different Taqman probes for the indicated genes of the amplifiedchr12p region in IDB-02S control and after short term treatment by qPCR. Each dot represents a tumor. Mean, SEM are indicated.

Supplementary Figure S4. Integrative genomic analysis using cBioPortal of samples from METABRIC and TCGA clinical setting. A) Representation of the most common cancer types harboring amplification of three selected genes located in chr12p amplified region. Black line indicate amplifications in breast cancer samples in different databases. **B)** Association between copy number and mRNA expression levels of three selected genes located at chr12p amplified region in METABRIC dataset. Each dot represents a tumor. Box and whiskers (min to max) and SEM are shown. **C)** Association between copy number of three selected genes located at chr12p amplified region and 3-gene classifier subtype in METABRIC dataset. **D)** Overall survival analysis of basal-like and claudin-low subtype METABRIC dataset patients separated by harboring or not the amplification or gain of three selected genes located at chr12p amplified region. Number of cases, median survival and log-

rank t-test p value was indicated. **E)** Representation of the most significantly altered pathways by differential gene expression between breast cancer tumors with or without chromosome 12p amplification from METABRIC.

Table 1. Somatic point mutations in the human metastatic sample of origin and derived PDX from model IDB-02. L, lymphocytes; PT, primary tumor; M, metastasis; IDB-02S, sensitive PDX tumors; IDB-02R, PDX tumors with acquired resistance to docetaxel .

Table 2. Putative somatic point mutations estimated in the human metastatic sample of origin and derived PDX from model IDB-01. M, metastasis. IDB-01S, sensitive PDX tumors; IDB-01R, PDX tumors with acquired resistance to docetaxel .

Table 3. Copy number variations (CNV) in the human metastatic sample of origin and derived PDX from model IDB-02. M, metastasis; IDB-02S, sensitive PDX; IDB-02R, resistant PDX. Colors indicate: Grey, common CNV between metastasis and PDX tumors; green, common CNV between PDX tumors absent in metastasis; red, specific CNV present in resistant PDX tumors and absent in sensitive PDX tumors.

Table 4. Copy number variations (CNV)estimated in metastatic sample of origin and PDX model IDB-01. Green, common CNV between PDX tumors absent in metastasis.M, metastasis; IDB-01S, sensitive PDX; IDB-01R, resistant PDX.

Supplementary Table 1. Co-ocurrence and mutual exclusivity analysis of alterations in queried genes: *ETV6, GABARAPL1* and *KLH42*.

Supplementary Table 2. Analysis of co-ocurrence and mutual exclusivity enrichment of copy number variation in breast cancers with alteration in the queried genes *ETV6, GABARAPL1* and *KLH42*.

Supplementary Table 3. Analysis of differential gene expression enrichment in breast cancers with alterations in the queried genes *ETV6, GABARAPL1* and *KLH42* compared to unaltered breast cancers.

Supplementary Table 4. Analysis of KEGG pathways and gene ontology terms of differentially expressed genes in breast cancers with alteration in the queried genes ETV6, GABARAPL1 and KLH42 compared to unaltered breast cancers.

ARTICLE 4

“Identification of epigenetic and transcriptomic pathways leading docetaxel resistance acquisition in triple-negative breast cancer patient derived xenografts”

Identification of epigenetic and transcriptomic pathways leading docetaxel resistance acquisition in triple-negative breast cancer patient derived xenografts

Jorge Gómez-Miragaya[1], Sebastián Morán[1], Maria Eréndira Calleja-Cervantes[1], Antonio Gómez[1], Laia Paré[2], Aleix Prat[3], Manel Esteller[1,4,5], Eva González-Suárez[1,*]

[1] Cancer Epigenetics and Biology Program (PEBC), Bellvitge Biomedical Research Institute (IDIBELL), Avinguda de la Gran Via, 199 – 203, L'Hospitalet deLlobregat, 08908 Barcelona, Spain

[2] Translational Genomics and Targeted Therapeutics in Solid Tumors, August Pi i Sunyer Biomedical Research Institute (IDIBAPS), 08036 Barcelona, Spain.

[3] Translational Genomics and Targeted Therapeutics in Solid Tumors, August Pi i Sunyer Biomedical Research Institute (IDIBAPS), 08036 Barcelona, Spain; Translational Genomics Group, Vall d'Hebron Institute of Oncology (VHIO), 08035 Barcelona, Spain.

[4] Department of Physiological Sciences II, School of Medicine, University of Barcelona, Barcelona, Catalonia, Spain.

[5] Institució Catalana de Recerca i Estudis Avançats, Barcelona, Catalonia, Spain.
[*] Corresponding author: Eva González Suárez.

Cancer Epigenetics and Biology Program, Bellvitge Institute for Biomedical Research, IDIBELL.
Av.Gran Via de L'Hospitalet, 199. 08908 L'Hospitalet de Llobregat. Barcelona. Spain
egsuarez@idibell.cat www.pebc.cat Phone: +34 932607139 Fax: +34 932607219

Abstract

Chemotherapy is a general treatment for most breast tumors and depending on breast cancer subtype combination with targeted anti-hormonal or anti-HER2 therapy is conducted. Chemoresistance relapse and metastatic disease are common events and count on being the main cause of death. Aiming to elucidate docetaxel-associated chemoresistance mechanisms, genome-wide DNA methylation and gene expression analysis have been performed in preclinical breast cancer patient-derived xenograft (PDX) models with primary and acquired chemoresistance. These analyses revealed that DNA methylation patterns from breast cancer PDX are closer to breast cancer clinical samples than breast cancer cell lines (BCCLs) and they maintain subtype specific methylation patterns. Triple negative PDX tumors show very stable methylation patterns accompanying chemoresistance acquisition but some critical genes/pathways were unraveled as differentially methylated. Transcriptomically, triple negative PDX tumors accumulate gene expression changes during chemoresistance acquisition with some common pathways between different triple negative PDX models. Integrative analysis reveals correlation of some differentially methylated genes as differentially expressed in resistant triple negative breast cancer PDX tumors. These findings identify a set of promising pathways that may contribute to the acquisition of chemoresistance in TNBC patients.

Introduction

Breast cancer chemotherapeutic treatment is a systemic anticancer therapy that affects whole body, killing cancer cells at the original cancer site and those that may have spread to another part of the body (Rapoport et al., 2014). Different chemotherapy regimens are used in combination, and also combined with targeted therapies for the treatment of some breast cancer subtypes (Rapoport et al., 2014). Triple-negative breast cancer (TNBC), the most heterogeneous and aggressive subtype of breast cancer, is associated with poor prognosis (Dent et al., 2007; Foulkes et al., 2010) and has higher rates of response to neoadjvant chemotherapy than other breast cancer subtypes (Liedtke et al., 2008). Despite initial responses, complete cure is not assured and relapse or metastatic disease become chemoresistant in some patients. Although new treatments have been developed during last years, metastatic resistant form of breast cancer has a 5-year survival rate of around 25% (Tai et al., 2004; http://seer.cancer.gov/csr/1975_2010/). In order to benefit outcome and survival rates from patients, it is essential to elucidate the mechanisms of chemoresistance.

In cancer, epigenetics, which includes methylation, has been revealed as an important mechanism responsible for disease. Methylation changes can contribute to cancer development through inactivation of tumor suppressor genes and, conversely, through activation of oncogenes (Stefansson and Esteller, 2013). The main breast cancer-associated methylation change is hypermethylation of tumor suppressor genes, as *BRCA1*, but also other genes as *CDH1*, *RARB2* and *GSTP1* (Stefansson and Esteller, 2013). Methylation has been also revealed as an important clinical marker of drug treatment and resistance in breast cancer, as acquired methylation of *BRCA1* is an epigenetic marker of good response to PARP inhibitors (Stefansson and Esteller, 2013) and DNA methylation of several other genes has been consistently associated with prognosis, acting as promising biomarkers in patients with distinct breast cancer subtypes (Győrffy et al., 2016). That points out the importance and relevance of DNA methylation in breast cancer studies in clinics.

Patient-derived xenografts (PDX) have been proposed as a preferred tool for conducting basic and translational preclinical research, being closer to patient tumors and recapitulating intra- and inter-tumoral heterogeneity that is reflected in human cancers (Byrne et al., 2017; Dobrolecki et al., 2016). Breast cancer PDX maintain not only histopathological features from human tumors but also retain main genomic, transcriptomic and proteomic profiles and drug response (Byrne et al., 2017; Network, 2012). However, methylation patterns of breast cancer PDX and their correlation with human breast tumors have never been studied. Multiple studies support the relevance of PDX models as powerful preclinical tools for the study of resistance mechanisms but it is necessary to determine if breast cancer methylation patterns are represented and maintained in PDX to establish their suitability for preclinical methylation studies.

Taxanes are considered among the most active classes of compounds against TNBC and metastatic breast cancer (King et al., 2009; O'Shaughnessy, 2005). Docetaxel, a taxane chemotherapeutic agent used broadly for treatment of different cancer types, acts by binding to microtubuls and avoiding tubulin subunits depolimerazation, inducing cell cycle arrest and apoptosis (Herbst and Khuri, 2003). Many general mechanisms have been suggested to confer

docetaxel resistance for different cancer types, as prostate (Lohiya et al., 2016), gastric (Kubo et al., 2016), ovarian (Duran et al., 2017) and non-small cell lung cancer (Wang et al., 2017a). In breast cancer, the most well known chemoresistance mechanism is the modulation of drug efflux proteins, which limits drug efficacy by removal at their site of action (Brooks et al., 2003; Murray et al., 2012). Circumvention or blocking resistance using small molecule inhibitors of drug efflux proteins have being tried in clinics with limited success (Murray et al., 2012). Other molecular mechanisms of docetaxel resistance implying gene expression deregulation or epigenetic mechanisms have been proposed (Dong et al., 2015; Kastl et al., 2010; Kulkarni et al., 2009; Rouzier et al., 2005; Wang et al., 2017a). However, most of these studies were performed *in vitro* using breast cancer cell lines (BCCL), the predictive value of which has been discussed because of the absence of correlation between BCCLs and clinical outcome (Byrne et al., 2017; Dobrolecki et al., 2016). Therefore, mechanisms of resistance to docetaxel are understudied and further investigations are urgently required. However, paired clinical samples before and after acquisition of resistance are difficult to obtain, limiting the viability of these studies.

We have generated a panel of five breast cancer PDX comprising all histopathological subtypes: two TNBC (IDB-01 and IDB-02, being the last one *BRCA1* mutant), two luminal (IDB-03 and IDB-04, being the first one *BRCA2* mutant) and an ER+PR+HER2+ (IDB-05) PDX models. Mimicking the clinical scenario, TNBC PDX models respond to docetaxel treatment while luminal PDX models proved to be resistant. Moreover, after *in vivo* continuous exposure to the chemotherapeutic agent, initially sensitive TNBC PDX models become resistant and do not respond to treatment (Gómez-Miragaya et al., 2017). These paired sensitive and resistant TNBC PDX models solve the gap between *in vitro* results and clinical samples, and constitute powerful tools to differentiate passenger from driver changes contributing to docetaxel chemoresistance.

We hypothesize that epigenetic and transcriptional changes contribute to the acquisition of chemoresistance to docetaxel in TNBC patients. Here we performed genome-wide DNA methylation and transcriptional analysis in our panel of PDX models and in chemoresistant derived TNBC PDX tumors. We demonstrate that human breast cancer methylation patterns are conserved in breast cancer PDX models and that global methylation is preserved during chemoresistance acquisition, with some gene-specific methylation changes detected. Transcriptionally, some genes were differentially expressed between sensitive and resistant TNBC tumors. Differentially methylated/expressed genes were associated to some important pathways. Similar pathways were found between methylation and expression analysis, suggesting that some gene expression changes are controlled by methylation during chemoresistance acquisition to docetaxel in TNBC PDX tumors, although most of the transcriptional changes identified were not related to methylation.

Materials and methods

Patient Characteristics and Generation of PDX

IDB PDX were generated by orthotopic transplantation of human fresh tumoral tissue or injection of cancer cells isolated from pleural effusions into the fat pad of immunodeficient mice, as described previously (Gómez-Miragaya et al., 2017). Generation of resistant TNBC PDX models from the original sensitive ones and maintenance of PDX models by serial transplantation in the intact fat pad of Nod/Scid mice was described previously (Gómez-Miragaya et al., 2017). All experimental procedures were performed according to Spanish regulations. Informed consent was obtained from all subjects and the study received approval from the institutional Ethics Committee. All research involving animals was performed at the IDIBELL animal facility in compliance with protocols approved by the IDIBELL Committee on Animal Care and following national and European Union regulations.

DNA extraction and RNAse treatment

Total DNA from tissue was prepared with *in house* lysis buffer (100mM NaCl, 10mM Tris-Cl pH 8, 25mM EDTA). Frozen tumor tissues were fractionated using the POLYTRON® system PT 1200 E (Kinematica) and incubated 12-16 hours with 0.25% SDS (Invitrogen, 24730020), 0.25 mg/ml Proteinase K (Sigma Aldrich, P4850) and RNAse A (Sigma Aldrich, R5503) at 55ºC in a termal block. For DNA purification, the homogenized sample was transferred to a phase lock gel heavy tube (VWR, 713-2538). Two steps of removal of proteins from nucleic acids using Phenol:Chloroform:Isoamyl Alcohol 25:24:1 (Sigma Aldrich, P3803) and three steps of nucleic acid washing with chloroform (VWR, 1024311000) were performed, centrifuging each time at 1500G during 5 minutes. After last spinning, remaining volume containing DNA was recovered and transferred to a solution containing 2.5x absolute ethanol (Merck Millipore, 1009832500) and 30 mM of sodium acetate pH 5.2 (Sigma Aldrich, S2889), mix and centrifuge at maximum for 5 minutes. Wash two times with 70% ethanol centrifuging at maximum for 5 minutes. Finally resuspension in TE buffer (10 mM Tris-HCl, 1 mM disodium EDTA, pH 8.0) or ultrapure water (MilliQ purification system) was performed. All DNA samples were quantified by the fluorometric method (Quant-iT PicoGreen dsDNA Assay, Life Technologies, CA, USA), and assessed for purity by NanoDrop-1000 Spectrophotometer (Thermo Scientific, MA, USA) 260/280 and 260/230 ratio measurements. DNA integrity of samples was checked by electrophoresis in an agarose gel.

Bisulfite conversion and genome-wide DNA methylation microarray

Two ug of purified genomic DNA were treated with sodium bisulfite using the EZ DNA methylation kit (Zymo Research, CA, USA). The incubation profile was 16 cycles at 95°C for 30 s, 50°C for 60 min and a final holding step at 4°C. 4 µl of bisulfite-converted DNA (50 ng/ul) were used for hybridization on Infinium HumanMethylation 450 BeadChip, following the Illumina Infinium HD Methylation protocol. This consisted of a whole genome amplification step followed by enzymatic end-point fragmentation, precipitation and resuspension. The resuspended samples were hybridized on HumanMethylation 450 BeadChips at 48°C for 16 h. Then unhybridized and non-specifically hybridized DNA were washed away, followed by a

single nucleotide extension using the hybridized bisulfite-treated DNA as a template. The nucleotides incorporated were labeled with biotin (ddCTP and ddGTP) and 2,4-dinitrophenol (DNP) (ddATP and ddTTP). After the singlebase extension, repeated rounds of staining were performed with a combination of antibodies that differentiated DNP and biotin by fixing them different fluorophores. Finally the BeadChip was washed and protected in order to scan it.

The Illumina HiScan SQ scanner (Illumina, CA, USA) is a two-color laser (532 nm/660 nm) fluorescent scanner with a 0.375 µm spatial resolution capable of exciting the fluorophores generated during the staining step of the protocol. The intensities of the images were extracted and raw IDAT files were processed with Illumina's GenomeStudio software. The methylation score for each CpG was represented as a β-value according to the fluorescent intensity ratio. β-values may take any value between 0 (nonmethylated) and 1 (completely methylated) and they were used for all downstream analyses. All downstream analysis was conducted using the hg19/GRCh37 human genome assembly.

Methylation clustering

Scatter plots of mean β-values for PDX models were produced to check if there was a degree of difference between the models. Afterwards, a variability filter, comparing PDX models was applied to β-values obtaining a total of 35,367 CpGs. An unsupervised heatmap representation of the PDX models was generated using those CpGs. Organizing the values by applying a hierarchical clustering method based on Manhattan distances aggregated by Ward's linkage. Methylation difference between at least one of the groups equal or higher to 75% and p-value <0.01. Among the reduced group of 35367 CpGs, 743 were differentially methylated between TNBC vs luminal subtype from TCGA breast cancer BCCLs, PDX models and TCGA clinical patients. Data from primary tumor samples were obtained from TCGA data portal (https://portal.gdc.cancer.gov/).

Unsupervised heatmap representation of the PDX models and 100 human normal mammary gland samples (from TCGA) was generated using randomly selected 1% of the CpG sites and organizing them by applying a hierarchical clustering method based on Manhattan distances aggregated by Ward's linkage

Correlation between Gene Expression Array and Methylation Array.

To study the association between gene expression and DNA methylation at gene level, data derived from both arrays was filtered to obtain the mean methylation value for each gene found in the expression array and annotated in the 450k Mehtylation Array. In the case of Methylation, CpG site probes falling on the promoter region of the known genes were considered, i.e., TSS1500, TSS200, 5'UTR, and 1st exon. Methylation beta values of CpG islands were averaged across CpG sites. A Pearson correlation test was performed for all the genes in the Expression Array, first correlating the genes intra models IDB-01 and IDB-02 and later calculating the correlation within the sensitive and resistant samples independently. Density plots were created with the correlation values per model, or based on the sensitive/resistant conditions. Also, for those genes that were previously considered as differentially expressed (logFC >=1.5 and adj.P.Val <=0.05). A heatmap with the most differentially expressed genes was generated organizing the mean expression values by applying a clustering method based

on Manhattan distances, and drawing its equivalent mean methylation values with its corresponding gene.

Statistical analysis and graphical representation were performed with R programming language (version 3.4 2017-04-21) and limma (version 3.30.13) and ggplot2 libraries. Significant differences between samples/models were assessed using Wilcoxon, Pearson or Chi-tests were appropriate with values of $p<0.05$ considered to be significant.

Pyrosequencing

Pyrosequencing assays were designed to analyze and validate the results obtained from the array under different scenarios. Sodium bisulfite modification of 1 µg of genomic DNA isolated from breast cancer PDX tumors was carried out with the EZ DNA Methylation Kit (Zymo Research Corporation) following the manufacturer's protocol. Bisulfite-treated DNA was eluted in 30-µL volumes with 2 µL used for each PCR. The set of primers for PCR amplification and sequencing were designed with a specific program (PyroMark assay design version 2.0.01.15). Primer sequences were designed to hybridize with CpG-free sites to ensure methylation-independent amplification. PCR was performed with primers biotinylated to convert the PCR product to single-stranded DNA templates. We used the Vacuum Prep Tool (Biotage) to prepare single-stranded PCR products according to the manufacturer's instructions. Pyrosequencing reactions and quantification of methylation were performed in a PyroMark Q24 System version 2.0.6 (QIAGEN). Primers indicated below are in 5' → 3' direction.

Primers

hSLC25A30 Forward	AGTTTTTATTGGTTTTTGTTAGTATTAGT
hSLC25A30 Reverse Biotinylated	[Btn]TTCCCCAAATTTCTCTTCCACC
hSLC25A30 Forward PyroSeq	TGATAGTTTTAGATGGGGATA

RNA extraction and gene expression microarray

Total RNA from tissue was prepared with Tripure Isolation Reagent (Roche). Frozen tumor tissues from sensitive and resistant IDB-01 and IDB-02 TNBC PDX models were fractionated using the POLYTRON® system PT 1200 E (Kinematica). Two-hundred-nanogram aliquots of total RNA were used for the production of fluorescent complementary RNA following the Two-Color Microarray-Based Gene Expression Analysis v. 6.5 (Agilent) protocol under manufacturer's instructions. All samples were hybridized to the SurePrint G3 Human Gene Expression 8 × 60 K microarray (Agilent Technologies). The signal values were extracted using the Feature Extraction software (Agilent Technologies). After scanning and normalization processes, all the statistical treatment was realized under an R programming environment using Bioconductor's package for gene expression analysis: Limma, RankProd, Marray, affy, pcaMethods, EMA y RamiGO.

Differentially expressed genes, after Limma analysis, were represented as a mean-centered gene expression graphs using web-based tool Morpheus from Broad Institute.

Gene Ontology/Pathway Analysis.

To identify functional clusters of genes differentially methylated and/or differentially expressed, we performed Functional Annotation Clustering using DAVID (Huang et al., 2009) on the candidate genes obtained from comparisons between sensitive and resistant tumors from IDB-01 and IDB-02 TNBC PDX models.

GSEA analysis

Gene Set Enrichment Analysis (GSEA) is freely available and is supported by the Broad Institute website (http://www.broadinstitute.org/gsea/index.jsp) [2] and includes versions compatible with Java, R or Gene Pattern. All GSEA analyses presented here were performed using the R GSEA implementation.

DNAse treatment and qRT-PCR

Prior to cDNA conversion, RNA was treated with DNA-free DNase I kit (Ambion, AM1906). cDNA was produced by reverse transcription using 1 µg of DNA-free RNA in a 35 µL reaction following TaqMan™ Reverse Transcription instructions (Applied Biosystems, N8080234). 20 ng/well of cDNA were used for the analysis performed in triplicate. Quantitative PCR was performed using the LightCycler® 480 SYBR green. Primer sequences are indicated below. Ct analysis was performed using LightCycler 480 software (Roche). All primers indicated below are in 5' → 3' direction.

hEGFR Forward	CCTGTCTGGAAGTACGCAG
hEGFR Reverse	GCGATGGACGGGATCTTAGG
hERBB3 Forward	CCGCTTGACTCAGCTCACC
hERBB3 Reverse	CACGATGTCCCTCCAGTCAAT
hSLC25A30 Forward	ACTGCTGAGTGCGGTACATT
hSLC25A30 Reverse	GTCCTCTTGTCCCCTCTTGC
hPPiA Forward	ATGCTGGACCCAACACAAAT
hPPiA Reverse	TCTTTCACTTTGCCAAACACC

Western blot

Total protein was isolated from sensitive and resistant tumors from IDB-01 PDX model using radioimmunoprecipitation assay (RIPA) with 1% NP-40, Complete protease inhibitor cocktail (Roche Diagnostics GmbH) and PhoStop inhibitor cocktail (Roche Diagnostics GmbH). Lysates were separated by 10% SDS-PAGE and blotted onto a nitrocellulose membrane. The membranes were blocked with 5% of non-fat milk and then blotted with the antibodies for anti-phosphorylated ERK1/2 antibody (Sigma, #M8159), anti-ERK1/2 antibody (Cell Signaling, #9102), monoclonal anti-phosphorylated EGFR antibody (Cell Signaling, #3777) and monoclonal anti-EGFR antibody (Cell Signaling, #4267). *Home-made* Ponceau S () was used for control staining of total protein normalization.

Statistical Analyses

All data are expressed as mean ± SEM. Statistical comparison was performed by Student's t test using GraphPad Prism version 5.04. $p \leq 0.05$ was considered statistically significant. The statistical significance of difference between groups is expressed by asterisks: *$0.01 < p < 0.05$; **$0.001 < p < 0.01$; ***$0.001 < p < 0.0001$; ****$p < 0.0001$.

Results and Discussion

Methylation patterns fidelity between subtypes of breast cancer PDX and human primary breast tumors

More than five hundred breast cancer PDX models have been established around the world (Dobrolecki et al., 2016), but to our knowledge whole-genome DNA methylation analysis has not yet been conducted. DNA methylation status was analyzed for each of our breast cancer PDX models. Two tumors from each TNBC PDX model sensitive to docetaxel, luminal and ER+PR+HER2+ PDX models were analyzed, and also three resistant tumors derived from each TNBC PDX model, using Infinium HumanMethylation 450k BeadChip Array from Illumina. The array contains 485,512 probes covering 99% of RefSeq genes.

A first approach comparing whole-genome DNA methylation using all CpG sites β-values between both sensitive TNBC PDX models (Figure 1A) or between a TNBC and a luminal PDX model (Figure 1B) displayed a higher correlation between tumors from the same breast cancer subtype. Then, unsupervised analysis of most differentially methylated CpGs between breast cancer PDX models showed two major clusters that correlate with hormone receptor expression: a cluster for estrogen receptor (ER) negative and a cluster for ER positive breast cancer PDX (Figure 1C). Interestingly, model IDB-03, which has lost hormone receptor expression in the PDX model (Gómez-Miragaya et al., 2017) clusters with TNBC PDX models (Figure 1C), but it is virtually as close to the ER- as to the ER+ cluster (Figure 1C, dendogram). This result suggests that loss of ER expression is accompanied by subtle methylation changes in the PDX model. Selection of an ER- population from tumor of origin during engraftment could explain this result. The disparity in clustering could be solved by analizing methylation status from adjacent ER+ and ER- cells from luminal tumors. Importantly, this result shows that the segregation in two major DNA methylation clusters based on hormone receptor expression observed in breast cancer patients (Network, 2012) is maintained in our breast cancer PDX models.

In order to know if methylation patterns from different TCGA breast cancer subtypes are conserved in our breast cancer PDX models and if they are closer to the clinical behaviour than breast cancer cell lines (BCCL), BCCLs, our breast cancer PDX and breast cancer primary tumors from TCGA (Network, 2012) were compared. A supervised cluster using the subtype methylation patterns extracted from TCGA (Network, 2012) revealed that each PDX model was classified with human breast cancer samples from the same subtype (Figure 1D), as well as BCCLs (Figure 1D). Most of our breast cancer PDX models were mixed with TCGA tumors, while virtually all BCCLs classify separately from TCGA tumors (Figure 1D). This result indicates that DNA methylation from breast cancer tumors is conserved in breast cancer PDX models and they are closer to clinics than BCCLs. Thus, BCCLs have accumulated irreversible methylation changes probably caused by long-term *ex vivo* culture that maintains subtype-specific methylation but induces other methylation changes not observed when tumors are passaged in mice. Note that here the IDB-03 model, despite the loss of ER expression, classifies with luminal TCGA tumors, suggesting that selected CpGs from TCGA classify better for subtype specific methylation than global methylation.

Distinctive DNA methylation patterns for the different breast cancer subtypes that correlate with clinical implications have been previously described (Stefansson et al., 2015). A supervised hierarchical clustering of our breast cancer PDX using these methylation signatures resulted in the classification of our TNBC models as EpiBasal and the luminals and HER2+ as EpiLumB (Supplementary Figure S1A). This data supports the idea that the subtype-specific methylation patterns showed in primary breast tumors are maintained in breast cancer PDX models with clinical significance.

Alterations in DNA methylation patterns between normal tissue and matched tumors for breast cancer and other cancer types have been described (Baylin et al., 2001; Narayan et al., 1998). Genome-wide DNA methylation status of our breast cancer PDX were compared with human normal mammary glands revealing a general hypomethylation pattern in breast cancer PDX while hypermethylation in some gene-specific CpG sites (Supplementary Figure S1B), which is also observed in patient´s tumors. This result shows that variations in methylome between normal mammary gland and human breast cancer are also conserved in breast cancer PDXs models.

Breast PDX tumors have demonstrated to resemble the heterogeneity, drug response, invasive capabilities and growth rates of human cancers better than established BCCLs (Byrne et al., 2017; Dobrolecki et al., 2016). Our results point out the relevance of the use of breast cancer PDX for methylation studies, as shown for other PDX tumors (Poirier et al., 2015; Tomar et al., 2016; Wang et al., 2017b). Genome-wide DNA methylation patterns of breast cancer PDX models are closer to primary breast tumors and breast cancer subtypes are preserved in breast cancer PDX models. These data reinforce the relevance of breast cancer PDXs to accelerate the translation into clinics of DNA methylation studies.

Genome-wide DNA methylation comparisons from sensitive and chemoresisant-derived TNBC PDX models.

Methylation studies have been conducted for different tumor PDX models showing their potential to investigate drug resistance mechanisms and to identify drug response biomarkers (Gupta et al., 2016; Min et al., 2017; Wong et al., 2014), however methylation studies in breast cancer PDX models unraveling chemoresistance mechanisms are still missed. As DNA methylation changes in BCCLs have also been shown to contribute to taxane chemoresistance (He et al., 2016; Kastl et al., 2010; Si et al., 2016), we investigated whether changes in DNA methylation patterns could be associated with chemoresistance acquisition in our TNBC PDX models.

DNA methylation patterns in paired sensitive and resistant TNBC PDX tumors were analyzed. Unsupervised methylation cluster using the ten thousand most variable CpGs between both TNBC PDX models showed a clear separation between the two TNBC PDX models (Figure 2A). Then an unsupervised methylation cluster using the ten thousand most variable CpGs between samples within each TNBC PDX model was performed. Separation between sensitive and resistant samples for IDB-01 (Figure 2B) but not for IDB-02 (Supplementary Figure 2A) was observed. Next, an analysis and comparison of methylomes using all CpG sites β-values between sensitive and resistant groups from IDB-01 and IDB-02 were accomplished (Figure

2C). CpG site methylation levels of paired sensitive and resistant tumors were strongly correlated in both models (Figure 2C), to a similar extent to that achieved when both sensitive tumors were compared between them (Figure 2C). Finally, a comparison of whole genome DNA methylation of sensitive and resistant groups from IDB-01 and IDB-02 (Figure 2D and 2E and Supplementary Figure 2B and 2C) based on CpG genomic region and CpG context was done. Interestingly, a significant genome-wide DNA methylation increase was found in the promoter (Figure 2D) and CpG island context (Figure 2E) in both chemoresistant TNBC PDX models, while some changes in other CpG genomic regions or CpG contexts between both chemoresistant TNBC PDX were not consistent between TNBC PDX models (Supplementary Figure 2B and 2C).

Together this data demonstrate that although acquisition of chemoresistance to docetaxel is not driven by global methylation changes but a few acquired methylation changes associated with hypermethylation of both promoter and CpG islands were observed in resistant TNBC PDX models.

Gene specific DNA methylation changes in TNBC breast cancer PDX are poorly associated with gene expression changes

Specific methylation changes in some critical genes have been described to directly mediate docetaxel acquired resistance in breast cancer, but also in other cancer types (Dong et al.; Tao et al., 2015; Yan et al., 2013). Then specific gene methylation changes in both TNBC PDXs that could provide chemoresistance to TNBC tumors were studied.

To identify key DNA methylation changes associated with response to docetaxel, differentially methylated CpGs between sensitive and resistant groups from both TNBC PDX models were extracted. Comparison of DNA methylation at single base pair resolution using a minimum methylation difference of 30% revealed a total of 262 and 1264 differentially methylated CpGs, corresponding to 148 and 622 genes, in resistant tumors of IDB-01 and IDB-02, respectively (Figure 3A and Table 1). Same number of differentially methylated sites was found to be hypo- and hypermethylated in resistant IDB-01 PDX tumors (Figure 3A), whereas hypermethylation was detected as predominant phenomenon in differentially methylated sites from resistant IDB-02 (86%, Figure 3A). Most of the differentially methylated sites in the IDB-01 were in promoter and in CpG island context (Supplementary Figure 3A) while in the IDB-02 were intergenic and open sea sites (Supplementary Figure 3A). Hypomethylated sites in IDB-01 resistant tumors were located preferentially in body and CpG island context while the hypermethylated sites were located preferentially in promoter, CpG island site and open sea (Supplementary Figure 3B). In the case of IDB-02, the whole resistant methylome is defined by the hypermethylated sites (86%, Figure 3A, Supplementary Figure 3A and 3B), mainly intergenic and open sea sites.

Comparison of differentially methylated CpGs between both resistant TNBC PDX models revealed that just one CpG was in common (Supplementary Figure 3C). It was a CpG island from an intergenic location and it was methylated in opposite direction between both models. The absence of common changes between both resistant TNBC PDX models may be explained

due to the high heterogeneity of the TNBC subtype and the multiple mechanisms that can influence chemoresistance.

It is well known the machinery and relationship between epigenetic changes, that includes methylation, and gene expression control in cancer (Perri et al., 2017; Pouliot et al., 2015). In order to know if methylation is controlling gene expression in chemosensitive and chemoresistant TNBC PDX, whole gene expression microarray analyses were performed. Three paired sensitive and resistant tumors from each TNBC PDX model using SurePrint G3 Human Gene Expression Microarray v2 platform from Agilent were analyzed. Correlations between methylation and gene expression were extracted for IDB-01 and IDB-02 TNBC PDX models showing that there are mostly a lineal positive correlation [Figure 3B (blue lines), Table 2]. This result demonstrates that global methylation is not driving gene expression in basal, global conditions. When sensitive or resistant PDX models were looked separately, no clear negative correlation was shown [Supplementary Figure 3D and 3E (blue lines)] except for IDB-01R, which clearly showed that half of the genes seem to be controlled by methylation (Supplementary Figure 3D, right). Taken together, these results do not show a general negative correlation between methylation and expression in basal conditions or during chemoresistance acquisition in TNBC PDX models, but some genes could be controlled by methylation, mostly in chemoresistant tumors from model IDB-01R.

In order to characterize the significance of changes in DNA methylation on gene expression during chemoresistance acquisition, a simple, initial parametric test was applied to infer most differentially expressed genes between sensitive and resistant IDB-01 and IDB-02 PDX and correlate it with methylation. Analysis revealed that most differentially expressed genes (adj. p-value < 0.05, LogFC > |1.5|) were negatively correlated with methylation in IDB-01 PDX model [Figure 3B (red lines) and 3C] and it was most clear when IDB-01S and IDB-01R were analyzed separately, as around half of the genes are negatively correlated [Supplementary Figure 3D (red lines)], suggesting a gene expression control by methylation. In the case of the IDB-02 model, there was not clear negative correlation between methylation and gene expression [Figure 3B, Supplementary Figure 3E (red lines) and 3F]. Taken together, these results show some gene-specific association between methylation and expression during chemoresistance acquisition in IDB-01 TNBC PDX model, while no correlation was found in the case of IDB-02 TNBC PDX model.

Finally, pair-wise comparisons between sensitive and resistant IDB-01 and IDB-02 PDX models were performed using *limma* test, a more complex ANOVA test that stabilizes the gene-specific variance estimates (Gentleman et al., 2004; Ritchie et al., 2015), to identify strongly, differentially expressed genes (adj. p-value < 0.05, fold change > |1.5|). A total of 702 candidate genes in IDB-01, 304 downregulated and 398 overexpressed (Figure 3D and Table 3), and 769 genes in IDB-02, 445 downregulated and 324 overexpressed (Figure 3D and Table 3), were identified in chemoresistants compared to chemosensitive. When differentially expressed genes between both chemoresistant TNBC models were compared, a common set of 35 genes were identified (Supplementary Figure 3G), 7 of them in the same direction in both TNBC PDX models (Supplementary Figure 3G).

Crosstalk between methylation- and gene expression-altered pathways reveal chemoresistance-involved pathways

For the purpose to know if methylation and expression altered genes were associated to common pathways, analysis from Gene Ontology (GO) and Kyoto Encyclopedia of Genes and Genomes (KEGG) pathways were conducted on DAVID bioinformatics web-based tool (https://david.ncifcrf.gov/). The analysis of the differentially methylated genes in resistant IDB-01 PDX model revealed alterations in some interesting pathways such as focal adhesion, ribosome and transport (Figure 4A and Table 4). In the other hand, analyses of expression changes in IDB-01R highlighted extracellular space as significant (Figure 4B and Table 5), but other pathways were deregulated (mitochondrion, amino acid transport, regulation of nitric oxide). In IDB-02R PDX model, methylation altered genes converge in some important pathways, as GABAergic synapse, cell junction, glutamaergic synapse and MAPK signaling pathway (Figure 4C and Table 4) and expression changes were related mainly with immune reponse pathways, but also with extracellular matrix organization and cell adhesion (Figure 4D and Table 5). Similar pathways were identified between methylation and gene expression data from each resistant TNBC PDX model. Interestingly, one of the gene expression pathways altered in chemoresistant tumors was shared between both TNBC PDX models, the extracellular space (Figure 4B and 4 D, Table 5).

In breast cancer, association between chemoresistance and mitochondria and ribosomal pathways has been demonstrated (Candas et al., 2014; Dave et al., 2017). In MCF7 breast cancer cell line, a breast cancer population overexpressing mitochondrial and ribosome-related proteins was consistently associated with an anabolic breast cancer stem-like phenotype (Lamb et al., 2015). Important mitochondrial proteins are solute carrier transporters (SLC) and ATP-binding proteins (ABC), which mediate the efflux and influx of different substrates, including cytotoxic drugs (Joyce et al., 2015). Some of these transporters have been associated with chemoresistance to many drugs in breast cancer, as BCRP/ABG2. SLC25A30 pertains to the family of solute carrier transporters and it appears to be consistently associated with ribosomal, mitochondrial and transport pathways. We identified that SLC25A30 is differentially methylated and expressed significantly in omics analysis from resistant IDB-01 TNBC PDX model, pyrosequencing and gene expression analysis in sensitive and resistant IDB-01 PDX tumors were performed. The analysis revealed that *SLC25A30* promoter was differentially methylated, showing a hypomethylation pattern in IDB-01R (Figure 4E). Next we asked if differential promoter methylation of SLC25A30 was associated with changes in gene expression in resistant IDB-01 tumors. Analysis by qRT-PCR showed higher mRNA expression levels of *SLC25A30* in resistant IDB-01 PDX models (Figure 4F). This data supports that *SLC25A30* expression is controlled by promoter methylation and increased expression in resistant IDB-01 PDX could contribute to chemoresistance acquisition.

Globally, some gene specific changes between sensitive and resistant tumors in both TNBC PDX models were unraveled. In IDB-01, half of the methylation changes were hypermethylations and the other half hypomethylations; in IDB-02, the methylation changes were mainly to CpG hypermethylation in chemoresistant TNBC PDX tumors. We have identified novel methylation and gene expression altered pathways between sensitive and resistant tumors from both IDB-01 and IDB-02 PDX models that could contribute to

chemoresistance acquisition. In IDB-01 SLC25A30 appears to be hypomethylated and overexpressed in docetaxel resistant PDX tumors. Chemoresistance properties of ABC transporters have been extensively studied for different types of cancer and chemotherapeutic compounds. Thus, ABC transporter inhibitors could be interesting chemosensitizers used in combination with standard chemotherapeutic agents to enhance their therapeutic efficacy (Kathawala et al., 2015). The BCRP/*ABCG2* is the most known ABC transporter playing a major role in breast cancer multidrug chemoresistance (Doyle et al., 1998; Kathawala et al., 2015). Solute carrier transporter (SLC) with similar functions, as movement of drugs across the cell membrane bidirectionally, has been less studied (Joyce et al., 2015). Further studies using paired breast cancer patient samples or bigger collections of TNBC PDX have to be performed to precisely select the most important pathways and to study the role of SLC transporters in acquired chemoresistance to taxanes.

Whole gene expression analysis independent on DNA methylation in TNBC PDX models revealed chemoresistance-associated pathways

Breast cancer PDXs recapitulate global gene expression patterns from tumors of origin (DeRose et al., 2011; Dobrolecki et al., 2016). Gene expression changes can increase chemoresistance to taxanes and other drugs (Ajabnoor et al., 2012; Antoon et al., 2012; Duhachek-Muggy et al., 2017). Taking into account that most gene expression changes identified in our sensitive/resistant pairs cannot be explained by methylation alterations, we studied gene expression changes independently of methylation.

GSEA revealed that resistant samples from IDB-02 showed enrichment in genes associated to pathways of regulation of mitosis, replication and cell cycle (Figure 5A and Table 6). Resistant samples from model IDB-01 showed enrichment in pathways involved in ECM receptor interaction, focal adhesion and cell differentiation, being the most enriched the EGFR pathway (Figure 5B and Table 6). EGFR and HER2 pathways, both tyrosine kinase receptors (TKR) pathways, have been associated with poor response to chemotherapy (Abdelrahman et al., 2017; Murray et al., 2012) and clinical combinations of taxanes plus TKR inhibitors regimens are under current study for the treatment of TNBC patients (Nabholtz et al., 2014, 2016). Differential mRNA expression levels were found by qRT-PCR from *EGFR* (Figure 5C) but also other partners of the pathway, as *ERBB3* (Figure 5C), between sensitive and resistant IDB-01 PDX tumors. No different expression of *HER2* was found between sensitive and resistant IDB-01 PDX tumors (Gómez-Miragaya et al., 2017). Validation of the EGFR pathway result by western blot was conducted showing an increase in EGFR expression and downstream activation of the pathway in chemoresistant IDB-01 tumors (Figure 5D).

Together these data evidence multiple changes in gene expression between sensitive and resistant TNBC PDX tumors. Some clinically relevant pathways, as tyrosine kinase receptor pathway, have been unravelled using our paired PDX models, pointing out the reliability of PDX models in the study of chemoresistance acquisition to chemotherapy drugs.

In conclusion, our findings demonstrate that sensitive/resistant matched breast cancer PDX are suitable models for elucidating mechanisms of drug resistance related to methylation and gene expression. These models are closer to clinical samples than cell lines; results obtained in

these matched models are easier to interpret than those obtained using heterogeneous patient´s populations under complex and variable drug regimens. Several key genes and pathways that could mediate chemoresistance in TNBC have been identified. Further studies using additional paired sensitive and resistant TNBC PDXs and clinical trials will be required to illustrate the translational relevance of our findings.

References

Abdelrahman, A.E., Rashed, H.E., Abdelgawad, M., and Abdelhamid, M.I. (2017). Prognostic impact of EGFR and cytokeratin 5/6 immunohistochemical expression in triple-negative breast cancer. Ann. Diagn. Pathol. *28*, 43–53.

Ajabnoor, G.M.A., Crook, T., and Coley, H.M. (2012). Paclitaxel resistance is associated with switch from apoptotic to autophagic cell death in MCF-7 breast cancer cells. Cell Death Dis. *3*, e260.

Antoon, J.W., Lai, R., Struckhoff, A.P., Nitschke, A.M., Elliott, S., Martin, E.C., Rhodes, L.V., Yoon, N.S., Salvo, V.A., Shan, B., et al. (2012). Altered death receptor signaling promotes epithelial-to-mesenchymal transition and acquired chemoresistance. Sci. Rep. *2*, 539.

Baylin, S.B., Esteller, M., Rountree, M.R., Bachman, K.E., Schuebel, K., and Herman, J.G. (2001). Aberrant patterns of DNA methylation, chromatin formation and gene expression in cancer. Hum. Mol. Genet. *10*, 687–692.

Brooks, T.A., Minderman, H., O'Loughlin, K.L., Pera, P., Ojima, I., Baer, M.R., Bernacki, R.J., and Brooks, T. (2003). Taxane-based reversal agents modulate drug resistance mediated by P-glycoprotein, multidrug resistance protein, and breast cancer resistance protein. Mol. Cancer Ther. *2*, 1195–1205.

Byrne, A.T., Alférez, D.G., Amant, F., Annibali, D., Arribas, J., Biankin, A.V., Bruna, A., Budinská, E., Caldas, C., Chang, D.K., et al. (2017). Interrogating open issues in cancer precision medicine with patient-derived xenografts. Nat. Rev. Cancer *17*, 254–268.

Candas, D., Lu, C.-L., Fan, M., Chuang, F.Y.S., Sweeney, C., Borowsky, A.D., and Li, J.J. (2014). Mitochondrial MKP1 is a target for therapy-resistant HER2-positive breast cancer cells. Cancer Res. *74*, 7498–7509.

Dave, B., Gonzalez, D.D., Liu, Z.-B., Li, X., Wong, H., Granados, S., Ezzedine, N.E., Sieglaff, D.H., Ensor, J.E., Miller, K.D., et al. (2017). Role of RPL39 in Metaplastic Breast Cancer. J. Natl. Cancer Inst. *109*.

Dent, R., Trudeau, M., Pritchard, K.I., Hanna, W.M., Kahn, H.K., Sawka, C.A., Lickley, L.A., Rawlinson, E., Sun, P., and Narod, S.A. (2007). Triple-negative breast cancer: clinical features and patterns of recurrence. Clin. Cancer Res. Off. J. Am. Assoc. Cancer Res. *13*, 4429–4434.

DeRose, Y.S., Wang, G., Lin, Y.-C., Bernard, P.S., Buys, S.S., Ebbert, M.T.W., Factor, R., Matsen, C., Milash, B.A., Nelson, E., et al. (2011). Tumor grafts derived from women with breast cancer authentically reflect tumor pathology, growth, metastasis and disease outcomes. Nat. Med. *17*, 1514–1520.

Dobrolecki, L.E., Airhart, S.D., Alferez, D.G., Aparicio, S., Behbod, F., Bentires-Alj, M., Brisken, C., Bult, C.J., Cai, S., Clarke, R.B., et al. (2016). Patient-derived xenograft (PDX) models in basic and translational breast cancer research. Cancer Metastasis Rev. *35*, 547–573.

Dong, T., Zhang, M., Dong, Y., Herman, J.G., Engeland, M. van, Zhong, G., and Guo, M. Methylation of RASSF10 Promotes Cell Proliferation and Serves as a Docetaxel Resistant Marker in Human Breast Cancer. Discov. Med. *20*, 261–271.

Doyle, L.A., Yang, W., Abruzzo, L.V., Krogmann, T., Gao, Y., Rishi, A.K., and Ross, D.D. (1998). A multidrug resistance transporter from human MCF-7 breast cancer cells. Proc. Natl. Acad. Sci. U. S. A. *95*, 15665–15670.

Duhachek-Muggy, S., Qi, Y., Wise, R., Alyahya, L., Li, H., Hodge, J., and Zolkiewska, A. (2017). Metalloprotease-disintegrin ADAM12 actively promotes the stem cell-like phenotype in claudin-low breast cancer. Mol. Cancer *16*.

Duran, G.E., Wang, Y.C., Moisan, F., Francisco, E.B., and Sikic, B.I. (2017). Decreased levels of baseline and drug-induced tubulin polymerisation are hallmarks of resistance to taxanes in ovarian cancer cells and are associated with epithelial-to-mesenchymal transition. Br. J. Cancer *116*, 1318–1328.

Foulkes, W.D., Smith, I.E., and Reis-Filho, J.S. (2010). Triple-Negative Breast Cancer. N. Engl. J. Med. *363*, 1938–1948.

Gentleman, R.C., Carey, V.J., Bates, D.M., Bolstad, B., Dettling, M., Dudoit, S., Ellis, B., Gautier, L., Ge, Y., Gentry, J., et al. (2004). Bioconductor: open software development for computational biology and bioinformatics. Genome Biol. *5*, R80.

Gómez-Miragaya, J., Palafox, M., Paré, L., Yoldi, G., Ferrer, I., Vila, S., Galván, P., Pellegrini, P., Pérez-Montoyo, H., Igea, A., et al. (2017). Resistance to Taxanes in Triple-Negative Breast Cancer Associates with the Dynamics of a CD49f+ Tumor-Initiating Population. Stem Cell Rep. *8*, 1392–1407.

Gupta, S.K., Kizilbash, S.H., Carlson, B.L., Mladek, A.C., Boakye-Agyeman, F., Bakken, K.K., Pokorny, J.L., Schroeder, M.A., Decker, P.A., Cen, L., et al. (2016). Delineation of MGMT Hypermethylation as a Biomarker for Veliparib-Mediated Temozolomide-Sensitizing Therapy of Glioblastoma. J. Natl. Cancer Inst. *108*.

Győrffy, B., Bottai, G., Fleischer, T., Munkácsy, G., Budczies, J., Paladini, L., Børresen-Dale, A.-L., Kristensen, V.N., and Santarpia, L. (2016). Aberrant DNA methylation impacts gene expression and prognosis in breast cancer subtypes. Int. J. Cancer *138*, 87–97.

He, D.-X., Gu, F., Gao, F., Hao, J., Gong, D., Gu, X.-T., Mao, A.-Q., Jin, J., Fu, L., and Ma, X. (2016). Genome-wide profiles of methylation, microRNAs, and gene expression in chemoresistant breast cancer. Sci. Rep. *6*, srep24706.

Herbst, R.S., and Khuri, F.R. (2003). Mode of action of docetaxel – a basis for combination with novel anticancer agents. Cancer Treat. Rev. *29*, 407–415.

Huang, D.W., Sherman, B.T., and Lempicki, R.A. (2009). Systematic and integrative analysis of large gene lists using DAVID bioinformatics resources. Nat. Protoc. *4*, 44–57.

Johnson, J.I., Decker, S., Zaharevitz, D., Rubinstein, L.V., Venditti, J.M., Schepartz, S., Kalyandrug, S., Christian, M., Arbuck, S., Hollingshead, M., et al. (2001). Relationships between drug activity in NCI preclinical in vitro and in vivo models and early clinical trials. Br. J. Cancer *84*, 1424–1431.

Joyce, H., McCann, A., Clynes, M., and Larkin, A. (2015). Influence of multidrug resistance and drug transport proteins on chemotherapy drug metabolism. Expert Opin. Drug Metab. Toxicol. *11*, 795–809.

Kastl, L., Brown, I., and Schofield, A.C. (2010). Altered DNA methylation is associated with docetaxel resistance in human breast cancer cells. Int. J. Oncol. *36*, 1235–1241.

Kathawala, R.J., Gupta, P., Ashby, C.R., and Chen, Z.-S. (2015). The modulation of ABC transporter-mediated multidrug resistance in cancer: a review of the past decade. Drug Resist. Updat. Rev. Comment. Antimicrob. Anticancer Chemother. *18*, 1–17.

Kawaguchi, T., Foster, B.A., Young, J., and Takabe, K. (2017). Current Update of Patient-Derived Xenograft Model for Translational Breast Cancer Research. J. Mammary Gland Biol. Neoplasia *22*, 131–139.

King, K.M., Lupichuk, S., Baig, L., Webster, M., Basi, S., Whyte, D., and Rix, S. (2009). Optimal use of taxanes in metastatic breast cancer. Curr. Oncol. Tor. Ont *16*, 8–20.

Kubo, T., Kawano, Y., Himuro, N., Sugita, S., Sato, Y., Ishikawa, K., Takada, K., Murase, K., Miyanishi, K., Sato, T., et al. (2016). BAK is a predictive and prognostic biomarker for the therapeutic effect of docetaxel treatment in patients with advanced gastric cancer. Gastric Cancer Off. J. Int. Gastric Cancer Assoc. Jpn. Gastric Cancer Assoc. *19*, 827–838.

Kulkarni, S.A., Hicks, D.G., Watroba, N.L., Murekeyisoni, C., Hwang, H., Khoury, T., Beck, R.A., Ring, B.Z., Estopinal, N.C., Schreeder, M.T., et al. (2009). TLE3 as a candidate biomarker of response to taxane therapy. Breast Cancer Res. BCR *11*, R17.

Lamb, R., Ozsvari, B., Bonuccelli, G., Smith, D.L., Pestell, R.G., Martinez-Outschoorn, U.E., Clarke, R.B., Sotgia, F., Lisanti, M.P., Lamb, R., et al. (2015). Dissecting tumor metabolic heterogeneity: Telomerase and large cell size metabolically define a sub-population of stem-like, mitochondrial-rich, cancer cells. Oncotarget *6*, 21892–21905.

Liedtke, C., Mazouni, C., Hess, K.R., André, F., Tordai, A., Mejia, J.A., Symmans, W.F., Gonzalez-Angulo, A.M., Hennessy, B., Green, M., et al. (2008). Response to neoadjuvant therapy and long-term survival in patients with triple-negative breast cancer. J. Clin. Oncol. Off. J. Am. Soc. Clin. Oncol. *26*, 1275–1281.

Lohiya, V., Aragon-Ching, J.B., and Sonpavde, G. (2016). Role of Chemotherapy and Mechanisms of Resistance to Chemotherapy in Metastatic Castration-Resistant Prostate Cancer. Clin. Med. Insights Oncol. *2016*, 57–66.

Min, H.-Y., Lee, S.-C., Woo, J.K., Jung, H.J., Park, K.H., Jeong, H.M., Hyun, S.Y., Cho, J., Lee, W., Park, J.E., et al. (2017). Essential Role of DNA Methyltransferase 1–mediated Transcription of Insulin-like Growth Factor 2 in Resistance to Histone Deacetylase Inhibitors. Clin. Cancer Res. *23*, 1299–1311.

Murray, S., Briasoulis, E., Linardou, H., Bafaloukos, D., and Papadimitriou, C. (2012). Taxane resistance in breast cancer: Mechanisms, predictive biomarkers and circumvention strategies. Cancer Treat. Rev. *38*, 890–903.

Nabholtz, J.M., Abrial, C., Mouret-Reynier, M.A., Dauplat, M.M., Weber, B., Gligorov, J., Forest, A.M., Tredan, O., Vanlemmens, L., Petit, T., et al. (2014). Multicentric neoadjuvant phase II study of panitumumab combined with an anthracycline/taxane-based chemotherapy in operable triple-negative breast cancer: identification of biologically defined signatures predicting treatment impact. Ann. Oncol. Off. J. Eur. Soc. Med. Oncol. *25*, 1570–1577.

Nabholtz, J.M., Chalabi, N., Radosevic-Robin, N., Dauplat, M.M., Mouret-Reynier, M.A., Van Praagh, I., Servent, V., Jacquin, J.P., Benmammar, K.E., Kullab, S., et al. (2016). Multicentric neoadjuvant pilot Phase II study of cetuximab combined with docetaxel in operable triple negative breast cancer. Int. J. Cancer *138*, 2274–2280.

Narayan, A., Ji, W., Zhang, X.Y., Marrogi, A., Graff, J.R., Baylin, S.B., and Ehrlich, M. (1998). Hypomethylation of pericentromeric DNA in breast adenocarcinomas. Int. J. Cancer *77*, 833–838.

Network, T.C.G.A. (2012). Comprehensive molecular portraits of human breast tumours. Nature *490*, 61–70.

O'Shaughnessy, J. (2005). Extending Survival with Chemotherapy in Metastatic Breast Cancer. The Oncologist *10*, 20–29.

Perri, F., Longo, F., Giuliano, M., Sabbatino, F., Favia, G., Ionna, F., Addeo, R., Scarpati, G.D.V., Lorenzo, G.D., and Pisconti, S. (2017). Epigenetic control of gene expression: Potential implications for cancer treatment. Crit. Rev. Oncol. Hematol. *111*, 166–172.

Poirier, J.T., Gardner, E.E., Connis, N., Moreira, A.L., de Stanchina, E., Hann, C.L., and Rudin, C.M. (2015). DNA methylation in small cell lung cancer defines distinct disease subtypes and correlates with high expression of EZH2. Oncogene *34*, 5869–5878.

Pouliot, M.-C., Labrie, Y., Diorio, C., and Durocher, F. (2015). The Role of Methylation in Breast Cancer Susceptibility and Treatment. Anticancer Res. *35*, 4569–4574.

Rapoport, B.L., Demetriou, G.S., Moodley, S.D., and Benn, C.A. (2014). When and How Do I Use Neoadjuvant Chemotherapy for Breast Cancer? Curr. Treat. Options Oncol. *15*, 86–98.

Ritchie, M.E., Phipson, B., Wu, D., Hu, Y., Law, C.W., Shi, W., and Smyth, G.K. (2015). limma powers differential expression analyses for RNA-sequencing and microarray studies. Nucleic Acids Res. *43*, e47.

Rouzier, R., Rajan, R., Wagner, P., Hess, K.R., Gold, D.L., Stec, J., Ayers, M., Ross, J.S., Zhang, P., Buchholz, T.A., et al. (2005). Microtubule-associated protein tau: A marker of paclitaxel sensitivity in breast cancer. Proc. Natl. Acad. Sci. U. S. A. *102*, 8315–8320.

Si, X., Liu, Y., Lv, J., Ding, H., Zhang, X.A., Shao, L., Yang, N., Cheng, H., Sun, L., Zhu, D., et al. (2016). ERα propelled aberrant global DNA hypermethylation by activating the DNMT1 gene to enhance anticancer drug resistance in human breast cancer cells. Oncotarget *7*, 20966–20980.

Stefansson, O.A., and Esteller, M. (2013). Epigenetic modifications in breast cancer and their role in personalized medicine. Am. J. Pathol. *183*, 1052–1063.

Stefansson, O.A., Moran, S., Gomez, A., Sayols, S., Arribas-Jorba, C., Sandoval, J., Hilmarsdottir, H., Olafsdottir, E., Tryggvadottir, L., Jonasson, J.G., et al. (2015). A DNA methylation-based definition of biologically distinct breast cancer subtypes. Mol. Oncol. *9*, 555–568.

Tai, P., Yu, E., Vinh-Hung, V., Cserni, G., and Vlastos, G. (2004). Survival of patients with metastatic breast cancer: twenty-year data from two SEER registries. BMC Cancer *4*, 60.

Tao, L., Huang, G., Chen, Y., and Chen, L. (2015). DNA methylation of DKK3 modulates docetaxel chemoresistance in human nonsmall cell lung cancer cell. Cancer Biother. Radiopharm. *30*, 100–106.

Tomar, T., de Jong, S., Alkema, N.G., Hoekman, R.L., Meersma, G.J., Klip, H.G., van der Zee, A.G., and Wisman, G.B.A. (2016). Genome-wide methylation profiling of ovarian cancer patient-derived xenografts treated with the demethylating agent decitabine identifies novel epigenetically regulated genes and pathways. Genome Med. *8*, 107.

Wang, D., Ma, J., Ji, X., Xu, F., and Wei, Y. (2017a). miR-141 regulation of EIF4E expression affects docetaxel chemoresistance of non-small cell lung cancer. Oncol. Rep. *37*, 608–616.

Wang, D., Pham, N.-A., Tong, J., Sakashita, S., Allo, G., Kim, L., Yanagawa, N., Raghavan, V., Wei, Y., To, C., et al. (2017b). Molecular heterogeneity of non-small cell lung carcinoma patient-derived xenografts closely reflect their primary tumors. Int. J. Cancer *140*, 662–673.

Wong, N.C., Bhadri, V.A., Maksimovic, J., Parkinson-Bates, M., Ng, J., Craig, J.M., Saffery, R., and Lock, R.B. (2014). Stability of gene expression and epigenetic profiles highlights the utility of patient-derived paediatric acute lymphoblastic leukaemia xenografts for investigating molecular mechanisms of drug resistance. BMC Genomics *15*, 416.

Yan, W., Wu, K., Herman, J.G., Brock, M.V., Fuks, F., Yang, L., Zhu, H., Li, Y., Yang, Y., and Guo, M. (2013). Epigenetic regulation of DACH1, a novel Wnt signaling component in colorectal cancer. Epigenetics *8*, 1373–1383.

Cancer of the Breast (Female) - Cancer Stat Facts.

Morpheus.

Figure 1

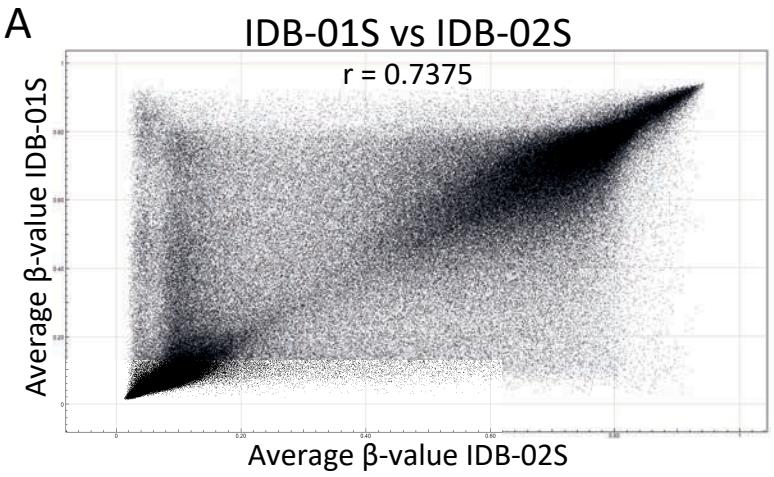

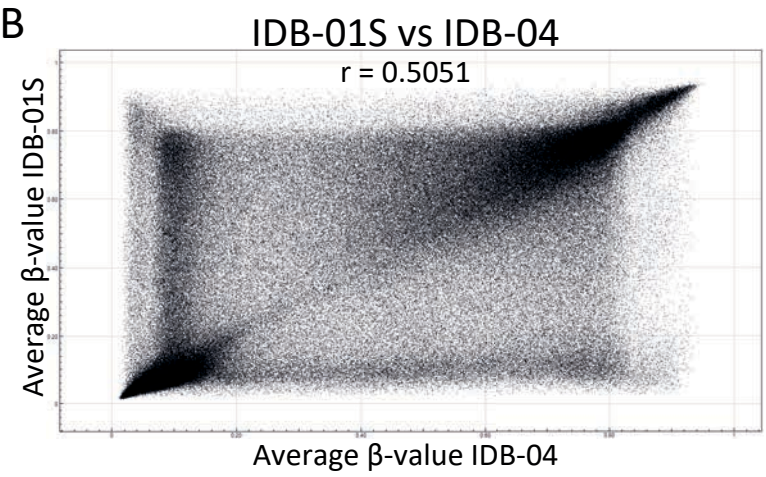

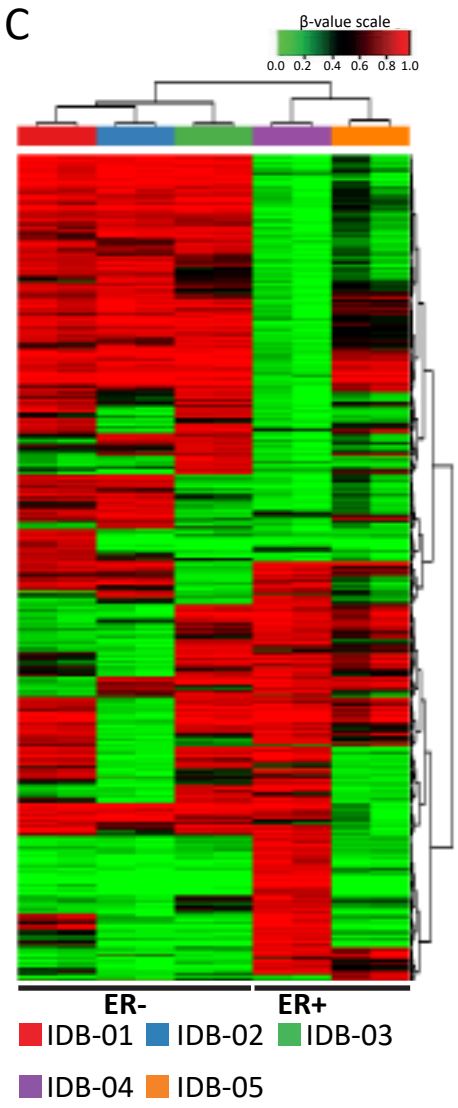

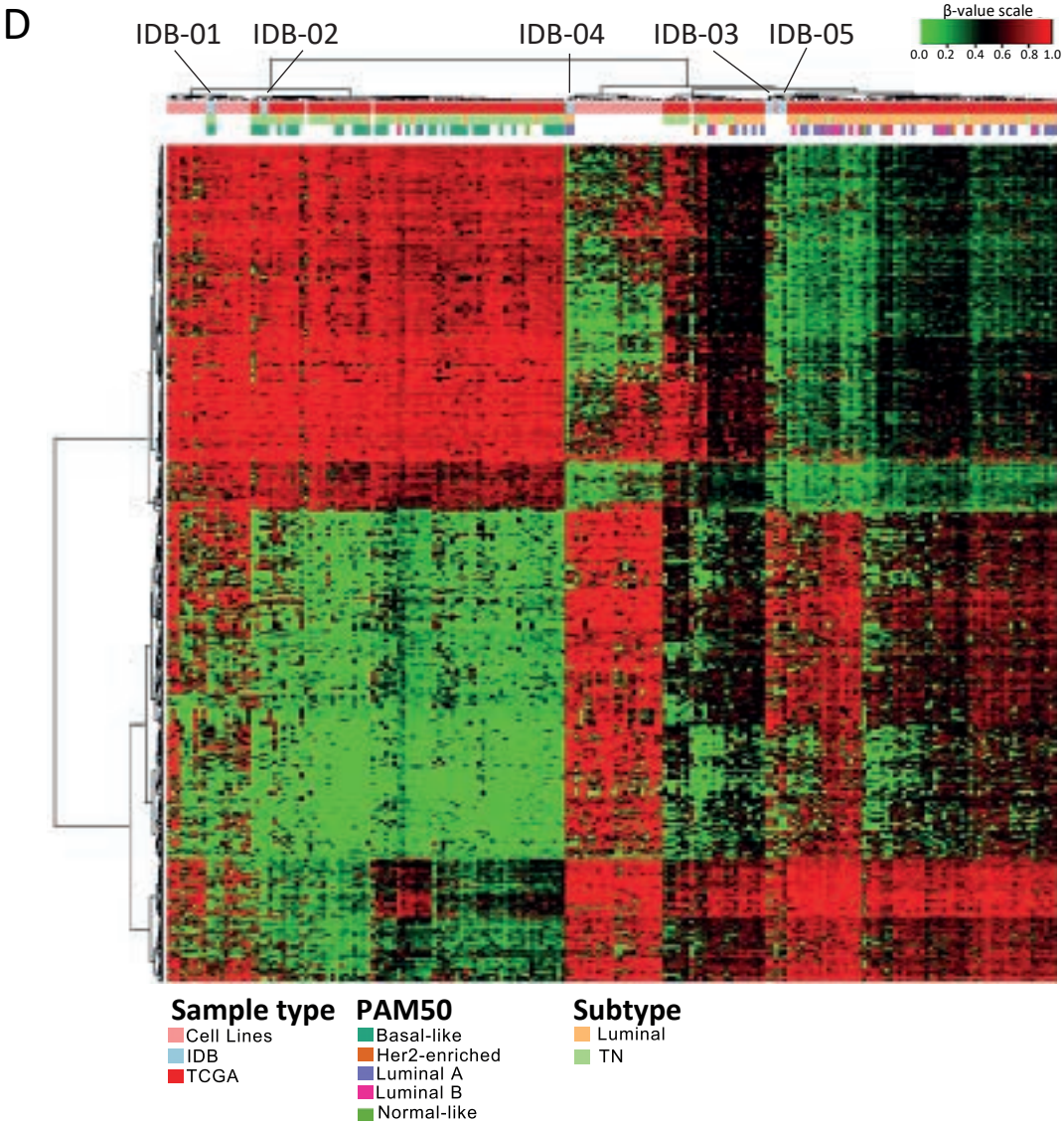

	BCCLs			PDX models			Marginal row totals
TCGA	4	(8)	[2]	6	(2)	[8]	10
Non-TCGA	36	(32)	[0.5]	4	(8)	[2]	40
Marginal column totals	40			10			50 (grand total)

Chi-square = 12.5
p-value = 0.000407

Figure 2

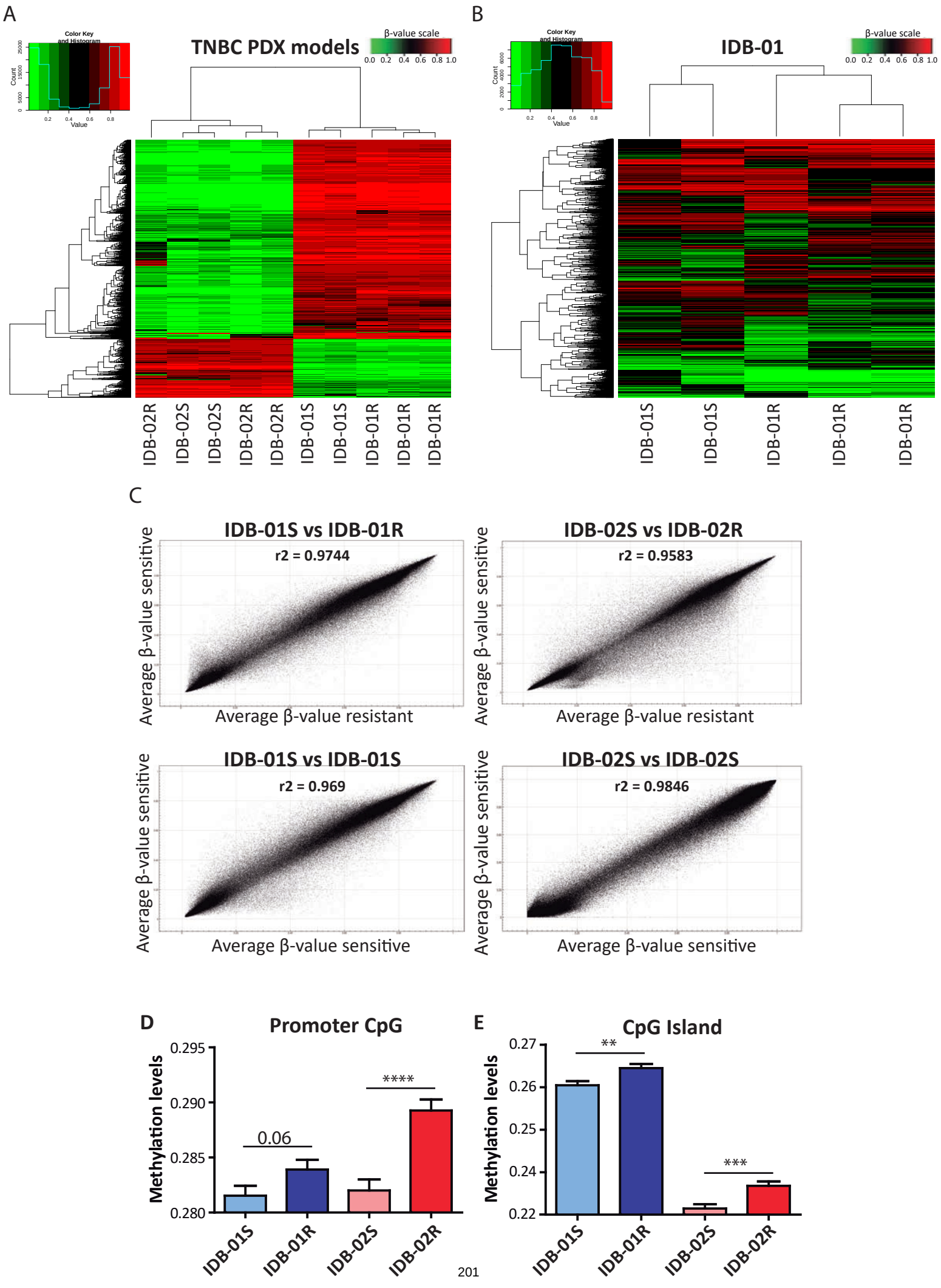
A
TNBC PDX models
β-value scale
0.0 0.2 0.4 0.6 0.8 1.0
Color Key and Histogram
Count
Value
IDB-02R
IDB-02S
IDB-02S
IDB-02R
IDB-02R
IDB-01S
IDB-01S
IDB-01R
IDB-01R
IDB-01R
B
IDB-01
β-value scale
0.0 0.2 0.4 0.6 0.8 1.0
Color Key and Histogram
Count
Value
IDB-01S
IDB-01S
IDB-01R
IDB-01R
IDB-01R
C
IDB-01S vs IDB-01R
r2 = 0.9744
Average β-value sensitive
Average β-value resistant
IDB-02S vs IDB-02R
r2 = 0.9583
Average β-value sensitive
Average β-value resistant
IDB-01S vs IDB-01S
r2 = 0.969
Average β-value sensitive
Average β-value sensitive
IDB-02S vs IDB-02S
r2 = 0.9846
Average β-value sensitive
Average β-value sensitive
D
Promoter CpG
Methylation levels
0.295
0.290
0.285
0.280
0.06
****
IDB-01S
IDB-01R
IDB-02S
IDB-02R
E
CpG Island
Methylation levels
0.27
0.26
0.25
0.24
0.22
**
***
IDB-01S
IDB-01R
IDB-02S
IDB-02R

Figure 3

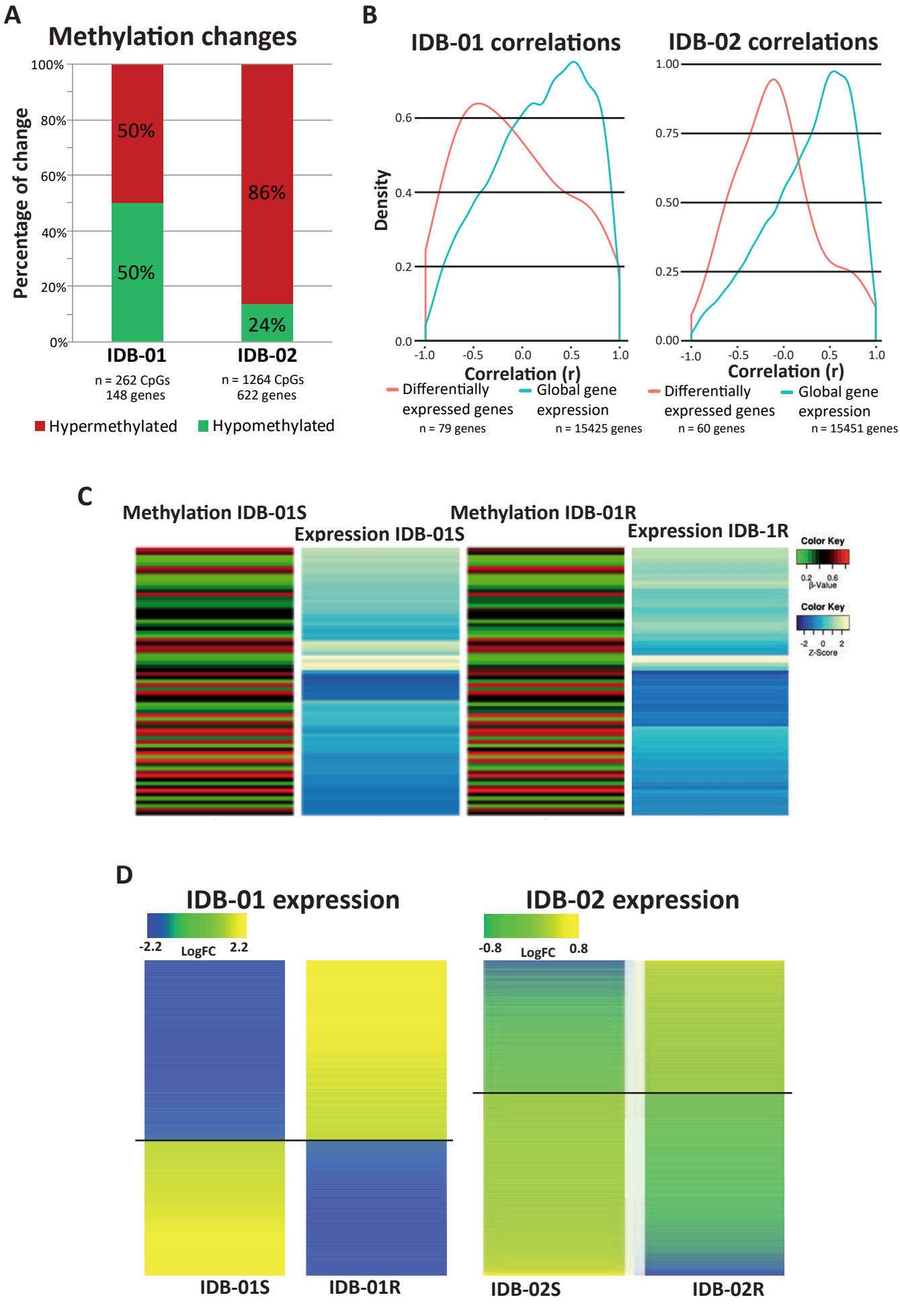
A
Methylation changes
100%
80%
60%
40%
20%
0%
Percentage of change
50%
50%
86%
24%
IDB-01
IDB-02
n = 262 CpGs
148 genes
n = 1264 CpGs
622 genes
Hypermethylated
Hypomethylated
B
IDB-01 correlations
IDB-02 correlations
Density
0.6
0.4
0.2
0.0
1.00
0.75
0.50
0.25
0.00
-1.0
-0.5
0.0
0.5
1.0
Correlation (r)
Differentially expressed genes
n = 79 genes
Global gene expression
n = 15425 genes
Differentially expressed genes
n = 60 genes
Global gene expression
n = 15451 genes
C
Methylation IDB-01S
Expression IDB-01S
Methylation IDB-01R
Expression IDB-1R
Color Key
0.2 0.6
β-Value
Color Key
-2 0 2
Z-Score
D
IDB-01 expression
-2.2
LogFC
2.2
IDB-02 expression
-0.8
LogFC
0.8
IDB-01S
IDB-01R
IDB-02S
IDB-02R

Figure 4

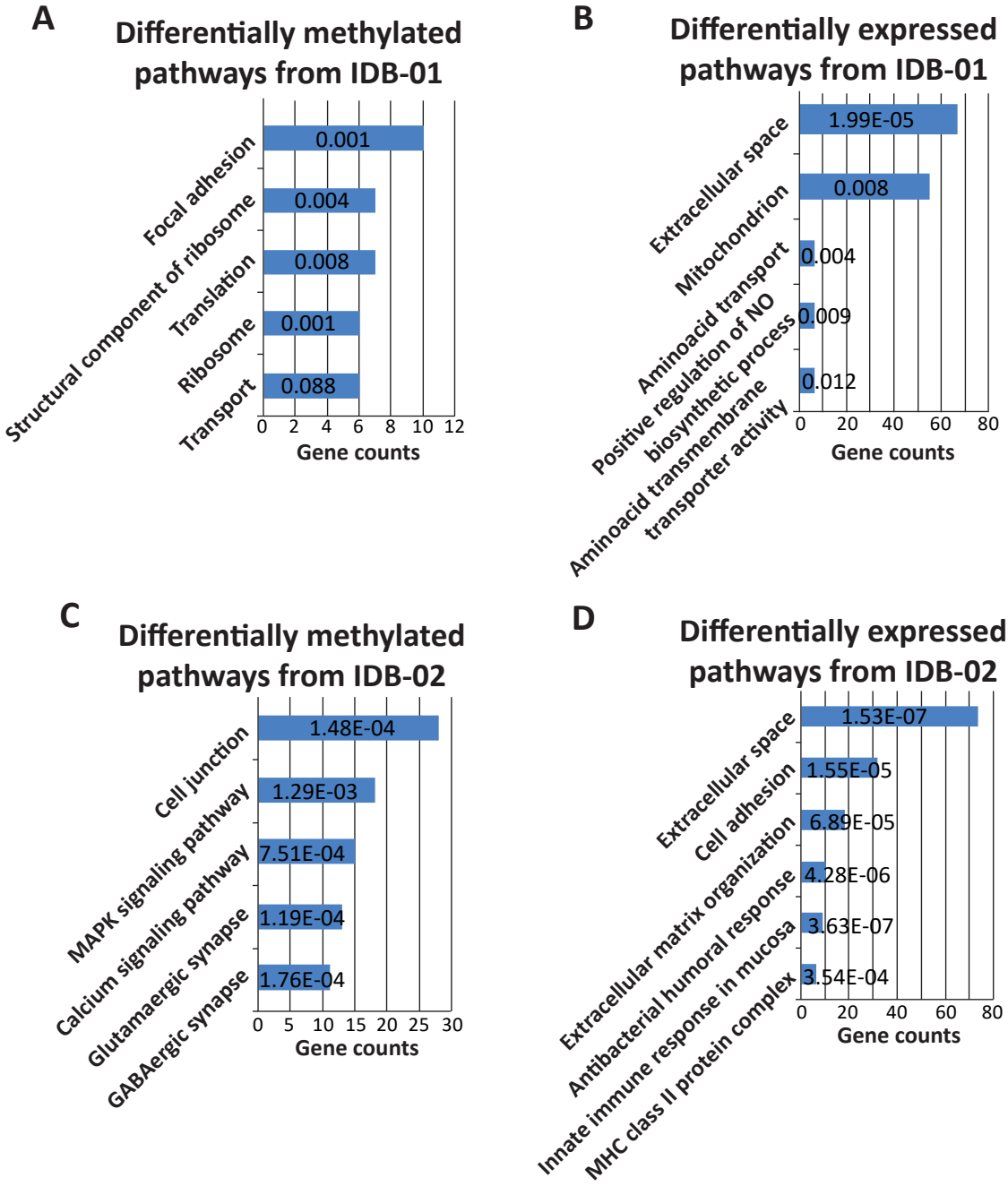
A
Differentially methylated pathways from IDB-01
Focal adhesion
Structural component of ribosome
Translation
Ribosome
Transport
0.001
0.004
0.008
0.001
0.088
0 2 4 6 8 10 12
Gene counts
B
Differentially expressed pathways from IDB-01
Extracellular space
Mitochondrion
Aminoacid transport
Positive regulation of NO biosynthetic process
Aminoacid transmembrane transporter activity
1.99E-05
0.008
0.004
0.009
0.012
0 20 40 60 80
Gene counts
C
Differentially methylated pathways from IDB-02
Cell junction
MAPK signaling pathway
Calcium signaling pathway
Glutamaergic synapse
GABAergic synapse
1.48E-04
1.29E-03
7.51E-04
1.19E-04
1.76E-04
0 5 10 15 20 25 30
Gene counts
D
Differentially expressed pathways from IDB-02
Extracellular space
Cell adhesion
Extracellular matrix organization
Antibacterial humoral response
Innate immune response in mucosa
MHC class II protein complex
1.53E-07
1.55E-05
6.89E-05
4.28E-06
3.63E-07
3.54E-04
0 20 40 60 80
Gene counts

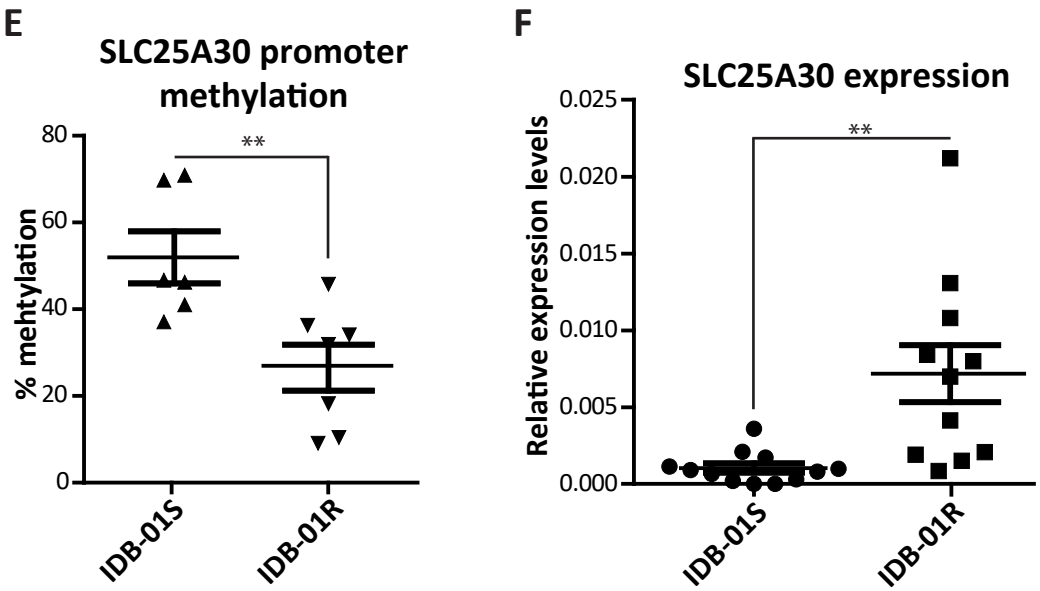
E
SLC25A30 promoter methylation
% mehtylation
80
60
40
20
0
**
IDB-01S
IDB-01R
F
SLC25A30 expression
Relative expression levels
0.025
0.020
0.015
0.010
0.005
0.000
**
IDB-01S
IDB-01R

Figure 5

A

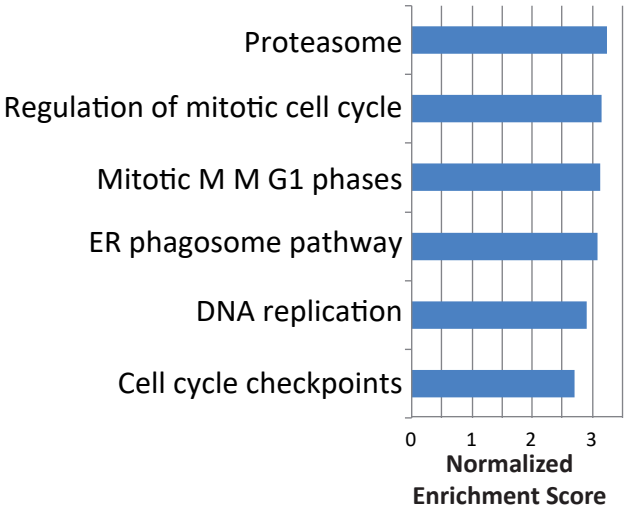

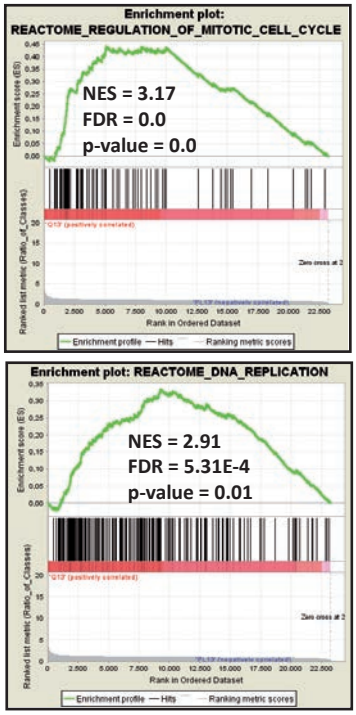

B

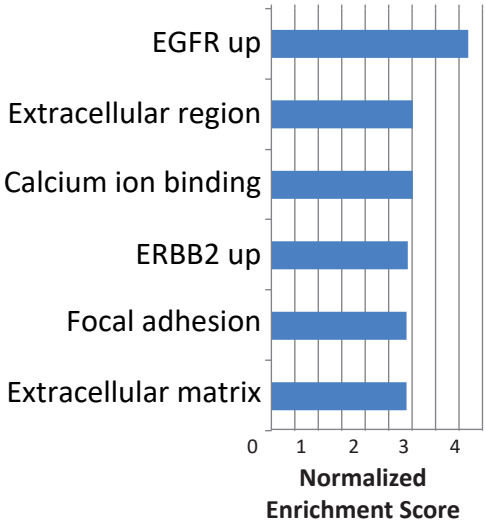

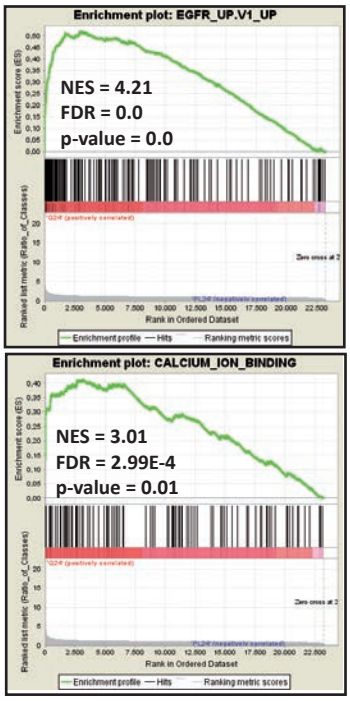

C

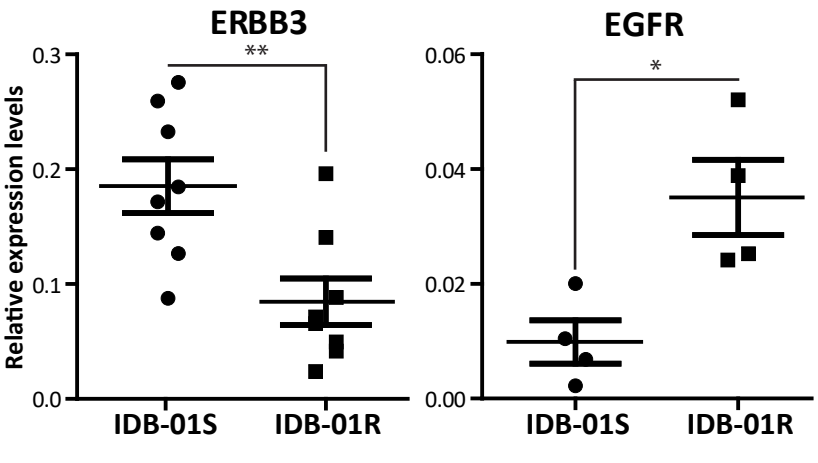

D

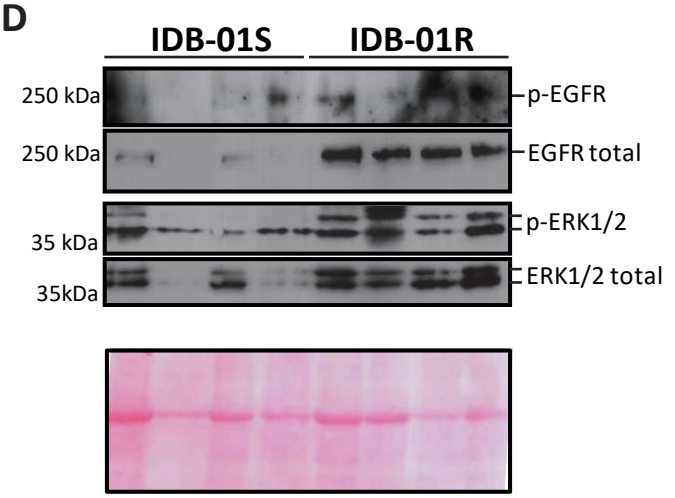

Supplementary Figure S1

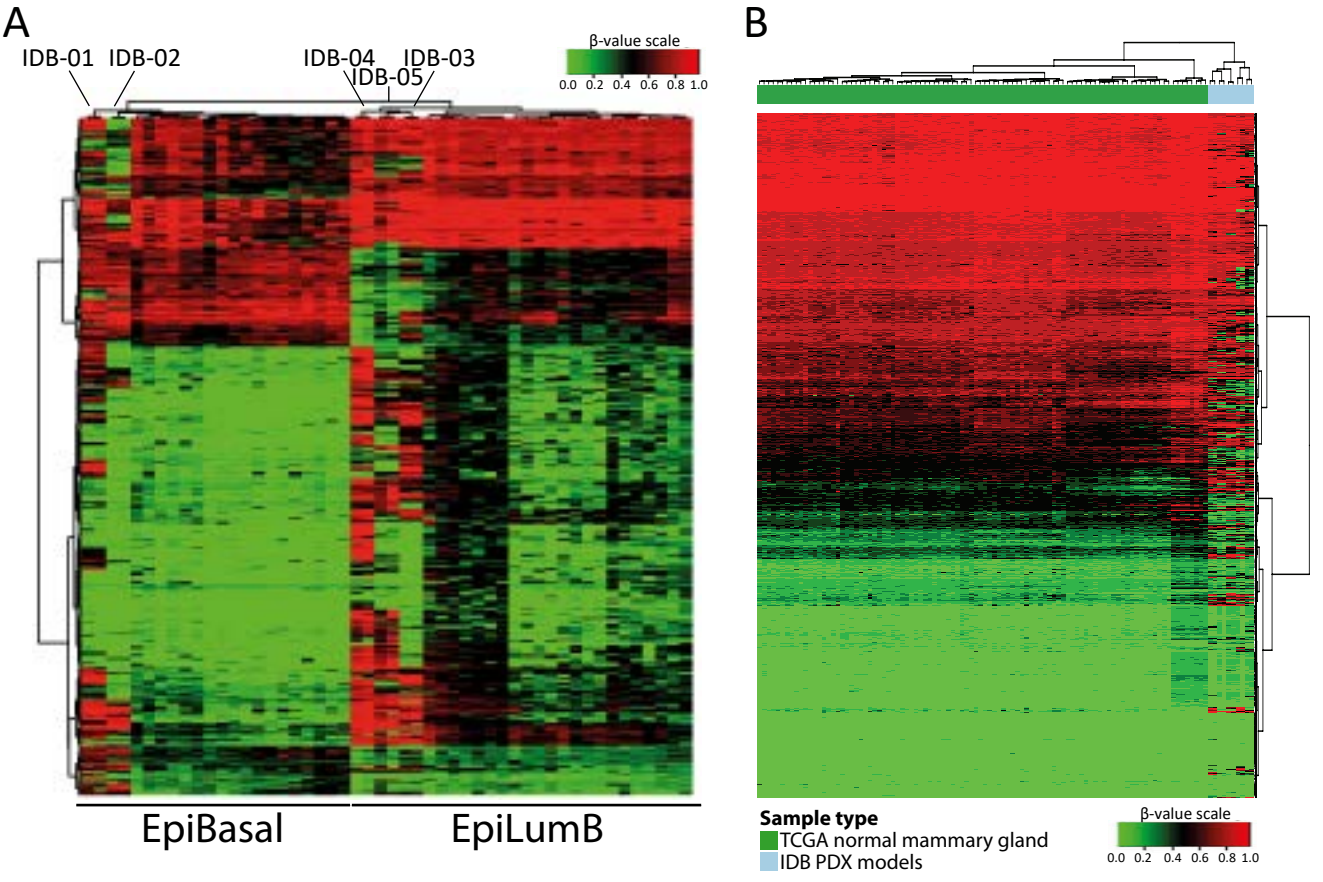

Supplementary Figure 2

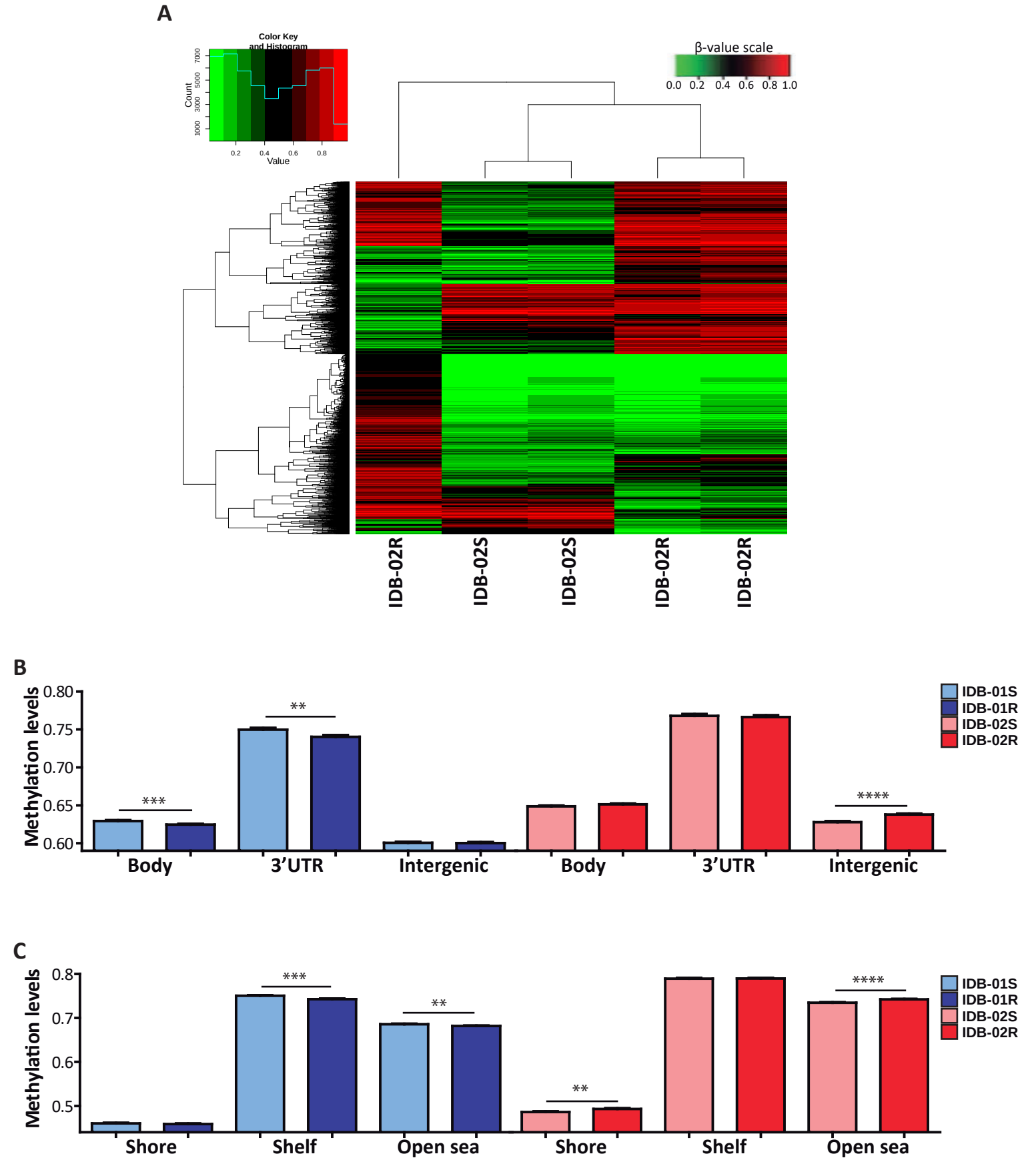

Supplementary Figure 3

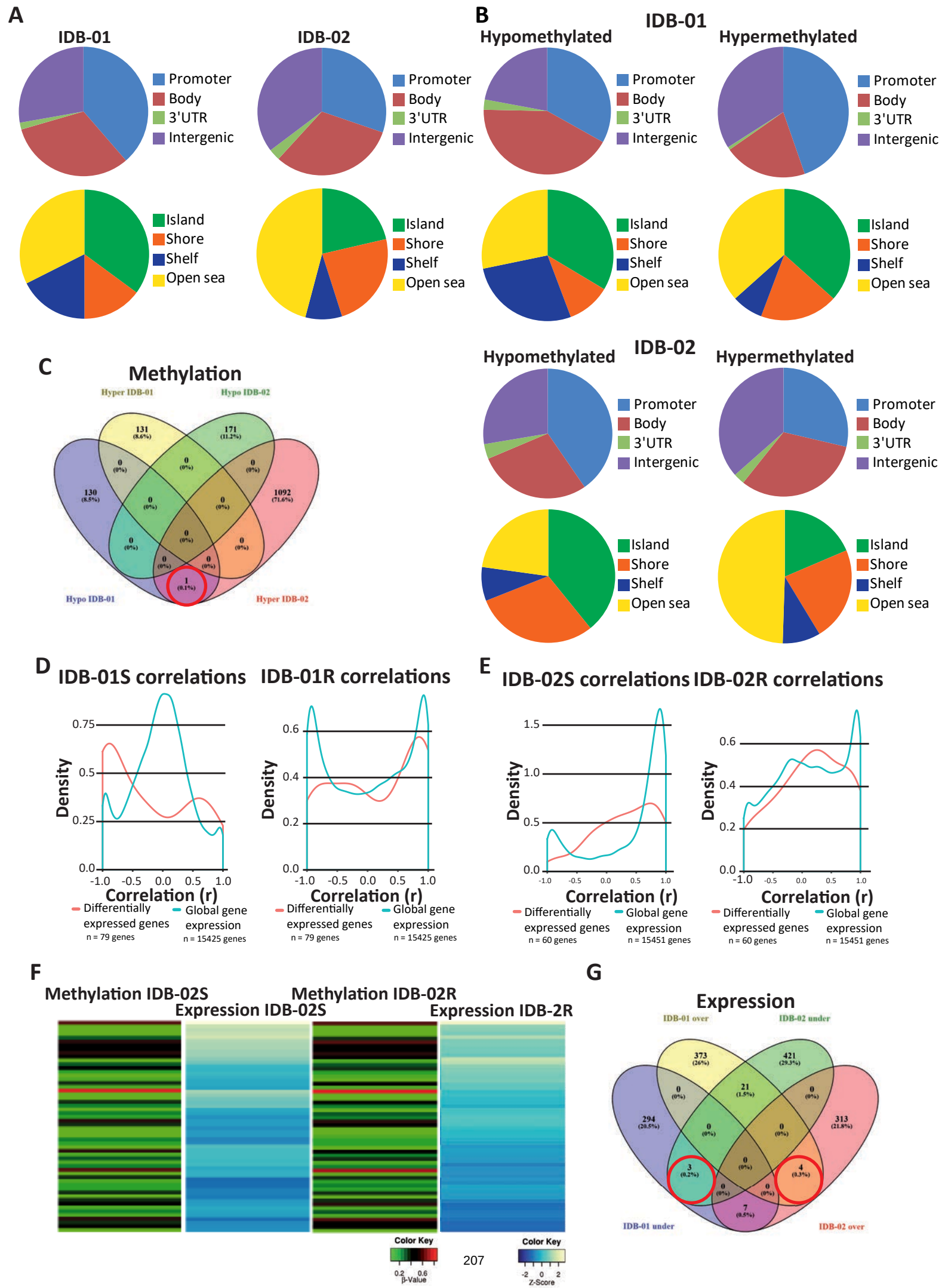

Figure legends

Figure 1. Global DNA methylation patterns of breast cancer PDX resemble breast cancer human samples and stratify in subtypes. A, B) Scatter plot of groupwise mean genome-wide DNA methylation levels analyzed by GenomeStudio between both sensitive TNBC PDX models (**A**) or between a TNBC and a luminal PDX model (**B**). Correlations are indicated as r^2. **C)** Unsupervised hierarchical clustering using 35.367 most differentially methylated CpGs between breast cancer PDX models. Methylation difference between at least one of the groups equal or higher to 75% and p-value < 0.01. Breast cancer PDX models and two major clusters, an ER+ and an ER-, are indicated. **D)** Supervised hierarchical clustering applying 743 selected CpGs that discriminate TNBC vs luminal subtype from TCGA breast cancer to BCCLs, PDX models and TCGA clinical samples. Breast cancer PDX models are indicated. Chi-square indicating association between TCGA breast tumors and PDX models from the same subtype is indicated below.

Figure 2. Genome-wide methylation patterns between docetaxel sensitive and resistant IDB-01 PDX model. A, B) Unsupervised hierarchical methylation clustering using the 10.000 most variable CpGs between TNBC PDX models (**A**) or between sensitive and resistant IDB-01 PDX tumors (**B**). **C)** Scatter plot of groupwise mean genome-wide DNA methylation levels analyzed by GenomeStudio between sensitive and resistant IDB-01 (top left) and IDB-02 (top right) PDX models and between sensitive tumors from IDB-01 (bottom left) and IDB-02 (bottom right) PDX models. Correlations are indicated as r^2. **D, E)** Mean methylation levels of CpGs located in promoter (**D**) and CpG island (**E**) in sensitive and resistant IDB-01 and IDB-02 PDX models. Mean, SEM and statistical significance are represented.

Figure 3. Association between point methylation and gene expression changes in sensitive and resistant TNBC PDX tumors. A) Representation of differentially methylated sites indicating direction of change when comparing sensitive and resistant TNBC PDX tumors from IDB-01 (left) and IDB-02 (right) PDX models. Percentage from total is indicated above. Total number of differentially methylated CpGs and genes for each TNBC PDX model are indicated. CpGs were selected by a methylation change higher than 30% and a standard deviation lower than 0.05 between samples from the same group. **B)** Mean-centered gene expression of differentially expressed genes between sensitive and resistant tumors from IDB-01 PDX model after *limma* test analysis. Genes are ordered vertically with regard to their expression. Overexpression (*yellow*) and underexpression (*blue*) are indicated. **C)** Density plot for correlation scores of methylation and gene expression for global, basal gene expression (blue line) and differentially expressed genes (red line) between sensitive and resistant IDB-01 PDX model. Number of genes used for correlations are indicated. **D)** Average methylation levels and gene expression of differentially expressed genes between sensitive and resistant tumors from IDB-01 PDX model. Genes are ordered vertically with regard to their expression.

Figure 4. Altered pathways by gene specific DNA methylation and gene expression changes and validation of SLC25A30. A, B, C, D) Representation of the most significative altered pathways by differential gene methylation (**A, C**) or gene expression (**B, D**) in resistant tumors from IDB-01 (**A, B**) and IDB-02 (**C, D**). p-value (left) is indicated, as well as number of genes

from each pathway. **E)** Mean methylation levels of 4 CpG islands from *SLC25A30* promoter in sensitive and resistant tumors from IDB-01 measured by pyrosequencing. Mean, SEM and statistical significance are represented. **F)** *SLC25A30* mRNA expression levels relative to *PPiA* in sensitive and resistant tumors from IDB-01 measured by qRT-PCR. Mean, SEM and statistical significance are represented.

Figure 5. Gene expression analysis independent of methylation and EGFR pathway validation. A, B) Representative plots of GSEA analysis showing enriched pathways derived from gene expression data from resistant IDB-01R (**A**) and IDB-02R (**B**) PDX models. **C)** *EGFR* and *ERBB3* mRNA expression levels relative to *PPiA* in sensitive and resistant tumors from IDB-01 measured by qRT-PCR. Mean, SEM and statistical significance are represented. **D)** Western blot for EGFR pathway from sensitive and resistant IDB-01 tumors.

Supplementary Figure 1. Clinical methylation signatures applied to breast cancer PDX models and comparison with human normal mammary glands. A) Supervised hierarchical clustering applying 202 and 254 CpGs that discriminate between EpiBasal and EpiLumB subtypes, respectively, to our PDX models. Breast cancer PDX models and two major clusters are indicated with luminal PDX samples being classified as EpiLumB signature and basal PDX models being classified as EpiBasal. **B)** Unsupervised hierarchical clustering from breast cancer PDX models and 100 human normal mammary gland samples using a representative 1% of the captured CpGs in the Infinium HumanMethylation450k from Illumina. Breast cancer PDX models are indicated.

Supplementary Figure 2. Methylation patterns between docetaxel sensitive and resistant IDB-02 PDX model. A) Unsupervised hierarchical methylation clustering using 10.000 most variable CpGs between sensitive and resistant IDB-02 PDX tumors. **B, C)** Mean methylation levels of the CpGs by genomic region (**B**) and CpG context (**C**) in sensitive and resistant IDB-01 and IDB-02 PDX models. Mean, SEM and statistical significance are represented.

Supplementary Figure 3. Dissection of point methylation changes between sensitive and resistant TNBC PDX tumors. A) Representation of differentially methylated sites between sensitive and resistant tumors from model IDB-01 (left) and IDB-02 (right) classified by genomic region (top) or CpG context (bottom). **B)** Representation of differentially methylated sites between sensitive and resistant tumors from model IDB-01 (left panels) and IDB-02 (right panels) classified by genomic region (top) or CpG context (bottom). CpG methylation change in resistant TNBC PDX tumors is indicated. **C, D)** Venn's diagram comparing differentially methylated CpGs (**C**) or differentially expressed genes (**D**) found in the comparisons between sensitive and resistant TNBC PDXs. Direction of the change in methylation and gene expression as well as TNBC PDX model is indicated. **E, F)** Density plot for correlation scores of methylation and gene expression for global, basal gene expression (blue line) and differentially expressed genes (orange line) in sensitive (left) and resistant (right) tumors of IDB-01 (**E**) and IDB-02 (**F**) PDX models. Number of genes used for correlations are indicated. **G)** Average methylation levels and mean-centered gene expression of differentially expressed genes between sensitive and resistant tumors from IDB-02 PDX model. Genes are ordered vertically with regard to their expression.

ARTICLE 5

“RANK Signaling Blockade Reduces Breast Cancer Recurrence by Inducing Tumor Cell Differentiation”

Published OnlineFirst August 1, 2016; DOI: 10.1158/0008-5472.CAN-15-2745

Tumor and Stem Cell Biology

Cancer Research

RANK Signaling Blockade Reduces Breast Cancer Recurrence by Inducing Tumor Cell Differentiation

Guillermo Yoldi[1], Pasquale Pellegrini[1], Eva M. Trinidad[1], Alex Cordero[1], Jorge Gomez-Miragaya[1], Jordi Serra-Musach[2], William C. Dougall[3], Purificación Muñoz[1], Miguel-Angel Pujana[2], Lourdes Planelles[4], and Eva González-Suárez[1]

Abstract

RANK expression is associated with poor prognosis in breast cancer even though its therapeutic potential remains unknown. RANKL and its receptor RANK are downstream effectors of the progesterone signaling pathway. However, RANK expression is enriched in hormone receptor negative adenocarcinomas, suggesting additional roles for RANK signaling beyond its hormone-dependent function. Here, to explore the role of RANK signaling once tumors have developed, we use the mouse mammary tumor virus-Polyoma Middle T (MMTV-PyMT), which mimics RANK and RANKL expression patterns seen in human breast adenocarcinomas. Complementary genetic and pharmacologic approaches demonstrate that therapeutic inhibition of RANK signaling drastically reduces the cancer stem cell pool, decreases tumor and metastasis initiation, and enhances sensitivity to chemotherapy. Mechanistically, genome-wide expression analyses show that anti-RANKL therapy promotes lactogenic differentiation of tumor cells. Moreover, RANK signaling in tumor cells negatively regulates the expression of *Ap2* transcription factors, and enhances the Wnt agonist *Rspo1* and the Sca1-population, enriched in tumor-initiating cells. In addition, we found that expression of *TFAP2B* and the RANK inhibitor, *OPG*, in human breast cancer correlate and are associated with relapse-free tumors. These results support the use of RANKL inhibitors to reduce recurrence and metastasis in breast cancer patients based on its ability to induce tumor cell differentiation. *Cancer Res; 76(19); 5857–69. ©2016 AACR.*

Introduction

Multiple lines of evidence support the existence of tumor-initiating cells (TICs) or cancer stem cells (CSC) in breast cancer (1). Recent efforts to develop CSC-related therapies explored elimination of the CSC population, removal of their self-renewal capability, and forced terminal differentiation. The first differentiation agent successfully used in the clinic was all-trans retinoic acid in acute promyelocytic leukemia (2). Retinoid signaling also regulates breast CSC self renewal and differentiation (3).

RANK ligand (RANKL) is expressed in progesterone receptor-positive (PR^+) mammary epithelial cells and acts as a paracrine mediator of progesterone in mouse and human mammary epithelia (4–9). Overexpression of RANKL's receptor, RANK in mammary epithelial cells enhances proliferation, impairs lactation, and induces the accumulation of mammary stem cells (MaSC) and progenitors (9–12). In human adenocarcinomas, RANK is predominantly expressed in hormone receptor-negative (HR^-) tumors, supporting a progesterone-independent role. In contrast to RANK, RANKL is rarely expressed on tumor cells, but it is expressed in tumor-infiltrating lymphocytes (7, 11, 13). RANK expression in human adenocarcinomas is associated with reduced overall survival (13, 14). However, the mechanisms underlying these aggressive tumor phenotypes and the therapeutic potential of RANKL inhibition once tumors have developed remain unexplored.

The MMTV-PyMT breast cancer mouse model displays widespread transformation of the mammary gland and a high incidence of lung metastasis (15, 16). Tumor cells of invasive PyMT adenocarcinomas do not express hormone receptors or RANKL, but do express high levels of RANK (7, 9). RANKL inhibitors are currently used for the treatment of bone-related pathologies, osteoporosis, and bone metastasis. Here we demonstrate that inhibition of RANK signaling acts as a differentiation therapy in breast cancer, depleting the cancer stem cells population and reducing recurrence and metastasis.

[1]Cancer Epigenetics and Biology Program, Bellvitge Biomedical Research Institute, IDIBELL, Barcelona, Spain. [2]Program Against Cancer Therapeutic Resistance (ProCURE), Breast Cancer and Systems Biology Lab, Catalan Institute of Oncology, IDIBELL, Barcelona, Spain. [3]Therapeutic Innovation Unit, Amgen Inc., Seattle, Washington. [4]Centro Nacional de Biotecnología/CSIC, UAM Cantoblanco, Madrid, Spain.

Note: Supplementary data for this article are available at Cancer Research Online (http://cancerres.aacrjournals.org/).

G. Yoldi, P. Pellegrini, and E.M. Trinidad contributed equally to this work.

Current address for P. Pellegrini: Gladstone Institutes, San Francisco, California; current address for W.C. Dougall: Department of Immunology in Cancer and Infection, QIMR Berghofer Medical Research Institute, Herston, QLD, Australia; current address for A. Cordero: Department of Neurological Surgery Feinberg School of Medicine, Northwestern University Chicago, IL.

Corresponding Author: Eva González-Suárez, Bellvitge Biomedical Research Institute (IDIBELL), Av. Gran Via de L'Hospitalet, 199-203, L'Hospitalet de Llobregat, Barcelona 08908, Spain. Phone: 932607347; Fax: 932607219; E-mail: egsuarez@idibell.cat

doi: 10.1158/0008-5472.CAN-15-2745

Published OnlineFirst August 1, 2016; DOI: 10.1158/0008-5472.CAN-15-2745

Materials and Methods

Animals, RANKL, RANK-Fc, and docetaxel treatments

All research involving animals was performed at the IDIBELL animal facility in compliance with protocols approved by the IDIBELL Committee on Animal Care and following National and European Union regulations. MMTV-PyMT (FVB/N-Tg(MMTV-PyVT)634Mul) were obtained from the Jackson Laboratory (15). MMTV-PyMT$^{-/+}$;RANK$^{-/-}$ mice were obtained by backcrossing the MMTV-PyMT (FvB/N) strain with RANK$^{+/-}$ mice into the C57BL/6 background (17). RANKL (1 mg/kg, Amgen) and RANK-Fc (10 mg/kg, Amgen) were injected subcutaneously three times a week (7, 10). Docetaxel (Actavis) was administered at 25 mg/kg intraperitoneally twice per week.

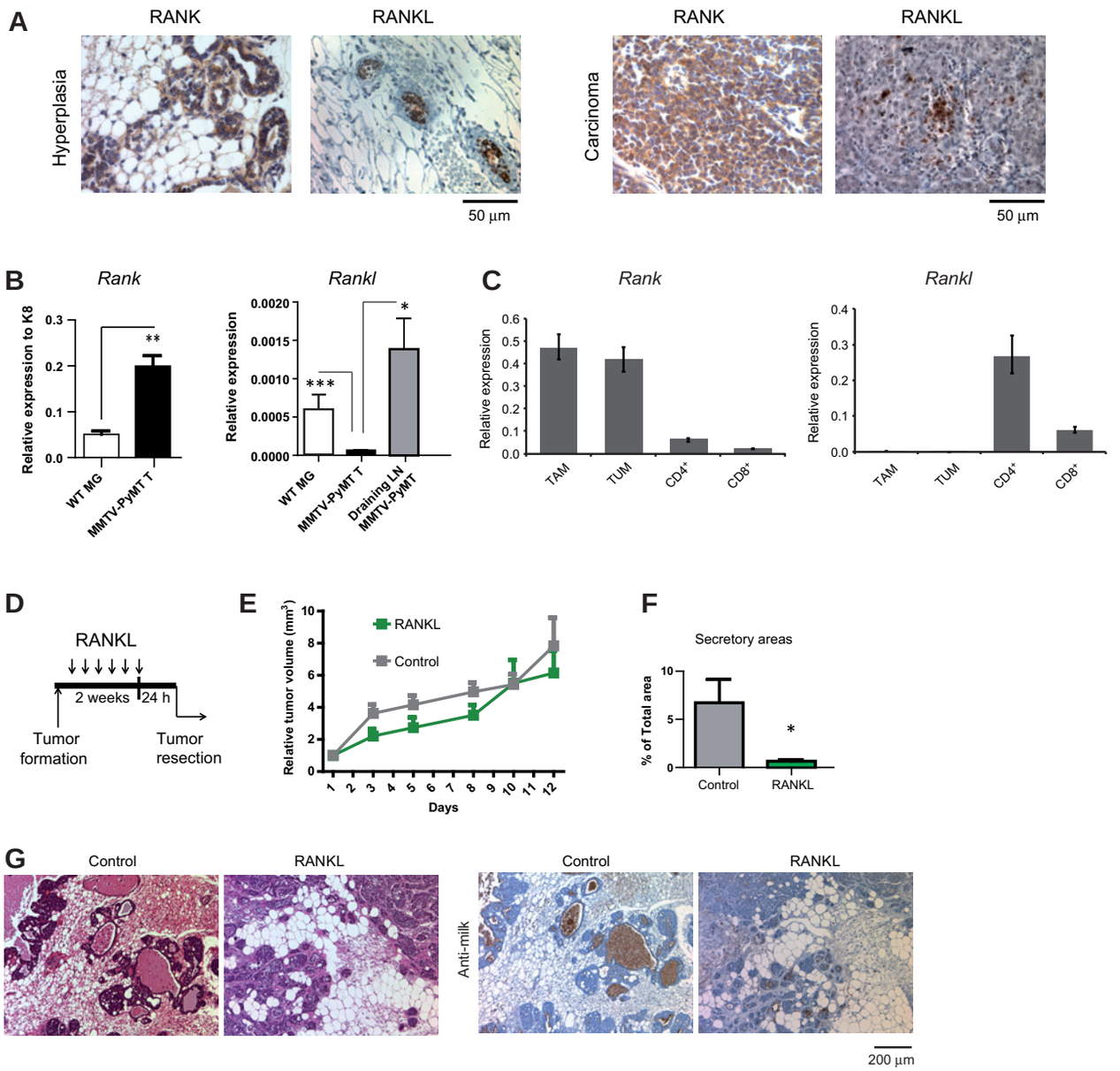

Figure 1.

RANKL decreases MMTV-PyMT tumor cell differentiation. **A,** representative images of RANK and RANKL protein expression. Note that in carcinomas, RANKL is not expressed in tumor cells but in tumor-infiltrating lymphocytes. **B,** *Rank* and *Rankl* mRNA expression relative to *K8* or b-*actin* in seven WT, eight MMTV-PyMT tumors, and three draining lymph nodes of MMTV-PyMT tumor-bearing mice. **C,** *Rank* and *Rankl* mRNA expression relative to *Rpl38* in FACS-sorted (Supplementary Fig. S2) tumor cells (TUM) CD45$^-$, macrophages (TAM) CD45$^+$CD11b$^+$F4/80$^+$Gr1$^-$, CD4$^+$, and CD8$^+$ T lymphocytes (CD45$^+$CD11b$^-$CD3$^+$CD4$^+$ or CD8) from four MMTV-PyMT tumors. **D,** schematic overview of short-term (2 weeks) RANKL treatment in MMTV-PyMT tumor-bearing females. **E,** tumor volume normalized to the first day of treatment of five MMTV-PyMT tumor-bearing mice undergoing RANKL treatment and controls. **F,** percentage of secretory areas relative to total tumor area in (3–5) MMTV-PyMT primary tumors after RANKL treatment. **G,** representative images of hematoxylin and eosin and milk protein staining in MMTV-PyMT primary tumors. **B, E, F,** mean, SEM, and *t* test probabilities are shown (*, 0.01 < *P* < 0.05; **, 0.001 < *P* < 0.01; ***, 0.001 < *P* < 0.0001).

Published OnlineFirst August 1, 2016; DOI: 10.1158/0008-5472.CAN-15-2745

Tumor cell isolation, tumor and metastasis initiation assays

Tumor cells were isolated as described (18). For orthotopic transplants and tumor-limiting dilution assays (LDA), tumor cells were mixed 1:1 with Matrigel matrix (BD Biosciences) and orthotopically implanted in the inguinal mammary gland of 6- to 10-week-old syngeneic females. For metastasis assays, tumor cells resuspended in cold PBS were injected intravenously in 6- to 10-week-old *Foxn1*^{nu} females.

Tissue histology and immunostaining

Tissue samples were fixed in formalin and embedded in paraffin. Three-micrometer sections were cut for histologic analysis and stained with hematoxylin and eosin. Entire lungs were step sectioned at 100 μm and 15 cuts per lung were quantified. Antigen heat retrieval with citrate was used for PR (DAKO), SMA-1 (Sigma-Aldrich), mRANKL (R&D Systems), Ki67 (Thermo Scientific), cleaved caspase-3 (Cell Signaling) antibodies, and rabbit anti-milk serum (kindly provided by Prof. Nancy E. Hynes). mRANK (R&D Systems) immunostaining was performed, pretreating sections with Protease XXIV 5 U/mL (Sigma-Aldrich) for 15 minutes at room temperature. All antibodies were incubated overnight at 4°C, detected with biotinylated secondary antibodies and streptavidin horseradish peroxidase (Vector), and revealed with DAB substrate (DAKO).

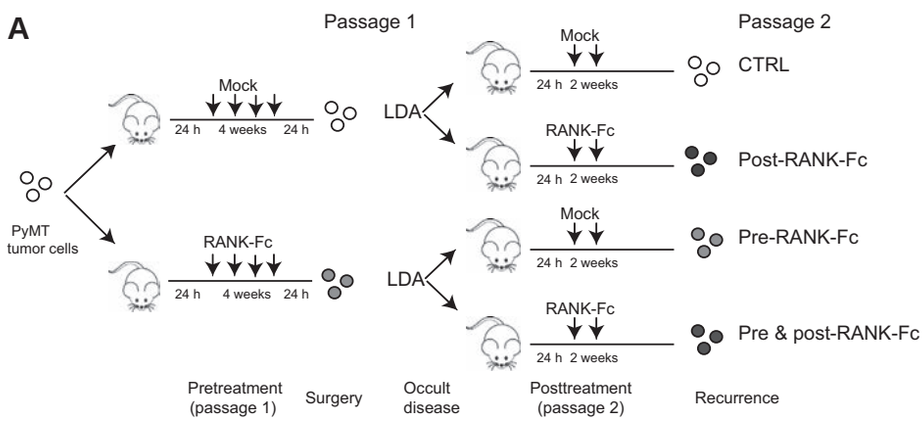

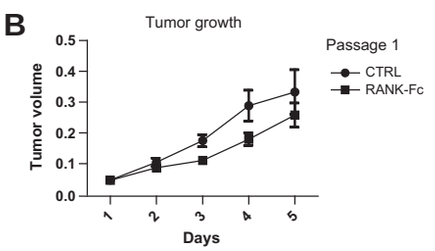

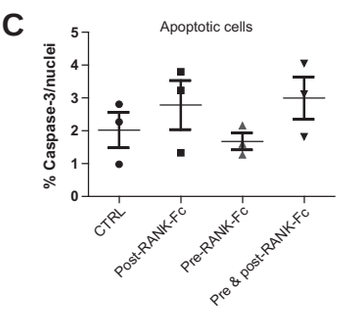

D

Group	*N* cells	*N* fat pad	*N* tumors	TIC frequency
CTRL	100,000	4	4	1/ 206 (CI 599–70.9)
	10,000	6	6	
	1,000	6	5	
	100	6	6	
Post-RANK-Fc	100,000	6	6	1/ 466 (CI 1,138–190.7)
	10,000	6	6	
	1,000	6	4	
	100	6	4	
Pre-RANK-Fc	100,000	6	6	1/ 1,929 (CI 5,431–685.1)
	10,000	6	5	
	1,000	6	5	
	100	6	2	
Pre & post RANK-Fc	100,000	6	6	1/ 2,353 (CI 6,378–868.3)
	10,000	6	5	
	1,000	6	3	
	100	6	3	

GROUP	*P*	χ^2
CTRL vs. post RANK-Fc	0.13	2.27
CTRL vs. pre RANK-Fc	2.99 E–5	17.4
CTRL vs. pre & post RANK-Fc	7.48 E–6	7.41
Pre RANK-Fc vs. pre & post RANK-Fc	0.701	0.147

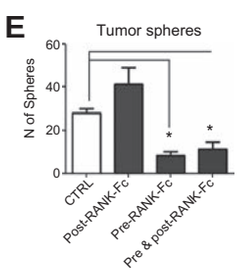

Figure 2.
Inhibition of RANK signaling depletes the pool of MMTV-PyMT TICs. **A,** schematic overview of RANK-Fc treatments in orthotopic MMTV-PyMT tumors. One million cells isolated from one MMTV-PyMT carcinoma were orthotopically injected into syngeneic WT mice (FVB), which were randomized 1:1 for RANK-Fc (10 mg/kg, 3 times per week, 4 weeks) or mock treatment starting 24 h later (passage 1). Cells isolated from three tumors from each treatment arm were pooled and orthotopically injected into WT (passage 2) mice in limiting dilutions and randomized 1:1 for additional RANK-Fc or mock treatment (2 weeks). Total number of tumors was scored after 26 weeks. **B,** tumor growth of passage 1 tumors. **C,** percentage of positive cleaved caspase-3 cells in passage 2 tumors. **D,** TIC frequencies (with confidence intervals), x^2 values, and associated probabilities. **E,** number of secondary tumorspheres formed by RANK-Fc-treated MMTV-PyMT tumors. Each bar represents data from four tumors plated in triplicates. **B, C, E,** mean, SEM, and *t* test statistics are shown (*, $0.01 < P < 0.05$).

Published OnlineFirst August 1, 2016; DOI: 10.1158/0008-5472.CAN-15-2745

Tumorsphere culture

Cells isolated from primary tumors were resuspended in serum-free DMEM F12 mammosphere medium containing 20 ng/mL of EFG, 1× B27, and 4 μg/mL heparin (Sigma-Aldrich), as previously described (19) with 2% of growth factor–reduced matrigel. Primary tumorspheres were derived by plating 20,000 cells/mL in 2 mL of medium onto cell-suspension culture plates. After 14 days, tumorspheres were isolated by 5 min treatment with PBS-EDTA 1 mmol/L + 5 min of trypsin at 37°C and plated for secondary tumorsphere formation at a concentration of 5,000 cells/mL in triplicate. Individual spheres from each replicate well were counted under a microscope.

Flow cytometry

Single cells were resuspended and blocked with PBS 2% FBS and IgG blocking reagent for 10 min on ice and incubated for 30 min on ice with CD45-APC-Cy7 (30-F11), CD4-PE-Cy7 (RM4-5), CD11b-APC (M1/70), CD8-PE or CD8-FITC (53-6.7), Gr1-FITC (RB6-8C5), F4/80-PE (BM8), CD49b-Alexa 647 (1HMa2), CD45-PECy7 or –APCCy7 (30-F11), and CD31-PECy7 (390), all from Biolegend, CD24-FITC (M1/69), CD61-FITC (2C9.G2), Sca-1-APC (Ly-6A/E) from BD Pharmingen, CD90-PE (HIS51; Bioscience) and CD49f-AF647 (GoH3; R&D Systems). FACS analysis was performed using FACS Canto, FACS Aria (Becton Dickinson) and Diva software. Cells were sorted using MoFlo (Beckman Coulter) at 25 psi (172 kPa) and a 100-μm tip.

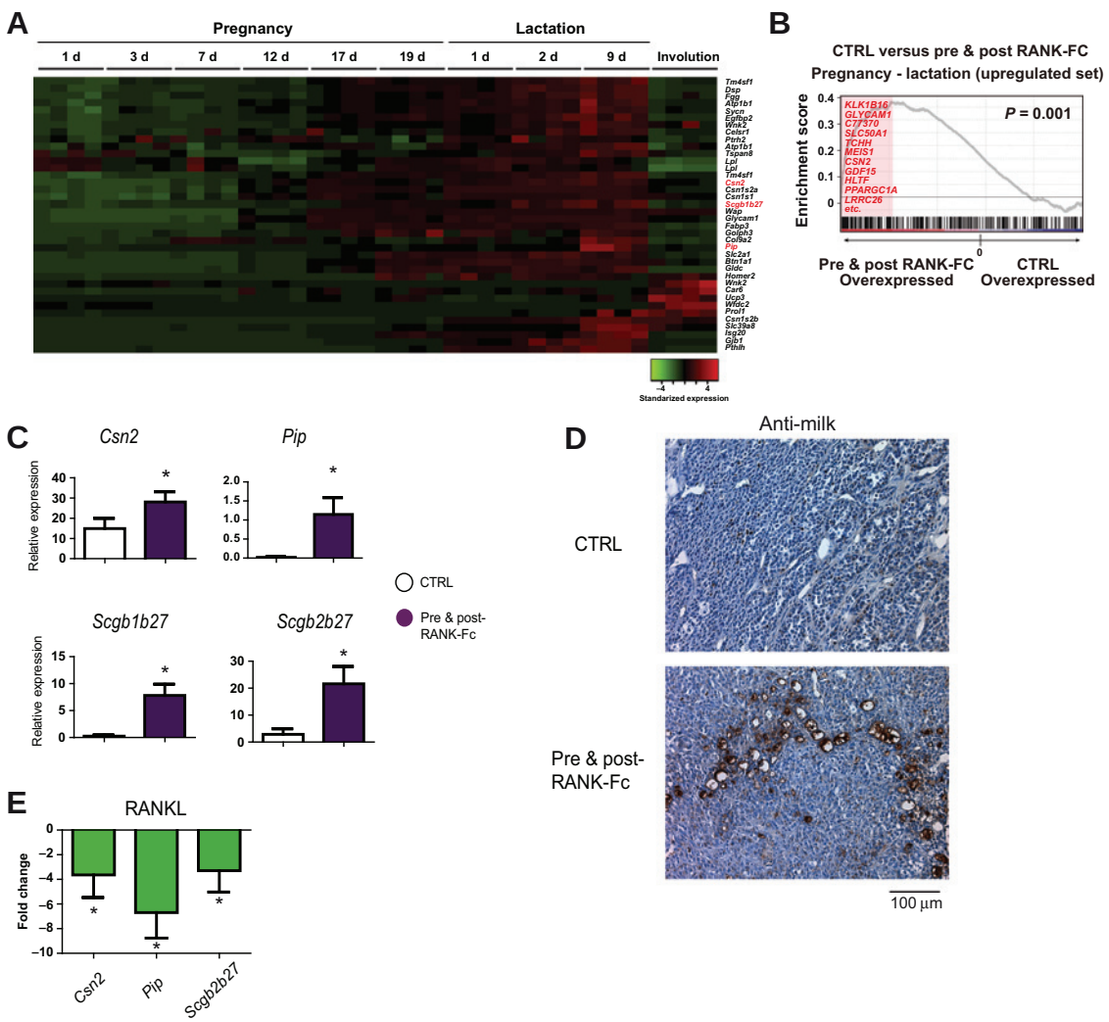

Figure 3.

RANKL inhibition induces differentiation of tumor cells into milk secreting cells. **A,** expression profile in mammary gland development of differentially expressed genes between RANK-Fc-treated tumors and controls (21). Genes further validated by reverse transcription-PCR are shown in red. **B,** GSEA graphical output for the association between lactation overexpressed genes and RANK-Fc treatment. The top genes contributing to this association are listed. **C,** mRNA expression levels of indicated genes relative to *HPRT*. Each bar is representative of three tumors. **D,** representative images of milk staining in RANK-Fc–treated tumors. **E,** fold change of mRNA expression levels of indicated genes in RANKL-treated acinar cultures of MMTV-PyMT tumor cells relative to untreated controls. Three tumors were analyzed. **B** and **E,** mean, SEM, and *t* test *P* values are shown (*, $0.01 < P < 0.05$).

Published OnlineFirst August 1, 2016; DOI: 10.1158/0008-5472.CAN-15-2745

RNA labeling and hybridization to Agilent microarrays

Hybridization to SurePrint G3 Mouse Gene Expression Microarray (ID G4852A; Agilent Technologies) was conducted following manufacturer's protocol (Two-Color Microarray-Based Gene Expression Analysis v. 6.5; Agilent Technologies), and dye swaps (Cy3 and Cy5) were performed for RNA amplified from each sample. Microarray chips were washed and scanned using a DNA Microarray Scanner (Model G2505C; Agilent Technologies).

Microarray analysis

Microarray data were feature extracted using Feature Extraction Software (v. 10.7) available from Agilent, using the default variables. Outlier features on the arrays were flagged by the same software package. Data analysis was performed using Bioconductor package, under R environment. Data preprocessing and differential expression analysis was performed using limma and RankProd package, and latest gene annotations available was used. Raw feature intensities were background corrected using normexp background correction algorithm. Within-array normalization was done using spatial and intensity-dependent loess. Aquantile normalization was used to normalize between arrays. The expression of each gene is reported as the *base 2 logarithm* of ratio of the value obtained of each condition relative to controls. A gene is considered differentially expressed if it displays a pfp (proportion of false positives) less than 0.05 by nonparametric test. The GSEA was run using default values for all parameters. Raw microarray data has been deposited in GEO, access number GSE66085. The mature luminal and stem cell gene sets were taken from the original publication (20). The differentially expressed genes between lactation and pregnancy were identified using the GEO GSE8191 dataset (21) and the TFAP2C-regulated genes in breast cancer cells using the GEO GSE8640 dataset (22). Cox proportional hazard regression analyses were applied to evaluate associations with prognosis (relapse or distant metastasis) at the level of microarray probes.

Statistical analysis

Differences were analyzed with a two-tailed Student *t* test or an *F* test, one sample *t* test against a reference value of 1. Two-way analysis of variance was used to compare tumor growth curves. The Mantel–Cox test was used for tumor-free survival studies. Frequency of tumor initiating was estimated using the extreme limiting dilution software (ELDA; ref. 23). The statistical significance of difference between groups is indicated by asterisks (*, $0.01 < P < 0.05$; **, $0.001 < P < 0.01$; ***, $0.001 < P < 0.0001$; ****, $P < 0.0001$).

Results

RANKL stimulation promotes tumor growth in MMTV-PyMT primary tumor cells

MMTV-PyMT preneoplasic lesions and adenocarcinomas expressed high levels of RANK (Fig. 1A and B). RANKL expression

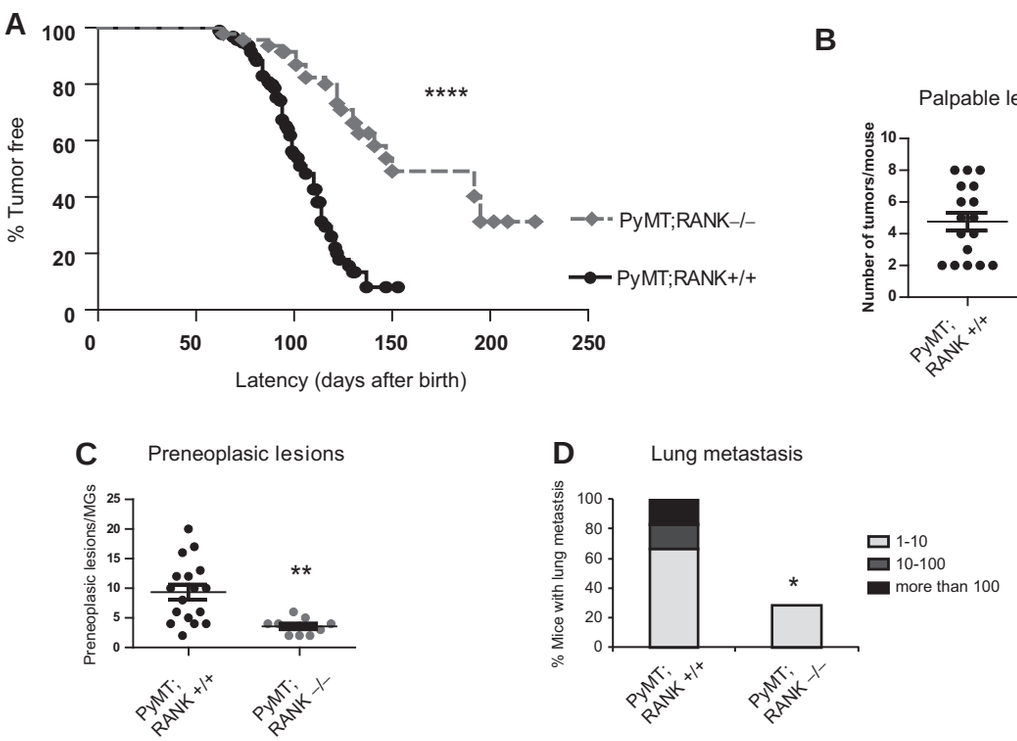

Figure 4.

Constitutive deletion of RANK increases tumor latency, decreases tumor incidence, and prevents lung metastasis of MMTV-PyMT tumors. **A,** kinetics of palpable tumor onset with age in 18 PyMT;RANK$^{+/+}$ and 10 PyMT;RANK$^{-/-}$ mice. Log-rank test (****, $P < 0.0001$). **B,** number of palpable lesions detected at necropsy in 17 PyMT;RANK$^{+/+}$ and 10 PyMT;RANK$^{-/-}$ mice. **C,** number of preneoplasic regions per mammary gland detected in mammary whole mounts of 9 PyMT;RANK$^{+/+}$ and 5 PyMT;RANK$^{-/-}$ mice 13 to 22 weeks old. Each dot represents one mammary gland. **D,** percentage of PyMT;RANK$^{+/+}$ ($n = 6$) and PyMT;RANK$^{-/-}$ ($n = 7$) mice with lung metastasis. The total number of metastatic foci per mouse is indicated. $x^2 = 6.96$, as calculated by contingency 2×2, $P = 0.01$. **B** and **C,** mean, SEM, and *t* test *P* values are shown (*, $0.01 < P < 0.05$).

Published OnlineFirst August 1, 2016; DOI: 10.1158/0008-5472.CAN-15-2745

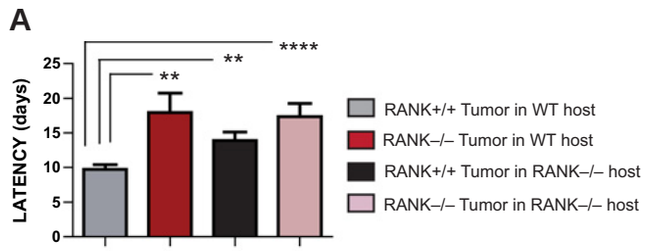

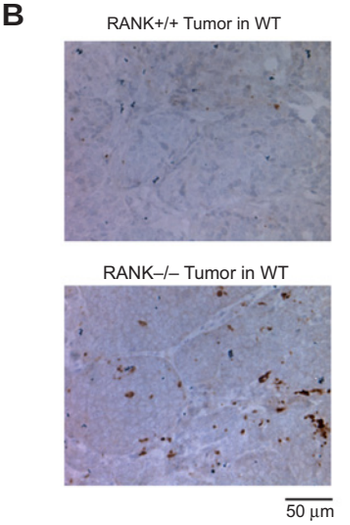

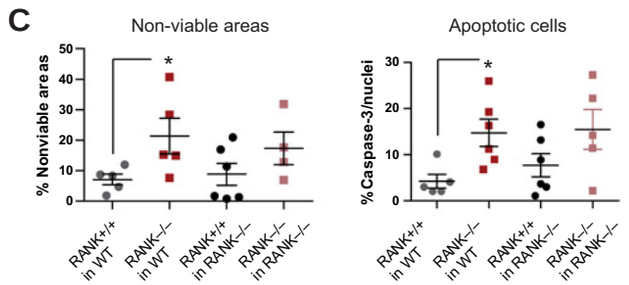

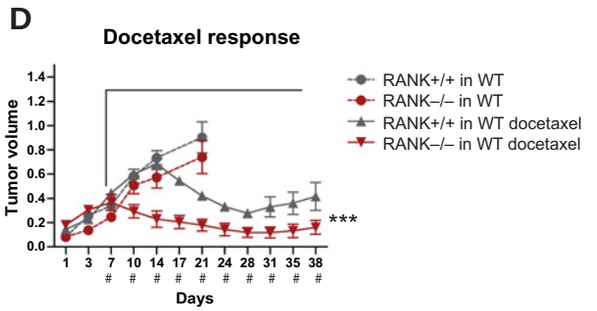

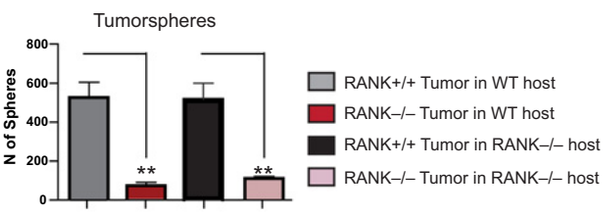

F

Group	*N* cells	*N* fat pad	*N* tumors
PyMT;RANK+/+	10,000	4	4
	1,000	4	3
	100	4	4
	10	4	0
PyMT;RANK–/–	10,000	4	4
	1,000	4	2
	100	4	1
	10	4	0

Tumor-initiating cell (TIC) frequency

PyMT;RANK +/+
1/ 285 (C.I. 913–89)

PyMT;RANK–/–
1/ 1,078 (C.I. 3,572–326)

P value : 0.05 χ^2: 3.58

G

Group	*N* cells	Mice	Metastasis incidence
PyMT;RANK+/+	100,000	4	4
	10,000	4	4
	1,000	4	0
	100	4	1
PyMT;RANK–/–	100,000	4	3
	10,000	4	3
	1,000	4	1
	100	4	0

Metastasis-initiating cell (MIC) frequency

PyMT;RANK +/+
1 / 2,952 (C.I. 9,374–929)

PyMT;RANK–/–
1/ 29,420 (C.I. 93,261–9,281)

P value : 0.00262 χ^2: 9.06

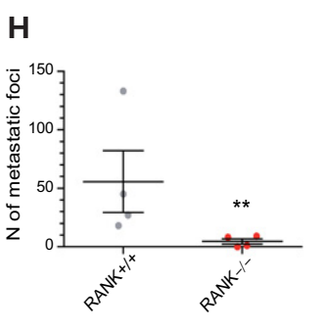

Published OnlineFirst August 1, 2016; DOI: 10.1158/0008-5472.CAN-15-2745

was found in nontumorigenic ducts and hyperplasias (Fig. 1A) but was lost in MMTV-PyMT adenocarcinomas, consistent with the loss of PR positivity (Fig. 1A and Supplementary Fig. S1; ref. 24). RANKL was expressed in draining lymph nodes and tumor-infiltrating leucocytes of tumor-bearing mice (Fig. 1A and B). *Rankl* mRNA was predominantly found in tumor-infiltrating $CD4^+$ and $CD8^+$ T lymphocytes ($CD45^+CD11b^-CD4^+$ and $CD45^+CD11b^-CD8^+$), whereas *Rank* mRNA was found in tumor cells and macrophages (Fig. 1C and Supplementary Fig. S2), consistent with the expression of RANK and RANKL in human breast adenocarcinomas (7, 11, 13), highlighting the relevance of the MMTV-PyMT tumor model to the study of human pathology.

Administration of RANKL resulted in increased acinar size in MMTV-PyMT tumor acini (Supplementary Fig. S3A and S3B; refs. 25, 26). No significant changes in proliferation were found, but decreased apoptosis was observed in RANKL-treated tumor cultures (Supplementary Fig. S3B). RANKL-treated acini showed an "invasive-like" phenotype, with isolated cells surrounding the acini (Supplementary Fig. S3A). Remarkably, 2-week RANKL-treated acini gave rise to faster growing tumors and more metastasis than untreated controls when injected in immunodeficient mice (Supplementary Fig. S3C and S3D). These results demonstrate that activation of RANK signaling could promote tumor growth and metastasis in MMTV-PyMT primary tumor cells.

Inhibition of RANKL signaling decreases the frequency of tumor-initiating cells

No significant changes in tumor growth, tumor cell proliferation, or apoptosis were observed after 2 weeks of RANKL treatment *in vivo* on tumor-bearing MMTV-PyMT mice (Fig. 1D–E and Supplementary Fig. S3E; ref. 10), but tumor cell density was higher in RANKL treated lesions, in contrast to control mice, where extensive areas of dilated ducts and hyperplasias full of milk secretions were observed (Fig. 1F–G). These results indicate that short-term *in vivo* activation of RANK signaling is not sufficient to change the growth of established tumors, but appears to prevent secretory differentiation of tumor cells.

The putative benefit of pharmacologic RANKL inhibition with RANK-Fc in tumor recurrence was interrogated (Fig. 2A; ref. 7). No significant differences in tumor growth or the frequency of apoptotic cells were observed after RANK-Fc treatments (Fig. 2B and C). However, LDAs revealed that tumor cells pretreated with RANK-Fc at passage 1 showed a 10-fold decrease in tumor-initiating ability, whereas RANK-Fc treatment only at passage 2 did not significantly change tumor-initiating cell (TIC) frequency (Fig. 2D). Concomitantly, the ability to form secondary tumorspheres was significantly impaired in cells derived from the RANK-Fc-pretreated pool (Fig. 2E), consistent with a reduction in the CSC population (19). These results demonstrate that pretreatment with RANK-Fc reduces tumor-initiating ability, and suggests that in clinics, RANKL inhibition may reduce the risk of relapse by depleting the population of CSCs.

Pharmacological inhibition of RANK signaling induces lactogenic differentiation of tumor cells

To investigate the molecular mechanism underlying the reduction in tumor-initiating ability, we analyzed global gene expression profiles from all RANK-Fc treatment arms. Genes induced by RANK-Fc included milk proteins such as *Pip*, *caseins*, *Wap*, or *Lpl*, which are expressed during differentiation of mammary cells into milk-secreting alveoli (21) and multiple members of the secretoglobin family (*Scgb1b27*, *Scgb1b30*, *Scgb2b2*), which are associated with differentiation and low risk of relapse in human breast cancer (Table S1 and Fig. 3A; refs. 3, 27). In fact, genes upregulated during lactation (21) were significantly overexpressed in the RANK-Fc-treated tumors (Fig. 3A–B). Upregulation of *Csn2*, *Pip*, *Scgb1b27*, and *Scgb2b27* mRNA was confirmed in the RANK-Fc -treated tumors (Fig. 3C). Immunostaining with an anti-milk antibody confirmed that RANKL inhibition induced differentiation of late-adenocarcinoma cells into milk secreting cells (Fig. 3D). Conversely, tumor acini cultured with RANKL showed lower *Csn2*, *Pip*, and *Scgb2b27* expression (Fig. 3E), in correlation with the reduced milk protein found *in vivo* (Fig. 1F–G). These results demonstrate that pharmacological inhibition of RANK signaling in PyMT tumor-bearing mice promotes tumor cell differentiation into an apocrine, milk-secreting phenotype that mimics mammary lactogenesis, concomitantly with the reduction in tumor-initiating ability.

RANK deletion increases tumor latency, decreases tumor incidence, and impairs lung metastasis in MMTV-PyMT mice

Genetic deletion of RANK in the MMTV-PyMT background significantly delayed tumor onset and reduced tumor incidence (Fig. 4A–B and Supplementary Fig. S4A). In accordance with their multifocal origin (24), PyMT;$RANK^{+/+}$ palpable lesions showed multiple stages of tumor progression, whereas one predominant stage was found throughout the whole PyMT;$RANK^{-/-}$ palpable mass (Supplementary Fig. S4B-C). Accordingly, the number of preneoplasic lesions quantified in mammary gland whole mounts was significantly reduced in PyMT;$RANK^{-/-}$ compared with control mice (Fig. 4C). PyMT;$RANK^{-/-}$ lesions contained extensive areas of early and/or late carcinoma, indicating that tumors can progress to the invasive stage in the absence of RANK. However, most of PyMT;$RANK^{-/-}$ mice were devoid of lung metastasis, whereas all PyMT;$RANK^{+/+}$ mice with early/late carcinomas developed lung metastasis, and several showed 30 to 200 metastatic foci per lung (Fig. 4D). Thus, RANK deletion increases tumor latency, decreases tumor incidence, and impairs lung metastasis in the MMTV-PyMT tumor-prone model.

Figure 5.

RANK-null tumors contain fewer tumor and metastasis-initiating cells have enhanced apoptosis and are more sensitive to docetaxel. **A,** latency to tumor formation of PyMT;$RANK^{+/+}$ and PyMT;$RANK^{-/-}$ tumor cells orthotopically implanted in WT and $RANK^{-/-}$ syngeneic mice. Twenty-two tumors from each group were quantified. **B,** representative pictures of cleaved caspase-3 staining in transplants. **C,** percentage of nonviable areas versus total tumor area and of cleaved caspase-3–positive nuclei in transplants. Each dot represents one tumor. **D,** relative tumor volume (length × width/100) of PyMT;$RANK^{+/+}$ and PyMT;$RANK^{-/-}$ tumors treated with docetaxel (25 mg/kg) twice per week. #, docetaxel doses. **E,** number of tertiary tumorspheres. Each bar represents four tumors. **F–G,** tumor-initiating (**F**) and metastasis-initiating frequencies (**G**; with confidence intervals) and x^2 values. Cells from two tumors per genotype were pooled for injections and metastasis was scored after 8 weeks. **H**, absolute number of lung metastatic foci. Each dot represents the lung of one mouse. **A, E, H,** mean, SEM, and *t* test (*F* test for **H**) probabilities are shown (*, $0.01 < P < 0.05$; **, $0.001 < P < 0.01$; ***, $0.001 < P < 0.0001$; ****, $P < 0.0001$).

Published OnlineFirst August 1, 2016; DOI: 10.1158/0008-5472.CAN-15-2745

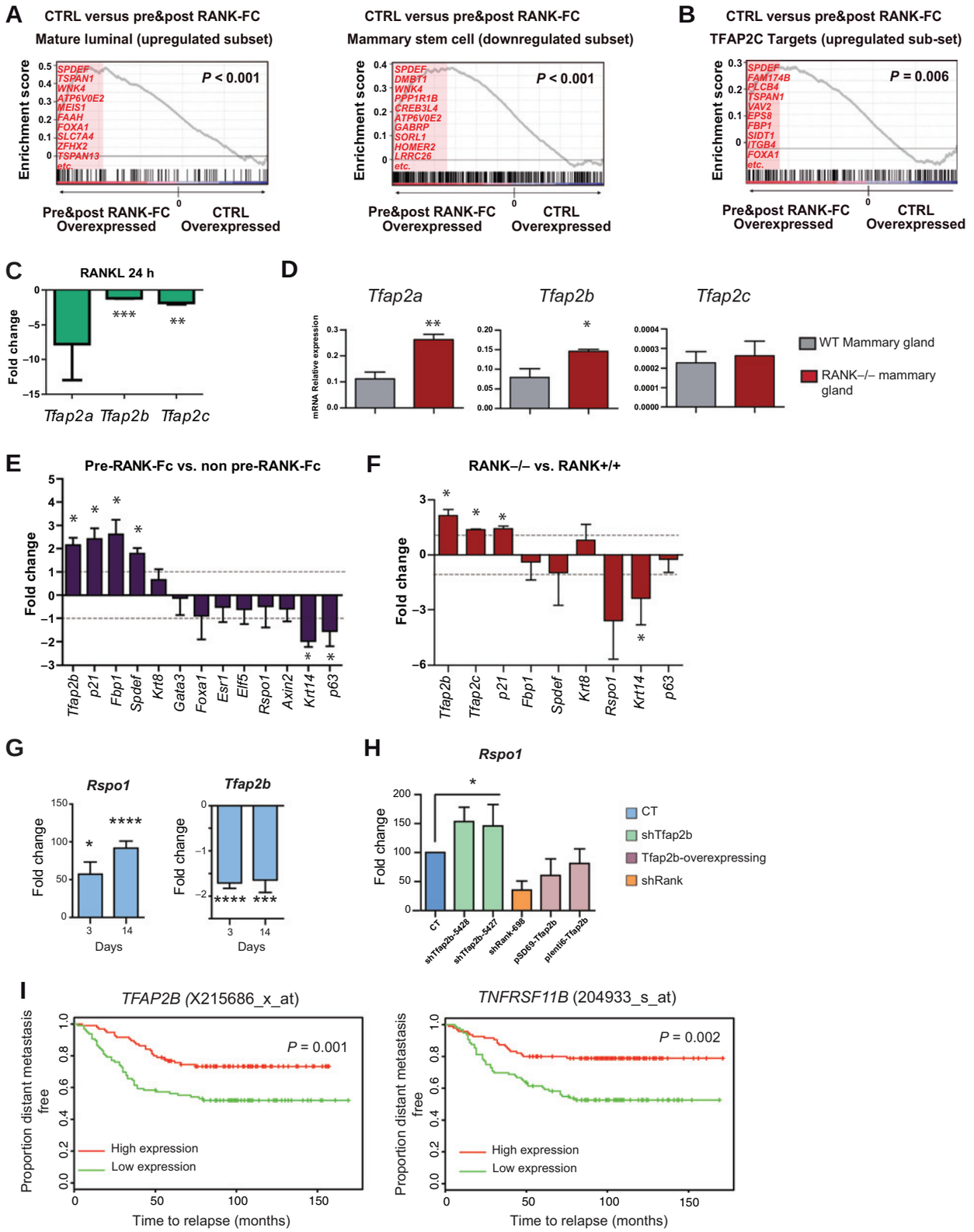

Published OnlineFirst August 1, 2016; DOI: 10.1158/0008-5472.CAN-15-2745

RANK loss in tumor cells depletes the tumor and metastasis-initiating cell pools and increases apoptosis and sensitivity to docetaxel

To rule out the progesterone/RANKL-mediated effects acting in early tumorigenesis (7) and the influence of the RANK-null microenvironment (17), PyMT;RANK$^{-/-}$ and PyMT;RANK$^{+/+}$ tumors cells, isolated from established carcinomas were orthotopically implanted in syngeneic wild-type (WT) females. PyMT;RANK$^{-/-}$ tumor cells showed a significantly longer latency to tumor formation than did PyMT;RANK$^{+/+}$ tumor cells, indicating a tumor cell autonomous defect (Fig. 5A). Longer latency was also observed when PyMT;RANK$^{+/+}$ tumor cells were implanted in RANK null mice compared with WT, but no synergic effect after implantation of PyMT;RANK$^{-/-}$ in RANK null hosts was found (Fig. 5A).

PyMT;RANK$^{-/-}$ tumors growing in WT hosts contained more apoptotic cells and extensive nonviable areas relative to PyMT;RANK$^{+/+}$ tumors (Fig. 5B–C). No significant differences in tumor cell survival were observed when the same tumor, either PyMT;RANK$^{+/+}$ or PyMT;RANK$^{-/-}$, was implanted on WT and RANK null hosts supporting a tumor cell intrinsic mechanism (Fig. 5C). This demonstrates that tumor cell survival is impaired in the absence of RANK, which may contribute to the delayed tumor formation observed. Moreover, the absence of RANK on tumor cells sensitized tumors to docetaxel (Fig. 5D).

Next, we aimed to determine whether loss of RANK signaling exclusively on tumor cells reduced the CSC pool as observed after RANKL inhibition. PyMT;RANK$^{-/-}$ tumor cells gave rise to less tumorspheres than controls, independently of the initial host (Fig. 5E), highlighting an extenuation of a self-renewal capability that is tumor cell-autonomous. LDA in WT hosts also revealed a significant reduction in the frequency of TICs in the absence of RANK (Fig. 5F). PyMT;RANK$^{+/+}$ tumor cells efficiently colonized the lung of *Foxn1*^{nu} mice and abundant metastatic foci were found (Fig. 5G–H). Strikingly, in the PyMT;RANK$^{-/-}$ pool a 10-fold decrease in the frequency of metastasis-initiating cells (MIC) was observed with very few metastatic foci (Fig. 5G–H), implying that RANK expression in tumor cells is determinant for metastasis. Thus, RANK loss in advanced adenocarcinomas depleted the pool of tumor and MICs, decreased survival and sensitized tumors to docetaxel.

RANKL negatively regulates the Ap2 transcription factors, drivers of luminal differentiation, and induces Rspo1

To further understand the molecular mechanism underlying tumor cell differentiation after RANKL inhibition, we focused on genes specifically induced in tumors that received RANK-Fc treatment at passage 1 such as *Tfap2b* (Supplementary Table S1). The AP2 transcription factor family is a set of retinoic acid inducible genes that governs the luminal epithelial phenotype in mammary development and carcinogenesis (28, 29) and whose expression is associated with survival (30, 31). Consistent with a tumor cell-luminal differentiation phenotype, GSEA analyses of the genes that characterize mammary differentiation hierarchy (20), revealed that the mature luminal upregulated set and the MaSC downregulated set, were overexpressed on the RANK-Fc-treated tumors (Fig. 6A). *Spdef*, which also promotes luminal differentiation (32) was the top gene in these associations (Fig. 6A). Genes upregulated by TFAP2C in human breast cancer cells (22) were significantly overexpressed in RANK-Fc-treated tumors (Fig. 6B). Moreover, an increase in *Tfap2a* and *Tfap2b* was observed in the RANK null mammary epithelia and RANKL treatment significantly reduced the *Tfap2a*, *Tfap2b*, and *Tfap2c* mRNA expression in tumor cultures of PyMT cells (Fig. 6C–D and G).

Gene expression analysis in the pre-RANK-Fc-treated tumors confirmed upregulation of *Tfap2b*, the luminal genes *Spdef* and *Fbp1* and *cdkn1a/p21* (known to be induced by Tfap2; ref. 29) and downregulation of the basal genes *p63*, *Krt14*. No significant changes were detected between groups in *Krt8*, *Foxa1*, *Gata3*, *Esr1*, *Elf5*, and *Rspo1* (Fig. 6E). Higher levels of *Tfap2b*, *Tfap2c*, and *p21* and lower levels of *Krt14* and *Rspo1* were found in PyMT;RANK$^{-/-}$ tumor cells isolated from transplants as compared to controls (Fig. 6F). R-spondin1 (*Rspo1*), a Wnt agonist that has been shown to be expressed on luminal progenitors and mediate RANK-driven expansion of mammary progenitors in the healthy gland (33, 34), was strongly induced by RANKL on PyMT acini cultures (Fig. 6G). Tfap2b-overexpressing and knockdown PyMT tumor cells were obtained as little is known about the specific role of Tfap2b on mammary tumors (Supplementary Fig. S5A and S5B). Gene expression analyses confirmed that *Spdef* was positively regulated by Tfap2b (Supplementary Fig. S5C). Analyses of PyMT tumor acini cultured for 2 weeks revealed that RANKL led to an increase on acini size irrespectively of Tfap2b expression (Supplementary Fig. S6A–B). However, in Tfap2b-overexpressing PyMT acini treated with RANKL, *Rspo1* mRNA expression was 30% lower than in RANKL-treated control acini. Conversely, in shTfap2b PyMT acini treated with RANKL, *Rspo1* expression was 50% higher than in controls, demonstrating that Tfap2b interfered with RANKL-driven increase in *Rspo1* (Fig. 6H). *Rspo1* expression decreased, whereas *Tfap2b* and *Spdef* expression increased in PyMT tumor cells infected with shRANK, further supporting that RANK pathway negatively regulates luminal differentiation (Supplementary Fig. S5D).

Figure 6.

RANK loss or inhibition induces the expression of AP2 transcription factors and reduces Rspo1. **A** and **B,** GSEA graphical outputs for the association between mammary mature luminal (upregulated genes) and mammary stem (downregulated genes) cells gene sets (**A**) and TFAP2C upregulated genes sets in human breast cancer (**B**) and RANK-Fc treatment. The top genes contributing to the association are listed. **C,** fold changes in mRNA expression of indicated genes in PyMT tumor acini cultures treated with RANKL for 24 h relative to untreated cultures. Each bar is representative of three tumors. **D,** mRNA expression levels of indicated genes relative to *Krt8* in PyMT RANK$^{+/+}$ and PyMT;RANK$^{-/-}$ mammary glands. Each bar is representative of three mammary glands. **E,** fold changes in mRNA expression of indicated genes in RANK-Fc treated PyMT tumors at passage 1 relative to expression in the other treatment arms. Each bar is representative of six tumors. **F,** fold changes in mRNA expression of indicated genes in PyMT;RANK$^{-/-}$ relative to expression in PyMT;RANK$^{+/+}$ sorted tumor cells. Each bar is representative of three-four independent tumors. **G,** fold change of *Rspo1* and *Tfap2b* mRNA expression levels in PyMT acini tumor acini cultured with RANKL for 3 and 14 days relative to untreated cultures. **H,** relative induction of *Rspo1* mRNA expression in Tfap2b-knockdown or -overexpressing PyMT tumor acini cultured with RANKL for 14 days relative to the induction in RANKL-treated controls (normalized as 100%). Induction of *Rspo1* mRNA in Rank-Knockdown PyMT acini is included. **I,** association between *TFAP2B* and *TNFRSF11B* tumor expression and distant metastasis in lymph-node negative breast cancer patients (GSE2034). Graphs show the proportion of distant metastasis-free patients over time (months) and are stratified according to the first (low expression) or the third (high expression) tertiles. **C, D, E, F,** mean, SEM and t-test statistics are shown. (*, $0.01 < P < 0.05$; **, $0.001 < P < 0.01$; ***, $0.001 < P < 0.0001$; ****, $P < 0.0001$).

Published OnlineFirst August 1, 2016; DOI: 10.1158/0008-5472.CAN-15-2745

To investigate the clinical relevance of TFAP2B, we analyzed an expression dataset from lymph-node negative breast cancer patients that developed distant metastasis (35). The expression of *TFAP2B* was found to be significantly associated with the absence of distant metastasis: Cox regression HR = 0.25; 95% confidence interval (CI), 0.11–0.57; $P = 0.001$ (Fig. 6I). Similar results were observed in tumors with a luminal phenotype (ER^+): HR = 0.24; 95% CI, 0.09–0.63, $P = 0.004$, and the same trend for (ER^-) tumors: HR = 0.24; 95% CI, 0.04–1.29; $P = 0.09$. Consistent with the proposed cancer-promoting role for enhanced RANK signaling, associations with relapse free were observed for *TNFRSF11B* (*OPG*), the canonical negative regulator of the RANK pathway: HR = 0.49; 95% CI, 0.31 – 0.78; $P = 0.002$ (Fig. 6I); in luminal tumors (ER^+): HR = 0.33; 95% CI, 0.17–0.62; $P = 0.0006$. Accordingly, *TFAP2B* and *TNFRSF11B* were found to be significantly coexpressed (Pearson's correlation coefficient = 0.14, $P = 0.018$). Together these data indicate that RANKL inhibition leads to tumor differentiation, metastasis impairment, and good prognosis.

RANK signaling inhibition depletes the pool of Sca1$^-$ TICs

Next, we aimed to identify the CSC population regulated by RANK in our models, which remains elusive in the MMTV-PyMT model (36–38). The levels of CD49f, CD49b, CD61, and CD90 within epithelial cells were comparable for all RANK-Fc treatment arms; in contrast, Sca1$^+$/hi cells were more abundant in tumors pretreated with RANK-Fc, which show a lower tumor-initiating ability (Fig. 7A and B). In the normal mammary gland, Sca1$^+$ identifies a population enriched in ER^+/PR^+ luminal mature cells (37). However, we could not detect an increase in PR^+ cells after RANK-Fc treatment (Fig. 7C). Similarly, an increase in the Sca1$^+$/hi population, but none of the other markers, was found in PyMT;RANK$^{-/-}$ tumors as compared to controls (Fig. 7D). Secondary tumorspheres of Sca1$^-$/lo tumor cells were larger and five times more numerous as those of Sca1$^+$/hi cells (Fig. 7E–F). Strikingly, LDA assays revealed the TIC frequency is significantly enhanced by 200-fold in Sca1$^-$/lo compared with Sca1$^+$/hi tumor cells (Fig. 7G), indicating that the Sca1$^-$/lo population is enriched in CSCs. Altogether these results demonstrate that RANK loss or RANKL inhibition reduced the frequency of the Sca1$^-$/lo CSC population.

Discussion

The work presented here reveals a central role of RANK signaling promoting recurrence and metastasis in aggressive breast tumors, providing a rationale for additional therapeutic applications of RANK inhibitors beyond its current use for the management of skeletal-related events. We found that constitutive deletion of RANK in MMTV-PyMT mice increases tumor latency and decreases tumor and lung metastasis incidence, as observed in MMTV-neu mice upon RANK-Fc preventive treatment (7), reinforcing the role of RANK signaling in early stages of tumorigenesis (8).

Our previous data showed that enhanced RANK activation promotes stemness in human and mouse mammary epithelia, leading to the accumulation of MaSC and progenitors (11, 12, 39). Importantly, now we demonstrate that inhibition of RANK signaling reduces CSC in invasive mammary tumors decreasing recurrence and metastasis, and induces tumor cell differentiation. LDA assays aim to mimic occult disease that remains in breast cancer patients after surgery. Our results suggest that neoadjuvant RANKL inhibition may be more efficient in reducing recurrence and metastasis than adjuvant treatment, as a significant reduction in the CSC population was observed on tumors treated at passage 1. Along with our previous data demonstrating that overactivation of RANK signaling at midgestation disrupts lactogenesis (12, 39), current results suggest that RANK signaling regulates the balance between self-renewal and differentiation not only during mammary gland development but also in breast adenocarcinomas.

The impaired tumor and metastasis initiation ability observed in RANK null tumor cells growing in WT hosts demonstrates that tumor cell intrinsic mechanisms mediate the observed reduction in CSC. However, we cannot discard that tumor cell extrinsic mechanisms induced by RANK signaling inhibition in the microenvironment can also contribute to reduce recurrence (40).

Mechanistically, we demonstrate that RANK signaling negatively regulates the AP2 transcription factor family that can mediate retinoic acid responsiveness (41, 42). TFAP2A functions as a tumor suppressor in several solid tumors including breast cancer (43, 44). Overexpression of Tfap2a and Tfap2c mimics the mammary phenotype of RANK null mice (5, 45, 46). Tfap2a and Tfap2c maintain the luminal phenotype (28, 29) and negatively regulate cancer stem cell markers (28). Although little is known about TFAP2B in mammary epithelia, our results suggest that, similarly to other members of the family, TFAP2B promotes luminal differentiation and is associated with good prognosis. The positive correlation between the RANKL inhibitor, *OPG*, and *TFAP2B* expression in human breast tumors and their association with metastasis-free phenotype support the clinical implication of our findings.

Although enhanced Tfap2b expression alone cannot prevent RANKL-driven increased in acinar size, it interferes with the induction of the Wnt agonist Rspo1. Rspo1 together with Wnt4 promote MaSC self-renewal and Rspo1 rescues some of the mammary developmental defects in RANK null epithelia (33, 34). Similarly to our previous results on mammary epithelial cells at midgestation where RANKL induces the expression of Rspo1, leads to the expansion of basal and bipotent cells and prevents lactogenic differentiation (39), we now observe that on PyMT tumor acini, RANK pathway also enhances Rspo1 and interferes with differentiation. Our results evidence a complex regulatory loop between RANK, Tfap2, and Rspo1 underlying the reduction in the CSC pool observed upon RANK pathway inhibition (Fig. 7H). Further experiments will be required to clarify their contribution to the protumorigenic role of RANK in cancer. Sca-1/Ly6A is found in the luminal differentiated ER^+/PR^+ cell cluster and according to our data it is likely to be induced by Tfap2, whereas Rspo1 is expressed on luminal Sca1$^-$ progenitor cells (33, 34). The decrease in Sca1$^-$ cells upon RANK loss or inhibition and their enhanced mammosphere-forming and tumor-initiating potential demonstrate that this population is enriched in CSCs in the PyMT tumors, as shown in the MMTV-wnt model (47). A negative regulation of Sca1$^+$ by RANK has been observed during mammary gland development (12, 34). The relevance of Sca1/Ly6a as a CSC marker in human luminal adenocarcinomas deserves further investigation.

Mortality in breast cancer is due to tumor recurrence and metastasis, which is driven by surviving CSC. RANKL inhibitors, although unable to reduce tumor growth, can be used as differentiation therapy of CSC (Fig. 7H). Moreover, RANK null tumor cells are more susceptible to taxanes than RANK-expressing tumor

Published OnlineFirst August 1, 2016; DOI: 10.1158/0008-5472.CAN-15-2745

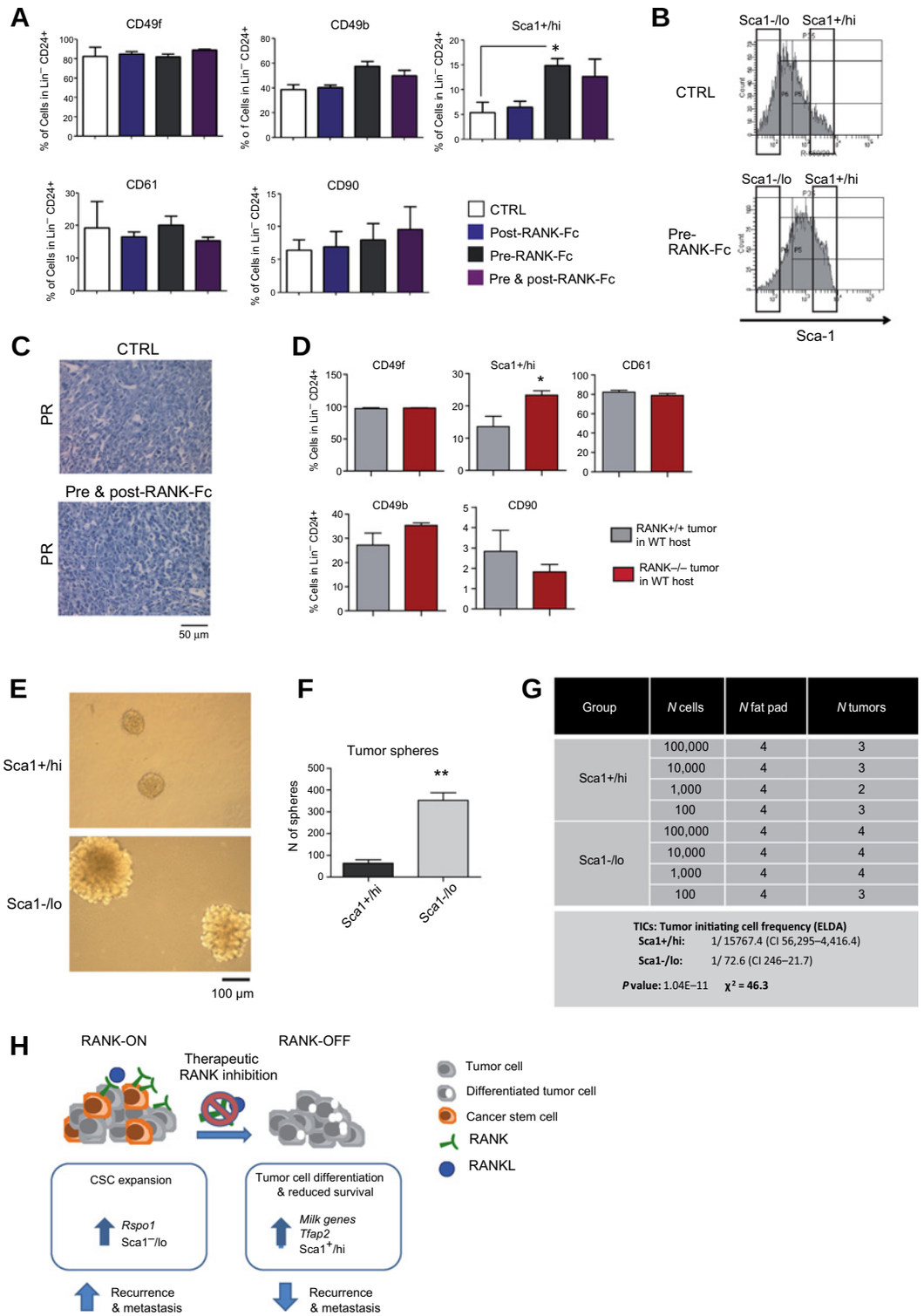

Group	*N* cells	*N* fat pad	*N* tumors
Sca1+/hi	100,000	4	3
	10,000	4	3
	1,000	4	2
	100	4	3
Sca1-/lo	100,000	4	4
	10,000	4	4
	1,000	4	4
	100	4	3

TICs: Tumor initiating cell frequency (ELDA)
Sca1+/hi: 1/ 15767.4 (CI 56,295–4,416.4)
Sca1-/lo: 1/ 72.6 (CI 246–21.7)
***P* value:** 1.04E–11 $\chi^2 = 46.3$

Figure 7.
RANK-Fc pretreatment reduces the Sca1$^-$ tumor cell population. **A,** frequency of the indicated populations within tumor CD45-CD31-CD24+ cells. Each bar represents data from four mice in two independent experiments. **B,** representative histograms of Sca1$^+$/hi and Sca1$^-$/lo populations. **C,** representative images of PR immunostaining. **D,** frequency of the indicated populations within tumor cell transplants. Each bar is representative of 3-5 tumors. **E** and **F,** representative images (**E**) and number (**F**) of tumorspheres derived from FACS-sorted Sca1$^+$/hi and Sca1$^-$ tumor cells. Each bar is representative of two tumors quantified in triplicates. **G,** tumor-initiating frequency (with confidence intervals), χ^2 values, and associated probabilities. **H,** graphical abstract indicating the multiple effects observed after therapeutic inhibition of RANK pathway in MMTV-PyMT tumors. **A, D, F,** mean, SEM and t-test statistics are shown (**, $0.001 < P < 0.01$).

Published OnlineFirst August 1, 2016; DOI: 10.1158/0008-5472.CAN-15-2745

cells, supporting the use of neoadjuvant RANKL inhibitors in the clinical setting to reduce the frequency of tumor relapse and metastasis and to increase sensitivity to chemotherapy. FDA-approved RANKL inhibitors are currently used in clinic for the management of skeletal-related events, therefore patients may quickly benefit from this therapeutic strategy to combat advanced breast cancer.

Disclosure of Potential Conflicts of Interest

W.C. Dougall has ownership interest (including patents) in a patent. No potential conflicts of interest were disclosed by the other authors.

Authors' Contributions

Conception and design: W.C. Dougall, E. González-Suárez

Development of methodology: G. Yoldi, P. Pellegrini, E.M. Trinidad, A. Cordero, E. González-Suárez

Acquisition of data (provided animals, acquired and managed patients, provided facilities, etc.): G. Yoldi, P. Pellegrini, E.M. Trinidad, A. Cordero, J. Gomez-Miragaya, E. González-Suárez

Analysis and interpretation of data (e.g., statistical analysis, biostatistics, computational analysis): G. Yoldi, P. Pellegrini, E.M. Trinidad, A. Cordero, J. Gomez-Miragaya, J. Serra-Musach, P. Muñoz, M.-A. Pujana, E. González-Suárez

Writing, review, and/or revision of the manuscript: G. Yoldi, P. Pellegrini, E.M. Trinidad, A. Cordero, J. Gomez-Miragaya, W.C. Dougall, P. Muñoz, M.-A. Pujana, L. Planelles, E. González-Suárez

Administrative, technical, or material support (i.e., reporting or organizing data, constructing databases): P. Pellegrini, J. Serra-Musach, E. González-Suárez

Study supervision: E. González-Suárez

Acknowledgments

We thank L. Alcaraz and D. Amoros (Bioarray) for microarray analyses; N.E. Hynes, M. Glukhova's group, M. Bentires-Alj, S. Duss, and K. Jin for sharing protocols and reagents; G. Boigues, A. Villanueva, E Castaño, and the IDIBELL animal facility for their technical assistance.

Grant Support

This work was supported by grants to E. González-Suárez by MINECO and ISCIII [SAF2011-22893 , SAF2014-55997; PIE13/00022, cofunded by FEDER funds/European Regional Development Fund (ERDF)—a way to build Europe-], by the Susan Komen Foundation CCR13262449, Concern Foundation, and by Fundació La Marató; to M.A. Pujana from ISCIII (PI12/01528) and AGAUR (SGR 2014-364), and to L. Planelles from ISCIII (PI10/01556). P Pellegrini and J. Gomez-Miragaya are recipients of an FPI grant from MINECO. The funders had no role in study design, data collection and analysis, decision to publish, or preparation of the manuscript.

Received October 5, 2015; revised June 15, 2016; accepted July 7, 2016; published OnlineFirst August 1, 2016.

References

1. Li X, Lewis MT, Huang J, Gutierrez C, Osborne CK, Wu MF, et al. Intrinsic resistance of tumorigenic breast cancer cells to chemotherapy. J Natl Cancer Inst 2008;100:672–9.
2. Tallman MS, Andersen JW, Schiffer CA, Appelbaum FR, Feusner JH, Ogden A, et al. All-trans-retinoic acid in acute promyelocytic leukemia. N Engl J Med 1997;337:1021–8.
3. Dontu G, Abdallah WM, Foley JM, Jackson KW, Clarke MF, Kawamura MJ, et al. In vitro propagation and transcriptional profiling of human mammary stem/progenitor cells. Genes Dev 2003;17:1253–70.
4. Beleut M, Rajaram RD, Caikovski M, Ayyanan A, Germano D, Choi Y, et al. Two distinct mechanisms underlie progesterone-induced proliferation in the mammary gland. Proc Natl Acad Sci U S A 2010;107:2989–94.
5. Fata JE, Kong YY, Li J, Sasaki T, Irie-Sasaki J, Moorehead RA, et al. The osteoclast differentiation factor osteoprotegerin-ligand is essential for mammary gland development. Cell 2000;103:41–50.
6. Tanos TSG, Echeverria PC, Ayyanan A, Gutierrez M, Delaloye JF, Raffoul W, et al. Progesterone/RANKL is a major regulatory axis in the human breast. Sci Transl Med 2013;5:182ra155.
7. Gonzalez-Suarez E, Jacob AP, Jones J, Miller R, Roudier-Meyer MP, Erwert R, et al. RANK ligand mediates progestin-induced mammary epithelial proliferation and carcinogenesis. Nature 2010;468:103–7.
8. Gonzalez-Suarez E. RANKL inhibition: a promising novel strategy for breast cancer treatment. Clin Transl Oncol 2011;13:222–8.
9. Schramek D, Leibbrandt A, Sigl V, Kenner L, Pospisilik JA, Lee HJ, et al. Osteoclast differentiation factor RANKL controls development of progestin-driven mammary cancer. Nature 2010;468:98–102.
10. Gonzalez-Suarez E, Branstetter D, Armstrong A, Dinh H, Blumberg H, Dougall WC. RANK overexpression in transgenic mice with mouse mammary tumor virus promoter-controlled RANK increases proliferation and impairs alveolar differentiation in the mammary epithelia and disrupts lumen formation in cultured epithelial acini. Mol Cell Biol 2007;27:1442–54.
11. Palafox M, Ferrer I, Pellegrini P, Vila S, Hernandez-Ortega S, Urruticoechea A, et al. RANK induces epithelial-mesenchymal transition and stemness in human mammary epithelial cells and promotes tumorigenesis and metastasis. Cancer Res 2012;72:2879–88.
12. Pellegrini P, Cordero A, Gallego MI, Dougall WC, Purificacion M, Pujana MA, et al. Constitutive activation of RANK disrupts mammary cell fate leading to tumorigenesis. Stem Cells 2013;31:1954–65.
13. Pfitzner BM, Branstetter D, Loibl S, Denkert C, Lederer B, Schmitt WD, et al. RANK expression as a prognostic and predictive marker in breast cancer. Breast Cancer Res Treat 2014;145:307–15.
14. Santini D, Schiavon G, Vincenzi B, Gaeta L, Pantano F, Russo A, et al. Receptor activator of NF-kB (RANK) expression in primary tumors associates with bone metastasis occurrence in breast cancer patients. PLoS One 2011;6:e19234.
15. Guy CT, Cardiff RD, Muller WJ. Induction of mammary tumors by expression of polyomavirus middle T oncogene: a transgenic mouse model for metastatic disease. Mol Cell Biol 1992;12:954–61.
16. Maglione JE, Moghanaki D, Young LJ, Manner CK, Ellies LG, Joseph SO, et al. Transgenic Polyoma middle-T mice model premalignant mammary disease. Cancer Res 2001;61:8298–305.
17. Dougall WC, Glaccum M, Charrier K, Rohrbach K, Brasel K, De Smedt T, et al. RANK is essential for osteoclast and lymph node development. Genes Dev 1999;13:2412–24.
18. Smalley MJ. Isolation, culture and analysis of mouse mammary epithelial cells. Methods Mol Biol 2010;633:139–70.
19. Dontu G, Wicha MS. Survival of mammary stem cells in suspension culture: implications for stem cell biology and neoplasia. J Mammary Gland Biol Neoplasia 2005;10:75–86.
20. Lim E, Wu D, Pal B, Bouras T, Asselin-Labat ML, Vaillant F, et al. Transcriptome analyses of mouse and human mammary cell subpopulations reveal multiple conserved genes and pathways. Breast Cancer Res 2010;12:R21.
21. Anderson SM, Rudolph MC, McManaman JL, Neville MC. Key stages in mammary gland development. Secretory activation in the mammary gland: it's not just about milk protein synthesis! Breast Cancer Res 2007;9:204–18.
22. Woodfield GW, Chen Y, Bair TB, Domann FE, Weigel RJ. Identification of primary gene targets of TFAP2C in hormone responsive breast carcinoma cells. Genes Chromosomes Cancer 2010;49:948–62.
23. Hu Y, Smyth GK. ELDA: extreme limiting dilution analysis for comparing depleted and enriched populations in stem cell and other assays. J Immunol Methods 2009;347:70–8.
24. Lin EY, Jones JG, Li P, Zhu L, Whitney KD, Muller WJ, et al. Progression to malignancy in the polyoma middle T oncoprotein mouse breast cancer

Published OnlineFirst August 1, 2016; DOI: 10.1158/0008-5472.CAN-15-2745

model provides a reliable model for human diseases. Am J Pathol 2003;163:2113–26.
25. Barcellos-Hoff MH, Aggeler J, Ram TG, Bissell MJ. Functional differentiation and alveolar morphogenesis of primary mammary cultures on reconstituted basement membrane. Development 1989; 105:223–35.
26. Lee GY, Kenny PA, Lee EH, Bissell MJ. Three-dimensional culture models of normal and malignant breast epithelial cells. Nat Methods 2007;4:359–65.
27. Span PN, Waanders E, Manders P, Heuvel JJ, Foekens JA, Watson MA, et al. Mammaglobin is associated with low-grade, steroid receptor-positive breast tumors from postmenopausal patients, and has independent prognostic value for relapse-free survival time. J Clin Oncol 2004;22:691–8.
28. Bogachek MV, Chen Y, Kulak MV, Woodfield GW, Cyr AR, Park J M, et al. Sumoylation pathway is required to maintain the basal breast cancer subtype. Cancer Cell 2014;25:748–61.
29. Cyr AR, Kulak MV, Park JM, Bogachek MV, Spanheimer PM, Woodfield GW, et al. TFAP2C governs the luminal epithelial phenotype in mammary development and carcinogenesis. Oncogene 2014;34:436–44.
30. Bar-Eli M. Role of AP-2 in tumor growth and metastasis of human melanoma. Cancer Metastasis Rev 1999;18:377–85.
31. Gee JM, Robertson JF, Ellis IO, Nicholson RI, Hurst HC. Immunohistochemical analysis reveals a tumour suppressor-like role for the transcription factor AP-2 in invasive breast cancer. J Pathol 1999;189:514–20.
32. Buchwalter G, Hickey MM, Cromer A, Selfors LM, Gunawardane R N, Frishman J, et al. PDEF promotes luminal differentiation and acts as a survival factor for ER-positive breast cancer cells. Cancer Cell 2013;23: 753–67.
33. Cai C, Yu QC, Jiang W, Liu W, Song W, Yu H, et al. R-spondin1 is a novel hormone mediator for mammary stem cell self-renewal. Genes Dev 2014;28:2205–18.
34. Joshi PA, Waterhouse PD, Kannan N, Narala S, Fang H, Di Grappa MA, et al. RANK signaling amplifies WNT-responsive mammary progenitors through R-SPONDIN1. Stem Cell Reports 2015;5:31–44.
35. Wang Y, Klijn JG, Zhang Y, Sieuwerts AM, Look MP, Yang F, et al. Gene-expression profiles to predict distant metastasis of lymph-node-negative primary breast cancer. Lancet 2005;365:671–9.
36. Malanchi I, Santamaria Martinez A, Susanto E, Peng H, Lehr HA, Delaloye JF, et al. Interactions between cancer stem cells and their niche govern metastatic colonization. Nature 2011;481:85–9.
37. Sleeman KE, Kendrick H, Robertson D, Isacke CM, Ashworth A, Smalley MJ. Dissociation of estrogen receptor expression and *in vivo* stem cell activity in the mammary gland. J Cell Biol 2007;176:19–26.
38. Vaillant F, Asselin-Labat ML, Shackleton M, Forrest NC, Lindeman GJ, Visvader JE. The mammary progenitor marker CD61/beta3 integrin identifies cancer stem cells in mouse models of mammary tumorigenesis. Cancer Res 2008;68:7711–7.
39. Cordero A, Pellegrini P, Sanz-Moreno A, Trinidad EM, Serra-Musach J, Deshpande C, et al. Rankl impairs lactogenic differentiation through inhibition of the prolactin/Stat5 pathway at midgestation. Stem Cells 2016;34:1027–39.
40. Gonzalez-Suarez E, Sanz-Moreno A. RANK as a therapeutic target in cancer. Febs J 2016;283:2018–33.
41. Bosher JM, Totty NF, Hsuan JJ, Williams T, Hurst HC. A family of AP-2 proteins regulates c-erbB-2 expression in mammary carcinoma. Oncogene 1996;13:1701–7.
42. McPherson LA, Woodfield GW, Weigel RJ. AP2 transcription factors regulate expression of CRABPII in hormone responsive breast carcinoma. J Surg Res 2007;138:71–8.
43. McPherson LA, Loktev AV, Weigel RJ. Tumor suppressor activity of AP2alpha mediated through a direct interaction with p53. J Biol Chem 2002;277:45028–33.
44. Scibetta AG, Wong PP, Chan KV, Canosa M, Hurst HC. Dual association by TFAP2A during activation of the p21cip/CDKN1A promoter. Cell Cycle 2010;9:4525–32.
45. Jager R, Werling U, Rimpf S, Jacob A, Schorle H. Transcription factor AP-2gamma stimulates proliferation and apoptosis and impairs differentiation in a transgenic model. Mol Cancer Res 2003;1:921–9.
46. Zhang J, Brewer S, Huang J, Williams T. Overexpression of transcription factor AP-2alpha suppresses mammary gland growth and morphogenesis. Dev Biol 2003;256:127–145.
47. Batts TD, Machado HL, Zhang Y, Creighton CJ, Li Y, Rosen JM. Stem cell antigen-1 (sca-1) regulates mammary tumor development and cell migration. PLoS One 2011;6:e27841.

Top genes upregulated in tumors pre-treated with RANK-Fc (more than 4-fold)

Genbank	EntrezGeneID	GeneSymbol	GeneName
NM_013467	11668	Aldh1a1	aldehyde dehydrogenase family 1, subfamily A1
NM_177744	245282	Apol10a	apolipoprotein L 10A
NM_001025574	433492	Bpifb9b	BPI fold containing family B, member 9B
NM_009802	12353	Car6	carbonic anhydrase 6
NM_009886	12614	Celsr1	cadherin, EGF LAG seven-pass G-type receptor 1 (flamingo homolog, Drosophila)
NM_001164320	214685	Chadl	chondroadherin-like
NM_001164320	214685	Chadl	chondroadherin-like
NM_021386	58187	Cldn10	claudin 10
NM_022319	64085	Clstn2	calsyntenin 2
NM_007729	12814	Col11a1	collagen, type XI, alpha 1
NM_007730	12816	Col12a1	collagen, type XII, alpha 1
NM_198711	77018	Col25a1	collagen, type XXV, alpha 1
NM_001113515	12824	Col2a1	collagen, type II, alpha 1
NM_053185	94216	Col4a6	collagen, type IV, alpha 6
NM_013496	12903	Crabp1	cellular retinoic acid binding protein I
NM_021282	13106	Cyp2e1	cytochrome P450, family 2, subfamily e, polypeptide 1
NM_019910	13184	Dcpp1	demilune cell and parotid protein 1
NM_001077633	620253	Dcpp3	demilune cell and parotid protein 3
NM_001159743	100294583	Fam150b	family with sequence similarity 150, member B
NM_001162532	100038347	Fam174b	family with sequence similarity 174, member B
NM_019395	14121	**Fbp1**	fructose bisphosphatase 1
NM_176959	448987	Fbxl7	F-box and leucine-rich repeat protein 7
NM_133862	99571	Fgg	fibrinogen gamma chain
NM_001081416	68655	Fndc1	fibronectin type III domain containing 1

NM_010251	14397	Gabra4	gamma-aminobutyric acid (GABA) A receptor, subunit alpha 4
NM_017370	15439	Hp	haptoglobin
BC108385	626347	Igkv3-4	immunoglobulin kappa variable 3-4
NM_033373	94179	Krt23	keratin 23
NM_028973	74488	Lrrc15	leucine rich repeat containing 15
NM_019471	17384	Mmp10	matrix metallopeptidase 10
NM_008607	17386	Mmp13	matrix metallopeptidase 13
NM_001012323	381530	Mup20	major urinary protein 20
NM_001039544	*17842*	*Mup3*	*major urinary protein 3*
NM_008648	17843	Mup4	major urinary protein 4
NM_008649	*17844*	*Mup5*	*major urinary protein 5*
NM_023456	109648	Npy	neuropeptide Y
NM_001167891	100042150	Nrg2	neuregulin 2
NM_020252	18189	Nrxn1	neurexin I
NM_198410	68957	Paqr6	progestin and adipoQ receptor family member VI
NM_146086	225600	Pde6a	phosphodiesterase 6A, cGMP-specific, rod, alpha
NM_008843	18716	**Pip**	prolactin induced protein
BC051068	18798	Plcb4	phospholipase C, beta 4
NM_144828	19049	Ppp1r1b	protein phosphatase 1, regulatory (inhibitor) subunit 1B
NM_008644	17830	Prol1	proline rich, lacrimal 1
NM_028903	71145	Scara5	scavenger receptor class A, member 5 (putative)
NM_001270543	545948	Scgb1b20	secretoglobin, family 1B, member 20
NM_009596	11354	**Scgb1b27**	secretoglobin, family 1B, member 27
NM_001256073	384585	Scgb1b3	secretoglobin, family 1B, member 3
NM_001099330	100043868	Scgb1b30	secretoglobin, family 1B, member 30
NM_001281523	624439	Scgb2b15	secretoglobin, family 2B, member 15
NM_207262	381970	Scgb2b2	secretoglobin, family 2B, member 2
NM_001009952	494519	Scgb2b20	secretoglobin, family 2B, member 20

NM_178308	110187	Scgb2b26	secretoglobin, family 2B, member 26
NM_001100464	233099	**Scgb2b27**	secretoglobin, family 2B, member 27
NM_009136	20284	Scrg1	scrapie responsive gene 1
NM_009189	20471	Six1	sine oculis-related homeobox 1
NM_022411	20500	Slc13a2	solute carrier family 13 (sodium-dependent dicarboxylate transporter), member 2
NM_026183	67473	Slc47a1	solute carrier family 47, member 1
NM_001025305	**21419**	**Tfap2b**	**transcription factor AP-2 beta**
NM_177839	329278	Tnn	tenascin N
NM_146010	216350	Tspan8	tetraspanin 8
NM_026323	67701	Wfdc2	WAP four-disulfide core domain 2

Supplemental Figure 1

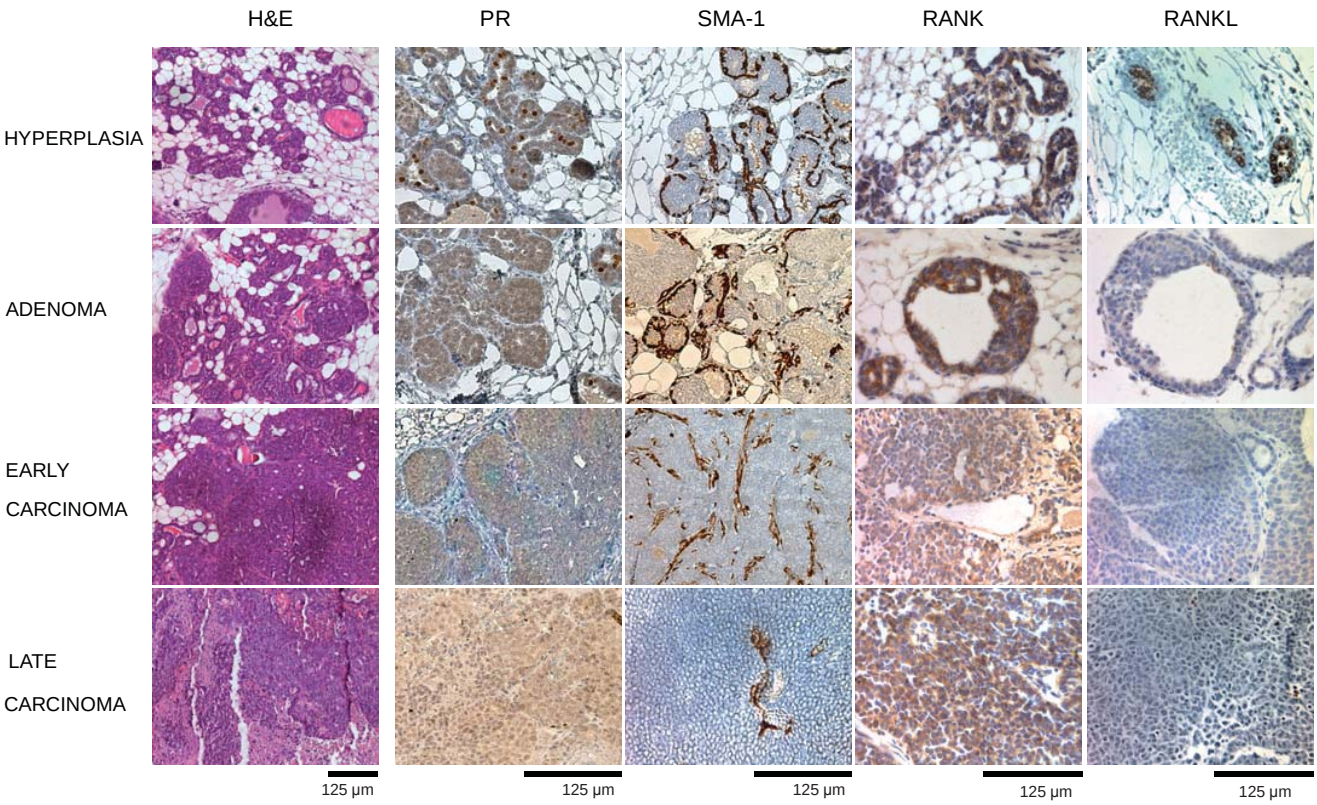

Supp. Figure 2

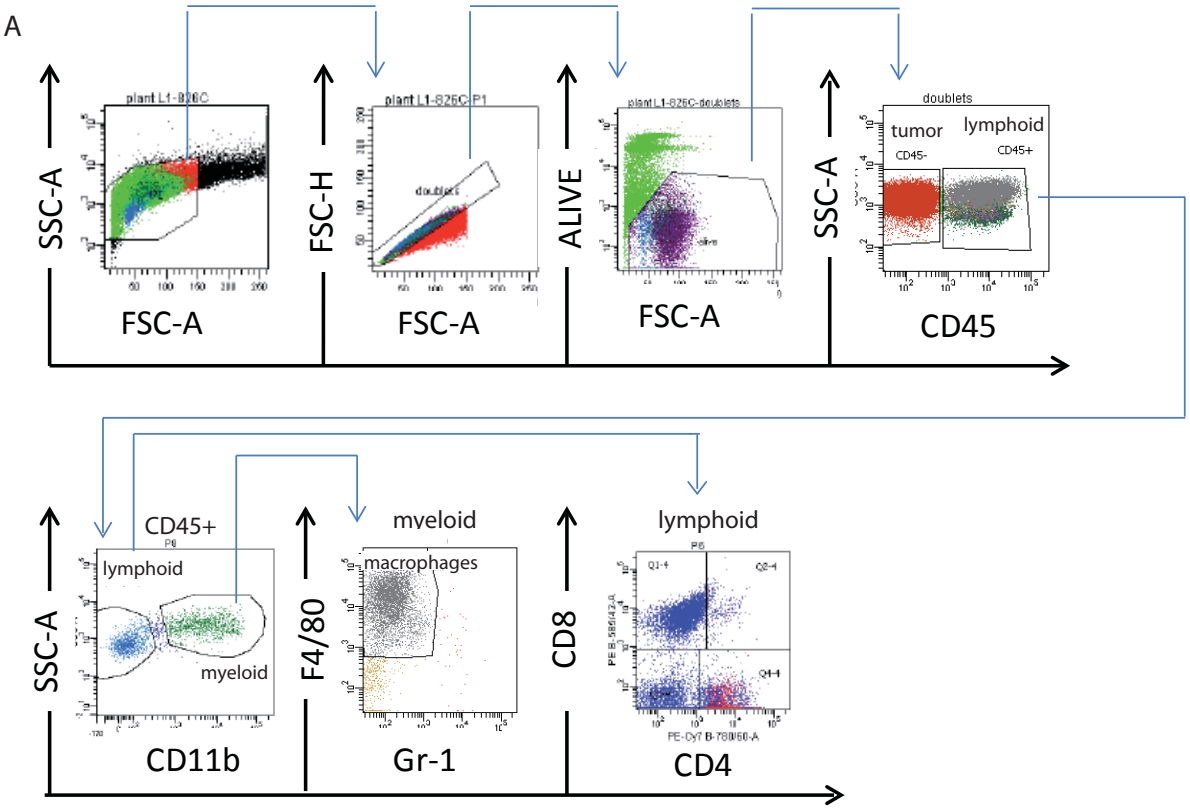

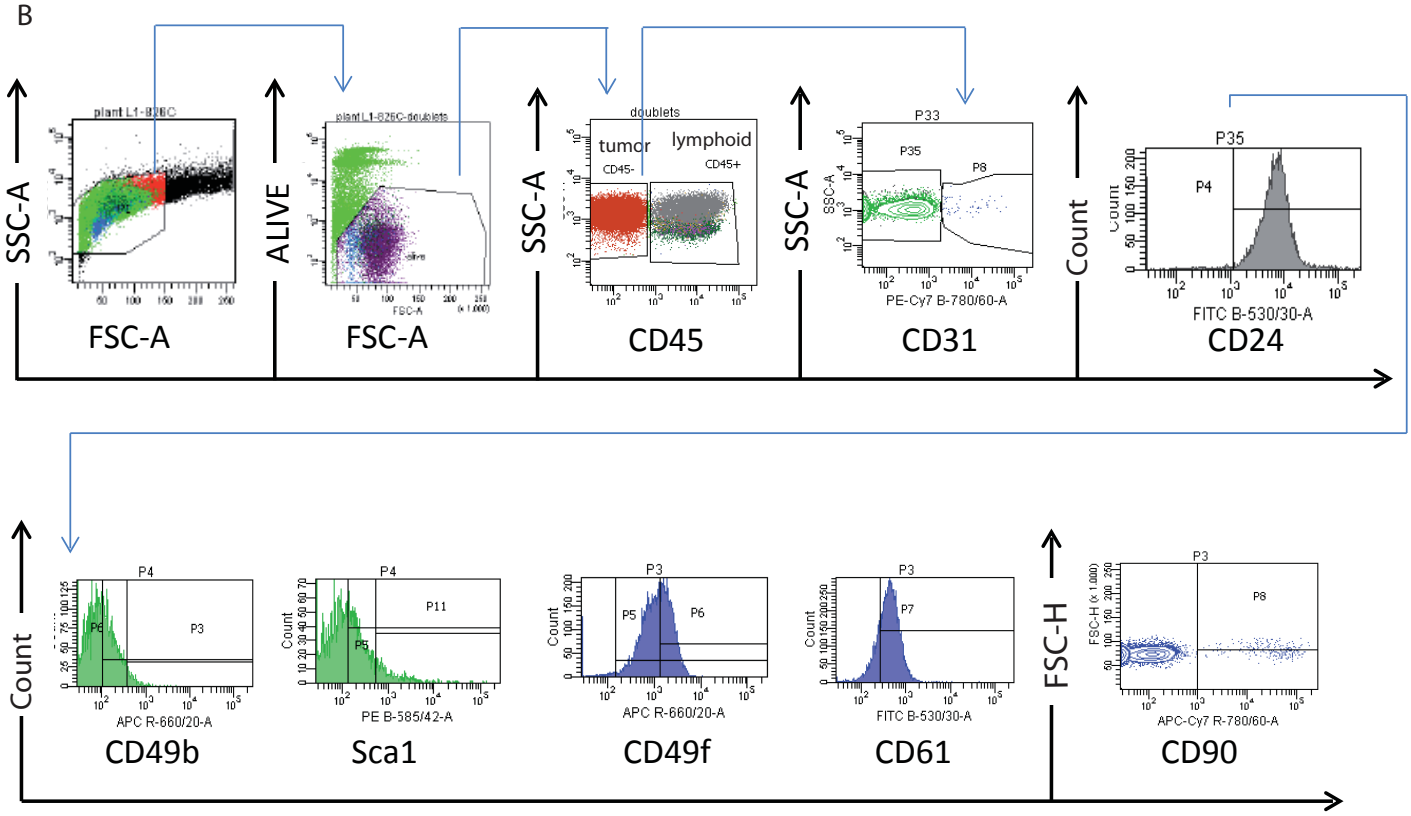

Figure S3

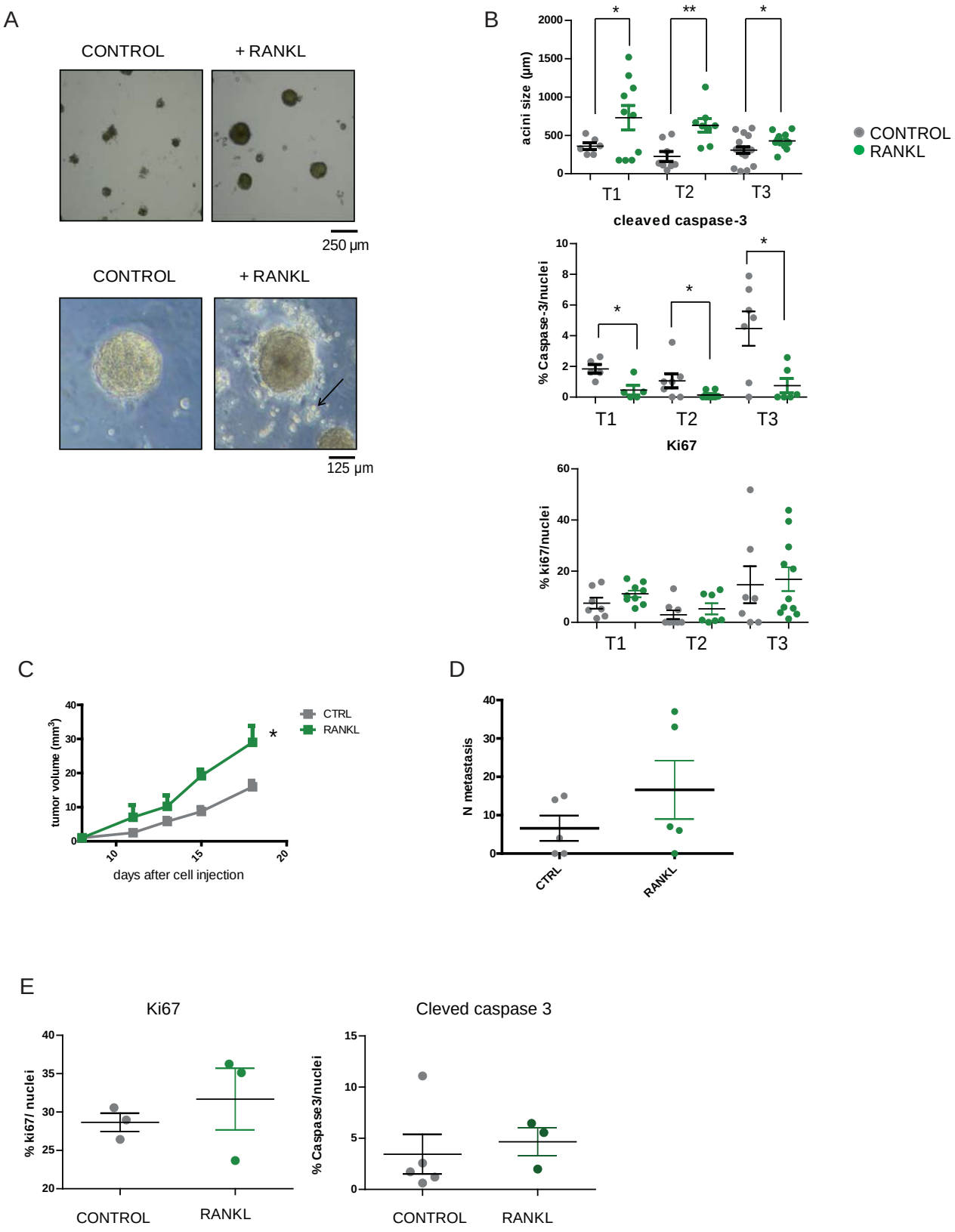
A
CONTROL
+ RANKL
250 µm
CONTROL
+ RANKL
125 µm
B
acini size (µm)
T1
T2
T3
CONTROL
RANKL
cleaved caspase-3
% Caspase-3/nuclei
Ki67
% ki67/nuclei
C
tumor volume (mm3)
days after cell injection
CTRL
RANKL
D
N metastasis
CTRL
RANKL
E
Ki67
% ki67/ nuclei
CONTROL
RANKL
Cleved caspase 3
% Caspase3/nuclei
CONTROL
RANKL

Supp. Figure 4

A

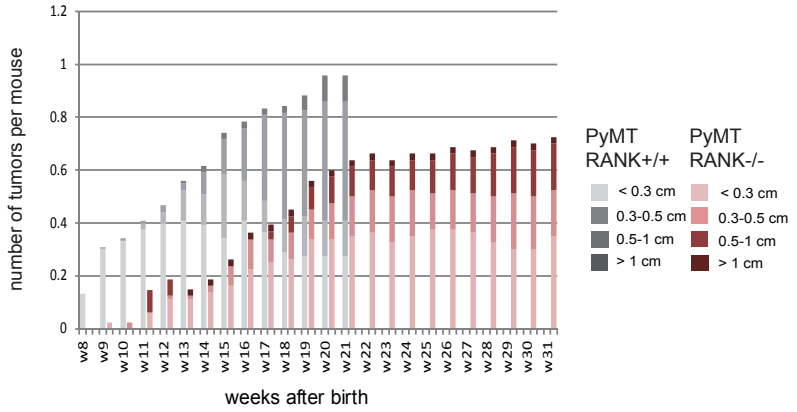

B

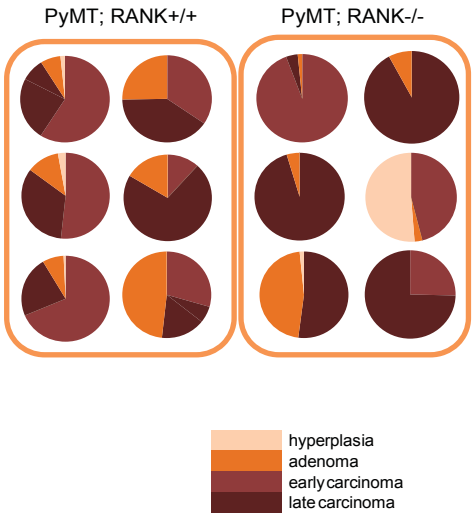

C

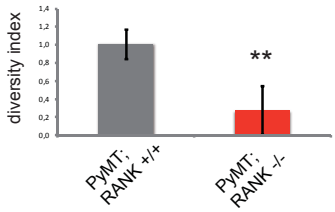

Supplementary Figure S5

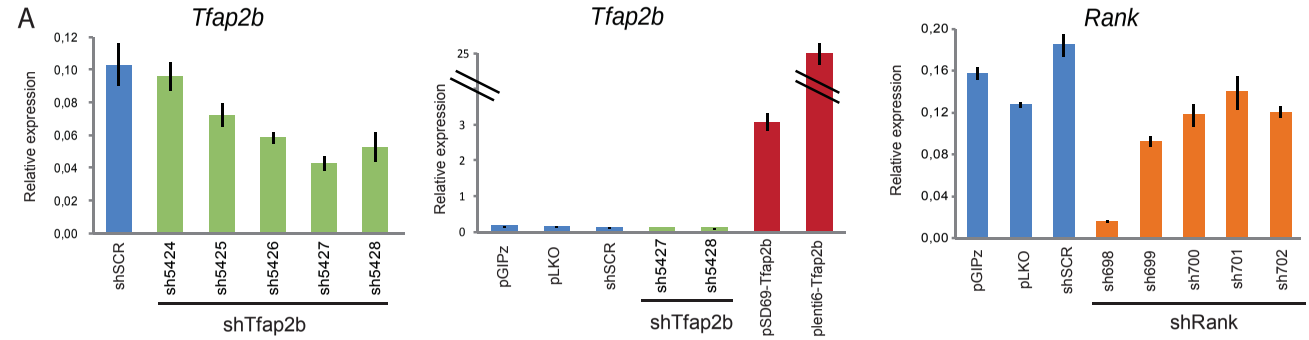

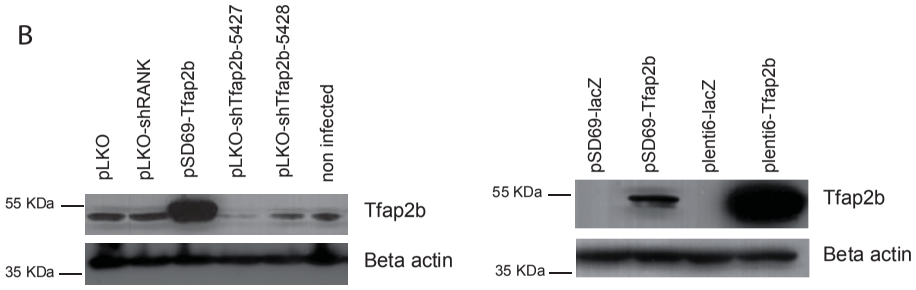

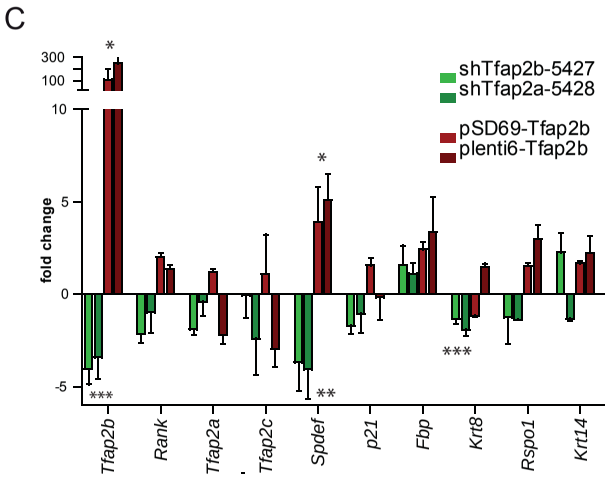

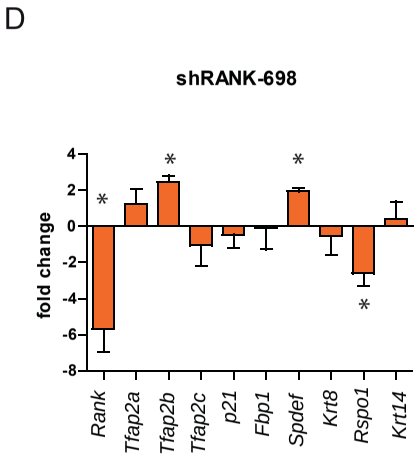

Supplementary Fig S6

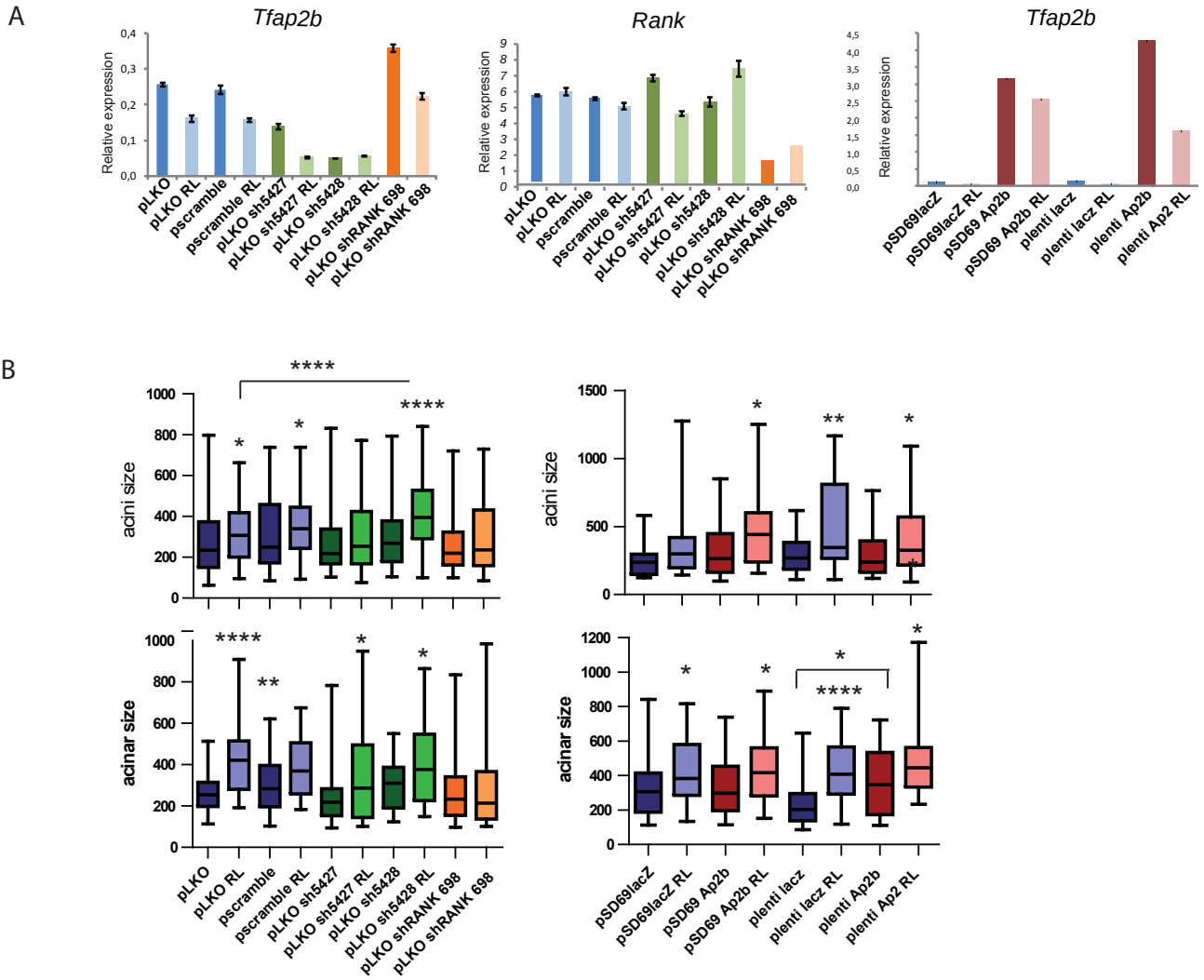

SUPPLEMENTARY TABLE AND FIGURE LEGENDS

SupplementaryTable S1. Genes differentially regulated by adjuvant and neoadjuvant RANK-Fc treatments.

Genes mentioned in the text or further validated by RT-PCR analyses are shown in bold letters.

Supplementary Figure S1. RANK and RANKL expression during MMTV-PyMT tumor progession

Representative pictures of hematoxylin eosin (H&E), PR (progesterone receptor), Sma-1, Rank and Rankl protein expression in MMTV-PyMT palpable lesions by immunostaining. Note the loss of PR (nuclear staining) and RANKL expression in adenoma and loss of a continuous layer of Sma-1 in the transition to carcinoma and late carcinoma.

Supplementary Figure S2.FACS gating scheme.

Dot-blots and histograms representing the hierarchy identified by flow cytometry analyses for the selection of tumor infiltrating leucocytes and epithelial cells in MMTV-PyMT tumors. Positive populations or mean values are defined based on isotope or FMO ("fluorescence minus one") controls.

Supplementary Figure S3. RANKL treatment decreases apoptosis in MMTV-PyMT-derived tumor cells *in vitro.*

A. Representative pictures of MMTV-PyMT tumor acini cultured in Matrigel with or without RANKL (1 μg/mL) for 15 days.

B. Diameter (μm), percentage of cleaved caspase 3+ and percentage of ki67+ nuclei of MMTV-PyMT tumor acini cultured in Matrigel, treated or not treated with RANKL for 15 days. Each dot represents one acinus, and results from three independent tumors (T1, T2 and T3) are shown. SEM and t-test statistics are shown.

C. Tumor growth curves derived from MMTV-PyMT tumor cells cultured for 15 days with or without RANKL after injection in the fat pads of Scid/Beige mice. Tumor volume is normalized to the first measurement. 100,000 cells per mammary gland were injected. Each mean and SEM is representative of six tumors and t-test statistics are shown.

D. Quantification of lung metastatic foci derived from tumor cells cultured for 15 days with or without RANKL after intravenous injection in Nod/Scid mice. 100,000 cells were injected and mice were sacrificed 9 weeks after tumor-cell injection. Each dot represents one mouse. Entire lungs were step-sectioned at 100 □m and individual metastases identified. The total number of metastatic foci per mouse is indicated.

E. Percentage of **t**umor cell proliferation (Ki67) and apoptosis (cleaved caspase-3) after 2 weeks of RANKL or control of MMTV-PyMT tumor-bearing mice. Each dot represents one independent tumor from one mouse. Six sections per tumor were quantified. The mean and SEM for each group is shown.

(*, 0.01 <P < 0.05; **, 0.001 <P < 0.01)

Supplementary Figure S4. Constitutive deletion of RANK decreases tumor incidence in MMTv-PyMT

A. Cumulative number of palpable lesions per mouse in 18 PyMT;RANK+/+ and 10 PyMT;RANK-/- mice with age (in weeks). Tumors were classified by diameter. All PyMT;RANK+/+ and PyMT;RANK-/- mice died after week 21 and 31, respectively; for mice dying before, total number of tumors detected at necropsy was considered.

B. Pie charts representing quantification of histological areas as defined in Supplemental Fig. S1 of PyMT;RANK-/- and PyMT;RANK+/+ tumors. Tumor size at sacrifice was similar for the two genotypes (1 cm diameter).

C. Shannon-Wiener diversity test of palpable PyMT;RANK-/- and PyMT;RANK+/+ lesions. Each bar represents the mean of 6 tumors and t-test statistics are shown. (**, $0.001 < P < 0.01$).

Supplementary Figure S5. Knock-down and overexpression of Tfap2b and knock down of Rank

A. mRNA expression levels of *Tfap2b* and *Rank* relative to *Hprt* in MMTV-PyMT tumor cells infected with control vectors pGIPZ, pLKO1, pLKO-scramble, and the indicated shRNA sequences against Tfap2b and Rank, and the overexpressing vectors pSD69-Tfap2b (PGK promoter) and plenti6-Tfap2b (CMV promoter).

B. Protein expression levels of Tfap2b determined by western blot in PyMT tumor cells infected with the indicated vectors using the anti-mouse Tfap2b antibody (SIGMA). Mouse Rank expression on PyMT cells could not be detected by western blot with the anti-mouse Rank (R&D Systems), data not shown. Beta-actin is used as a loading control.

C. Fold change in the mRNA expression of the indicated genes in MMTV-PyMT cells infected with pLKO-shTfap2b-5427 and 5428 knock-down and pSD69-Tfap2b and pCMV-Tfap2b overexpressing vectors relative to cells infected with the corresponding control vectors growing

in plastic. Each bar is representative of two-three independent tumors infected. Mean, SEM and t test statistics for knock-down and overexpressing vectors are shown.

D. Fold change in the mRNA expression of the indicated genes in MMTV-PyMT cells infected with pLKO-shRANK-698 knock-down, relative to cells infected with the corresponding control vectors growing in plastic after selection with puromycin. Each bar is representative of four or five independent tumors infected. Mean, SEM and t test statistics are shown.

(*, 0.01 <P < 0.05; **, 0.001 <P < 0.01; ***, 0.001<P < 0.0001; ****, P<0.0001).

Supplementary Figure 6. Tfap2b expression does not interfere with Rankl-driven proliferation or apoptosis of MMTV-PyMT acini

A. mRNA expression levels of indicated genes relative to *Hprt* in MMTV-PyMT tumor acini infected with the indicated vectors and cultured on matrigel, with or without RANKL for 14 days. Results are representative of two independent tumors infected. Measurements were obtained in triplicates, and mean and SD values are shown.

B. Acini size in MMTV-PyMT tumor acini infected with the indicated vectors and cultured on matrigel, with or without RANKL for 14 days. Each dot represents one acinus. Results for two independent tumors infected are shown. They are representative of four independent tumors infected. Mean, SEM and t-test statistics for RANKL-treated vs untreated cultures are shown. Significant differences between RANKL treated vs untreated cultures are indicated and were consistent in all infected tumors. Other significant comparisons (ie: bigger acini in shTfap2b-5427 RL vs pLKO RL) were not observed in all tumors. Note that in freshly isolated tumor cells RANKL treatment leads to reduced apoptosis, whereas in infected tumor cells RANKL

treatments leads to increased proliferation. This was observed in three independent infected tumors.

(*, 0.01 <P < 0.05; **, 0.001 <P < 0.01; ***, 0.001<P < 0.0001; ****, P<0.0001).

SUPPLEMENTAL MATERIALS AND METHODS

Animals

Littermates with the same genetic background were used as controls in all experiments. Mice were backcrossed for at least five generations with $RANK^{+/-}$ (C57BL/6) before transplantation into syngeneic C57BL/6 mice. *Foxn1*^{nu}, Scid/Beige and Nod/Scid mice were obtained from Charles River.

Whole-mounts analysis

Preneoplasic lesions were quantified in the mammary glands of mice between 90 and 150 days of age by fixation with Carnoy's solution (ethanol 95%, chloroform and glacial acetic acid at 6:3:1) 2 hours at RT. Then, they were washed 15 minutes with ethanol 70% and rinsed in distilled water. Overnight staining was performed at 4ºC with carmine alum at 0,002% and then dehydrated at RT.

Tumor cell isolation

Fresh tissues were mechanically dissected with a McIlwain tissue chopper and enzymatically digested with appropriate medium (DMEM F-12, 0.3% Collagenase A, 2.5 U/mL dispase, 20 mM HEPES and antibiotics) for 30 min at 37°C. Samples were washed with Leibowitz L15 medium containing 10% fetal bovine serum (FBS) between each step. Erythrocytes were eliminated by treating samples with hypotonic lysis buffer (Lonza Iberica). Single epithelial cells were isolated by treating with trypsin (PAA Laboratories) for 2 min at 37°C. Cell aggregates were removed by filtering the cell suspension with a 40-μm filter and counted.

Orthotopic transplants, metastasis and limiting dilution assays

For orthotopic transplants and tumor-limiting dilution assays tumor cells isolated from MMTV-PyMT (FVB), MMTV-PyMT;RANK$^{+/+}$ (C57BL/6) or MMTV-PyMT;RANK$^{-/-}$ (C57BL/6) mice were mixed 1:1 with Matrigel matrix (BD Biosciences) and orthotopically implanted in the inguinal mammary gland of 6-10-week-old syngeneic females. Mice were monitored for tumor formation for a maximum of 38 weeks. In all assays, tumor-initiating potential was defined as the ability to form palpable, growing tumors of ≥2 mm diameter. For metastasis assays, the indicated number of tumor cells were resuspended in 200 μL of cold PBS and injected intravenously in 6-10-week-old *Foxn1*^{nu} females. Lungs were recovered 8-10 weeks later for histological analysis. For metastasis scoring entire lungs were step-sectioned at 100 μm and individual metastases identified histologically.

Tumor acinar cultures and growth/metastasis assays from acinar cultures

For 3D acinar cultures, isolated MMTV-PyMT tumor cells were seeded on top of growth factor reduced matrigel (10,000 cells/well in 8-well chamber slides; 500,000 cells/well in 6-well paltes) in growth medium (DMEM-F12, 5% FBS, 10 ng/ml of EGF, 100 ng/ml cholerin toxin, 5 μg/ml insulin and 1x Penicillin/Streptomycin with or without RANKL (1 μg/mL). After 24 h cells were collected for RNA analyses or medium was changed to differentiation medium containing DMEM F-12, prolactin 3 μg/mL (Sigma-Aldrich), hydrocortisone 1 μg/mL, ITS (Sigma-Aldrich), cholera toxin 100 ng/mL and penicillin/streptomycin, as previously described (1) with or without RANKL (1 μg/mL). Medium was replenished three times a week and maintained in culture for 15 days. Acinar diameters were quantified with ImageJ software (Wayne Rasband, NIH). Matrigel was

dissolved by treatment with cold PBS-EDTA 5 mM for 25 min on ice, washed with PBS, and tumor cells were obtained after digestion with trypsin for 5 min at 37°C.

Immunofluorescence

Immunofluorescence of Ki67 and cleaved caspase-3 in acinar cultures were performed as previously described (2). Briefly, acini were fixed in 2% paraformaldehyde (20 min), permeabilized with PBS containing 0.5% Triton X-100 (15 min), and washed with PBS-Glycine 100 mM (three washes of 15 min each). Antigens were blocked with IF buffer (PBS, 7.7 mM NaN_3, 0.1% bovine serum albumin, 0.2% Triton x-100, 0.05% Tween-20) + 10% goat serum for 1 h and then with IF buffer + goat serum + 20 µg/mL F(ab') fragment (Jackson ImmunoResearch) for 30 min. Primary antibodies were incubated overnight in a humid chamber. Antibody-antigen complexes were detected using Alexa-488-conjugated anti-rabbit (Invitrogen) diluted 1:500 in IF buffer + 10% goat serum and incubated for 40 min. Acini were then washed with IF buffer and the nuclei stained with DAPI. Confocal analysis was carried out using a Leica confocal microscope. Images were captured using LasAF software (Leica). The percentage of Ki67 or caspase-3+ cells was calculated with ImageJ software.

RNA extraction and RT-PCR

Total RNA of tissue, sorted cells and acinar cultures were prepared with Tripure Isolation Reagent (Roche); Matrigel cultures were dissolved with cold PBS-EDTA (5 mM) on ice for 30 min. Matrigel-free cell suspensions were then pelleted at maximum speed and resuspended in TriPure Isolation Reagent for RNA isolation. Frozen tumor tissues were fractionated using glass beads (Sigma-Aldrich) and the PrecCellys® 24 tissue homogenizer

(Berting Technologies). cDNA was produced by reverse transcription using 1 μg of RNA in a 35 μL reaction following the kit instructions (Applied Biosystems). 20 ng/well of RNA/cDNA were used for tissue/acinar cultures and 5,000 cells/well for sorted cells. Analyses were performed in triplicate. Quantitative PCR was performed using TaqMan or LightCycler® 480 SYBR green.Primer sequences and TaqMan probes are indicated below.

Primers

NAME		**SEQUENCE 5'→3'**
mRANK	TaqMan	Mm00437135_m1
mRANKL	TaqMan	Mm00441908_m1
mACTINβ	TaqMan	4352341e-1003012
Rank	FWD	CAGATGCGAACCAGGAAAGT
	REV	TCTTCATTCCAGGTGTCCAAG
Rankl	FWD	TCCTGAGACTCCATGAAAACG
	REV	CCCACAATGTGTTGCAGTTC
Rpl38	FWD	AGGATGCCAAGTCTGTCAAGA
	REV	TCCTTGTCTGTGATAACCAGGG
Csn2	FWD	TCCACAACATTCCGTTTCTG
	REV	AGCATGATCCAAAGGTGAAAA
Pip	FWD	TCAGTGCTGTGACACTCTTCT
	REV	GTGTTTCAACTGTAACTTGCACA
Scgb1b27	FWD	TCTGATAGGACCTTGACCGAG
	REV	GGCAATTGGTTTCCGTGAGA
Scgb2b27	FWD	AGGGGACACTTCTTCTGCTG
	REV	TGGGGACTCTTTAATTTGGTGG
p21	FWD	CGCGGTGTCAGAGTCTAGG
	REV	GGACATCACCAGGATTGGAC
Hprt	FWD	TCAGTCAACGGGGGACATAAA
	REV	GGGGCTGTACTGCTTAACCAG
Rspo1	FWD	CTGAGCTGGACACACATCG
	REV	AACAGAGCTCACAGCCCTTG
Krt14	FWD	TGAGAGCCTCAAGGAGGAGC
	REV	TCTCCACATTGACGTCTCCAC
	FWD	GAGTGGGGAAGGAGTTGGAC

Krt5	REV	GCCACTGCCAACACCAAT
p63	FWD	GCATGGGAGCCAACATTCC
	REV	TGTCTCCAGCCATTGGCAT
Axin2	FWD	TGTGAGATCCACGGAAACA
	REV	GTGGCTGGTGCAAAGACATA
Tfap2a	FWD	CTTACCTCACGCCATCGAG
	REV	TTGCTGTTGGACTTGGACAG
Tfap2b	FWD	GACAGCCTCTCGTTGCAC
	REV	TGACTGACTGGTCCAATAGGTTC
Tfap2c	FWD	AGTATGAAGAGGATTGCGAGGA
	REV	CGCGGGACTGTAGAGATGTT
Krt8	FWD	ATTGACAAGGTGCGCTTCCT
	REV	CTCCACTTGGTCTCCAGCATC
Gata3	FWD	GCAGGCATTGCAAAGGTAGT
	REV	AGCACAGGCAGGGAGTGT
Foxa1	FWD	CACGCAGGAGGCCTACTCCT
	REV	TGTTGGCGTAGGACATGTTG
Esr1	FWD	GGAAGCTCCTGTTTGCTCCT
	REV	CGGAACCGACTTGACGTAG
Spdef	FWD	AGGTGCAATCGATGGTTGTG
	REV	AAAAGCCACTTCTGCACGTT
Fbp1	FWD	CGCTACCTGTGTTCTTGTGTCT
	REV	CACAAGGCAGTCAATGTTGG
Elf5	FWD	GGACTCCGTAACCCATAGCA
	REV	TACTGGTCGCAGCAGAATTG

Plasmid construction

Knockdown of Tfap2b and Rank expression was performed using MISSION short hairpin RNA (shRNA) of Dharmacon or Sigma in pLKO1 vector with puromycin or neomycin selection. Tfap2b overexpressing plasmids were prepared using Gateway technology. Briefly, the ORFeome collaboration sequence of mouse Tfap2b inserted in a pENTR223.1 vector (clone ID: 100015850) was inserted into pSD69 (PGK promoter, generously donated by S Duss and M Bentires-Alj) expressing vector and pLENTI-CMV (CMV promoter, Addgene, #17452) expressing vector using Gateway LR Clonase Enzyme Mix (Invitrogen).

The resultant plasmids were designated pSD69-Tfap2b or pLENTI-Tfap2b, respectively. Control vectors were generated inserting lacZ from a pLENTI6-v5-lacZ vector into p201 donor vector using Gateway BP Clonase Enzyme Mix (Invitrogen) and then, into pSD69 and pLENTI-CMV using Gateway LR Clonase Enzyme Mix (Invitrogen).

NAME		**SEQUENCE 5´ 3´**
shTfap2b	sh5424 (TRCN0000095424)	TTATCAGATAAATGTAGCCGG
	Sh5425 (TRCN0000095425)	AACTGAGTAGAGATAAACGGC
	sh5426 (TRCN0000095426)	TTTCTAGCCTTTCTCTCAAGG
	sh5427 (TRCN0000095427)	TTAGTGGTGTTGTTCAAGAAC
	sh5428 (TRCN0000095428)	AATCCCGAGCTAAGTGAACAG
shRank	sh698 (TRCN0000065698)	TATTTCCACTTAGACTACTGC
	sh699 (TRCN0000065699)	CGACAGTTTAAGCCAGTGTTTC
	sh700 (TRCN0000065700)	CCAGCAGGGAAGCAAATCTAT
	sh701 (TRCN0000065701)	AATGGTCCACATTTCAGGGAC
	sh702 (TRCN0000065702)	TTTATGCAGCAAGCATTTATCT

Lentiviral infection

Lentiviral infection was done following the manufacturer´s indications (Invitrogen). Briefly 293FT cells were used for the production of the virus. 293FT cells ($5x10^6$) were transfected with correspongding vectors and packaging (gag-pol, vsvg, rev) plasmids (Addgene) by calcium phosphate method. HEPES was added 24 h later. Virus was harvested 72 h post transfection and concentrated by centrifugation. Tumor cells were isolated from MMTV-PyMT mice 24 h before infection and 600,000 cells per well were plated in 6-well plates (BD). Cells were transduced with the different vectors in a ratio 1:3 with fresh growth medium and with 8 µg/ml of polybrene. Plates were centrifuged 1 h at 1000 rpm at 37ºC. After 24 h cells were lifted up with trypsin (Labclinics) and plated (20,000 cells/well in 8-well chamber slides (BD); 500,000 cells/well in 6-well plates) on matrigel. After 24 h medium was changed for differentiation medium and RL (1 µg/mL) was added. Puromycin

(Sigma-Aldrich, 1.5 µg/ml) or neomicin (sc-29065A, Santa Cruz, 500 µg/uL) were added 48h later. The resulting stable cell lines infected were maintained with 0.75 µg/ml of puromycin or 250 µg/uL of neomycin during two weeks. Medium was replenished three times a week. Acinar diameters were quantified from 6-well plates after 2 weeks of culture with ImageJ software (Wayne Rasband, NIH). For RNA analyses, acini were collected 3 days and 2 weeks after infection from 6-well plates.

Western blot

Infected PyMT tumor cells in 6-well plates were isolated and total protein lysates were prepared. Cells were lysed with RIPA buffer (50 mM Tris-HCl at pH 7.6, 150 mM NaCl, 1% NP-40, 0,5% Sodium deoxycholate, 0,1% SDS, 5 mM EDTA). Proteases and phosphatases inhibitors (Roche) were added freshly to the lysis buffer. Western blotting was performed with standard protocols. In brief, blots were blocked for 1 h at room temperature with 5% milk in 10 mM Tris-HCl pH 7.5, 150 mM NaCl containing 0.1% Tween 20 (TBST) and incubated overnight with primary antibody at 4°C. Primary antibodies reactive to mouse Tfap2b (SIGMA-6178) and β-actin (AC-74, Sigma) were used. After washing, blots were incubated with horseradish peroxidase-conjugated secondary antibodies (1:2000) for 1 h at 20–25 °C, and revealed with enhanced chemiluminescence.

SUPPLEMENTARY REFERENCES

1. Hathaway, H. J. and Shur, B. D. Mammary gland morphogenesis is inhibited in transgenic mice that overexpress cell surface beta1,4-galactosyltransferase. Development, *122:* 2859-2872, 1996.
2. Debnath, J., Muthuswamy, S. K., and Brugge, J. S. Morphogenesis and oncogenesis of MCF-10A mammary epithelial acini grown in three-dimensional basement membrane cultures. Methods, *30:* 256-268, 2003.

ANNEX 1

Breast cancer PDX models for the study of RANK/RANKL signalling pathway

Jorge Gómez-Miragaya[1], Héctor Pérez-Montoyo[1, 2,] Eva María Trinidad[1], Clara Gómez-Aleza[1], Marina Ciscar[1], MT Lewis, A Welm, J Arribas, R Clarke, Antonio Martínez Aranda[3], Angels Sierra[3,4], Eva González-Suárez[1,*]

[1] Cancer Epigenetics and Biology Program (PEBC), Bellvitge Biomedical Research Institute (IDIBELL), Avinguda de la Gran Via, 199 – 203, L'Hospitalet deLlobregat, 08908 Barcelona, Spain

[2] Present address: Ability Pharmaceuticals, SL, Edifici Eureka, Campus UAB, Bellaterra, Barcelona, Catalonia, Spain.

[3] Laboratory of Molecular and Translational Oncology, Institut d'Investigacions Biomèdiques August Pi i Sunyer-IDIBAPS, Centre de Recerca Biomèdica CELLEX, Barcelona, Spain,

[4] Faculty of Medicine, Universitat de VIC-Universitat Central de Catalunya, Barcelona, Spain

[*]Corresponding author: Eva González Suárez.
Cancer Epigenetics and Biology Program, Bellvitge Institute for Biomedical Research, IDIBELL.
Av.Gran Via de L'Hospitalet, 199. 08908 L'Hospitalet de Llobregat. Barcelona. Spain
egsuarez@idibell.cat www.pebc.cat Phone: +34 932607139 Fax: +34 932607219

Abstract

Receptor activator of NF-κB (RANK) is expressed in human breast tumors and has been associated with aggressive breast cancers. In this study we used breast cancer PDX models to investigate the functional role of RANK and its ligand (RANKL) in clinical human breast cancer. RANK expression in human breast cancer is more frequent in ER/PR-negative than in hormone receptor positive tumors and that is maintained in breast cancer PDX models. RANKL is generally poorly expressed in human breast cancer, but some RANKL-positive breast cancer PDX models were identified. Selection of RANK/RANKL-positive breast cancer PDX models expressing different levels of RANK or RANKL was done in order to functionally study the role of RANK signalling in human breast cancer. *In vitro* RANKL treatment on breast cancer cells isolated from RANK/RANKL-positive PDX models show modulation of NF-κB pathway, even in tumors where RANK expression was very low.

Introduction

RANK/RANKL signaling pathway has an essential role controlling activation and survival of osteoclasts (Kearns et al., 2008). Knockout mice lacking either RANK or RANKL develop osteopetrosis resulting from a block of osteoclasts differentiation and absence of bone resorption (Dougall et al., 1999; Kang et al., 2003). Because of the key function of these players in bone remodeling misregulation of RANK/RANKL signaling pathway has been associated with postmenopausal osteoporosis, cancer-associated bone disease and bone metastasis (Dougall, 2012). Denosumab, a monoclonal antibody against human RANKL (Kostenuik et al., 2011), is currently approved for the treatment of osteoporosis associated with postmenopausal period (Kostenuik et al., 2011; Ominsky et al., 2011) and also for bone metastasis associated to several solid tumors, as breast and prostate cancer among others (Coleman, 2012; Fizazi et al., 2009; Henry et al., 2011).

In the mammary gland RANK participates in the normal epithelial development and RANK overexpression or deletion originate a similar phenotype, a defect on lactation (Cordero et al., 2016; Fata et al., 2000; Gonzalez-Suarez et al., 2007). RANKL is expressed on ER/PR positive cells and its expression is induced by progesterone, mediating the proliferative effect of this hormone on mammary gland (Gonzalez-Suarez et al., 2010; Tanos et al., 2013). Paracrine signaling through RANKL binding on RANK-positive/ER-negative cells maintains and expands the niche of mammary stem cells (Asselin-Labat et al., 2010; Joshi et al., 2010; Schramek et al., 2010).

RANKL also mediates the protumorigenic effect of progesterone in the mammary gland (Gonzalez-Suarez et al., 2010; Schramek et al., 2010) and the inhibition of RANK signaling prevents or attenuates mammary carcinogenesis in multiple tumor prone mouse models or mouse under chemical carcinogenic protocols (Gonzalez-Suarez et al., 2010; Nolan et al., 2016; Sigl et al., 2016; Yoldi et al., 2016). In oncogene-driven mammary tumors expressing high levels of RANK (MMTV-neu and MMTV-PyMT), inhibition of RANK signaling by pharmacological or genetic approaches also reduces the number of lung metastasis (Gonzalez-Suarez et al., 2010; Yoldi et al., 2016).

Previous studies demonstrated that RANK-KO mammary tumors from the MMTV-PyMT tumor model have higher sensitivity to the chemotherapeutic agent docetaxel than the corresponding RANK-WT breast tumors (Yoldi et al., 2016). RANK-KO tumor cells gave rise to less tumorspheres than RANK-WT, highlighting an extenuation of a self-renewal capability. Limiting dilution assays also revealed a significant reduction in the frequency of tumor initiating cells in the absence of RANK. These results confirm that the absence of RANK in spontaneous murine mammary tumors depletes the pool of breast cancer stem cells, sensitizing tumors to chemotherapy treatment. Mortality of breast cancer patients is mainly due to treatment failure and tumor recurrence, which is driven by intrinsically resistant breast cancer stem cells (Creighton et al., 2009; Li et al., 2008). The achieved observation suggests that treatment with RANKL inhibitors in the clinical setting could reduce the frequency of tumor relapse and increase sensitivity to taxanes.

RANK overexpression in human, non-transformed breast cell lines induces epithelial-to-mesenchymal transition, acquisition of stem cell features and a transformed phenotype, increases migration capacity (Palafox et al., 2012). On the other hand, RANK overexpression in breast cancer cell lines induces *in vitro* invasiveness, tumorigenicity, metastatic capacity and increases the $CD44^{+}/CD24^{-}$ breast cancer stem cell population (Palafox et al., 2012). In human breast cancer, RANK

expression has been associated to more aggressive, triple negative breast cancer, high histological grade, high proliferative index and metastatic ability (Palafox et al., 2012), and decreased survival (Pfitzner et al., 2014; Santini et al., 2011). However, these associations were biased by the high frequency of RANK expression in the ER-PR- subgroup, which has poor prognosis as compared to ER+ PR+ tumors.

Encouraging results obtained in mouse models prompted us to evaluate the functional role of the pathway in the clinical breast cancer disease using breast cancer PDX models.

Materials and methods

RANK and RANKL immunohistochemistry

RANK and RANKL expression was evaluated by immunohistochemistry (IHC) in formalin-fixed paraffin-embedded (FFPE) sections from human breast adenocarcinomas and *in house*-generated PDX models and other PDX models from collaborations. Dried tissue sections were deparaffinized, hydrated, and prepared by heat retrieval in Diva Decloaker (Biocare Medical) at 90ºC overnight in a water bath. Tissue sections were blocked against endogenous proteins and staining reagents. Tissue sections were stained with a mouse anti-human RANK antibody, Amgen N1H8 (5 µg/mL; Amgen Inc.) and mouse anti-human RANKL antibody, Amgen M366 (0.75 mg/mL; Amgen Inc.) with goat anti-mouse secondary antibody. An isotype control mouse IgG1 slide was analyzed for each specimen and each antibody. The streptavidin–biotin peroxidase detection system was used with 3,3'-diaminobenzidine as a substrate (DAKO), and counterstaining was performed with hematoxylin before adding a coverslip and imaging on a Zeiss upright microscope using Zen software (Zeiss). The positivity and distribution of RANK and RANKL-positive cells in the tumor specimen were assessed for all samples.

RNA extraction and qRT-PCR

Total RNA from tissue was prepared with Tripure Isolation Reagent (Roche). Frozen tumor tissues from *in house*-generated PDX models and other PDX models from collaborations were fractionated using the POLYTRON® system PT 1200 E (Kinematica). cDNA was produced by reverse transcription using 1 µg of DNA-free RNA in a 35 µL reaction following TaqMan™ Reverse Transcription instructions (Applied Biosystems, N8080234). 20 ng/well of cDNA were used for the analysis performed in triplicate. Quantitative PCR was performed using the LightCycler® 480 SYBR green. Primer sequences are indicated below. Ct analysis was performed using LightCycler 480 software (Roche). All primers indicated below are in 5' → 3' direction.

hRANK Forward	GCAGGTGGCTTTGCAGAT
hRANK Reverse	GCATTTAGAAGACATGTACTTTCCTG
hRANKL Forward	TGATTCATGTAGGAGAATTAAACAGG
hRANKL Reverse	GATGTGCTGTGATCCAACGA
hPPiA Forward	ATGCTGGACCCAACACAAAT
hPPiA Reverse	TCTTTCACTTTGCCAAACACC

Breast cancer cells isolation, culture and treatments

Fresh PDX tumors were mechanically cut using the McIlwain tissue chopper and enzymatically digested with appropriate medium (Dulbecco's modified Eagle's medium [DMEM] F-12 (BioWest, Product #L0093), 0.3% Collagenase A (Roche Diagnostics, S.L.), 2.5U/mL Dispase (Gibco), 20 mM HEPES (Sigma-Aldrich), and antibiotics) 60 minutes at 37ºC with shacking. Samples were washed with Leibowitz-L15 medium (Gibco) supplemented with 10% fetal bovine serum (FBS) and penicillin/streptomycin (PAA) between each step. Erythrocytes were eliminated by treating samples with hypotonic lysis buffer (ACK lysing buffer, Lonza Iberica) and incubated overnight at 4ºC in the aforementioned Leibowitz-L15 medium. The following day, single epithelial cells were isolated by

treating with trypsin (PAA Laboratories) 5 minutes at 37ºC and a mix of Dispase (Gibco life technologies, Invitrogen) and DNAse (Invitrogen) for 10 minutes at 37ºC. Dead cells were first excluded by centrifugation with Lympholyte (Cedarlane laboratories) 800xg for 20 minutes and then 250xg for 10 minutes at room temperature. Cell aggregates were removed by filtering cell suspension with 40 µm filter and counted with Trypan Blue. Cells were plated in 6-well plates (Corning, Product #353046) with medium DMEM-F12 w/ L-Glutamine w/ 15 mM Hepes (BioWest, Product #L0093) supplemented with 5% fetal bovine serum (FBS), epidermal growth factor (10ng/ml, Sigma-Aldrich #E9644), choleric toxin (100ng/ml, Sigma-Aldrich #C8052), insulin (5ug/ml, Sigma-Aldrich #I1882) and penicillin/streptomycin (PAA) during 24 hours at 37ºC and 5% CO_2. Next day, non-attached cells were collected, centrifugated during 5' at 250xg and replated in 2 millilitres of starving medium DMEM-F12 w/ L-Glutamine w/ 15 mM Hepes supplemented with 0.5% fetal bovine serum (FBS), choleric toxin, insulin and penicillin/streptomycin (PAA) during 24 hours at 37ºC and 5% CO_2. Next day, cells were treated with RANKL (500 ng/ml) and total proteis from control and RANKL treated cells was extracted.

Western blot

Total protein from PDX cell cultures was isolated using radioimmunoprecipitation assay (RIPA) with 1% NP-40, Complete protease inhibitor cocktail (Roche Diagnostics GmbH) and PhoStop inhibitor cocktail (Roche Diagnostics GmbH). Lysates were separated by 10% SDS-PAGE and blotted onto a nitrocellulose membrane. The membranes were blocked with 5% of non-fat milk and then blotted with the antibodies for anti-phosphorylated p65 antibody (Cell Signaling, #3033), anti-p65 antibody (Cell Signaling, #8242), anti-phosphorylated IκB antibody (Cell Signaling, #9246), anti-IκB antibody (Santa Cruz, #sc-371) and anti-β-tubulin antibody (Abcam, AB21058). Home-made Ponceau S [Poceau S 0,2% (w/v), Glacial acetic acid 0,5% (v/v)] was used for control staining of total protein normalization.

Flow cytometry

Breast cancer single cells were isolated as described before. Single cells were resuspended and blocked with PBS 2% fetal bovine serum (FBS), 2 mM EDTA, and immunoglobulin G blocking reagent for 10 min on ice. Then they were labelled with antibodies against CD24-PE (555428), CD44-APC (559942), EpCAM-FITC (347197), CD10-PECy5 (555376), and CD49f-A647 (562473) (all from BD Pharmingen), CD133/1-PE (130-098-826 from Miltenyi Biotec), CD49f-APC (FAB13501A from R&D Systems) and CD45-PE (304008 from BioLegend). Mouse cells were excluded in flow cytometry using H2Kd-PECy7 (116622 from BioLegend). Gating was based on ''Fluorescence Minus One'' controls. A population of 10,000 living cells was captured in all FACS experiments. FACS analysis was performed using Gallios (Beckman Coulter) flow cytometer. Data was analyzed using the FlowJo software.

Results and discussion

Analyses of a collection of 300 breast adenocarcinomas demonstrated that 46% of ER-PR- and 21% of ER+PR+ tumors expressed RANK, and only 3% of ER-PR- and 5% of ER+PR+ expressed RANKL (Fig 1A). These results are in accordance with previous data generated in our laboratory and others (Azim et al., 2015; Palafox et al., 2012; Pfitzner et al., 2014).

In order to study the relevance of RANK/RANKL pathway in human breast cancer, RANK and RANKL expression screening at mRNA and protein was performed in breast cancer PDX models generated *in house* or obtained through collaborations (DeRose et al., 2011; Eyre et al., 2016; Zhang et al., 2013; Joaquín Arribas). Frequency of RANK-positivity in breast cancer PDX was slightly lower than the frequency found in clinical tumors (Figure 1A) but RANK expression was more frequently found in hormone receptor-negative breast cancer than in luminal tumors.

In the case of RANKL, its expression was exclusively restricted to hormone receptor-negative PDX models (Figure 1A), and the frequency of RANKL-positive breast tumors was increased in PDX models compared to clinical samples (Figure 1A Thus, as engraftment has been considered by itself as a prognostic marker, RANKL expression in breast cancer may be associated with increased aggressiveness. . No RANK expression was detected in tumor cells from RANKL positive tumors suggesting an unexplored mechanism of action. This subgroup of patients with RANKL+ breast tumors could benefit treatment with the RANKL inhibitor, denosumab.

PDX models indicated in Figure 1B-C were selected for functional studies based on the RNA and protein expression of RANK and RANKL. Further characterization of the models based on surface markers and histology revealed that B0047, a strongly RANK+ PDX, and IDB-07, a RANKL+ PDX, were lymphoproliferative lesions and not breast adenocarcinomas. Both models expressed human CD45 and lack the common epithelial marker EpCAM (Fig 1D). Although these models were originally derived from patients harbouring breast adenocarcinomas, during the process of engraftment and selection, a human lymphoproliferative lesion that was kept under control by the immune system of the pacient, got amplified and expanded once implanted in animmunodeficient environment overgrowing the breast tumor. This “selection” has been repeatedly observed in several collections of solid adenocarcinomas (Bondarenko et al., 2015; Chen et al., 2012; Fujii et al., 2014). Based on the high levels of RANK and RANKL, respectively, both CD45+ models were included in the study. In addition, RANK-positive PDX from TNBC and luminal subtype were selected (IDB-08 and B3277, respectively) as well as a RANKL-positive TNBC PDX (HCI-001) (Figure 1C). Both CD45+ models expressed high levels of CD44. Low levels of CD24 and CD49f were found in B0047, whereas CD49f and EpCAM were detected in IDB-07, which may reflect the remaining breast tumor cells. The breast adenocarcinomas PDX expressed high levels of CD24, CD49f, EpCAM and CD133 and some expressed CD10, expression patterns similar to that observed in the initial PDX collection we generated (Gómez-Miragaya et al., 2017).

To confirm functionality of the pathway in breast tumor cells expressing different levels of RANK, tumor cells were isolated from each tumor, stimulated *in vitro* with RANKL and analyzed for NF-κB signaling activation (Figure 1E). NF-κB activation, based on increased phosphorylation of p65 and IκB was observed in 3 out of the 4 RANK-positive PDX models tested, irrespectively of being from the

luminal or the TNBC subtype, or CD45+ (Figure 1D). Expression levels of RANK in IDB-08, where NF-κB activation was not observed, were higher than in BB3RC32 (Figure 1B – C). These results suggest that high variability in the downstream response to RANK pathway activation is driven by intrinsic differences between tumors and not only by the expression levels of RANK. Similarly, we have observed activation of RANK signaling upon RANKL stimulation even in breast cancer cell lines with very low levels of RANK expression (Palafox et al., 2012; unpublished observations). In the case of RANKL-positive PDX models high variability between different tumors even within the same model was observed. In some cases activation or even inhibition of the pathway was observed (Figure 1E and data not shown). Heterogeneity on the stromal content may be responsible of this variability. It is unclear how RANKL could signal in these tumors. We cannot rule out that RANK although at very low levels could be mediating the effect. RANKL tumor cells could also signal to RANK being expressed in stromal cells (macrophages, NK cells, dendritic cells). Other alternatives include RANKL binding to other receptors, such as Lgr4 recently described to bing RANKL in the bone suppressing canonical signalling. (Luo et al., 2016). . It has been described that RANKL can induce reverse signaling in acute myeloid leukemias (Schmiedel et al., 2013). Taken together these results suggest that RANK- and RANKL-positive breast cancers may respond to RANKL activation or inhibition. Currently functional experiments are undergoing in the laboratory to determine the impact of RANKL, RANK-Fc or denosumab treatment on tumor growth, recurrence and chemotherapy treatments using the selected RANK+ and RANKL+ PDX.

References

Asselin-Labat, M.-L., Vaillant, F., Sheridan, J.M., Pal, B., Wu, D., Simpson, E.R., Yasuda, H., Smyth, G.K., Martin, T.J., Lindeman, G.J., et al. (2010). Control of mammary stem cell function by steroid hormone signalling. Nature *465*, 798–802.

Azim, H.A., Peccatori, F.A., Brohée, S., Branstetter, D., Loi, S., Viale, G., Piccart, M., Dougall, W.C., Pruneri, G., and Sotiriou, C. (2015). RANK-ligand (RANKL) expression in young breast cancer patients and during pregnancy. Breast Cancer Res. BCR *17*, 24.

Bondarenko, G., Ugolkov, A., Rohan, S., Kulesza, P., Dubrovskyi, O., Gursel, D., Mathews, J., O'Halloran, T.V., Wei, J.J., and Mazar, A.P. (2015). Patient-Derived Tumor Xenografts Are Susceptible to Formation of Human Lymphocytic Tumors. Neoplasia N. Y. N *17*, 735–741.

Chen, K., Ahmed, S., Adeyi, O., Dick, J.E., and Ghanekar, A. (2012). Human solid tumor xenografts in immunodeficient mice are vulnerable to lymphomagenesis associated with Epstein-Barr virus. PloS One *7*, e39294.

Coleman, R.E. (2012). Adjuvant bone-targeted therapy to prevent metastasis: lessons from the AZURE study. Curr. Opin. Support. Palliat. Care *6*, 322–329.

Cordero, A., Pellegrini, P., Sanz-Moreno, A., Trinidad, E.M., Serra-Musach, J., Deshpande, C., Dougall, W.C., Pujana, M.A., and González-Suárez, E. (2016). Rankl Impairs Lactogenic Differentiation Through Inhibition of the Prolactin/Stat5 Pathway at Midgestation. Stem Cells Dayt. Ohio *34*, 1027–1039.

Creighton, C.J., Li, X., Landis, M., Dixon, J.M., Neumeister, V.M., Sjolund, A., Rimm, D.L., Wong, H., Rodriguez, A., Herschkowitz, J.I., et al. (2009). Residual breast cancers after conventional therapy display mesenchymal as well as tumor-initiating features. Proc. Natl. Acad. Sci. U. S. A. *106*, 13820–13825.

DeRose, Y.S., Wang, G., Lin, Y.-C., Bernard, P.S., Buys, S.S., Ebbert, M.T.W., Factor, R., Matsen, C., Milash, B.A., Nelson, E., et al. (2011). Tumor grafts derived from women with breast cancer authentically reflect tumor pathology, growth, metastasis and disease outcomes. Nat. Med. *17*, 1514–1520.

Dougall, W.C. (2012). Molecular Pathways: Osteoclast-Dependent and Osteoclast-Independent Roles of the RANKL/RANK/OPG Pathway in Tumorigenesis and Metastasis. Clin. Cancer Res. *18*, 326–335.

Dougall, W.C., Glaccum, M., Charrier, K., Rohrbach, K., Brasel, K., Smedt, T.D., Daro, E., Smith, J., Tometsko, M.E., Maliszewski, C.R., et al. (1999). RANK is essential for osteoclast and lymph node development. Genes Dev. *13*, 2412–2424.

Eyre, R., Alférez, D.G., Spence, K., Kamal, M., Shaw, F.L., Simões, B.M., Santiago-Gómez, A., Sarmiento-Castro, A., Bramley, M., Absar, M., et al. (2016). Patient-derived Mammosphere and Xenograft Tumour Initiation Correlates with Progression to Metastasis. J. Mammary Gland Biol. Neoplasia *21*, 99–109.

Fata, J.E., Kong, Y.Y., Li, J., Sasaki, T., Irie-Sasaki, J., Moorehead, R.A., Elliott, R., Scully, S., Voura, E.B., Lacey, D.L., et al. (2000). The osteoclast differentiation factor osteoprotegerin-ligand is essential for mammary gland development. Cell *103*, 41–50.

Fizazi, K., Lipton, A., Mariette, X., Body, J.-J., Rahim, Y., Gralow, J.R., Gao, G., Wu, L., Sohn, W., and Jun, S. (2009). Randomized phase II trial of denosumab in patients with bone metastases from

prostate cancer, breast cancer, or other neoplasms after intravenous bisphosphonates. J. Clin. Oncol. Off. J. Am. Soc. Clin. Oncol. *27*, 1564–1571.

Fujii, E., Kato, A., Chen, Y.J., Matsubara, K., Ohnishi, Y., and Suzuki, M. (2014). Characterization of EBV-related lymphoproliferative lesions arising in donor lymphocytes of transplanted human tumor tissues in the NOG mouse. Exp. Anim. *63*, 289–296.

Gómez-Miragaya, J., Palafox, M., Paré, L., Yoldi, G., Ferrer, I., Vila, S., Galván, P., Pellegrini, P., Pérez-Montoyo, H., Igea, A., et al. (2017). Resistance to Taxanes in Triple-Negative Breast Cancer Associates with the Dynamics of a CD49f+ Tumor-Initiating Population. Stem Cell Rep. *8*, 1392–1407.

Gonzalez-Suarez, E., Branstetter, D., Armstrong, A., Dinh, H., Blumberg, H., and Dougall, W.C. (2007). RANK overexpression in transgenic mice with mouse mammary tumor virus promoter-controlled RANK increases proliferation and impairs alveolar differentiation in the mammary epithelia and disrupts lumen formation in cultured epithelial acini. Mol. Cell. Biol. *27*, 1442–1454.

Gonzalez-Suarez, E., Jacob, A.P., Jones, J., Miller, R., Roudier-Meyer, M.P., Erwert, R., Pinkas, J., Branstetter, D., and Dougall, W.C. (2010). RANK ligand mediates progestin-induced mammary epithelial proliferation and carcinogenesis. Nature *468*, 103–107.

Henry, D.H., Costa, L., Goldwasser, F., Hirsh, V., Hungria, V., Prausova, J., Scagliotti, G.V., Sleeboom, H., Spencer, A., Vadhan-Raj, S., et al. (2011). Randomized, double-blind study of denosumab versus zoledronic acid in the treatment of bone metastases in patients with advanced cancer (excluding breast and prostate cancer) or multiple myeloma. J. Clin. Oncol. Off. J. Am. Soc. Clin. Oncol. *29*, 1125–1132.

Joshi, P.A., Jackson, H.W., Beristain, A.G., Di Grappa, M.A., Mote, P.A., Clarke, C.L., Stingl, J., Waterhouse, P.D., and Khokha, R. (2010). Progesterone induces adult mammary stem cell expansion. Nature *465*, 803–807.

Kang, Y., Siegel, P.M., Shu, W., Drobnjak, M., Kakonen, S.M., Cordón-Cardo, C., Guise, T.A., and Massagué, J. (2003). A multigenic program mediating breast cancer metastasis to bone. Cancer Cell *3*, 537–549.

Kearns, A.E., Khosla, S., and Kostenuik, P.J. (2008). Receptor Activator of Nuclear Factor κB Ligand and Osteoprotegerin Regulation of Bone Remodeling in Health and Disease. Endocr. Rev. *29*, 155–192.

Kostenuik, P.J., Smith, S.Y., Jolette, J., Schroeder, J., Pyrah, I., and Ominsky, M.S. (2011). Decreased bone remodeling and porosity are associated with improved bone strength in ovariectomized cynomolgus monkeys treated with denosumab, a fully human RANKL antibody. Bone *49*, 151–161.

Li, X., Lewis, M.T., Huang, J., Gutierrez, C., Osborne, C.K., Wu, M.-F., Hilsenbeck, S.G., Pavlick, A., Zhang, X., Chamness, G.C., et al. (2008). Intrinsic resistance of tumorigenic breast cancer cells to chemotherapy. J. Natl. Cancer Inst. *100*, 672–679.

Luo, J., Yang, Z., Ma, Y., Yue, Z., Lin, H., Qu, G., Huang, J., Dai, W., Li, C., Zheng, C., et al. (2016). LGR4 is a receptor for RANKL and negatively regulates osteoclast differentiation and bone resorption. Nat. Med. *22*, 539–546.

Nolan, E., Vaillant, F., Branstetter, D., Pal, B., Giner, G., Whitehead, L., Lok, S.W., Mann, G.B., Kathleen Cuningham Foundation Consortium for Research into Familial Breast Cancer (kConFab),

Rohrbach, K., et al. (2016). RANK ligand as a potential target for breast cancer prevention in BRCA1-mutation carriers. Nat. Med. *22*, 933–939.

Ominsky, M.S., Stouch, B., Schroeder, J., Pyrah, I., Stolina, M., Smith, S.Y., and Kostenuik, P.J. (2011). Denosumab, a fully human RANKL antibody, reduced bone turnover markers and increased trabecular and cortical bone mass, density, and strength in ovariectomized cynomolgus monkeys. Bone *49*, 162–173.

Palafox, M., Ferrer, I., Pellegrini, P., Vila, S., Hernandez-Ortega, S., Urruticoechea, A., Climent, F., Soler, M.T., Muñoz, P., Viñals, F., et al. (2012). RANK induces epithelial-mesenchymal transition and stemness in human mammary epithelial cells and promotes tumorigenesis and metastasis. Cancer Res. *72*, 2879–2888.

Pfitzner, B.M., Branstetter, D., Loibl, S., Denkert, C., Lederer, B., Schmitt, W.D., Dombrowski, F., Werner, M., Rüdiger, T., Dougall, W.C., et al. (2014). RANK expression as a prognostic and predictive marker in breast cancer. Breast Cancer Res. Treat. *145*, 307–315.

Santini, D., Schiavon, G., Vincenzi, B., Gaeta, L., Pantano, F., Russo, A., Ortega, C., Porta, C., Galluzzo, S., Armento, G., et al. (2011). Receptor activator of NF-kB (RANK) expression in primary tumors associates with bone metastasis occurrence in breast cancer patients. PloS One *6*, e19234.

Schmiedel, B.J., Grosse-Hovest, L., and Salih, H.R. (2013). A “vicious cycle” of NK-cell immune evasion in acute myeloid leukemia mediated by RANKL? Oncoimmunology *2*.

Schramek, D., Leibbrandt, A., Sigl, V., Kenner, L., Pospisilik, J.A., Lee, H.J., Hanada, R., Joshi, P.A., Aliprantis, A., Glimcher, L., et al. (2010). Osteoclast differentiation factor RANKL controls development of progestin-driven mammary cancer. Nature *468*, 98–102.

Sigl, V., Jones, L.P., and Penninger, J.M. (2016). RANKL/RANK: from bone loss to the prevention of breast cancer. Open Biol. *6*.

Tanos, T., Sflomos, G., Echeverria, P.C., Ayyanan, A., Gutierrez, M., Delaloye, J.-F., Raffoul, W., Fiche, M., Dougall, W., Schneider, P., et al. (2013). Progesterone/RANKL is a major regulatory axis in the human breast. Sci. Transl. Med. *5*, 182ra55.

Yoldi, G., Pellegrini, P., Trinidad, E.M., Cordero, A., Gomez-Miragaya, J., Serra-Musach, J., Dougall, W.C., Muñoz, P., Pujana, M.-A., Planelles, L., et al. (2016). RANK Signaling Blockade Reduces Breast Cancer Recurrence by Inducing Tumor Cell Differentiation. Cancer Res. *76*, 5857–5869.

Zhang, X., Claerhout, S., Prat, A., Dobrolecki, L.E., Petrovic, I., Lai, Q., Landis, M.D., Wiechmann, L., Schiff, R., Giuliano, M., et al. (2013). A Renewable Tissue Resource of Phenotypically Stable, Biologically and Ethnically Diverse, Patient-Derived Human Breast Cancer Xenograft Models. Cancer Res. *73*, 4885–4897.

Receptor Activator for NF-κB Ligand in Acute Myeloid Leukemia: Expression, Function, and Modulation of NK Cell Immunosurveillance | The Journal of Immunology.

Figure 1

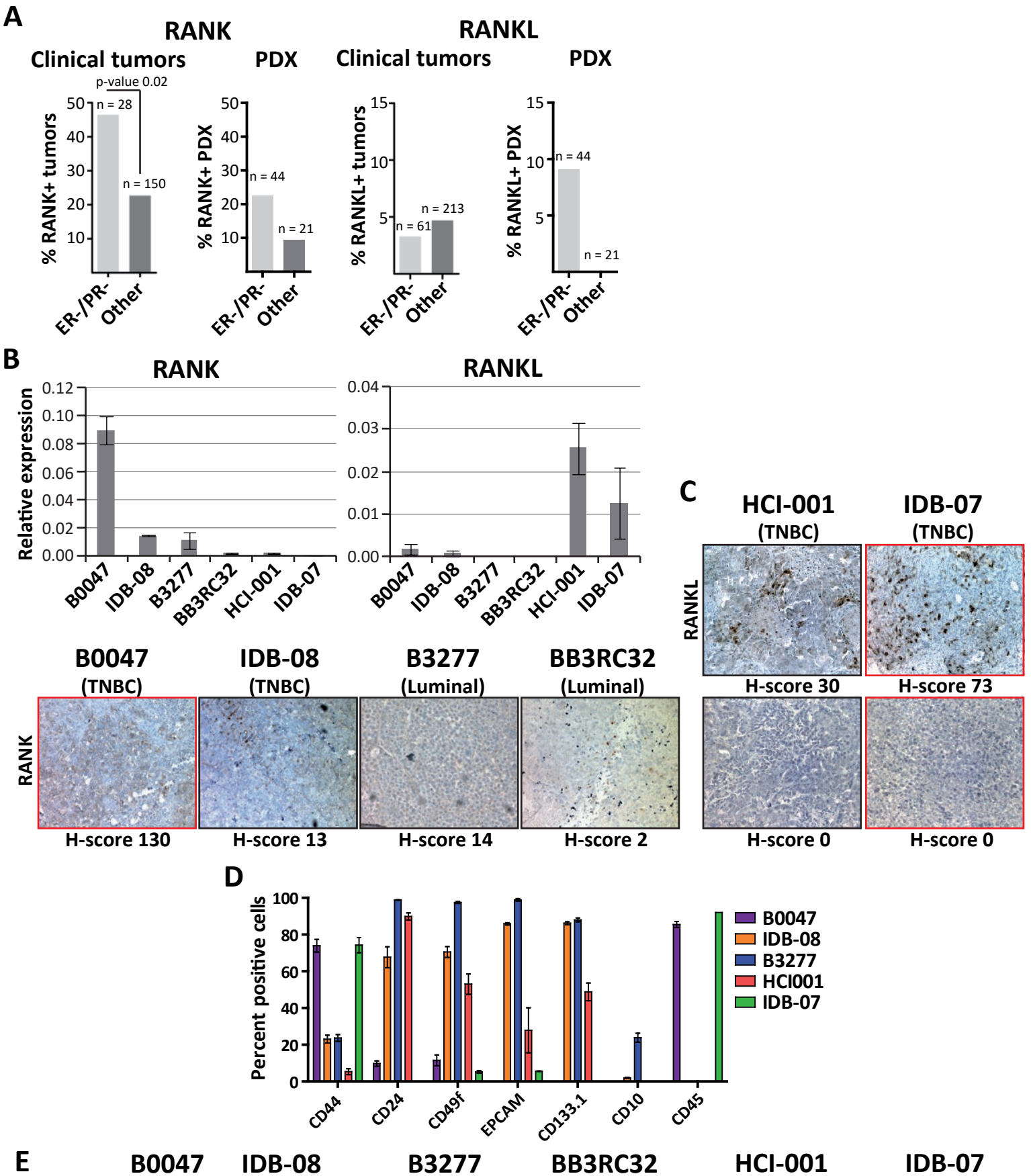
A
RANK
RANKL
Clinical tumors
PDX
Clinical tumors
PDX
p-value 0.02
n = 28
n = 150
n = 44
n = 21
n = 61
n = 213
n = 44
n = 21
% RANK+ tumors
% RANK+ PDX
% RANKL+ tumors
% RANKL+ PDX
ER-/PR-
Other
B
RANK
RANKL
Relative expression
B0047
IDB-08
B3277
BB3RC32
HCI-001
IDB-07
C
HCI-001
(TNBC)
IDB-07
(TNBC)
RANKL
H-score 30
H-score 73
B0047
(TNBC)
IDB-08
(TNBC)
B3277
(Luminal)
BB3RC32
(Luminal)
RANK
H-score 130
H-score 13
H-score 14
H-score 2
H-score 0
H-score 0
D
Percent positive cells
B0047
IDB-08
B3277
HCI001
IDB-07
CD44
CD24
CD49f
EPCAM
CD133.1
CD10
CD45
E
B0047
(TNBC)
IDB-08
(TNBC)
B3277
(Luminal)
BB3RC32
(Luminal)
HCI-001
(TNBC)
IDB-07
(TNBC)
RANKL
U
30'
10'
60'
1'
p-p65
p65
p-IKBα
IKBα
β-tubulina

Figure legends

Figure 1. Establishment, characterization and response to RANKL treatment of RANK + and RANKL+ PDX. A) Frequency of RANK and RANKL protein expression determined by immunohistochemistry (IHC) in a collection of human breast adenocarcinomas REFand in 65 models of patient-derived xenografts (PDX). **B, C)** *RANK* and *RANKL* mRNA expression levels determined by RT-PCR (**B**) and RANK and RANKL protein levels determined by IHC (**C**) in the selected PDX models. The red-framed models are the ones CD45+. **D)** Frequency of indicated markers within the H2Kd– population in RANK+ and RANKL+ PDX models. Total number of tumors analyzed (n), mean values and SDs are shown. **E)** Western blot of canonical NF-κB pathway activation in tumor cells from the indicated PDX cultures in starving conditions after activation with RANKL (500 ng/ml).

DISCUSSION

Discussion

Patient-derived xenografts (PDX) have emerged as useful tools to address clinically relevant questions and improve translational research and preclinical drug testing in breast cancer and other cancer types. This thesis has been mainly focus on the study of mechanisms of acquired chemoresistance to taxanes in human triple negative breast cancer using breast cancer PDX models and the selection of PDX models for the study of of the role of RANK/RANKL signalling pathway in human breast cancer.

Breast cancer patient-derived xenografts: more powerful cancer research tools?

Histopathological features and molecular subtyping in PDX

The importance of using patient-derived xenograft models in the study of cancer has been widely recognized, being considered as promising, powerful tools. More than 1850 PDX models have been established from 14 different cancer types just in the EuroPDX consortium from Europe (Byrne et al., 2017). From breast cancer, more than 500 well established and characterized PDX models have been established (and published) around the world (Dobrolecki et al., 2016), and probably many more are established but still unpublished. Breast cancer PDX models have shown to reflect human tumors of origin, in terms of histology, transcriptomics, genomics, signaling pathways, metastasis and response to anticancer therapy better than long-term established human breast cancer cell lines and transgenic mouse models (Bruna et al., 2016; Cassidy et al., 2015; DeRose et al., 2011; Eirew et al., 2015; Li et al., 2013b; Marangoni et al., 2007). The key feature of breast cancer PDX models is the fact that they mirror the biological features and retain the intratumoral heterogeneity from tumors of origin, being used as an ideal model for complex cancer studies representing a diverse pool of human breast cancer patients.

In order to generate breast cancer PDX models, fresh tumor pieces from primary breast cancers or metastatic breast cancer cells isolated from pleural effusions are implanted/injected in the mammary fat pad from immunodeficient mice.

Using these procedures, we have been able to establish a panel of breast cancer PDX models. As reported in other collections (Dobrolecki et al., 2016) our breast cancer PDX models resemble human primary tumors of origin in terms of the main histopathological markers and the intrinsic molecular subtypes. That is independent if they come from a primary tumor, where there is more intratumoral heterogeneity, or from a metastasis, which is more homogeneous and enriched in breast cancer stem cells (Krøigård et al., 2015; Tiran et al., 2017). That indicates that breast cancer cells isolated from pleural effusions are able to reconstitute tumors with histopathological and molecular subtype features similar to those present in human patients of origin as previously seen (Al-Hajj et al., 2003; Dobrolecki et al., 2016).

There is just a PDX that does not correlate exactly with the histopathological markers and the molecular intrinsic subtype from the tumor of origin. This breast cancer PDX model derives from a solid tumor piece. This tumor in the patient was hormone receptor-positive/HER2-negative and was classified as Luminal B subtype. The hormone receptor expression was maintained at early passages in mice, but during progressive, late passages ER and PR expression were lost, hormone independency to grow was achieved and molecular intrinsic subtype changed to HER2-enriched without overexpression of *HER2*.

In clinics, hormone receptor expression in at least 1% of tumor cells is enough to determine the tumors as hormone receptor positive (Hammond et al., 2010; Prabhu et al., 2014), while the vast majority of the tumor cells from hormone receptor-positive tumors could be hormone receptor-negative. In the process of xenografting and during serial passages, clonal selection events that can range from a minor to a extreme clonal selection can result in the selection of a population that was scarce in the original patient´s tumor (Eirew et al., 2015). As the hormone receptor-positive population was maintained during generation of the breast cancer PDX model, the selection of this hormone receptor-negative population takes place during later passages, indicating that the hormone receptor-negative population has an advantage to grow in mice.

The change in intrinsic molecular subtype from tumor of origin to breast cancer PDX model, to the best of our knowledge, has never been reported (DeRose et al., 2011; Ma et al., 2012; Petrillo et al., 2012; Reyal et al., 2012). Two hypotheses may explain that phenomenon: the correlation of the hormone

receptor-negative population in the tumor of origin with a HER2-enriched intrinsic molecular subtype and the expansion of this population in the PDX model during late passages or a complete gene expression switch in the PDX model. Single cell clonal analyses in the tumor of origin studying this hormone receptor-negative population are required to validate these hypotheses.

Initially, immunodeficient mouse strains used were *Foxn1nu*, originated at the NIH in the 60s, being them unable to produce mature T cells due to thymus deficiency. Afterwards, severe combined immune deficient (SCID)/Beige mice were generated in the 90s, lacking both the B and T lymphocytes and having defective natural killer cells. Closely in time to SCID/Beige mice generation, another immunodeficient mice strain was developed: the non-obese diabetic (NOD)/SCID mice, which present defects also in dendritic cells, macrophages and complement system. Nowadays breast cancer PDX are typically generated and propagated in highly immunodeficient mice that were developed during 2000s: the NOD/SCID-gamma (NSG) mice, which have also defects in signaling of multiple cytokines, resulting in significantly improved engraftment of human tissues, hematopoietic stem cells, and peripheral blood mononuclear cells (The Jackson Laboratory; https://www.jax.org/). Our studies using these different strains demonstrate that some tumors can grow equally in mouse strains with different grades of immunodeficiency whereas others exclusively grow or grow better in the most immunodeficient strains.

Early breast cancer PDX studies using mainly *Foxn1nu* mice suffered from low xenografting rates, with around 10% of positive xenografting, and consequently a limitation in diversity of breast cancer panels occurred. It was also described that the most aggressive breast cancers show higher xenografting rates, as triple negative breast cancers (TNBC) and high histological grade tumors (DeRose et al., 2011; Zhang et al., 2013), being xenografting by itself an independent prognostic marker of patient outcome.

Our breast cancer PDX models come from different, clinically relevant subtypes, demonstrating that the limitation in diversity of breast cancer PDX subtypes can be solved at least partially by using more immunodeficient mice. We confirm better xenografting from more aggressive tumors (TNBC, grade 3 and metastasis derived models) Similar xenografting rates to those published were obtained during generation of our breast cancer PDX panel, around 10%. The better

engraftment that has been usually shown for metastasis correlates with the idea of enrichment in breast cancer stem cells, with anchorage-independent growth ability, stromal-independent growth and suffering EMT processes.

The lower number of established, hormone receptor-positive PDX models in our collection compared to TNBC is in concordance with the aforementioned overrepresentation of TNBC/basal-like tumors in breast cancer PDX collections (Dobrolecki et al., 2016, 2016). That point may be explained because the hormone receptor-positive cells from luminal tumors show a disadvantage to xenotransplant or to be maintained as stable breast cancer PDX models.

Another important point during xenografting of breast cancer PDX models that could be biasing the establishment of different breast cancer PDX subtypes, affecting mainly hormone receptor-positive and HER2-positive breast tumors, is the lack of human stromal component, such as fibroblasts, endothelial cells and adipocytes, as it is rapidly replaced by mouse stroma after xenotransplantation (DeRose et al., 2011). The tumor microenvironment has newly recognised crucial and roles in breast cancer disease and metastasis have been described (Gangadhara et al., 2012; Hanahan and Weinberg, 2011; Swartz et al., 2012). Cancer-associated fibroblasts, tumor-associated macrophages and different secreted growth factors, as cytokines, present in human stroma have demonstrated to play important roles in tumor initiation, maintenance and progression of breast cancer. However, it is uncertain how closely the murine stroma and human tumor cell interactions resemble that of the human stroma/human tumor. This new murine stroma probably results in changes in paracrine regulation of the tumor as well as in physical properties such as interstitial pressure. Lack of human stroma can be biasing xenografting rates, being the most stroma-independent tumors overrepresented in breast cancer PDX models. It has been demonstrated that TNBC/basal-like tumors are enriched in breast cancer stem cells and it is widely accepted that breast cancer stem cells has the inner ability to grow in anchorage-independent conditions *in vitro* and undergo EMT processes (Chekhun et al., 2015; Ricardo et al., 2011; Schmitt et al., 2012). On the other hand, the luminal/ER-positive breast tumors have shown lower metabolic activity but more reverse Warburg effect mediated by stroma and also response to an activated stroma microenvironment (Choi et al., 2013; Merlino et al., 2017). This idea suggests that hormone receptor- and HER2-positive tumors are more dependent on human stromal cross-talk signaling and

its removal during xenografting can be reducing its xenografting rates, again concomitantly with the idea of the biasing against ER-positive and Her2-positive breast tumors xenotransplantation in mice.

To be useful as preclinical models, the early bias towards aggressive TNBCs had to be overcome and panels of different breast cancer subtypes achieved. In this context, the use of more immunodeficient mice strains and some new implantation protocols, as co-implantation of Luminal/ER-positive breast tumors with estrogen/progesterone-releasing pellets, have demonstrated to dramatically increase engraftment and maintainance rates especially in less aggressive, low-dividing breast tumors, from up to 20% of all tumors engrafted (DeRose et al., 2013; Ishikawa et al., 2005; Sflomos et al., 2016; Shultz et al., 2005; Telli et al., 2016). It does not seem a high rate increase but it is approximately the double than initial xenografting rates. Moreover, the injection of ER-positive breast tumors intraductally into the mouse mammary gland increases the xenografting rates without estrogen supplementation, allowing them to maintain ER signaling and response to steroid hormones and endocrine therapy, being the resulting breast cancer PDX faithful to the primary tumors that they arise from (Sflomos et al., 2016). A prospective analysis implementing novel methodology would be necessary to validate whether the less aggressive luminal subtypes can be faithfully represented in PDX collections.

Most of our breast cancer PDX models evolve to more aggressive phenotype during passages in mice, indicated by a reduced latency and higher growing rates. That is another sign of malignancy and could be explained because of an enrichment in tumor cells and a cleanning of stroma and immune cells from the patient that could be fighting the tumors , but also by the selection of a more aggressive clonal population present initially in the tumors of origin (Eirew et al., 2015; Polyak, 2007).

Although limited in number, similarities between patient outcome and PDX responses to anti-neoplastic therapies have been reported. Zhang and colleagues reported comparable treatment responses in breast cancer PDX models as those observed clinically in the tumors of origin (Zhang et al., 2013). In another study, Marangoni and co-workers demonstrated that drug response of

breast cancer PDX models was concordant with that of the patient's tumor in five of seven cases (Marangoni et al., 2007). More studies are necessary to confirm the power of breast cancer PDX in resistance studies by direct comparison of clinical response with that of the corresponding breast cancer PDX to the same drug. However, these correlations are difficult to be performed because of the complex treatment regimens administered in patients. Once the similarity in drug response will be established between primary breast tumors and PDX models using high cohorts of both, they will be useful to perform co-clinical trials, becoming a revolution.

Our breast cancer PDX models mimic clinical behaviour also in terms of drug response. In that way, TNBC PDX models are sensitive to docetaxel while luminal PDX models are resistant. But we show for the first time that, as occurs in clinics, continuous exposure *in vivo* to the drug induce acquisition of chemoresistance in breast cancer PDX models. This point reinforces the value of breast cancer PDX models as useful, reliable and cleaner tools to study chemoresistance acquisition mechanisms better than breast cancer cell lines or comparisons between different cohorts of patients. Thus, breast cancer PDX models constitute a superior approach than breast cancer cell lines in terms of the stroma presence: murine stroma supports tumor cells by mechanical and secreted factors, being closer to clinical scenario. One limitation in PDX models is the role of the immune system in fighting breast cancer, which has been demonstrated to have an important task in drug response, especially on targeted therapies (Bianchini and Gianni, 2014; Schmidt et al., 2017; Solinas et al., 2017). The immune system is important in terms of initiation and progression, controlling tumor development (Boyle and Kochetkova, 2014; Jiang and Shapiro, 2014; Savas et al., 2016). However, in our approach the role of immune system is not so important: chemotherapy, as docetaxel imposes an immunodeficient environment by targeting the rapid dividing cells contained in the bone marrow and blood (Fontanella et al., 2014; Mozaffari et al., 2007; Wijayahadi et al., 2007). Chemotherapy regimens are also administered in combination with glucocorticoids, immune system depressants, to avoid hypersensitivity-mediated effects and fluid retention (Chouhan and Herrington, 2011; Piccart et al., 1997; Weiss et al., 1990). For these reasons, PDX models constitute an ideal scenario for the study of chemoresistance, where all the players are present (tumor cells, murine stroma cells and chemotherapy) in the same field and under the same

rules (*in vivo* physiological conditions with attenuation of the immune system) than in patients.

Genomic analysis in PDX: genetic stable instability!

The genomic landscape from breast cancer has been extensively studied in the last years, taking advantage from next generation sequencing technologies and platforms (Ciriello et al., 2015; Network, 2012; Nik-Zainal et al., 2016; Stephens et al., 2012). The analysis of all this genomic data generated from human primary breast tumors and metastasis has allowed to establish or to improve some important aspects in the field of breast cancer genomics.

Since mutations in *BRCA1/2* genes can explain just 30% of hereditary breast cancer, , the study and identification of new genes with low or moderate penetrance conferring risk of hereditary breast cancer, (Economopoulou et al., 2015; Shiovitz and Korde, 2015), will improve assessment of breast cancer risk. The study and analysis of circulating tumor cells or DNA will be useful as a non-invasive test for the advanced detection of primary tumors (Desmedt et al., 2016; Esposito et al., 2014; Heidary et al., 2014; Murtaza et al., 2015). The identification of subtype-associated mutations (Ciriello et al., 2015; Network, 2012; Nik-Zainal et al., 2016; Stephens et al., 2012) will benefit the identification of subtype-specific drug treatment. The genomic evolution and dynamics of breast cancer, from the primary tumor to lymph node and distant metastatis at whole tumor or single cell genetic resolution level (Moelans et al., 2014; Wang et al., 2014; Yates et al., 2017), showing the plasticity and existence of intratumoral populations, will benefit the treatment and establish checkpoints of tumor evolution as potential targets to be disrupted.

Likewise, other genomic entities, involving chromosomal abnormalities, have been studied in human breast cancer. Different studies associate genetic alterations with gene expression-based, molecular intrinsic subtypes (Bergamaschi et al., 2006; Hu et al., 2009), elucidating the relevance of these genomic changes and their relationship with different clinicopathological features and oncogenic pathways in breast cancer. Substantial variability in copy number is displayed even inside each molecular intrinsic subtypes, being basal-like tumors the ones having the greatest intrinsic diversity (Chin et al., 2006, 2007; Kreike et al., 2007; Shah et al., 2012). Genomic diversity combining copy number

variation (CNV) and transcriptomic analysis allowed the characterization of new genome-driven integrative clusters of breast cancer (Ali et al., 2014; Curtis et al., 2012; Dawson et al., 2013; Pereira et al., 2016; Russnes et al., 2017), refining genomic breast cancer classification with clinical implications. Taken together, all these genomic studies demonstrate a new discovery horizon in our understanding of the pathophysiology and genomics of this complex disease.

Different genomic associations have been performed through the analysis of big cohort of breast cancer patients. Thus, TNBC/basal-like and HER2+ breast tumors have been identified as the subtypes displaying the highest number of mutational rates and chromosomal aberrations and, as aforementioned, subtype-associated mutations have been also unrevealed (Network, 2012). Exome-wide analysis of single nucleotide variants and CNV in our metastatic samples of origin revealed somatic mutational rates and copy number alterations similar to those described in primary human TNBC/basal-like subtype (Network, 2012). Most common mutations associated to primary TNBC have been found in the metastatic samples of origin, as mutations in *TP53*, *PIK3CA* or *BRCA1*, while mutations associated with other breast cancer subtypes (Network, 2012) were not detected. These results indicate that TNBC/basal-like metastasis maintain main genomic features from primary breast tumors, in concordance with other previous studies (Ding et al., 2010; Moelans et al., 2014; Yates et al., 2017). Also, the fact of this positive correlation between studies validates the use of exome-sequencing for breast cancer PDX studies.

Some genomic studies have been also performed in breast cancer PDX models (Bruna et al., 2016; Li et al., 2013b; du Manoir et al., 2014; Zhang et al., 2013). Most of these genomic studies using breast cancer PDX are related with tumor evolution and intratumoral dynamics (Bruna et al., 2016; Eirew et al., 2015), which is a consequence of the intratumoral heterogeneity present in breast tumors, and with the study of treatment response and resistance (Cottu et al., 2014; Li et al., 2013b; Ma et al., 2012; Zhang et al., 2013).

Here, using exome-wide comparisons between both sensitive TNBC PDX models and corresponding metastatic samples of origin we showed very similar genotypes, with most of the single nucleotide variants and CNV being maintained in TNBC PDX models during engraftment and also during early to late passages in mice. Only a few specific point mutations or chromosomal

aberrations have been selected in our models during xenotransplantation, showing a minor selective pressure in that process. This point demonstrates that despite the high number of DNA alterations, these are stable, evidencing a conserved genomic instability that is in equilibrium, with no accumulation of point mutations or chromosomal aberrations during passages. These observations about stability of DNA alteration during transplantation in mice corroborate recent results (Bruna et al., 2016; Eirew et al., 2015).

Previous literature showed two main possibilities to explain intratumoral dynamics: a huge selection during engraftment and then a stable genotype during passages in mice or a small selection during engraftment and a huge variability/clonal selection during passages in mice (Bruna et al., 2016; Eirew et al., 2015). It is important to emphasize again that we have not done single cell analysis to clearly conclude stability during intratumoral evolution. But, if a major clonal dynamics occur and some specific genomic clone/subpopulation overcomes the rest during first xenograft or during xenotransplantation in mice, it will be detectable at global tumor analysis and that does not seem to be the case. An explanation for this discrepancy could be that, while their breast cancer PDX models used in these previous studies come from a primary tumor piece at surgery or diagnostic core biopsy (Eirew et al., 2015), our sample of origin is a pleural metastasis.

Then, a combination of different studies can explain our observation of genomic stability not only during PDX model generation but also during xenotransplantation in mice. Tumor evolution from primary tumor to metastasis, leading to the selection of a more aggressive population from a minority of cells within primary tumor (Ding et al., 2010) would be the first step. An enrichment in breast cancer stem cells in the metastatic population found in pleural effusions from patients has also been demonstrated (Tiran et al., 2017). Next, population enrichment or selection from primary tumor oftenly occurs during xenotransplantation in mice (Bruna et al., 2016; Eirew et al., 2015), being the most aggressive tumors the ones with higher percentage of engratment (DeRose et al., 2011; Zhang et al., 2013). These three points (clonal metastatic development, breast cancer stem cell enrichment and clonal selection during engraftment) converge in a situation where a first step of selection of a more aggressive/CSC population occurs during metastatic event in patient and a second, minor round of selection occurs during xenografting in mice.

We identified an homozygous germline mutation in *BRCA1* in the normal lymphocytic DNA and the primary tumor from patient. In the metastatic population from the patient, this *BRCA1* mutation was detected as predominant but not homozygous, while in the TNBC PDX model it was observed as an homozygous *BRCA1* mutation. It is important to highlight two points: first, the *BRCA1*-mutant metastasis of origin showed a lot of chromosomal aberrations, showing chromothrypsis, a phenomenon associated to *BRCA1*-mutant breast cancer derived from the loss of the homologous repair machinery (Kass et al., 2016; Menghi et al., 2016; Moynahan, 2002), what is maintained in TNBC PDX model. Second, *BRCA1*-mutated breast cancer patients have an increased propensity for brain relapse (Lee et al., 2011), a metastatic pattern that is shown in our *BRCA1*-mutated, TNBC PDX model (Gómez-Miragaya et al., 2017). Findings in this *BRCA1*-mutated model are broadly consistent with previous literature showing that an expansion of a more aggressive subclonal population enriched in oncogenic mutations can take place during engrafment of TNBC PDX models. Thus, our *BRCA1*-mutant PDX model mimics main features associated to *BRCA1*-mutated, TNBC in patients.

Methylation analysis in PDX

Genome-wide methylation patterns using high-throughput microarrays of our panel of breast cancer PDX models revealed higher correlation between PDX models from the same intrinsic molecular or histological subtype than with other subtypes . Thus, DNA methylation patterns from breast cancer PDX models correlate with intrinsic molecular and histological subtype. Also, breast cancer PDX models, but not breast cancer cell lines, cluster together with patient tumors from the same intrinsic molecular/histological subtype.

Breast cancer cell lines have been widely used for breast cancer methylation studies (Fang et al., 2010; Lin et al., 2013; Tang et al., 2006). However, DNA methylation profiles of cells grown in culture tend to be distinct from those of primary tissues with both random and highly consistent changes in methylation being observed (Varley et al., 2013; Ziller et al., 2013). During last years, epigenetics, including methylation, has been studied for different PDX cancer types (Guilhamon et al., 2014; Poirier et al., 2015; Tomar et al., 2016; Wang et al., 2017; Wong et al., 2014). Some studies showed that different small cell lung cancer subtypes (Poirier et al., 2015), non-small cell lung cancer subtypes (Wang

et al., 2017) and ovarian carcinomas (Ricci et al., 2014) can be differentiated by DNA methylation patterns in PDX models. Also the association of methylation mechanisms with breast cancer tumorigenesis, tumor progression and metastasis, among others, has been elucidated (Baylin et al., 2001; Karsli-Ceppioglu et al., 2014; Pouliot et al., 2015; Stefansson and Esteller, 2013). Recently, The Cancer Genome Atlas identified five distinct DNA methylation groups based on methylation arrays of 802 breast tumors (Network, 2012). We found that breast cancer PDX models maintain a DNA methylation pattern consistent with primary breast cancer from the same molecular subtype even after multiple passages. This supports our earlier hypothesis and shows the fidelity, stability and diversity of breast cancer methylation patterns in PDX models illustrating their superiority as preclinical tools.

Curiously, the luminal PDX model that loses ER expression and changes intrinsic molecular subtype show a DNA methylation pattern associated with TNBC/ER-negative PDX models, but when compared with primary breast tumors it clusters with Luminal/ER-positive breast tumors. This result is confusing and no clear response is obvious. Genome-wide DNA methylation from this breast cancer PDX model was analyzed at late passage, when it losses expression of hormone receptor. In the case of the association with TNBC/ER-negative PDX models, the ten thousand most variable CpG islands are used while in the association with primary Luminal/ER-positive breast tumors the methylation signature described by (Network, 2012) to differentiate breast cancer subtypes was applied. The main putative hypothesis include: i) a change in the tumoral population of the breast cancer PDX model; ii) a selection of an ER-negative population with a corresponding ER-negative methylation profile in the breast cancer PDX model; iii) a better discrimination using a curated, supervised methylation signature derived from primary breast cancer. Microdissection and analysis of the ER-positive and ER-negative cells from human tumor of origin will clarify if these cells clearly form two different clusters based on ER expression as occurs between molecular subtypes.

Chemoresistance acquisition: a competition between breast cancer stem cell populations?

Overall survival of TNBC patients is poorer than for non-TNBC patients. That is mostly because after surgery, the majority of TNBC patients have residual disease in the breast and lymph nodes, but also because, even after an initial good response to non-targeted treatment, resistant relapses and metastasis develop (Crown et al., 2012).

There is a consensus that TNBC shows increased chemosensitivity compared with ER-positive breast cancer, although no optimal cytotoxic regimen has been identified. The “standard of care” chemotherapeutic approach to treat TNBC is based on anthracycline and taxane combinations for the first line (Oakman et al., 2010).

Recently, signatures predicting chemoresponse were extracted from breast cancer cell lines, with very low translation into clinics (Liedtke et al., 2010). PDX have been used to extract resistance signatures for targeted therapies (Jiménez-Valerio et al., 2016; Johnson et al., 2015; Simões et al., 2015), but the value of using breast cancer PDX models to investigate chemoresistance acquisition has not been shown. Our study using paired sensitive and resistant breast cancer PDX models is the first to highlight breast cancer PDX models for *in vivo* chemoresistance studies, accelerating the process to translation from bench-to-bedside.

Breast Cancer Stem Cell Population: the “intrinsic” resistance

The theory of CSC plasticity to explain tumor evolution as well as drug resistance has been extensively discussed. This hypothesis implies the existence of a breast CSC population in the tumor with stem cell characteristics, responsible for tumor growth, resistance, and recurrence. Different CSC markers for breast and other cancer types have been identified and CSCs have been proposed to be able to overpass chemotherapy treatment (Al-Hajj et al., 2004). However, the relationship of these BCSC markers with therapy resistance has been poorly demonstrated.

A low or no expression of CD24 in combination with a high expression of CD44 has been utilized as a CSC marker in breast and prostate cancers (Hermann et al., 2010). High CD44 protein levels have been used as a key characteristic of

CSCs in solid tumors with epithelial origin, such as breast, colon, prostate and pancreas (Zöller, 2011). Thus, the classical BCSCs were initially identified as the CD44+/CD24- (Al-Hajj et al., 2003). Also, an expansion of the CD44+/CD24- BCSC population has been demonstrated after chemotherapy treatment (Li et al., 2008). However, in pancreatic cancer, CD44-positive cells expressing CD24 have been isolated as CSCs (Hermann et al., 2010). That point indicates that CSC and/or their markers can differ depending on the types of cancer. More studies conducted not only in CSC markers but also combining CSC populations from different cancer types to know if the same gene signatures are altered, seem to be required.

Other markers used alone or in combination with the classical BCSC markers are commonly used. Thus, expression of EpCAM was utilized as a cell surface marker in a combination with CD44 to further identify CSCs, and specifically BCSC (Al-Hajj et al., 2003; Hermann et al., 2010). CD133, also known as Prominin 1, is expressed in stem cells from neural, epithelial, endothelial and hematopoietic tissues, but also it is a marker for BCSC, brain, lung, colon, pancreas and liver cancers (Hermann et al., 2010). Aldehyde dehydrogenease-1 (ALDH-1) is an enzyme oxidizing cellular aldehydes, and its high activity has been a useful CSC marker for breast and pancreatic cancers (Hermann et al., 2010; Ma and Allan, 2011), a population that has been demonstrated to be resistant to some drug therapies (Charafe-Jauffret et al., 2009, 2010; Ginestier et al., 2007). CD49f/integrin α6, a receptor for laminins, has been presented as a good indicator for CSCs in breast, colon and brain cancers (Goel et al., 2013; Klonisch et al., 2008; Meyer et al., 2010; Vieira et al., 2012). Many studies looking for additional stem cell markers are in progress with the goal to isolate defined CSCs from different types of cancers (Bachelard-Cascales et al., 2010; Clevers, 2011; Liu et al., 2013; Mostert et al., 2012; Osta et al., 2004). And importantly it has been demonstrated that different breast cancer subtypes are composed by different BCSC populations (Schmitt et al., 2012).

In our study, and in contrast with previous publications, no changes have been observed in the classical CD44+/CD24- or ALDH+ populations with chemotherapy resistance acquisition using TNBC PDX models. Instead of that, an expansion of CD49f+ population and an increase in EpCAM+ cells occurred in both chemoresistant TNBC PDX models, suggesting some common patterns in

the mechanisms of chemoresistance acquisition to docetaxel in TNBC PDX models.

It has been proposed that CD49f by itself is an independent prognostic marker in ER-negative breast cancer, more than the classical BCSC markers CD44/CD24 o ALDH (Ali et al., 2011), but association between CD49f and chemoresistance was not described. Our associations with clinical features demonstrate that CD49f-positive population is an aggressive population that correlates with metastasis in distant organs and relapse, what could be translated to poor prognosis in ER-/basal-like breast cancer in the clinical scenario.

By definition, disease recurrence originates from residual, treatment-resistant cells, which regenerate at least the initial breast cancer phenotype. Treatment of breast cancer has demonstrated to enrich in BCSC in residual disease (Phillips et al., 2006). In our experiments, the treatment of sensitive TNBC PDX models with docetaxel shows that in residual disease, the remaining cells are the CD49f+ cells. These docetaxel-resistant BCSC CD49f+ are not completely eliminated and then will be the ones with capabilities to give rise to new tumors that likely will be resistant to treatment. The increase in CD49f+ population observed in residual disease of most sensitive TNBC PDX models reinforces the idea of CD49f expansion as a common feature of resistance to docetaxel.

A decrease in the population heterogeneity in *in vitro* cultured breast cancer cell lines compared to clinical samples has been so far demonstrated (Lacroix and Leclercq, 2004; Thompson et al., 2008). In an evolutionary manner, breast cancer cell lines have drift from the initial primary tumors or metastasis from which breast cancer cells were isolated and a subset of clones were selected for *in vitro* propagation and maintenance. Despite this drift, the presence of BCSCs in breast cancer cell lines has been shown (Calcagno et al., 2010; Charafe-Jauffret et al., 2009; Fillmore and Kuperwasser, 2008).

We observed that treatment with chemotherapy in TNBC cell lines kills most tumor cells, reducing population heterogeneity and, as occurs with PDX, selecting for a population expressing high levels of CD49f. Our results demonstrate that the enrichment in a CD49f+ population is observed in most of the analyzed TNBC cell lines, highlighting the relevance of this population in

breast cancer resistance acquisition not only in *in vivo* TNBC PDX models but also in *in vitro* TNBC cell lines.

Similarly to docetaxel Treatment with paclitaxel selects again for a population expressing high levels of CD49f in half of the analyzed TNBC cell lines. Thus, CD49f+ population demonstrates resistance to different taxanes, unravelling enrichment in CD49f+ population as a general marker of resistance to taxanes. These common markers of resistance to different taxanes seem to be the most reliable, as they are specifically selecting for BCSCs resistant to more than one drug.

Although CSC markers are mainly cell surface markers, some intracellular CSC markers have also been described (Badve and Nakshatri, 2012; Bozorgi et al., 2015; Iqbal et al., 2013; Schmitt et al., 2012). Currently most of the CSC markers aforementioned can be used to identify CSCs in various cancer and tissue types. Many CSC markers have been extensively studied in clinical settings, providing important therapeutic information and potential treatments (Cheng et al., 2009; Dean, 2009; Tsang et al., 2012; Zeppernick et al., 2008). However, it is still unclear if the clinical relevance of individual CSC markers stems directly from the specific biological function of the marker, or is incidental to their expression on a specific population of tumourigenic cells. Although the expression of markers are directly correlated with some clinical outcomes, there are a few instances of direct functional correlation with individual CSC markers (Angelastro and Lamé, 2010; Mallard and Tiralongo, 2017; Tamada et al., 2012). However, our results demonstrate that downregulation of CD49f in TNBC cell lines does not alter response to docetaxel, indicating that CD49f by itself do not exhibit chemoresistant functions but it is selecting for a more aggressive breast cancer population with BCSC properties.

ITGB1 and ITGB4 have been described to be the most common partners of CD49f when heterodimerization and binding to laminins occur (Chung and Mercurio, 2004; Mercurio et al., 2001; Shaw, 1999), and their role in tumorigenesis has been studied (Goel et al., 2013; Hoshino et al., 2015; Vassilopoulos et al., 2014). Interestingly, the β4 partner subunit appears to be expressed at very low levels in CSCs compared to non-CSCs, indicating that α6β1 is the dominant α6 integrin expressed by CSCs (Goel et al., 2013; Lathia et al., 2010). Although the α6β1 integrin has been implicated in the function of breast and other CSCs (Cariati et

al., 2008; Goel et al., 2013; Lathia et al., 2010), much needs to be learned about the contribution of this integrin to the genesis of CSCs. Similar results were obtained in our study: very low expression levels of *ITGB4* and higher expression levels of *ITGB1* were observed in whole tumor population of all analyzed TNBC sensitive PDX models but no changes in ITGB1 or ITGB4 were observed in residual disease or resistant TNBC PDX models. This, together with the lack of changes in chemosensitivity after CD49f downregulation speaks against a functional effect of CD49f by itself on our setting. However, we cannot rule out that CD49f could have a functional role in chemoresistance acquisition. Previous studies revealed that while knockdown of *ITGB1* or *CD49f* alone slightly reduced cell migration ability in *BRCA1*-mutant cancer cell lines, knockdown of both genes caused a profound effect, blocking migration, suggesting an overlapping, yet critical function of both genes in the migration of BCSCs (Vassilopoulos et al., 2008). Also, the fact that CD49f exists as two distinct cytoplasmic domain variants, α6A and α6B, which are generated by alternative mRNA splicing (Hogervorst et al., 1991; Tamura et al., 1991), could be relevant to the understanding of the function of this integrin in CSCs, but little is known about the relative contribution of these variants to self-renewal and tumor initiation. More studies involving downregulation or inhibition of both proteins and/or the different isoforms of CD49f, will elucidate if they are only markers or they play a functional role in resistance.. Recently an increase of the CD49f-positive population has been associated with resistance to radiotherapy (Hu et al., 2016) and we also showed that expansion of CD49f+ population occurs in breast cancer cell lines resistant to everolimus, an mTOR inhibitor (Mateo et al., 2017).

Breast CSC properties include not only chemoresistance but also tumor initiating ability and assimetric cell division (Badve and Nakshatri, 2012; Smalley et al., 2013). There are two main assays to determine cancer stem cell ability: *in vitro* culture of CSC in anchorage-independent conditions or *in vivo* injection in the immunodeficient mice, which is the gold standard of CSC assessment (Beck and Blanpain, 2013; Magee et al., 2012). These FACS-isolated and injected breast CSC have demonstrated to give rise tumors that recapitulate intratumoral heterogeneity (Al-Hajj et al., 2003). Upon injection in the mammary fat pad of immunodeficient mice of CD49f+/- cells isolated from sensitive TNBC PDX models, we observed that CD49f+ cells have higher tumor initiating ability than CD49f-. Importantly, both CD49f+ and CD49f- cells are able to generate the other

population, evidencing high plasticity. However, CD49f+ derived tumors are more resistant and present higher levels of CD49f+ cells than tumors derived from CD49f- cells or sensitive TNBC tumors of origin.

Recent studies suggest that the state of CSCs is plastic, as CSCs are able to differentiate into non-CSC but also non-CSC can give rise to CSC (Gupta et al., 2011; Nguyen et al., 2012). This phenomenon has been described not only for CSC but also for mature, specialized cells that can be reprogrammed by external factors to become immature cells capable of developing into all tissues of the body (Takahashi and Yamanaka, 2006). The plasticity of the CSC state adds complexity to both CSC regulation and cancer in general. More studies aiming to identify the factors that can influence this interconversions and drug therapies that target these cells are needed.

It is important to note that the resistance to therapy in the CD49f+-derived tumors is not so acute as in the really resistant TNBC PDX, showing an intermediate phenotype. That could be because CD49f is enriched in breast CSC but not all of them are resistant to the therapy or because the CD49f population may acquire more specific changes during long term treatments that further increases its resistance to chemotherapy. Transcriptional analysis on CD49f+ cells from sensitive tumors and from resistant tumors showed that the CD49f+ population in resistant TNBC PDX tumors acquire transcriptional changes during chemoresistance acquisition, as high proliferation score, that are not present in CD49f+ cells from sensitive tumors of origin. Further studies looking for the progression of this CD49f+ population from sensitive tumors and studying transcriptional and tumor initiating ability changes would shed light CD49f role in chemoresistance acquisition to taxanes.

Other possibility is an enrichment in a small CD49f+ population defined by another marker and present in the sensitive TNBC tumors. It has been demonstrated that a combination of CSC markers define better a subpopulation enriched in CSC features than just one CSC marker (Al-Hajj et al., 2003; Liu et al., 2011). Then, a subpopulation inside the CD49f+ cells could be the one enriched in CSC features and proliferation. This will be the population selected and expanded during treatment. Despite considerable efforts we have not found expansion in other integrins, as ITGB1 and ITGB4, or any other CSC marker analyzed common to all PDX . Thus, a limitation in our study is the lack of a

second CSC marker that would define better the chemoresistant BCSC population.

Over the past decades, clinical evidence has suggested a role for unstable, non-heritable mechanisms of acquired drug resistance pertaining to chemotherapy and targeted agents. Reintroduction of the same therapy dates back to the 1970s with the retreatment using combination chemotherapy in patients with Hodgkin lymphoma (Young et al., 1973) and multiple myeloma (Alexanian et al., 1978). There are many examples of circumstances where patients respond to reintroduction of the same therapy in other cancer types after a drug holiday period following disease relapse or progression during therapy (Colombo and Gore, 2007; Muss et al., 1987; Seruga and Tannock, 2008). But, in the case of breast cancer, once the tumors do not respond to a chemotherapeutic regimen, this will never be administered again.

Both TNBC PDX models derive from metastatic breast cancer cells isolated from pleural effusions that were heavily treated with different chemotherapeutic agents, including taxanes, showing minimal clinical response. Nevertheless, TNBC PDX tumors prove to be initially sensitive to the treatment. Surprisingly, chemoresistant derived TNBC PDX that were left during some passages without treatment recover sensitivity to docetaxel and that correlates with a decrease in expression of CD49f, showing a shrinking in that chemoresistant population when no treatment is executing a selective pressure. This result reveals for the first time the drug holidays effect in breast cancer for cytotoxic, non-targeted therapy. This could be also shown in cancer cell lines, where under no selective pressure, the sensitive CD49f- population overcomes the resistant CD49f+ population.

Thus, the drug holidays effect we identified in breast cancer has clear, direct clinical implications, as breast cancer patients that respond to taxanes but relapse can be also treated with taxanes. Previous studies in prostate cancer have shown that intermittent taxane-based chemotherapy regimens may prevent selection for taxane-resistant cells, circumventing in some way the acquisition of therapeutic resistance (Madan et al., 2011). Some other clinical trials have also suggested that intermittent taxane chemotherapy could be a valuable approach for increasing survival in patients (Beer et al., 2008; Lin et al., 2007). These results suggest that intermittent chemotherapy regimens in breast cancer would be useful, avoiding the acquisition of chemoresistance, but clinical

trials proving that hypothesis have to be performed. Then, “drug holidays” effect is important in terms to establish a rationale schedule of treatment.

Taken together this work revealed some important results that demonstrate the rationale by which ER-/basal-like CD49f-high tumors are associated with poor outcome in patients. It demonstrates, in concordance with other works, that there are no universal markers for CSCs. However, once a marker can be confirmed to be overly expressed on CSCs, such a marker can be exploited for targeted cancer therapy (Karsten and Goletz, 2013). CSC markers are informative to understand the population being studied and promising for active targeting, but they alone cannot define CSCs (Lathia, 2013). That shows the importance to find another markers of CSC and resistance to define properly this population.

In fact, a clinical trial using antibody-based therapy (EpCAM-targeting antibody), targeting specifically BCSCs, in combination with docetaxel has shown to improve clinical benefit in patients with primary refractory advanced-stage breast cancer and EpCAM positive relapsed tumors (Schmidt et al., 2012). Similar clinical trials using CD49f antibodies in combination with chemotherapy or conjugated CD49f antibody with other chemotherapeutic agents could address the relevance of these findings in patients.

Clinical trials of TNBC patients treated neoadjuvantlly with taxane-based therapies are required to clinically validate our findings. CD49f+ population enrichment has to be evaluated both during residual disease, but also during relapse. The screening of CD49f during relapse compared to initial levels would suggest if retreatment with taxane-based therapies would be beneficial or not for patients. Then, novel anticancer drugs targeting the CD49f+ population in TNBC sensitive tumors combined with chemotherapy would be useful. The performed study of the CD49f+ gene expression signature from resistant tumors could allow to define better this population and to elucidate new therapeutic targets.

Another important point is that this enrichment in the chemoresistant population can also be accompanied by changes in (epi)genomics and transcriptomics, associated or not with the enrichment in BCSCs population. So other molecular mechanisms could be driving or influencing the acquisition of chemoresistance, as it has been described. Then, these three omics were screened.

Genetic changes (mutations or CNVs): looking for a resistant clone that hides during drug holidays

Genomics on breast cancer has allowed the establishment of different survival trends, being for example complex amplifications around 11q in ER-positive tumors or *PIK3CA* mutation predictors of lower survival (Curtis et al., 2012; Pereira et al., 2016). Associations between genomic alterations and drug resistance has been developed (Ellis et al., 2012; Robinson et al., 2013; Toy et al., 2013). Recently the Triple-Negative Breast Cancer Trial (TNT) presented at the San Antonio Breast Cancer Symposium that, while no statistically differences were shown for progression-free survival, patients with *BRCA* mutations showed an overall-response rate better for carboplatin treatment than for docetaxel treatment. Other studies showed similar results in response to PARP inhibitors, which are more effective in the treatment of TNBC, *BRCA1*-mutation carrier patients (O'Shaughnessy et al., 2011, 2014). These studies highlight the importance to investigate genomics in breast cancer prior to establish conclusions about biomarkers that could predict treatment benefit for patients and that could provide insights into resistance mechanisms.

Nonetheless, despite TNBC tumors are the ones with higher rates of mutations and chromosomal abnormalities (Network, 2012), just a couple of clinical studies associate genomic alterations with chemoresistance in TNBC (Balko et al., 2014, 2016; Goetz et al., 2017). More studies are needed to unravel if there are targetable mutations causing chemoresistance acquisition in TNBC or demonstrating that genomic alterations are or not drivers of chemoresistance.

Regardless of the powerful tools that constitute breast cancer PDX models for the study of genomics and resistance (Dobrolecki et al., 2016; Hidalgo et al., 2014; Marangoni and Poupon, 2014; Whittle et al., 2015), genomics have never been studied in matched sensitive and resistant TNBC PDX models to extract chemoresistance markers/mechanisms or actionable targets. Aiming to overcome these limitations the present study investigates the contribution of genomics as mechanism of resistance acquisition to docetaxel in TNBC patients using matched sensitive and resistant TNBC PDX models.

A remaining question in the chemotherapy field is whether resistant mutations appear *de novo* spontaneously in the presence of the treatment or they are pre-

existing mutations present in clonal populations that could be, but not necessary, rare in the initially sensitive tumor. Here we show that very few mutations have been acquired not only during engraftment and passages, but also during chemoresistance acquisition and no common mutations between resistant tumors absent in the sensitive ones were identified. Then it seems more feasible that pre-existing mutations in sensitive tumors enrich/select during chemoresistance acquisition. This result converges with the idea of the intratumoral heterogeneity (previously discussed) and with recent reports demonstrating the emergence of pre-existing populations in metastasis, relapses or after chemotherapy (Balko et al., 2014; Eirew et al., 2015; Goetz et al., 2017; Hoadley et al., 2016; Yates et al., 2017).

Another factor reinforcing the pre-existence of heterogenic intratumoral populations, some of them chemoresistance, in the initially sensitive PDX models is that these PDX models are generally passed in mice as a piece of tumor, not dissociated until single cells, acting also the passing methodology as a selection of different genomic resistant clones. Then, it is also possible that different mutations affecting multiple genes from a common biological pathway could be responsible for resistance or that different genomic alterations could induce chemoresistance acquisition to the same drug. Unfortunately, in this study we have not been able to test these hypothesis and to perform the analysis to know if mutations affecting different genes alter the same biological pathway. Further genomic studies using our approach with sensitive and resistant derived tumors as well as single cell analysis in sensitive tumors to see intratumoral heterogeneity and population dynamics during chemoresistance acquisition would need to be conducted.

Correlations between copy number alterations and chromosomal abnormalities with drug resistance have been previously established for different tumors types, as small cell lung cancer, ovarian, prostate and colorectal (Abida et al., 2017; Carter et al., 2017; Ge et al., 2017; Lee et al., 2017; Suzuki et al., 2017), but not for breast cancer. As copy number variation can be inferred from whole-exome sequencing data (Kadalayil et al., 2015; Serratì et al., 2016; Valdés-Mas et al., 2012), in this study we investigate the implication of DNA copy number variation on resistance acquisition to docetaxel in TNBC PDX models.

Comparisons between sensitive and resistant TNBC PDX models revealed that, in both PDX models, very few CNV were differentially present in resistant tumors, supporting the genomic stability during chemoresistance acquisition shown by point mutations. However, the *BRCA1*-mutated TNBC PDX model IDB-02 showed two chromosomal amplifications detected in all resistant tumors and in the metastasis but absent in sensitive tumors, involving a small fragment of chr3 and a large fragment of chr12p.

The chr12p amplification is a known, common chromosomal alteration present in testicular germ cell tumors, nasopharyngeal carcinomas (Almstrup et al., 2005; Cheng et al., 2017; Lo et al., 2012) and other cancer types as pancreatic carcinomas (Heidenblad et al., 2002) and gastrointestinal stromal tumors (Lourenço et al., 2014). Translocations of chr12p resulting in complex gene fusions have also been associated to some haematological malignancies, as leukaemia and myelodysplastic syndrome (De Braekeleer et al., 2012). It has also been associated with poor prognosis after surgery in esophageal squamous cell carcinoma (Kwong et al., 2004) and with metastatic events in testicular germ cell tumors (Kernek et al., 2004). Association of 12p amplification with ER-negative/TNBC tumors has also been described (Han et al., 2008; Hannemann et al., 2006; Natrajan et al., 2009; Turner et al., 2010), but no associations with drug resistance have been described.

Genomic and transcriptomic association studies have demonstrated that in cancer disease, amplifications can induce a regulation of gene expression (Chin et al., 2006; Pollack et al., 2002), but not always CNV associates with changes in gene expression (Jia et al., 2016), as amplification of untranslated genes or genes transcriptionally repressed will not increase their gene expression. The fact that all the expression-analyzed genes from chr12p amplified region tend to be overexpressed strengthen the idea that chr12p amplification is inducing gene overexpression. All these evidences demonstrate the relevance of the amplification of this region in cancer disease and drug resistance.

As discussed previously, intratumoral heterogeneity has become actually a trending topic in, but not restricted to, breast cancer (Bruna et al., 2016; Dobrolecki et al., 2016; Eirew et al., 2015; Nguyen et al., 2014; Whittle et al., 2015). The role of genetic heterogeneity within breast tumors is increasingly recognized as important for understanding the dynamics of cancer progression,

CSC, but also therapeutic resistance (Eirew et al., 2015; Nguyen et al., 2014), and there is interest in intratumoral heterogeneity measurements as potential biomarkers for risk stratification. The detection of an extra chr12p copy in the metastasis of origin and in the chemoresistant TNBC PDX model that it is not detected in the initial sensitive model concur with the idea of the intratumoral heterogeneity and the selection of a chemoresistant population present initially in the metastasis that is masked/overcome by the expansion of another population in the sensitive PDX model.

The “drug holidays effect” shown previously in resistant tumors during absence of selective drug pressure is a phenomenon that could explain this clonal dynamics. To investigate this possibility, treatment was performed in sensitive TNBC PDX model to check if an enrichment in chr12p amplified population takes place. Analysis at residual disease for the amplification revealed that there was a clear selection of a more homogeneous genomic population but this one was not carrying chr12p amplification. But when transcriptional analysis were performed, overexpression of genes located at chr12p was detected, not only in that model, but also a trend of overexpression was detected in residual disease from other sensitive TNBC PDX models. These data suggested that overexpression of some chr12p-located genes is predominant in TNBC PDX and is selected for by chemotherapy. These results establish a clear connection between chemoresistance, chromosome amplification and gene overexpression that is difficult to explain and has to be unravelled.

I hypothesize some possibilities to explain that point, but most of them are starting hypothesis as no concluding data from this thesis can support them. Modulation of gene expression has been proposed to play a central role in cellular adaptation to short- or long-term environmental changes, demonstrating plasticity and dynamics (López-Maury et al., 2008). Gene expression changes can occur at both transcriptional and post-transcriptional levels (López-Maury et al., 2008). So in an evolutionary manner, at short term it will be easier to select a population expressing genes just to survive to the chemotherapy treatment (residual disease state); while after a long-term exposure to the drug, it will be easier to select the population harbouring the amplification for the survival genes to a more rapid response to chemotherapy treatment, similar to what happens with immune system after a pathogenic infection (chemoresistant tumor state). For that, we propose chemoresistance acquisition in a two-step

model: first, selection of a population overexpressing chemotherapy survival genes, and second, selection for population with chr12p amplification as a mechanism for maintenance the overexpression of chemotherapy survival genes and a faster response to chemotherapy treatment.

Another possibility to explain the amplification and the acquisition of chemoresistance relationship are the double minute chromosomes and the multinucleation of tumoral cells. Metastatic sample of origin is hugely destroyed, as aforementioned, and that could be related with a mutational phenomenon in cancer called chromothripsis. Chromothripsis is characterized by extensive genomic aberrations and rearrangements and an oscillating pattern of DNA copy number levels, which could be restricted normally to a few genes or megabases (Kloosterman et al., 2012; Stephens et al., 2011). The origin of chromothripsis is unknown, but it could occur through the physical isolation of chromosomes in aberrant nuclear structures in the cytoplasm of the cell called micronuclei (Crasta et al., 2012) containing the named double minute chromosomes. Micronuclei are a common outcome of many cell division defects, including mitotic errors that miss-segregate intact chromosomes, and errors in DNA replication or repair that generate acentric chromosome fragments, and it has been associated in some types of cancer to mutation in mismatch repair genes (Nones et al., 2014). After mitosis, chromosomes from micronuclei can be reincorporated into daughter nuclei (Crasta et al., 2012), potentially integrating mutations from the micronucleus into the genome. This micronuclei during cell division, as do not have centromers or telomers found in normal chromosomes and similarly to mitochondrial DNA, will be randomly, non-uniformly segregated to just one daughter cell but the other one will be normally diploid. Then this micronucleated population after serial rounds of cell division will be reduced to a minimal population, overcome by the non-micronucleated population. Just in the presence of chemotherapy this population can be selected as to be resistant, enriching a definite population.

Double minute chromosomes have been shown to confer resistance to certain drugs, but most of these data were obtained by studying amplified mutants selected *in vitro* for their resistance to various cytotoxic drugs. Also, as distribution of these micronuclei is independent from mitotic spindle during cell division, this process is not altered and cells can continue dividing. All these

hypotheses have to be tested to clearly demonstrate if chromothripsis is responsible of chemoresistance to taxanes.

In breast cancer patients, the tumors harbouring chr12p amplification when compared with the rest of tumors show a gene expression signature enriched in cell cycle, cell division, mitosis and cytoskeletal pathways. As these gene expression signatures have been associated with chemoresistance to taxanes, these chr12p amplified tumors could be intrinsically resistant to taxanes.

Ten different integrative clusters (IntClust) have been described on breast cancer clinical tumors associating genomic and transcriptomic data, displaying each IntClust different CNV and gene expression profiles (Ali et al., 2014; Curtis et al., 2012; Dawson et al., 2013; Russnes et al., 2017). These CNV affect gene expression not only in *cis* but also in *trans*, it means that expression of genes contained in amplified and deleted regions are affected but also expression of genes that are not modified by CNV, that could be located in regions with no CNV (Curtis et al., 2012; Dawson et al., 2013). It implies that genomic and transcriptomic profiles can be used as biomarkers, classifying tumors into subtypes as it was done in the past with the histopathological classification (Dawson et al., 2013; Russnes et al., 2017), having not only a cause-effect relationship the CNVs. The IntClust10 is the subtype including mostly triple-negative/basal-like tumors with poor prognosis and characterized by 5q loss and 8q, 10p and 12p gain. This group of tumors represents a high-risk group during first 5 years from diagnoses but they also show better pCR, associate to young women (what is also associated with hereditary breast cancer/*BRCA1* mutations), high histological grade, high Nothingam prognostic index, poorly differentiated tumors and high mitotic index. These tumors also are enriched for DNA damage repair genes and apoptotic genes, as *BCL2*, *IGF1R* and *AURKB* (Ali et al., 2014; Curtis et al., 2012; Dawson et al., 2013; Russnes et al., 2017). Most of these features have been widely associated to taxane resistance, as overexpression of Bcl2 and other antiapoptotic genes and the high mitotic index due to mitotic arrest scape.

Our results indicate that tumors harbouring chr12p amplification, which are mainly included in the IntClust10, are not responders to taxane treatment. Actual data difficults these associations between IntClust10 and taxane resistance, because TNBC are treated with a mix of chemotherapeutic agents, normally

consisting in three or four different chemotherapies. Heterogeneous treatments can mask any chemoresistance and IntClust10 relationship, since IntClust10 is enriched in DNA damage repair is more sensitive to anthraciclines, PARP inhibitors, mTOR inhibitors, etc. The treatment with taxanes in this subtype would not be necessary and, in some cases, it would be counterproductive, improving patient outcome and diminishing side effects a simple, cost-benefit genetic tests based on FISH, saving also time and money in clinical research. Clinical trials dividing tumors harbouring all CNV of IntClust10 and with chr12p amplification in arms treated with or without taxanes would be needed to validate this study.

Together gene expression and genomic results, a loop between mitotic slippage, which has been related with resistance to taxanes (Flores et al., 2012; Huang et al., 2009; Kolesnick et al., 2007; Mittal et al., 2017; Visconti and Grieco, 2017), chromothripsis and cell cycle, mitosis and replication pathways seem to be altered, and the chromosome 12p amplification can be a cause or a marker of chemoresistance. More studies associating chr12p amplification/IntClust10 tumors to taxane resistance have to be performed.

Epigenetics: an independent role leading to resistance acquisition

Genome-wide methylation studies using breast cancer cell lines or human breast tumors have shown the relevance of methylation in drug response and chemoresistance acquisition (Du et al., 2014; He et al., 2016; Klajic et al., 2014; Liu et al., 2014; Takada et al., 2017). Ter Brugge and colleagues have studied for the first time methylation processes involved in chemoresistance acquisition in *BRCA1*-mutated breast cancer PDX models using methylation-specific multiplex ligation-dependent probe amplification (MLPA) (Ter Brugge et al., 2016). They demonstrated a novel resistance mechanism in *BRCA1*-methylated PDX tumors involving de novo rearrangements at the *BRCA1* locus. The limitation of this technique is that an initial hypothesis is required to know where to look.

The screening of genome-wide methylation patterns of resistant TNBC PDX models showed that resistance acquisition in TNBC PDX models is accompanied by very few methylation changes, as evidences the high correlation in methylation between resistant and sensitive tumors. This result demonstrates a very stable methylation profile during chemoresistance acquisition, but also

during passages in mice, as both variables are present in resistant TNBC PDX tumors. The methylation stability during passages in mice upon xenografting was proved in osteosarcoma and colorectal PDX models, but just for two passages in mice (Guilhamon et al., 2014). Our results show that global methylation changes are not involved in resistance acquisition to docetaxel but demonstrate the stability and reproducibility of methylation studies in early or late established breast cancer PDX models. This is in contrast with *in vitro* cultured cell lines, which acquire accumulative epigenetic changes with passaging, making some late-passage cell lines unusable for therapeutic purposes (Maitra et al., 2005).

Breast CSC enrichment in resistant TNBC PDX tumors showed previously is not reflected in changes in global DNA methylation profiles. Two main hypotheses can explain that result: the first is that methylation profiles in BCSC and non-BCSC are similar and the second is an underrepresentation of the BCSC DNA methylation in the whole tumor DNA methylation. Very few studies have shown different DNA methylation patterns in the promoter of genes between BCSC and non-BCSC (El Helou et al., 2014) or mammosphereres relative to their parental cells (Hernandez-Vargas et al., 2011). On the other hand, the CSC increase in resistant TNBC PDX tumors is probably not high enough to change DNA methylation patterns in a crystal clear manner. More studies defining methylation signatures in BCSC compared to non-BCSC are needed to elucidate that point.

Despite no global changes were detected between sensitive and resistant TNBC PDX models, some specific, differentially methylated CpGs could be potentially modulating resistance. Differentialmethylation in promoter regions from different genes has been identified in resistant TNBC PDX models.

The promoter of the Solute Carrier Family 25 Member 30 (SLC25A30) showed decreased methylation in one resistant TNBC PDX model, affecting gene expression which is upregulated. There are two main protein superfamilies of transporters: the ATP-binding cassette (ABC) transporters and the solute carrier (SLC) transporters (Dean et al., 2001; He et al., 2009). Mainly, ABC transporters function like efflux transporters, such as p-glycoprotein (*ABCB1*), the breast cancer resistant protein (*ABCG2*) and the multidrug resistance protein (*MRP2*) (Hee Choi and Yu, 2014) and they have shown to induce resistance to different antineoplasic compounds in breast cancer (Nigam, 2015). SLC transporters participate as uptake or bi-directional transporters for organic anions and organic

cations among other substrates (He et al., 2009). The importance of ABC transporters in cancer therapy has been well documented (Deeley et al., 2006; Ross and Nakanishi, 2010) being the most studied transporters in drug resistance, while the impact of SLC transporters on cancer therapy has not been extensively characterized. Our data reveal than in one TNBC PDX model acquisition of chemoresistance could be mediated by modulation of transport pathways, which includes SLC. That points out the relevance in the study not only of ABC transporters, which has been used in clinics to overcome breast cancer resistance but showed side effects (Karthikeyan and Hoti, 2015), but also the study of the SLCas potential targets to resensitize breast cancer to taxanes.

In the BRCA1 mutated IDB-02 model even less methylation changes between sensitive and resistant tumors were observed; these include alteration of calcium signaling pathways, which includes most of the genes that form both glutamaergic and GABAergic neuronal networks, mainly voltage-dependent calcium channels, was showed. These calcium channels play a pivotal role in proliferation and tumorigenesis of breast cancer cells, and participate in the modulation of resistance, yet the underlying mechanism are not completely understood (Al-Taweel et al., 2014; Coogan, 2013; Phan et al., 2017; Roger et al., 2004). In that way, calcium-channel blockers used from 1970s for the treatment of heart diseases, such as verapamil, that also blocks ABC transporters (Karthikeyan and Hoti, 2015; Timcheva and Todorov, 1996), has been widely used for the treatment of breast cancer in combination with other drugs, mostly chemotherapy. Verapamil acts as a sensitizer to other chemotherapeutic agents, not only in breast cancer cell lines (Chen et al., 2014; Guo et al., 2017; Zhang et al., 2007), but also in human breast cancer patients, where a synergistic effect and beneficial outcome was observed (Belpomme et al., 2000; Silva et al., 2012). However, some other large population-based case-control study suggests that long-term use of calcium-channel blockers is associated with a greater than 2-fold increase in the risk of breast cancer in postmenopausal women (Li et al., 2013a). Additional research is needed to confirm this finding and to evaluate potential underlying biological mechanisms before to administer calcium-channel blockers as standard of care for multidrug resistant breast cancer.

Taken together, our results validate the use of breast cancer PDX models for the study of mechanisms of resistance acquisition at early or late passages, as methylation is conserved during passages in mice, and demonstrate a very

stable methylation profiles during chemoresistance acquisition. No global methylation changes have been observed in our chemoresistant TNBC PDX tumor models while some specific alterations in different genes and pathways could explain the different response from patients to therapy. More studies increasing number of breast cancer PDX models are necessary to confirm no global methylation changes during chemoresistance acquisition.

It has been widely demonstrated that methylation controls gene expression. Instead very few changes were elucidated affecting epigenomics, gene expression was investigated to unravel the role of methylation controlling gene expression in chemoresistant tumors, but also transcriptomic mechanisms independent from epigenomics.

Gene expression changes in chemoresistant PDX models associated with methylation

Gene expression microarray analysis was performed in paired sensitive and resistant TNBC PDX tumors, and connection with methylation was assessed. Very few significant differentially methylated genes in resistant TNBC PDX tumors led to differences in gene expression. In concordance with previous works, while most gene specific promoter methylation analysis is correlated with gene expression (Jiao et al., 2014; Liu et al., 2016; Shargh et al., 2014), global methylation status and gene expression do not correlate for breast cancer, or other cancer types (Moarii et al., 2015).

Some methylation- and gene expression-affected pathways from a TNBC PDX model are concordant, indicating common altered mechanisms, such as transport pathway alteration by methylation and mitochondria, aminoacid transport and regulation of NOS affected by expression. However, most of the methylation- and gene expression-affected pathways are different. There seems to be some genes and pathways controlled by methylation, but in the acquisition of chemoresistance to docetaxel in breast cancer, most gene expression changes observed between sensitive and resistant tumors were not driven by methylationFurther methylation/gene expression studies using different breast cancer PDX models from different subtypes and to different drug treatments would unravel crossed mechanisms.

Additional transcriptomic changes in chemoresistant PDX models

Gene set enrichment analysis (GSEA) from gene expression data was performed in both resistant TNBC PDX models. Analyses of one chemoresistant model IDB-01R showed that the most altered network is the upregulation of the EGFR pathway. Validation of EGFR upregulation in chemoresistant PDX tumors was done, showing correlation with increased downstream pathway activation. Around 50% to 70% of TNBC patients have shown to (over)express EGFR (Lehmann et al., 2011; Nielsen et al., 2004) and its expression has been associated with poor prognosis (Park et al., 2014). Despite some TNBC tumors express EGFR, making them potentially susceptible to anti-EGFR therapies, initial studies have demonstrated minimum benefit or a worsening of clinical outcomes, associated with their use in the clinical setting alone or in combination with chemotherapy (Gelmon et al., 2012; Hsia et al., 2013; Masuda et al., 2012; Press et al., 2008), being an ineffective clinical option for breast cancer. However more recent studies showed that EGFR-targeted therapy in combination with other targeted therapies is a clinically available option for treatment of TNBC patients overexpressing EGFR (Jamdade et al., 2015; Scaltriti et al., 2016; Tao et al., 2014), which will be supported by our findings.

High expression levels of both *CD49f* and *EGFR* have been observed in the chemoresistant IDB-01R model. In the *BRCA1*-mutant TNBC IDB-02 model, higher initial expression levels have been demonstrated for both genes, what could correlate with a less responsive phenotype to chemotherapy. Crosstalk and crossactivation between EGFR and CD49f has been described (Marcoux and Vuori, 2003; Mariotti et al., 2001; Yamada and Even-Ram, 2002). There are many mechanisms by which adhesion and growth-factor receptors cooperate to control cell behaviour. For example, growth-factor receptor and downstream signaling intermediates are recruited to sites of integrin ligation (Yamada and Even-Ram, 2002), what could enhance autophosphorylation of growth-factor receptors (Bromann et al., 2004) and then this can activate PI3K intracellular pathway (Burridge and Wennerberg, 2004). But also the other way around, integrins can induce activation of growth factor receptors independently of growth-factor binding. Then integrin activation induce phosphorylation of EGFR different from that induced by the binding of EGF to EGFR (Moro et al., 2002). All this interactions between growth factor receptors, as EGFR, and integrins participate

in signaling pathways required for DNA synthesis, control of receptor turnover, cytoskeleton rearrangements, motility and survival.

Overexpression of both *CD49f* and *EGFR* genes has been associated with chemo and radioresistance in cancer. Thus, non-responding ovarian PDX models to cisplatinum have displayed higher expression levels for *CD49f* and *EGFR*, a CSC and an EMT marker, than the responders (Ricci et al., 2017). Also overexpression of EGFR by transcription factors as YAP1 in esophageal cancer results in docetaxel and 5-fluorouracil resistance in clinics (Song et al., 2015). In head and neck squamous cell carcinoma, integrin and EGFR targeting has been proposed as a powerful and promising approach to overcome radioresistance (Eke et al., 2015), and CD49f signaling by itself has also been proposed as a radioresistance pathway in breast cancer (Hu et al., 2016). Actually, new studies using EGFR inhibitors in combination with chemotherapy and other inhibitors, as dasatinib and mTOR/PI3K inhibitors, seem to be more encouraging for the treatment (André and Zielinski, 2012; Costa et al., 2017; Masuda et al., 2012), but it is important to highlight that there is a need to know the role of CD49f and EGFR in TNBC to better understand the best way to use targeted therapy.

This data suggest a functional role of CD49f, but, as aforementioned, downregulation of CD49f in breast cancer cell lines of CD49f has not shown differences in resistance to docetaxel, at least in our hands. We have not studied the role of EGFR in resistance to taxanes neither the interaction between other β partner subunits and EGFR. More studies unravelling this relationship are required.

Taken together our these results show the importance of the cooperation between integrins and growth factor receptors in the chemoresistance acquisition process in triple negative breast cancer. A good selection and characterization of the TNBC patients treated with combination of integrin inhibitors and/or EGFR inhibitors with chemotherapy will be essential to demonstrate the usefulness of this kind of more target-specific treatment.

GSEA analysis in the *BRCA1*-mutant, TNBC chemoresistant model associates with cell cycle, replication and mitosis pathways, which have been described to be related to breast cancer chemoresistance in patients (Reeder et al., 2015; Sanders et al., 2017; Visconti and Grieco, 2017). Paclitaxel and vincristine are

unable to work efficiently in cells, which are halted at the G1 phase of the cell cycle thereby promoting drug resistance (Reeder et al., 2015). DNA replication inhibition induces a compromised DNA repair and chemosensitization to platinum-based regimens (Sanders et al., 2017).

Mitotic slippage is another mechanism of resistance associated with cell cycle and mitosis. It has been suggested that the cells responding to an arrest in mitosis can activate the mitotic catastrophe pathway to overcome mitotic arrest bypassing the spindle-associated checkpoint (SAC), and exit mitosis without dividing in a process termed mitotic slippage (Brito and Rieder, 2006; Orth et al., 2011). Most cells bypassing mitosis by mitotic slippage, will stop dividing, becoming senescent and dying, but a small fraction of cancer cells may continue dividing through aberrant mitosis, becoming aneuploid but also resistant to treatment (Chittajallu et al., 2015; Gascoigne and Taylor, 2009; Orth et al., 2011; Topham and Taylor, 2013).

In conclusion, we have demonstrated that gene expression pathways associate with chemoresistance in the clinics are also observed using TNBC PDX models. Then, these models are useful tools for the study of methylation and gene expression, as they correlate with clinical breast cancer. Also these models can be used for the study or development of new therapies affecting some important, here highlighted pathways, shortening the consuming time invested in clinics, and reducing the heterogeneity between patients and the use of drug combinations that occurs in clinics, maybe masking resistance mechanisms. Further studies using breast cancer PDX models for the study of resistance will illustrate the relevance of these models in clinical translation.

CONCLUSIONS

Conclusions

1. Most breast cancer PDX models resemble human primary tumors of origin in terms of the main histopathological markers and the intrinsic molecular subtypes, but changes are observed in some models (IDB-03), evidencing population selection during xenografting and/or serial passages (intratumoral dynamics).

2. Some breast cancer PDX models can grow equally in different immunodeficient mouse strains, while other breast cancer PDX models just grow or grow better in the most immunodeficient strains.

3. Increased engraftment is observed for the most aggressive tumors, grade 3, metastatis, TNBC subtype.

4. TNBC PDX models have similar point mutation and chromosomal aberration rates than human tumors from the same molecular subtype. Genomic alterations present in initial TNBC PDX models are maintained with serial passages in mice. The most important selection was detected during xenografting.

5. Subtype-specific methylation patterns from different breast cancer subtypes are maintained in breast cancer PDX models.

6. Breast cancer PDX models mimic clinical behaviour in terms of chemotherapy response: luminal PDX models are resistant and triple negative breast cancer PDX models are initially sensitive but acquired resistance after continuous exposure to docetaxel *in vivo*.

7. Expansion of a CD49f+ population, but not of the breast cancer stem cell markers, CD44+ CD24- or ALDH activity, are observed during the acquisition of resistance to docetaxel in TNBC. This CD49f+ population is initially present in sensitive TNBC PDX models and breast cancer cell lines (BCCLs) and is enriched in residual disease after docetaxel treatment.

8. The CD49f+ population has increased chemoresistance and tumor-initiating properties compared to the corresponding CD49f- cells.

9. Resistance to taxanes in TNBC PDX models is reversible in the absence of the drug, the so called “drug holidays”, and associates with the dynamics of a CD49f+ population.

10. The CD49f+ population has a gene expression signature associated with resistance in breast cancer patients after treatment with anthracycline/taxane-based chemotherapy regimens.

11. Few genetic changes are found in docetaxel resistant TNBC PDX tumors indicating that acquisition of chemoresistance to docetaxel is not driven by the acquisition of point mutations or small INDELs. Continuous exposure to docetaxel does not induce genetic changes in breast cancer PDX.

12. Chr12p amplification may be associated to docetaxel resistance in BRCA1 TNBC tumors. Overexpression of genes located in Chr12p was found not only in resistant IDB-02 tumors but also in residual disease from this model and additional basal like PDX.

13. In breast cancer patients the chr12 amplification is associated to basal-like disease and is associated with poor survival.

    Algo respecto a los cambios en mitotic, gene expression signature associated to chr12p amplification?¿

14. Acquisition of resistance to docetaxel does not result in global methylation changes, however, changes in methylation and expression of some specific genes, such as *SCL25A30* may contribute to the acquisition of chemoresistance .

15. Increased expression levels of EGFR and overactivation of downstream pathway were detected in a chemoresistant TNBC PDX model, similar to clinics.

16. Gene expression changes between sensitive and resistant TNBC PDX models are associated with chemoresistance mechanisms described in human breast tumors, highlighting the preclinical use of breast cancer PDX models.

17. Breast cancer PDX models and their resistant variants constitute powerful tools for the study of chemoresistance in breast cancer.

BIBLIOGRAPHY

Abida, W., Armenia, J., Gopalan, A., Brennan, R., Walsh, M., Barron, D., Danila, D., Rathkopf, D., Morris, M., Slovin, S., et al. (2017). Prospective Genomic Profiling of Prostate Cancer Across Disease States Reveals Germline and Somatic Alterations That May Affect Clinical Decision Making. JCO Precis. Oncol. *2017*.

Afify, A., Purnell, P., and Nguyen, L. (2009). Role of CD44s and CD44v6 on human breast cancer cell adhesion, migration, and invasion. Exp. Mol. Pathol. *86*, 95–100.

Aigner, S., Sthoeger, Z.M., Fogel, M., Weber, E., Zarn, J., Ruppert, M., Zeller, Y., Vestweber, D., Stahel, R., Sammar, M., et al. (1997). CD24, a Mucin-Type Glycoprotein, Is a Ligand for P-Selectin on Human Tumor Cells. Blood *89*, 3385–3395.

Aigner, S., Ramos, C.L., Hafezi-Moghadam, A., Lawrence, M.B., Friederichs, J., Altevogt, P., and Ley, K. (1998). CD24 mediates rolling of breast carcinoma cells on P-selectin. FASEB J. Off. Publ. Fed. Am. Soc. Exp. Biol. *12*, 1241–1251.

Albain, K.S., Barlow, W.E., Shak, S., Hortobagyi, G.N., Livingston, R.B., Yeh, I.-T., Ravdin, P., Bugarini, R., Baehner, F.L., Davidson, N.E., et al. (2010). Prognostic and predictive value of the 21-gene recurrence score assay in postmenopausal women with node-positive, oestrogen-receptor-positive breast cancer on chemotherapy: a retrospective analysis of a randomised trial. Lancet Oncol. *11*, 55–65.

Alevizos, L., Kataki, A., Derventzi, A., Gomatos, I., Loutraris, C., Gloustianou, G., Manouras, A., Konstadoulakis, M.M., and Zografos, G. (2014). Breast cancer nodal metastasis correlates with tumour and lymph node methylation profiles of Caveolin-1 and CXCR4. Clin. Exp. Metastasis *31*, 511–520.

Alexanian, R., Gehan, E., Haut, A., Saiki, J., and Weick, J. (1978). Unmaintained remissions in multiple myeloma. Blood *51*, 1005–1011.

Al-Hajj, M., Wicha, M.S., Benito-Hernandez, A., Morrison, S.J., and Clarke, M.F. (2003). Prospective identification of tumorigenic breast cancer cells. Proc. Natl. Acad. Sci. U. S. A. *100*, 3983–3988.

Al-Hajj, M., Becker, M.W., Wicha, M., Weissman, I., and Clarke, M.F. (2004). Therapeutic implications of cancer stem cells. Curr. Opin. Genet. Dev. *14*, 43–47.

Ali, H.R., Dawson, S.-J., Blows, F.M., Provenzano, E., Pharoah, P.D., and Caldas, C. (2011). Cancer stem cell markers in breast cancer: pathological, clinical and prognostic significance. Breast Cancer Res. *13*, R118.

Ali, H.R., Rueda, O.M., Chin, S.-F., Curtis, C., Dunning, M.J., Aparicio, S.A., and Caldas, C. (2014). Genome-driven integrated classification of breast cancer validated in over 7,500 samples. Genome Biol. *15*.

Almendro, V., Cheng, Y.-K., Randles, A., Itzkovitz, S., Marusyk, A., Ametller, E., Gonzalez-Farre, X., Muñoz, M., Russnes, H.G., Helland, A., et al. (2014). Inference of tumor evolution during chemotherapy by computational modeling and in situ analysis of genetic and phenotypic cellular diversity. Cell Rep. *6*, 514–527.

Almstrup, K., Ottesen, A.M., Sonne, S.B., Hoei-Hansen, C.E., Leffers, H., Rajpert-De Meyts, E., and Skakkebaek, N.E. (2005). Genomic and gene expression

signature of the pre-invasive testicular carcinoma in situ. Cell Tissue Res. *322*, 159–165.

Al-Taweel, N., Varghese, E., Florea, A.-M., and Büsselberg, D. (2014). Cisplatin (CDDP) triggers cell death of MCF-7 cells following disruption of intracellular calcium ([Ca(2+)]i) homeostasis. J. Toxicol. Sci. *39*, 765–774.

Ando, K., Mori, K., Rédini, F., and Heymann, D. (2008). RANKL/RANK/OPG: key therapeutic target in bone oncology. Curr. Drug Discov. Technol. *5*, 263–268.

André, F., and Zielinski, C.C. (2012). Optimal strategies for the treatment of metastatic triple-negative breast cancer with currently approved agents. Ann. Oncol. Off. J. Eur. Soc. Med. Oncol. *23 Suppl 6*, vi46-51.

Andre, F., Job, B., Dessen, P., Tordai, A., Michiels, S., Liedtke, C., Richon, C., Yan, K., Wang, B., Vassal, G., et al. (2009). Molecular characterization of breast cancer with high-resolution oligonucleotide comparative genomic hybridization array. Clin. Cancer Res. Off. J. Am. Assoc. Cancer Res. *15*, 441–451.

Angelastro, J.M., and Lamé, M.W. (2010). Overexpression of CD133 promotes drug resistance in C6 glioma cells. Mol. Cancer Res. MCR *8*, 1105–1115.

Ansieau, S. (2013). EMT in breast cancer stem cell generation. Cancer Lett. *338*, 63–68.

Antoniou, A.C., Beesley, J., McGuffog, L., Sinilnikova, O.M., Healey, S., Neuhausen, S.L., Ding, Y.C., Rebbeck, T.R., Weitzel, J.N., Lynch, H.T., et al. (2010). Common breast cancer susceptibility alleles and the risk of breast cancer for BRCA1 and BRCA2 mutation carriers: implications for risk prediction. Cancer Res. *70*, 9742–9754.

Aparicio, S., and Caldas, C. (2013). The implications of clonal genome evolution for cancer medicine. N. Engl. J. Med. *368*, 842–851.

Armstrong, A., and Eck, S.L. (2003). EpCAM: A New Therapeutic Target for an Old Cancer Antigen. Cancer Biol. Ther. *2*, 320–325.

Armstrong, L., Stojkovic, M., Dimmick, I., Ahmad, S., Stojkovic, P., Hole, N., and Lako, M. (2004). Phenotypic characterization of murine primitive hematopoietic progenitor cells isolated on basis of aldehyde dehydrogenase activity. Stem Cells Dayt. Ohio *22*, 1142–1151.

Asselin-Labat, M.-L., Vaillant, F., Sheridan, J.M., Pal, B., Wu, D., Simpson, E.R., Yasuda, H., Smyth, G.K., Martin, T.J., Lindeman, G.J., et al. (2010). Control of mammary stem cell function by steroid hormone signalling. Nature *465*, 798–802.

Auvinen, P., Tammi, R., Tammi, M., Johansson, R., and Kosma, V.-M. (2005). Expression of CD 44 s, CD 44 v 3 and CD 44 v 6 in benign and malignant breast lesions: correlation and colocalization with hyaluronan. Histopathology *47*, 420–428.

Azad, N., Zahnow, C.A., Rudin, C.M., and Baylin, S.B. (2013). The future of epigenetic therapy in solid tumours--lessons from the past. Nat. Rev. Clin. Oncol. *10*, 256–266.

Bachelard-Cascales, E., Chapellier, M., Delay, E., Pochon, G., Voeltzel, T., Puisieux, A., Caron de Fromentel, C., and Maguer-Satta, V. (2010). The CD10 enzyme is a key player to identify and regulate human mammary stem cells. Stem Cells Dayt. Ohio *28*, 1081–1088.

Badve, S., and Nakshatri, H. (2012). Breast-cancer stem cells-beyond semantics. Lancet Oncol. *13*, e43-48.

Baird, R.D., and Caldas, C. (2013). Genetic heterogeneity in breast cancer: the road to personalized medicine? BMC Med. *11*, 151.

Balko, J.M., Giltnane, J.M., Wang, K., Schwarz, L.J., Young, C.D., Cook, R.S., Owens, P., Sanders, M.E., Kuba, M.G., Sánchez, V., et al. (2014). Molecular profiling of the residual disease of triple-negative breast cancers after neoadjuvant chemotherapy identifies actionable therapeutic targets. Cancer Discov. *4*, 232–245.

Balko, J.M., Schwarz, L.J., Cook, R.S., Estrada, M.V., Giltnane, J.M., Sanders, M.E., Sánchez, V., Dean, P.T., Wang, K., Combs, S.E., et al. (2016). Triple negative breast cancers with amplification of JAK2 at the 9p24 loci demonstrate JAK2-specific dependence. Sci. Transl. Med. *8*, 334ra53.

Bapat, S.A. (2007). Evolution of cancer stem cells. Semin. Cancer Biol. *17*, 204–213.

Bastien, R.R.L., Rodríguez-Lescure, Á., Ebbert, M.T.W., Prat, A., Munárriz, B., Rowe, L., Miller, P., Ruiz-Borrego, M., Anderson, D., Lyons, B., et al. (2012). PAM50 breast cancer subtyping by RT-qPCR and concordance with standard clinical molecular markers. BMC Med. Genomics *5*, 44.

Batlle, E., and Clevers, H. (2017). Cancer stem cells revisited. Nat. Med. *23*, 1124–1134.

Baumann, P., Cremers, N., Kroese, F., Orend, G., Chiquet-Ehrismann, R., Uede, T., Yagita, H., and Sleeman, J.P. (2005). CD24 Expression Causes the Acquisition of Multiple Cellular Properties Associated with Tumor Growth and Metastasis. Cancer Res. *65*, 10783–10793.

Baylin, S.B., Esteller, M., Rountree, M.R., Bachman, K.E., Schuebel, K., and Herman, J.G. (2001). Aberrant patterns of DNA methylation, chromatin formation and gene expression in cancer. Hum. Mol. Genet. *10*, 687–692.

Beck, B., and Blanpain, C. (2013). Unravelling cancer stem cell potential. Nat. Rev. Cancer *13*, 727–738.

Beer, T.M., Ryan, C.W., Venner, P.M., Petrylak, D.P., Chatta, G.S., Ruether, J.D., Chi, K.N., Young, J., and Henner, W.D. (2008). Intermittent chemotherapy in patients with metastatic androgen-independent prostate cancer. Cancer *112*, 326–330.

Belpomme, D., Gauthier, S., Pujade-Lauraine, E., Facchini, T., Goudier, M.J., Krakowski, I., Netter-Pinon, G., Frenay, M., Gousset, C., Marié, F.N., et al. (2000). Verapamil increases the survival of patients with anthracycline-resistant metastatic breast carcinoma. Ann. Oncol. Off. J. Eur. Soc. Med. Oncol. *11*, 1471–1476.

Bendell, J., Saleh, M., Rose, A.A.N., Siegel, P.M., Hart, L., Sirpal, S., Jones, S., Green, J., Crowley, E., Simantov, R., et al. (2014). Phase I/II study of the antibody-drug conjugate glembatumumab vedotin in patients with locally advanced or metastatic breast cancer. J. Clin. Oncol. Off. J. Am. Soc. Clin. Oncol. *32*, 3619–3625.

Bergamaschi, A., Kim, Y.H., Wang, P., Sørlie, T., Hernandez-Boussard, T., Lonning, P.E., Tibshirani, R., Børresen-Dale, A.-L., and Pollack, J.R. (2006). Distinct patterns of DNA copy number alteration are associated with different clinicopathological features and gene-expression subtypes of breast cancer. Genes. Chromosomes Cancer *45*, 1033–1040.

Bernard-Marty, C., Treilleux, I., Dumontet, C., Cardoso, F., Fellous, A., Gancberg, D., Bissery, M.C., Paesmans, M., Larsimont, D., Piccart, M.J., et al. (2002). Microtubule-associated parameters as predictive markers of docetaxel activity in advanced breast cancer patients: results of a pilot study. Clin. Breast Cancer *3*, 341–345.

Bianchini, G., and Gianni, L. (2014). The immune system and response to HER2-targeted treatment in breast cancer. Lancet Oncol. *15*, e58-68.

Bibikova, M., Barnes, B., Tsan, C., Ho, V., Klotzle, B., Le, J.M., Delano, D., Zhang, L., Schroth, G.P., Gunderson, K.L., et al. (2011). High density DNA methylation array with single CpG site resolution. Genomics *98*, 288–295.

Bines, J., Earl, H., Buzaid, A.C., and Saad, E.D. (2014). Anthracyclines and taxanes in the neo/adjuvant treatment of breast cancer: does the sequence matter? Ann. Oncol. Off. J. Eur. Soc. Med. Oncol. *25*, 1079–1085.

Birgisdottir, V., Stefansson, O.A., Bodvarsdottir, S.K., Hilmarsdottir, H., Jonasson, J.G., and Eyfjord, J.E. (2006). Epigenetic silencing and deletion of the BRCA1 gene in sporadic breast cancer. Breast Cancer Res. BCR *8*, R38.

Bjerkvig, R., Tysnes, B.B., Aboody, K.S., Najbauer, J., and Terzis, A.J.A. (2005). Opinion: the origin of the cancer stem cell: current controversies and new insights. Nat. Rev. Cancer *5*, 899–904.

Bolós, V., Blanco, M., Medina, V., Aparicio, G., Díaz-Prado, S., and Grande, E. (2009). Notch signalling in cancer stem cells. Clin. Transl. Oncol. Off. Publ. Fed. Span. Oncol. Soc. Natl. Cancer Inst. Mex. *11*, 11–19.

Bonnefoi, H., Litière, S., Piccart, M., MacGrogan, G., Fumoleau, P., Brain, E., Petit, T., Rouanet, P., Jassem, J., Moldovan, C., et al. (2014). Pathological complete response after neoadjuvant chemotherapy is an independent predictive factor irrespective of simplified breast cancer intrinsic subtypes: a landmark and two-step approach analyses from the EORTC 10994/BIG 1-00 phase III trial. Ann. Oncol. Off. J. Eur. Soc. Med. Oncol. *25*, 1128–1136.

Bonnet, D., and Dick, J.E. (1997). Human acute myeloid leukemia is organized as a hierarchy that originates from a primitive hematopoietic cell. Nat. Med. *3*, 730–737.

Boyle, S.T., and Kochetkova, M. (2014). Breast cancer stem cells and the immune system: promotion, evasion and therapy. J. Mammary Gland Biol. Neoplasia *19*, 203–211.

Boyle, W.J., Simonet, W.S., and Lacey, D.L. (2003). Osteoclast differentiation and activation. Nature *423*, 337–342.

Bozorgi, A., Khazaei, M., and Khazaei, M.R. (2015). New Findings on Breast Cancer Stem Cells: A Review. J. Breast Cancer *18*, 303–312.

Bratton, M.R., Duong, B.N., Elliott, S., Weldon, C.B., Beckman, B.S., McLachlan, J.A., and Burow, M.E. (2010). Regulation of ERalpha-mediated transcription of Bcl-2 by PI3K-AKT crosstalk: implications for breast cancer cell survival. Int. J. Oncol. *37*, 541–550.

Braun, S., Vogl, F.D., Naume, B., Janni, W., Osborne, M.P., Coombes, R.C., Schlimok, G., Diel, I.J., Gerber, B., Gebauer, G., et al. (2005). A pooled analysis of bone marrow micrometastasis in breast cancer. N. Engl. J. Med. *353*, 793–802.

Brennan, K., Garcia-Closas, M., Orr, N., Fletcher, O., Jones, M., Ashworth, A., Swerdlow, A., Thorne, H., KConFab Investigators, Riboli, E., et al. (2012). Intragenic ATM methylation in peripheral blood DNA as a biomarker of breast cancer risk. Cancer Res. *72*, 2304–2313.

Brenner, C., and Fuks, F. (2006). DNA methyltransferases: facts, clues, mysteries. Curr. Top. Microbiol. Immunol. *301*, 45–66.

Brito, D.A., and Rieder, C.L. (2006). Mitotic Checkpoint Slippage in Humans Occurs via Cyclin B Destruction in the Presence of an Active Checkpoint. Curr. Biol. *16*, 1194–1200.

Broadley, K.W.R., Hunn, M.K., Farrand, K.J., Price, K.M., Grasso, C., Miller, R.J., Hermans, I.F., and McConnell, M.J. (2011). Side population is not necessary or sufficient for a cancer stem cell phenotype in glioblastoma multiforme. Stem Cells Dayt. Ohio *29*, 452–461.

Bromann, P.A., Korkaya, H., and Courtneidge, S.A. (2004). The interplay between Src family kinases and receptor tyrosine kinases. Oncogene *23*, 7957–7968.

Bruna, A., Rueda, O.M., Greenwood, W., Batra, A.S., Callari, M., Batra, R.N., Pogrebniak, K., Sandoval, J., Cassidy, J.W., Tufegdzic-Vidakovic, A., et al. (2016). A Biobank of Breast Cancer Explants with Preserved Intra-tumor Heterogeneity to Screen Anticancer Compounds. Cell *167*, 260–274.e22.

Burridge, K., and Wennerberg, K. (2004). Rho and Rac take center stage. Cell *116*, 167–179.

Byrne, A.T., Alférez, D.G., Amant, F., Annibali, D., Arribas, J., Biankin, A.V., Bruna, A., Budinská, E., Caldas, C., Chang, D.K., et al. (2017). Interrogating open issues in cancer precision medicine with patient-derived xenografts. Nat. Rev. Cancer *17*, 254–268.

Byrski, T., Gronwald, J., Huzarski, T., Grzybowska, E., Budryk, M., Stawicka, M., Mierzwa, T., Szwiec, M., Wisniowski, R., Siolek, M., et al. (2010). Pathologic complete response rates in young women with BRCA1-positive breast cancers after neoadjuvant chemotherapy. J. Clin. Oncol. Off. J. Am. Soc. Clin. Oncol. *28*, 375–379.

Cai, F.-F., Kohler, C., Zhang, B., Wang, M.-H., Chen, W.-J., and Zhong, X.-Y. (2011). Epigenetic Therapy for Breast Cancer. Int. J. Mol. Sci. *12*, 4465–4476.

Calcagno, A.M., Salcido, C.D., Gillet, J.-P., Wu, C.-P., Fostel, J.M., Mumau, M.D., Gottesman, M.M., Varticovski, L., and Ambudkar, S.V. (2010). Prolonged drug selection of breast cancer cells and enrichment of cancer stem cell characteristics. J. Natl. Cancer Inst. *102*, 1637–1652.

Carey, L.A., Dees, E.C., Sawyer, L., Gatti, L., Moore, D.T., Collichio, F., Ollila, D.W., Sartor, C.I., Graham, M.L., and Perou, C.M. (2007). The triple negative paradox: primary tumor chemosensitivity of breast cancer subtypes. Clin. Cancer Res. Off. J. Am. Assoc. Cancer Res. *13*, 2329–2334.

Cariati, M., Naderi, A., Brown, J.P., Smalley, M.J., Pinder, S.E., Caldas, C., and Purushotham, A.D. (2008). Alpha-6 integrin is necessary for the tumourigenicity of a stem cell-like subpopulation within the MCF7 breast cancer cell line. Int. J. Cancer *122*, 298–304.

Carter, L., Rothwell, D.G., Mesquita, B., Smowton, C., Leong, H.S., Fernandez-Gutierrez, F., Li, Y., Burt, D.J., Antonello, J., Morrow, C.J., et al. (2017). Molecular analysis of circulating tumor cells identifies distinct copy-number profiles in patients with chemosensitive and chemorefractory small-cell lung cancer. Nat. Med. *23*, 114–119.

Cassidy, J.W., Caldas, C., and Bruna, A. (2015). Maintaining Tumor Heterogeneity in Patient-Derived Tumor Xenografts. Cancer Res. *75*, 2963–2968.

Cassidy, J.W., Batra, A.S., Greenwood, W., and Bruna, A. (2016). Patient-derived tumour xenografts for breast cancer drug discovery. Endocr. Relat. Cancer *23*, T259–T270.

Charafe-Jauffret, E., Ginestier, C., Iovino, F., Wicinski, J., Cervera, N., Finetti, P., Hur, M.-H., Diebel, M.E., Monville, F., Dutcher, J., et al. (2009). Breast cancer cell lines contain functional cancer stem cells with metastatic capacity and a distinct molecular signature. Cancer Res. *69*, 1302–1313.

Charafe-Jauffret, E., Ginestier, C., Iovino, F., Tarpin, C., Diebel, M., Esterni, B., Houvenaeghel, G., Extra, J.-M., Bertucci, F., Jacquemier, J., et al. (2010). Aldehyde dehydrogenase 1-positive cancer stem cells mediate metastasis and poor clinical outcome in inflammatory breast cancer. Clin. Cancer Res. Off. J. Am. Assoc. Cancer Res. *16*, 45–55.

Chedin, F., Lieber, M.R., and Hsieh, C.-L. (2002). The DNA methyltransferase-like protein DNMT3L stimulates de novo methylation by Dnmt3a. Proc. Natl. Acad. Sci. U. S. A. *99*, 16916–16921.

Chekhun, S.V., Zadvorny, T.V., Tymovska, Y.O., Anikusko, M.F., Novak, O.E., and Polishchuk, L.Z. (2015). CD44+/CD24- markers of cancer stem cells in patients with breast cancer of different molecular subtypes. Exp. Oncol. *37*, 58–63.

Chen, S., and Parmigiani, G. (2007). Meta-analysis of BRCA1 and BRCA2 penetrance. J. Clin. Oncol. Off. J. Am. Soc. Clin. Oncol. *25*, 1329–1333.

Chen, Y., Zheng, X.-L., Fang, D.-L., Yang, Y., Zhang, J.-K., Li, H.-L., Xu, B., Lei, Y., Ren, K., and Song, X.-R. (2014). Dual agent loaded PLGA nanoparticles enhanced

antitumor activity in a multidrug-resistant breast tumor eenograft model. Int. J. Mol. Sci. *15*, 2761–2772.

Cheng, J.-X., Liu, B.-L., and Zhang, X. (2009). How powerful is CD133 as a cancer stem cell marker in brain tumors? Cancer Treat. Rev. *35*, 403–408.

Cheng, L., Lyu, B., and Roth, L.M. (2017). Perspectives on testicular germ cell neoplasms. Hum. Pathol. *59*, 10–25.

Cherciu, I., Bărbălan, A., Pirici, D., Mărgăritescu, C., and Săftoiu, A. (2014). Stem cells, colorectal cancer and cancer stem cell markers correlations. Curr. Health Sci. J. *40*, 153–161.

Cheung-Ong, K., Giaever, G., and Nislow, C. (2013). DNA-damaging agents in cancer chemotherapy: serendipity and chemical biology. Chem. Biol. *20*, 648–659.

Chin, K., DeVries, S., Fridlyand, J., Spellman, P.T., Roydasgupta, R., Kuo, W.-L., Lapuk, A., Neve, R.M., Qian, Z., Ryder, T., et al. (2006). Genomic and transcriptional aberrations linked to breast cancer pathophysiologies. Cancer Cell *10*, 529–541.

Chin, S.F., Teschendorff, A.E., Marioni, J.C., Wang, Y., Barbosa-Morais, N.L., Thorne, N.P., Costa, J.L., Pinder, S.E., van de Wiel, M.A., Green, A.R., et al. (2007). High-resolution aCGH and expression profiling identifies a novel genomic subtype of ER negative breast cancer. Genome Biol. *8*, R215.

Chittajallu, D.R., Florian, S., Kohler, R.H., Iwamoto, Y., Orth, J.D., Weissleder, R., Danuser, G., and Mitchison, T.J. (2015). In vivo cell-cycle profiling in xenograft tumors by quantitative intravital microscopy. Nat. Methods *12*, 577–585.

Choesmel, V., Anract, P., Høifødt, H., Thiery, J.-P., and Blin, N. (2004). A relevant immunomagnetic assay to detect and characterize epithelial cell adhesion molecule-positive cells in bone marrow from patients with breast carcinoma: immunomagnetic purification of micrometastases. Cancer *101*, 693–703.

Choi, J., Kim, D.H., Jung, W.H., and Koo, J.S. (2013). Metabolic interaction between cancer cells and stromal cells according to breast cancer molecular subtype. Breast Cancer Res. BCR *15*, R78.

Chung, J., and Mercurio, A.M. (2004). Contributions of the alpha6 integrins to breast carcinoma survival and progression. Mol. Cells *17*, 203–209.

Ciriello, G., Miller, M.L., Aksoy, B.A., Senbabaoglu, Y., Schultz, N., and Sander, C. (2013). Emerging landscape of oncogenic signatures across human cancers. Nat. Genet. *45*, 1127–1133.

Ciriello, G., Gatza, M.L., Beck, A.H., Wilkerson, M.D., Rhie, S.K., Pastore, A., Zhang, H., McLellan, M., Yau, C., Kandoth, C., et al. (2015). Comprehensive Molecular Portraits of Invasive Lobular Breast Cancer. Cell *163*, 506–519.

Clark, M.J., Chen, R., Lam, H.Y.K., Karczewski, K.J., Chen, R., Euskirchen, G., Butte, A.J., and Snyder, M. (2011). Performance comparison of exome DNA sequencing technologies. Nat. Biotechnol. *29*, 908–914.

Clevers, H. (2011). The cancer stem cell: premises, promises and challenges. Nat. Med. *17*, 313–319.

Cokus, S.J., Feng, S., Zhang, X., Chen, Z., Merriman, B., Haudenschild, C.D., Pradhan, S., Nelson, S.F., Pellegrini, M., and Jacobsen, S.E. (2008). Shotgun bisulphite sequencing of the Arabidopsis genome reveals DNA methylation patterning. Nature *452*, 215–219.

Coleman, R., Gnant, M., Morgan, G., and Clezardin, P. (2012). Effects of bone-targeted agents on cancer progression and mortality. J. Natl. Cancer Inst. *104*, 1059–1067.

Coloff, J.L., Macintyre, A.N., Nichols, A.G., Liu, T., Gallo, C.A., Plas, D.R., and Rathmell, J.C. (2011). Akt-dependent glucose metabolism promotes Mcl-1 synthesis to maintain cell survival and resistance to Bcl-2 inhibition. Cancer Res. *71*, 5204–5213.

Colombo, N., and Gore, M. (2007). Treatment of recurrent ovarian cancer relapsing 6-12 months post platinum-based chemotherapy. Crit. Rev. Oncol. Hematol. *64*, 129–138.

Conley, S.J., Gheordunescu, E., Kakarala, P., Newman, B., Korkaya, H., Heath, A.N., Clouthier, S.G., and Wicha, M.S. (2012). Antiangiogenic agents increase breast cancer stem cells via the generation of tumor hypoxia. Proc. Natl. Acad. Sci. U. S. A. *109*, 2784–2789.

Coogan, P.F. (2013). Calcium-channel blockers and breast cancer: a hypothesis revived. JAMA Intern. Med. *173*, 1637–1638.

Cook, J.A., Gius, D., Wink, D.A., Krishna, M.C., Russo, A., and Mitchell, J.B. (2004). Oxidative stress, redox, and the tumor microenvironment. Semin. Radiat. Oncol. *14*, 259–266.

Cordon-Cardo, C., O'Brien, J.P., Boccia, J., Casals, D., Bertino, J.R., and Melamed, M.R. (1990). Expression of the multidrug resistance gene product (P-glycoprotein) in human normal and tumor tissues. J. Histochem. Cytochem. Off. J. Histochem. Soc. *38*, 1277–1287.

Corte, M.D., González, L.O., Junquera, S., Bongera, M., Allende, M.T., and Vizoso, F.J. (2010). Analysis of the expression of hyaluronan in intraductal and invasive carcinomas of the breast. J. Cancer Res. Clin. Oncol. *136*, 745–750.

Costa, R., Shah, A.N., Santa-Maria, C.A., Cruz, M.R., Mahalingam, D., Carneiro, B.A., Chae, Y.K., Cristofanilli, M., Gradishar, W.J., and Giles, F.J. (2017). Targeting Epidermal Growth Factor Receptor in triple negative breast cancer: New discoveries and practical insights for drug development. Cancer Treat. Rev. *53*, 111–119.

Cottu, P., Bièche, I., Assayag, F., El Botty, R., Chateau-Joubert, S., Thuleau, A., Bagarre, T., Albaud, B., Rapinat, A., Gentien, D., et al. (2014). Acquired resistance to endocrine treatments is associated with tumor-specific molecular changes in patient-derived luminal breast cancer xenografts. Clin. Cancer Res. Off. J. Am. Assoc. Cancer Res. *20*, 4314–4325.

Crasta, K., Ganem, N.J., Dagher, R., Lantermann, A.B., Ivanova, E.V., Pan, Y., Nezi, L., Protopopov, A., Chowdhury, D., and Pellman, D. (2012). DNA breaks and chromosome pulverization from errors in mitosis. Nature *482*, 53–58.

Creighton, C.J., Li, X., Landis, M., Dixon, J.M., Neumeister, V.M., Sjolund, A., Rimm, D.L., Wong, H., Rodriguez, A., Herschkowitz, J.I., et al. (2009). Residual breast cancers after conventional therapy display mesenchymal as well as tumor-initiating features. Proc. Natl. Acad. Sci. U. S. A. *106*, 13820–13825.

Criscitiello, C., Esposito, A., Gelao, L., Fumagalli, L., Locatelli, M., Minchella, I., Adamoli, L., Goldhirsch, A., and Curigliano, G. (2014). Immune approaches to the treatment of breast cancer, around the corner? Breast Cancer Res. BCR *16*, 204.

Crown, J., O'Shaughnessy, J., and Gullo, G. (2012). Emerging targeted therapies in triple-negative breast cancer. Ann. Oncol. Off. J. Eur. Soc. Med. Oncol. *23 Suppl 6*, vi56-65.

Cruet-Hennequart, S., Glynn, M.T., Murillo, L.S., Coyne, S., and Carty, M.P. (2008). Enhanced DNA-PK-mediated RPA2 hyperphosphorylation in DNA polymerase eta-deficient human cells treated with cisplatin and oxaliplatin. DNA Repair *7*, 582–596.

Curtis, C., Shah, S.P., Chin, S.-F., Turashvili, G., Rueda, O.M., Dunning, M.J., Speed, D., Lynch, A.G., Samarajiwa, S., Yuan, Y., et al. (2012). The genomic and transcriptomic architecture of 2,000 breast tumours reveals novel subgroups. Nature *486*, 346–352.

Daniel, A.R., Hagan, C.R., and Lange, C.A. (2011). Progesterone receptor action: defining a role in breast cancer. Expert Rev. Endocrinol. Metab. *6*, 359–369.

Daniel, V.C., Marchionni, L., Hierman, J.S., Rhodes, J.T., Devereux, W.L., Rudin, C.M., Yung, R., Parmigiani, G., Dorsch, M., Peacock, C.D., et al. (2009). A Primary Xenograft Model of Small-Cell Lung Cancer Reveals Irreversible Changes in Gene Expression Imposed by Culture In vitro. Cancer Res. *69*, 3364–3373.

Darnay, B.G., Haridas, V., Ni, J., Moore, P.A., and Aggarwal, B.B. (1998). Characterization of the intracellular domain of receptor activator of NF-kappaB (RANK). Interaction with tumor necrosis factor receptor-associated factors and activation of NF-kappab and c-Jun N-terminal kinase. J. Biol. Chem. *273*, 20551–20555.

Dawson, S.-J., Rueda, O.M., Aparicio, S., and Caldas, C. (2013). A new genome-driven integrated classification of breast cancer and its implications. EMBO J. *32*, 617–628.

De Braekeleer, E., Douet-Guilbert, N., Morel, F., Le Bris, M.-J., Basinko, A., and De Braekeleer, M. (2012). ETV6 fusion genes in hematological malignancies: a review. Leuk. Res. *36*, 945–961.

De Palma, M., and Hanahan, D. (2012). The biology of personalized cancer medicine: facing individual complexities underlying hallmark capabilities. Mol. Oncol. *6*, 111–127.

Dean, M. (2009). ABC transporters, drug resistance, and cancer stem cells. J. Mammary Gland Biol. Neoplasia *14*, 3–9.

Dean, M., Rzhetsky, A., and Allikmets, R. (2001). The human ATP-binding cassette (ABC) transporter superfamily. Genome Res. *11*, 1156–1166.

Deeley, R.G., Westlake, C., and Cole, S.P.C. (2006). Transmembrane transport of endo- and xenobiotics by mammalian ATP-binding cassette multidrug resistance proteins. Physiol. Rev. *86*, 849–899.

DeGorter, M.K., Xia, C.Q., Yang, J.J., and Kim, R.B. (2012). Drug transporters in drug efficacy and toxicity. Annu. Rev. Pharmacol. Toxicol. *52*, 249–273.

Denisov, E.V., Litviakov, N.V., Zavyalova, M.V., Perelmuter, V.M., Vtorushin, S.V., Tsyganov, M.M., Gerashchenko, T.S., Garbukov, E.Y., Slonimskaya, E.M., and Cherdyntseva, N.V. (2014). Intratumoral morphological heterogeneity of breast cancer: neoadjuvant chemotherapy efficiency and multidrug resistance gene expression. Sci. Rep. *4*, 4709.

DeRose, Y.S., Wang, G., Lin, Y.-C., Bernard, P.S., Buys, S.S., Ebbert, M.T.W., Factor, R., Matsen, C., Milash, B.A., Nelson, E., et al. (2011). Tumor grafts derived from women with breast cancer authentically reflect tumor pathology, growth, metastasis and disease outcomes. Nat. Med. *17*, 1514–1520.

DeRose, Y.S., Gligorich, K.M., Wang, G., Georgelas, A., Bowman, P., Courdy, S.J., Welm, A.L., and Welm, B.E. (2013). Patient-derived models of human breast cancer: protocols for in vitro and in vivo applications in tumor biology and translational medicine. Curr. Protoc. Pharmacol. *Chapter 14*, Unit14.23.

Desmedt, C., Yates, L., and Kulka, J. (2016). Catalog of genetic progression of human cancers: breast cancer. Cancer Metastasis Rev. *35*, 49–62.

Dey, N., Leyland-Jones, B., and De, P. (2015). MYC-xing it up with PIK3CA mutation and resistance to PI3K inhibitors: summit of two giants in breast cancers. Am. J. Cancer Res. *5*, 1–19.

van Dijk, E.L., Auger, H., Jaszczyszyn, Y., and Thermes, C. (2014). Ten years of next-generation sequencing technology. Trends Genet. TIG *30*, 418–426.

Ding, L., Ellis, M.J., Li, S., Larson, D.E., Chen, K., Wallis, J.W., Harris, C.C., McLellan, M.D., Fulton, R.S., Fulton, L.L., et al. (2010). Genome Remodeling in a Basal-like Breast Cancer Metastasis and Xenograft. Nature *464*, 999–1005.

Dobrolecki, L.E., Airhart, S.D., Alferez, D.G., Aparicio, S., Behbod, F., Bentires-Alj, M., Brisken, C., Bult, C.J., Cai, S., Clarke, R.B., et al. (2016). Patient-derived xenograft (PDX) models in basic and translational breast cancer research. Cancer Metastasis Rev. *35*, 547–573.

Donnenberg, V.S., and Donnenberg, A.D. (2005). Multiple drug resistance in cancer revisited: the cancer stem cell hypothesis. J. Clin. Pharmacol. *45*, 872–877.

Dougall, W.C., and Chaisson, M. (2006). The RANK/RANKL/OPG triad in cancer-induced bone diseases. Cancer Metastasis Rev. *25*, 541–549.

Dougall, W.C., Glaccum, M., Charrier, K., Rohrbach, K., Brasel, K., Smedt, T.D., Daro, E., Smith, J., Tometsko, M.E., Maliszewski, C.R., et al. (1999). RANK is

essential for osteoclast and lymph node development. Genes Dev. *13*, 2412–2424.

Doyle, L.A., and Ross, D.D. (2003). Multidrug resistance mediated by the breast cancer resistance protein BCRP (ABCG2). Oncogene *22*, 7340–7358.

Doyle, L.A., Yang, W., Abruzzo, L.V., Krogmann, T., Gao, Y., Rishi, A.K., and Ross, D.D. (1998). A multidrug resistance transporter from human MCF-7 breast cancer cells. Proc. Natl. Acad. Sci. U. S. A. *95*, 15665–15670.

Du, M., Su, X.-M., Zhang, T., and Xing, Y.-J. (2014). Aberrant promoter DNA methylation inhibits bone morphogenetic protein 2 expression and contributes to drug resistance in breast cancer. Mol. Med. Rep. *10*, 1051–1055.

Dumontet, C., and Sikic, B.I. (1999). Mechanisms of action of and resistance to antitubulin agents: microtubule dynamics, drug transport, and cell death. J. Clin. Oncol. Off. J. Am. Soc. Clin. Oncol. *17*, 1061–1070.

Dylla, S.J., Beviglia, L., Park, I.-K., Chartier, C., Raval, J., Ngan, L., Pickell, K., Aguilar, J., Lazetic, S., Smith-Berdan, S., et al. (2008). Colorectal cancer stem cells are enriched in xenogeneic tumors following chemotherapy. PloS One *3*, e2428.

Early Breast Cancer Trialists' Collaborative Group (EBCTCG), Darby, S., McGale, P., Correa, C., Taylor, C., Arriagada, R., Clarke, M., Cutter, D., Davies, C., Ewertz, M., et al. (2011). Effect of radiotherapy after breast-conserving surgery on 10-year recurrence and 15-year breast cancer death: meta-analysis of individual patient data for 10,801 women in 17 randomised trials. Lancet Lond. Engl. *378*, 1707–1716.

Economopoulou, P., Dimitriadis, G., and Psyrri, A. (2015). Beyond BRCA: new hereditary breast cancer susceptibility genes. Cancer Treat. Rev. *41*, 1–8.

Eirew, P., Stingl, J., Raouf, A., Turashvili, G., Aparicio, S., Emerman, J.T., and Eaves, C.J. (2008). A method for quantifying normal human mammary epithelial stem cells with in vivo regenerative ability. Nat. Med. *14*, 1384–1389.

Eirew, P., Steif, A., Khattra, J., Ha, G., Yap, D., Farahani, H., Gelmon, K., Chia, S., Mar, C., Wan, A., et al. (2015). Dynamics of genomic clones in breast cancer patient xenografts at single cell resolution. Nature *518*, 422–426.

Eke, I., Zscheppang, K., Dickreuter, E., Hickmann, L., Mazzeo, E., Unger, K., Krause, M., and Cordes, N. (2015). Simultaneous β1 integrin-EGFR targeting and radiosensitization of human head and neck cancer. J. Natl. Cancer Inst. *107*.

El Helou, R., Wicinski, J., Guille, A., Adélaïde, J., Finetti, P., Bertucci, F., Chaffanet, M., Birnbaum, D., Charafe-Jauffret, E., and Ginestier, C. (2014). Brief reports: A distinct DNA methylation signature defines breast cancer stem cells and predicts cancer outcome. Stem Cells Dayt. Ohio *32*, 3031–3036.

Ellis, G.K., Bone, H.G., Chlebowski, R., Paul, D., Spadafora, S., Smith, J., Fan, M., and Jun, S. (2008). Randomized trial of denosumab in patients receiving adjuvant aromatase inhibitors for nonmetastatic breast cancer. J. Clin. Oncol. Off. J. Am. Soc. Clin. Oncol. *26*, 4875–4882.

Ellis, M.J., Ding, L., Shen, D., Luo, J., Suman, V.J., Wallis, J.W., Van Tine, B.A., Hoog, J., Goiffon, R.J., Goldstein, T.C., et al. (2012). Whole-genome analysis informs breast cancer response to aromatase inhibition. Nature *486*, 353–360.

ENCODE Project Consortium (2012). An integrated encyclopedia of DNA elements in the human genome. Nature *489*, 57–74.

Ergüner, B., Üstek, D., and Sağıroğlu, M.Ş. (2015). Performance comparison of Next Generation sequencing platforms. In 2015 37th Annual International Conference of the IEEE Engineering in Medicine and Biology Society (EMBC), pp. 6453–6456.

Eroles, P., Bosch, A., Pérez-Fidalgo, J.A., and Lluch, A. (2012). Molecular biology in breast cancer: intrinsic subtypes and signaling pathways. Cancer Treat. Rev. *38*, 698–707.

Esposito, A., Bardelli, A., Criscitiello, C., Colombo, N., Gelao, L., Fumagalli, L., Minchella, I., Locatelli, M., Goldhirsch, A., and Curigliano, G. (2014). Monitoring tumor-derived cell-free DNA in patients with solid tumors: clinical perspectives and research opportunities. Cancer Treat. Rev. *40*, 648–655.

Esteller, M. (2007). Cancer epigenomics: DNA methylomes and histone-modification maps. Nat. Rev. Genet. *8*, 286–298.

Esteller, M., and Almouzni, G. (2005). How epigenetics integrates nuclear functions. Workshop on epigenetics and chromatin: transcriptional regulation and beyond. EMBO Rep. *6*, 624–628.

Fan, M., Yan, P.S., Hartman-Frey, C., Chen, L., Paik, H., Oyer, S.L., Salisbury, J.D., Cheng, A.S.L., Li, L., Abbosh, P.H., et al. (2006). Diverse gene expression and DNA methylation profiles correlate with differential adaptation of breast cancer cells to the antiestrogens tamoxifen and fulvestrant. Cancer Res. *66*, 11954–11966.

Fang, Z., Yao, W., Xiong, Y., Zhang, J., Liu, L., Li, J., Zhang, C., and Wan, J. (2010). Functional elucidation and methylation-mediated downregulation of ITGA5 gene in breast cancer cell line MDA-MB-468. J. Cell. Biochem. *110*, 1130–1141.

Fata, J.E., Kong, Y.Y., Li, J., Sasaki, T., Irie-Sasaki, J., Moorehead, R.A., Elliott, R., Scully, S., Voura, E.B., Lacey, D.L., et al. (2000). The osteoclast differentiation factor osteoprotegerin-ligand is essential for mammary gland development. Cell *103*, 41–50.

Fiebig, H.H., Neumann, H.A., Henss, H., Koch, H., Kaiser, D., and Arnold, H. (1985). Development of three human small cell lung cancer models in nude mice. Recent Results Cancer Res. Fortschritte Krebsforsch. Progres Dans Rech. Sur Cancer *97*, 77–86.

Fillmore, C.M., and Kuperwasser, C. (2008). Human breast cancer cell lines contain stem-like cells that self-renew, give rise to phenotypically diverse progeny and survive chemotherapy. Breast Cancer Res. BCR *10*, R25.

Finn, R.S., Crown, J.P., Lang, I., Boer, K., Bondarenko, I.M., Kulyk, S.O., Ettl, J., Patel, R., Pinter, T., Schmidt, M., et al. (2015). The cyclin-dependent kinase 4/6 inhibitor palbociclib in combination with letrozole versus letrozole alone as first-line treatment of oestrogen receptor-positive, HER2-negative, advanced breast

cancer (PALOMA-1/TRIO-18): a randomised phase 2 study. Lancet Oncol. *16*, 25–35.

Fisher, B., Jeong, J.-H., Anderson, S., Bryant, J., Fisher, E.R., and Wolmark, N. (2002a). Twenty-five-year follow-up of a randomized trial comparing radical mastectomy, total mastectomy, and total mastectomy followed by irradiation. N. Engl. J. Med. *347*, 567–575.

Fisher, B., Anderson, S., Bryant, J., Margolese, R.G., Deutsch, M., Fisher, E.R., Jeong, J.-H., and Wolmark, N. (2002b). Twenty-year follow-up of a randomized trial comparing total mastectomy, lumpectomy, and lumpectomy plus irradiation for the treatment of invasive breast cancer. N. Engl. J. Med. *347*, 1233–1241.

Fitzmaurice, C., Allen, C., Barber, R.M., Barregard, L., Bhutta, Z.A., Brenner, H., Dicker, D.J., Chimed-Orchir, O., Dandona, R., Dandona, L., et al. (2017). Global, Regional, and National Cancer Incidence, Mortality, Years of Life Lost, Years Lived With Disability, and Disability-Adjusted Life-years for 32 Cancer Groups, 1990 to 2015: A Systematic Analysis for the Global Burden of Disease Study. JAMA Oncol. *3*, 524–548.

Flores, M.L., Castilla, C., Ávila, R., Ruiz-Borrego, M., Sáez, C., and Japón, M.A. (2012). Paclitaxel sensitivity of breast cancer cells requires efficient mitotic arrest and disruption of Bcl-xL/Bak interaction. Breast Cancer Res. Treat. *133*, 917–928.

Fontanella, C., Bolzonello, S., Lederer, B., and Aprile, G. (2014). Management of breast cancer patients with chemotherapy-induced neutropenia or febrile neutropenia. Breast Care Basel Switz. *9*, 239–245.

Forbes, S.A., Bindal, N., Bamford, S., Cole, C., Kok, C.Y., Beare, D., Jia, M., Shepherd, R., Leung, K., Menzies, A., et al. (2011). COSMIC: mining complete cancer genomes in the Catalogue of Somatic Mutations in Cancer. Nucleic Acids Res. *39*, D945-950.

Frank, N.Y., Schatton, T., and Frank, M.H. (2010). The therapeutic promise of the cancer stem cell concept. J. Clin. Invest. *120*, 41–50.

Friedrichs, K., Ruiz, P., Franke, F., Gille, I., Terpe, H.J., and Imhof, B.A. (1995). High expression level of alpha 6 integrin in human breast carcinoma is correlated with reduced survival. Cancer Res. *55*, 901–906.

Fujita, M., Ieguchi, K., Davari, P., Yamaji, S., Taniguchi, Y., Sekiguchi, K., Takada, Y.K., and Takada, Y. (2012). Cross-talk between integrin α6β4 and insulin-like growth factor-1 receptor (IGF1R) through direct α6β4 binding to IGF1 and subsequent α6β4-IGF1-IGF1R ternary complex formation in anchorage-independent conditions. J. Biol. Chem. *287*, 12491–12500.

Gangadhara, S., Barrett-Lee, P., Nicholson, R.I., and Hiscox, S. (2012). Pro-metastatic tumor-stroma interactions in breast cancer. Future Oncol. Lond. Engl. *8*, 1427–1442.

Ganta, S., and Amiji, M. (2009). Coadministration of Paclitaxel and curcumin in nanoemulsion formulations to overcome multidrug resistance in tumor cells. Mol. Pharm. *6*, 928–939.

Gascoigne, K.E., and Taylor, S.S. (2009). How do anti-mitotic drugs kill cancer cells? J. Cell Sci. *122*, 2579–2585.

Gastl, G., Spizzo, G., Obrist, P., Dünser, M., and Mikuz, G. (2000). Ep-CAM overexpression in breast cancer as a predictor of survival. Lancet Lond. Engl. *356*, 1981–1982.

Ge, L., Li, N., Liu, M., Xu, N.-Z., Wang, M.-R., and Wu, L.-Y. (2017). Copy number variations of neurotrophic tyrosine receptor kinase 3 (NTRK3) may predict prognosis of ovarian cancer. Medicine (Baltimore) *96*, e7621.

Geenen, J.J.J., Linn, S.C., Beijnen, J.H., and Schellens, J.H.M. (2017). PARP Inhibitors in the Treatment of Triple-Negative Breast Cancer. Clin. Pharmacokinet. 1–11.

Gelmon, K., Dent, R., Mackey, J.R., Laing, K., McLeod, D., and Verma, S. (2012). Targeting triple-negative breast cancer: optimising therapeutic outcomes. Ann. Oncol. *23*, 2223–2234.

Geng, S.-Q., Alexandrou, A.T., and Li, J.J. (2014). Breast cancer stem cells: Multiple capacities in tumor metastasis. Cancer Lett. *349*, 1–7.

Gerashchenko, T.S., Zavyalova, M.V., Denisov, E.V., Krakhmal, N.V., Pautova, D.N., Litviakov, N.V., Vtorushin, S.V., Cherdyntseva, N.V., and Perelmuter, V.M. (2017). Intratumoral Morphological Heterogeneity of Breast Cancer As an Indicator of the Metastatic Potential and Tumor Chemosensitivity. Acta Naturae *9*, 56–67.

Gewirtz, D.A. (1999). A critical evaluation of the mechanisms of action proposed for the antitumor effects of the anthracycline antibiotics adriamycin and daunorubicin. Biochem. Pharmacol. *57*, 727–741.

Geyer, C.E., Forster, J., Lindquist, D., Chan, S., Romieu, C.G., Pienkowski, T., Jagiello-Gruszfeld, A., Crown, J., Chan, A., Kaufman, B., et al. (2006). Lapatinib plus Capecitabine for HER2-Positive Advanced Breast Cancer. N. Engl. J. Med. *355*, 2733–2743.

Giancotti, F.G., and Ruoslahti, E. (1999). Integrin signaling. Science *285*, 1028–1032.

Gianni, L., Baselga, J., Eiermann, W., Porta, V.G., Semiglazov, V., Lluch, A., Zambetti, M., Sabadell, D., Raab, G., Cussac, A.L., et al. (2009). Phase III trial evaluating the addition of paclitaxel to doxorubicin followed by cyclophosphamide, methotrexate, and fluorouracil, as adjuvant or primary systemic therapy: European Cooperative Trial in Operable Breast Cancer. J. Clin. Oncol. Off. J. Am. Soc. Clin. Oncol. *27*, 2474–2481.

Gillet, J.-P., Calcagno, A.M., Varma, S., Marino, M., Green, L.J., Vora, M.I., Patel, C., Orina, J.N., Eliseeva, T.A., Singal, V., et al. (2011). Redefining the relevance of established cancer cell lines to the study of mechanisms of clinical anti-cancer drug resistance. Proc. Natl. Acad. Sci. *108*, 18708–18713.

Ginestier, C., Hur, M.H., Charafe-Jauffret, E., Monville, F., Dutcher, J., Brown, M., Jacquemier, J., Viens, P., Kleer, C.G., Liu, S., et al. (2007). ALDH1 is a marker of normal and malignant human mammary stem cells and a predictor of poor clinical outcome. Cell Stem Cell *1*, 555–567.

Girault, I., Tozlu, S., Lidereau, R., and Bièche, I. (2003). Expression analysis of DNA methyltransferases 1, 3A, and 3B in sporadic breast carcinomas. Clin. Cancer Res. Off. J. Am. Assoc. Cancer Res. *9*, 4415–4422.

Goel, H.L., Pursell, B., Chang, C., Shaw, L.M., Mao, J., Simin, K., Kumar, P., Vander Kooi, C.W., Shultz, L.D., Greiner, D.L., et al. (2013). GLI1 regulates a novel neuropilin-2/α6β1 integrin based autocrine pathway that contributes to breast cancer initiation. EMBO Mol. Med. *5*, 488–508.

Goetz, M.P., Kalari, K.R., Suman, V.J., Moyer, A.M., Yu, J., Visscher, D.W., Dockter, T.J., Vedell, P.T., Sinnwell, J.P., Tang, X., et al. (2017). Tumor Sequencing and Patient-Derived Xenografts in the Neoadjuvant Treatment of Breast Cancer. JNCI J. Natl. Cancer Inst. *109*.

Goldhirsch, A., Wood, W.C., Coates, A.S., Gelber, R.D., Thürlimann, B., and Senn, H.-J. (2011). Strategies for subtypes—dealing with the diversity of breast cancer: highlights of the St Gallen International Expert Consensus on the Primary Therapy of Early Breast Cancer 2011. Ann. Oncol. *22*, 1736–1747.

Gómez-Miragaya, J., Palafox, M., Paré, L., Yoldi, G., Ferrer, I., Vila, S., Galván, P., Pellegrini, P., Pérez-Montoyo, H., Igea, A., et al. (2017). Resistance to Taxanes in Triple-Negative Breast Cancer Associates with the Dynamics of a CD49f+ Tumor-Initiating Population. Stem Cell Rep. *8*, 1392–1407.

Gonzaga-Jauregui, C., Lupski, J.R., and Gibbs, R.A. (2012). Human genome sequencing in health and disease. Annu. Rev. Med. *63*, 35–61.

Gonzalez-Angulo, A.M., Morales-Vasquez, F., and Hortobagyi, G.N. (2007). Overview of resistance to systemic therapy in patients with breast cancer. Adv. Exp. Med. Biol. *608*, 1–22.

Gonzalez-Suarez, E., Jacob, A.P., Jones, J., Miller, R., Roudier-Meyer, M.P., Erwert, R., Pinkas, J., Branstetter, D., and Dougall, W.C. (2010). RANK ligand mediates progestin-induced mammary epithelial proliferation and carcinogenesis. Nature *468*, 103–107.

Götte, M., and Yip, G.W. (2006). Heparanase, hyaluronan, and CD44 in cancers: a breast carcinoma perspective. Cancer Res. *66*, 10233–10237.

Gottesman, M.M., Fojo, T., and Bates, S.E. (2002). Multidrug resistance in cancer: role of ATP–dependent transporters. Nat. Rev. Cancer *2*, 48–58.

Greaves, M., and Maley, C.C. (2012). CLONAL EVOLUTION IN CANCER. Nature *481*, 306–313.

Greve, B., Kelsch, R., Spaniol, K., Eich, H.T., and Götte, M. (2012). Flow cytometry in cancer stem cell analysis and separation. Cytom. Part J. Int. Soc. Anal. Cytol. *81*, 284–293.

Gucalp, A., Tolaney, S., Isakoff, S.J., Ingle, J.N., Liu, M.C., Carey, L.A., Blackwell, K., Rugo, H., Nabell, L., Forero, A., et al. (2013). Phase II trial of bicalutamide in patients with androgen receptor-positive, estrogen receptor-negative metastatic Breast Cancer. Clin. Cancer Res. Off. J. Am. Assoc. Cancer Res. *19*, 5505–5512.

Guilhamon, P., Butcher, L.M., Presneau, N., Wilson, G.A., Feber, A., Paul, D.S., Schütte, M., Haybaeck, J., Keilholz, U., Hoffman, J., et al. (2014). Assessment of patient-derived tumour xenografts (PDXs) as a discovery tool for cancer epigenomics. Genome Med. *6*, 116.

Günthert, U., Hofmann, M., Rudy, W., Reber, S., Zöller, M., Haussmann, I., Matzku, S., Wenzel, A., Ponta, H., and Herrlich, P. (1991). A new variant of glycoprotein CD44 confers metastatic potential to rat carcinoma cells. Cell *65*, 13–24.

Guo, Y., He, W., Yang, S., Zhao, D., Li, Z., and Luan, Y. (2017). Co-delivery of docetaxel and verapamil by reduction-sensitive PEG-PLGA-SS-DTX conjugate micelles to reverse the multi-drug resistance of breast cancer. Colloids Surf. B Biointerfaces *151*, 119–127.

Gupta, A., Godwin, A.K., Vanderveer, L., Lu, A., and Liu, J. (2003). Hypomethylation of the synuclein gamma gene CpG island promotes its aberrant expression in breast carcinoma and ovarian carcinoma. Cancer Res. *63*, 664–673.

Gupta, P.B., Fillmore, C.M., Jiang, G., Shapira, S.D., Tao, K., Kuperwasser, C., and Lander, E.S. (2011). Stochastic state transitions give rise to phenotypic equilibrium in populations of cancer cells. Cell *146*, 633–644.

Gurden, M.D., Westwood, I.M., Faisal, A., Naud, S., Cheung, K.-M.J., McAndrew, C., Wood, A., Schmitt, J., Boxall, K., Mak, G., et al. (2015). Naturally Occurring Mutations in the MPS1 Gene Predispose Cells to Kinase Inhibitor Drug Resistance. Cancer Res. *75*, 3340–3354.

Gusterson, B.A., Ross, D.T., Heath, V.J., and Stein, T. (2005). Basal cytokeratins and their relationship to the cellular origin and functional classification of breast cancer. Breast Cancer Res. BCR *7*, 143–148.

Guzmán-Ramírez, N., Völler, M., Wetterwald, A., Germann, M., Cross, N.A., Rentsch, C.A., Schalken, J., Thalmann, G.N., and Cecchini, M.G. (2009). In vitro propagation and characterization of neoplastic stem/progenitor-like cells from human prostate cancer tissue. The Prostate *69*, 1683–1693.

Hall, J.M., Lee, M.K., Newman, B., Morrow, J.E., Anderson, L.A., Huey, B., and King, M.C. (1990). Linkage of early-onset familial breast cancer to chromosome 17q21. Science *250*, 1684–1689.

Halsted, W.S. (1894). I. The Results of Operations for the Cure of Cancer of the Breast Performed at the Johns Hopkins Hospital from June, 1889, to January, 1894. Ann. Surg. *20*, 497–555.

Han, E.K., Kyu-Ho Han, E., Gehrke, L., Tahir, S.K., Credo, R.B., Cherian, S.P., Sham, H., Rosenberg, S.H., and Ng, S. (2000). Modulation of drug resistance by alpha-tubulin in paclitaxel-resistant human lung cancer cell lines. Eur. J. Cancer Oxf. Engl. 1990 *36*, 1565–1571.

Han, W., Jung, E.-M., Cho, J., Lee, J.W., Hwang, K.-T., Yang, S.-J., Kang, J.J., Bae, J.-Y., Jeon, Y.K., Park, I.-A., et al. (2008). DNA copy number alterations and expression of relevant genes in triple-negative breast cancer. Genes. Chromosomes Cancer *47*, 490–499.

Hanahan, D., and Weinberg, R.A. (2011). Hallmarks of cancer: the next generation. Cell *144*, 646–674.

Hannemann, J., Velds, A., Halfwerk, J.B.G., Kreike, B., Peterse, J.L., and van de Vijver, M.J. (2006). Classification of ductal carcinoma in situ by gene expression profiling. Breast Cancer Res. BCR *8*, R61.

Hausser, H.-J., and Brenner, R.E. (2005). Phenotypic instability of Saos-2 cells in long-term culture. Biochem. Biophys. Res. Commun. *333*, 216–222.

He, D.-X., Gu, F., Gao, F., Hao, J., Gong, D., Gu, X.-T., Mao, A.-Q., Jin, J., Fu, L., and Ma, X. (2016). Genome-wide profiles of methylation, microRNAs, and gene expression in chemoresistant breast cancer. Sci. Rep. *6*, srep24706.

He, K., Xu, T., and Goldkorn, A. (2011). Cancer cells cyclically lose and regain drug-resistant highly tumorigenic features characteristic of a cancer stem-like phenotype. Mol. Cancer Ther. *10*, 938–948.

He, L., Vasiliou, K., and Nebert, D.W. (2009). Analysis and update of the human solute carrier (SLC) gene superfamily. Hum. Genomics *3*, 195–206.

Hebbard, L., Steffen, A., Zawadzki, V., Fieber, C., Howells, N., Moll, J., Ponta, H., Hofmann, M., and Sleeman, J. (2000). CD44 expression and regulation during mammary gland development and function. J. Cell Sci. *113 (Pt 14)*, 2619–2630.

Hee Choi, Y., and Yu, A.-M. (2014). ABC Transporters in Multidrug Resistance and Pharmacokinetics, and Strategies for Drug Development. Curr. Pharm. Des. *20*, 793–807.

Hehlgans, S., Haase, M., and Cordes, N. (2007). Signalling via integrins: implications for cell survival and anticancer strategies. Biochim. Biophys. Acta *1775*, 163–180.

Heidary, M., Auer, M., Ulz, P., Heitzer, E., Petru, E., Gasch, C., Riethdorf, S., Mauermann, O., Lafer, I., Pristauz, G., et al. (2014). The dynamic range of circulating tumor DNA in metastatic breast cancer. Breast Cancer Res. BCR *16*, 421.

Heidenblad, M., Jonson, T., Mahlamäki, E.H., Gorunova, L., Karhu, R., Johansson, B., and Höglund, M. (2002). Detailed genomic mapping and expression analyses of 12p amplifications in pancreatic carcinomas reveal a 3.5-Mb target region for amplification. Genes. Chromosomes Cancer *34*, 211–223.

Hermann, P.C., Bhaskar, S., Cioffi, M., and Heeschen, C. (2010). Cancer stem cells in solid tumors. Semin. Cancer Biol. *20*, 77–84.

Hernandez-Vargas, H., Ouzounova, M., Le Calvez-Kelm, F., Lambert, M.-P., McKay-Chopin, S., Tavtigian, S.V., Puisieux, A., Matar, C., and Herceg, Z. (2011). Methylome analysis reveals Jak-STAT pathway deregulation in putative breast cancer stem cells. Epigenetics *6*, 428–439.

Herrera-Gayol, A., and Jothy, S. (1999). Adhesion proteins in the biology of breast cancer: contribution of CD44. Exp. Mol. Pathol. *66*, 149–156.

Hess, D.A., Meyerrose, T.E., Wirthlin, L., Craft, T.P., Herrbrich, P.E., Creer, M.H., and Nolta, J.A. (2004). Functional characterization of highly purified human hematopoietic repopulating cells isolated according to aldehyde dehydrogenase activity. Blood *104*, 1648–1655.

Hidalgo, M., Amant, F., Biankin, A.V., Budinská, E., Byrne, A.T., Caldas, C., Clarke, R.B., de Jong, S., Jonkers, J., Mælandsmo, G.M., et al. (2014). Patient-derived xenograft models: an emerging platform for translational cancer research. Cancer Discov. *4*, 998–1013.

Hing, B., Ramos, E., Braun, P., McKane, M., Jancic, D., Tamashiro, K.L.K., Lee, R.S., Michaelson, J.J., Druley, T.E., and Potash, J.B. (2015). Adaptation of the targeted capture Methyl-Seq platform for the mouse genome identifies novel tissue-specific DNA methylation patterns of genes involved in neurodevelopment. Epigenetics *10*, 581–596.

Hoadley, K.A., Yau, C., Wolf, D.M., Cherniack, A.D., Tamborero, D., Ng, S., Leiserson, M.D.M., Niu, B., McLellan, M.D., Uzunangelov, V., et al. (2014). Multiplatform analysis of 12 cancer types reveals molecular classification within and across tissues of origin. Cell *158*, 929–944.

Hoadley, K.A., Siegel, M.B., Kanchi, K.L., Miller, C.A., Ding, L., Zhao, W., He, X., Parker, J.S., Wendl, M.C., Fulton, R.S., et al. (2016). Tumor Evolution in Two Patients with Basal-like Breast Cancer: A Retrospective Genomics Study of Multiple Metastases. PLoS Med. *13*.

Hogervorst, F., Kuikman, I., van Kessel, A.G., and Sonnenberg, A. (1991). Molecular cloning of the human alpha 6 integrin subunit. Alternative splicing of alpha 6 mRNA and chromosomal localization of the alpha 6 and beta 4 genes. Eur. J. Biochem. *199*, 425–433.

Hoshino, A., Costa-Silva, B., Shen, T.-L., Rodrigues, G., Hashimoto, A., Tesic Mark, M., Molina, H., Kohsaka, S., Di Giannatale, A., Ceder, S., et al. (2015). Tumour exosome integrins determine organotropic metastasis. Nature *527*, 329–335.

Houghton, J.A., Houghton, P.J., and Green, A.A. (1982). Chemotherapy of Childhood Rhabdomyosarcomas Growing as Xenografts in Immune-deprived Mice. Cancer Res. *42*, 535–539.

Hsia, T.-C., Tu, C.-Y., Chen, Y.-J., Wei, Y.-L., Yu, M.-C., Hsu, S.-C., Tsai, S.-L., Chen, W.-S., Yeh, M.-H., Yen, C.-J., et al. (2013). Lapatinib-mediated cyclooxygenase-2 expression via epidermal growth factor receptor/HuR interaction enhances the aggressiveness of triple-negative breast cancer cells. Mol. Pharmacol. *83*, 857–869.

Hu, T., Zhou, R., Zhao, Y., and Wu, G. (2016). Integrin α6/Akt/Erk signaling is essential for human breast cancer resistance to radiotherapy. Sci. Rep. *6*, srep33376.

Hu, X., Stern, H.M., Ge, L., O'Brien, C., Haydu, L., Honchell, C.D., Haverty, P.M., Peters, B.A., Wu, T.D., Amler, L.C., et al. (2009). Genetic Alterations and Oncogenic Pathways Associated with Breast Cancer Subtypes. Mol. Cancer Res. *7*, 511–522.

Hu, Z., Fan, C., Oh, D.S., Marron, J.S., He, X., Qaqish, B.F., Livasy, C., Carey, L.A., Reynolds, E., Dressler, L., et al. (2006). The molecular portraits of breast tumors are conserved across microarray platforms. BMC Genomics *7*, 96.

Huang, H.-C., Shi, J., Orth, J.D., and Mitchison, T.J. (2009). Evidence that mitotic exit is a better cancer therapeutic target than spindle assembly. Cancer Cell *16*, 347–358.

Huang, Y., Ibrado, A.M., Reed, J.C., Bullock, G., Ray, S., Tang, C., and Bhalla, K. (1997). Co-expression of several molecular mechanisms of multidrug resistance and their significance for paclitaxel cytotoxicity in human AML HL-60 cells. Leukemia *11*, 253–257.

Ieguchi, K., Fujita, M., Ma, Z., Davari, P., Taniguchi, Y., Sekiguchi, K., Wang, B., Takada, Y.K., and Takada, Y. (2010). Direct binding of the EGF-like domain of neuregulin-1 to integrins ({alpha}v{beta}3 and {alpha}6{beta}4) is involved in neuregulin-1/ErbB signaling. J. Biol. Chem. *285*, 31388–31398.

Ingham, S.L., Warwick, J., Byers, H., Lalloo, F., Newman, W.G., and Evans, D.G.R. (2013). Is multiple SNP testing in BRCA2 and BRCA1 female carriers ready for use in clinical practice? Results from a large Genetic Centre in the UK. Clin. Genet. *84*, 37–42.

Iorns, E., Turner, N.C., Elliott, R., Syed, N., Garrone, O., Gasco, M., Tutt, A.N.J., Crook, T., Lord, C.J., and Ashworth, A. (2008). Identification of CDK10 as an important determinant of resistance to endocrine therapy for breast cancer. Cancer Cell *13*, 91–104.

Iqbal, J., Chong, P.Y., and Tan, P.H. (2013). Breast cancer stem cells: an update. J. Clin. Pathol. *66*, 485–490.

Ishikawa, F., Yasukawa, M., Lyons, B., Yoshida, S., Miyamoto, T., Yoshimoto, G., Watanabe, T., Akashi, K., Shultz, L.D., and Harada, M. (2005). Development of functional human blood and immune systems in NOD/SCID/IL2 receptor {gamma} chain(null) mice. Blood *106*, 1565–1573.

Jamdade, V.S., Sethi, N., Mundhe, N.A., Kumar, P., Lahkar, M., and Sinha, N. (2015). Therapeutic targets of triple-negative breast cancer: a review. Br. J. Pharmacol. *172*, 4228–4237.

Janiszewska, M., and Polyak, K. (2015). Clonal evolution in cancer: a tale of twisted twines. Cell Stem Cell *16*, 11–12.

Jia, Y., Chen, L., Jia, Q., Dou, X., Xu, N., and Liao, D.J. (2016). The well-accepted notion that gene amplification contributes to increased expression still remains, after all these years, a reasonable but unproven assumption. J. Carcinog. *15*.

Jiang, X., and Shapiro, D.J. (2014). The immune system and inflammation in breast cancer. Mol. Cell. Endocrinol. *382*, 673–682.

Jiao, F., Bai, S.-Y., Ma, Y., Yan, Z.-H., Yue, Z., Yu, Y., Wang, X., and Wang, J. (2014). DNA methylation of heparanase promoter influences its expression and associated with the progression of human breast cancer. PloS One *9*, e92190.

Jiménez-Valerio, G., Martínez-Lozano, M., Bassani, N., Vidal, A., Ochoa-de-Olza, M., Suárez, C., García-Del-Muro, X., Carles, J., Viñals, F., Graupera, M., et al. (2016). Resistance to Antiangiogenic Therapies by Metabolic Symbiosis in Renal Cell Carcinoma PDX Models and Patients. Cell Rep. *15*, 1134–1143.

Jin, Z., Tamura, G., Tsuchiya, T., Sakata, K., Kashiwaba, M., Osakabe, M., and Motoyama, T. (2001). Adenomatous polyposis coli (APC) gene promoter hypermethylation in primary breast cancers. Br. J. Cancer *85*, 69–73.

Johnson, J., Ascierto, M.L., Mittal, S., Newsome, D., Kang, L., Briggs, M., Tanner, K., Marincola, F.M., Berens, M.E., Vande Woude, G.F., et al. (2015). Genomic profiling of a Hepatocyte growth factor-dependent signature for MET-targeted therapy in glioblastoma. J. Transl. Med. *13*, 306.

Johnson, J.I., Decker, S., Zaharevitz, D., Rubinstein, L.V., Venditti, J.M., Schepartz, S., Kalyandrug, S., Christian, M., Arbuck, S., Hollingshead, M., et al. (2001). Relationships between drug activity in NCI preclinical in vitro and in vivo models and early clinical trials. Br. J. Cancer *84*, 1424–1431.

Jones, K.L., and Buzdar, A.U. (2004). A review of adjuvant hormonal therapy in breast cancer. Endocr. Relat. Cancer *11*, 391–406.

Jones, P.A., and Baylin, S.B. (2002). The fundamental role of epigenetic events in cancer. Nat. Rev. Genet. *3*, 415–428.

Jones, P.A., and Baylin, S.B. (2007). The epigenomics of cancer. Cell *128*, 683–692.

Joshi, P.A., Jackson, H.W., Beristain, A.G., Di Grappa, M.A., Mote, P.A., Clarke, C.L., Stingl, J., Waterhouse, P.D., and Khokha, R. (2010). Progesterone induces adult mammary stem cell expansion. Nature *465*, 803–807.

Joyce, H., McCann, A., Clynes, M., and Larkin, A. (2015). Influence of multidrug resistance and drug transport proteins on chemotherapy drug metabolism. Expert Opin. Drug Metab. Toxicol. *11*, 795–809.

Juric, D., Castel, P., Griffith, M., Griffith, O.L., Won, H.H., Ellis, H., Ebbesen, S.H., Ainscough, B.J., Ramu, A., Iyer, G., et al. (2015). Convergent loss of PTEN leads to clinical resistance to a PI(3)Kα inhibitor. Nature *518*, 240–244.

Kadalayil, L., Rafiq, S., Rose-Zerilli, M.J.J., Pengelly, R.J., Parker, H., Oscier, D., Strefford, J.C., Tapper, W.J., Gibson, J., Ennis, S., et al. (2015). Exome sequence read depth methods for identifying copy number changes. Brief. Bioinform. *16*, 380–392.

Kandoth, C., McLellan, M.D., Vandin, F., Ye, K., Niu, B., Lu, C., Xie, M., Zhang, Q., McMichael, J.F., Wyczalkowski, M.A., et al. (2013). Mutational landscape and significance across 12 major cancer types. Nature *502*, 333–339.

Karamboulas, C., and Ailles, L. (2013). Developmental signaling pathways in cancer stem cells of solid tumors. Biochim. Biophys. Acta *1830*, 2481–2495.

Karsli-Ceppioglu, S., Dagdemir, A., Judes, G., Ngollo, M., Penault-Llorca, F., Pajon, A., Bignon, Y.-J., and Bernard-Gallon, D. (2014). Epigenetic mechanisms of breast cancer: an update of the current knowledge. Epigenomics *6*, 651–664.

Karsten, U., and Goletz, S. (2013). What makes cancer stem cell markers different? SpringerPlus *2*, 301.

Karthikeyan, S., and Hoti, S.L. (2015). Development of Fourth Generation ABC Inhibitors from Natural Products: A Novel Approach to Overcome Cancer Multidrug Resistance. Anticancer Agents Med. Chem. *15*, 605–615.

Kass, E.M., Moynahan, M.E., and Jasin, M. (2016). When Genome Maintenance Goes Badly Awry. Mol. Cell *62*, 777–787.

Kearns, A.E., Khosla, S., and Kostenuik, P.J. (2008). Receptor Activator of Nuclear Factor κB Ligand and Osteoprotegerin Regulation of Bone Remodeling in Health and Disease. Endocr. Rev. *29*, 155–192.

Keller, P.J., Arendt, L.M., Skibinski, A., Logvinenko, T., Klebba, I., Dong, S., Smith, A.E., Prat, A., Perou, C.M., Gilmore, H., et al. (2012). Defining the cellular precursors to human breast cancer. Proc. Natl. Acad. Sci. U. S. A. *109*, 2772–2777.

Kernek, K.M., Brunelli, M., Ulbright, T.M., Eble, J.N., Martignoni, G., Zhang, S., Michael, H., Cummings, O.W., and Cheng, L. (2004). Fluorescence in situ hybridization analysis of chromosome 12p in paraffin-embedded tissue is useful for establishing germ cell origin of metastatic tumors. Mod. Pathol. Off. J. U. S. Can. Acad. Pathol. Inc *17*, 1309–1313.

Kim, H.I., Huang, H., Cheepala, S., Huang, S., and Chung, J. (2008). Curcumin inhibition of integrin (alpha6beta4)-dependent breast cancer cell motility and invasion. Cancer Prev. Res. Phila. Pa *1*, 385–391.

Klajic, J., Busato, F., Edvardsen, H., Touleimat, N., Fleischer, T., Bukholm, I., Børresen-Dale, A.-L., Lønning, P.E., Tost, J., and Kristensen, V.N. (2014). DNA Methylation Status of Key Cell-Cycle Regulators Such as CDKNA2/p16 and CCNA1 Correlates with Treatment Response to Doxorubicin and 5-Fluorouracil in Locally Advanced Breast Tumors. Clin. Cancer Res. *20*, 6357–6366.

Klinge, C.M. (2001). Estrogen receptor interaction with estrogen response elements. Nucleic Acids Res. *29*, 2905–2919.

Klonisch, T., Wiechec, E., Hombach-Klonisch, S., Ande, S.R., Wesselborg, S., Schulze-Osthoff, K., and Los, M. (2008). Cancer stem cell markers in common cancers - therapeutic implications. Trends Mol. Med. *14*, 450–460.

Kloosterman, W.P., Tavakoli-Yaraki, M., van Roosmalen, M.J., van Binsbergen, E., Renkens, I., Duran, K., Ballarati, L., Vergult, S., Giardino, D., Hansson, K., et al. (2012). Constitutional chromothripsis rearrangements involve clustered double-stranded DNA breaks and nonhomologous repair mechanisms. Cell Rep. *1*, 648–655.

Kolesnick, R., Altieri, D., and Fuks, Z. (2007). A CERTain role for ceramide in taxane-induced cell death. Cancer Cell *11*, 473–475.

Kreike, B., van Kouwenhove, M., Horlings, H., Weigelt, B., Peterse, H., Bartelink, H., and van de Vijver, M.J. (2007). Gene expression profiling and histopathological characterization of triple-negative/basal-like breast carcinomas. Breast Cancer Res. BCR *9*, R65.

Kreso, A., and Dick, J.E. (2014). Evolution of the cancer stem cell model. Cell Stem Cell *14*, 275–291.

Krøigård, A.B., Larsen, M.J., Lænkholm, A.-V., Knoop, A.S., Jensen, J.D., Bak, M., Mollenhauer, J., Kruse, T.A., and Thomassen, M. (2015). Clonal expansion and linear genome evolution through breast cancer progression from pre-invasive stages to asynchronous metastasis. Oncotarget *6*, 5634–5649.

Kruh, G.D., and Belinsky, M.G. (2003). The MRP family of drug efflux pumps. Oncogene *22*, 7537–7552.

Kuczynski, E.A., Sargent, D.J., Grothey, A., and Kerbel, R.S. (2013). Drug rechallenge and treatment beyond progression—implications for drug resistance. Nat. Rev. Clin. Oncol. *10*, 571–587.

Kwong, D., Lam, A., Guan, X., Law, S., Tai, A., Wong, J., and Sham, J. (2004). Chromosomal aberrations in esophageal squamous cell carcinoma among Chinese: gain of 12p predicts poor prognosis after surgery. Hum. Pathol. *35*, 309–316.

Lacroix, M., and Leclercq, G. (2004). Relevance of breast cancer cell lines as models for breast tumours: an update. Breast Cancer Res. Treat. *83*, 249–289.

Lathia, J.D. (2013). Cancer stem cells: moving past the controversy. CNS Oncol. *2*, 465–467.

Lathia, J.D., Gallagher, J., Heddleston, J.M., Wang, J., Eyler, C.E., Macswords, J., Wu, Q., Vasanji, A., McLendon, R.E., Hjelmeland, A.B., et al. (2010). Integrin alpha 6 regulates glioblastoma stem cells. Cell Stem Cell *6*, 421–432.

Lee, J.M., Dedhar, S., Kalluri, R., and Thompson, E.W. (2006). The epithelial-mesenchymal transition: new insights in signaling, development, and disease. J. Cell Biol. *172*, 973–981.

Lee, K.J., Lee, K.H., Yoon, K.-A., Sohn, J.Y., Lee, E., Lee, H., Eom, H.-S., and Kong, S.-Y. (2017). Chromothripsis in Treatment Resistance in Multiple Myeloma. Genomics Inform. *15*, 87–97.

Lee, L.J., Alexander, B., Schnitt, S.J., Comander, A., Gallagher, B., Garber, J.E., and Tung, N. (2011). Clinical outcome of triple negative breast cancer in BRCA1 mutation carriers and noncarriers. Cancer *117*, 3093–3100.

Lee, Y.K., Jin, S., Duan, S., Lim, Y.C., Ng, D.P., Lin, X.M., Yeo, G.S., and Ding, C. (2014). Improved reduced representation bisulfite sequencing for epigenomic profiling of clinical samples. Biol. Proced. Online *16*, 1.

Lehmann, B.D., Bauer, J.A., Chen, X., Sanders, M.E., Chakravarthy, A.B., Shyr, Y., and Pietenpol, J.A. (2011). Identification of human triple-negative breast cancer subtypes and preclinical models for selection of targeted therapies. J. Clin. Invest. *121*, 2750–2767.

Leis, O., Eguiara, A., Lopez-Arribillaga, E., Alberdi, M.J., Hernandez-Garcia, S., Elorriaga, K., Pandiella, A., Rezola, R., and Martin, A.G. (2012). Sox2 expression in breast tumours and activation in breast cancer stem cells. Oncogene *31*, 1354–1365.

Li, C., Heidt, D.G., Dalerba, P., Burant, C.F., Zhang, L., Adsay, V., Wicha, M., Clarke, M.F., and Simeone, D.M. (2007). Identification of pancreatic cancer stem cells. Cancer Res. *67*, 1030–1037.

Li, C.I., Daling, J.R., Tang, M.-T.C., Haugen, K.L., Porter, P.L., and Malone, K.E. (2013a). Use of antihypertensive medications and breast cancer risk among women aged 55 to 74 years. JAMA Intern. Med. *173*, 1629–1637.

Li, S., Shen, D., Shao, J., Crowder, R., Liu, W., Prat, A., He, X., Liu, S., Hoog, J., Lu, C., et al. (2013b). Endocrine-Therapy-Resistant ESR1 Variants Revealed by Genomic Characterization of Breast-Cancer-Derived Xenografts. Cell Rep. *4*, 1116–1130.

Li, X., Lewis, M.T., Huang, J., Gutierrez, C., Osborne, C.K., Wu, M.-F., Hilsenbeck, S.G., Pavlick, A., Zhang, X., Chamness, G.C., et al. (2008). Intrinsic resistance of tumorigenic breast cancer cells to chemotherapy. J. Natl. Cancer Inst. *100*, 672–679.

Li, X., Zhao, H., Gu, J., and Zheng, L. (2015). Prognostic value of cancer stem cell marker CD133 expression in pancreatic ductal adenocarcinoma (PDAC): a systematic review and meta-analysis. Int. J. Clin. Exp. Pathol. *8*, 12084–12092.

Liedtke, C., Wang, J., Tordai, A., Symmans, W.F., Hortobagyi, G.N., Kiesel, L., Hess, K., Baggerly, K.A., Coombes, K.R., and Pusztai, L. (2010). Clinical evaluation of chemotherapy response predictors developed from breast cancer cell lines. Breast Cancer Res. Treat. *121*, 301–309.

Lim, E., Vaillant, F., Wu, D., Forrest, N.C., Pal, B., Hart, A.H., Asselin-Labat, M.-L., Gyorki, D.E., Ward, T., Partanen, A., et al. (2009). Aberrant luminal progenitors as the candidate target population for basal tumor development in BRCA1 mutation carriers. Nat. Med. *15*, 907–913.

Lin, A.M., Ryan, C.J., and Small, E.J. (2007). Intermittent chemotherapy for metastatic hormone refractory prostate cancer. Crit. Rev. Oncol. Hematol. *61*, 243–254.

Lin, X., Li, J., Yin, G., Zhao, Q., Elias, D., Lykkesfeldt, A.E., Stenvang, J., Brünner, N., Wang, J., Yang, H., et al. (2013). Integrative analyses of gene expression and DNA methylation profiles in breast cancer cell line models of tamoxifen-resistance indicate a potential role of cells with stem-like properties. Breast Cancer Res. BCR *15*, R119.

Lindholm, E.M., Krohn, M., Iadevaia, S., Kristian, A., Mills, G.B., Mælandsmo, G.M., and Engebraaten, O. (2014). Proteomic characterization of breast cancer xenografts identifies early and late bevacizumab-induced responses and predicts effective drug combinations. Clin. Cancer Res. Off. J. Am. Assoc. Cancer Res. *20*, 404–412.

Ling, V. (1992). Charles F. Kettering Prize. P-glycoprotein and resistance to anticancer drugs. Cancer *69*, 2603–2609.

Litvinov, S.V., Velders, M.P., Bakker, H.A., Fleuren, G.J., and Warnaar, S.O. (1994). Ep-CAM: a human epithelial antigen is a homophilic cell-cell adhesion molecule. J. Cell Biol. *125*, 437–446.

Litvinov, S.V., van Driel, W., van Rhijn, C.M., Bakker, H.A., van Krieken, H., Fleuren, G.J., and Warnaar, S.O. (1996). Expression of Ep-CAM in cervical squamous epithelia correlates with an increased proliferation and the disappearance of markers for terminal differentiation. Am. J. Pathol. *148*, 865–875.

Liu, C., Lu, Y., Wang, B., Zhang, Y., Zhang, R., Lu, Y., Chen, B., Xu, H., Jin, F., and Lu, P. (2011a). Clinical implications of stem cell gene Oct-4 expression in breast cancer. Ann. Surg. *253*, 1165–1171.

Liu, G., Liu, Y.-J., Lian, W.-J., Zhao, Z.-W., Yi, T., and Zhou, H.-Y. (2014). Reduced BMP6 expression by DNA methylation contributes to EMT and drug resistance in breast cancer cells. Oncol. Rep. *32*, 581–588.

Liu, H., Patel, M.R., Prescher, J.A., Patsialou, A., Qian, D., Lin, J., Wen, S., Chang, Y.-F., Bachmann, M.H., Shimono, Y., et al. (2010). Cancer stem cells from human breast tumors are involved in spontaneous metastases in orthotopic mouse models. Proc. Natl. Acad. Sci. U. S. A. *107*, 18115–18120.

Liu, J., Sun, X., Qin, S., Wang, H., Du, N., Li, Y., Pang, Y., Wang, C., Xu, C., and Ren, H. (2016). CDH1 promoter methylation correlates with decreased gene expression and poor prognosis in patients with breast cancer. Oncol. Lett. *11*, 2635–2643.

Liu, L.-L., Fu, D., Ma, Y., and Shen, X.-Z. (2011b). The power and the promise of liver cancer stem cell markers. Stem Cells Dev. *20*, 2023–2030.

Liu, T.J., Sun, B.C., Zhao, X.L., Zhao, X.M., Sun, T., Gu, Q., Yao, Z., Dong, X.Y., Zhao, N., and Liu, N. (2013). CD133+ cells with cancer stem cell characteristics associates with vasculogenic mimicry in triple-negative breast cancer. Oncogene *32*, 544–553.

Liu, W., Xu, D., Yang, H., Xu, H., Shi, Z., Cao, X., Takeshita, S., Liu, J., Teale, M., and Feng, X. (2004). Functional identification of three receptor activator of NF-kappa B cytoplasmic motifs mediating osteoclast differentiation and function. J. Biol. Chem. *279*, 54759–54769.

Lo, K.-W., Chung, G.T.-Y., and To, K.-F. (2012). Deciphering the molecular genetic basis of NPC through molecular, cytogenetic, and epigenetic approaches. Semin. Cancer Biol. *22*, 79–86.

Lønning, P.E. (2012). Poor-prognosis estrogen receptor- positive disease: present and future clinical solutions. Ther. Adv. Med. Oncol. *4*, 127–137.

López-Maury, L., Marguerat, S., and Bähler, J. (2008). Tuning gene expression to changing environments: from rapid responses to evolutionary adaptation. Nat. Rev. Genet. *9*, 583–593.

Lourenço, N., Hélias-Rodzewicz, Z., Bachet, J.-B., Brahimi-Adouane, S., Jardin, F., Tran van Nhieu, J., Peschaud, F., Martin, E., Beauchet, A., Chibon, F., et al. (2014). Copy-neutral loss of heterozygosity and chromosome gains and losses are frequent in gastrointestinal stromal tumors. Mol. Cancer *13*, 246.

Ma, I., and Allan, A.L. (2011). The role of human aldehyde dehydrogenase in normal and cancer stem cells. Stem Cell Rev. *7*, 292–306.

Ma, C.X., Cai, S., Li, S., Ryan, C.E., Guo, Z., Schaiff, W.T., Lin, L., Hoog, J., Goiffon, R.J., Prat, A., et al. (2012). Targeting Chk1 in p53-deficient triple-negative breast cancer is therapeutically beneficial in human-in-mouse tumor models. J. Clin. Invest. *122*, 1541–1552.

Mabuchi, S., Ohmichi, M., Nishio, Y., Hayasaka, T., Kimura, A., Ohta, T., Kawagoe, J., Takahashi, K., Yada-Hashimoto, N., Seino-Noda, H., et al. (2004). Inhibition of inhibitor of nuclear factor-kappaB phosphorylation increases the efficacy of paclitaxel in in vitro and in vivo ovarian cancer models. Clin. Cancer Res. Off. J. Am. Assoc. Cancer Res. *10*, 7645–7654.

Madan, R.A., Pal, S.K., Sartor, O., and Dahut, W.L. (2011). Overcoming Chemotherapy Resistance in Prostate Cancer. Clin. Cancer Res. *17*, 3892–3902.

Maetzel, D., Denzel, S., Mack, B., Canis, M., Went, P., Benk, M., Kieu, C., Papior, P., Baeuerle, P.A., Munz, M., et al. (2009). Nuclear signalling by tumour-associated antigen EpCAM. Nat. Cell Biol. *11*, 162–171.

Magdalena, J., and Goval, J.-J. (2009). Methyl DNA immunoprecipitation. Methods Mol. Biol. Clifton NJ *567*, 237–247.

Magee, J.A., Piskounova, E., and Morrison, S.J. (2012). Cancer stem cells: impact, heterogeneity, and uncertainty. Cancer Cell *21*, 283–296.

Maitra, A., Arking, D.E., Shivapurkar, N., Ikeda, M., Stastny, V., Kassauei, K., Sui, G., Cutler, D.J., Liu, Y., Brimble, S.N., et al. (2005). Genomic alterations in cultured human embryonic stem cells. Nat. Genet. *37*, 1099–1103.

Malhotra, G.K., Zhao, X., Band, H., and Band, V. (2010). Histological, molecular and functional subtypes of breast cancers. Cancer Biol. Ther. *10*, 955–960.

Mallard, B.W., and Tiralongo, J. (2017). Cancer stem cell marker glycosylation: Nature, function and significance. Glycoconj. J. *34*, 441–452.

du Manoir, S., Orsetti, B., Bras-Gonçalves, R., Nguyen, T.-T., Lasorsa, L., Boissière, F., Massemin, B., Colombo, P.-E., Bibeau, F., Jacot, W., et al. (2014). Breast tumor PDXs are genetically plastic and correspond to a subset of aggressive cancers prone to relapse. Mol. Oncol. *8*, 431–443.

Mao, Q., and Unadkat, J.D. (2015). Role of the breast cancer resistance protein (BCRP/ABCG2) in drug transport--an update. AAPS J. *17*, 65–82.

Marangoni, E., and Poupon, M.-F. (2014). Patient-derived tumour xenografts as models for breast cancer drug development. Curr. Opin. Oncol. *26*, 556–561.

Marangoni, E., Vincent-Salomon, A., Auger, N., Degeorges, A., Assayag, F., Cremoux, P. de, Plater, L. de, Guyader, C., Pinieux, G.D., Judde, J.-G., et al. (2007). A New Model of Patient Tumor-Derived Breast Cancer Xenografts for Preclinical Assays. Clin. Cancer Res. *13*, 3989–3998.

Marcoux, N., and Vuori, K. (2003). EGF receptor mediates adhesion-dependent activation of the Rac GTPase: a role for phosphatidylinositol 3-kinase and Vav2. Oncogene *22*, 6100–6106.

Mariotti, A., Kedeshian, P.A., Dans, M., Curatola, A.M., Gagnoux-Palacios, L., and Giancotti, F.G. (2001). EGF-R signaling through Fyn kinase disrupts the function of integrin α6β4 at hemidesmosomes: role in epithelial cell migration and carcinoma invasion. J Cell Biol *155*, 447–458.

Martinet, N., Michel, B.Y., Bertrand, P., and Benhida, R. (2012). Small molecules DNA methyltransferases inhibitors. MedChemComm *3*, 263–273.

Marusyk, A., and Polyak, K. (2010). Tumor heterogeneity: causes and consequences. Biochim. Biophys. Acta *1805*, 105–117.

Marusyk, A., Almendro, V., and Polyak, K. (2012). Intra-tumour heterogeneity: a looking glass for cancer? Nat. Rev. Cancer *12*, 323–334.

Masuda, H., Zhang, D., Bartholomeusz, C., Doihara, H., Hortobagyi, G.N., and Ueno, N.T. (2012). Role of epidermal growth factor receptor in breast cancer. Breast Cancer Res. Treat. *136*, 331–345.

Mateo, F., Arenas, E.J., Aguilar, H., Serra-Musach, J., de Garibay, G.R., Boni, J., Maicas, M., Du, S., Iorio, F., Herranz-Ors, C., et al. (2017). Stem cell-like transcriptional reprogramming mediates metastatic resistance to mTOR inhibition. Oncogene *36*, 2737–2749.

Matsen, C.B., and Neumayer, L.A. (2013). Breast cancer: a review for the general surgeon. JAMA Surg. *148*, 971–979.

McCarthy, A.M., and Armstrong, K. (2014). The Role of Testing for BRCA1 and BRCA2 Mutations in Cancer Prevention. JAMA Intern. Med. *174*, 1023–1024.

McGrogan, B.T., Gilmartin, B., Carney, D.N., and McCann, A. (2008). Taxanes, microtubules and chemoresistant breast cancer. Biochim. Biophys. Acta *1785*, 96–132.

Meacham, C.E., and Morrison, S.J. (2013). Tumour heterogeneity and cancer cell plasticity. Nature *501*, 328–337.

Melchor, L., and Benítez, J. (2013). The complex genetic landscape of familial breast cancer. Hum. Genet. *132*, 845–863.

Menghi, F., Inaki, K., Woo, X., Kumar, P.A., Grzeda, K.R., Malhotra, A., Yadav, V., Kim, H., Marquez, E.J., Ucar, D., et al. (2016). The tandem duplicator phenotype as a distinct genomic configuration in cancer. Proc. Natl. Acad. Sci. U. S. A. *113*, E2373-2382.

Mercurio, A.M., Bachelder, R.E., Chung, J., O'Connor, K.L., Rabinovitz, I., Shaw, L.M., and Tani, T. (2001). Integrin laminin receptors and breast carcinoma progression. J. Mammary Gland Biol. Neoplasia *6*, 299–309.

Merkel, D.E., Fuqua, S.A., and McGuire, W.L. (1989). P-glycoprotein in breast cancer. Cancer Treat. Res. *48*, 97–105.

Merlino, G., Miodini, P., Callari, M., D'Aiuto, F., Cappelletti, V., and Daidone, M.G. (2017). Prognostic and functional role of subtype-specific tumor–stroma interaction in breast cancer. Mol. Oncol. *11*, 1399–1412.

Metzger-Filho, O., Tutt, A., de Azambuja, E., Saini, K.S., Viale, G., Loi, S., Bradbury, I., Bliss, J.M., Azim, H.A., Ellis, P., et al. (2012). Dissecting the heterogeneity of triple-negative breast cancer. J. Clin. Oncol. Off. J. Am. Soc. Clin. Oncol. *30*, 1879–1887.

Meyer, M.J., Fleming, J.M., Lin, A.F., Hussnain, S.A., Ginsburg, E., and Vonderhaar, B.K. (2010). CD44posCD49fhiCD133/2hi defines xenograft-initiating cells in estrogen receptor-negative breast cancer. Cancer Res. *70*, 4624–4633.

Michailidou, K., Hall, P., Gonzalez-Neira, A., Ghoussaini, M., Dennis, J., Milne, R.L., Schmidt, M.K., Chang-Claude, J., Bojesen, S.E., Bolla, M.K., et al. (2013). Large-scale genotyping identifies 41 new loci associated with breast cancer risk. Nat. Genet. *45*, 353–361, 361e1-2.

Miller, K., Wang, M., Gralow, J., Dickler, M., Cobleigh, M., Perez, E.A., Shenkier, T., Cella, D., and Davidson, N.E. (2007). Paclitaxel plus bevacizumab versus paclitaxel alone for metastatic breast cancer. N. Engl. J. Med. *357*, 2666–2676.

Miller, W.R., Larionov, A., Anderson, T.J., Evans, D.B., and Dixon, J.M. (2012). Sequential changes in gene expression profiles in breast cancers during treatment with the aromatase inhibitor, letrozole. Pharmacogenomics J. *12*, 10–21.

Minotti, A.M., Barlow, S.B., and Cabral, F. (1991). Resistance to antimitotic drugs in Chinese hamster ovary cells correlates with changes in the level of polymerized tubulin. J. Biol. Chem. *266*, 3987–3994.

Miraglia, S., Godfrey, W., Yin, A.H., Atkins, K., Warnke, R., Holden, J.T., Bray, R.A., Waller, E.K., and Buck, D.W. (1997). A novel five-transmembrane hematopoietic stem cell antigen: isolation, characterization, and molecular cloning. Blood *90*, 5013–5021.

Mittal, K., Donthamsetty, S., Kaur, R., Yang, C., Gupta, M.V., Reid, M.D., Choi, D.H., Rida, P.C.G., and Aneja, R. (2017). Multinucleated polyploidy drives resistance to Docetaxel chemotherapy in prostate cancer. Br. J. Cancer *116*, 1186–1194.

Mizukami, J., Takaesu, G., Akatsuka, H., Sakurai, H., Ninomiya-Tsuji, J., Matsumoto, K., and Sakurai, N. (2002). Receptor activator of NF-kappaB ligand (RANKL) activates TAK1 mitogen-activated protein kinase kinase kinase through a signaling complex containing RANK, TAB2, and TRAF6. Mol. Cell. Biol. *22*, 992–1000.

Moarii, M., Boeva, V., Vert, J.-P., and Reyal, F. (2015). Changes in correlation between promoter methylation and gene expression in cancer. BMC Genomics *16*, 873.

Moelans, C.B., van der Groep, P., Hoefnagel, L.D.C., van de Vijver, M.J., Wesseling, P., Wesseling, J., van der Wall, E., and van Diest, P.J. (2014). Genomic evolution from primary breast carcinoma to distant metastasis: Few copy number changes of breast cancer related genes. Cancer Lett. *344*, 138–146.

Moreb, J.S., Mohuczy, D., Muhoczy, D., Ostmark, B., and Zucali, J.R. (2007). RNAi-mediated knockdown of aldehyde dehydrogenase class-1A1 and class-3A1 is

specific and reveals that each contributes equally to the resistance against 4-hydroperoxycyclophosphamide. Cancer Chemother. Pharmacol. *59*, 127–136.

Moro, L., Dolce, L., Cabodi, S., Bergatto, E., Erba, E.B., Smeriglio, M., Turco, E., Retta, S.F., Giuffrida, M.G., Venturino, M., et al. (2002). Integrin-induced Epidermal Growth Factor (EGF) Receptor Activation Requires c-Src and p130Cas and Leads to Phosphorylation of Specific EGF Receptor Tyrosines. J. Biol. Chem. *277*, 9405–9414.

Morris, P.G., and Fornier, M.N. (2008). Microtubule Active Agents: Beyond the Taxane Frontier. Clin. Cancer Res. *14*, 7167–7172.

Mostert, B., Kraan, J., Sieuwerts, A.M., van der Spoel, P., Bolt-de Vries, J., Prager-van der Smissen, W.J.C., Smid, M., Timmermans, A.M., Martens, J.W.M., Gratama, J.W., et al. (2012). CD49f-based selection of circulating tumor cells (CTCs) improves detection across breast cancer subtypes. Cancer Lett. *319*, 49–55.

Moynahan, M.E. (2002). The cancer connection: BRCA1 and BRCA2 tumor suppression in mice and humans. Oncogene *21*, 8994–9007.

Mozaffari, F., Lindemalm, C., Choudhury, A., Granstam-Björneklett, H., Helander, I., Lekander, M., Mikaelsson, E., Nilsson, B., Ojutkangas, M.-L., Osterborg, A., et al. (2007). NK-cell and T-cell functions in patients with breast cancer: effects of surgery and adjuvant chemo- and radiotherapy. Br. J. Cancer *97*, 105–111.

Mukhopadhyay, R., Theriault, R.L., and Price, J.E. (1999). Increased levels of alpha6 integrins are associated with the metastatic phenotype of human breast cancer cells. Clin. Exp. Metastasis *17*, 325–332.

Müller, H.M., Widschwendter, A., Fiegl, H., Ivarsson, L., Goebel, G., Perkmann, E., Marth, C., and Widschwendter, M. (2003). DNA methylation in serum of breast cancer patients: an independent prognostic marker. Cancer Res. *63*, 7641–7645.

Mulrane, L., McGee, S.F., Gallagher, W.M., and O'Connor, D.P. (2013). miRNA dysregulation in breast cancer. Cancer Res. *73*, 6554–6562.

Muluhngwi, P., and Klinge, C.M. (2015). Roles for miRNAs in endocrine resistance in breast cancer. Endocr. Relat. Cancer *22*, R279-300.

Munster, P.N., Thurn, K.T., Thomas, S., Raha, P., Lacevic, M., Miller, A., Melisko, M., Ismail-Khan, R., Rugo, H., Moasser, M., et al. (2011). A phase II study of the histone deacetylase inhibitor vorinostat combined with tamoxifen for the treatment of patients with hormone therapy-resistant breast cancer. Br. J. Cancer *104*, 1828–1835.

Murray, S., Briasoulis, E., Linardou, H., Bafaloukos, D., and Papadimitriou, C. (2012). Taxane resistance in breast cancer: Mechanisms, predictive biomarkers and circumvention strategies. Cancer Treat. Rev. *38*, 890–903.

Murtaza, M., Dawson, S.-J., Pogrebniak, K., Rueda, O.M., Provenzano, E., Grant, J., Chin, S.-F., Tsui, D.W.Y., Marass, F., Gale, D., et al. (2015). Multifocal clonal evolution characterized using circulating tumour DNA in a case of metastatic breast cancer. Nat. Commun. *6*, 8760.

Muss, H.B., Smith, L.R., and Cooper, M.R. (1987). Tamoxifen rechallenge: response to tamoxifen following relapse after adjuvant chemohormonal therapy for breast cancer. J. Clin. Oncol. Off. J. Am. Soc. Clin. Oncol. *5*, 1556–1558.

Nadal, R., Ortega, F.G., Salido, M., Lorente, J.A., Rodríguez-Rivera, M., Delgado-Rodríguez, M., Macià, M., Fernández, A., Corominas, J.M., García-Puche, J.L., et al. (2013). CD133 expression in circulating tumor cells from breast cancer patients: potential role in resistance to chemotherapy. Int. J. Cancer *133*, 2398–2407.

Natrajan, R., Lambros, M.B., Rodríguez-Pinilla, S.M., Moreno-Bueno, G., Tan, D.S.P., Marchió, C., Vatcheva, R., Rayter, S., Mahler-Araujo, B., Fulford, L.G., et al. (2009). Tiling Path Genomic Profiling of Grade 3 Invasive Ductal Breast Cancers. Clin. Cancer Res. *15*, 2711–2722.

Naundorf, H., Fichtner, I., Büttner, B., and Frege, J. (1992). Establishment and characterization of a new human oestradiol- and progesterone-receptor-positive mammary carcinoma serially transplantable in nude mice. J. Cancer Res. Clin. Oncol. *119*, 35–40.

Network, T.C.G.A. (2012). Comprehensive molecular portraits of human breast tumours. Nature *490*, 61–70.

Nguyen, L.V., Vanner, R., Dirks, P., and Eaves, C.J. (2012). Cancer stem cells: an evolving concept. Nat. Rev. Cancer *12*, 133–143.

Nguyen, L.V., Cox, C.L., Eirew, P., Knapp, D.J.H.F., Pellacani, D., Kannan, N., Carles, A., Moksa, M., Balani, S., Shah, S., et al. (2014). DNA barcoding reveals diverse growth kinetics of human breast tumour subclones in serially passaged xenografts. Nat. Commun. *5*, 5871.

Nielsen, T.O., Hsu, F.D., Jensen, K., Cheang, M., Karaca, G., Hu, Z., Hernandez-Boussard, T., Livasy, C., Cowan, D., Dressler, L., et al. (2004). Immunohistochemical and Clinical Characterization of the Basal-Like Subtype of Invasive Breast Carcinoma. Clin. Cancer Res. *10*, 5367–5374.

Nigam, S.K. (2015). What do drug transporters really do? Nat. Rev. Drug Discov. *14*, 29–44.

Nik-Zainal, S., Davies, H., Staaf, J., Ramakrishna, M., Glodzik, D., Zou, X., Martincorena, I., Alexandrov, L.B., Martin, S., Wedge, D.C., et al. (2016). Landscape of somatic mutations in 560 breast cancer whole-genome sequences. Nature *534*.

Nishizaki, T., DeVries, S., Chew, K., Goodson, W.H., Ljung, B.M., Thor, A., and Waldman, F.M. (1997). Genetic alterations in primary breast cancers and their metastases: direct comparison using modified comparative genomic hybridization. Genes. Chromosomes Cancer *19*, 267–272.

Noguchi, S. (2006). Predictive factors for response to docetaxel in human breast cancers. Cancer Sci. *97*, 813–820.

Nones, K., Waddell, N., Wayte, N., Patch, A.-M., Bailey, P., Newell, F., Holmes, O., Fink, J.L., Quinn, M.C.J., Tang, Y.H., et al. (2014). Genomic catastrophes frequently arise in esophageal adenocarcinoma and drive tumorigenesis. Nat. Commun. *5*, 5224.

Nugoli, M., Chuchana, P., Vendrell, J., Orsetti, B., Ursule, L., Nguyen, C., Birnbaum, D., Douzery, E.J., Cohen, P., and Theillet, C. (2003). Genetic variability in MCF-7 sublines: evidence of rapid genomic and RNA expression profile modifications. BMC Cancer *3*, 13.

Oakman, C., Viale, G., and Leo, A.D. (2010). Management of triple negative breast cancer. The Breast *19*, 312–321.

O'Brien, C.A., Pollett, A., Gallinger, S., and Dick, J.E. (2007). A human colon cancer cell capable of initiating tumour growth in immunodeficient mice. Nature *445*, 106–110.

Okamoto, I., Tsuiki, H., Kenyon, L.C., Godwin, A.K., Emlet, D.R., Holgado-Madruga, M., Lanham, I.S., Joynes, C.J., Vo, K.T., Guha, A., et al. (2002). Proteolytic cleavage of the CD44 adhesion molecule in multiple human tumors. Am. J. Pathol. *160*, 441–447.

Okano, H., Imai, T., and Okabe, M. (2002). Musashi: a translational regulator of cell fate. J. Cell Sci. *115*, 1355–1359.

Okano, M., Bell, D.W., Haber, D.A., and Li, E. (1999). DNA methyltransferases Dnmt3a and Dnmt3b are essential for de novo methylation and mammalian development. Cell *99*, 247–257.

Orth, J.D., Kohler, R.H., Foijer, F., Sorger, P.K., Weissleder, R., and Mitchison, T.J. (2011). Analysis of mitosis and antimitotic drug responses in tumors by in vivo microscopy and single-cell pharmacodynamics. Cancer Res. *71*, 4608–4616.

O'Shaughnessy, J., Osborne, C., Pippen, J.E., Yoffe, M., Patt, D., Rocha, C., Koo, I.C., Sherman, B.M., and Bradley, C. (2011). Iniparib plus chemotherapy in metastatic triple-negative breast cancer. N. Engl. J. Med. *364*, 205–214.

O'Shaughnessy, J., Schwartzberg, L., Danso, M.A., Miller, K.D., Rugo, H.S., Neubauer, M., Robert, N., Hellerstedt, B., Saleh, M., Richards, P., et al. (2014). Phase III study of iniparib plus gemcitabine and carboplatin versus gemcitabine and carboplatin in patients with metastatic triple-negative breast cancer. J. Clin. Oncol. Off. J. Am. Soc. Clin. Oncol. *32*, 3840–3847.

Osta, W.A., Chen, Y., Mikhitarian, K., Mitas, M., Salem, M., Hannun, Y.A., Cole, D.J., and Gillanders, W.E. (2004). EpCAM Is Overexpressed in Breast Cancer and Is a Potential Target for Breast Cancer Gene Therapy. Cancer Res. *64*, 5818–5824.

Ottaviano, Y.L., Issa, J.P., Parl, F.F., Smith, H.S., Baylin, S.B., and Davidson, N.E. (1994). Methylation of the estrogen receptor gene CpG island marks loss of estrogen receptor expression in human breast cancer cells. Cancer Res. *54*, 2552–2555.

Pàez-Ribes, M., Allen, E., Hudock, J., Takeda, T., Okuyama, H., Viñals, F., Inoue, M., Bergers, G., Hanahan, D., and Casanovas, O. (2009). Antiangiogenic therapy elicits malignant progression of tumors to increased local invasion and distant metastasis. Cancer Cell *15*, 220–231.

Pakneshan, P., Szyf, M., Farias-Eisner, R., and Rabbani, S.A. (2004). Reversal of the hypomethylation status of urokinase (uPA) promoter blocks breast cancer growth and metastasis. J. Biol. Chem. *279*, 31735–31744.

Palafox, M., Ferrer, I., Pellegrini, P., Vila, S., Hernandez-Ortega, S., Urruticoechea, A., Climent, F., Soler, M.T., Muñoz, P., Viñals, F., et al. (2012). RANK induces epithelial-mesenchymal transition and stemness in human mammary epithelial cells and promotes tumorigenesis and metastasis. Cancer Res. *72*, 2879–2888.

Park, H.S., Jang, M.H., Kim, E.J., Kim, H.J., Lee, H.J., Kim, Y.J., Kim, J.H., Kang, E., Kim, S.-W., Kim, I.A., et al. (2014). High EGFR gene copy number predicts poor outcome in triple-negative breast cancer. Mod. Pathol. Off. J. U. S. Can. Acad. Pathol. Inc *27*, 1212–1222.

Parker, J.S., Mullins, M., Cheang, M.C.U., Leung, S., Voduc, D., Vickery, T., Davies, S., Fauron, C., He, X., Hu, Z., et al. (2009). Supervised risk predictor of breast cancer based on intrinsic subtypes. J. Clin. Oncol. Off. J. Am. Soc. Clin. Oncol. *27*, 1160–1167.

Pattabiraman, D.R., and Weinberg, R.A. (2014). Tackling the cancer stem cells - what challenges do they pose? Nat. Rev. Drug Discov. *13*, 497–512.

PAWAR, S.C., DOUGHERTY, S., PENNINGTON, M.E., DEMETRIOU, M.C., STEA, B.D., DORR, R.T., and CRESS, A.E. (2007). α6 Integrin Cleavage: Sensitizing human prostate cancer to ionizing radiation. Int. J. Radiat. Biol. *83*, 761–767.

Pearce, D.J., Taussig, D., Simpson, C., Allen, K., Rohatiner, A.Z., Lister, T.A., and Bonnet, D. (2005). Characterization of cells with a high aldehyde dehydrogenase activity from cord blood and acute myeloid leukemia samples. Stem Cells Dayt. Ohio *23*, 752–760.

Pece, S., Tosoni, D., Confalonieri, S., Mazzarol, G., Vecchi, M., Ronzoni, S., Bernard, L., Viale, G., Pelicci, P.G., and Fiore, P.P.D. (2010). Biological and Molecular Heterogeneity of Breast Cancers Correlates with Their Cancer Stem Cell Content. Cell *140*, 62–73.

Peitzsch, C., Kurth, I., Kunz-Schughart, L., Baumann, M., and Dubrovska, A. (2013). Discovery of the cancer stem cell related determinants of radioresistance. Radiother. Oncol. J. Eur. Soc. Ther. Radiol. Oncol. *108*, 378–387.

Pellegrini, P., Pasquale, P., Cordero, A., Alex, C., Gallego, M.I., Marta Ines, G., Dougall, W.C., William, D.C., Muñoz, P., Purificación, M., et al. (2013). Constitutive activation of RANK disrupts mammary cell fate leading to tumorigenesis. Stem Cells Dayt. Ohio *31*, 1954–1965.

Peng, S., Lü, B., Ruan, W., Zhu, Y., Sheng, H., and Lai, M. (2011). Genetic polymorphisms and breast cancer risk: evidence from meta-analyses, pooled analyses, and genome-wide association studies. Breast Cancer Res. Treat. *127*, 309–324.

Pereira, B., Chin, S.-F., Rueda, O.M., Vollan, H.-K.M., Provenzano, E., Bardwell, H.A., Pugh, M., Jones, L., Russell, R., Sammut, S.-J., et al. (2016). The somatic mutation profiles of 2,433 breast cancers refines their genomic and transcriptomic landscapes. Nat. Commun. *7*.

Perou, C.M., Sørlie, T., Eisen, M.B., van de Rijn, M., Jeffrey, S.S., Rees, C.A., Pollack, J.R., Ross, D.T., Johnsen, H., Akslen, L.A., et al. (2000). Molecular portraits of human breast tumours. Nature *406*, 747–752.

Perrone, G., Gaeta, L.M., Zagami, M., Nasorri, F., Coppola, R., Borzomati, D., Bartolozzi, F., Altomare, V., Trodella, L., Tonini, G., et al. (2012). In situ identification of CD44+/CD24- cancer cells in primary human breast carcinomas. PloS One *7*, e43110.

Petrillo, L.A., Wolf, D.M., Kapoun, A.M., Wang, N.J., Barczak, A., Xiao, Y., Korkaya, H., Baehner, F., Lewicki, J., Wicha, M., et al. (2012). Xenografts faithfully recapitulate breast cancer-specific gene expression patterns of parent primary breast tumors. Breast Cancer Res. Treat. *135*.

Pfefferle, A.D., Spike, B.T., Wahl, G.M., and Perou, C.M. (2015). Luminal progenitor and fetal mammary stem cell expression features predict breast tumor response to neoadjuvant chemotherapy. Breast Cancer Res. Treat. *149*, 425–437.

Pfitzner, B.M., Branstetter, D., Loibl, S., Denkert, C., Lederer, B., Schmitt, W.D., Dombrowski, F., Werner, M., Rüdiger, T., Dougall, W.C., et al. (2014). RANK expression as a prognostic and predictive marker in breast cancer. Breast Cancer Res. Treat. *145*, 307–315.

Phan, N.N., Wang, C.-Y., Chen, C.-F., Sun, Z., Lai, M.-D., and Lin, Y.-C. (2017). Voltage-gated calcium channels: Novel targets for cancer therapy. Oncol. Lett. *14*, 2059–2074.

Pharoah, P.D.P., Antoniou, A., Bobrow, M., Zimmern, R.L., Easton, D.F., and Ponder, B.A.J. (2002). Polygenic susceptibility to breast cancer and implications for prevention. Nat. Genet. *31*, 33–36.

Phillips, T.M., McBride, W.H., and Pajonk, F. (2006). The response of CD24(-/low)/CD44+ breast cancer-initiating cells to radiation. J. Natl. Cancer Inst. *98*, 1777–1785.

Piekarz, R.L., Frye, R., Turner, M., Wright, J.J., Allen, S.L., Kirschbaum, M.H., Zain, J., Prince, H.M., Leonard, J.P., Geskin, L.J., et al. (2009). Phase II multi-institutional trial of the histone deacetylase inhibitor romidepsin as monotherapy for patients with cutaneous T-cell lymphoma. J. Clin. Oncol. Off. J. Am. Soc. Clin. Oncol. *27*, 5410–5417.

Pisani, P., Bray, F., and Parkin, D.M. (2002). Estimates of the world-wide prevalence of cancer for 25 sites in the adult population. Int. J. Cancer *97*, 72–81.

Poirier, J.T., Gardner, E.E., Connis, N., Moreira, A.L., de Stanchina, E., Hann, C.L., and Rudin, C.M. (2015). DNA methylation in small cell lung cancer defines distinct disease subtypes and correlates with high expression of EZH2. Oncogene *34*, 5869–5878.

Poklar, N., Pilch, D.S., Lippard, S.J., Redding, E.A., Dunham, S.U., and Breslauer, K.J. (1996). Influence of cisplatin intrastrand crosslinking on the conformation, thermal stability, and energetics of a 20-mer DNA duplex. Proc. Natl. Acad. Sci. U. S. A. *93*, 7606–7611.

Pollack, J.R., Sørlie, T., Perou, C.M., Rees, C.A., Jeffrey, S.S., Lonning, P.E., Tibshirani, R., Botstein, D., Børresen-Dale, A.-L., and Brown, P.O. (2002). Microarray analysis reveals a major direct role of DNA copy number alteration in the transcriptional program of human breast tumors. Proc. Natl. Acad. Sci. U. S. A. *99*, 12963–12968.

Polyak, K. (2007). Breast cancer: origins and evolution. J. Clin. Invest. *117*, 3155–3163.

Ponti, D., Costa, A., Zaffaroni, N., Pratesi, G., Petrangolini, G., Coradini, D., Pilotti, S., Pierotti, M.A., and Daidone, M.G. (2005). Isolation and in vitro propagation of tumorigenic breast cancer cells with stem/progenitor cell properties. Cancer Res. *65*, 5506–5511.

Poole, C.J., Earl, H.M., Hiller, L., Dunn, J.A., Bathers, S., Grieve, R.J., Spooner, D.A., Agrawal, R.K., Fernando, I.N., Brunt, A.M., et al. (2006). Epirubicin and cyclophosphamide, methotrexate, and fluorouracil as adjuvant therapy for early breast cancer. N. Engl. J. Med. *355*, 1851–1862.

Pouliot, M.-C., Labrie, Y., Diorio, C., and Durocher, F. (2015). The Role of Methylation in Breast Cancer Susceptibility and Treatment. Anticancer Res. *35*, 4569–4574.

Pourteimoor, V., Mohammadi-Yeganeh, S., and Paryan, M. (2016). Breast cancer classification and prognostication through diverse systems along with recent emerging findings in this respect; the dawn of new perspectives in the clinical applications. Tumour Biol. J. Int. Soc. Oncodevelopmental Biol. Med. *37*, 14479–14499.

Prat, A., and Perou, C.M. (2009). Mammary development meets cancer genomics. Nat. Med. *15*, 842–844.

Prat, A., and Perou, C.M. (2011). Deconstructing the molecular portraits of breast cancer. Mol. Oncol. *5*, 5–23.

Prat, A., Parker, J.S., Karginova, O., Fan, C., Livasy, C., Herschkowitz, J.I., He, X., and Perou, C.M. (2010). Phenotypic and molecular characterization of the claudin-low intrinsic subtype of breast cancer. Breast Cancer Res. BCR *12*, R68.

Prat, A., Adamo, B., Cheang, M.C.U., Anders, C.K., Carey, L.A., and Perou, C.M. (2013). Molecular characterization of basal-like and non-basal-like triple-negative breast cancer. The Oncologist *18*, 123–133.

Prat, A., Lluch, A., Albanell, J., Barry, W.T., Fan, C., Chacón, J.I., Parker, J.S., Calvo, L., Plazaola, A., Arcusa, A., et al. (2014). Predicting response and survival in chemotherapy-treated triple-negative breast cancer. Br. J. Cancer *111*, 1532–1541.

Prat, A., Pineda, E., Adamo, B., Galván, P., Fernández, A., Gaba, L., Díez, M., Viladot, M., Arance, A., and Muñoz, M. (2015). Clinical implications of the intrinsic molecular subtypes of breast cancer. Breast Edinb. Scotl. *24 Suppl 2*, S26-35.

Press, M.F., Finn, R.S., Cameron, D., Di Leo, A., Geyer, C.E., Villalobos, I.E., Santiago, A., Guzman, R., Gasparyan, A., Ma, Y., et al. (2008). HER-2 gene amplification, HER-2 and epidermal growth factor receptor mRNA and protein expression, and lapatinib efficacy in women with metastatic breast cancer. Clin. Cancer Res. Off. J. Am. Assoc. Cancer Res. *14*, 7861–7870.

Printz, C. (2017). Genomic sequencing of treatment-resistant metastatic breast cancer reveals key alterations. Cancer *123*, 904–904.

Qu, H., Li, R., Liu, Z., Zhang, J., and Luo, R. (2013). Prognostic value of cancer stem cell marker CD133 expression in non-small cell lung cancer: a systematic review. Int. J. Clin. Exp. Pathol. *6*, 2644–2650.

Quintana, E., Shackleton, M., Foster, H.R., Fullen, D.R., Sabel, M.S., Johnson, T.M., and Morrison, S.J. (2010). Phenotypic heterogeneity among tumorigenic melanoma cells from patients that is reversible and not hierarchically organized. Cancer Cell *18*, 510–523.

Rack, B., Schindlbeck, C., Jückstock, J., Andergassen, U., Hepp, P., Zwingers, T., Friedl, T.W.P., Lorenz, R., Tesch, H., Fasching, P.A., et al. (2014). Circulating tumor cells predict survival in early average-to-high risk breast cancer patients. J. Natl. Cancer Inst. *106*.

Rae-Venter, B., and Reid, L.M. (1980). Growth of Human Breast Carcinomas in Nude Mice and Subsequent Establishment in Tissue Culture. Cancer Res. *40*, 95–100.

Ramaswamy, B., Fiskus, W., Cohen, B., Pellegrino, C., Hershman, D.L., Chuang, E., Luu, T., Somlo, G., Goetz, M., Swaby, R., et al. (2012). Phase I-II study of vorinostat plus paclitaxel and bevacizumab in metastatic breast cancer: evidence for vorinostat-induced tubulin acetylation and Hsp90 inhibition in vivo. Breast Cancer Res. Treat. *132*, 1063–1072.

Ramos, P., and Bentires-Alj, M. (2015). Mechanism-based cancer therapy: resistance to therapy, therapy for resistance. Oncogene *34*, 3617–3626.

Rangaswami, H., Bulbule, A., and Kundu, G.C. (2006). Osteopontin: role in cell signaling and cancer progression. Trends Cell Biol. *16*, 79–87.

Rapoport, B.L., Demetriou, G.S., Moodley, S.D., and Benn, C.A. (2014). When and How Do I Use Neoadjuvant Chemotherapy for Breast Cancer? Curr. Treat. Options Oncol. *15*, 86–98.

Reeder, A., Attar, M., Nazario, L., Bathula, C., Zhang, A., Hochbaum, D., Roy, E., Cooper, K.L., Oesterreich, S., Davidson, N.E., et al. (2015). Stress hormones reduce the efficacy of paclitaxel in triple negative breast cancer through induction of DNA damage. Br. J. Cancer *112*, 1461–1470.

Reya, T., Morrison, S.J., Clarke, M.F., and Weissman, I.L. (2001). Stem cells, cancer, and cancer stem cells. Nature *414*, 105–111.

Reyal, F., Guyader, C., Decraene, C., Lucchesi, C., Auger, N., Assayag, F., De Plater, L., Gentien, D., Poupon, M.-F., Cottu, P., et al. (2012). Molecular profiling of patient-derived breast cancer xenografts. Breast Cancer Res. BCR *14*, R11.

Rhee, W.J., and Bao, G. (2009). Simultaneous detection of mRNA and protein stem cell markers in live cells. BMC Biotechnol. *9*, 30.

Ricardo, S., Vieira, A.F., Gerhard, R., Leitão, D., Pinto, R., Cameselle-Teijeiro, J.F., Milanezi, F., Schmitt, F., and Paredes, J. (2011). Breast cancer stem cell markers CD44, CD24 and ALDH1: expression distribution within intrinsic molecular subtype. J. Clin. Pathol. *64*, 937–946.

Ricci, F., Bizzaro, F., Cesca, M., Guffanti, F., Ganzinelli, M., Decio, A., Ghilardi, C., Perego, P., Fruscio, R., Buda, A., et al. (2014). Patient-derived ovarian tumor xenografts recapitulate human clinicopathology and genetic alterations. Cancer Res. *74*, 6980–6990.

Ricci, F., Fratelli, M., Guffanti, F., Porcu, L., Spriano, F., Dell'Anna, T., Fruscio, R., and Damia, G. (2017). Patient-derived ovarian cancer xenografts re-growing after a cisplatinum treatment are less responsive to a second drug re-challenge: a new experimental setting to study response to therapy. Oncotarget *8*, 7441–7451.

Robert, N.J., Diéras, V., Glaspy, J., Brufsky, A.M., Bondarenko, I., Lipatov, O.N., Perez, E.A., Yardley, D.A., Chan, S.Y.T., Zhou, X., et al. (2011). RIBBON-1: randomized, double-blind, placebo-controlled, phase III trial of chemotherapy with or without bevacizumab for first-line treatment of human epidermal growth factor receptor 2-negative, locally recurrent or metastatic breast cancer. J. Clin. Oncol. Off. J. Am. Soc. Clin. Oncol. *29*, 1252–1260.

Robinson, D.R., Wu, Y.-M., Vats, P., Su, F., Lonigro, R.J., Cao, X., Kalyana-Sundaram, S., Wang, R., Ning, Y., Hodges, L., et al. (2013). Activating ESR1 mutations in hormone-resistant metastatic breast cancer. Nat. Genet. *45*, 1446–1451.

Roger, S., Le Guennec, J.-Y., and Besson, P. (2004). Particular sensitivity to calcium channel blockers of the fast inward voltage-dependent sodium current involved in the invasive properties of a metastastic breast cancer cell line. Br. J. Pharmacol. *141*, 610–615.

Roll, J.D., Rivenbark, A.G., Jones, W.D., and Coleman, W.B. (2008). DNMT3b overexpression contributes to a hypermethylator phenotype in human breast cancer cell lines. Mol. Cancer *7*, 15.

Ross, D.D., and Nakanishi, T. (2010). Impact of breast cancer resistance protein on cancer treatment outcomes. Methods Mol. Biol. Clifton NJ *596*, 251–290.

Rouzier, R., Rajan, R., Wagner, P., Hess, K.R., Gold, D.L., Stec, J., Ayers, M., Ross, J.S., Zhang, P., Buchholz, T.A., et al. (2005). Microtubule-associated protein tau: A marker of paclitaxel sensitivity in breast cancer. Proc. Natl. Acad. Sci. U. S. A. *102*, 8315–8320.

Rudd, G.N., Hartley, J.A., and Souhami, R.L. (1995). Persistence of cisplatin-induced DNA interstrand crosslinking in peripheral blood mononuclear cells from elderly and young individuals. Cancer Chemother. Pharmacol. *35*, 323–326.

Runz, S., Mierke, C.T., Joumaa, S., Behrens, J., Fabry, B., and Altevogt, P. (2008). CD24 induces localization of beta1 integrin to lipid raft domains. Biochem. Biophys. Res. Commun. *365*, 35–41.

Russnes, H.G., Lingjærde, O.C., Børresen-Dale, A.-L., and Caldas, C. (2017). Breast Cancer Molecular Stratification: From Intrinsic Subtypes to Integrative Clusters. Am. J. Pathol. *187*, 2152–2162.

Rycaj, K., and Tang, D.G. (2015). Cell-of-Origin of Cancer versus Cancer Stem Cells: Assays and Interpretations. Cancer Res. *75*, 4003–4011.

Sabatier, R., Finetti, P., Guille, A., Adelaide, J., Chaffanet, M., Viens, P., Birnbaum, D., and Bertucci, F. (2014). Claudin-low breast cancers: clinical, pathological, molecular and prognostic characterization. Mol. Cancer *13*.

Sakakibara, T., Xu, Y., Bumpers, H.L., Chen, F.A., Bankert, R.B., Arredondo, M.A., Edge, S.B., and Repasky, E.A. (1996). Growth and metastasis of surgical specimens of human breast carcinomas in SCID mice. Cancer J. Sci. Am. *2*, 291–300.

Sanders, M.A., Haynes, B., Nangia-Makker, P., Polin, L.A., and Shekhar, M.P. (2017). Pharmacological targeting of RAD6 enzyme-mediated translesion synthesis overcomes resistance to platinum-based drugs. J. Biol. Chem. *292*, 10347–10363.

Sanfilippo, O., Ronchi, E., De Marco, C., Di Fronzo, G., and Silvestrini, R. (1991). Expression of P-glycoprotein in breast cancer tissue and in vitro resistance to doxorubicin and vincristine. Eur. J. Cancer Oxf. Engl. 1990 *27*, 155–158.

Sano, A., Kato, H., Sakurai, S., Sakai, M., Tanaka, N., Inose, T., Saito, K., Sohda, M., Nakajima, M., Nakajima, T., et al. (2009). CD24 expression is a novel prognostic factor in esophageal squamous cell carcinoma. Ann. Surg. Oncol. *16*, 506–514.

Santini, D., Schiavon, G., Vincenzi, B., Gaeta, L., Pantano, F., Russo, A., Ortega, C., Porta, C., Galluzzo, S., Armento, G., et al. (2011). Receptor activator of NF-kB (RANK) expression in primary tumors associates with bone metastasis occurrence in breast cancer patients. PloS One *6*, e19234.

Saux, O.L., You, B., and Freyer, G. (2014). Antiangiogenic Therapy in Patients With HER2-Positive Metastatic Breast Cancer: A Case Series. Clin. Breast Cancer *14*, e89–e94.

Savas, P., Salgado, R., Denkert, C., Sotiriou, C., Darcy, P.K., Smyth, M.J., and Loi, S. (2016). Clinical relevance of host immunity in breast cancer: from TILs to the clinic. Nat. Rev. Clin. Oncol. *13*, 228–241.

Scaltriti, M., Elkabets, M., and Baselga, J. (2016). Molecular Pathways: AXL, a Membrane Receptor Mediator of Resistance to Therapy. Clin. Cancer Res. Off. J. Am. Assoc. Cancer Res. *22*, 1313–1317.

Scheel, C., Eaton, E.N., Li, S.H.-J., Chaffer, C.L., Reinhardt, F., Kah, K.-J., Bell, G., Guo, W., Rubin, J., Richardson, A.L., et al. (2011). Paracrine and autocrine signals induce and maintain mesenchymal and stem cell states in the breast. Cell *145*, 926–940.

Schmidt, M., Hasenclever, D., Schaeffer, M., Boehm, D., Cotarelo, C., Steiner, E., Lebrecht, A., Siggelkow, W., Weikel, W., Schiffer-Petry, I., et al. (2008). Prognostic effect of epithelial cell adhesion molecule overexpression in untreated node-negative breast cancer. Clin. Cancer Res. Off. J. Am. Assoc. Cancer Res. *14*, 5849–5855.

Schmidt, M., Rüttinger, D., Sebastian, M., Hanusch, C.A., Marschner, N., Baeuerle, P.A., Wolf, A., Göppel, G., Oruzio, D., Schlimok, G., et al. (2012). Phase IB study of the EpCAM antibody adecatumumab combined with docetaxel in patients with

EpCAM-positive relapsed or refractory advanced-stage breast cancer. Ann. Oncol. Off. J. Eur. Soc. Med. Oncol. *23*, 2306–2313.

Schmidt, T., van Mackelenbergh, M., Wesch, D., and Mundhenke, C. (2017). Physical activity influences the immune system of breast cancer patients. J. Cancer Res. Ther. *13*, 392–398.

Schmidt-Kittler, O., Ragg, T., Daskalakis, A., Granzow, M., Ahr, A., Blankenstein, T.J.F., Kaufmann, M., Diebold, J., Arnholdt, H., Muller, P., et al. (2003). From latent disseminated cells to overt metastasis: genetic analysis of systemic breast cancer progression. Proc. Natl. Acad. Sci. U. S. A. *100*, 7737–7742.

Schmitt, F., Ricardo, S., Vieira, A.F., Dionísio, M.R., and Paredes, J. (2012). Cancer stem cell markers in breast neoplasias: their relevance and distribution in distinct molecular subtypes. Virchows Arch. Int. J. Pathol. *460*, 545–553.

Schramek, D., Leibbrandt, A., Sigl, V., Kenner, L., Pospisilik, J.A., Lee, H.J., Hanada, R., Joshi, P.A., Aliprantis, A., Glimcher, L., et al. (2010). Osteoclast differentiation factor RANKL controls development of progestin-driven mammary cancer. Nature *468*, 98–102.

Sena, L.A., and Chandel, N.S. (2012). Physiological roles of mitochondrial reactive oxygen species. Mol. Cell *48*, 158–167.

Serratì, S., De Summa, S., Pilato, B., Petriella, D., Lacalamita, R., Tommasi, S., and Pinto, R. (2016). Next-generation sequencing: advances and applications in cancer diagnosis. OncoTargets Ther. *9*, 7355–7365.

Seruga, B., and Tannock, I.F. (2008). Intermittent androgen blockade should be regarded as standard therapy in prostate cancer. Nat. Clin. Pract. Oncol. *5*, 574–576.

Sflomos, G., Dormoy, V., Metsalu, T., Jeitziner, R., Battista, L., Scabia, V., Raffoul, W., Delaloye, J.-F., Treboux, A., Fiche, M., et al. (2016). A Preclinical Model for ERα-Positive Breast Cancer Points to the Epithelial Microenvironment as Determinant of Luminal Phenotype and Hormone Response. Cancer Cell *29*, 407–422.

Shafi, H., Astvatsaturyan, K., Chung, F., Mirocha, J., Schmidt, M., and Bose, S. (2013). Clinicopathological significance of HER2/neu genetic heterogeneity in HER2/neu non-amplified invasive breast carcinomas and its concurrent axillary metastasis. J. Clin. Pathol. *66*, 649–654.

Shah, S.P., Morin, R.D., Khattra, J., Prentice, L., Pugh, T., Burleigh, A., Delaney, A., Gelmon, K., Guliany, R., Senz, J., et al. (2009). Mutational evolution in a lobular breast tumour profiled at single nucleotide resolution. Nature *461*, 809–813.

Shah, S.P., Roth, A., Goya, R., Oloumi, A., Ha, G., Zhao, Y., Turashvili, G., Ding, J., Tse, K., Haffari, G., et al. (2012). The clonal and mutational evolution spectrum of primary triple-negative breast cancers. Nature *486*, 395–399.

Shapiro, C.L., Manola, J., and Leboff, M. (2001). Ovarian failure after adjuvant chemotherapy is associated with rapid bone loss in women with early-stage breast cancer. J. Clin. Oncol. Off. J. Am. Soc. Clin. Oncol. *19*, 3306–3311.

Shargh, S.A., Sakizli, M., Khalaj, V., Movafagh, A., Yazdi, H., Hagigatjou, E., Sayad, A., Mansouri, N., Mortazavi-Tabatabaei, S.A., and Khorram Khorshid, H.R. (2014). Downregulation of E-cadherin expression in breast cancer by promoter hypermethylation and its relation with progression and prognosis of tumor. Med. Oncol. Northwood Lond. Engl. *31*, 250.

Shaw, L.M. (1999a). Integrin function in breast carcinoma progression. J. Mammary Gland Biol. Neoplasia *4*, 367–376.

Shaw, L.M. (1999b). Integrin function in breast carcinoma progression. J. Mammary Gland Biol. Neoplasia *4*, 367–376.

Shiovitz, S., and Korde, L.A. (2015). Genetics of breast cancer: a topic in evolution. Ann. Oncol. Off. J. Eur. Soc. Med. Oncol. *26*, 1291–1299.

Shipitsin, M., Campbell, L.L., Argani, P., Weremowicz, S., Bloushtain-Qimron, N., Yao, J., Nikolskaya, T., Serebryiskaya, T., Beroukhim, R., Hu, M., et al. (2007). Molecular definition of breast tumor heterogeneity. Cancer Cell *11*, 259–273.

Shultz, L.D., Lyons, B.L., Burzenski, L.M., Gott, B., Chen, X., Chaleff, S., Kotb, M., Gillies, S.D., King, M., Mangada, J., et al. (2005). Human lymphoid and myeloid cell development in NOD/LtSz-scid IL2R gamma null mice engrafted with mobilized human hemopoietic stem cells. J. Immunol. Baltim. Md 1950 *174*, 6477–6489.

Silva, A.S., Kam, Y., Khin, Z.P., Minton, S.E., Gillies, R.J., and Gatenby, R.A. (2012). Evolutionary approaches to prolong progression-free survival in breast cancer. Cancer Res. *72*, 6362–6370.

Silver, D.P., Richardson, A.L., Eklund, A.C., Wang, Z.C., Szallasi, Z., Li, Q., Juul, N., Leong, C.-O., Calogrias, D., Buraimoh, A., et al. (2010). Efficacy of neoadjuvant Cisplatin in triple-negative breast cancer. J. Clin. Oncol. Off. J. Am. Soc. Clin. Oncol. *28*, 1145–1153.

Simões, B.M., O'Brien, C.S., Eyre, R., Silva, A., Yu, L., Sarmiento-Castro, A., Alférez, D.G., Spence, K., Santiago-Gómez, A., Chemi, F., et al. (2015). Anti-estrogen Resistance in Human Breast Tumors Is Driven by JAG1-NOTCH4-Dependent Cancer Stem Cell Activity. Cell Rep. *12*, 1968–1977.

Siolas, D., and Hannon, G.J. (2013). Patient-Derived Tumor Xenografts: Transforming Clinical Samples into Mouse Models. Cancer Res. *73*, 5315–5319.

Skibinski, A., and Kuperwasser, C. (2015). The origin of breast tumor heterogeneity. Oncogene *34*, 5309–5316.

Sládek, N.E. (2003). Human aldehyde dehydrogenases: potential pathological, pharmacological, and toxicological impact. J. Biochem. Mol. Toxicol. *17*, 7–23.

Slamon, D., Eiermann, W., Robert, N., Pienkowski, T., Martin, M., Press, M., Mackey, J., Glaspy, J., Chan, A., Pawlicki, M., et al. (2011). Adjuvant trastuzumab in HER2-positive breast cancer. N. Engl. J. Med. *365*, 1273–1283.

Smalley, M., Piggott, L., and Clarkson, R. (2013). Breast cancer stem cells: obstacles to therapy. Cancer Lett. *338*, 57–62.

Soares, J., Pinto, A.E., Cunha, C.V., André, S., Barão, I., Sousa, J.M., and Cravo, M. (1999). Global DNA hypomethylation in breast carcinoma: correlation with prognostic factors and tumor progression. Cancer *85*, 112–118.

Solinas, C., Ceppi, M., Lambertini, M., Scartozzi, M., Buisseret, L., Garaud, S., Fumagalli, D., de Azambuja, E., Salgado, R., Sotiriou, C., et al. (2017). Tumor-infiltrating lymphocytes in patients with HER2-positive breast cancer treated with neoadjuvant chemotherapy plus trastuzumab, lapatinib or their combination: A meta-analysis of randomized controlled trials. Cancer Treat. Rev. *57*, 8–15.

Song, S., Honjo, S., Jin, J., Chang, S.-S., Scott, A.W., Chen, Q., Kalhor, N., Correa, A.M., Hofstetter, W.L., Albarracin, C.T., et al. (2015). The Hippo Coactivator YAP1 Mediates EGFR Overexpression and Confers Chemoresistance in Esophageal Cancer. Clin. Cancer Res. Off. J. Am. Assoc. Cancer Res. *21*, 2580–2590.

Sordillo, E.M., and Pearse, R.N. (2003). RANK-Fc: a therapeutic antagonist for RANK-L in myeloma. Cancer *97*, 802–812.

Sørlie, T., Perou, C.M., Tibshirani, R., Aas, T., Geisler, S., Johnsen, H., Hastie, T., Eisen, M.B., van de Rijn, M., Jeffrey, S.S., et al. (2001). Gene expression patterns of breast carcinomas distinguish tumor subclasses with clinical implications. Proc. Natl. Acad. Sci. U. S. A. *98*, 10869–10874.

Sorlie, T., Tibshirani, R., Parker, J., Hastie, T., Marron, J.S., Nobel, A., Deng, S., Johnsen, H., Pesich, R., Geisler, S., et al. (2003). Repeated observation of breast tumor subtypes in independent gene expression data sets. Proc. Natl. Acad. Sci. U. S. A. *100*, 8418–8423.

Stahl, M., Ge, C., Shi, S., Pestell, R.G., and Stanley, P. (2006). Notch1-Induced Transformation of RKE-1 Cells Requires Up-regulation of Cyclin D1. Cancer Res. *66*, 7562–7570.

Stefansson, O.A., and Esteller, M. (2013). Epigenetic modifications in breast cancer and their role in personalized medicine. Am. J. Pathol. *183*, 1052–1063.

Stephens, P.J., Greenman, C.D., Fu, B., Yang, F., Bignell, G.R., Mudie, L.J., Pleasance, E.D., Lau, K.W., Beare, D., Stebbings, L.A., et al. (2011). Massive genomic rearrangement acquired in a single catastrophic event during cancer development. Cell *144*, 27–40.

Stephens, P.J., Tarpey, P.S., Davies, H., Van Loo, P., Greenman, C., Wedge, D.C., Nik-Zainal, S., Martin, S., Varela, I., Bignell, G.R., et al. (2012). The landscape of cancer genes and mutational processes in breast cancer. Nature *486*, 400–404.

Strobel, T., Swanson, L., Korsmeyer, S., and Cannistra, S.A. (1996). BAX enhances paclitaxel-induced apoptosis through a p53-independent pathway. Proc. Natl. Acad. Sci. U. S. A. *93*, 14094–14099.

Struewing, J.P., Hartge, P., Wacholder, S., Baker, S.M., Berlin, M., McAdams, M., Timmerman, M.M., Brody, L.C., and Tucker, M.A. (1997). The Risk of Cancer Associated with Specific Mutations of BRCA1 and BRCA2 among Ashkenazi Jews. N. Engl. J. Med. *336*, 1401–1408.

Suzuki, Y., Ng, S.B., Chua, C., Leow, W.Q., Chng, J., Liu, S.Y., Ramnarayanan, K., Gan, A., Ho, D.L., Ten, R., et al. (2017). Multiregion ultra-deep sequencing reveals

early intermixing and variable levels of intratumoral heterogeneity in colorectal cancer. Mol. Oncol. *11*, 124–139.

Swain, S.M., Baselga, J., Kim, S.-B., Ro, J., Semiglazov, V., Campone, M., Ciruelos, E., Ferrero, J.-M., Schneeweiss, A., Heeson, S., et al. (2015). Pertuzumab, Trastuzumab, and Docetaxel in HER2-Positive Metastatic Breast Cancer. N. Engl. J. Med. *372*, 724–734.

Swanton, C. (2012). Intratumor heterogeneity: evolution through space and time. Cancer Res. *72*, 4875–4882.

Swartz, M.A., Iida, N., Roberts, E.W., Sangaletti, S., Wong, M.H., Yull, F.E., Coussens, L.M., and DeClerck, Y.A. (2012). Tumor microenvironment complexity: emerging roles in cancer therapy. Cancer Res. *72*, 2473–2480.

Szakács, G., Annereau, J.-P., Lababidi, S., Shankavaram, U., Arciello, A., Bussey, K.J., Reinhold, W., Guo, Y., Kruh, G.D., Reimers, M., et al. (2004). Predicting drug sensitivity and resistance: profiling ABC transporter genes in cancer cells. Cancer Cell *6*, 129–137.

Tajima, S., and Suetake, I. (1998). Regulation and function of DNA methylation in vertebrates. J. Biochem. (Tokyo) *123*, 993–999.

Takada, M., Nagai, S., Haruta, M., Sugino, R.P., Tozuka, K., Takei, H., Ohkubo, F., Inoue, K., Kurosumi, M., Miyazaki, M., et al. (2017). BRCA1 alterations with additional defects in DNA damage response genes may confer chemoresistance to BRCA-like breast cancers treated with neoadjuvant chemotherapy. Genes. Chromosomes Cancer *56*, 405–420.

Takahashi, K., and Yamanaka, S. (2006). Induction of pluripotent stem cells from mouse embryonic and adult fibroblast cultures by defined factors. Cell *126*, 663–676.

Takai, D., and Jones, P.A. (2002). Comprehensive analysis of CpG islands in human chromosomes 21 and 22. Proc. Natl. Acad. Sci. U. S. A. *99*, 3740–3745.

Tamada, M., Nagano, O., Tateyama, S., Ohmura, M., Yae, T., Ishimoto, T., Sugihara, E., Onishi, N., Yamamoto, T., Yanagawa, H., et al. (2012). Modulation of glucose metabolism by CD44 contributes to antioxidant status and drug resistance in cancer cells. Cancer Res. *72*, 1438–1448.

Tamura, R.N., Cooper, H.M., Collo, G., and Quaranta, V. (1991). Cell type-specific integrin variants with alternative alpha chain cytoplasmic domains. Proc. Natl. Acad. Sci. U. S. A. *88*, 10183–10187.

Tan, W., Zhang, W., Strasner, A., Grivennikov, S., Cheng, J.Q., Hoffman, R.M., and Karin, M. (2011). Tumour-infiltrating regulatory T cells stimulate mammary cancer metastasis through RANKL-RANK signalling. Nature *470*, 548–553.

Tanei, T., Morimoto, K., Shimazu, K., Kim, S.J., Tanji, Y., Taguchi, T., Tamaki, Y., and Noguchi, S. (2009). Association of Breast Cancer Stem Cells Identified by Aldehyde Dehydrogenase 1 Expression with Resistance to Sequential Paclitaxel and Epirubicin-Based Chemotherapy for Breast Cancers. Clin. Cancer Res. *15*, 4234–4241.

Tang, D., Sivko, G.S., and DeWille, J.W. (2006). Promoter methylation reduces C/EBPdelta (CEBPD) gene expression in the SUM-52PE human breast cancer cell line and in primary breast tumors. Breast Cancer Res. Treat. *95*, 161–170.

Tao, J.J., Castel, P., Radosevic-Robin, N., Elkabets, M., Auricchio, N., Aceto, N., Weitsman, G., Barber, P., Vojnovic, B., Ellis, H., et al. (2014). Antagonism of EGFR and HER3 enhances the response to inhibitors of the PI3K-Akt pathway in triple-negative breast cancer. Sci. Signal. *7*, ra29.

Tashireva, L.A., Denisov, E.V., Gerashchenko, T.S., Pautova, D.N., Buldakov, M.A., Zavyalova, M.V., Kzhyshkowska, J., Cherdyntseva, N.V., and Perelmuter, V.M. (2017). Intratumoral heterogeneity of macrophages and fibroblasts in breast cancer is associated with the morphological diversity of tumor cells and contributes to lymph node metastasis. Immunobiology *222*, 631–640.

Telli, M.L., Timms, K.M., Reid, J., Hennessy, B., Mills, G.B., Jensen, K.C., Szallasi, Z., Barry, W.T., Winer, E.P., Tung, N.M., et al. (2016). Homologous Recombination Deficiency (HRD) Score Predicts Response to Platinum-Containing Neoadjuvant Chemotherapy in Patients with Triple-Negative Breast Cancer. Clin. Cancer Res. Off. J. Am. Assoc. Cancer Res. *22*, 3764–3773.

Tentler, J.J., Tan, A.C., Weekes, C.D., Jimeno, A., Leong, S., Pitts, T.M., Arcaroli, J.J., Messersmith, W.A., and Eckhardt, S.G. (2012). Patient-derived tumour xenografts as models for oncology drug development. Nat. Rev. Clin. Oncol. *9*, 338–350.

Ter Brugge, P., Kristel, P., van der Burg, E., Boon, U., de Maaker, M., Lips, E., Mulder, L., de Ruiter, J., Moutinho, C., Gevensleben, H., et al. (2016). Mechanisms of Therapy Resistance in Patient-Derived Xenograft Models of BRCA1-Deficient Breast Cancer. J. Natl. Cancer Inst. *108*.

Thiery, J.P., Acloque, H., Huang, R.Y.J., and Nieto, M.A. (2009). Epithelial-Mesenchymal Transitions in Development and Disease. Cell *139*, 871–890.

Thompson, A., Brennan, K., Cox, A., Gee, J., Harcourt, D., Harris, A., Harvie, M., Holen, I., Howell, A., Nicholson, R., et al. (2008). Evaluation of the current knowledge limitations in breast cancer research: a gap analysis. Breast Cancer Res. BCR *10*, R26.

Timcheva, C.V., and Todorov, D.K. (1996). Does verapamil help overcome multidrug resistance in tumor cell lines and cancer patients? J. Chemother. Florence Italy *8*, 295–299.

Tiran, V., Stanzer, S., Heitzer, E., Meilinger, M., Rossmann, C., Lax, S., Tsybrovskyy, O., Dandachi, N., and Balic, M. (2017). Genetic profiling of putative breast cancer stem cells from malignant pleural effusions. PLoS ONE *12*.

Tomar, T., de Jong, S., Alkema, N.G., Hoekman, R.L., Meersma, G.J., Klip, H.G., van der Zee, A.G., and Wisman, G.B.A. (2016). Genome-wide methylation profiling of ovarian cancer patient-derived xenografts treated with the demethylating agent decitabine identifies novel epigenetically regulated genes and pathways. Genome Med. *8*, 107.

Topham, C.H., and Taylor, S.S. (2013). Mitosis and apoptosis: how is the balance set? Curr. Opin. Cell Biol. *25*, 780–785.

Toy, W., Shen, Y., Won, H., Green, B., Sakr, R.A., Will, M., Li, Z., Gala, K., Fanning, S., King, T.A., et al. (2013). ESR1 ligand-binding domain mutations in hormone-resistant breast cancer. Nat. Genet. *45*, 1439–1445.

Traverso, N., Ricciarelli, R., Nitti, M., Marengo, B., Furfaro, A.L., Pronzato, M.A., Marinari, U.M., and Domenicotti, C. (2013). Role of glutathione in cancer progression and chemoresistance. Oxid. Med. Cell. Longev. *2013*, 972913.

Trock, B.J., Leonessa, F., and Clarke, R. (1997). Multidrug resistance in breast cancer: a meta-analysis of MDR1/gp170 expression and its possible functional significance. J. Natl. Cancer Inst. *89*, 917–931.

Tsai, H.-C., Li, H., Van Neste, L., Cai, Y., Robert, C., Rassool, F.V., Shin, J.J., Harbom, K.M., Beaty, R., Pappou, E., et al. (2012). Transient low doses of DNA-demethylating agents exert durable antitumor effects on hematological and epithelial tumor cells. Cancer Cell *21*, 430–446.

Tsang, J.Y.S., Huang, Y.-H., Luo, M.-H., Ni, Y.-B., Chan, S.-K., Lui, P.C.W., Yu, A.M.C., Tan, P.H., and Tse, G.M. (2012). Cancer stem cell markers are associated with adverse biomarker profiles and molecular subtypes of breast cancer. Breast Cancer Res. Treat. *136*, 407–417.

Turner, N.C., and Reis-Filho, J.S. (2012). Genetic heterogeneity and cancer drug resistance. Lancet Oncol. *13*, e178-185.

Turner, N., Lambros, M.B., Horlings, H.M., Pearson, A., Sharpe, R., Natrajan, R., Geyer, F.C., van Kouwenhove, M., Kreike, B., Mackay, A., et al. (2010). Integrative molecular profiling of triple negative breast cancers identifies amplicon drivers and potential therapeutic targets. Oncogene *29*, 2013–2023.

Valdés-Mas, R., Bea, S., Puente, D.A., López-Otín, C., and Puente, X.S. (2012). Estimation of copy number alterations from exome sequencing data. PloS One *7*, e51422.

Varley, K.E., Gertz, J., Bowling, K.M., Parker, S.L., Reddy, T.E., Pauli-Behn, F., Cross, M.K., Williams, B.A., Stamatoyannopoulos, J.A., Crawford, G.E., et al. (2013). Dynamic DNA methylation across diverse human cell lines and tissues. Genome Res. *23*, 555–567.

Vassilopoulos, A., Wang, R.-H., Petrovas, C., Ambrozak, D., Koup, R., and Deng, C.-X. (2008). Identification and characterization of cancer initiating cells from BRCA1 related mammary tumors using markers for normal mammary stem cells. Int. J. Biol. Sci. *4*, 133–142.

Vassilopoulos, A., Chisholm, C., Lahusen, T., Zheng, H., and Deng, C.-X. (2014). A critical role of CD29 and CD49f in mediating metastasis for cancer-initiating cells isolated from a Brca1-associated mouse model of breast cancer. Oncogene *33*, 5477–5482.

Velasco-Velázquez, M.A., Popov, V.M., Lisanti, M.P., and Pestell, R.G. (2011). The role of breast cancer stem cells in metastasis and therapeutic implications. Am. J. Pathol. *179*, 2–11.

Venditti, J.M., Wesley, R.A., and Plowman, J. (1984). Current NCI preclinical antitumor screening in vivo: results of tumor panel screening, 1976-1982, and future directions. Adv. Pharmacol. Chemother. *20*, 1–20.

Vieira, A.F., Ricardo, S., Ablett, M.P., Dionísio, M.R., Mendes, N., Albergaria, A., Farnie, G., Gerhard, R., Cameselle-Teijeiro, J.F., Seruca, R., et al. (2012). P-cadherin is coexpressed with CD44 and CD49f and mediates stem cell properties in basal-like breast cancer. Stem Cells Dayt. Ohio *30*, 854–864.

Visconti, R., and Grieco, D. (2017). Fighting tubulin-targeting anticancer drug toxicity and resistance. Endocr. Relat. Cancer *24*, T107–T117.

Visus, C., Ito, D., Amoscato, A., Maciejewska-Franczak, M., Abdelsalem, A., Dhir, R., Shin, D.M., Donnenberg, V.S., Whiteside, T.L., and DeLeo, A.B. (2007). Identification of Human Aldehyde Dehydrogenase 1 Family Member A1 as a Novel CD8+ T-Cell–Defined Tumor Antigen in Squamous Cell Carcinoma of the Head and Neck. Cancer Res. *67*, 10538–10545.

Visvader, J.E. (2011). Cells of origin in cancer. Nature *469*, 314–322.

Visvader, J.E., and Lindeman, G.J. (2010). Stem cells and cancer - the promise and puzzles. Mol. Oncol. *4*, 369–372.

Vora, S.R., Juric, D., Kim, N., Mino-Kenudson, M., Huynh, T., Costa, C., Lockerman, E.L., Pollack, S.F., Liu, M., Li, X., et al. (2014). CDK 4/6 inhibitors sensitize PIK3CA mutant breast cancer to PI3K inhibitors. Cancer Cell *26*, 136–149.

Voulgari, A., and Pintzas, A. (2009). Epithelial-mesenchymal transition in cancer metastasis: mechanisms, markers and strategies to overcome drug resistance in the clinic. Biochim. Biophys. Acta *1796*, 75–90.

Wada, T., Nakashima, T., Hiroshi, N., and Penninger, J.M. (2006). RANKL-RANK signaling in osteoclastogenesis and bone disease. Trends Mol. Med. *12*, 17–25.

Wang, D., Pham, N.-A., Tong, J., Sakashita, S., Allo, G., Kim, L., Yanagawa, N., Raghavan, V., Wei, Y., To, C., et al. (2017). Molecular heterogeneity of non-small cell lung carcinoma patient-derived xenografts closely reflect their primary tumors. Int. J. Cancer *140*, 662–673.

Wang, Y., Waters, J., Leung, M.L., Unruh, A., Roh, W., Shi, X., Chen, K., Scheet, P., Vattathil, S., Liang, H., et al. (2014a). Clonal evolution in breast cancer revealed by single nucleus genome sequencing. Nature *512*, 155–160.

Wang, Y., Waters, J., Leung, M.L., Unruh, A., Roh, W., Shi, X., Chen, K., Scheet, P., Vattathil, S., Liang, H., et al. (2014b). Clonal evolution in breast cancer revealed by single nucleus genome sequencing. Nature *512*, 155–160.

Ward, E.M., DeSantis, C.E., Lin, C.C., Kramer, J.L., Jemal, A., Kohler, B., Brawley, O.W., and Gansler, T. (2015). Cancer statistics: Breast cancer in situ. CA. Cancer J. Clin. *65*, 481–495.

Wei, X., Dombkowski, D., Meirelles, K., Pieretti-Vanmarcke, R., Szotek, P.P., Chang, H.L., Preffer, F.I., Mueller, P.R., Teixeira, J., MacLaughlin, D.T., et al. (2010). Mullerian inhibiting substance preferentially inhibits stem/progenitors in human

ovarian cancer cell lines compared with chemotherapeutics. Proc. Natl. Acad. Sci. U. S. A. *107*, 18874–18879.

Wewer, U.M., Shaw, L.M., Albrechtsen, R., and Mercurio, A.M. (1997). The integrin alpha 6 beta 1 promotes the survival of metastatic human breast carcinoma cells in mice. Am. J. Pathol. *151*, 1191–1198.

Whittaker, S.J., Demierre, M.-F., Kim, E.J., Rook, A.H., Lerner, A., Duvic, M., Scarisbrick, J., Reddy, S., Robak, T., Becker, J.C., et al. (2010). Final results from a multicenter, international, pivotal study of romidepsin in refractory cutaneous T-cell lymphoma. J. Clin. Oncol. Off. J. Am. Soc. Clin. Oncol. *28*, 4485–4491.

Whittle, J.R., Lewis, M.T., Lindeman, G.J., and Visvader, J.E. (2015). Patient-derived xenograft models of breast cancer and their predictive power. Breast Cancer Res. *17*, 17.

Widschwendter, M., and Menon, U. (2006). Circulating methylated DNA: a new generation of tumor markers. Clin. Cancer Res. Off. J. Am. Assoc. Cancer Res. *12*, 7205–7208.

Wijayahadi, N., Haron, M.R., Stanslas, J., and Yusuf, Z. (2007). Changes in cellular immunity during chemotherapy for primary breast cancer with anthracycline regimens. J. Chemother. Florence Italy *19*, 716–723.

Wilding, J.L., and Bodmer, W.F. (2014). Cancer cell lines for drug discovery and development. Cancer Res. *74*, 2377–2384.

Wong, N.C., Bhadri, V.A., Maksimovic, J., Parkinson-Bates, M., Ng, J., Craig, J.M., Saffery, R., and Lock, R.B. (2014). Stability of gene expression and epigenetic profiles highlights the utility of patient-derived paediatric acute lymphoblastic leukaemia xenografts for investigating molecular mechanisms of drug resistance. BMC Genomics *15*, 416.

Wooster, R., Neuhausen, S.L., Mangion, J., Quirk, Y., Ford, D., Collins, N., Nguyen, K., Seal, S., Tran, T., and Averill, D. (1994). Localization of a breast cancer susceptibility gene, BRCA2, to chromosome 13q12-13. Science *265*, 2088–2090.

Wright, M.H., Calcagno, A.M., Salcido, C.D., Carlson, M.D., Ambudkar, S.V., and Varticovski, L. (2008). Brca1 breast tumors contain distinct CD44+/CD24- and CD133+ cells with cancer stem cell characteristics. Breast Cancer Res. BCR *10*, R10.

Yamada, K.M., and Even-Ram, S. (2002). Integrin regulation of growth factor receptors. Nat. Cell Biol. *4*, E75-76.

Yang, X.-R., Xu, Y., Yu, B., Zhou, J., Li, J.-C., Qiu, S.-J., Shi, Y.-H., Wang, X.-Y., Dai, Z., Shi, G.-M., et al. (2009). CD24 Is a Novel Predictor for Poor Prognosis of Hepatocellular Carcinoma after Surgery. Clin. Cancer Res. *15*, 5518–5527.

Yap, T.A., Lorente, D., Omlin, A., Olmos, D., and de Bono, J.S. (2014). Circulating tumor cells: a multifunctional biomarker. Clin. Cancer Res. Off. J. Am. Assoc. Cancer Res. *20*, 2553–2568.

Yardley, D.A., Noguchi, S., Pritchard, K.I., Burris, H.A., Baselga, J., Gnant, M., Hortobagyi, G.N., Campone, M., Pistilli, B., Piccart, M., et al. (2013). Everolimus

plus exemestane in postmenopausal patients with HR(+) breast cancer: BOLERO-2 final progression-free survival analysis. Adv. Ther. *30*, 870–884.

Yasuda, H., Shima, N., Nakagawa, N., Mochizuki, S.-I., Yano, K., Fujise, N., Sato, Y., Goto, M., Yamaguchi, K., Kuriyama, M., et al. (1998). Identity of Osteoclastogenesis Inhibitory Factor (OCIF) and Osteoprotegerin (OPG): A Mechanism by which OPG/OCIF Inhibits Osteoclastogenesis in Vitro. Endocrinology *139*, 1329–1337.

Yates, L.R., Gerstung, M., Knappskog, S., Desmedt, C., Gundem, G., Loo, P.V., Aas, T., Alexandrov, L.B., Larsimont, D., Davies, H., et al. (2015). Subclonal diversification of primary breast cancer revealed by multiregion sequencing. Nat. Med. *21*, 751–759.

Yates, L.R., Knappskog, S., Wedge, D., Farmery, J.H.R., Gonzalez, S., Martincorena, I., Alexandrov, L.B., Van Loo, P., Haugland, H.K., Lilleng, P.K., et al. (2017). Genomic Evolution of Breast Cancer Metastasis and Relapse. Cancer Cell *32*, 169–184.e7.

Yazici, H., Terry, M.B., Cho, Y.H., Senie, R.T., Liao, Y., Andrulis, I., and Santella, R.M. (2009). Aberrant methylation of RASSF1A in plasma DNA before breast cancer diagnosis in the Breast Cancer Family Registry. Cancer Epidemiol. Biomark. Prev. Publ. Am. Assoc. Cancer Res. Cosponsored Am. Soc. Prev. Oncol. *18*, 2723–2725.

Yoldi, G., Pellegrini, P., Trinidad, E.M., Cordero, A., Gomez-Miragaya, J., Serra-Musach, J., Dougall, W.C., Muñoz, P., Pujana, M.-A., Planelles, L., et al. (2016). RANK Signaling Blockade Reduces Breast Cancer Recurrence by Inducing Tumor Cell Differentiation. Cancer Res. *76*, 5857–5869.

Young, R.C., Canellos, G.P., Chabner, B.A., Schein, P.S., and DeVita, V.T. (1973). Maintenance chemotherapy for advanced Hodgkin’s disease in remission. Lancet Lond. Engl. *1*, 1339–1343.

Yu, F., Yao, H., Zhu, P., Zhang, X., Pan, Q., Gong, C., Huang, Y., Hu, X., Su, F., Lieberman, J., et al. (2007). let-7 Regulates Self Renewal and Tumorigenicity of Breast Cancer Cells. Cell *131*, 1109–1123.

Yusuf, R.Z., Duan, Z., Lamendola, D.E., Penson, R.T., and Seiden, M.V. (2003). Paclitaxel resistance: molecular mechanisms and pharmacologic manipulation. Curr. Cancer Drug Targets *3*, 1–19.

Zardavas, D., Irrthum, A., Swanton, C., and Piccart, M. (2015). Clinical management of breast cancer heterogeneity. Nat. Rev. Clin. Oncol. *12*, 381–394.

Zeppernick, F., Ahmadi, R., Campos, B., Dictus, C., Helmke, B.M., Becker, N., Lichter, P., Unterberg, A., Radlwimmer, B., and Herold-Mende, C.C. (2008). Stem cell marker CD133 affects clinical outcome in glioma patients. Clin. Cancer Res. Off. J. Am. Assoc. Cancer Res. *14*, 123–129.

Zhang, G., Wang, J., Yang, J., Li, W., Deng, Y., Li, J., Huang, J., Hu, S., and Zhang, B. (2015a). Comparison and evaluation of two exome capture kits and sequencing platforms for variant calling. BMC Genomics *16*, 581.

Zhang, L., Yang, Y., Wei, X.Y., Shi, Y.R., Liu, H.Y., Niu, R.F., and Hao, X.S. (2007). Reversing adriamycin resistance of human breast cancer cells by hyperthermia

combined with Interferon alpha and Verapamil. J. Exp. Clin. Cancer Res. CR *26*, 201–207.

Zhang, M., Tsimelzon, A., Chang, C.-H., Fan, C., Wolff, A., Perou, C.M., Hilsenbeck, S.G., and Rosen, J.M. (2015b). Intratumoral heterogeneity in a Trp53-null mouse model of human breast cancer. Cancer Discov. *5*, 520–533.

Zhang, X., Claerhout, S., Prat, A., Dobrolecki, L.E., Petrovic, I., Lai, Q., Landis, M.D., Wiechmann, L., Schiff, R., Giuliano, M., et al. (2013). A Renewable Tissue Resource of Phenotypically Stable, Biologically and Ethnically Diverse, Patient-Derived Human Breast Cancer Xenograft Models. Cancer Res. *73*, 4885–4897.

Zheng, J., Li, Y., Yang, J., Liu, Q., Shi, M., Zhang, R., Shi, H., Ren, Q., Ma, J., Guo, H., et al. (2011). NDRG2 inhibits hepatocellular carcinoma adhesion, migration and invasion by regulating CD24 expression. BMC Cancer *11*, 251:1-9.

Zielske, S.P., Spalding, A.C., Wicha, M.S., and Lawrence, T.S. (2011). Ablation of breast cancer stem cells with radiation. Transl. Oncol. *4*, 227–233.

Ziller, M.J., Gu, H., Müller, F., Donaghey, J., Tsai, L.T.-Y., Kohlbacher, O., De Jager, P.L., Rosen, E.D., Bennett, D.A., Bernstein, B.E., et al. (2013). Charting a dynamic DNA methylation landscape of the human genome. Nature *500*, 477–481.

Zöller, M. (2011). CD44: can a cancer-initiating cell profit from an abundantly expressed molecule? Nat. Rev. Cancer *11*, 254–267.

Immunodeficient Mouse and Xenograft Host Comparisons.